UNIVERSITY OF LONDON THESIS

Degree PhD Year 2006 Name of Author BALA'AWI, Fadi

Salt Damage at Petra, Jordan: A Study of the Effects of Wind on Salt Distribution and Crystallisation

F. Bala'awi

PhD Thesis

A thesis submitted for the degree of Doctor of Philosophy in Archaeology (Conservation)

Institute of Archaeology
University College London

May 2006

ProQuest LLC
789 East Eisenhower Parkway
P.O. Box 1346
Ann Arbor, MI 48106-1346

Abstract

The crystallisation of salts in porous building materials is a principle agent of decay in historic monuments and archaeological sites, including the World Heritage Site of Petra, Jordan. Nonetheless, the mechanism of salt damage is still inadequately understood. This research was undertaken in order to examine the role of wind speed in the salt damage process.

The first aim of the research was to evaluate the role of wind speed in salt crystallisation and distribution. The second aim was to monitor the microclimate conditions and salt distribution at selected monuments in Petra, in order to understand the extent and mechanism of salt damage at these monuments. The monitoring of the microclimate conditions included spot readings for wind speed, temperature and relative humidity taken during four fieldwork visits as well as continuous logging. The salt distribution was assessed by analysis of samples that were collected from different locations, depths and heights at the same monuments. The research also took into account the role of clay minerals in salt damage. The third aim of the research was to develop a salt simulation test that would include the effects of wind. The tests were undertaken with sandstone and limestone specimens under controlled environmental conditions, including low, high and fluctuating wind speed.

The results have shown that wind speed has a significant impact on salt crystallisation and distribution in porous materials, and thus on decay rates, and that fluctuating wind speed enhances salt damage more than steady speeds. In addition, the research has suggested an unexpected relationship between pore structure and the behaviour of salts under different environmental conditions.

The thesis concludes with recommendations for the conservation of the site of Petra. These include proposals for reducing the salt content of certain monuments and for protection against the effects of wind.

Contents

Volume I

Volume II

Appendices

List of Figures

List of Tables

Acknowledgements

I owe a great debt of gratitude to my principal supervisor Prof. Clifford Price (Institute of Archaeology, UCL) for all his support and encouragement throughout this work. This project would have been impossible without his close supervision and invaluable academic and personal support. I am also very grateful to my second supervisor Ms. Kathryn Tubb (Institute of Archaeology, UCL) for her constant support, academic advice and guidance throughout this project. I must also thank Prof. Talal Akasheh (Hashemite University, Jordan) for his regular advice and support.
I am deeply indebted to the Hashemite University in Jordan, the Karim Rida Said Foundation and University College London for providing me with the financial support for this project. I must express my deepest gratitude to Ms. Ita Gallagher, Further Education Programme Officer at the Karim Rida Said Foundation, for her support and encouragement. I would also like to express my deepest thanks to Prof. Michael Worton, Vice Provost at UCL for his help and support.

I would like to thank a number of people who have provided invaluable technical support for this project: James Hales (Institute of Archaeology, UCL) for his invaluable contribution during the building of the experiment chamber and the provision of consumables, Kevin Reeves (Institute of Archaeology, UCL) for the practical support and guidance in the SEM analysis, and his constructive ideas concerning other practical issues in this project, Dr. Tim Yates (Building Research Establishment) for the provision of stone samples for the experimental work of this project and for all his advice regarding the selection of the stone types, Ms. Jacqui Duffet (Geochemistry Department, Royal Holloway, University of London) for her help with the ICP-AES analysis, Dr. Martin King (Geology Department, Royal Holloway, University of London) and Tony Osben (Earth Sciences Department, UCL) for their help with the IC analysis, Sandra Bond (Institute of Archaeology, UCL) for her help with optical microscopy and the provision of equipment and consumables for this project, Simon Groom (Institute of Archaeology, UCL) for his help with the XRF analysis, Neil Holloway (Geology Department, Royal Holloway, University of London) for preparing the thin sections of the samples, Dr. Graham Lott (British Geological Survey) for his help with the petrographic analysis and the selection of the stone types for this project, Simon Hiorns (Earth Sciences Department, UCL) for his help with the XRD analysis and Dr. Alison Sawdy (Institute of Archaeology, UCL) for the provision of materials for the experimental chamber.

I must express my deepest thanks to Elpiniki Psalti for her enormous and continuous support throughout this project and for the brilliant ideas that helped the completion of this project.

I am also grateful to all my friends and colleagues at the Institute of Archaeology (UCL), and especially to Aude Mongiatti for her help and support.

Last but not least, I would like to extend my thanks to my mother, brothers and sisters. Without their help this project would never have seen the light.

Chapter 1
Introduction

1.1. General

Archaeological sites are an essential part of our cultural heritage, with cultural, historical, architectural, social and economic values. Unfortunately, this important part of the world's cultural heritage is gradually being diminished. This can be due to the nature of the building materials of these sites, which are mainly porous inorganic materials, and the uncontrolled environmental conditions around them.

From a geological point of view, porous materials are more susceptible to weathering agents than non-porous materials. This is related to the fact that porous media are able to exchange their moisture content with the surrounding environments. The change in the moisture content of a porous material, especially stone, usually results in damaging features through a wide range of mechanisms.

1.2. Deterioration factors of porous building materials

The literature includes many reviews, which discuss the main factors that influence the deterioration of porous building materials, and stone in particular (Charola 2004, Price 1996, Honeyborne 1990). Based on these reviews the main causes of deterioration in porous building materials can be summarised as follows:

- **Air pollution:** Many scholars consider air pollution to be as the principle agent of deterioration in porous building materials, especially when it contains acid pollutants that interact with calcareous materials. In particular, sulphur oxides are considered to be the main aggressive compounds, their reaction with calcareous

materials resulting in the formation of slightly soluble calcium sulfate. Sabbioni (2003) presented a detailed review of air pollution damage to stone materials.

- **Soluble salts**: The relation between weathering and the presence of salt has been observed since antiquity (Herodotus 420 B.C., in Luquer 1895). Since the beginning of the last century, the salt damage process in porous materials has been given more attention. Generally, the growth of salt crystals within the pore structure creates pressure inside the porous materials. When the pressure is higher than the tensile strength of these materials, they break down. Chapter 2 will discuss this factor in more detail.
- **Biological activities:** These include the hazards caused by biological organisms and microorganisms. While it is easy to recognise the damage from complex organisms (for example the growth of shrubs and trees within stone buildings), the effect of microorganisms on porous building materials is not easy to observe and more research is still needed in this field (see Griffin, Indictor and Koestler 1991 and Koestler *et al.* 1997 for more details). In addition, animal by-products can have a major effect on porous materials as will be discussed later in this study.
- **Frost attack:** Frost damage in porous materials takes place when these materials become frozen when wet. Honeyborne (1990) states that the damage from this stone deterioration agent is different to the soluble salts and air pollution damage, since it appears dramatically in the form of cracking, that can cause large fragments or many small pieces to become detached, rather than powdering of the host materials.
- **Wet-dry cycling of clay containing materials:** Stones with high clay content may suffer significant decay when subjected to continuous cycles of wetting and

drying. Some clay minerals (swelling clays) have the ability to absorb water into their internal structure, which results in expansion of their volume, and to lose the absorbed water under dry conditions, which causes contraction of their volume. The cycles of expansion-contraction will ultimately weaken the structure of porous materials. This deterioration agent will be discussed in more detail in chapter 4.

- **Thermal cycling:** While some authors do not recognise this as a principal agent of deterioration in porous building materials (Charola 2004), others consider it a primary cause of weathering of stone (Paradise 2005). This type of weathering is related to the difference in expansion and contraction of different minerals within the same porous materials.
- **Other weathering agents in porous materials:** Besides the above mentioned causes of decay in porous materials, there is a long list of other factors also involved in the deterioration of porous building materials, including natural hazards (such as tectonic activities, wind erosion, rainfall and water erosion) and anthropogenic hazards (such as previous conservation treatments, tourism activities and many others) (Charola 2004, Price 1996, Honeyborne 1990).

Among all the above stated deterioration factors, salt damage is one of the most common phenomena in archaeological sites, since salts can absorb moisture, dissolve, crystallise and recrystallise, and many of them can exist in both hydrous and anhydrous forms (Goudie and Viles 1997). Despite the vast amount of research in the salt damage processes (see, for example, Correns 1949, Winkler and Singer 1972, Arnold and Zehnder 1991, Steiger and Zeunert 1996, Goudie and Viles 1997, Rodriguez-Navarro and Doehne 1999a & 1999b, Scherer 1999 & 2000, Pender 2000,

Sawdy 2001, Flatt 2002), the overall understanding of this phenomenon is still open to question. This is due to its complexity, which is mainly related to the wide range of factors involved and the difficulty in monitoring the exact details of the entire process that occurs on a microscopic scale within the pore structure of porous materials.

This research has been undertaken with the aim of exploring one particular factor in the salt damage process that is not yet fully understood: the role of wind speed in the crystallisation and distribution of salts in porous building materials in general, and in selected monuments of the World Heritage Site of Petra, Jordan in particular.

1.3. Petra: an introduction

The archaeological site of Petra is located in the southern part of Jordan. This World Heritage Site has more than 2000 monuments, most hewed into the coloured sandstone and limestone mountains, and is the biggest tourist attraction in Jordan. However, most of its monuments have been deteriorating at a very fast pace over the last few years and in 1995 the site was included on the World Monuments Fund list of the world's 100 most endangered archaeological sites (American Centre of Oriental Research (ACOR) 1997). The city suffers from weathering and erosion problems, both natural and human-in origin. Salt damage is one of the main weathering factors. The detailed description of the site of Petra and its weathering problem is presented in chapter 6.

1.4. Aims and objectives of the current research

The ultimate aim of the research described in this thesis is to examine the effects of wind speed on salt damage in porous building materials, and in Petra monuments in particular. To achieve this, the following objectives were identified:

- Monitor the salt distribution and microclimate conditions at selected monuments in Petra in order to understand the extent and the mechanism of salt damage at these monuments.

- Evaluate the main characteristics of Petra stones, in particular their clay content and their potential role in stone decay generally and in the salt damage process specifically.

- Develop and apply a salt damage simulation test that would take into account the wind speed factor in the evaluation of the salt damage process.

The research objectives were achieved through fieldwork investigation, data and sample analysis and laboratory simulation tests.

1.5. Thesis outline

The thesis starts with a literature review and discussion of the concepts of salt damage in porous materials. It also includes a critical literature review of the different methods used for the simulation of salt damage in order to develop a simulation test suitable for the purposes of the current research.

Chapter 3 presents a literature review of the role of environmental conditions in salt damage. The review includes an evaluation of the role of relative humidity, temperature and wind speed conditions in the activation of salt damage in porous materials. The outcome of this chapter is the starting point of this research, as it outlines the areas where further research in the field is needed.

Chapter 4 introduces and discusses the main physical and chemical properties of clay minerals, their classification, as well as their possible role in stone decay generally and in salt damage specifically. The elaboration of the properties of clay minerals and their role in stone decay in this chapter derives from the fact that the literature review and the petrographic analysis of Petra stone revealed high percentages of clay minerals. Therefore, any evaluation of stone decay in these monuments must take this into account.

The aims and objectives of the current research are described and discussed in chapter 5. Chapter 6 introduces the case study site (Petra), its location, climate, monuments, geological background, main deteriorating agents and weathering forms.

The methodology of both the fieldwork investigations and the laboratory work are discussed in detail in chapter 7. The microclimate data of Petra are presented and evaluated in chapter 8, while the salts contents and distribution in the case study monuments are discussed in chapter 9. The thermodynamic behaviour of the soluble salts in Petra is evaluated in chapter 10.

Chapter 11 includes a discussion of the current research's simulation test procedures, materials and results. Chapter 12 presents the research limitations, summary of findings and a general discussion of the research outcomes, where the results have been linked and correlated. It also includes proposals for preventive conservation measures at Petra, based on the research findings.

The general discussion of the outcomes of the current research points towards areas where further research in this field is needed, and some proposals for further research are described in chapter 13. The conclusion in chapter 14 is a presentation of the answers to the questions raised in this research.

Chapter 2
Porous Materials, Salts and Salts Damage

2.1. Introduction

The deterioration of porous building materials due to crystallisation of salts within their pore structure is a widespread weathering process and the main cause of decay of many archaeological sites, including the World Heritage Site of Petra.

This chapter presents a brief review of the literature on salt damage in porous materials and introduces the main concepts of this phenomenon. The latter includes a discussion about salt origins, sources of moisture, salt solutions, porous materials characterisation, moisture movements in porous materials, salt transport, crystallisation and distribution in porous materials, salt damage mechanisms, and, finally, a critical review of the main salt damage simulation tests. Understanding these concepts will be a key factor in shaping the research questions and formulating its hypothesis.

2.2. Salt damage: a literature review

The relation between weathering and the presence of salt has been noted since antiquity (Herodotus 420 B.C., in Luquer 1895). Since the beginning of the last century, the salt damage process in porous materials has been given more attention by researchers and has attracted scholars from many different fields including geomorphology, geology, chemistry, conservation, environmental and materials sciences. It should be stated that the current research does not intend to present an extensive review of all the literature on salt damage, but rather to provide a brief and clear account of the main developments in this field. A detailed literature review in

this field has been included in other studies (see for example Doehne 2002, Goudie and Viles 1997 and Price 1996).

As mentioned above, the presence of salts in porous building materials has been documented since antiquity; however, it was not until the nineteenth century that salt damage to porous materials became the subject of serious scientific investigations. One of the earliest accounts is Brard's discussion of salt damage simulation tests as summarised by de Thury (de Thury 1828). Steiger (2005) reported that it was Lavalle (1853) who presented for the first time experimental evidence that the growing salt crystals within porous materials can exert pressure. Luquer (1895) reviewed Brard's sodium sulfate simulation test and concluded that the action of sodium sulfate in porous materials is much more powerful than that of freezing water.

Taber (1916) and Hobbs (1917) recognised and tested the relation between salt crystallisation pressure and deterioration mechanisms in porous materials. In addition, Cooling (1930) demonstrated the role of the drying rate in the location of salt accumulation and crystallisation. Cooling's work was one of the primary studies that related the structure of porous materials to the salt damage phenomenon.

Mortensen (1933), in a further attempt to understand the salt weathering mechanism, proposed hydration pressure as a potential mechanism of salt damage in porous materials. Mortensen's study is further discussed later in this chapter.

Correns (1949) discussed the relationship between the supersaturation ratios of salt solutions and the pressure exerted by these solutions. Correns was able to devise an equation to calculate the pressure exerted by growing salt crystals based on their supersaturation ratios. Winkler and Singer (1972) used Correns' equation to calculate the exerted pressure by two salts (halite and gypsum), while Duttlinger and Knöfel (1993) have limited the application of Correns' equation to low supersaturation ratios only (see section 2.10 for more details).

Wellman and Wilson presented a different model for salt damage in 1965 (Wellman and Wilson 1965). In their model, they suggested that the initial crystallisation takes place in the larger pores by solution supply from the smaller pores.

Evans (1970) produced an excellent review of the research that discussed the main characteristic rock weathering forms associated with salt crystallisation, such as cavernous weathering (chapter 3 of the current research discusses this type of weathering). Evans also included a review of the procedures and outcomes of the main salt simulation tests.

Lewin (1982) presented a mathematical model for the salt dynamics in a single stone prism that is continuously fed with salt-bearing moisture from the bottom. The model was criticised by Senthlage and Wendler (1997), who stated that it is different from the natural situation, since stone prisms do not have moisture gradients between the evaporation zone and the bottom surface of the prism, while in a brick or stone wall there is a gradient in moisture content and consequently in salt concentration from top to bottom.

Rossi-Manaresi and Tucci (1991) discussed the relation between pore geometry and salt damage in porous materials. In their study they correlated the pore structure of porous materials with the weathering forms in these materials.

Arnold and Zehnder (1991) pointed out an important aspect of salt weathering in historic buildings. They observed that buildings are unlikely to be contaminated with single salts. They also stated that salts mixtures behave differently than individual salts. This study was a key point in many following studies.

Price and Brimblecombe (1994) discussed some of the principles concerning crystallisation from solutions containing more than one salt. In their study, they used a computer program (PITZ93) to calculate the equilibrium relative humidity of a mixed salt solution and concluded that, while preventing the salt damage of single salts was a straightforward process because the crystallisation and hydration took place at fixed relative humidity, the salt crystallisation and hydration of a mixed salts solution created a more complicated situation since it took place across a range of relative humidities. As a result, the 'safe' condition for the prevention of salt damage in the case of a mixed salt solution is a range of relative humidities rather than a particular value. Chapter 10 discusses this in more detail.

Doehne (1994) presented a new method of studying the salt weathering mechanism based on the combined use of an environmental scanning electron microscope (ESEM) and a time-lapse video to record the actual sequence of hydration and dehydration of sodium sulfate. This method demonstrated that the recrystallisation of mirabilite crystals from the dehydrated sodium sulfate (thenardite) results in more

damage than the breakdown of large crystals of mirabilite during the dehydration cycle to form thenardite.

Price (1996) carried out a significant review of the recent research in stone conservation. In this, he not only reviewed critically the research in stone decay factors, but also addressed the effectiveness of the different preventive and remedial treatments presented in various studies.

Goudie and Viles (1997) provided a very detailed literature review on many aspects regarding the salt damage nature, mechanisms, simulation tests and diagnosis as well as methods of managing and containing salt weathering hazards. They also pointed out that salt damage is widespread in many of the world's most important archaeological sites.

Rodriguez-Navarro and Doehne (1999a) studied the role of wind in enhancing the formation of honeycomb (alveolar) weathering. Their experimental work was able to reproduce the honeycomb weathering in a homogenous limestone by subjecting this stone to wind exposure and salt crystallisation (see chapter 3).

Rodriguez-Navarro and Doehne (1999b) combined their salt simulation tests with a critical literature review on the salt damage mechanism to develop a model that was able to demonstrate the reasons for the salt damage variations when using different salts, substrate and environmental conditions. They presented the supersaturation of the solution and the location of crystallisation as the controlling factors in the salt

damage mechanism. The results of their experimental research were in agreement with Correns' equation (Correns 1949).

Scherer's research on salt crystallisation pressure in porous materials (1999 & 2000) was a new approach to the study of the salt damage process. The research reinforced the importance of pore structure in salt damage and predicted that most of the salt damage takes place when a salt solution migrates from the larger to the smaller pores. Scherer's theories will be discussed in more detail later in this chapter.

Based on the work of Price and Brimblecombe (1994) and other researchers, such as Steiger (1994) and Steiger and Zeunert (1996), who used the Pitzer model in preventive conservation studies, a collaborative European research project was able to produce an expert chemical model (ECOS) for determining the environmental conditions needed to prevent salt damage in porous materials (Price 2000a). This work is discussed in detail in chapter 10.

Steiger (2002) reviewed the basic thermodynamic aspects required to understand the relevant phase equilibria in porous materials and the influence of room climate conditions. Steiger (2002) also discussed the current thermodynamic models used in understanding the behaviour of salt solutions and their limitations and ways for improvement. In particular, the influence of temperature on the relevant phase equilibria was discussed and evaluated.

A critical review of the literature on the pressure exerted by growing crystals in porous materials was carried out by Steiger (2005). Steiger developed an equation for

the calculation of the salt crystallisation pressure based on the chemical potential of the loaded and unloaded faces of a growing crystal. He also concluded that the assumption of non-uniform pressure is fundamental for the understanding of the dynamics of salt crystallisation pressure in porous materials (Steiger 2005).

Lubelli (2006) carried out fieldwork and laboratory investigations to study sodium chloride damage to porous materials. The research results demonstrated that environmental conditions (temperature, relative humidity and wind speed) had not only a strong influence on the pattern of sodium chloride decay, but also on the rate of decay this salt causes.

All in all, it can be stated that our knowledge in the field of salt damage has been significantly advanced in the last few years, but some fundamental questions have not yet been fully answered. The literature review highlights the need to direct the research more towards the understanding of salt damage as it happens in the field rather than continuing to develop theories and carry out simulation tests under conditions that do not reproduce actual conditions. The current research will combine fieldwork investigation with a laboratory simulation test in order to assess an important aspect of salt damage, the role of wind speed in the salt crystallisation process.

2.3. Salts and weathering

From the previous literature review, it can be noted that salts and their relationship to decay of porous building materials has been subjected to intensive research. Nevertheless, a number of aspects in this field are still not fully addressed.

Generally, the main factors that cause salt damage in stone materials are well known (Winkler 1994). However, the mechanisms by which this process occurs are very complex and hotly contested. In the coming sections the factors involved in the salt damage process in porous building materials (figure 2.1) will be presented and discussed briefly.

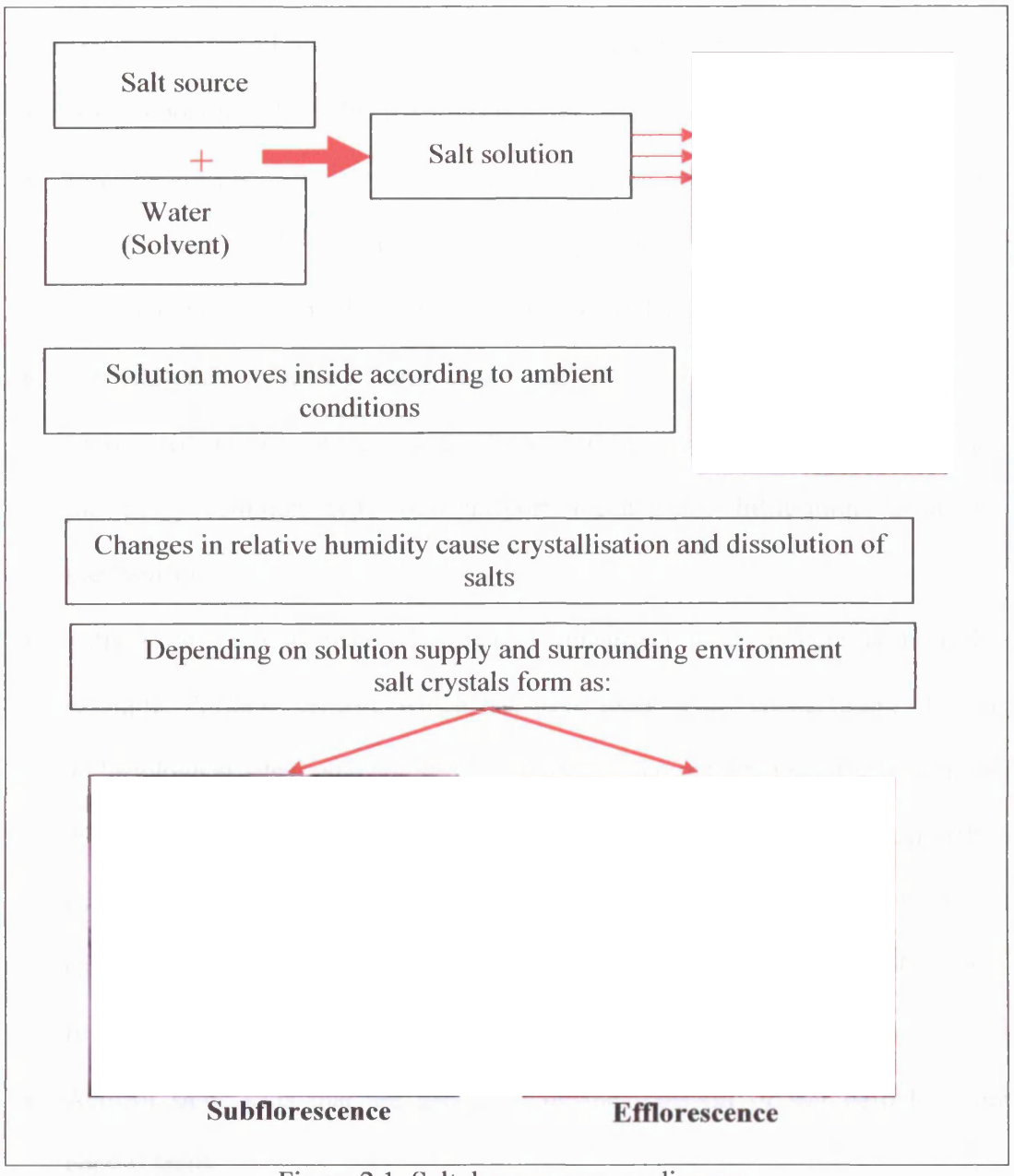

Figure 2.1: Salt damage process diagram
Images from the salt research project: Paul Getty Trust (2005)

2.4. The origins of salts

The determination of the sources of the salt(s) involved in the deterioration of porous materials is a vital issue in understanding the mechanisms of this process. Generally, salt can originate from a wide range of sources. These sources have been categorised by a number of researchers, including Arnold and Zehnder (1991) and Price (1996), who identified the following sources of salts in porous materials:

- Autochthonous salts: salts that are part of the original object.
- Biogenical salts: salts that are a by-product of the deterioration process of some organic material. For example, animal by-products contain ammonia, which is oxidised to nitrous and then nitric acid by bacterial action.
- Groundwater dissolved salts: salts that dissolve in groundwater and are transported into the porous system through different mechanisms. Capillarity is the most common type of transport mechanism. Infiltration is another mechanism.
- Salts from external materials, such as materials used in conservation. For example, Portland cement, which has been used in the conservation of many archaeological sites, was found to have a considerable amount of salts that can participate in the deterioration process of these sites. Arnold and Zehnder (1990) estimated that 100 kg of Portland cement could produce 460 g of sodium carbonate ($Na_2CO_3.10H_2O$) or 520 g of mirabilite ($Na_2SO_4.10H_2O$) when reacting with sulphuric acid.
- Aerosol salts: salts that are generated by the transport of salt particles from coastal areas.

- De-icing salts: sodium chloride (NaCl) has been used extensively in the last few decades to minimise the impact of ice on busy roads and pavements (Goudie and Viles 1997).
- Storage places used for meat preservation or gunpowder.
- Salts from atmospheric pollutants: salts that are produced by the reaction of some oxides and calcareous rocks. Sulphur and nitrogen oxides are the most common pollutants that are usually considered as a significant source of salts in porous building materials.

Despite the fact that the sources of salts seem obvious, their practical identification proved to be challenging in many case studies (see Arnold 1996). This is mainly due to the fact that, in porous building materials, salts originate from more than one source. It is worth remembering that only soluble salts are involved in the deterioration of porous materials, since they can dissolve in a solution and become transported into the material, where they can crystallise, dissolve and recrystallise (see table 2.1).

Name of salt	Chemical formula
Alunite	$(K,Na)Al_3(SO_4)_2(OH)_6$
Ammonia niter	NH_4NO_3
Anhydrite	$CaSO_4$
Antarcticite	$CaCl_2.6H_2O$
Aphthitalite	$K_2SO_4.(Na,K)SO_4$
Aragonite	$CaCO_3$
Arcanite	K_2SO_4
Bassanite	$CaSO_4.1/2H_2O$
Bischofite	$MgCl.6H_2O$
Bloedite	$Na_2Mg(SO_4).4H_2O$
Burkeite	$Na_2CO_3.2Na_2SO_4$
Calcite	$CaCO_3$
Darapaskite	$Na(NO_3)(SO_4).H2O$
Dolomite	$CaMg\ (CO_3)_2$
Epsomite	$MgSO_4.7H_2O$
Gypsum	$CaSO_4.2H_2O$
Halite	$NaCl$
Heptahydrite	$Na_2CO_3.7H_2O$
Hexahydrite	$MgSO_4.6H_2O$
Kieserite	$MgSO_4.H_2O$
Magnesite	$MgCO_3$
Mirabilite	$Na_2SO_4.10H_2O$
Nahcolite	$NaHCO_3$
Natrite	$Na_2CO_3.10H_2O$
Niter	KNO_3
Nitratine	$NaNO_3$
Nitrocalcite	$Ca(NO_3).4H_2O$
Nitromagnesite	$Mg(NO_3).6H_2O$
Pentahydrite	$MgSO_4.5H_2O$
Rosenite	$FeSO_4.4H_2O$
Sanderite	$MgSO_4.2H2O$
Shoenite	$MgSO_4.K_2SO_4.6H_2O$
Shortite	$2CaCO_3.Na_2CO_3$
Sylvite	KCl
Syrgenite	$CaSO_4.K_2SO_4.H_2O$
Tachyhydrite	$CaCl_2.2MgCl_2.12H_2O$
Thenardite	Na_2SO_4
Thermonatrite	$Na_2CO_3.H_2O$
Trona	$Na_3(CO_3)(HCO_3).2H_2O$
Vanthoffite	$MgSO_4.3Na_2SO_4$
Weddellite	$CaC_2O_4.2H_2O$
Whewellite	$CaC_2O_4.H_2O$

Table 2.1: The major evaporite minerals (salts) and their chemical composition (after Goudie and Viles 1997).

2.5. Sources of moisture

The second crucial factor in the salt damage mechanism is the presence of moisture (solvent), which dissolves the soluble salts and allows them to migrate within the pore system.

A number of scholars, including Winkler (1994) and Goudie and Viles (1997), listed the main sources of moisture in masonry walls as follows:

- Rain: rainwater is the main source of moisture in porous materials, even in arid areas.
- Dew: in some desert areas, a considerable amount of dewfall may occur in a surprisingly large number of nights during the year, resulting in hydration of the hygroscopic salts and providing a moisture source for these salts.
- Fog: fog can provide porous materials with a significant amount of moisture. Also, fog itself could be a potential source of salts, particularly in coastal desert areas.
- Groundwater: it has been considered to be one of the major sources of moisture, especially in areas where the water table is high.

2.6. Salt solutions

The combination of soluble salt(s) with any moisture sources results in the formation of salt solutions. The physical and chemical properties of the salt solutions play a major role in the salt weathering process.

As a soluble salt dissolves in water, the water vapour pressure over the solution decreases and continues to do so until it reaches its minimum in the saturation state (Charola 2000). This vapour pressure depends on temperature and the nature of the salts in the solution and can be expressed as the 'equilibrium relative humidity', since water vapour pressure can be expressed as relative humidity (Steiger 2002).

$$RH = (P_w / P_{w^\circ}) \times 100\%$$

Where:
RH: relative humidity
P_w: partial pressure of water vapour
P_{w°: saturation vapour pressure at the same temperature

So:

$$ERH = (P_{w\ saturated} / P_{w^\circ}) \times 100\ \%$$

Arnold and Zehnder (1991) demonstrated that the dynamics of salt damage in porous materials are largely determined by the salt solution and the surrounding temperature and relative humidity. If the surrounding relative humidity at a given temperature is higher than the equilibrium relative humidity of the salt solution, the salt will remain in its soluble condition and the solution will become more diluted. But if the surrounding relative humidity is lower than the equilibrium relative humidity of the salt solution, the salt will crystallise out of the solution. The equilibrium relative humidity of salts ranges between 99.9 % [for calcium sulfate ($CaSO_4.2H_2O$)] and 11 % [for lithium chloride ($LiCl.H_2O$)] (Greenspan 1977). From the previous statement it might seem that to predict and control the behaviour of salt solutions in porous materials would be a straightforward task. Unfortunately this is not the case, as it is unusual to have a single salt in the salt solution that contaminates a porous material.

The presence of a mixture of salts not only affects the chemical and physical properties of the solution, but, more importantly, the equilibrium relative humidity ranges (Steiger and Zeunert 1996). Generally, the solubility of one salt increases in the presence of another salt, when there are no common ions between them and vice versa. However, Steiger and Dannecker (1995) observed some anomalies in this theory, when they found that the solubility of potassium nitrate increased in the presence of other nitrates. Price and Brimblecombe (1994) and Steiger (1994) used the thermodynamic properties of aqueous electrolyte solutions to predict the properties of salt mixture solutions. As a result of a European collaboration project, an expert computerised model was introduced (ECOS) (Price 2000a), which can predict the different states (solid or soluble) of certain salt mixtures at any given relative humidity or temperature using a thermodynamic calculation. The model is a very useful tool for the study of the behaviour of salt mixture solutions in different atmospheric conditions (namely relative humidity and temperature). This is discussed in more detail in chapter 10.

2.7. Characterisations of porous materials

The salt weathering process is greatly affected by the physical properties of the porous materials. The resistance of porous materials to weathering agents varies considerably from one type to another depending on their pore structure (Honeyborne and Harris 1958). In particular, the pore structure of a porous material could affect the solutions pathways and their interaction with original materials and with the surrounding microclimate conditions (Sawdy 2001).

Porosity, permeability, water absorption capacity, capillary water uptake, specific surface area and bulk density are the main structural factors that affect the movements of salt solutions; these factors will be described briefly in the following sections.

2.7.1. Porosity and pore size distribution

Porosity (ϕ) is of key importance to this study. It is defined as the ratio of the pore volume to the bulk volume (Robertson 1982).

The pore space can occur in a wide range of sizes (from less than a micron to several centimetres) and in a variety of shapes (angular, circular, oval, uneven and so forth). According to Robertson (1982) the pore space can be classified into the following categories:

- Effective porosity (open): where the pore spaces are connected to each other.
- Ineffective porosity: where the pore spaces are disconnected from each other.
- Total porosity: effective porosity + ineffective porosity.

Due to the microscopic nature of the pore space, the determination of the porosity and pore size distribution is usually carried out through indirect methods. Mercury intrusion porosimetry and microscopic analysis of thin sections using transmitted light microscopes are the main methods used in measuring the diameter of the pore space as well as the total porosity of the material. Mercury intrusion porosimetry is based on the capillary law, which states that the intrusion into pores of an unwetting liquid, such as mercury, depends upon the pressure applied to that liquid (Nicholson 2001). Thus, under a given pressure the intrusion of liquid into porous materials will

be related to the diameter of the pore space in that material according to Washburn's equation (Washburn 1921):

$$D = \frac{-4\gamma \cos \theta}{P}$$

Where:
D: pore throat diameter
P: applied pressure of introducing mercury
γ: surface tension
θ: contact angle

On the other hand, the microscopic analysis of thin sections can provide us with more accurate information about the structure of the porous system, but not about the quantity distribution of the pores.

Another frequently used method of evaluating the total open porosity of porous materials is to saturate them under vacuum and then dry them to constant weight in an oven. The difference between the saturated and the dried weight represents the amount of water that entered the porous material. This amount of water in turn represents the total open porosity (Leary 1983). This method will be used in the present study in order to calculate the total open porosity of the laboratory specimens, while the petrographic microscopic analysis will be used to evaluate their pore structure and total porosity.

As a result, one can say that the determination of the pore size distribution in porous systems has a high level of uncertainty, since it is measured indirectly, such as by intrusion of liquid into the pores under a certain pressure. Moreover, the determination of the morphology of the pore system depends on the characteristics of the liquid used in the determination process.

In their laboratory investigations of the salt damage in various stone types, Honeyborne and Harris (1958) attributed the durability of these materials to their pore structure and showed that the stones with higher microporosity[1] were the least durable ones.

Rossi-Manaresi and Tucci (1991) have studied the relation between pore structure and salt crystallisation pressure. They concluded that only when soluble salts are found in particular types of pore structure can they be considered harmful. In their experimental work Rossi-Manaresi and Tucci (1991) showed that high crystallisation pressure in the tested stone samples was associated with those stones where a substantial percentage of fine pores existed alongside coarse pore spaces. Ordóñez *et al.* (1997), Nicholson (2001) and Flatt (2000a) carried out similar evaluations.

It is worth remembering that the pore size distribution is the main factor determining the movement of solutions within porous materials and that not all porous materials allow the movement of solutions within their system, rather, only those that have a connected pore system will allow the migration of solutions within their structures. Consequently, other parameters, such as permeability, are needed to clarify the relationship of the solution movement and the pore system.

2.7.2. Permeability

Permeability can be defined as the ability of a material to permit fluids to flow through it (Pavia and Bolton 2000). Permeability depends basically on the pore size,

[1] Microporosity: is defined as 'the volume of water retained (expressed as percentage of the total available pore space) when a suction equivalent to 6.4 m head of water applied to the specimen. In essence, it measures the percentage of pore with an effective diameter less than 5 μm' (Leary 1983).

the sorting of the grains (number of similar grain sizes), the roundness of the grains and the characteristics of the cement materials.

The measurement of permeability is based on Darcy's law, which states that the volumetric flow rate of a liquid through a cross section of a porous material is proportional to its hydraulic gradient.

$$F = k \frac{A}{\mu} \frac{\Delta P}{L}$$

Where:
F: volumetric rate
k: permeability measured in Darcy unit[2]
A: the cross-sectional area
L: the distance of flow
μ: the viscosity of fluid
Δ P: the difference in hydraulic pressure

From the previous statement, it is obvious that permeability is governed by the effective pores and not the total porosity. In other words, materials could be porous but not permeable, and so the permeability does not reflect the total amount of fluid that can be present in a porous material.

2.7.3. Water absorption capacity (WAC)

The water absorption capacity (WAC), or what is also called saturation coefficient, is one of the properties most commonly used to evaluate stone materials before applying any salt simulation tests to them (Goudie 1974, Goudie and Viles 1995 and Goudie 1999). The WAC is usually defined as the ratio of the volume of water absorbed under standard conditions to the volume of the available pore space and it is mainly controlled by the porosity and permeability, pore structure and chemical

[2] Darcy: is defined to be the permeability of a 1 cm^3 of material, if a pressure difference of 1 atmosphere will induce a flow rate of 1 cm^3 /s in a fluid viscosity of 1 cP.

composition of the porous materials (Honeyborne and Harris 1958). The methodology for measuring the WAC is discussed in chapter 7.

It is also worth mentioning that, in salt simulation tests, many researchers measure the weight increase of porous materials due to saturation with different salts and call this 'salt uptake ratio'. Generally, the higher the water absorption capacity and salt uptake ratios in specimens, the more susceptible to salt damage these will be.

2.7.4. Capillary water uptake

The capillary water uptake is also one of the properties that could reveal important information about water penetration and movement within porous materials. Considering the fact that most archaeological and stone building damage is located in the lower parts of the monuments and is mainly attributed to rising damp, the capillary water uptake becomes an important aspect in the evaluation of water movement in these materials (Al Naddaf 2002). However, despite the fact that the capillary water uptake is undoubtedly important for the evaluation of water penetration and movement in porous materials, it could be argued that the evaluation of these properties in a laboratory experiment using a single sample could not possibly represent the capillary water uptake of an entire monument.

2.7.5. Specific surface area

The specific surface area is defined as the ratio of the surface area to the volume of a particle. The smaller the size of a particle the larger is the ratio of its surface area to volume. The specific area of a porous material is affected by porosity, grain size and shape (Bear 1988). This physical parameter is a crucial characteristic that affects the

salt damage problem in a porous system (Torraca 1988, Goudie and Viles 1997). This is mainly related to the fact that the specific surface area governs the amount of moisture that can be absorbed onto the surface of the pores, which is the main factor in damaging phenomena. The coarser the stone's grains or crystals, the lower the specific surface area of this stone and vice-versa. Therefore, porous materials with very fine grains have a very high specific surface area, which results in more interaction with the surrounding environment. The specific surface is usually measured by the gas sorption technique (for more information about this technique, see Skaling and Hearn 2000).

2.7.6. Bulk density

Bulk density, or apparent density, is defined as the total mass per unit of total volume. In non-porous materials the true density equals the bulk density. Therefore, the bulk density can provide information about the porosity of these materials (Kenkel 2002). The test procedure for measuring the bulk density can be found in the British Standard BS EN 14617-1: 2005.

$$\text{Porosity (\%)} = 1 - (\text{bulk density} / \text{actual density}) \times 100$$

In general, the higher the bulk density of porous materials, the higher is their resistance to salt damage weathering.

2.8. Moisture movement in porous systems

Understanding moisture movement in a porous material is a key point in understanding the salt damage phenomena in that system. This is due to the fact that the location of salt crystallisation or hydration in the porous system is governed by

the dynamic balance between the rate of moisture uptake into the system and the rate of moisture escape from it (Lewin 1982). Despite the fact that salts are transported only in liquid state, their pathways and distribution are affected by the vapour as well as the liquid phase of water.

2.8.1. Mechanisms of liquid and vapour water movements

- Liquid water movement mechanisms

Many mechanisms have been proposed for the transport of liquid water in porous materials, but the predominant mechanism is the viscous flow due to capillarity.

Massari and Massari (1993), when discussing capillary action, point out the fact that the liquid in two communicating containers ought to settle at the same level. But when the diameter of one of these containers is very fine (as fine as a hair), the liquid will not be at the same level as the other containers but will rise to a higher level (figure 2.2).

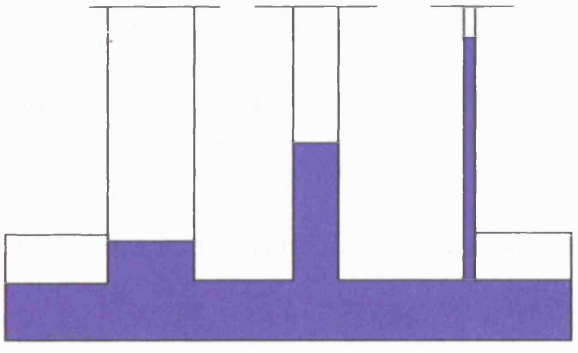

Figure 2.2: Water levels under the capillary rise forces.

The behaviour of water in the above illustration describes the capillarity in porous materials and can be explained as follows: When two fluids come in contact, an interface is created between them (meniscus). This interface is then curved towards

the medium of lower pressure. The equilibrium of the convex and concave pressure can be expressed by Laplace's equation:

$$P_1 - P_2 = \frac{2\gamma \cos\theta}{r}$$

Where:
P_1: the pressure of the concave side of the interface
P_2: the pressure of the convex side of the interface
γ: the surface tension
θ: contact angle
r: the radius of the curvature

As the pressure on the convex side is lower than the concave side in the fine container, the water will rise (capillary rise). As water rises in the capillary and in the absence of evaporation, the hydrostatic pressure increases from the column of liquid inside the capillary. The water stops rising when the driving forces, namely capillary rise and hydrostatic pressure, are balanced.

From the previous equations, it can be stated that the capillary rise in porous materials is a complex system that depends not only on the diameter of the pore space, but also on the surface tension of the water surface. The water surface tension can be explained according to the variation in the physical properties between the water molecules on the water surface and the inside molecules. The latter are surrounded by other molecules and experience the same degree of intermolecular bonding; on the other hand, the surface molecules have less bonding and so have the ability to leave the surface. In other words, the surface molecules could be attracted by other molecules, because their bonding is not fully fulfilled.

The application of Laplace's equation to the behaviour of water in porous materials resulted in Kelvin's equation, which also explains the capillary condensation of water vapour.

$$P\text{-}P^* = (2\gamma/r) + (d\ RT/m)\ \ln\ (P/P^*)$$

Where:
P: vapour pressure of liquid water within the capillary
P*: vapour pressure of liquid water (flat surface)
γ: surface tension
r: radius of curvature
d: the density of liquid water
R: gas constant
T: temperature in degree Kelvin
m: water molecular weight
V: molar volume of water

Capillary condensation is the phenomenon by which condensation occurs in the fine pores even when the relative humidity is less than 100 %.

- Water vapour movement mechanisms

Generally the movement of water vapour can take place either by convection or diffusion. The former is the vapour movement due to airflow, while the latter is a movement due to concentration gradient. In porous materials diffusion is the main, if not the only, water vapour movement mechanism.

The vapour diffusion is governed by Fick's First Law, which describes the proportional relationship between the rate of mass transfer by diffusion and the concentration gradient:

$$J_x = -D \frac{dc}{dx}$$

Where:
J_x: flux
D: diffusion constant for the material that is diffused in the specific solvent
dc/dx: concentration gradient

Even though the previous models describe clearly both the liquid and vapour water transport mechanisms, none of them has considered the correspondence of these two

mechanisms. Philip and de Vries (1957) have described the liquid and vapour as inter-related mechanisms of moisture movement within the porous materials. While at high relative humidity the main transport mechanism of moisture is the liquid continuity, at low relative humidity this continuity breaks down forming liquid islands within the pores. These liquid islands have liquid/gas interface with equal curvature in equilibrium conditions, but in the presence of a vapour pressure gradient the condensation and evaporation take place simultaneously at opposite sides of the curvature, resulting in water build-up on one side and vapour-liquid draw back on the other side. This process results in capillary flow due to the increase of the curvature on one side of the liquid/gas interface. The work of Phillip and de Vries (1957) has proved that moisture transport in porous materials continues in the absence of liquid continuity through a vapour diffusion mechanism.

Pender (2000) illustrated the nature of problems associated with moisture changes in wall paintings and presented an overview of the theoretical models underlying the moisture behaviour in porous materials. Pender's experimental work showed that the type of a porous material (stones) governed the speed and pattern of moisture movements within it, with permeability being the main controlling factor.

2.9. Salt transport, crystallisation and distribution in porous materials

The understanding of the salt and moisture transport in porous materials is a key factor in the evaluation of their damage potential. The previous section discussed the different transport mechanisms of pure water. But how do these differ from salt solution movements?

As mentioned earlier, salts are only transported in porous materials when in liquid phase. The movement of a salt solution is slower than pure water, since it has higher viscosity and density (Kaufmann 1971). Therefore, in porous materials the capillarity will force the salt solution to rise at a rate slower than pure water up to a certain level, where evaporation starts. With evaporation increasing, the concentration of the salt solution will increase resulting in lower mobility rates, higher supersaturation ratio and ultimately crystallisation of the salt out of the solution.

In addition, salt solutions have designated solubilities, and therefore, while moving within porous materials through capillary rise forces, they will fractionate according to their solubility. Those with low solubility will crystallise out of the solution at earlier stages than salts with higher solubility. Arnold and Zehnder (1991) presented a model for the fractionation of salts with heights depending on the solubility of salts. Their paper was one of the first studies that linked the rate of stone decay with the surrounding environments. In addition, this study included a comprehensive summary of the characterisation of the soluble salts in porous building materials.

The salt solution's behaviour in porous materials is largely controlled by the ambient environmental conditions, namely relative humidity and temperature, the salt types and the pore size and structure of the materials. As mentioned earlier, each salt solution has its equilibrium relative humidity (ERH), which is the transition point between crystallisation and dissolution. If the ambient relative humidity is lower than the ERH of the solution, then the salt(s) crystallise out of the solution. While, if the ambient RH is higher than the ERH of the solution, the salt(s) stay in solution state. The presence of other salt(s) in the salt solution is another factor that affects the salt

behaviour inside a porous system. The presence of other salt(s) in the salt solution will reduce the ERH of that solution and, therefore, change its thermodynamic behaviour (Price and Brimblecombe 1994).

Benavente *et al.* (2004) have studied the influence of the pore structure of porous materials in salt crystallisation and distribution. In their experimental work, they used the SEM and XRD techniques to identify the salt distribution in three stone samples, each with a designated type of porosity, after these had been immersed in two different salt solutions, sodium sulfate and sodium chloride, for 48 hours and then dried in laboratory conditions (20 $\pm$ 3 C° and 40 $\pm$ 5% RH). The results of the test showed that halite (NaCl) tends to grow on the stone surface and its location was similar in all samples, while mirabilite and thenardite crystallised inside the stone and their distance from the surface was linked to the pore size distribution in the stones, with more salts towards the inner part of the stones with fine pores. Benavente *et al.* (2004) concluded that the pore size distribution had a major influence not only on the salt crystallisation pressure in porous materials, with materials of fine pores having higher crystallisation pressure than materials of coarse pores, but also on the salt distribution within these materials.

From the above studies in salt crystallisation and distribution, it may seem that these processes are straightforward and that their mechanisms have been identified to the full. Unfortunately, this is not the case since most of the above discussed results were based on a simplified test or observation of a more complicated situation. Prokos (2005) criticised Arnold and Zehnder's (1991) model for not taking into consideration the interaction between different species of salts as well as for using

conditions that are not representative of the environmental conditions at the case study site. Moreover, in many simulation tests, such as the test by Benavente *et al.* (2004), the identification of the role of pore structure in salt crystallisation and distribution is mainly based on observations from a small cube of stone (less than 4 cm cube), while the actual pore structure of a bigger porous system is much more complicated. Turkington and Smith (2000) also questioned the traditional view of examining the salt distribution within individual building stones, where neither the scale of the samples, the experiment conditions and materials nor the post-test method for the evaluation of the salt distribution provided an accurate model of the salt distribution in stone buildings. They concluded that the variability in stone decay features should be understood in a better way, emphasising the need for a three-dimensional model for the evaluation of the main characteristics and salt distribution in porous materials.

The transport patterns of moisture and salt ions have been recently evaluated using the Nuclear Magnetic Resonance (NMR) technique (Pel *et al.* 2000 & 2001, Pel and Huinink and Kopinga 2003). This non-destructive method evaluates the moisture and salt ions transport by monitoring and recording the moisture content and amount of dissolved salt during a steady drying process (for more information about the NMR technique see Gummerson *et al.* 1979 and Rijniers 2004).

All in all, the processes of salt crystallisation and distribution in porous building materials are mainly controlled by the salt solution, the surrounding environmental conditions and the pore size and structure of these materials. Consequently, the understanding of salt crystallisation and distribution in the monuments at Petra will need to take all these factors and their interrelationship into account.

2.10. Salt damage mechanisms

There is no doubt that salts cause damage to porous materials. However, great uncertainty lies in determining the mechanism by which salt damage in porous materials occurs. Basically, crystallisation of salt(s) outside the system, namely 'efflorescence', causes no or minor damage. On the other hand, crystallisation of salt(s) inside the porous system, namely 'subflorescence', causes significant damage. But the question is how do salts cause damage to porous materials?

2.10.1. Crystallisation pressure

Crystallisation pressure is one of the most accepted explanations for the salt damage mechanism in porous materials. The basic principle of this theory is that when salt crystals grow inside the pore space, they will exert pressure and when this pressure is higher than the tensile strength of the host material, it breaks the pore wall and ultimately causes damage to this material.

As mentioned earlier, it was Lavalle (1853) who provided experimental evidence that crystal growth exerts pressure (Steiger 2005). In the following decades, scholars were in disagreement about the crystallisation pressure theory, since some of the simulation tests that were carried out based on this theory did not result in the anticipated damage.

Taber (1916) reviewed the research in salt damage up to that time and proposed a hypothesis for the absence of damage in some simulation tests. He stated that during evaporation, if a crystal present in a saturated solution is under pressure from the weight above, the solution will supersaturate and the crystal will grow causing

damage. But if at the same time another crystal that does not have any weight on it is present, it will grow instead of the first crystal, which is under pressure, resulting in no damage. In other words, the supersaturation is eliminated by the presence of a crystal without pressure in the solution (Rijiners 2004).

Correns (1949) presented the idea of a linear crystal growth pressure mechanism, in which he showed that the exerted crystal growth pressure is related to the degree of supersaturation. He based his theory on Thomson's work (1862), known as Rieke's principle, that a 'crystal under linear pressure has greater solubility than unstressed crystals' (Winkler 1994).

$$P = R\,(T/\,V)\,\ln\,(C/Cs)$$

Where:
P: crystallisation pressure
R: ideal gas constant
T: temperature
V: molar volume of the solid salt
C: the actual concentration of the solution during crystallisation
Cs: the concentration of solute at saturation

Correns (1949) considered the supersaturation state to be a key factor in the crystallisation of salts, pointing out that no supersaturation means no crystallisation.

Mullin (1961) studied the relation between salt supersaturation state, temperature and crystallisation behaviour. He presented three different situations involving these factors, which are:

- Unsaturated solutions and no crystallisation.
- Saturated solutions and crystallisation through cooling (or evaporation).
- Supersaturated solutions and direct crystallisation.

Winkler and Singer (1972) used Correns' equation to calculate the value of crystallisation pressure of different salts at different supersaturation ratios and temperatures. However, in 1993, Duttlinger and Knöfel questioned Correns' equation and concluded that it is only applicable for lower supersaturation ratios and not for all supersaturation levels. They found that Correns' data for supersaturation ratio above 1.2 showed a significant diversion from the theoretical values. Moreover, Sawdy (2001) criticised Correns' equation for ignoring the inevitable complexities of porous media.

Fitzner and Snethlage (1982) developed an equation for calculating the crystallisation pressure that considers the geometry of pore structure in porous materials. The equation was based on the theoretical model of frost damage by Everett (1961). According to this, crystal growth will take place preferentially in large pores due to the differences in the chemical potential between large and small crystals, and stress will be generated when the large pores are filled and crystals growth continues (Steiger 2003).

$$P = 2\gamma (1/r - 1/R)$$

Where:
P: crystallisation pressure
γ: surface tension
r: smaller pore radius
R: larger pore radius

Price (1991) put forward a very interesting argument that questions the reality of having high supersaturation ratios in porous building materials outside laboratory conditions.

> *How realistic is to think that one can get significant degrees of supersaturation in a dirty piece of stone, with any number of possible nucleation sites?*
>
> *(Price 1991, 180)*

Rodriguez-Navarro and Doehne (1999b) in their critical review of salt damage concluded that salt damage due to crystallisation pressure is a function of the supersaturation ratio and the location of crystallisation, with salt types and evaporation rates being the main controlling factors of these parameters. Their experimental observations were in agreement with Correns' equation for salt crystallisation pressure, but they also emphasised the fact that more studies are needed, especially in the field of the kinetics in the salt crystallisation process.

Scherer (1999 and 2000) developed a new approach for the salts crystallisation pressure mechanism in porous materials. He stated that when supersaturation increases, the crystal grows and, when it reaches the pore entry, it adopts a curvature. This surface curvature of a crystal gives rise to capillary pressure, and consequently crystal growth is established parallel to the pore's walls. Moreover, Scherer developed an equation to measure the radial stress on the pore walls as follows:

$$\sigma_r = - Ps - Pd + \gamma_{wl} K_{wl}$$

Where:
σ_r: radial stress on the pore wall
Ps: pressure in the solution
Pd: disjointing pressure
γ_{wl}: interfacial energy of wall / liquid interface
K_{wl}: the curvature of the wall / liquid interface

In addition, Scherer (1999) explained the continuity of crystal growth from the thin water film according to the interfacial energies between pore, solution and salts as follows:

> *If the balance of interfacial energies between the crystal, solution and pore wall is such that contact between the crystal and pore wall is energetically unfavorable, liquid is drawn into the gap between the two, thus maintaining a thin film of solution from which the crystal can continue to grow.*
>
> Scherer (1999, 1349)

According to this statement, the interfacial tension between the support and the salt crystal ($\gamma_{support\text{-}crystal}$) should be higher than the interfacial tension between the salt and the solution ($\gamma_{salt\text{-}solution}$) plus the interfacial tension between the support and the solution ($\gamma_{support\text{-}solution}$) in order to form a film of solution from which the crystal can continue to grow. Scherer added that as the crystal expands, the tensile stress rises and, consequently, damage occurs.

Scherer's thermodynamic calculations (1999 and 2000) demonstrated that crystallisation pressure is a function of the pore space size, with lower pressure in the larger pores than the fine ones. However, Scherer (2000) also pointed out that high stress can occur in large pores when they are nearly filled with salts. He explained this theory as follows: if the pore and salt crystals are both large, the curvature of the crystal/liquid interface (K_{cl}) and the curvature of the wall/liquid interface (K_{wl}) are negligible, which means that stress is bounded only by the disjointing pressure. In other words, crystallisation pressure can occur in stones with large pores, as the large pores are effectively converted to fine ones when filled with salts. In addition, Scherer's calculations predicted that the maximum damage from salt crystallisation in porous materials will take place when the salt crystals migrate from large to smaller pores (less than 4 nm). But the question is how often does this pore size exist within porous building materials? In a more recent paper, Scherer (2004) evaluated the crystallisation pressure in a pore structure similar to the ones usually present in porous building materials and developed a hypothesis. The formation of isolated

pockets of salts within the pores was the suggested mechanism for the development of crystallisation pressure in porous materials. Scherer (2004, 1615) stated that 'due to evaporation, solution is trapped between the crystals and the pore walls, whereas the free ends of the crystals are not in contact with the solution' and as a result crystallisation pressure will develop even in large pores.

Flatt (2002a) linked Scherer's theory of interfacial energies to supersaturation levels and pore sizes. He noticed that in the case of damage attributed to sodium sulfate, the dissolution of thenardite (Na_2SO_4) produces a solution highly supersaturated with respect to mirabilite ($Na_2SO_4.10H_2O$). Consequently, the crystallisation of mirabilite from such a solution generates crystallisation pressure resulting in tensile pressure substantially larger than the tensile strength of most stones or concrete material. Moreover, the results of his experiment were in agreement with Scherer's (1999) hypothesis regarding the relation between pore structure and salt crystallisation pressure and he concluded that the materials with micropores (in the mesopore range[3]) are more susceptible to crystallisation pressure.

Flatt and Scherer's observations regarding the potential for higher crystallisation pressure in fine pores than larger ones were in agreement with the findings on the relation between supersaturation ratios and crystallisation pressure by Putnis *et al.* (1995). They demonstrated that in fine pores the rate of nucleation is contained resulting in higher supersaturation ratios and thereby higher crystallisation pressure.

[3] Mesopore pore: a pore with a size between 2-100 nm (Duong 1998).

Steiger (2005) pointed out the need for considering the dynamics and the non-ideal behaviour of the supersaturation solution when evaluating the salt crystallisation pressure. The evaluation of the non-ideal behaviour of the liquid phase was carried out using the Pitzer model. Steiger (2005) was able to develop and apply an equation for the salt crystallisation pressure based on the assumption of the non-uniform stress of growing crystals.

2.10.2. Hydration pressure

The hydration pressure is the pressure that supposedly develops by increase of salt volume due to absorption of water (hydration). Mortensen (1933) was the first one to propose hydration pressure as a potential mechanism of salt damage in porous materials. In his investigation, he argued that no damage could result from salt crystallisation pressure, since the newly formed salt crystals occupied less volume than the original solution. Instead, he proposed that the increase of salt volume after crystallisation through the hydration process is an alternative mechanism of salt damage in porous materials.

$$P = [nRT/ (V_h - V_a)] \ln (P_w/ P'_w)$$

Where:
P: hydration pressure
n: number of moles of water gained upon hydration
R: ideal gas constant
T: temperature
V_h: molar volume of the hydrate salt
V_a: molar volume of the anhydrate salt
P_w: water vapour pressure at temperature T
P'_w: water vapour pressure of the hydrated salts

Winkler and Wilhelm (1970) used Mortensen's equation to calculate the hydration pressure of some common salts at different temperatures and relative humidities.

Duttlinger and Knöfel (1993) also attempted to measure the hydration pressure under controlled conditions using Mortensen's equation. They studied the hydration process thoroughly and produced a different equation that resulted in far smaller values of hydration pressure (Charola 2000).

The experiments of Doehne (1994) and Rodriguez-Navarro and Doehne (1999b) on the hydration and de-hydration of sodium sulfate ruled out the potential of salt damage from hydration of salts. In their work, they observed that thenardite dissolved first during the hydration stage resulting in a supersaturated salt solution of mirabilite. During the de-hydration stage, mirabilite crystals were formed and caused damage by salt crystallisation pressure.

Flatt (2002b) confirmed the findings by Rodriguez-Navarro and Doehne (1999b) and stated that hydration pressure is just a sub-set of crystallisation pressure, in which supersaturation comes from the dissolution of the anhydrous salt and is followed by the crystallisation of the hydrated salt.

2.10.3. Thermal expansion

Thermal expansion is another mechanism by which salt could cause damage to porous materials. Cooke and Smalley (1968) were the first to propose this mechanism and they built their argument on the fact that salts enclosed in the pores may expand much more than the stone that contains them, namely, salts have higher coefficients of expansion than the minerals of the support system (rock), and so thermal disruption takes place.

Through an experimental approach, Johannessen *et al.* (1982) illustrated the effect of this mechanism by using sodium sulfate on a quartz crystal with a temperature change of 50 °C. According to their results, the pressure from thermal expansion could break the quartz crystal from its surrounding cement.

The efficiency of such a mechanism in damaging porous materials has caused disagreement among scholars. Given that salt damage has been observed at many sites, where temperature is relatively steady, considering this mechanism as the primary cause for salt damage is unrealistic. On the other hand, this mechanism should not be ruled out as one of the parameters for salt damage, especially in areas with significant variation in their diurnal temperature values.

All in all, it can be stated that recent research was able to prove that salt crystallisation pressure is the primary mechanism for salt damage in porous materials. However, the exact mechanism of salt crystallisation pressure has not yet been fully explored.

2.11. Experimental simulation of salt damage

In order to understand the salt damage process, experimental simulations are needed to replicate and verify the different parameters involved in this process. Because of the uncertainty about the exact mechanism of salt damage, the experimental simulations vary considerably in the literature (see for example, Goudie 1974, Cooke 1979, RILEM 1980, Smith and McGreevy 1983, Goudie 1986, Ross and Butlin 1989, Goudie 1993, British-European: *BS EN 12370*, Rodriguez-Navarro and Doehne 1999a and 1999b, Goudie 1999a and 1999b, Benavente *et al.* 2001). The

variations are mainly due to the use of different methods, tested materials, environmental conditions and simulation techniques. These variations have resulted not only in extreme difficulty in comparing the different salt damage simulating methods, but also in a lack of clear conclusions from their outcomes. Goudie and Viles (1997) presented most of the salt simulation methods and the main differences between them.

2.11.1. Salt crystallisation test

One of the most widely used techniques for simulation of salt damage, often called salt crystallisation test, is the testing of building stones or aggregates by the use of sodium sulfate to estimate their soundness when subjected to weathering actions.

In 1828, Brard suggested for the first time the use of saturated sodium sulfate solution to study the frost behaviour of building materials (De Thury 1828). In his test, the specimens were soaked in saturated sodium sulfate solution and dried in the atmosphere. Despite the fact that this test included the main parameters in the salt damage process, it was unable to reproduce the frost behaviour in building materials.

In the 1930s, the Building Research Station developed Brard's original test in another attempt to reproduce the effect of frost in building materials (Bonnell 1965). The test was more systematic and included more controlled testing parameters. The testing procedure was as follows:

1- Specimens (cubes of 4 cm) were dried for 18 hours at 90-100 °C and 40 % relative humidity.
2- Specimens were cooled for 2 hours in a desiccator at 20 °C and weighed.

3- Specimens were immersed in sodium sulfate solution (14 % $Na_2SO_4.10H_2O$ by weight) for 2 hours at 20 °C.
4- Specimens were drained for 2 hours on a perforated tray above the solution.
5- Finally, specimens were dried for 18 hours at unspecified temperature, cooled for 2 hours and weighed again.
6- Steps 1-5 were repeated 15 times.

In this test, the stone with the greatest relative disintegration after 15 cycles was considered as the one with the lowest resistance to weathering. Despite the fact that this test was very useful as a comparative technique, it revealed very little information as to how the disintegration occurred. Also, there was no explanation of why the test was performed in these conditions (90-100 °C and 40 % relative humidity) or why that particular solution concentration (14 %) was used.

Price (1978) studied the results of the crystallisation test on two types of French limestone carried out by three collaborative institutions. He noted that the testing procedures followed by those institutions varied in the used concentration of sodium sulfate solution, the solution's temperature, the drying conditions and the duration of the samples' immersion in the salt solution. Following this investigation Price (1978) conducted a set of experiments to investigate whether these parameters affect the ranking order of three British stones. He concluded that the quantitative results of the crystallisation test were strongly dependent on the solution's concentration, the solution's temperature and the drying rate. According to Price's experiments (1978), only one of these parameters was found to affect the stones ranking: the total drying of the samples between the cycles. The results suggested that these parameters

should be strictly controlled during the test, even if they did not affect the ranking order of the tested stones.

The crystallisation test developed by the Building Research Establishment (Ross and Butlin 1989) was used intensively over many years. The procedure was based on the test developed by the Building Research Station and can be summarised as follows:

1- A large stock of sodium sulfate solution (14 %) is prepared by dissolving 1.4 kg of sodium sulfate decahydrate in 8.6 litres of water. The solution should be kept at 20 °C.
2- Stone samples are cut into cubes of 4 cm.
3- Samples are washed in fresh water to remove any loose materials and then dried to a constant weight at 103±2 °C.
4- Samples are removed from the oven and are allowed to cool in a desiccator to 20±2 °C. They are weighed to 0.01 grams (W_o).
5- Samples are labelled and weighed again (W_1).
6- Each sample is placed in a 250 ml container, covered with fresh sodium sulfate solution to about 8 mm at a constant room temperature and left for 2 hours. After samples have soaked for 1.5 h, a shallow tray of 300 ml of water is placed in the oven.
7- After 2 hours of soaking, samples are removed from the solution and dried in the oven at 103±2 °C for 16 hours.
8- Samples are removed from the oven and are allowed to cool in a desiccator to 20±2 °C.
9- Steps 6-8 are repeated until 15 cycles are completed.

10- Samples are weighed (W_f). The weight loss can be calculated from the expression % weight loss = 100 (W_f–W_1)/ W_o

The BRE test used three types of limestone, Portland White Bed, Box Ground and Monks Park of good, moderate and poor durability respectively, as internal reference samples. The last stone has been used extensively as a reference sample in many salt simulation tests (Doehne, Selwitz and Carson 2002, Rodriguez-Navarro and Doehne 1999b, Goudie 1999a, Goudie 1999b and Gabriel and Inkpen 1996). Monks Park limestone was also used as a reference stone in the current research (see chapter 7). Even though the BRE test was a comparative test that took into account certain environmental conditions, one could argue that it is still far from representing the mechanism of salt damage in the porous materials. First of all, there was no quantitative control over the relative humidity and no explanation was provided why the test performed better in humid conditions (namely, the variation between one stone behaviour and another was more easily spotted when the test was carried out in high humidity conditions) (Ross and Butlin 1989). Moreover, it was not obvious why the drying period was chosen to be 16 hours, apart from the intention to complete each test cycle in 24 hours. Nevertheless, considering the drying period, drying temperature and the specimens size, the total drying of the stone samples must have been achieved after each cycle. In addition, the test did not consider a major environmental factor: air speed, which can have a direct effect on the salt crystallization process. Finally, the drying temperature was far higher than those temperatures where salt crystallises in real situations.

In their standard test for the soundness of aggregates by the use of sodium sulfate or magnesium sulfate (C-88), The American Society for Testing Materials (ASTM 1990 and ASTM 2004) applied a different simulation test for salt damage. In this test, a saturated solution with an excess of crystals was used instead of the 14 % solution used in the BRE test. Also, the immersion period was increased from 2 hours to 16-18 hours. In addition, the samples were dried to a constant weight at 110±5 °C instead of the fixed 16 hour drying period at 103±2 °C used in the BRE test. However, the number of cycles (immersion and drying) was not specified. From the point view of the current research, the main advantages of this test compared to the BRE test, are using the saturated solution and ensuring complete drying after each cycle of immersion. However, because this test was mainly designed to test aggregates rather than building stones, the relative humidity and the air speed parameters were again not taken into account.

Goudie (1993) proposed a simulation method slightly different from the previous ones. In his simulation, Goudie used a single immersion technique rather than repeated immersion cycles. Mortar samples made of Portland cement and sand were immersed in different saturated single salt solutions and monitored in an environmental cabinet for 24 hours. The experiment was carried out under six different environmental conditions. These conditions represented a 24-hour direct field observation of ground surface temperature and relative humidity at six different locations. Each set of samples was exposed to 25 daily runs of the appropriate cycle. The main advantage of this test was the introduction of the field's environmental conditions instead of the extremely unrealistic conditions used in previous tests. In addition, the study provided a comparison of the behaviour of different salts at

different environmental conditions. However, one can still argue that the single immersion technique represents a very special situation, where salt solutions enter the porous system all at once and no supply follows afterwards. In other words, the porous system is closed after the first immersion, which is not a common situation in reality.

Goudie and Viles (1995) carried out the same simulation procedure as Goudie (1993) with six different rock types. In this test, samples were immersed in only two salt solutions (sodium sulfate and sodium carbonate) and the 24-hour cycle was based on actual observation of ground surface temperature and relative humidity that were recorded on two consecutive days in Avdat, the Negev Desert, Israel in 1967. The simulation procedure can be summarised as follows:

1- The blocks of stones were dried to a constant weight at 40 °C temperature and 50 % relative humidity.
2- Two sets of samples were immersed in a saturated solution of either sodium carbonate or sodium sulfate for 24 hours.
3- Samples were dried at 40 °C and 50 % relative humidity.
4- The cycle was repeated for 100 days, however, the blocks were saturated only once: i.e. only at the first immersion and not each day during the 100-day cycle of the test.

This test was more representative than Goudie's (1993), not only because it provided a comparison of two salts in six different types of natural rocks, but also because its runs were repeated 100 times, which gave a more detailed observation of the

damage. However, the previously mentioned limitations of Goudie's test (1993) remain the same.

The current British-European Standard (BS-EU) for the determination of the natural stone's resistance to salt crystallisation was approved and put into use in March 1999 (British Standard BS EN 12370: 1999). The BS EN Standard was very similar to the BRE test. However, the test stated that at least six samples should be used instead of the four to six specified in the BRE test. Also, the drying temperature was 105±5 °C instead of 103 ±2 °C of the BRE test, but the drying period remained the same (16 hours). The test was carried out under high relative humidity in the early stages of drying, which was achieved by placing a tray of water (300 ± 25 ml) in the cold oven and switching the heater on for 30 ± 5 minutes before introducing the specimens in. After the 15th cycle, the specimens were removed from the oven and stored for 24 ± 1 hours in water at 23 ± 5 °C. Then, they were washed thoroughly with water and after drying they were weighed to constant weight.

2.11.2. Partial immersion testing methods

Despite the fact that many researchers used the total immersion technique in simulating the salt crystallisation mechanism, others considered this approach unrealistic in simulating the salt damage in porous stones (Goudie 1986, Benavente *et al.* 2001, and Rodriguez-Navarro, Doehne and Sebastian 2000). Instead they proposed the partial immersion of stone samples, which would allow salt and moisture to migrate within the samples, creating what is often called *the wick effect* (Goudie 1986). The conditions and the procedure of the partial immersion varied from one study to another.

In Goudie (1986), the partial immersion test was carried out by placing 18 cm long York sandstone samples in different solutions that were topped up each day to maintain a level of 1.5 cm so that the rest of the sample would be available for moisture and salt migration. The temperature cycle consisted of 7 hours at 55 °C and the rest of the 24 hour cycle at 22 °C. Even though continuous partial immersion is more representative of salt damage in the field, Goudie's method did not attempt to control the relative humidity and required much longer time to achieve complete drying compared to total immersion simulation methods, where drying is done at much elevated temperatures.

On the other hand, Benavente *et al.* (2001) carried out simulation tests using both the total and the partial immersion techniques. In the latter, 12 types of stone were partially immersed to one-tenth of their height in 14 % sodium sulfate solution. The test cycle composed of two stages, the capillary stage (12 hours at 40 °C and 80 % RH) and the cooling stage (12 hours at 10 °C and 70 % RH). The test cycle was repeated 15 times. In this test, both the relative humidity and temperature conditions were selected according to the sodium sulfate - water system and not based on field observations. In the capillary stage (40 °C and 80 % RH) hydration-dehydration does not occur due to the fact that no solid phase is present and so the most stable phase is the sodium sulfate solution. This stage was set to represent the day-time period. Benavente *et al.* (2001) argued that, in the capillary stage, mirabilite crystallisation does not depend on the relative humidity value, and even though the relative humidity used at this stage was high in relation to the day-time conditions, it was chosen to avoid evaporation in this stage. On the other hand, in the cooling stage (10 °C and 70 % RH), the most stable mineral phase is mirabilite and the stage conditions

were set to represent the night-time period. In other words, the authors used the hydration-dehydration transformation of the Na_2SO_4-H_2O system when setting up the different conditions for the experiment. The air speed parameter was not included in the test.

Doehne *et al.* (2002) introduced the air speed parameter to the partial immersion simulation test. Two limestone columns were immersed partially in 20 % sodium sulfate solution and placed in two different conditions: the first was at a relative humidity of about 43 % in a well-ventilated laboratory and the second at a high relative humidity in a large, draft-free, plastic box that was not hermetically sealed. These conditions were chosen to represent two different air speed conditions: high and low. The experiment was the first to include the air speed parameter in laboratory salt damage simulation tests. However, the air speed conditions represented two extreme conditions, while field observations (as stated in chapter 8) show that air speed fluctuates vastly and, therefore, a salt simulation test needs not only to introduce the air speed conditions, but also to include all the possible expressions of this parameter. The laboratory experiment of the current research is an attempt to achieve this purpose (see chapter 7).

Lubelli (2006) presented a set of salt simulation tests aimed at improving the effectiveness of the salt weathering simulation test using sodium chloride. The environmental parameters of these tests were based on a literature review as well as on data from the case studies of her research. Three types of porous materials were used in this test: a lime-cement mortar, a fired clay brick and a cement-based restoration plaster. The experiment was composed of three main tests:

1- A test to evaluate the effect of accelerated drying on sodium chloride damage.
2- A test to evaluate the effect of relative humidity cycles on sodium chloride damage.
3- An accelerated weathering test based on the results of the two previous tests.

Lubelli's work was able to demonstrate how important it is to include all possible factors when designing a salt simulation test and how different the outcomes can be when different conditions are applied. In addition, Lubelli's tests were able to demonstrate that sodium chloride could cause significant damage in porous materials at certain environmental conditions. This finding contradicts many previous simulation test results that regarded sodium chloride as a harmless salt in regards to weathering of porous materials.

All things considered, it can be said that the salt crystallisation test has been applied in many different ways. Each way has revealed certain information. However, most of the tests have neglected or modified some aspects of the salt damage process. One of the main aspects that has been neglected is the effect of air speed in the mechanism of salt damage. On the other hand, the partial immersion tests were more representative of salt damage as it happens in the field. In addition, the visual appearance of the damage from the partial immersion tests is more similar to the damage as it appears on an actual building compared to the damage from total immersion tests. But, in order to have a realistic simulation, the test needs to be carried out for comparatively long periods. Also, more sophisticated environmental

chambers are needed in order to control the different environmental conditions in the partial immersion test.

Therefore, one could argue that the selection of the best salt damage simulation technique will vary from one situation to another, since each of these techniques (partial and total immersion) has its advantages and disadvantages. While the partial immersion is more representative of the actual damage mechanism in both damaging features and procedure, the more intensive total immersion technique can simulate long-term damage within a relatively short testing period.

In this study, the total immersion test was chosen as the basis for the research's modified salt crystallisation test. The research needed to test the salt damage on five different stones under six different environmental conditions using two different salt solutions. This meant that the test should include 12 runs, and if the partial immersion technique were followed, a minimum of three years of laboratory work would be needed to complete it; a time scale not available for this research. The experiment conditions, procedure and limitations of the actual experiment are discussed in detail in chapter 7.

2.12. Salt damage in porous materials: the way forward

The previous discussion of the main aspects of salt damage demonstrates strongly how the understanding of this process has advanced significantly in the last few years. But, has the main question regarding the salt damage process been fully answered, and if not, what should be the next step? Unfortunately, the salt damage mechanism has not yet been fully explored, despite the numerous and

interdisciplinary studies in this field. So, what is the way forward? The answer depends on another question: why do we need to understand how salt damage happens? The ultimate goal behind every investigation into salt damage is to understand this mechanism in order to preserve the many cultural heritage sites and buildings that undergo a continuous loss of material due to salt action within them. As a result, the research on salt damage should be directed towards the more practical side of the problem and combine the theoretical knowledge with field observations. This broad direction can be specified by two areas where more research in salt damage is needed:

- Studies that discuss the salt damage mechanism as it happens in nature. In other words, the theoretical models and simulation tests that aim to understand salt damage should be based on field observations and realistic conditions rather than using complicated models and theories that are based on conditions different to the existing ones.
- Studies that focus on possible ways of tackling the salt damage problem. The conservation practices could be remedial, preventive or even managerial matter. Considering the size of the salt damage problem in archaeological sites and buildings, the remedial conservation practices are limited to a certain degree, and it is more realistic to focus the research on the other aspects of conservation practice, namely prevention and management practices. In regards to preventive conservation, the use of thermodynamic models (see chapter 10) to predict the salts behaviour seems very promising. Undoubtedly, more studies are needed to test the practicality of these models.

As a result, and based on field observations and data collection, the current research identified an important factor with significant impact on the salt damage in porous materials and examined it under realistic conditions. Petra monuments deteriorate at a fast rate, and one of the main obvious weathering factors is salt damage. In addition, one of the main environmental conditions at the site is the high rate of wind speed fluctuation. Therefore, it was deemed necessary to explore the role of wind speed in salt damage. Moreover, this study encountered other factors that can have an impact on the salt damage in the Petra monuments, as is shown in the following chapters (chapters 5-11).

Chapter 3
The Role of Microclimate Conditions in the Activation of Salt Damage

3.1. Introduction

The presence of high levels of moisture and salt supply in porous materials is the prerequisite for salt weathering (Goudie and Viles 1997). However, environmental conditions such as relative humidity, temperature and wind speed also play a crucial role in activating the salt weathering process. The following is a brief description of the role of these environmental factors in the salt damage process.

3.2. Relative humidity

Relative humidity (RH) can be defined as the amount of water vapour (vapour pressure) in a given volume of air divided by the maximum amount of water vapour that this same volume of air could contain at a given temperature (saturation vapour pressure) before it would begin to condense into water droplets (Visualisation and Analysis System Project Glossary 1996). This environmental condition (RH) is crucial in the salt damage process since it plays a major role in the transition states of salts. As discussed in chapter 2 (section 2.6), when a soluble salt dissolves in water, the water vapour pressure over the solution decreases and continues to do so until it reaches its minimum in the saturation state. Raoult's law, as shown in the following equation, partially describes this property of the solute, although the dissolved salt ions establish strong bonding forces with water molecules and with each other and cause further decrease in the solution's vapour pressure. (Steiger 2002, Sawdy 2001 and Steiger and Zeunert 1996).

$$P = P^{o} X$$

Where:
P^{o}: the vapour pressure of the pure solvent
X: the mole fraction of the solvent in the solution

The mole fraction of water in saline solutions is less than one, and so the vapour pressure of the saline solution will be less than the vapour pressure of the pure water.

The vapour pressure above a saturated single salt solution is expressed as the 'equilibrium relative humidity' (ERH). As discussed in chapter 2, the relation between the surrounding relative humidity and the ERH of a salt solution defines the behaviour of the salt solution in porous materials (see section 2.6 for more details).

3.3. Temperature

It is well known that temperature has a strong influence on the relevant phase equilibria. Increase in temperature leads to evaporation of water, which in turn causes increase in salt concentration and decrease in the vapour pressure of the solution until finally the salt starts to crystallise. It is very important to state that the vapour pressure is the absolute measurement of moisture in the air. The relative humidity on its own can be a misleading measure of the moisture content in the air. For instance, two different relative humidity measurements 70 % and 55 % could reflect exactly the same absolute moisture content of the air at different temperatures (16 °C and 20 °C respectively).

Moreover, temperature has a wide effect on the solubility of different materials. As the temperature increases, the solubility of most salts increases too. An increase in

the solubility of a salt results in increase of its mole fraction and thereby in decrease of the water vapour pressure. In other words, increase in temperature causes a gradual decrease in the equilibrium relative humidity (ERH) of soluble salts. For instance, the ERH of magnesium nitrate is 58.86 % at 5 °C, but it decreases to 48.42 % as the temperatures goes up to 40 °C. This process is also typical for hydrated salts and the anhydrous nitrates of sodium and potassium (Steiger 2002). On the other hand, some salts have a more stable ERH at different temperatures. For example, the ERH of sodium chloride is around 75.65 % at 5 °C and 74.68 % at 40 °C. The ERH of potassium sulfate is also fairly stable at different temperatures.

In brief, the ambient temperature affects the phase equilibria of salts as well as the solubility of most soluble salts. This has a direct effect on the salt damage mechanism since dissolution/crystallisation is a fundamental aspect of this process.

3.4. Wind

Wind is another environmental condition that affects the salt damage process through different mechanisms. First of all, wind speed has a major effect on the evaporation rate. According to Bird *et al.* (1960), an increase in wind speed results in higher evaporation rate. When water evaporates from the solution, the air in the boundary layer usually has a partial pressure very close to the vapour pressure of that solution at the temperature of its surface. Normally, a large amount of water evaporates and immediately recondenses in equilibrium within this thin layer. The diffusion and convection of the water molecules away from this thin layer is what really drives the rate of evaporation. So, in windy conditions, the evaporation rate increases, as the wind takes away the moist air and replaces it with dry air. As a result, the water

vapour decreases, the supersaturation ratio of saline solutions increases and salt crystals form more rapidly.

Secondly, the wind has a crucial role in the cooling rate of the solution. Wind acts as a factor that removes energy from a surface and therefore affects the cooling rate. High wind speed increases the cooling rate and therefore the solubility of salt(s) decreases. As the solubility decreases, the water vapour decreases as well and a highly supersaturated solution is formed. Doehne, Selwitz and Carson (2002) stated that rapid cooling is an effective way to obtain a high supersaturation ratio in the sodium sulfate system.

Moreover, the wind has a direct influence on the crystallisation location of salts. The location where the salt(s) precipitate(s) out of the solution is a dynamic balance between moisture uptake and moisture loss in the system. If the moisture uptake is higher than the moisture loss, the solution moves towards the surface of the porous material and salts deposit on the outer surface forming what is called 'efflorescence'. But, if the drying rate is higher than the moisture uptake, then the salt precipitates out of the solution inside the porous system causing what is called 'subflorescence'. Lewin (1982) presented a mathematical model to determine the depth of solute precipitation in a steady state, where the rate of diffusion of water through a thin layer of porous solid at the surface is balanced by the rate of replenishment of water to that area from the solution. As mentioned earlier, under windy conditions, the evaporation rate is higher and therefore the salts crystallise deep below the surface of the porous host materials. Mossoti and Castainer (1990) monitored the evaporation of water from porous limestone using computer-aided tomography (CAT-Scan).

They confirmed that under windy conditions water evaporation is promoted deep under the stone surface. Doehne, Selwitz and Carson (2002) carried out two sets of experiments to test the non-equilibrium crystallisation of thenardite (Na_2SO_4) and the generation of high supersaturation ratios and rapid mirabilite crystallisation ($Na_2SO_4.10H_2O$). The first test was a macro experiment of 'rising damp' crystallisation of sodium sulfate in limestone blocks under conditions of high and low air exchange rate, while the second involved dynamic environmental scanning electron microscope crystallisation experiments. These experiments showed that draught-free, high humidity environments enhanced efflorescence and reduced damage. On the other hand, high airflow encouraged crystallisation under the surface of the stone resulting in extensive damage. They concluded that the drying rate is a key parameter in salt weathering. It follows that the air exchange rate is a fundamental factor in the salt damage process since it controls the drying rate of saline solutions.

It is worth mentioning that the rate of airflow affects the morphology of the salt crystals. In wind-exposed faces, salt crystals are usually non-equilibrium and anhedral, while euhedral or whisker-like crystals usually appear in low airflow rates (Rodriguez-Navarro and Doehne 1999b). The morphology of salt crystals is a direct indicator of the supersaturation ratio before crystallisation (Doehne, Selwitz and Carson 2002). The non-equilibrium crystals are formed from highly supersaturated solutions, while euhedral or whisker-like crystals are formed from solutions with low supersaturation ratios.

Wind is also a direct factor affecting the wetting of the stone by wind-driven rain (Smith and McGreevy 2004). This affects the moisture content, which in turn is a crucial factor in salt damage.

3.4.1. Wind, salt and cavernous weathering

Cavernous weathering is a relatively common phenomenon in earthen architecture and natural stone, especially in coastal and arid areas (Goudie and Viles 1997). It is a weathering feature characterised by the fact that disaggregation proceeds preferentially in some areas of the stone, forming deep cavities (alveoles) while the nearby surface remains unaffected (Torraca 1988) (See figure 3.1). The small scale of this weathering form is called honeycomb (or alveolar weathering) while the larger scale is called tafoni.

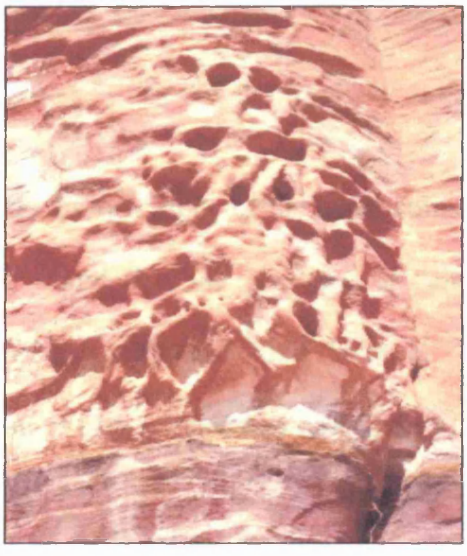

Figure 3.1: Alveolar weathering in the Palace Tomb, Petra, Jordan. Height of shown rock façade: approximately 1 m. (Fitzner and Heinrichs 2004)

The origin of cavernous weathering and its causes have been studied extensively by many scholars (see for example, Viles 2005b, McBride and Picard 2004, Turkington

and Phillips 2004, Rodriguez-Navarro and Doehne 1999a, Goudie and Viles 1997, Pye and Mottershead 1995, Pauly 1976, Martini 1978, Smith and McAlister 1986). In general, these studies concluded that salt solutions and wind speed are the main controlling factors in this type of weathering.

Pauly (1976) noticed that alveolar weathering developed in a homogeneous rock where local wind speed fluctuation had been observed. Torraca (1988) supported Pauly's theory and added a further explanation for the formation of alveoles, that the acceleration of wind causes more evaporation in the cavities than in the surrounding area.

Matsukura and Matsuoka (1991) carried out experimental work to study the degree of tafoni formation on the faces of marine cliffs. They stated that salt weathering is essential for tafoni development, while wind and sun were the main factors determining its severity.

Pye and Mottershed (1995), in their study of the honeycomb weathering of sandstone in the west of England, found that the presence of salt solutions enhanced the swelling and contraction of clay minerals within the rock. The effect of salt solutions in swelling and contraction of clay is discussed in chapter 4.

Rodriguez-Navarro and Doehne (1999a) studied the role of wind in the formation of honeycomb (alveolar) weathering. After a laboratory experiment to reproduce the honeycomb weathering in homogeneous rocks under windy conditions, they pointed out that wind enhanced the evaporation of a saline solution and that this in turn

resulted in a random development of small cavities. The introduction of heterogeneous wind flow caused more rapid evaporation within these cavities and consequently led to the formation of honeycomb weathering.

Honeycomb weathering is one of the common weathering forms observed in the Petra monuments (see chapter 6). As mentioned earlier, these monuments are located in an arid area, where both salt damage and fluctuating wind speed are common features (see chapters 8 and 9). This strongly supports the idea that wind and salt damage are involved in the formation and development of cavernous weathering.

In brief, the formation of cavernous weathering is strongly linked to saline solutions and fluctuating wind speed conditions. Despite some uncertainty about how cavernous weathering is formed, previous research has shown that the salt weathering process initiates the formation of these features, while wind speed is the main environmental factor in their development process.

3.3. Summary

From what has been discussed so far, it can be concluded that in order to understand the salt damage process, all the surrounding environmental conditions should be taken into account. Also, relating one environmental parameter to the others is very important in order to get an overview of the salt damage process. In particular, the wind effect on salt damage needs more detailed research and a comprehensive study that includes both fieldwork and laboratory data.

Chapter 4

Clay Minerals and Salt: Their Combined Role in Porous Materials Decay

4.1. Introduction

It has long been known that soluble salts and clay minerals, as individual factors, have a significant role in damaging inorganic porous materials such as stone and masonry (Evans 1970, Delgado-Rodrigues 1976, Brattlie and Broch 1995, Price 1996 and Goudie and Viles 1997). However, very few inclusive studies have been focused on the relation of these two factors, as combined agents, in the stone damage mechanism (McGreevy and Smith 1983 and Rodriguez-Navarro, Hansen, Sebastian and Ginell 1997). This chapter will first present and discuss the clay minerals terminology, their physical and chemical properties and their mineralogical classification. Secondly, the role of clay minerals in the stone damage process will be discussed and evaluated. Moreover, the possible role of clay minerals in the salt damage mechanism as well as the impact of salt ions on the weathering behaviour of clay minerals in stone will be examined.

In addition to this, chapter 11 will present some experimental procedures undertaken to understand the effect of clay minerals on the salt damage mechanism under different environmental conditions, with special consideration of the wind speed factor.

4.2. Clay and clay minerals: an introduction

From a geological point of view, clay is a term that applies to materials that have a particle size less than 2 micrometers, while clay minerals are clays that have a definite chemical composition and common crystal structure characteristics (Velde 1995). In other words, clay minerals have not only physical but also chemical features. More precisely, clay minerals can be defined as fine crystalline hydrous minerals formed by the weathering of silicate minerals such as feldspar, pyroxene and amphibole (Grimshaw 1971).

4.3. Physical and chemical properties of clay minerals

Both the physical and the chemical properties of clay minerals affect their behaviour (Velde 1995). Therefore, in order to understand the complexity of clay minerals and their activity, their physical and chemical properties should be addressed with care.

4.3.1. Particle size

As mentioned earlier, it is important to emphasise the difference between clay and clay minerals. Clays are any fine-grained materials with a particle size less than 2 micrometers, while clay minerals, apart from their particle size, have a definite internal structure and chemical composition. In other words, not all clays are clay minerals, but the reverse is true. The particle size of clay minerals is a key factor in their activity, since it gives them a large surface area compared to their volume (Velde 1992 and 1995). The importance of such a special property, the large surface area, will be discussed later along with other clay mineral properties.

4.3.2. Structure

Clay minerals are the most important part of a large mineral family called phyllosilicates, which are minerals with layer structure composed of shared sheets. This layer structure is composed of interlinked polyhedrals between the anions and the cations. Oxygen forms half of the present ions, while silicon and aluminium are the major cations. The basic clay minerals structure is called tetrahedral and is built of two-dimensional sheets, which are composed of T_2O_5 compounds (T: cation, usually silica (Si), aluminium (Al) or iron (Fe)) (Bailey 1980). The other polyhedral clay mineral structure is called octahedral, where aluminium, magnesium or ferrous iron composes a structure with six oxygen anions, instead of four, in octahedral coordination. In this structure, the number of cations and anions vary between two and three, but the positive charge is usually +6 (Velde 1995). The structure is called dioctahedral (gibbsite) in the case of two cations and trioctahedral (burcite) in the case of three cations. These two categories of octahedral structures are the basic features for the clay minerals classification (Newman and Brown 1987, Brindley 1980). Tetrahedral and octahedral structures are very rarely found alone (Velde 1992). The two sheets are usually joined together in a sheet structure through a plane of shared apical oxygen anions and unshared OH groups (Bailey 1980). The thickness of the layer of linked tetrahedral and octahedral structures is the fundamental means of identifying clay minerals (Velde 1995) and can be measured by X-ray diffraction. The thickness of the interlinked tetrahedral and octahedral structures is less than that of the two individual layers put together since they share oxygen atoms in their combined network structure. Accordingly, the main building structure in natural clay minerals is as follows:

- One tetrahedral + one octahedral = 1:1 structure, with a thickness of 7 Å.

- Two tetrahedral + one octahedral = 2:1 structure, with a thickness of 10 Å.
- Two tetrahedral + two octahedral = 2:1+1 structure, with a thickness of 14 Å.

4.3.3. Clay minerals and water

It was mentioned earlier that clay minerals have a large surface area compared to their volume. Therefore, water molecules are usually adsorbed to the clay mineral surface. Furthermore, some clay minerals, called swelling clay minerals, not only adsorb the water molecules, but also absorb them into their structure (Velde 1992). According to Velde (1995), the absorbed water changes the dimension of the clay particles as it goes into or out of the clay structure. The water exchange process is quite reversible under atmospheric conditions, where relative humidity and temperature are the main controlling factors.

In brief, the swelling property of a certain type of clay is a key factor in the interaction between the clay-bearing rock and its surrounding environmental conditions.

4.3.4. Clay minerals cation exchange capacity (CEC)

Clay minerals are chemically active due to the fact that they have charged surfaces. Moreover, the surface charge usually increases from the absorbed ion molecules that find a way to enter the internal crystallographic network of these minerals. Velde (1995) stated that the property of adsorbing and absorbing ionic species in solutions is called cation exchange capacity. The cation exchange capacity can be expressed as the total sum of the exchangeable cations that clay minerals can absorb. It is usually expressed in milli-equivalents of charge (moles) / 100 g. In addition, it is

worth mentioning that some cations are more attracted to clay minerals than others. As a result, when clay minerals interact with cations in aqueous solution, a process of cation selectivity takes place (Laudelout 1987).

4.4. Clay minerals groups

The swelling properties and the layer structure distance are the main categories in the clay minerals classification. As mentioned above, clay minerals can be divided into three groups according to their layer thickness: 7, 10 and 14 Å. However, only the 10 Å thick layer (smectite group) has swelling properties, due to its capacity to accept and exchange hydrated cations and other molecules within the interlayer position, which means that this is the only category that needs to be subdivided according to such properties. The classification of clay minerals varies from very basic schemes, such as Newman and Brown (1987), to very detailed and precise ones, such as Bailey (1980) and Velde (1995).

4.5. Clay minerals and stone weathering

Clay minerals are a common component of sedimentary rock and can cause severe weathering to it. Many researchers, such as Grimshaw (1971), Wendler *et al.* (1991) and Brattli and Broch (1995), have confirmed that clay minerals have a vital role in the stone weathering process. Other scholars, such as Delgado-Rodrigues (1976), Rodriguez-Navarro, Hansen, Sebastian and Ginell (1997) and Warke and Smith (2000), have reported types of stone damage, which are caused by a very small amount of clay minerals within the composition of the stone. Clay minerals can cause both physical and chemical changes to their hosting rock when they are

subjected to different environmental conditions, and more precisely when they interact with water. In this section the factors that control the weathering behaviour of clay minerals will be presented and discussed. Secondly, the swelling behaviour of clay minerals and its effect on stone decay will be discussed and evaluated. Finally the role of clay minerals in the salt damage process will be addressed in some detail.

4.5.1. Factors controlling the weathering behaviour of clay minerals in stones

The role of clay minerals in stone decay is controlled by a group of factors. First of all, it is the type and amount of clay minerals in the host rock. It was mentioned earlier that some clay minerals (smectite group) absorb water and add it to their internal structure, while the rest of clay minerals only adsorb water to their surface. In other words, some clay minerals can cause more damage to host rocks than others, because the absorbed water changes their internal structure. Consequently, the identification of the type of clay mineral and its quantity in particular stone should be the first step in understanding the role of such minerals.

Secondly, the way in which clay minerals are distributed in the rocks is a basic factor in determining the stability of these rocks. For instance, Rodriguez-Navarro (1994) has reported that the presence of 5 % of clay minerals in limestone along its bedding planes causes rapid decay when the stone is in contact with water. However, Dunn and Hudec (1966) have stated that, in other situations, similar rocks (limestone) were very stable and sound, even with higher clay minerals content (30 %). This was mainly because of a homogenous distribution of clays in these rocks.

Another important factor is the chemistry of the water with which the clay minerals interact (Grimshaw 1971, Velde 1992, and Rodriguez-Navarro, Hansen, Sebastian and Ginell 1997). For instance, changing the pH of the pore water affects the ability of clay minerals to absorb it.

Moreover, the existence of other weathering agents within the same rock, such as contamination with salts, could enhance the role of clay minerals as deterioration agents and vice-versa (McGreevy and Smith 1984). The relationship between clay minerals and salt damage will be discussed and evaluated later in this chapter.

Furthermore, the pore structure of the host rock has a primary role in the way clay minerals behave (Grimshaw 1971). Some rocks have connected pore structures, while others have dead end or disconnected structures. Those with connected pore structures will allow the water to go through their internal structure, which will result in clay minerals becoming swelled and hence cause more damage.

Finally, the amount and type of exchangeable ions associated with clay has a fundamental role in determining the swelling features of clay. These ions cause what is called osmotic swelling, in which the negative charge of the clay surface adsorbs polar liquid (water) as well as various ions present, which later hydrate and produce initial swelling of fibrous clay crystals (Grimshaw 1971 and Rodriguez-Navarro, Hansen, Sebastian and Ginell 1997). Rodriguez-Navarro *et al.* (1997), in their study of the role of clay minerals in the decay of Egyptian limestone sculptures, reported that the presence of sodium chloride and sodium nitrate within the stone offers a supply of sodium ions to the solution formed when water enters the pore system of

the limestone. After that, the sodium ions become hydrated and, as a consequence, crystalline swelling takes place.

4.5.2. The swelling of clay minerals and its role in stone decay

Dunn and Hudec (1966) and McGreevy and Smith (1984) reported that the absorption of water molecules is the main deterioration factor in clay-bearing materials. Because of this, the process of swelling and its role in stone decay will be discussed briefly.

It is important to remember that not all clay minerals have the ability to absorb water molecules. But, does that mean that only the smectites group (being the only one with absorption abilities) can cause stone decay? Surprisingly, this is not the case. It has been stated that other clay minerals such as kaolinite and illite have a swelling behaviour (Van Olphen 1977, McEwan and Wilson 1980 and Rodriguez-Navarro *et al.* 1997).

When a swelling clay mineral is immersed in water, swelling deformation and swelling pressure occurs. The swelling deformation and swelling pressure are proportional to the volume of water absorbed by swelling clay minerals. The absorbed volume is related to the surface fractality of the minerals (Grimshaw 1971). Warke and Smith's (2000) experimental results for clay (smectite) - rich weathered sandstone are very straightforward examples of such swelling deformation and pressure.

Scherer and Jimenz Gonzalez (2005) carried out a set of laboratory experiments to assess the risk of stone damage from swelling clay minerals. Alongside performing the method of direct swelling measurement[4], their research introduced a new method for evaluating the swelling stress, which is to observe the warping of a thin plate of stone by wetting one side only. The research concluded that some stones could suffer destructive stress as a result of differential strains from wetting and swelling. On the other hand, the research demonstrated the importance of considering that the very small pores that usually exist in stones containing clay minerals generate high crystallisation pressure and, thereby, these stones become more susceptible to damage from crystallisation of ice or salt. The current research will discuss the effect of pore space in the evaluation of salt damage in more detail in chapter 11.

4.5.3. Clay minerals and salt concentration: the potential hazards

Many researchers have examined the potential hazards of clay minerals and salt accumulation as individual agents in stone building materials (Dunn and Hudec 1966, Evans 1970, Delgado- Rodrigues 1976, Cook 1979, Price 1996 and 2002). However, only a few scholars, such as McGreevy and Smith (1984), Rodriguez-Navarro *et al.* (1997) and Warke and Smith (2000) have examined the relationship between these two factors and their combined effect in stone weathering. It has to be emphasised that neither factor can be fully understood without consideration of the other. This is mainly related to the fact that both factors have a direct or indirect consequence on the mechanism of each other. For example, the existence of clay minerals in the stone can increase the attraction of water molecules, which is a key

[4] Direct measurement of swelling pressure is a method to evaluate the swelling pressure by placing a sample of stone into a rigid frame and then saturating it with water. As a result the stone swells and exerts pressure on the confining frame (for more details see Scherer and Jimenz Gonzalez 2005).

factor in the salt damage mechanism, while salt can play a major role in the swelling behaviour of some clay minerals.

4.5.3.1. The possible role of clay minerals in salt damage of stone materials

Fookes and Poole (1981) mention that salt damage might be enhanced by the presence of clay minerals. In their model of the possible role of clay in salt damage, McGreevy and Smith (1984) proposed two explanations as to how clay minerals could promote breakdown through salt weathering. Firstly, the swelling of clay minerals could weaken the internal structure of the stone and, therefore, make it less resistant to salt damage. Secondly, the clay minerals could play a vital role in the modification of the pore space within the rocks. Keighin (1980) reported that the consequence of the formation of authigenic[5] clays within sandstone results in developing secondary porosity, with mesopore ranges. Flatt (2002b) carried out a set of experiments in order to evaluate the relation between pore geometry of stone and salt damage. He concluded that the materials with mesopores are more susceptible to crystallisation pressure. Consequently, in the presence of authigenic clays, the salt weathering process is more active.

4.5.3.2. The role of salts in clay mineral weathering

Rodriguez-Navarro *et al.* (1997) carried out an extensive survey on Egyptian limestone sculptures that had suffered serious damages while being kept in storage in the Metropolitan Museum. The mineralogical and petrographic studies of that research revealed that these sculptures contained approximately 10 % of non-swelling clays (sepiolite-palygorskite). Moreover, both halite (NaCl) and sodium

[5] Authigenic clays: pertaining to clay minerals crystallised with enclosing sediment during or after deposition, either infilling voids or replacing pre-existing rock constituents.

nitrate ($NaNO_3$) were identified. After a series of laboratory tests, such as wetting/drying cycles, relative humidity changes and thermo-mechanical analyses, it was found that clay minerals and not salt growth, were the main cause of the sculptures' decay. Furthermore, this study revealed the role of salt accumulation in the clay swelling behaviour and, hence, in the stone decay mechanism. The existence of a mixture of salts reduces the equilibrium relative humidity of the individual salts (Price and Brimblecombe 1994). This means that water was present within the pore space at a relative humidity lower than the equilibrium relative humidity of each individual salt. In addition, the salts ions play a further role in the swelling process by providing sodium ions, which promote the osmotic swelling of clays.

All in all, it can be concluded that both clay minerals and salt have a direct influence on weathering of porous materials. As a result, any evaluation of either mechanism must consider the effect of the other, as appropriate.

Chapter 5
The Current Research

5.1. Introduction

As discussed in the previous chapter, the salt damage mechanism in porous materials cannot be understood without consideration of the role of the environmental conditions in this process. Consequently, this research was undertaken to investigate the particular role of the wind speed factor in the salt damage mechanism. Considering the complexity of the salt damage mechanism, the current research project required a combination of fieldwork observation, data collection and analysis and a laboratory simulation experiment.

5.2. Aims and objectives

There were four main research aims. The first aim was to monitor the salt distribution and microclimate conditions at selected monuments in Petra in order to understand the extent and the mechanism of salt damage at these monuments. Moreover, the research was extended to examine the role of clay minerals in salt damage. This last objective derived from the fact that the petrographic analysis of Petra stone revealed high percentages of clay.

The second aim of the research was to develop a salt damage simulation test that would take into account the wind speed factor in the evaluation of the salt damage process.

The third and overall aim of this research was to examine the effects of the wind speed on salt damage. The theoretical base of this research is built on the hypothesis

that the fluctuation of wind speed enhances salt damage in porous materials since it causes an alteration of crystallisation and dissolution. As wind speed increases, the evaporation increases too and so the salt crystallises. At low wind speed the salt takes up moisture and dissolves again. Moreover, the dissolution of the salt could take away part of the supportive material or even weaken it. The succession of high and low wind speed will result in succession of crystallisation and dissolution, which will cause more damage than a steady rate of crystallisation would cause. This research took into consideration other environmental conditions that affect the salt damage process, namely temperature and relative humidity.

The last aim of the research was to use all fieldwork observations and laboratory simulation test results in order to recommend some conservation measures that could minimize the salt damage at Petra.

The research's overall aim was achieved by combining and correlating the results of the fieldwork observation and data collection with the laboratory simulation test results.

The monitoring of the microclimate conditions was achieved firstly by taking spot readings for the temperature, relative humidity and wind speed around four different monuments on four fieldwork visits and also by recording the relative humidity and temperature at one location for a period of 20 months using a Tinytag logger. Unfortunately, the wind speed conditions could not be recorded in the same way due to the lack of data loggers that could monitor this environmental factor for a long period of time, and the spot readings were the only reliable source of information.

The salt distribution in the studied monuments was determined by collecting and analysing samples from different locations at the studied monuments during four fieldwork visits. Samples were collected from different depths and heights at each monument. The fieldwork visits covered the main seasonal changes in the area of Petra.

It must be stated that the variation in salt distribution in the collected samples and the changing microclimate conditions that were recorded around the studied monuments made the author aware of the importance of introducing the observed fieldwork conditions in the laboratory simulation test. This test was undertaken to examine the role of the wind speed in the salt damage process in porous sandstone and limestone specimens under controlled environments and consisted of two experiments.

The first experiment monitored the salt damage in different sandstone and limestone specimens after immersion in a certain salt solution in controlled environmental conditions. A specially developed microclimate chamber with air speed controlling facilities was connected to a microclimate generator to enable control of the temperature and relative humidity (see chapter 7). This experiment consisted of two parts: firstly, the evaluation of the salt damage caused in specimens using a single salt (sodium sulfate), and secondly, the evaluation of the salt damage caused in similar specimens using a salt mixture similar to the one found at the case-study monuments. The conditions for the first part were based on the Na_2SO_4-H_2O phase diagram (figure 7.3), while the second part was mainly based on the microclimate data collected from the studied monuments. Unfortunately, irreparable breakdown of

the microclimate generator denied the completion of this experiment, and the second experiment had to be devised in its place.

The second experiment was a modified version of the salt crystallisation test used by the Building Research Establishment (BRE) (Ross and Butlin 1989) that introduced the wind speed factor based on the conditions recorded at the studied monuments. This experiment also consisted of two parts: the first evaluated the salt damage process in 5 different stone specimens under controlled environment using a saturated single salt solution (sodium sulfate), and the second part was carried out using a salt solution similar to that found in one of the studied monuments (Palace Tomb). A vacuum oven connected to gas bottles placed in a water bath, which were connected at the other end to an air pump, was used to provide the required conditions (see chapter 7). The conditions in both parts (the sodium sulfate and the 'Petra' solutions) were based on the collected microclimate data from the studied monuments. The main reason for not carrying out the sodium sulfate test in similar conditions to those used in the microclimate generator experiment was the difficulty of producing accurate conditions with the available equipment.

The evaluation of the effect of the different environmental conditions, and especially the different wind speed conditions, was observed through the weight loss or gain and also through the examination of salt distribution at the end of each set of experiments.

Chapter 6
Petra, the Site and the Problem

6.1. Introduction

Jordan lies at the heart of one of the most historically important and intellectually intriguing regions on earth. The Kingdom has more than 10,000 known archaeological sites with many yet to be discovered. One of the most famous sites in Jordan is the World Heritage Site of Petra. The archaeological city of Petra with its 2000 sandstone rock cut façades is considered by many to be the eighth wonder of the world. It is a Nabatean[6] city that was hewed into coloured sandstone and limestone mountains. Petra is the biggest tourist attraction in Jordan; however the city suffers from weathering and erosion problems, both natural and human in origin. The following sections will briefly introduce the location, the climate, the monuments, the geological setting, and the major weathering problems in the city of Petra.

6.2. Petra, the location

The city of Petra lies hidden in the Desert Mountains in the southern part of Jordan, half way between the Dead Sea and the Gulf of Aqaba. It is 255 km away from Amman (the capital of Jordan) (Figure 6.1). The international coordinates for the city are 35° 25′ E - 35° 28′ E and 30° 19′ N - 30° 21′ N. The archaeological city of Petra occupies about 15 km^2 and is 900 to 1500 m above sea level. Figure 6.1.b. shows the most important carved monuments in the city, some of which will be discussed in more detail later on in this chapter.

[6] The Nabateans were nomadic Arabic people who ranged between Syria and Arabia from the 7th century BC to the 2nd century AD (Burgen 2000).

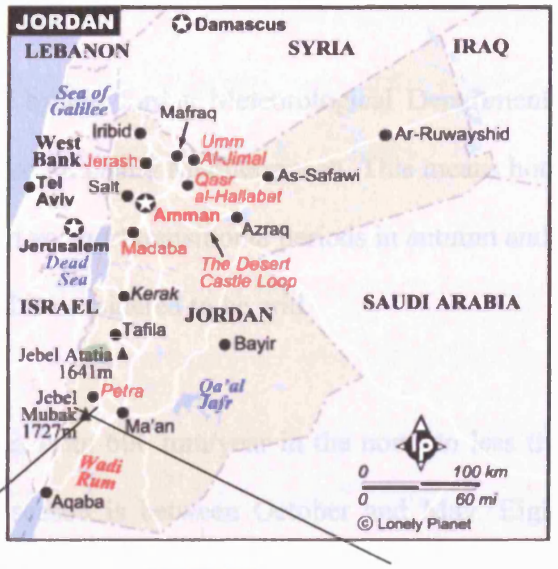

6.1.a

6.1.b

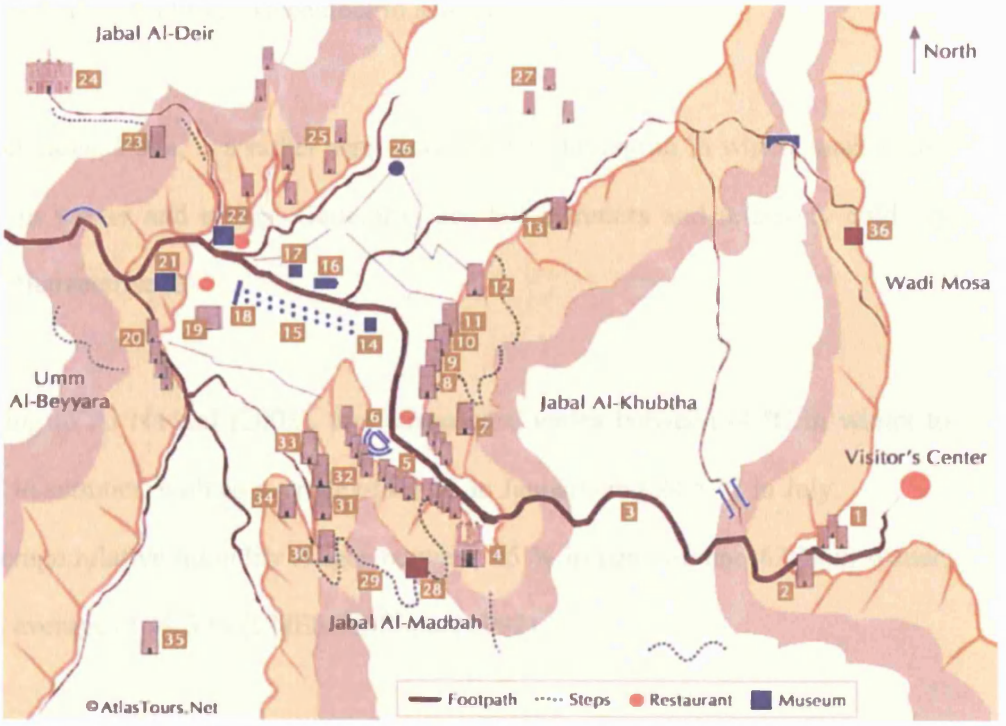

1. Djin Blocks	7. Aneisho Tomb	13. House of Dorotheos	19. Qasr Al-Bint	25. Turkmaniya Tomb	31. Triclinium
2. Obelisk Tomb	8. Urn Tomb	14. The Nymphaeum	20. Unfinished Tomb	26. Conway Tower	32. Renaissance Tomb
3. Al Siq	9. Silk Tomb	15. Colonnaded Street	21. Al-Habees Museum	27. Moghar Annassara	33. Broken Pediment Tomb
4. The Treasury	10. Corinthian Tomb	16. Byzantine Church	22 Petra Archaeological Museum	28. High Place of Sacrifice	34. Roman Soldier Tomb
5. Street of Façades	11. Palace Tomb	17. Winged Lion Temple	23. Lion Triclinium	29. Lion Monument	35. Snake Monument
6. The Theatre	12. Sextus Florentinus Tomb	18. The Arched Gate	24. Al-Deir	30. Garden Temple Complex	36. Crusader Fort

Figure 6.1.a: Map of Jordan and its main archaeological sites. (Lonely Planet 2004)
Figure 6.1.b: The main monuments at the city of Petra (Atlas Tours Net 2004)

6.3. Petra, the climate

According to a report by the Jordan Meteorological Department (JMD 2003), the climate in Jordan is predominantly Mediterranean. This means hot, dry summers and cool, wet winters with two short transitional periods in autumn and spring. More than 80 % of Jordanian land is considered to be arid.

Average rainfall ranges from 600 mm/year in the north to less than 50 mm/year in the south. The rainy season is between October and May. Eighty percent of the annual rainfall occurs from December to March.

The study area, Petra, is a rather semi-arid, steppe-like region in which small plants survive in winter and spring. Generally, dry hot summers and relatively cold dry winters characterise it.

According to Al Naddaf (2002), the temperature varies between -4 °C in winter to 38.5 °C in summer, with an average of 8.1 °C in January and 24.5 °C in July.
The average relative humidity ranges between 45 % in summer and 62 % in winter, with an average of 49.5 % (UNESCO Report 1992).

The annual rainfall varies between 250 mm on the surrounding mountains (Al-Sharah Mountain) to less than 50 mm at the foot of the massif of Petra (Al Naddaf 2002). Moreover, when it rains heavily for a short time, the area is apt to suffer a number of flash floods, due to the nature of its soil. One of these floods occurred during the second fieldwork visit of this research and the city was closed for two days.

Due to the high temperature and the long duration of sunshine (around 8.6 hours per day), the daily evaporation rate is generally very high, with higher readings in the summer months (end of May - beginning of November).

The daily climatological data from Wadi Mousa station, the nearest meteorological station to the site, reveal that the annual wind speed varies between 6 knots (3.1 m/s) in the summer and 13 knots (6.6 m/s) in the winter, with an average of 7 knots (3.6 m/s) in the summer and 11.4 knots (5.8 m/s) in the winter. Winds usually originate from the west and south-west.

6.4. Petra, the monuments

The monuments of Petra are unique in their architecture, structure and durability. The presentation of the monuments of Petra is beyond the scope of this research; however, four of the monuments will be presented in detail. These monuments are the case study tombs, where the samples and the microclimate data for this research project were collected.

6.4.1. The Bab al Siq Triclinium Tomb

The Bab al Siq Triclinium Tomb is the first carved monument that appears on the trail leading to the Siq (the main entrance to Petra) (Figure 6.2). It has a very complex classical Nabatean design, which is characterised by one large chamber flanked by two smaller ones and with carved stone benches at the back of the large chamber. The Triclinium displays the variety and the contradiction of the Nabateans' architecture (Kühlenthal 2000). The tomb was used as a room for wakes and feasts to honour the dead (Browning 1989). The Bab al Siq Tomb was carved between 40-70

A.D., a later date than the Obelisk Tomb, even though it is located almost immediately below the Obelisk Tomb (Vivekanand 1995). This monument was chosen as a sampling point for its topographic location (on the left-hand side of the Wadi), its highly deteriorated state and its accessibility for sampling.

Figure 6.2: The Bab al Siq Triclinium Tomb, Petra, Jordan (August 2003)

6.4.2. The Palace Tomb

The Palace Tomb is one of the three large façades at the eastern side of the city, known as The Royal Tombs. It is so-called because it is a copy of the design of a Roman palace (Ulama 1997, Khouri 1986, Kennedy 1925) (figure 6.3). It consists of three different levels, the first level being completely inconsistent with the upper two levels. The lower part is a rock-cut façade, while the two upper parts are built as freestanding façades (Markoe 2003). In front of the tomb is a large stage and in front of that a large courtyard. The Palace Tomb is one of the most impressive monuments in Petra, as it is located at the edge of a mountain cliff, has a complicated architectural structure and is unusual in appearance. The location of the monument at

the edge of a mountain and in a very open area as well as its highly deteriorated state were the main reasons for its selection as a sampling point. Many writers such as Taylor (2001), Vivekanand (1995) and Maqsood (1994) have suggested that the Palace Tomb housed the last Nabatean kings (King Rabbel II, 75-106 AD).

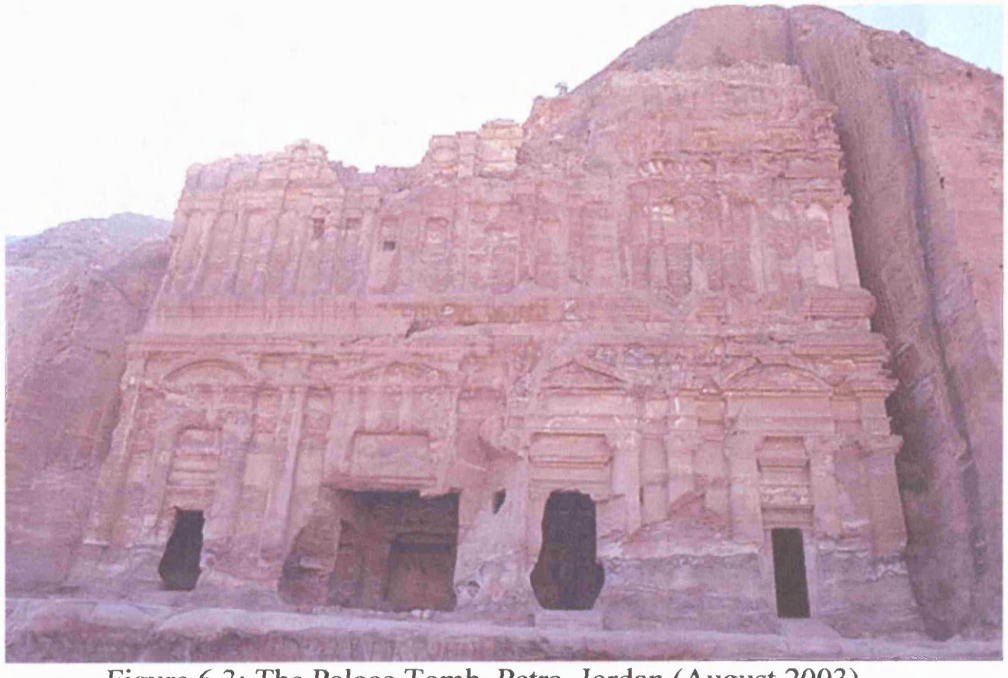

Figure 6.3: The Palace Tomb, Petra, Jordan (August 2003)

6.4.3. The Corinthian Tomb

The Corinthian Tomb (figure 6.4) is 27.5 m wide and 28 m high. It is one of the most beautiful tombs in Petra, but unfortunately has lost most of its features due to deterioration. The upper part of this tomb shows the clear influence of Hellenistic architecture, while the lower part is a typical Nabatean style. As with most of the Nabatean monuments, there is no historical record of the absolute date of its construction. Many authors such as Bourbon (1999) and Maqsood (1994) reported that this tomb was built for either Aretas II (120-110 BC) or Malchus II (40-70 AD). In contrast, Vivekananda (1995) suggested that it is more likely that Aretas III (84-62

BC) constructed the Corinthian Tomb, because its structure is similar to his famous monument in Petra, The Treasury (The Khazneh). The Corinthian Tomb is the most deteriorated carved monument of the site and thus, having a sampling profile from this monument was considered essential for this research.

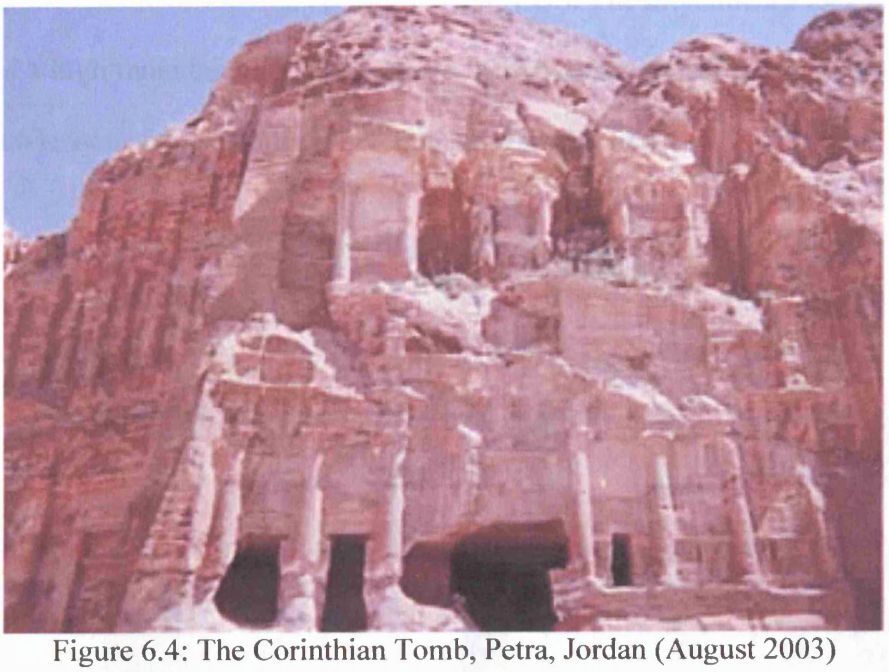

Figure 6.4: The Corinthian Tomb, Petra, Jordan (August 2003)

6.4.4. The Deir Tomb (The Monastery)

The Deir (figure 6.5) (meaning monastery in Arabic) received its name from the cave that is known as the Hermit's Cell. No one knows where this name comes from, and it may have only come into use after the Middle Ages. The journey to the Deir Tomb requires the climbing of more than 2000 steps carved into the mountain. It is the largest and most impressive façade in Petra. The façade is about 50 m wide and 45 m high (Khouri 1986). It is divided into two storeys; the lower one has a simple doorway (8 m high) with six columns topped by Nabatean capitals, the upper storey, which is better preserved, has eight columns with a conical central roof crowned with an urn. The main chamber in the Deir is huge (11.5 m by 10 m). A small part of it

was used as a meeting room (symposium), whereas the main part was a mausoleum for the king. A huge area in front of the monument was levelled, and seems to have been used for great congregations of people. There is no actual dating for the Deir. However, many writers such as Bourbon (1999), Taylor (2001) and Khouri (1986) suggest the middle of the first century (44-70 A.D.). The monument's location on the edge of a high mountain and the presence of two different levels of stone decay are the main reasons for selecting this monument for sampling.

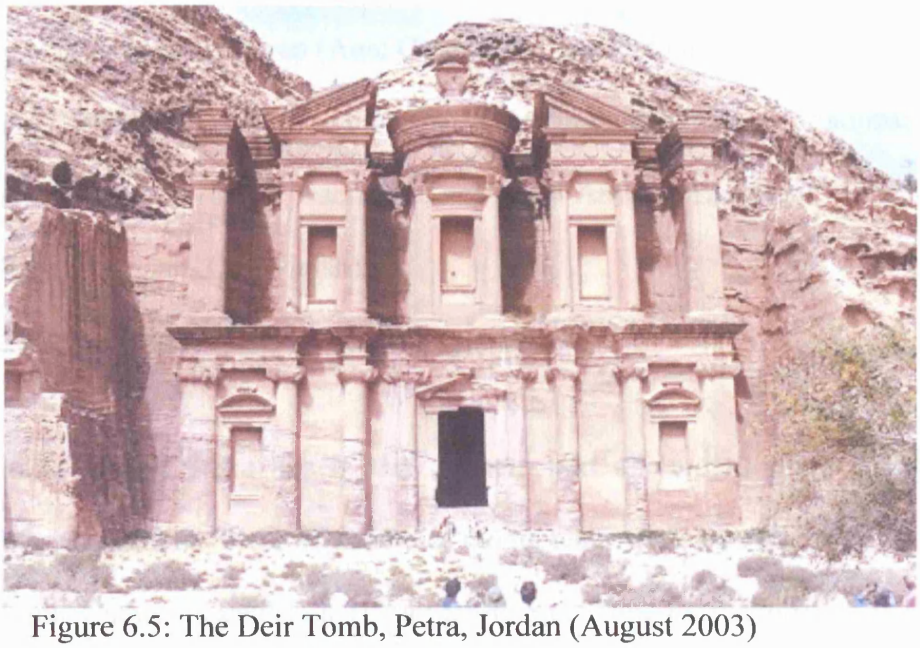

Figure 6.5: The Deir Tomb, Petra, Jordan (August 2003)

6.5. Petra, the geological background

In order to understand the mechanisms of stone deterioration at the Petra monuments, the geological and structural setting of the area should be considered. In this section the lithostratigraphy of the formation from which the Petra tombs were carved out will be discussed and evaluated. After that, the main features of the geological structure in the Petra area will be identified. Finally, the main geotechnical properties of Petra sandstone will be summarised and assessed.

6.5.1. Lithostratigraphy

Jaser and Barjous (1992), Pflüger (1995) and Heinrichs and Fitzner (2000) have studied the geology of Petra. Jaser and Bargous (1992) outlined the main chronological sequences in Petra as follows (figure 6.6), in increasing age order:

- Soil, soil cover over Pleistocene sediment (Age: Holocene - Recent)
- Alluvium and Wadi Sediments (Age: Holocene - Recent)
- Debris apron over ancient settlement (Age: Holocene - Recent)
- Pleistocene Gravel (Age: Pleistocene)
- Kurnub Sandstone Group (Age: Cretaceous Neocomian)
- Ram Sandstone Group, which includes three different formations: Disi Sandstone, Umm Ishrin Sandstone and Salib Arkosic Sandstone Formations. (Age: Cambrian- Ordovician).
- Al Bayda Porphyry Unit (Age: Pre-Cambrian).

As mentioned earlier, Petra lies in the southern part of Jordan, where Cambrian sediments are dominant. Most of the Petra monuments were carved out of the late lower - middle Cambrian sandstone (Umm Ishrin Sandstone Formation) and the early Ordovician sandstone (Disi Sandstone) (figure 6.7).

The Umm Ishrin Sandstone Formation consists predominantly of red-brown, yellow and mauve, medium to coarse-grained sandstone (Jaser and Bargous 1992)

The formation is subdivided into three main parts as follows:

- Upper Umm Ishrin: called Honeycomb Sandstone in Jaser and Bargous (1992), Ed-Deir Sandstone and Al Habis Sandstone in Pflüger's classification of 1995. This part is multicoloured, mainly medium-grained, massive sandstone (Heinrichs and Fitzner 2000).

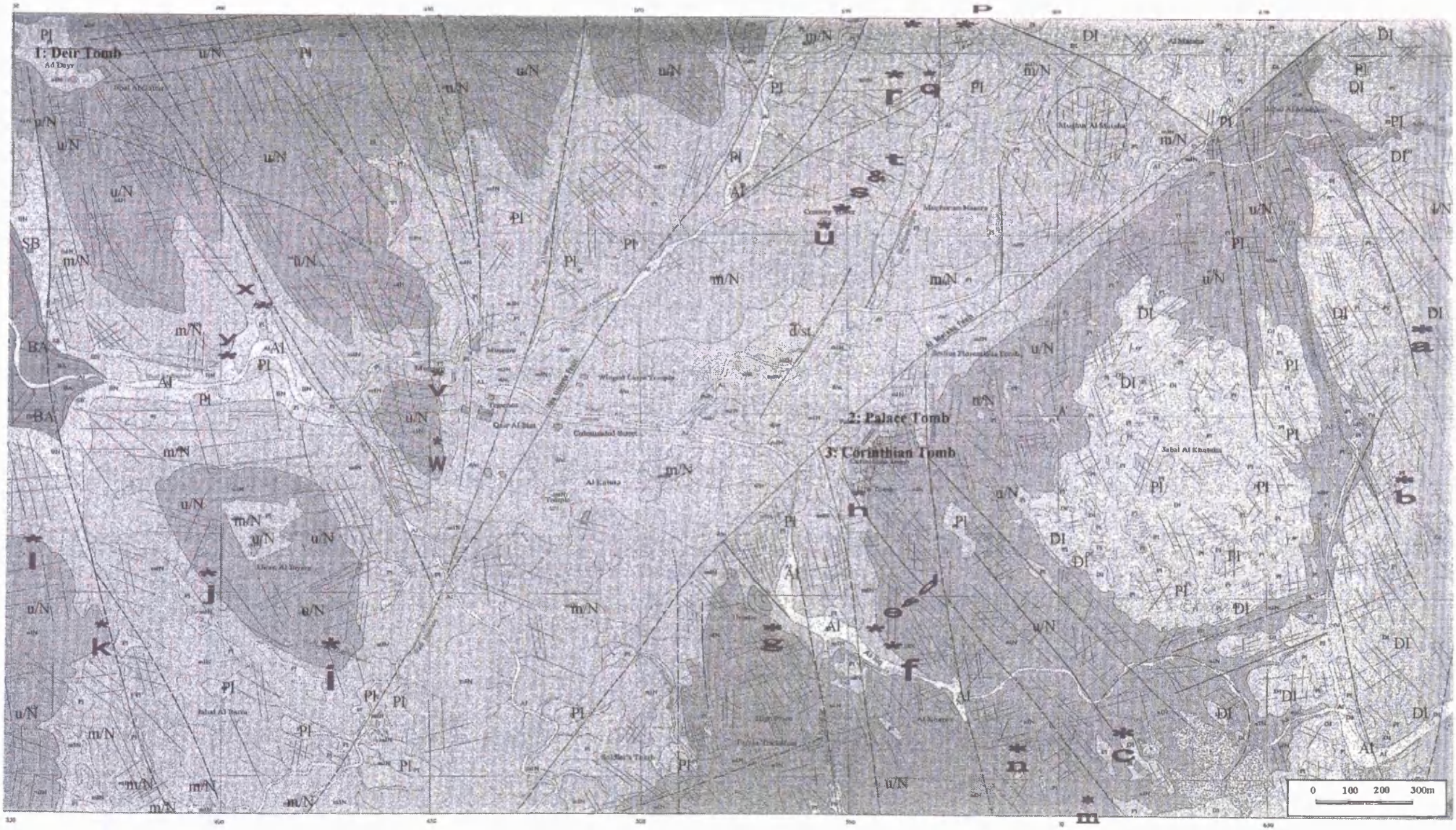

Figure 6.6: Geological map of Petra area (after Al Naddaf 2002).

Map legend: S.K/P: soil cover. Al: alluvium sediment. d/st: Debris. Pl: Pleist-Gravel. KS: Kurnub s.st. DI: Disi s.st. u/N: upper Umm Ishrin. m/N: Middle Umm Ishrin. I/N: lower Umm Ishrin s.st. SB: Salib Arkosic s.st. BA: Al Bayda porphyry.

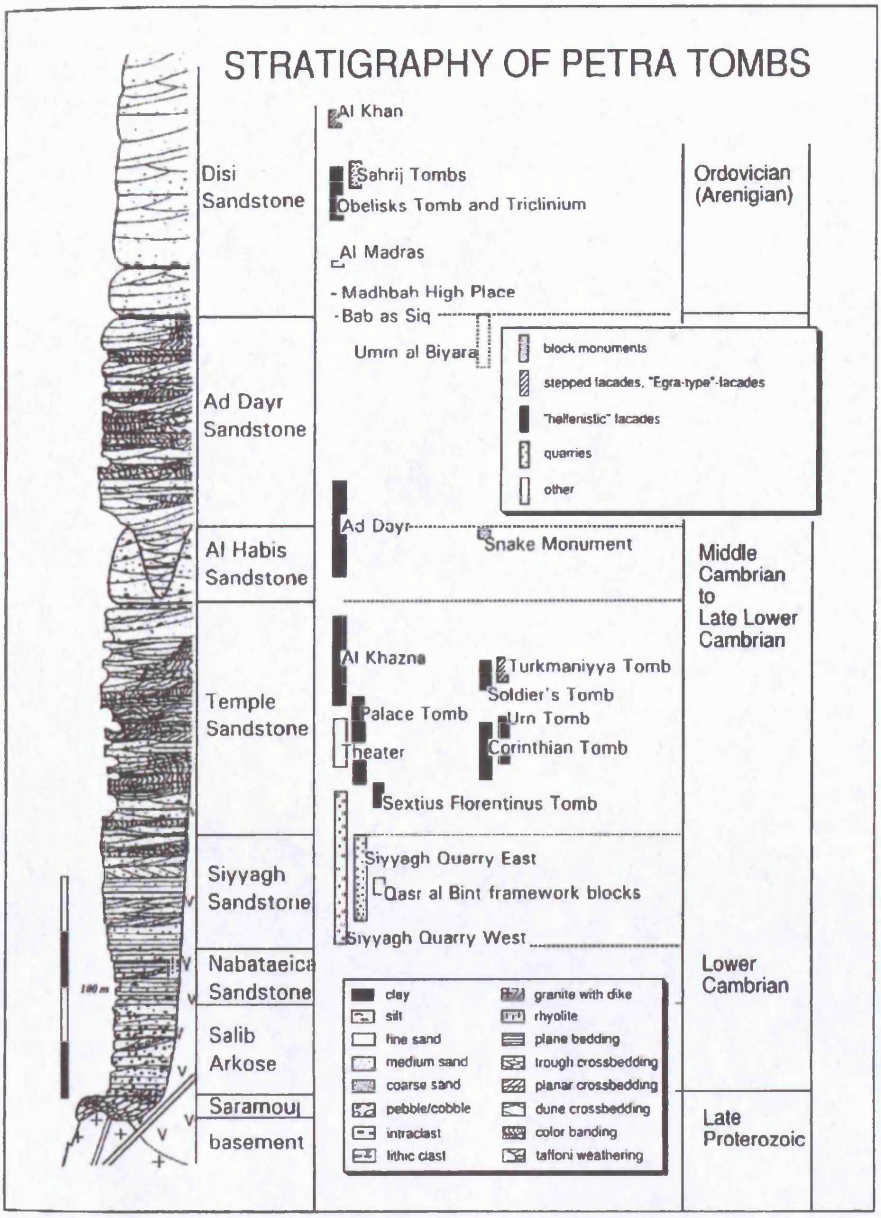

Figure 6.7: Stratigraphy of the Cambrian and Ordovician Sandstone with the most important monuments carved in it (Pflüger 1995).

Three main monuments were carved out of this part: the Deir Tomb, the Snake Monument and Umm al Biyara (Pflüger 1995).

- Middle Umm Ishrin: called Tear Sandstone in Jaser and Bargous' classification (1992), and Temple Sandstone in Pflüger's classification of 1995. This is the most important part of the Umm Ishrin unit since most of the Petra monuments were

carved out of it. For instance, Al Khazan (The Treasury), the Palace Tomb, the Theatre, the Corinthian Tomb, the Urn Tomb, the Turkmanbiyya Tomb and many other tombs were hewed from this part of the Umm Ishrin Formation. This part is multicoloured, mainly fine-grained massive sandstone. Heinrichs and Fitzner (2000) subdivided this part into six further lithotypes.

- Lower Umm Ishrin: called Smooth Sandstone in Jaser and Bargous' classification (1992), and Siyyagh and Nabateica Sandstone in Pflüger's classification of 1995. This part consists of mauve-white, medium to coarse-grained, hard, massive sandstone with scattered quartz pebbles (Jaser and Bargous 1992). Due to its hardness, both the Nabateans and the Romans used this sandstone as building and decorative material. The two main quarries in Petra, Siyyagh Quarry East and Siyyagh Quarry West as well as the framework blocks of Qasr Al Bint were cut out of this part of the Umm Ishrin Formation.

The Disi Sandstone Formation is the other formation used by the Nabateans to carve out their city. Only a small part of this formation is exposed in Petra. It crops out in the east, forming the upper part of Jabal Kuhubtha and the entrance of the Siq (Jaser and Bargous 1992). The sandstone of this formation is mainly white, medium-grained and massive. Several monuments, such as the Bab al Siq Triclinium Tomb, the Obelisk Tomb, the Sahrij Tombs and Madhbah High Place, were hewed from this formation.

6.5.2. Physical and mechanical properties of Petra sandstone

The physical and mechanical properties of porous materials have a vital role in controlling their weathering mechanisms. Therefore, this section will address the main structural, physical and chemical properties of two of the main formations in

Petra monuments (Umm Ishrin Sandstone Formation and Disi Sandstone Formation).

6.5.2.1. Mineral composition

Quartz is the main mineral in all Petra sandstone formations (see table 6.1). Generally, the Umm Ishrin Formation (both in its middle and upper parts) contains a high percentage of clay minerals (Heinrichs and Fitzner 2000 and Al Naddaf 2002). Kaolinite, the main clay mineral in Petra sandstones, is the main matrix in the Umm Ishrin Sandstone Formation. In the Disi Sandstone Formation, on the other hand, the rock fragments are the second predominant component and its matrix is mainly of kaolinite and calcite (Heinrichs and Fitzner 2000).

Two cross-sections of random samples from Umm Ishrin Sandstone Formation were made and interpreted by Graham Lott from the British Geological Society (Lott 2004) at the request of the author. The first sample was a laminated, fine-grained, quartzose sandstone in which kaolinite was the principle cement, while the second one was much coarser in grain size with a mix of carbonate and ferromagnesian cement (Lott 2004).

It can be concluded that clay minerals are a major component of the Petra rock and therefore they should be included in the evaluation of its decay mechanism. The evaluation in this research will include additional identifications of the clay mineral types present in the Petra stone and a wetting and drying test to evaluate the swelling behaviour of these clay minerals. It will also examine the effect of clay minerals in the salt damage process in porous materials by comparing the results of a salt crystallisation test of two stone samples, one with clay and one without, but with similar physical and chemical properties (chapters 7 and 11).

6.5.2.2. Grain size

The grain size of the Umm Ishrin Sandstone Formation ranges between fine grained (middle part), medium grained (upper part) and medium to coarse grained (lower part). The Disi Sandstone Formation is mainly a medium-grained sandstone (Jaser and Bargous 1992 and Heinrichs and Fitzner 2000).

Rock Properties	Disi Sandstone	Upper Umm Ishrin Sandstone	Middle Umm Ishrin Sandstone
Grain Size	Medium-grained	Medium-grained	Fine-grained
Mean Grain Size	0.305 mm	0.21 mm	0.17 mm
Maximum Grain Size	1.185 mm	0.7 mm	0.615 mm
Chemical Composition	quartz 83.1 %, rock fragments 8.4 %, clay 5.1 %, calcite 3.2 %	quartz 78.1 %, rock fragments 3 %, clay 18.6 %, other 0.2 %	quartz 78 %, rock fragments 3 %, clay 18.6 %, other 0.3 %
Total Porosity	21.3 %	19.6 %	17.4 %
Pore surface	0.14 m^2/g	0.24 m^2/g	0.36 m^2/g
Porosity % in Radii Classes	(0.001-0.01µm): 0.02, (0.01-0.1µm): 0.21, (0.1-1µm): 0.68, (1-10 µm): 1.23, (10-100 µm): 7.19, (100-1000 µm): 11.98	(0.001-0.01µm):0.05, (0.01-0.1µm): 0.44, (0.1-1µm): 1.54, (1-10 µm): 2.96, (10-100 µm): 8.64, (100-1000 µm): 6.84	(0.001-0.01µm): 0.08, (0.01-0.1µm): 0.63, (0.1-1µm): 2.72, (1-10 µm): 4.65, (10-100 µm): 7.65, (100-1000 µm): 1.69
Medium Pore Radius	115 µm	55 µm	13 µm
Bulk Density	2.19 g/cm^3	2.14 g/cm^3	2.19 g/cm^3
Sphericity	moderate to high	moderate	low to moderate
Roundness	sub-rounded to well rounded	sub-rounded to well rounded	sub-angular to rounded
Sorting	moderate	moderate	good
Fabric	grain support fabric	grain support fabric	grain support fabric

Table 6.1: Properties of Petra rocks (after Heinrichs and Fitzner 2000).

6.5.2.3. Roundness and sphericity

Roundness is the degree of abrasion of a clastic particle as shown by the sharpness of its edges and corners. It is expressed by Wadell (1932) as the ratio of the average radius of curvature of the several edges or corners of the particle to the radius of curvature of the maximum inscribed sphere (or to one-half of the nominal diameter of the particle) (Bates and Jackson 1980). The clastic grains can be divided into six classes according to their roundness (see figure 6.8)

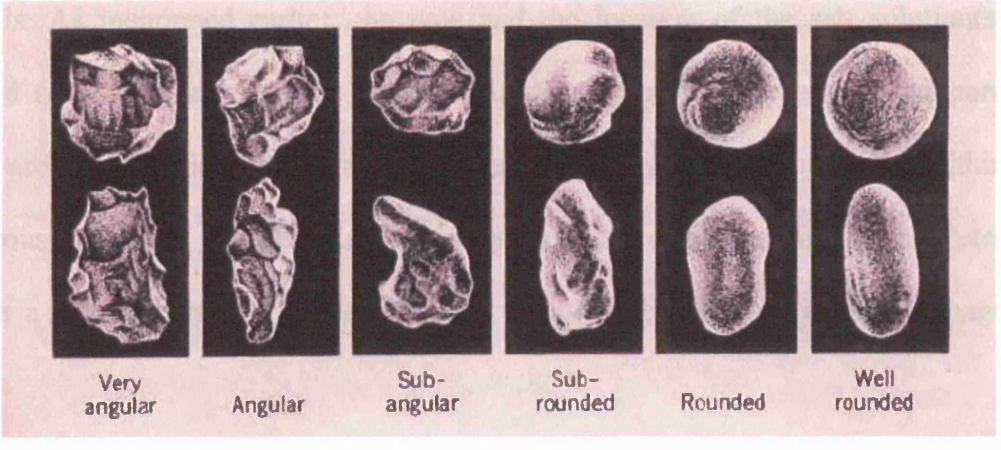

Figure 6.8: Various classes of roundness (Powers 1953)

Umm Ishrin sandstone grains range from sub-angular to rounded in the middle part, sub-rounded to well rounded in the upper part and rounded to well rounded in the lower part. Meanwhile, the grains of the Disi Sandstone Formation are mainly sub-rounded to well-rounded (Jaser and Bargous 1992, Heinrichs and Fitzner 2000).

On the other hand, sphericity is the relation between the various diameters (length, width, thickness) of a particle, specifically the degree to which the shape of a sedimentary particle approaches that of a sphere (Bates and Jackson 1980). Sphericity is usually classified into five categories: very low, low, moderate, high and very high.

The sphericity of Umm Ishrin Sandstone grains varied between low and moderate in its middle part and moderate in its lower and upper parts. The sphericity of the Disi Sandstone grains was mainly moderate to high (Heinrichs and Fitzner 2000).

6.5.2.4. Porosity

Porosity plays an important role in the deterioration processes in porous materials. It affects the water, the vapour and any other movement of solutions in porous materials. As mentioned earlier, the type and the location of the salt solution(s) involved affect the salt damage mechanism. Since porosity, pore size and pore surface are the main factors in determining the location of the salt solution(s) within the porous materials, the identification of the porosity characteristics of the Petra stone is a crucial part in the understanding of the mechanism of its salt damage process.

The porosity properties of Petra sandstone were studied by many researchers such as Jaser and Bargous (1992), Heinrichs and Fitzner (2000) and Al Naddaf (2002). This research will place more emphasis on the Heinrichs and Fitzner's study (2000), due to its detailed survey that includes all the lithotypes of each formation. (The main porosity characteristics from the above-mentioned studies are summarised in table 6.1.). In order to rate the total porosity Heinrichs and Fitzner (2000) used the following classification:

- less than 5%: very low porosity
- 5 - 10%: low porosity
- 10-15 %: moderate porosity
- 15-20%: high porosity

- more than 20%: very high porosity

The main porosity was in ranges of moderate to high in the Middle Umm Ishrin Sandstone Formation and high to very high in the Upper Umm Ishrin Sandstone Formation and the Disi Sandstone Formation.

6.5.2.5. Permeability

Jaser and Bargous (1992) examined the permeability of the different sandstone formations of Petra monuments in terms of the coefficient of permeability. They used the I.A.E.G (1979) semi-quantitative classification, which classifies porous materials into five different categories according to their permeability as follows:

- Class 1 with permeability higher than 10^{-2} m/s: Very high
- Class 2 with permeability between 10^{-2} and 10^{-4} m/s: High
- Class 3 with permeability between 10^{-4} and 10^{-5} m/s: Moderate
- Class 4 with permeability between 10^{-5} and 10^{-7} m/s: Slight
- Class 5 with permeability between 10^{-7} and 10^{-9} m/s: Very slight

Jaser and Bargous' (1992) data showed that most Petra sandstone permeability measurements ranged between slight (class 4) in Disi, Upper Umm Ishrin and Middle Umm Ishrin Sandstone and very slight (class 5) in Lower Umm Ishrin Sandstone.

6.5.3. Water system and main hydroscopic properties

6.5.3.1. Hydrological basin

According to the UNESCO survey in 1992, the regional hydrology is characterised by a strong hypsometric gradient[7]. The difference in the height between the Shara mountains (the major mountain series in the area) and Wadi Arab is around 1500 m. Consequently, the water flows westward following the slope of the land.

The map of the catchment area (figure 6.9) shows that five main Wadis pass through the Petra site, namely Wadi Mousa, Wadi al Matah, Wadi Turkmaniya, Wadi Kharobit-ibn-Jraimah and Wadi Beidha.

6.5.3.2. The main source of moisture in the Petra area

The determination of moisture sources and movement is essential in the understanding of the weathering mechanism of porous materials. Petra monuments are mainly deteriorated either in their lower part or near the old water channels and pipes. Such observations could give an indication as to the source of moisture in Petra monuments.

One of the main sources of moisture is the groundwater. According to McKenzie (1990), the water in Petra runs underground, from the main streams to the centre of the city. This source of moisture is of high importance to the current study, since it has a direct influence on the movements of soluble salts inside the monuments. Unfortunately, the hydrology of the area has not yet been fully studied (chapter 13).

[7] Hypsometric: from the Greek words 'hypsos' = height and 'metron' = measurement. In cartography it is the representation of a relief (difference in elevation) by the systematic application of sequences of colours, each representing a class of elevation above or of depth below a datum (Reitz 2005).

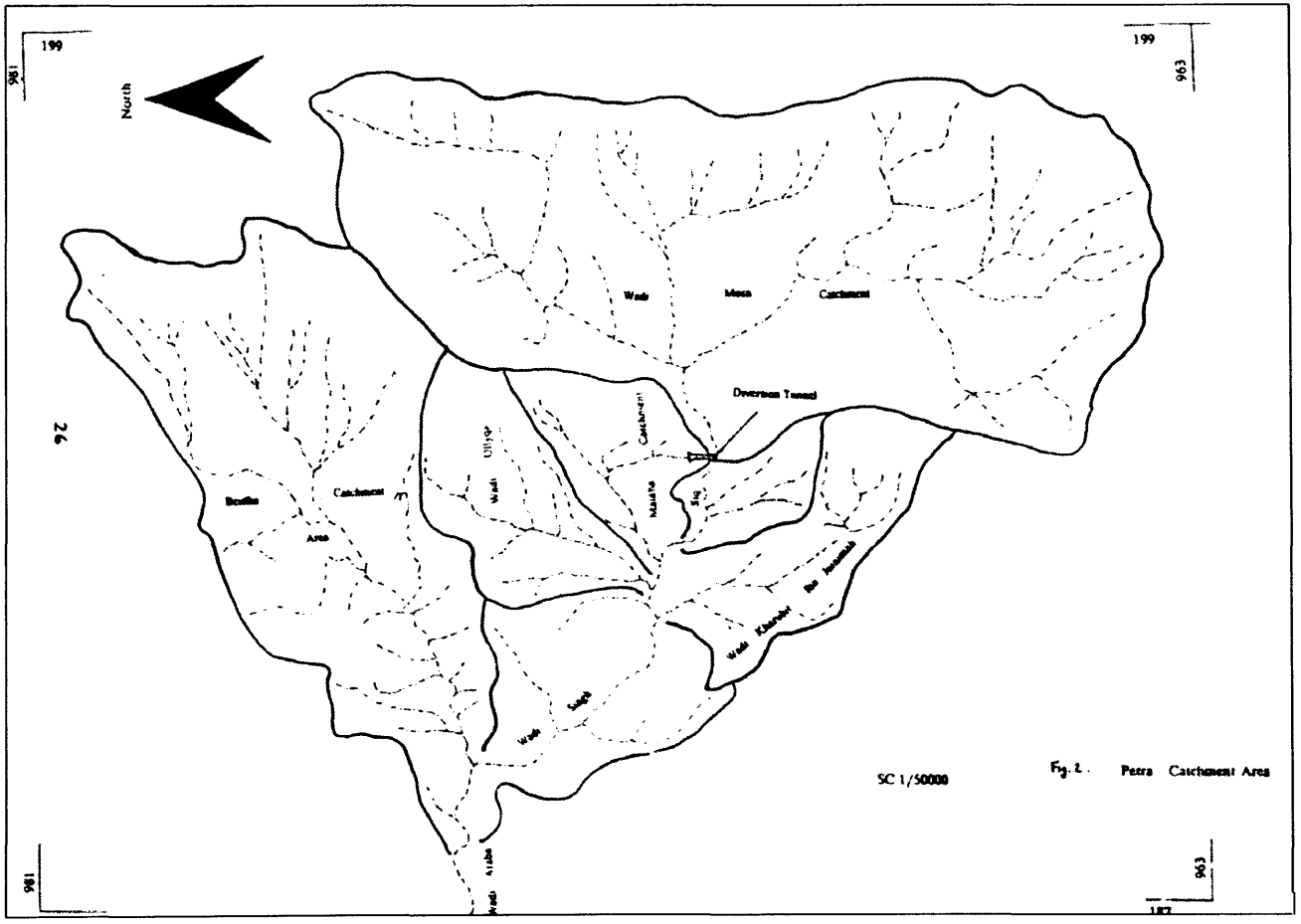

Figure 6.9: The catchment area in Petra (UNESCO report 1992)

Another source of moisture in Petra monuments is the penetration of rainwater. Despite the fact that the average rainfall in Petra is less than 150 mm/year, rainfall is a major source of moisture in the monuments for two main reasons: the Nabatean hydrological system and the period of precipitation. One of the main accomplishments of the Nabateans was the management of their water system. They developed a system to collect rainwater, using channels, pipes and underground cisterns (figure 6.10). Waterproof cement was applied to these features in antiquity to prevent water penetrating the monument façades.

6.10.a

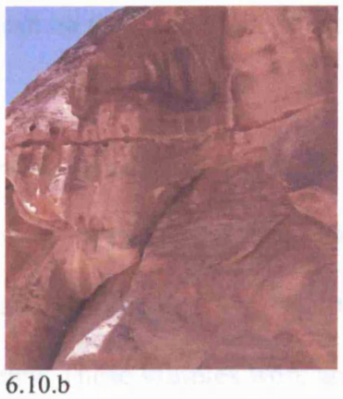

6.10.b

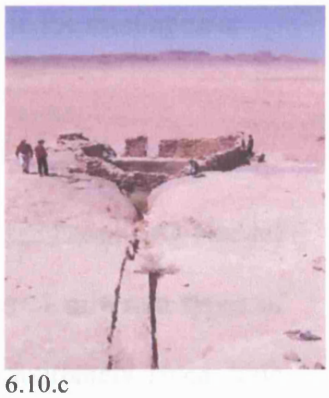

6.10.c

Figure 6.10.a: Water channel at the Siq (main entrance to Petra) (Nabataea.net 2005)
Figure 6.10.b: Water pipe at the Street of the Façades (Nabataea.net 2005)
Figure 6.10.c: Water channel at the top of a mountain near the archaeological site of Petra leading to a cistern (Nabataea.net 2005)

Unfortunately, due to lack of maintenance, to the natural hazards of the area and to the erosion of the waterproof cement, the Nabatean water system has turned into a major problem for the façades concentrating the rainwater collected from the surrounding mountains on them. The second reason for the rainwater being a major source of moisture in Petra monuments is the fact that the precipitation period is very short. Most of the rainfall takes place in 20 or less days within the year and, due to the nature of the soil in Petra as well as the high slope at the site, the rainwater

usually creates floods, which ultimately become a significant source of moisture in the monuments (UNESCO Report 1992).

Running water (springs) is another source of moisture in Petra monuments. Currently, there are two main perennial springs in Petra: one in Wadi Siyyagh and another in Wadi Abu Ollegoh (McKenzie 1990). The location of these two springs does not suggest any direct influence on the salt behaviour in the monuments. However, they can have a significant effect on the groundwater level of the area, which will ultimately have an impact on the movement of salts in the monuments.

6.5.3.3. Main hygroscopic properties of Petra sandstone

In order to study the main hygroscopic properties of Petra sandstone, Al Naddaf (2002) carried out a laboratory survey on drilled core samples of different types of sandstone from the Petra monuments. These samples were approximately 10 cm long and, in each investigation, both their surface and internal sides were examined and correlated. Three main experiments were conducted in this survey and the main outcomes can be summarised as follows:

- **Water uptake under atmospheric pressure and under vacuum**: this kind of investigation is used to find out the ratio of the pore space in a porous material, which can be filled with water and from which the saturation coefficient[8] is calculated. The water uptake in the internal zones (the water in contact with the deep zone of the sample) under atmospheric pressure ranged between 3.14 and 8.07 in weight percent, while the out-surface samples generally showed much lower values.

[8] Saturation coefficient of a rock sample (S) is the volume of water present in the pores after immersion for 24 hours under atmospheric pressure in relation to the total volume of accessible pores (Al Naddaf 2002).

The values of the water uptake under vacuum were generally higher than the water uptake under atmospheric pressure due to the quantity of micropores, which can only be filled under vacuum. The saturation coefficient values ranged between 0.3 and 0.7, indicating a wide range of pore properties in the stones.

- **Capillary Water Uptake**: Many of the Petra monuments, such as the Deir Tomb, are mostly damaged in their lower parts. This evidence can indicate that dampness rising through capillary action is the main force of moisture movement that results in such condition. Two main coefficients usually express the capillary process in porous materials: the absorption coefficient (W-value) and the water penetration coefficient (B-value). Samples are put on sponge saturated with distilled water and the increasing of the sample weight and water height level is monitored for fixed time intervals. The W-value is the slope of the relation between square root of time and weight increase, while the B-value is the slope of the relation between the square root of time and water height (Wendler and Snethlage 1989). The results of Al Naddaf's (2002) experiment showed that the Disi sandstone had the highest capillary water uptake values, while the Lower Umm Ishrin sandstone had the lowest. Moreover, the internal samples showed higher W- and B- values. This is mainly due to the superficial precipitation on the surface, which resulted in the formation of a repellent hard thin layer on the external surface, which could slow down the free movement of water through these stones. In general, the results showed a positive correlation between the water uptake W- and B- values, indicating that the pores of Petra stones are homogenous.

- **Water vapour diffusion**: In his analysis of the vapour diffusion resistance number (μ) of Petra stones, Al Naddaf (2002) concluded that Petra sandstone is partially impermeable to vapour in dry conditions (Relative Humidity less than 50 %), while

in wet conditions (RH between 50 and 100 %), surface diffusion of water vapour could take place within the micropores (less than 10 μm) (For more details see Al Naddaf 2002). These results indicated that surface diffusion is a determining factor in the water vapour transport in Petra stones, since many of these stones had a remarkable pore size distribution within the <10 μm range.

6.6. Petra, the problem

Most Petra monuments are endangered due to weathering processes (Heinrichs and Fitzner 2000). Fischer (1997) claims that more than 80 % of the sandstone façades in Petra have been eroded beyond recognition. It is worth remembering that in 1995 the World Monuments Fund inscribed Petra on its list of 100 Most Endangered Sites (Fitzner and Heinrichs 1998).

6.6.1. The weathering agents in Petra monuments

Natural processes and human activities as well as lack of maintenance in the ancient city are all involved in the weathering process. The natural causes of weathering are summarised below:

6.6.1.1. Tectonic movements (earthquakes)

According to a UNESCO Report (1992) and Jaser and Barjous (1992), Petra is located in a tectonically active region. Jaser and Barjous (1992) traced three major faults in the area (see figure 6.11), which are:

- The Al Matahan Fault (NE-SW): a regional fault and a branch of the sinistral Al Quwayra Fault system.
- The Wadi Arab Fault: the most important fault in the area (186 km long and 10 km deep) running from the Gulf of Aqaba to the Dead Sea.

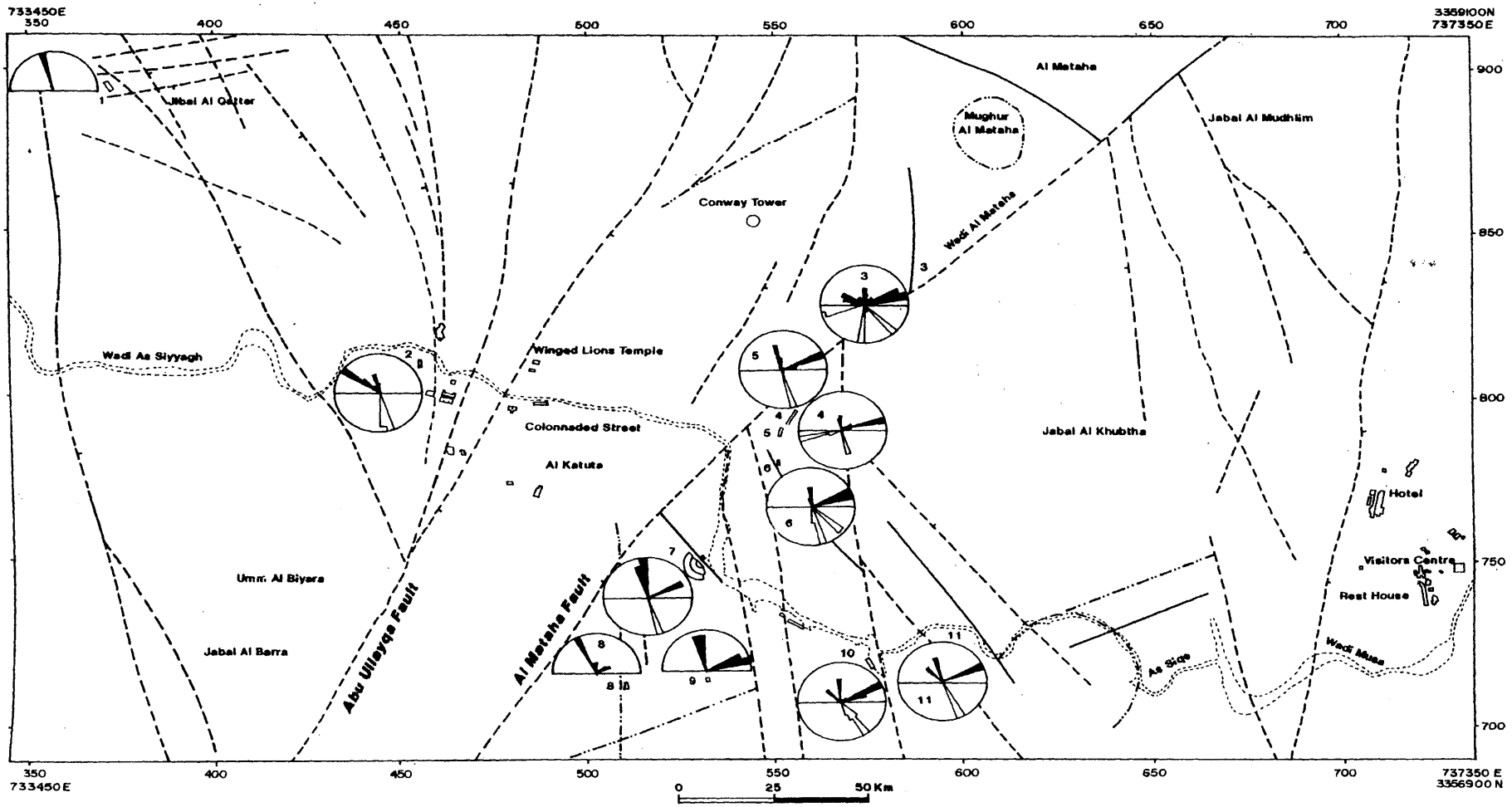

Figure 6.11: Structural Map of Petra area after (Jaser and Barjous 1992). The rose digram show the major trends of the joints system, where the northern hemisphere represents the vertical joints and the southern hemisphere represents the inclined joints.

Map legend: 1: Dier Tomb. 2: Museum area. 3. Wadi al Mataha. 4: Palace Tomb. 5. Corinthian Tomb. 6: Um Tomb area. 7: Theatre. 8: Wadi Farasa. 9: High Place area. 10: Al Khazna. 11: The Siq. Fault is indicated as: ----.

- The Abu Ullayqa Fault: run in the same direction as the Al Matahan Fault but with a downturn to the east (Al Naddaf 2002).

Due to the high seismic slip between these faults, the area has suffered a series of serious earthquakes. The monuments of Petra have suffered from a wide range of destructive earthquakes, such as the earthquake of 363 AD that destroyed most of the Theatre, and the earthquake of 747 AD that destroyed most of the monuments in the centre of the city. Generally, statistics showed that an earthquake with a magnitude above 6 on the Richter scale occurs every 100 years or so in the area of Petra (UNESCO Report 1992).

6.6.1.2. Water erosion

As mentioned earlier, the rainfall in Petra is very low, but happens in a very short period. Subsequently, water erosion is a very active agent in such an environment. The Nabatean hydrological systems prove that the Nabateans were very much aware of the water erosion problem in their area; they constructed ceramic pipes along the bedrock and the face of the monuments to protect them from the running water (figure 6.12). Moreover, the horizontal surfaces were covered with multilayered mortar to minimise the effect of running water on these features (Shaer and Aslan 2000).

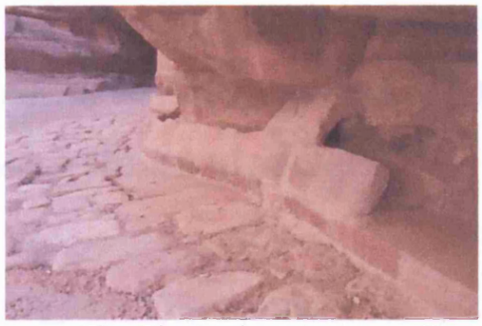

Figure 6.12: Ceramic pipes at The Siq (main entrance to Petra) (Nabataea net 2005)

Unfortunately, nowadays, the Nabatean water system is the main cause of water erosion at the site. Joints and cracks that were created by earthquakes as well as the clogging of the Nabatean water channels allow the water to attack the Petra monuments from within and from outside (Fischer 2000).

The American Centre of Oriental Research in Amman (ACOR 1997) reported that the water table in Petra is actually much higher at the dawn of the 21st century than it was at the dawn of the last millennium. The rising of the water table in the area has had a major impact on many other deterioration mechanisms such as the salt crystallisation process and the dissolution or leaching of materials (clay materials, for example). These weathering agents will be discussed separately, later in this section. In short, the water is a major factor in the deterioration process in the city of Petra through flood damage, rainwater, runoff water, and capillary action (and their subsequent effects).

6.6.1.3. Wind erosion

Wind is another important weathering agent for the Petra monuments. Not only does it cause the destruction of monuments due to wind-blown sand (UNESCO Report 1992), but it also enhances other weathering agents, such as salt crystallisation (which is the main scope of this study). The effect of the wind-blown sand is mainly restricted to the lower parts of the monuments (1-2 m height), as these parts come into contact with sand particles (UNESCO Report 1992).

6.6.1.4. Salt crystallisation process

Salt crystallisation is another, if not the major, weathering agent in Petra monuments. This study carried out a detailed survey of the salt types, locations and variations within the monuments (see chapter 8). Previous studies, such as Al Naddaf's (2002), showed that drilled samples from the Petra monuments are rich in sodium chloride and calcium sulfate, while the scraped samples were dominated by calcium sulfate.

6.6.1.5. Thermal shock

Due to wide variations in temperature, both daily and seasonally, the monuments in Petra suffer from what is known as 'thermal shock'. This kind of weathering is related to the fact that some minerals expand more than others at high temperatures and contract at low temperatures. A study of the temperature variations within a 24-hour cycle in Petra carried out by Fitzner and Heinrichs (1991) showed a difference of 20 °C in the stone temperature and a difference of 21.1 °C in the air temperature. In another study of the effect of thermal shock, Paradise (1999) concluded that, as a weathering agent, thermal shock was more effective in calcite-cemented sandstones due to the fact that calcite expands $25x10^{-6}$ μm/°C parallel to the C-axis and contracts $4.9x10^{6}$ μm/°C normal to the same axis in temperatures between 18 and 50 °C.

The evaluation of the effect of the thermal shock in the mechanical degradation of Petra monuments varies between scholars. Franchi and Pallecchi (1996) concluded that this is the main cause of stone deterioration in the Petra monuments, while others, such as a UNESCO Report (1992) considered it to be a minor cause. In accordance with this, this research supports the idea of the temperature variation having a minor effect and does not consider it to be a main cause of stone deterioration in Petra.

6.6.1.6. Biological weathering

The main biological weathering feature in Petra is the overgrowth of grass in and around the monuments. The availability of water allows vegetation to grow on some of the façades, such as the Corinthian Tomb (figure 6.4), causing considerable destruction of the façades' structure. Insect colonisation in certain monuments also enhances the damage by trapping the water under their nests and blocking its evaporation (Al Naddaf 2002). It should be stated that the impact, if any, of micro-organisms on stone decay in Petra, which could have a significant role in the biological weathering of the monuments, has not been studied.

6.6.1.7. Human activities

The human activities in the city make a considerable contribution to the deterioration of the monuments. Tourism is one of the main destructive factors. For example, Paradise (1999, 355) estimated that '20 percent of the original masonry marks were visible on the amphitheatre in 1990; however, only 5-10 remained in 1999 due to traffic pollution as well as the type of footwear tourists used at the turn of the century'. Moreover, the uncontrolled urban developments, in and around the archaeological site affect it negatively. This includes the hotel development, as well as the uncontrolled expansion of the villages around the site (Umm Sayhun and Wadi Mousa). This unrestrained development has not only impacted on the aesthetic integrity of the site, but has also increased the rate of pollution in the area.

6.6.2. Weathering forms in Petra monuments

The identification, classification, documentation and evaluation of the stone weathering forms are crucial stages prior to the start of any remedial or preventive conservation work. The field survey is the starting point, where the weathering forms are identified. The classification and documentation of these forms are the second step. Due to the many forms of stone decay, various methods are used to classify and document the damage state of the stones.

Viles *et al.* (1997) presented a very basic scheme for the classification of the visible deterioration of historical stone monuments. The scheme has three different levels: microscale (cm or less), mesoscale (cm to m) and macroscale (whole façades, entire monuments).

According to Heinrichs and Fitzner (1999), the term "weathering form" is used for stone deterioration visible at the mesoscale. The Natural Stones and Weathering Group at Aachen University of Technology presented a comprehensive monument-mapping method for in situ studies of weathering damage on natural stone (Fitzner and Heinrichs 2002). This mapping method offered a detailed documentation of all weathering forms, according to the exact type, intensity and distribution. It is based on a comprehensive classification scheme of stone weathering forms, which resulted from the detailed investigation of different monuments around the world (Fitzner, Heinrichs and Kownatzki 1995).

Bala'awi (2002) studied the general condition of the most famous monuments in Petra and indicated the main causes of deterioration in each monument. Table 6.2 summarises these investigations.

Monuments	General Condition	Main Cause of Deterioration
Obelisk Tomb	Fair to good	Winds (eolian weathering) + (rain) water + salts crystallisation
Bab al-Siq Triclinium Tomb	Fair to poor	Salts crystallisation + winds (eolian weathering) + (rain) water + horse traffic + heavy foot + the nature of the bedrock (soft sandstone)
The Siq	Fair to good	Earthquakes + winds + rain + water from the clogged water channels + tourist activity + animals by-product + floods + runoff water
The Khazneh	Fair to good	Salts crystallisation + earthquakes + tourist activity + rain
The Theatre	Fair to poor	Variation in the rock matrix chemistry and its related annual solar flux (Paradise 1999) + rain + wind + earthquakes
Palace Tomb	Poor	Salts crystallisation + runoff water earthquakes + rain + wind + sun + human activities
Corinthian Tomb	Very poor	Tectonic movements + water + wind + human + salt crystallisation + runoff water + biological agents (plants growth within the façade)
The monuments of the city centre	Poor to fair	Earthquakes + tourist activities + rain + war + wind ++
The Deir Tomb	Fair to good	Earthquakes + tourist activities + rain + war + wind + runoff water + salt crystallisation + biological agents

Table 6.2: The general condition of the most important monuments in Petra, their rate of deterioration and the main causes of decay (Bala'awi 2002)

The observation of the current research determined the main weathering forms in the case study monuments as follows:

6.6.2.1. Bab al Siq Tomb

Main weathering group	Main weathering forms	Main individual weathering forms
1. Loss of stone materials	1.1. Back weathering: uniform loss of stone material parallel to the original surface	1.1.1. Back weathering due to loss of scale
	1.2. Relief	1.2.1. Rounding 1.2.2. Alveolar weathering
2. Deposits on stones	2.1. Loose salt deposits 2.2. Biological colonisation	2.1.1. Efflorescence 2.2.1. Microbiological colonisation
3. Detachments	3.1. Flaking: detachment of small, thin stone elements parallel to the stone surface	3.1.1. Flaking
4. Fractures	4.1. Fractures	4.1.1. Cracks: fractures due to structural movement

Table 6.3: The main weathering groups, weathering forms and individual weathering forms at the Bab al Siq Triclinium Tomb, Petra-Jordan

Figure 6.13[9]: The main weathering groups, weathering forms and individual weathering forms at the Bab al Siq Triclinium Tomb, Petra, Jordan

[9] Photogrammetric elevations for the four monuments after McKenzie (1990).

6.6.2.2. Palace Tomb

Main weathering group	Main weathering forms	Main individual weathering forms
1. Loss of stone materials	1.1. Break out: loss of compact stone elements	1.1.1. Break out due to natural causes
	1.2. Spalling: breaking away due natural weathering in localised area	
	1.3. Relief	1.3.1. Rounding weathering 1.3.2. Alveolar weathering
	1.4. Washout: erosion of small parts of the monument surface due to the action of running water	
2. Deposits on stones	2.1. Loose salt deposits	2.1.1. Efflorescence
	2.2. Biological colonisation	2.2.1. Microbiological colonisation
3. Detachments	3.1. Flaking	3.1.1. Flaking
	3.2. Granular disintegration: disintegration of stone into individual grains	
	3.3. Cantour scaling: detachment of larger, platy stone elements parallel to the stone surface, not following any stone structure	3.3.1. Single scaling
4. Fractures	4.1. Fractures	4.1.1. Cracks

Table (6.4): The main weathering groups, weathering forms and individual weathering forms at the Palace Tomb, Petra, Jordan

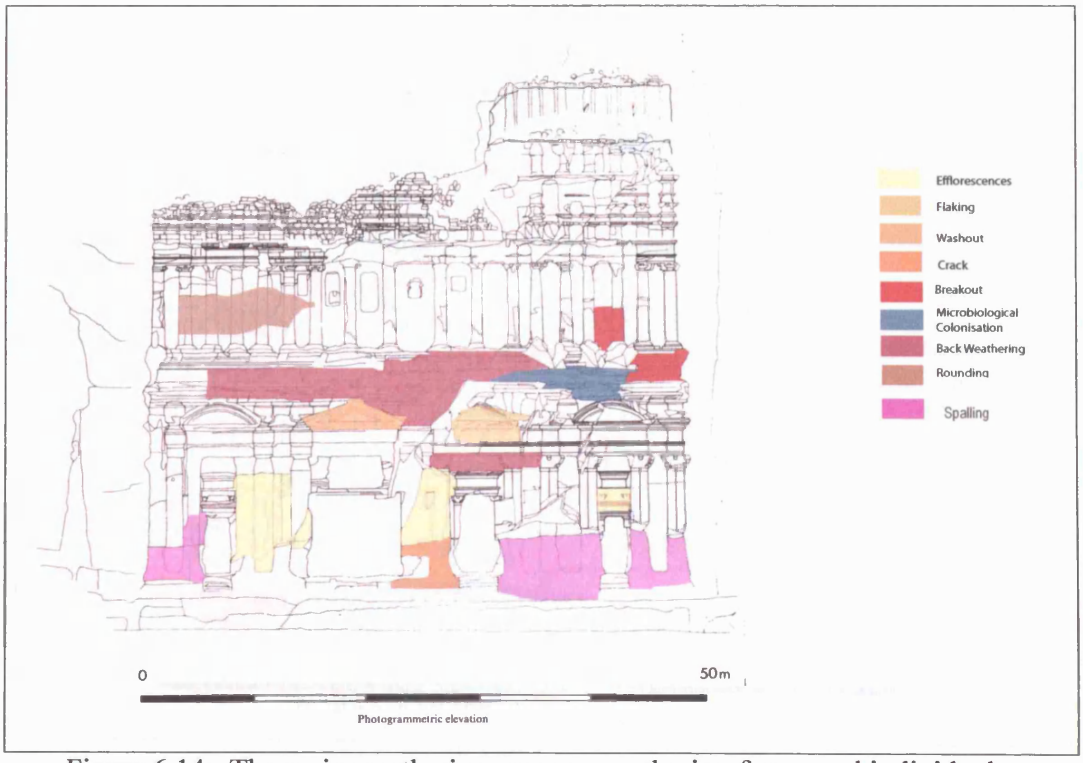

Figure 6.14: The main weathering groups, weathering forms and individual weathering forms at the Palace Tomb, Petra, Jordan

6.6.2.3. Corinthian Tomb

Main weathering	Main weathering forms	Main individual weathering
1. Loss of stone materials	1.1. Break out	1.1.1. Break out due to natural causes
	1.2. Relief	1.2.1. Rounding weathering
	1.3. Back weathering	1.3.1. Back weathering due to loss of scale
	1.4. Washout	
	1.5. Pitting: punctiform corrosion evidenced by the formation of small holes or pits, developed as a result of the selective weathering of non-homogenous stone surfaces	
2. Deposits on stones	2.1. Loose salt deposits	2.1.1. Efflorescence
	2.2. Biological colonisation	2.2.1. Colonisation of high plants
3. Detachments	3.1. Detachment of stone elements dependent on stone structure	3.1.1. Exfoliation
	3.2. Flaking	3.1.2. Flaking
	3.3. Cantour scaling	3.3.1. Single scaling
		3.3.2. Multi scaling
4. Fractures	4.1. Fractures	4.1.1. Faults
		4.1.2. Cracks

Table 6.5: The main weathering groups, weathering forms and individual weathering forms at the Corinthian Tomb, Petra, Jordan

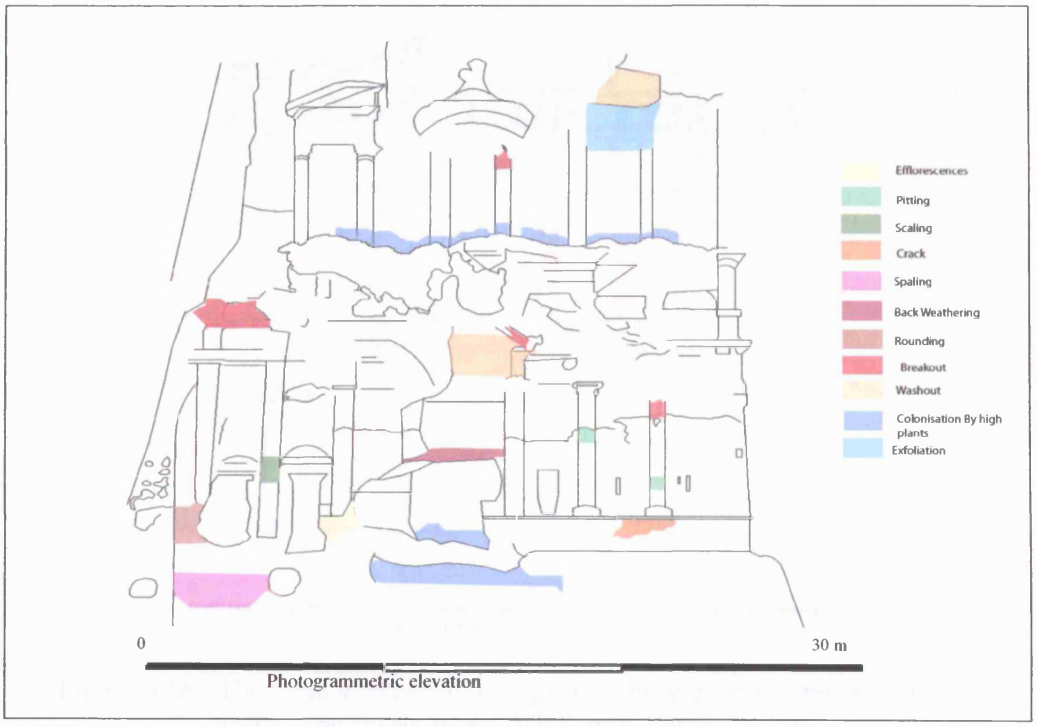

Figure 6.15: The main weathering groups, weathering forms and individual weathering forms at the Corinthian Tomb, Petra, Jordan

6.6.2.4. Deir Tomb

Main weathering group	Main weathering forms	Main individual weathering forms
1. Loss of stone materials	1.1. Break out 1.2. Back weathering 1.3. Relief 1.4. Pitting 1.5. Washout	1.1.1. Break out due to natural causes 1.2.1. Back weathering due to loss of scale 1.3.1. Rounding weathering
2. Deposits on stones	2.1. Loose salt deposits 2.2. Biological colonisation	2.1.1. Efflorescence 2.2.1. Colonisation of high plants
3. Detachments	3.1. Flaking 3.2. Cantour scaling	3.1.1. Flaking 3.2.1. Single scaling 3.2.2. Multi scaling
4. Fractures	4.1 Fractures	4.1.1. Cracks 4.1.2. Faults

Table 6.6: The main weathering groups, weathering forms and individual weathering forms at the Deir Tomb, Petra, Jordan

Figure 6.16: The main weathering groups, weathering forms and individual weathering forms at the Deir Tomb, Petra, Jordan

All in all, considering the importance of the world heritage city of Petra and the overall poor condition of its monuments, the weathering mechanisms that affect the site should be studied in order to prevent its deterioration. This study will focus on the examination of the salt crystallisation process with some emphasis on the role of wind speed in this process.

Chapter 7
Methodology

7.1. Introduction

A series of fieldwork investigations and laboratory work was undertaken in order to study the effect of wind speed in the salt crystallisation process. The methodology of these two aspects of the research will be presented in this chapter.

7.2. Fieldwork investigations methodology

The fieldwork part of the research consisted of four visits to Petra, dated as follows:

- August 2003
- January 2004
- June 2004
- April 2005

These dates represent periods within the two extreme climatic conditions on the site, namely summer (August) and winter (January), and two intermediate intervals (June and April).

In each visit, the fieldwork included the following:

- Collection of samples from the selected monuments (Bab al Siq Triclinium Tomb, Corinthian Tomb, Palace Tomb and the Deir Tomb) at four different periods (see chapter 8 for the criteria regarding the selection of these monuments). The samples were collected from different depths and different heights in order to build an overview of the salts distribution in these monuments. The samples were in powder form and a manual drill was used for their collection. The profiles of the samples from the fieldwork visits are listed in chapter 9.

- Recording of the wind speed at each sampling point at different times during the day (see chapter 8 for more details).
- Collection of environmental microclimate data (i.e. relative humidity and temperature) from two environmental loggers that were installed at two sites (the Corinthian Tomb and the Deir Tomb) in the first fieldwork visit. (Unfortunately, in the second fieldwork visit only one of the loggers was found, while the second had gone missing).
- Collection of climatic data from the meteorological station at Wadi Mousa (the nearest to the site), as a backup for the research data. These data included measurements of relative humidity, temperature and wind speed at two different times on each day, morning and afternoon.
- Photographic documentation in order to record the state of the monuments and any noticeable changes.

7.3. Laboratory work methodology

The laboratory work consisted of two main parts: the analysis of the collected samples and the laboratory experiment.

7.3.1. Fieldwork sample analysis

The cation and anion content of each sample was analysed. Before carrying out the analysis, the samples were diluted with distilled water. A sample of 0.2 ± 0.0005 g was diluted with 10 ± 0.05 ml of distilled water. The samples were filtered in order to avoid any metal debris from the drills affecting the results. The cation analysis was carried out by using an Inductively Coupled Plasma Atomic Emission Spectrometer

(ICP-AES).[10] The machine was capable of measuring the following cations: calcium, sodium, iron, aluminium, magnesium, potassium, titanium and zinc. The machine was calibrated automatically every tenth sample. The anion content was measured by using Ion Chromatography (IC)[11]. The experiment was carried out with the same diluted samples that were used for the ICP-AES in order to maintain homogeneous results. The samples were diluted further when the anion concentration exceeded the capacity of the machine reading. Standard solutions were analysed at the beginning of each test and after every tenth sample. The machine could measure the following anions: fluoride, chloride, bromide, nitrate, phosphate and sulfate. Unfortunately, this type of machine was unable to measure the carbonate and, therefore, pH measurements were taken for each analysed sample in order to give an indication of the carbonate content in the samples. Samples with high carbonate content give high pH readings (above 7) (White 1988, 134). The best way to determine the carbonate content is by titration with acid. However, the amount of the collected samples was far too small for what is required for such analysis.

7.3.2. Laboratory experiment

The experiment was designed as follows: firstly, sandstone specimens were immersed in certain types of salts for a certain period, and then the saturated specimens were monitored in an environmental chamber under controlled microenvironment conditions. The experiment started with using a single salt

[10] The Perkin Elmer Optima 3300RL Inductively Coupled Plasma Atomic Emission Spectrometer (ICP-AES) at Royal Holloway, University of London, UK, was used. The specifications of this machine are in appendix (Za).

[11] The Dionex DX 100 Ion Chromatography (IC) at Royal Holloway, University of London, UK, was used for the first and second fieldwork samples and the Dionex modular system (IC) at the Department of Earth Sciences at University College London, UK, was used for the third and fourth fieldwork samples. The specifications of these machines are in appendix (Za).

solution of sodium sulfate, since this type is well known as a major damage-causing salt. After that, the other salt mixtures that were used for the experiment were chosen according to the types of salts that were detected present at the case study sites (see chapter 9).

Both experiments (single and mixed salts) were carried out at fixed temperatures and relative humidities and under different wind speed conditions. During the sodium sulfate experiment, three tests were carried out at different temperature and relative humidity conditions. Each test was carried out at four different wind speed conditions: no wind, low, high and fluctuating wind speed (section 7.3.2.3.2. discusses the experiment procedure and conditions in detail).

Unfortunately, the microclimate generator that was used to provide controlled relative humidity conditions in the experiment chamber broke down during the preliminary tests. A new generator was bought as a replacement, but it was also faulty. After nine months of delay and with the machine still unable to be fixed, an alternative experiment was designed in order to be used from that point on to complete the laboratory work. Nevertheless, the results of this first experiment with the microclimate generator were recorded and are evaluated in chapter 11.

The second experiment was a modified version of the sodium sulfate crystallisation test that introduced the wind speed as a significant factor in the test. The procedure of this modified crystallisation test is presented in detail in the following section.

7.3.2.1. Specimen selection and preparation

- *Specimen selection:* The selection of specimens that would be used in the laboratory experiment was one of the most difficult tasks the research faced.

For reasons related to the authenticity and integrity of the site, it was impossible to extract large quantities of stone from Petra for the test purposes, and it was therefore necessary to use comparable British stone instead.

The literature review of the petrographical properties of Petra monuments concluded that Petra stones are mainly highly porous sandstones (19-20 %) with a high concentration of kaolinite (~19 %) (Jaser and Barjous 1992, Pflüger 1995 and Heinrichs and Fitzner 2000). However, Lott's (2004) study of two random sandstone specimens from Petra presented different results. While it emphasised the high percentage of kaolinite in one of the samples, it showed that the porosity was slightly lower in both samples than is stated in other reports. The current research carried out additional porosity and petrography tests on selected samples from Petra (see chapter 11).

Matching these results with sandstone specimens from the United Kingdom was a real problem, mainly because United Kingdom sandstone does not have such a high percentage of clay minerals.

Following consultation with Lott of the British Geological Survey and Yates of the Building Research Establishment, Locharbriggs sandstone was chosen. This stone has a similar porosity to Petra stone (The BRE / British Stone Stone List 2000), but

does not contain a high percentage of clay minerals. The current research carried out a porosity test for three different sandstones from Petra, Locharbriggs sandstone and Monks Park limestone[12]. Results of these tests confirmed the similarity of the total porosity between Locharbriggs and Petra sandstones. On the other hand, X-ray diffraction analysis confirmed the high percentage of clay minerals in Petra sandstone and the lack of such minerals in the Locharbriggs sandstone (see chapter 11).

In addition, in order to evaluate the role of clay minerals in the weathering process of Petra stone, a drying/wetting test was carried out on selected samples from three different tombs in Petra (Bab al Siq, Palace and Deir). The drying and wetting test procedures are presented in section 7.3.2.2.

Moreover, and due to the alteration of the laboratory experiment, Monks Park limestone was used in association with the Locharbriggs sandstone. The reason for introducing the Monks Park limestone is that this stone is commonly used as the reference stone for crystallisation tests. Since the main experiment of this research would be based on a modified crystallisation test, it was seen as necessary to introduce this stone for comparison and evaluation of the results. Therefore, 7 specimens were tested at each run (1 sample from each monument: Bab al Siq Tomb, Palace Tomb and Deir Tomb, 2 Locharbriggs sandstone specimens and 2 Monks Park limestone specimens) and the average readings of each group were recorded and evaluated. Due to the limited number of samples available from the case study

[12] Monks Park Limestone: limestone that is largely used in the BRE and ASTM standards crystallisation test to evaluate stone durability in the UK. The stone properties and composition will be discussed in chapter 11.

monuments, only one sample from each monument was used in each set of the experiment, as opposed to two UK specimens.

- *Specimen preparation*: Both Locharbriggs sandstone and Monks Park limestone samples were cut into cubes of 40 × 40 × 40 mm[13]. All Petra laboratory samples were collected from strata nearby the carved façades of the case study monuments based on geological correlation of the façades and the surrounding rock formations. A geological hammer was used to collect the samples, which resulted in samples with mainly irregular shapes but with size similar to the other laboratory samples (Locharbriggs sandstone and Monks Park limestone samples). No other attempts were made to modify the shape of Petra samples, since they were very weak and any intervention could result in loss of significant material.

7.3.2.2. Characterisation tests for the laboratory specimens

Prior to the start of the main laboratory test (crystallisation test), a group of other tests was carried out on the different laboratory specimens in order to determine and evaluate the main properties of each tested stone. These tests included petrographical study, total porosity analysis and water absorption. The information from each of these tests had an important role to play in the evaluation of the stone behaviour in the main research experiment.

Petrography

Petrographic examination is considered to be an essential analytical method for the evaluation of the durability of stone materials (Robertson 1982). It identifies the

[13] The samples were provided and cut into cubes in the Building Research Establishment, Garston, Watford, UK, with the generous help of Tim Yates

mineral composition, homogeneity, pore space types and percentages and bedding planes of the sample. All these properties have a direct effect on the salt crystallisation process; (Nicholson 2001 and Ordóñez *et al.* 1997). Therefore, two thin sections from each laboratory tested stone were prepared and examined prior to the start of any test. Furthermore, after each set of experiments, a thin section from each tested stone was prepared in order to evaluate the changes before and after each cycle.

All thin-sections were prepared without using water in order to minimise the loss of salt crystals[14]. The preparation procedure can be summarised as follows:

- Samples were cut and trimmed with a 150 mm diameter diamond saw.
- Samples were vacuum impregnated for porosity with blue dye Stuers 'Epofix' epoxy resin.
- Samples were lapped flat with 230 grit silicon carbide powder mixed with kerosene on a glass plate.
- Samples were washed in kerosene.
- Samples were lapped with 600 grit silicon carbide mixed with kerosene on a glass plate.
- Samples were washed in kerosene and dried.
- Remaining kerosene residue was removed with methanol.
- Samples were glued with 'EpoTek 301' epoxy resin to round/ashed 75mm x 26mm glass slides and left under a spring press at 70 °C for 1 hour.
- Sections were trimmed to 0.3 mm thickness using Buhler 'Petro Trim' diamond saw/grinding heel.
- Sections were lapped to 30 micron thickness on Logitech 'LP30' using 600 grit

[14] The thin sections were prepared with the kind help of Neil Holloway, Department of Geology, Royal Holloway, University of London, UK.

silicon arbide/kerosene slurry.

- Thin sections were washed with kerosene and methanol.
- Cover slips were mounted to some of the thin sections with Canada Balsam. The samples to be tested in the ESEM were left without cover slips in order to apply carbon coating.

Samples were examined using a Leica DM LP Polarised Light Microscope (specifications in appendix Za) and using magnifications of 40x and 100x. A digital camera attached to the microscope was used to record the features of the tested samples.

X-Ray Fluorescence (XRF) and X-Ray Diffraction (XRD) tests

In order to determine the chemical composition of the laboratory test specimens, two other methods were used alongside the petrography analysis: X-Ray Fluorescence (XRF) and X-ray Diffraction (XRD).

XRF: A SPECTRO X-LAP 2000 (for specifications see appendix Za) at the Institute of Archaeology, University College London with Menu-based X-LAP Pro software was used to determine the main elements in the laboratory test specimens. An 8 g portion of each sample was crushed to powder and pressed with a binding material, to produce a 32 mm diameter pellet. Each sample measurement was repeated three times.

XRD: The main minerals phases in the Petra simulation test specimens, and more importantly their clay minerals types were identified using the XRD technique. Two types of XRD analysis were carried out: the first for the whole rock and the second for a less than 2 μ fraction (clay fraction), using Phillips PW 1710 diffractometer at

the Department of Earth Sciences, University College London (see appendix Za for specifications).

For the whole rock analysis, a small portion of each sample was crushed in an agate pestle and mortar until the fragments passed a 72-mesh sieve (210 μm). Frequent sieving served to avoid over-grinding. The resultant powder was then mounted on a standard sample holder using the back-packing method. This method theoretically avoids preferred orientation. The samples were then examined in the diffractometer scanning through 2-60°.

For the clay mineral analysis (preferred orientation test), a small portion of each sample was taken and crushed in an agate pestle and mortar until the fragments passed a 72-mesh sieve (210 μm), with frequent sieving to avoid over-grinding. The powder was then put into test tubes containing distilled water, was disaggregated using an ultrasonic tank and, after the necessary settling intervals, the <2 μ fraction was removed with a pipette and recovered from suspension by centrifuging. The recovered slurry was then smeared onto two glass slips and air-dried at 20 °C. The samples were then examined in the diffractometer scanning through 2-40°.

In both analyses, the whole rock and the clay mineral analysis, the evaluation of the mineral phase was then carried out using the Philips PC-APD software.

Open porosity test

As mentioned earlier in chapter 2, porous materials are more susceptible to weathering agents than non-porous ones and the pore space affects the solutions' pathways and their interaction with surrounding materials and with the surrounding

microclimate. Accordingly, the determination and evaluation of the effective porosity in all laboratory samples were essential prior to the start of the crystallisation test.

A group of selected samples from the three case study tombs in Petra (Bal al Siq, Palace and Deir) and the sandstone and limestone samples which were used in the laboratory experiment (Locharbriggs sandstone and Monks Park limestone), were tested using the following procedures:

1- Three samples from each category were randomly chosen and labelled (T1, T2 and T3 for Bab al Siq Tomb samples, C1, C2 and C3 for Palace Tomb samples, D1, D2 and D3 for Deir Tomb samples, S1, S2 and S3 for Locharbriggs sandstone samples and L1, L2 and L3 for Monks Park limestone samples).
2- The samples were dried in the oven at 105 °C until a constant weight was reached.
3- The samples were allowed to cool in dry air in a desiccator to a temperature of 20 $\pm$2 °C.
4- The dry weight of each sample was recorded (W_d).
5- The dimensions of each sample were measured in centimetres. For Petra stones, three hemispherical samples were chosen so that their approximate dimensions could be determined. The Locharbriggs sandstone and Monks Park limestone samples were cubic in shape, and therefore easy to measure.
6- The volume of each sample was calculated.
7- The samples were put in a desiccator and then immersed in distilled water.
8- The desiccator was closed, a vacuum pump connected to the lid was switched on and the samples were kept in the water for two hours.
9- After that, the samples were taken out of the desiccator using a wet cloth and

weighed again. The saturated weight of each sample was recorded (W_s).

10- The weight of water in each sample was then calculated by subtracting the dry weight from the saturated weight.

$$W_W = W_s - W_d$$

11- The volume of water in each sample was calculated as follows:

$$V_w = \text{weight/ density}$$

Since water density equals 1g/cm^3, the water volume will equal the water weight.

12- The porosity of each sample was calculated by dividing the volume of water in each sample by its original volume and multiplying by 100 %.

$$P = (V_w/V) \times 100\ \%$$

Water absorption test

Various testing methods have been applied by different standard tests such as RILEM, ASTM and ISRM to measure water absorption. In this research, the American Society of Testing and Materials procedure (ASTM C 642-97) was used (Annual Book of ASTM Standards 2004: Volume 04.02, 334-335). In this procedure the water absorption of the laboratory tested stone after immersion and also after immersion and boiling were determined as follows:

1- Three samples from each group of the laboratory test samples (Bal al Siq, Palace, Deir, Locharbriggs sandstone and Monks Park Limestone samples) were dried in an oven at 105 °C for 24 hours. Then they were allowed to cool in a desiccator to a temperature of 20 $\pm$2 °C and the dry weight of each sample was measured.

2- The samples were dried to constant weight. The dry weight of each sample was measured (W_d).

3- Then the samples were immersed in distilled water for 48 hours, and the wet

weight of each sample was measured twice, after 24 hours and at the end of the 48-hour immersion cycle (W_w).

4- The processed samples were placed in a large glass container, covered with tap water and boiled for 5 hours.

5- The samples were allowed to cool naturally to about 20 $\pm$2 °C for about 14-hours.

6- The samples were then removed from the container with a wet cloth and the wet weight of each sample after boiling was recorded (W_{wb}).

7- The water absorption percentage was calculated as follows:

Water absorption (%) after immersion = $[(W_w-W_d)/W_d] \times 100$

Water absorption (%) after immersion and boiling = $[(W_{wb}-W_d)/W_d] \times 100$

Wetting and drying test

15 cycles of wetting and drying were carried out on three samples from each laboratory test groups (Bal al Siq, Palace, Deir, Locharbriggs sandstone and Monks Park limestone samples). This test was carried out on both Locharbriggs sandstone and Monks Park limestone samples, even though the petrographical studies illustrated that the clay minerals content in these samples is negligible, in order to have a comprehensive comparison between these stones and the Petra stone in both the wetting and drying test and the salt crystallisation test as well as in the evaluation of the clay minerals effect during the salt crystallisation test with Petra samples.

The Building Research Establishment (BRE) procedure for the wetting and drying test (Ross and Butlin 1989) was followed in this test and each cycle was carried out as follows:

1- Three samples of each laboratory test stone were immersed in distilled water for

6 hours.

2- The samples were then removed using a wet cloth and the wet weight of each samples was recorded (W_w).

3- The samples were then dried in an oven at 105 $\pm$ 2 °C for 17 hours.

4- The samples were allowed to cool naturally until they reached a temperature of around 20 $\pm$ 2 °C and the dry weight of each sample was recorded (W_d).

5- Steps 1-4 were repeated for 15 cycles.

7.3.2.3. The original experiment chamber (microclimate generator test)

In order to identify the role of the wind speed fluctuation in the salt damage process, an environmentally controlled[15] chamber was used in this laboratory experiment.

The chamber (figure 7.1) is a box (dimensions 1.5 m x 0.5 m x 0.5 m), made from 5mm thick Perspex. Its joints were sealed by dissolving the join edges with chloroform. The chamber had a double lid to reduce the fluctuation of the internal climate conditions. Moreover, in order to be able to reach every part of the chamber with a minimum impact on the internal environmental conditions, the inner lid had three portholes cut into it, each with a replaceable lid.

A thick section of aluminium honeycomb box was fitted to the left end of the chamber in an attempt to produce a uniform linear air stream inside the box.

[15] The materials for the chamber were generously donated by Alison Sawdy, and rebuilt with the help of James Hales.

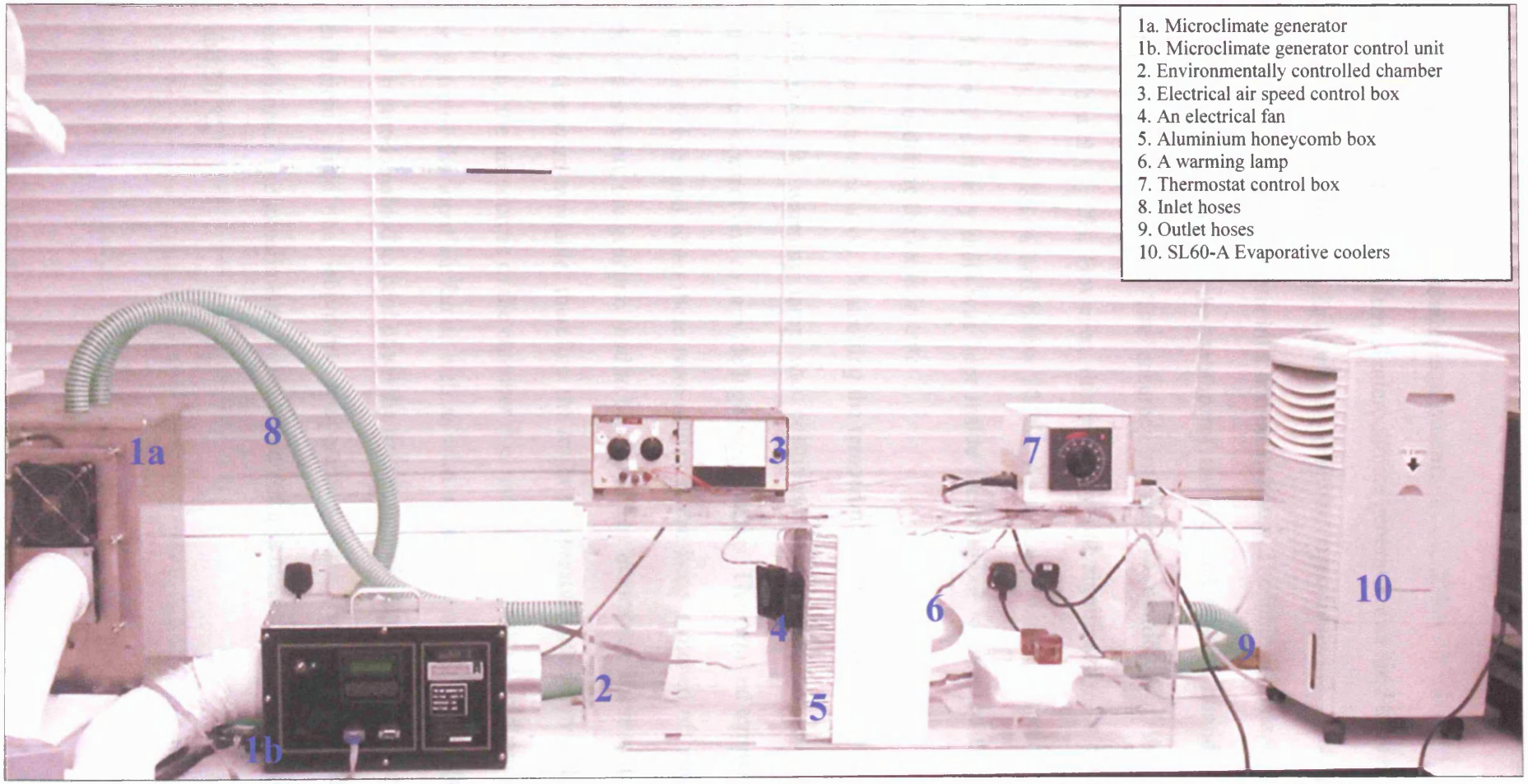

Figure 7.1: The microclimate experiment chamber

The chamber had the following equipment:

-*RH control:* A 92 MCG external microclimate generator was used to control the relative humidity (see appendix Za for the generator specifications). The generator was connected to the chamber via inlet and outlet hoses. The main advantage of the generator is its ability to maintain the stability of the required relative humidity regardless of temperature fluctuations. The accuracy of relative humidity of this machine was approximately $\pm$ 2%. However, this accuracy fell significantly for relative humidity readings above 80 % and below 30 %. As a double check, a radio-monitoring unit (Hanwell telemetry unit) was kept inside the chamber to measure the environmental conditions during the experiment.

- *Temperature control:* Controlling the temperature of the chamber was one of the main difficulties. A warming lamp was positioned in the chamber and connected to a thermostat control box to provide high temperatures. The required temperatures were set up in this box and when these were achieved, the lamp switched off automatically. On the other hand, the generator had to be placed in a laboratory where no air-conditioning facilities were available, therefore the lower temperature conditions were achieved by cooling the air sources of the chamber (i.e. the input air) with a cold water vessel placed in front of the input air fan as well as with a small air condition unit (see figure 7.1). This method enabled to cool down the temperatures by 2 or 3 °C, and these results were sufficient since the laboratory temperatures were mostly below the experiment conditions. The experiments were carried out at temperature zones ranging between 22 and 30 °C.

- *Air speed control:* The air speed was the most important environmental condition in this experiment. An electrical fan fitted to a small box inside the chamber was used to control the air speed. The electrical fan was connected to an external control box, where the air speed could be adjusted. Moreover, prior to the start of each set of experiments, a Lutron Am-4201 hand anemometer was used to measure the wind speed inside the chamber at the location where the samples would be placed.

7.3.2.3.1. Solution preparation

The sodium sulfate solution was prepared by mixing 400 g of anhydrous sodium sulfate with 1000 ml of distilled water at 20 °C.

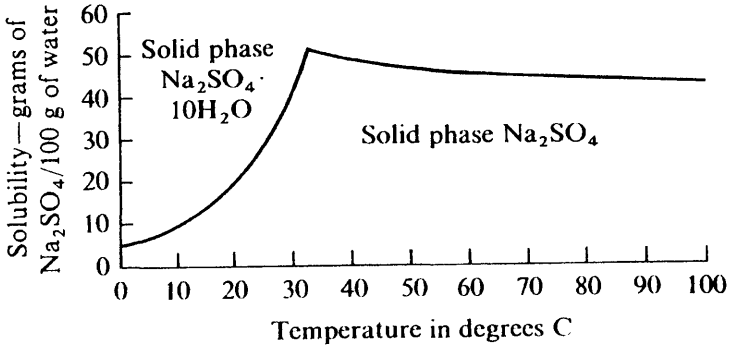

Figure 7.2: The solubility of sodium sulfate in water (Pauling 1970)

This was enough to ensure that the solution is saturated. The solubility of sodium sulfate (Na_2SO_4) at 20 °C is 19.3 g in 100 ml of distilled water (Pauling 1970), however the experimental work showed that up to 40 g of sodium sulfate (Na_2SO_4) can be dissolved in 100 ml of de-ionised water in the laboratory conditions (20 $\pm$ 2 °C). This solution mixture was the result of sets of laboratory tests that were carried out in order to identify the amount of sodium sulfate needed to prepare 1 litre of saturated sodium sulfate solution. Large quantities (20 litres) of salt solution were prepared at once, and kept in

large containers in order to achieve the highest homogeneity and reduce the variation of salt concentration during the test. The saturated solution was chosen so that the maximum damage could be obtained in the experiment.

7.3.2.3.2. Experiment procedure

The proposed method of measuring the amount of stone decay caused by salt crystallisation pressure in a controlled chamber environment was as follows:

1- The stone sample was dried in an oven at a temperature of 105 °C until a constant weight was reached.

2- The weight of the sample was recorded. This was called the sample's original dry weight (W_0).

3- The sample was immersed into salt(s) solution for 2 hours.

4- The sample was put in the environmental chamber for 24 hours under selected environmental conditions.

5- The sample was carefully taken out of the chamber and the loose debris on its outer surface was scratched off by scalpel and weighed. This weight was called loose weight (W_L).

6- The remaining sample was dried in an oven at a temperature of 105 °C until it reached a constant weight. This weight represented the remaining weight of the original dry sample (W_0) plus the weight of the salt crystals inside the sample and was called weight after crystallisation (W).

7- The salt content of the loose weight was dissolved by adding suitable solvent (deionised water) and the loose content was then dried in an oven at a temperature of 105 °C

8- The remaining particles were then weighed. This weight represented the amount of decay through salt crystallisation (W_s).

9- The amount of salts deposit on the outer surface (efflorescence) was calculated by subtracting the amount of decay (W_s) from the loose weight (W_L):

$$\text{Efflorescence } (W_E) = \text{loose weight } (W_L) - \text{amount of decay } (W_s)$$

9- The amount of salt(s) crystals inside the samples (subflorescence) was calculated by subtracting the weight of the original dry sample (W_0) from the weight of the dry sample after crystallisation (W) plus the amount of decay (W_s):

$$\text{Subflorescence } (S_{b)} = (W) + (W_s) - (W_0)$$

- The crystallisation of sodium sulfate in the environmentally controlled chamber

The first experiment was designed to investigate the crystallisation behaviour of sodium sulfate (in both hydrous and anhydrous states) in four different environmental conditions as follows:

- *First Stage*: The crystallisation of sodium sulfate in wind free conditions. In this stage three experiments were performed:

1- The formation of mirabilite crystals: RH 80 $\pm$2 % and temperature 22$\pm$2 °C. According to the equilibrium diagram (relative humidity vs. temperature) of sodium sulfate (see figure 7.3), mirabilite should crystallise immediately from the saturated solution.

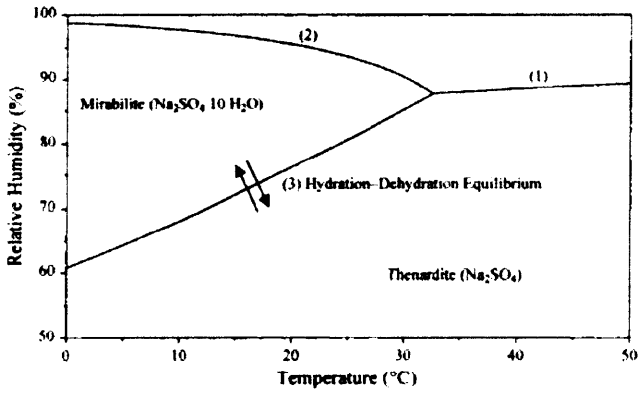

Figure 7.3: The Na_2SO_4-H_2O system from 0-50 °C (Steiger 2003)

2- The formation of thenardite crystals: RH 70 ±2 % and temperature 30 ±2 °C. Thenardite should instantly crystallise from the saturated solution of sodium sulfate without the formation of mirabilite.

3- The transition from mirabilite to thenardite: RH 75 ± 2 % and temperature 20 ± 2 °C. This condition represents the transition zone where either salt could be formed depending on the slight variations of the ambient conditions. Since the accuracy of the machine is ± 2 % for RH and ± 2 °C for temperature, the system should fluctuate between the formation of each salt (mirabilite or thenardite). At this condition the highest stone damage was expected.

By considering the three previous conditions, the experiment would cover the three different crystallisation pressure mechanisms that could be formed from the sodium sulfate salt solution under different environmental conditions.

- *Second Stage*: The tests under the three previous conditions were repeated, this time introducing a low wind speed condition.

- *Third Stage*: The tests under the same conditions were repeated, but with a high wind speed condition.
- *Fourth Stage*: The tests were repeated under fluctuated wind speed conditions. The experiment started with low wind speed for three hours, then changed to high wind speed for another three hours, and the same process was repeated throughout the duration of the drying cycle. In other words, there were four periods of low wind speed and four periods of high wind speed alternating throughout the duration of each cycle (24 hours). The 3-hour interval was chosen to simulate the wind speed trends at Petra (see chapter 8).

The second part of this experiment was designed to carry out the same tests with a saturated salt solution mixture similar to the Petra salt solution mixture. However, as the microclimate generator broke down after the completion of the first part of the test, the author was unable to continue this experiment.

A modified salt crystallisation test was designed as an alternative to the microclimate generator one in order to complete the experiment.

7.3.2.4. The modified salt crystallisation test

7.3.2.4.1. Solution preparation

Two different salt solutions were used in the modified salt crystallisation test. The first was a saturated sodium sulfate solution and the second was a saturated salt solution similar to the salts solution found at Petra (see chapter 9).

The sodium sulfate solution used in this experiment was the same as the solution used for the salt crystallisation test in the microclimate chamber. By using the saturated sodium sulfate solution in the crystallisation test the dissolution of the existing sodium sulphate that had crystallised in the stone sample at earlier cycles was avoided. This point is discussed in more detail in chapter 12.

In order to prepare a standard salt solution that could be used to represent the Petra salt mixture, two different types of salt mixtures were tested.

The first solution was prepared by considering averages of main cations and anions in all the samples (from the four tombs: Bab al Siq, Palace, Corinthian and Deir) that were collected on the four fieldwork visits. The Petra overall average of the main cations and anions was considerably low when compared to the averages of individual sites such as the Palace and Corinthian Tombs. Nevertheless, a set of laboratory experiments was carried out using this salt solution mixture (i.e. salt solution based on the overall averages of the cations and anions from the four different tombs on the four fieldwork visits).

	Ca %	Na %	Mg %	K %	Cl %	NO_3 %	SO_4 %
Petra overall averages (from the four different tombs)	31.4	18.3	2.3	48.0	16.0	48.3	35.4
Palace Tomb averages	50.3	24.6	3.6	74.6	36.3	137.8	109.1
Corinthian Tomb averages	37.3	33.9	7.3	36.2	32.0	72.8	37.7
Deir Tomb averages	40.6	17.2	1.8	2.3	8.7	5.7	74.3
Bab al Siq Triclinium Tomb averages	14.9	22.8	1.3	19.7	12.4	18.4	37.8

Table 7.1: Overall average (as weight percentage) of the main cations and anions of samples from the four case study tombs (Analysis was carried out by dissolving 0.2 g of the stone material in 10 ml of water. The cation and anion measurements were in ppm and the weight percentage was calculated from these measurements).

In order to prepare the salt mixture solution from the previous data the following steps were followed:

- The molar proportion of each cation and anion average was calculated by dividing these averages by the weight of each ion.
- Then, each molar proportion was multiplied by the ion charge, in order to obtain the charge balance between the cations and the anions.

In this case, the solution was more balanced if the calcium was taken out, suggesting that the calcium ions were bound with carbonate and bicarbonate ions which the IC is not capable of detecting. The total charge of the cations was 3.68, while the total charge of the anions is 1.97, but by eliminating the calcium from the solution, the solution charge was more balanced (2.10 the total charge of the cations and 1.97 the total charge of the anions). Therefore, the salt mixture was prepared with the consideration of the molecular weight of sodium, magnesium, potassium, chloride, nitrate and sulfate (see table 7.2).

	Ca %	Na %	Mg %	K %	Cl %	NO_3 %	SO_4 %
Overall averages	31.4	18.3	2.3	48.0	16.0	48.3	35.4
molar proportion	0.8	0.8	0.05	1.2	0.5	0.8	0.4
molar proportion X charge	1.6	0.8	0.1	1.2	0.5	0.8	0.7

Table 7.2: Molar proportion and molar proportion x charge from the overall averages of cations and anions of samples from the four case study tombs.

- The cation and anion molecular weights multiplied by the charges were then rounded (0.8 Na, 0.1 Mg, and 1.2 K, 0.5 Cl, 0.8 NO_3 and 0.8 SO_4).

- Based on these data, the salt solution mixture was prepared with the following molar proportions:
    - 0.8 sodium nitrate
    - 0.4 potassium sulfate
    - 0.4 potassium chloride
    - 0.05 magnesium chloride

Following the first results of laboratory work with this salt mixture (see chapter 11) and due to the fact that a major cation (calcium) was eliminated from the mixtures, as well as the significant variation in salt concentration from one case study to the other, this salt mixture was subsequently replaced by a more representative mixture.

The new salt mixture was based on the overall averages of cations and anions weights of samples taken from one site (Palace Tomb) during the four fieldwork visits (Table 7.3).

	Ca %	Na %	Mg %	K %	Cl %	NO_3 %	SO_4 %
1st fieldwork	40.3	14.4	2.2	8.6	17.1	12.1	90.6
2nd fieldwork	53.0	13.0	2.6	109.8	16.1	315.8	105.1
3rd fieldwork	68.9	38.5	5.4	144.0	56.4	166.6	181.2
4th fieldwork	16.5	37.8	2.8	12.3	96.1	65.2	33.3
Overall average	50.3	24.6	3.6	74.6	36.3	137.8	109.1

Table 7.3: Averages of the main cations and anions of samples from the Palace Tomb at the four fieldwork visits

The same procedures that had been previously used to prepare the first mixtures were followed (i.e. calculating the molar proportions of the main cations and anions, multiplying them with the charge and then grouping them together). As shown in table

7.4, the cation and anion charges were balanced without removing or adding any elements, which meant that this solution mixture was more balanced. The average sum of the molecular weight of each cation and anion multiplied by their charges was also balanced (5.8 for both cations and anions).

	Ca %	Na %	Mg %	K %	Cl %	NO_3 %	SO_4 %
Average weight ppm	50.25	24.58	3.59	74.55	36.27	137.84	109.09
Molar proportions: weight/atomic weight	1.26	1.07	0.15	1.91	1.02	2.22	1.13
Molar proportions X charge	2.52	1.07	0.30	1.91	1.02	2.22	2.56

Table 7.4: Molar proportions and molar proportions x charge from the overall averages of cations and anions of samples from the four case study tombs

The salt mixtures from these data could be prepared in different ways but the most important factor in this solution is the final salt mixture and not the individual salts that will be used to prepare this mixture.

In this test, the salt mixture was prepared with the following molar proportions:

- sodium chloride (1.02)
- sodium nitrate (0.05)
- calcium nitrate (1.085)
- calcium sulfate (0.35)
- potassium sulfate (0.955)
- magnesium sulfate (0.30)

- A solid mixture was made with these molar proportions and was stirred for 10 minutes in order to ensure homogeneity.

- Then a solution was prepared from the previous mixture. The preparation of the solution started by dissolving 5 g of the Palace Tomb salts mixture in 1 litre of distilled water using a magnetic stirrer. The process of adding 5 g continued until no more salt would dissolve. It was possible to dissolve only 70 g of the Palace Tomb salts mixture in 1 litre of distilled water.

7.3.2.4.2. Experiment procedure

This test was mainly based on the BRE (Building Research Establishment) test for the evaluation of stone building materials, especially limestone (Ross and Butlin 1989). The test procedure was modified and developed in order to respond to the purposes of this research. The main modifications to this test were the drying temperature and duration, the solution concentration and, more importantly, the introduction of the controlled wind speed and relative humidity to the test procedure.

The drying temperature was reduced from 103 $\pm$ 2 °C to 60 °C. This change was made in order to have a drying condition closer to that in Petra. Though one could argue that the chosen temperature was still higher than in Petra, the reason for not having the exact Petra drying conditions is the fact that under those conditions the complete drying would take a very long time, and, due to the time limit of this research, this was not possible.

In addition, the drying duration of each cycle was changed from 16 hours to 24 hours. The increase of the drying period was fundamental to balance the reduction of the drying temperature.

A saturated solution was used in this modified crystallisation test instead of the 14 % weight concentration used in the BRE. A saturated solution could produce more damage than the unsaturated ones and due to the limited time period for each set of tests (around 15 days) and the slightly low drying temperature, this type of solution was considered more suitable for this experiment. Therefore, a saturated solution of sodium sulfate and a saturated solution of Petra salt mixture were used in this test.

Furthermore, as the study and evaluation of the wind speed factor is a crucial part of this study, it was essential to introduce this factor into the crystallisation test. The wind speed was controlled using an electrical air pump that was connected to the vacuum oven by a plastic tube (this equipment and its function are discussed in detail in the following section). The experiment was carried out at three different wind speed conditions: low, high and fluctuating wind speed.

Moreover, previous studies of the salt crystallisation test (as reported in Price 1978) showed that the variations in the behaviour of different types of stone were much clearer, when a tray of water was placed in the drying oven. However, no explanation was given for such a phenomenon. Consequently, introducing a controlled relative humidity was necessary not only in order to compare the test results at different relative humidity conditions, but also to reduce the variables of the testing conditions, thereby increasing the accuracy of the test. The test was carried out under low and high relative humidity conditions. The relative humidity was introduced and controlled by connecting the air pump to gas wash bottles filled with water and placed in a controlled water bath

(see the experiment equipment section). For the high relative humidity conditions, the water bath was adjusted at 70 °C, while for the low relative humidity conditions the air pump was connected directly to the vacuum oven without passing through the gas wash bottles.

7.3.2.4.3. Equipment[16]

The modified salt crystallisation test chamber (figure 7.4) was composed of the following equipment:

- Vacuum Oven: Gallenkamp vacuum oven with temperature control range between 0 and 210 °C. The oven was not operated under the vacuum pump, but its outlets have been used for the wind control. The oven had two outlets, one for the incoming air, and one for the return air. Inside the oven, the two holes (incoming and return holes) were too close to each other and, in order to create better air circulation inside the oven, a plastic tube (10 cm) was attached to the incoming air hole and fixed at a 45° angle. This not only enhanced the internal air circulation, but also increased the wind speed and created direct wind, which is very similar to the wind speed conditions in Petra.

[16] For the specification of the simulation test see appendix Za.

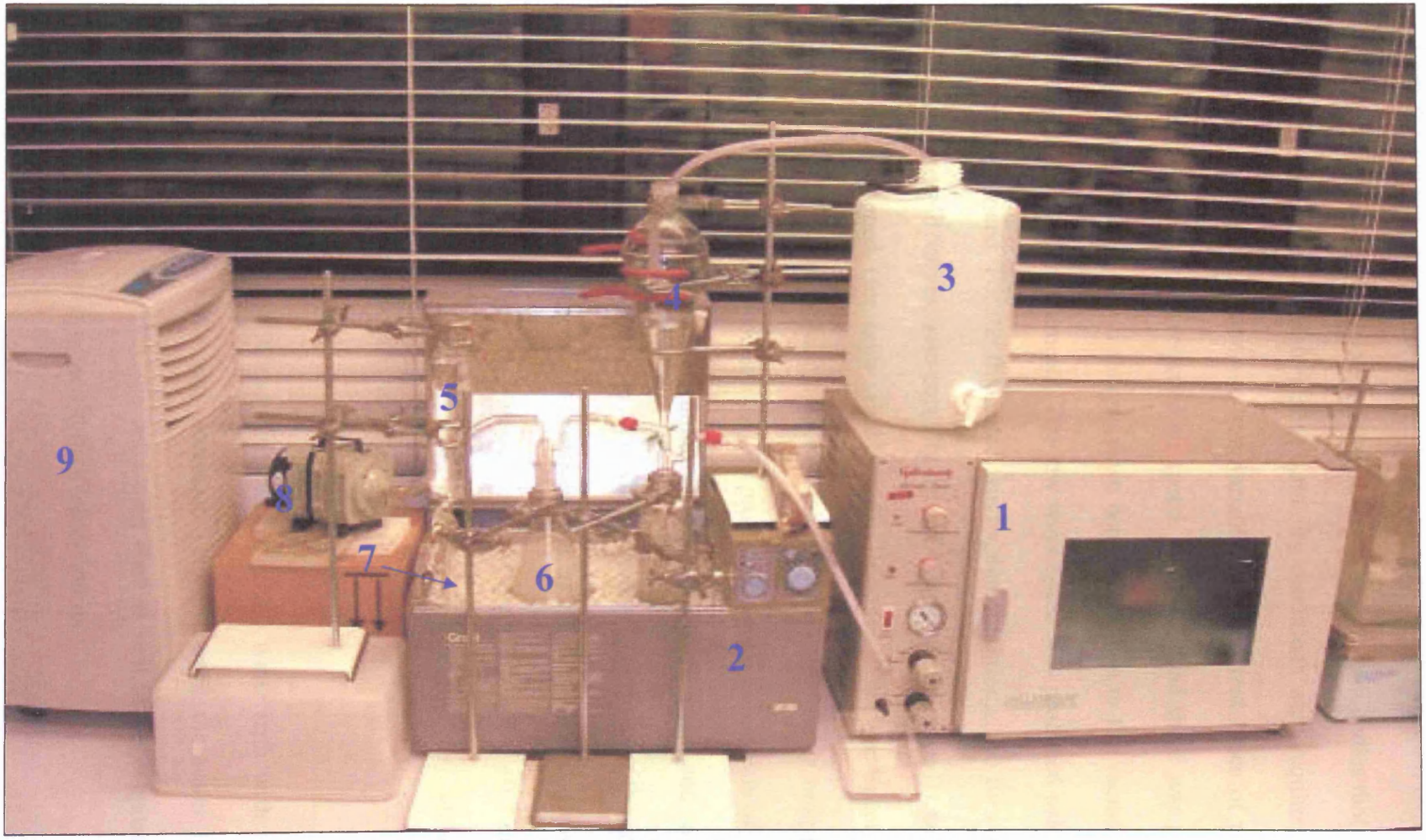

Figure 7.4: The modified salt crystallisation test chamber

Figure index: 1. Vacuum oven 2. Controlled temperature water bath 3. Water supplier container 4. Liquid separation funnel 5. 1L Gas wash bottle 6. 3L Gas wash bottle 7. Polyethylene balls 8. Electrical air pump 9. Evaporative coolers

- Electrical Air Pump: (Hailea ACO-328): An air compressor capable of pumping 75 litres per minute. The pump was connected directly to the vacuum oven, when low relative humidity conditions were applied, or to the gas wash bottles that were placed in the water bath, when high relative humidity conditions were required. Since the air speed through the pump was not variable, two different types of plastic tubes were used to produce the required air speed. The high wind speed was produced by connecting the air pump to the gas wash bottles and then to the vacuum oven to a plastic tube of 0.8 cm diameter. The low wind speed was produced using the same tube but perforated. For the fluctuated wind speed conditions, two two-way general purpose solenoid valves, one partially closed (for low wind speed) and the other completely opened (for high wind speed) (Burkert: ½ in, see specifications in appendix Za), were connected to two multifunction time delay relays (Crouzet: TAR1: specifications in appendix Z), to produce fluctuation intervals of three hours of low wind speed followed by three hours of high wind speed, and so on for the duration of each cycle (see figure 7.5). The average measurement at the points where the specimens were placed was carried out using the Lutron Am-4201 hand anemometer in all different tests conditions. The reading was 3.6 $\pm$0.2 m/s for high air speed conditions, 0.6 $\pm$0.2 m/s for low air speed conditions, while the same figures alternated for the fluctuated wind speed conditions.

- Temperature Controlled Water Bath: Grant (W28) water bath with temperature control sensors. The water bath thermostat could control the water temperature between 0-100 °C. Polyethylene balls were used to reduce the evaporation of the water when the machine operated at high temperatures.

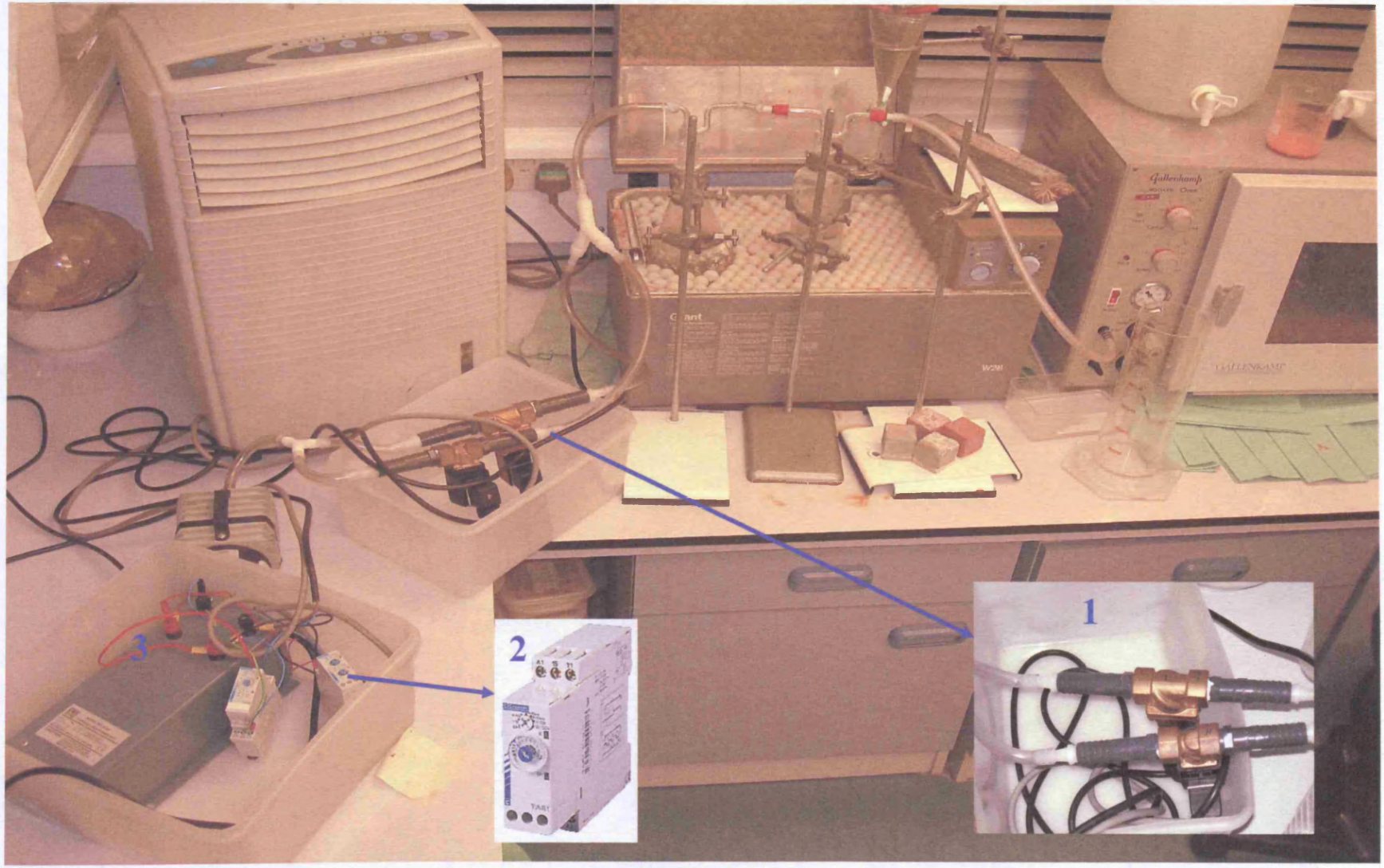

Figure 7.5: The modified salt crystallisation test chamber during fluctuating wind speed runs

Figure index: 1. Two-way general purpose solenoid valves 2. Multifunction time delays 3. Electrical power supply

- Gas wash bottles: Two gas wash bottles, of 3 litres and 1 litre volume, were used to create high relative humidity conditions. The bottles were filled with water, connected to each other and placed in the water bath. The 3-litre bottle was connected to the air pump, while the 1-litre bottle was connected to the vacuum oven (see figure 7.4). Having both bottles in the design was to ensure the application of high relative humidity conditions when needed, and because most of the moisture would be picked up from the first bottle, this needed to be larger.

- SL60-A Evaporative Coolers: this multifunction unit (Cooler/Humidifier/Fan/Air Cleaner) was used to cool down the ambient conditions. As the test was running continuously for a period of 16 days for each set of the experiment, it was important to keep the equipment at low temperatures to avoid damage to the equipment.

- Water supplier: a 10-litre water container was connected to a 1-litre liquid separation funnel with a plastic tube (see figure 7.4) in order to create a siphon effect between them. In this case, the liquid separation funnel provided the water bath with drops of water, while the big water container provided a controlled and consistent supply of water to the liquid separation funnel. A second liquid separation funnel (500 ml) was used to provide extra supply of water to the bath when needed.

- Tinytag Extra Logger: A water-proof dual logger to record both relative humidity and temperature was placed inside the vacuum oven. The temperature range of this logger is between -30 to 85 °C, and the relative humidity range between 0-100 %.

Chapter 8
Petra: The Microclimate Data

8.1. Introduction

The activation of salt damage is highly controlled by the surrounding environmental conditions. Relative humidity, temperature, solar radiation and air speed are the main factors with a direct influence on the salt damage process. Therefore, the collection of climatic data from the case study sites was an essential part of the current research.

The methodologies of climatic monitoring programmes vary considerably in the literatures of cultural heritage studies. Some scholars such as Tricio and Viloria (2002) and Camuffo and Bernadi (1995) have undertaken a very detailed microclimate investigation in evaluating the effect of the environmental parameters on historical buildings, while others, such as Al Naddaf (2004), preferred a basic monitoring programme in evaluating the stone weathering behaviour. The detailed monitoring approach was considered more appropriate for the current research because it would provide a more systematic way of evaluating the salt damage process at different locations by comparing the microclimate data of each location with its salts content. This is unlike basic monitoring programmes where the variation of the microclimate conditions between one location and another would not be considered. Therefore, it was decided to use two climatic monitoring programmes in order to evaluate the microclimate of the studied areas. The first was a spot reading monitoring programme at each site during each fieldwork visit. This included spot readings of the temperature, relative humidity and wind speed. The second monitoring programme involved a more

detailed recording of the temperature and the relative humidity over a period of 18 months (August 2003- April 2005), using Tinytag loggers.

Unfortunately, data loggers were not available for the recording of the wind speed and, therefore, spot readings were the basis for the evaluation of this environmental parameter. During each fieldwork visit to the case study locations, a group of detailed wind speed spot readings were taken.

In the first fieldwork visit, the wind speed readings were taken in front of each of the three case study monuments (Bab al Siq, Palace and Deir tombs) and on an average frequency of one reading every 15 minutes for six days. A more detailed recording of the wind speed was undertaken during the other three fieldwork visits, during which the wind speed readings were taken from above each sampling point. Five readings were taken every hour for 13 hours above each sampling point (the maximum, minimum and average readings for each visit are presented in appendices D, G and K).

In addition, the climatic data records for the period between August 2003 and April 2005 were collected from the nearest meteorological station (Wadi Mousa, approximately 7 km from the site). These data included two daily readings for the temperature and relative humidity (one in the morning and one in the late afternoon) and one daily reading for the wind speed and rainfall.

8.2. First fieldwork visit (August 2003)

This first fieldwork trip to the site took place between the 1st and 10th of August 2003. During this visit, two Gemini Tinytag Plus (TGP-1500) loggers (figure 8.1) were installed inside two monuments: the Deir Tomb and the Corinthian Tomb.

The reason for choosing this type of logger was mainly because they are designed for tough locations and they are ideal for external environmental monitoring due to their waterproofing and large detection range. The temperature ranges of these loggers are between -30 and 50° C, and the relative humidity ranges are from 0 to 100%. Also, these loggers are capable of recording more than 15,000 readings, which means that they can run unattended for more than 20 months if set up to record one reading every hour (Gemini Data Loggers 2005).

Figure 8.1: Tinytag Plus logger (TGP-1500) (Gemini Data Loggers, 2005)
(For specifications see appendix Za)

The selection of the monuments where the loggers were installed was based on the fact that these monuments are located at two quite different geographical areas (the first one is in a sheltered and high level area, while the second is at an open and low-level location).

In order to have an initial profile during the first fieldwork visit, spot readings for temperature, relative humidity and wind speed were taken near three of the case study monuments. The relative humidity and temperature were recorded using a Digitron SP3R temperature and relative humidity recorder (figure 8.2). The temperature range of this recorder is between -20 and 60 °C with 0.1 °C resolution, while the relative humidity range is between 0 to 90 % with 1 % resolution. The recorder accuracy for temperature was ±1 °C for temperatures between 0-40 °C and ±2 °C for temperatures outside this range, while the accuracy for relative humidity was ±5 % for relative humidity between 40-80 %, and ±7 % for relative humidity outside this range. These features were suitable for the purpose of getting an initial profile of the temperature and relative humidity at the selected monuments.

Figure 8.2: The SP3R temperature and relative humidity recorder
(For specifications see appendix Za)

A Lutron hand anemometer (Am-4201) was used to measure the wind speed at the case study monuments (figure 8.3). This portable anemometer provides fast, accurate readings with digital readability and the convenience of a remote sensor. It also has a

multi-function for air flow measurement: m/s, km/h, ft/min and knots. In this research the airflow measurements were recorded in m/s.

Figure 8.3: The Lutron Am-4201 hand anemometer (Ginza Marketing 2005)
(For specifications see appendix Za)

8.2.1. Relative humidity and temperature spot readings

For three consecutive days, spot readings of relative humidity and temperature were recorded every 5 minutes at three different locations. The first set was taken in front of the Bab al Siq Triclinium Tomb (Tables A1, A2: Appendix A), the second in front of the Palace Tomb (Tables A4, A5: Appendix A), and the last in front of the Deir Tomb (Tables A7, A8: Appendix A).

Generally, a day could be divided into three intervals (see figure 8.4). In the first interval (07.40 to 09.30) the temperature was quite low, with an average of 24.4, 24.7 and 22.3 °C, at Bab al Siq Triclinium, Palace and Deir Tombs respectively. The relative humidity was slightly high for this area, with an average of 29.9, 26.9 and 29.1 % respectively.

It is worth mentioning that the terms 'high' and 'low' used in this section are comparative and not absolute values.

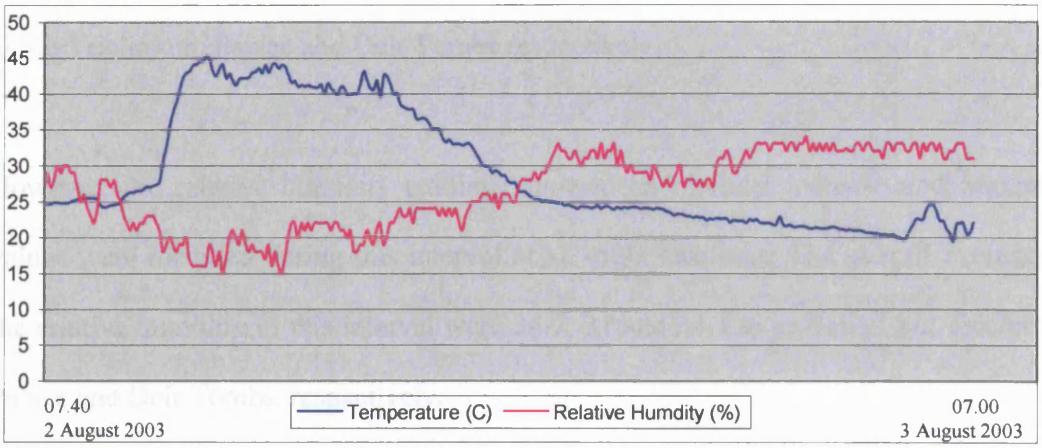

Figure 8.4: Temperature and relative humidity spot readings.
First fieldwork visit. Location: Palace Tomb.

After 9.30am the temperature increased gradually until it reached its maximum during the mid-day hours.

Conversely, the relative humidity decreased gradually until it reached its minimum during this interval. On this particular day, the average temperatures of the second interval (09.35-19.30) were 33.5, 37.6 and 35.5 °C and the average relative humidity readings were 20.7, 21.1 and 19.7 % at Bab al Siq Triclinium, Palace and Deir Tombs respectively.

The general trend of this interval (the day-time interval) was a considerable gradual increase in temperature and noticeable fluctuations in relative humidity.

The temperature readings of the third interval (19.35-07.00 next day, namely the night-time interval) at the three locations showed a gradual decrease throughout the night. During this interval, the average temperature readings were 18.8, 22 and 20.4 °C at Bab al Siq Triclinium, Palace and Deir Tombs respectively.

However, the relative humidity readings showed an obvious increase and maximum values were recorded during this interval at all three locations. The overall averages of the relative humidity in this interval were 34.7, 31 and 34.1 % at Bab al Siq Triclinium, Palace and Deir Tombs, respectively.

8.2.2. Wind speed spot readings

During the day-time hours, the wind speed values were recorded in front of the same monuments where temperature and relative humidity readings were taken and during the night hours at the Nabateans Hotel (10 minutes walking distance from the archaeological site). The readings were taken on three successive days, each day from a different site. Spot readings were taken every 15 minutes (Tables A1, A3, A4, A6, A7 and A9: Appendix A and figure 8.5).

Generally, the airflow measurements showed a wide fluctuation at the three locations (see figure 8.5 for example). For instance, the wind speed at the Palace Tomb was very slow between 07.40 and 10.00 with an average of 0.2 m/s. Between 10.15 and 12.45, the wind speed values increased slightly with an average of 0.7 m/s. Between 13.00 and

17.45 the wind speed continued to increase with an average of 1.9 m/s. Such fluctuations remained the main trend of the wind speed throughout the day.

The data from the three other sites showed a very similar trend in the wind speed, with slightly lower wind speed at the Deir Tomb, and the lowest overall wind speed measurement at the Bab al Siq Triclinium Tomb. In addition, the fluctuation rates at the Deir Tomb and Bab al Siq Triclinium Tomb were considerably lower than those at the Palace Tomb.

During the night-time, the wind speed increased significantly between 20.00 and 05.00 of the next day with averages of about 3 m/s. Generally, the wind speed reached its maximum during the early hours of the day (between 03.00 and 05.00). Then, between 05.15 and 07.00, the wind speed started to decrease gradually with an average of approximately 0.9-1.0 m/s.

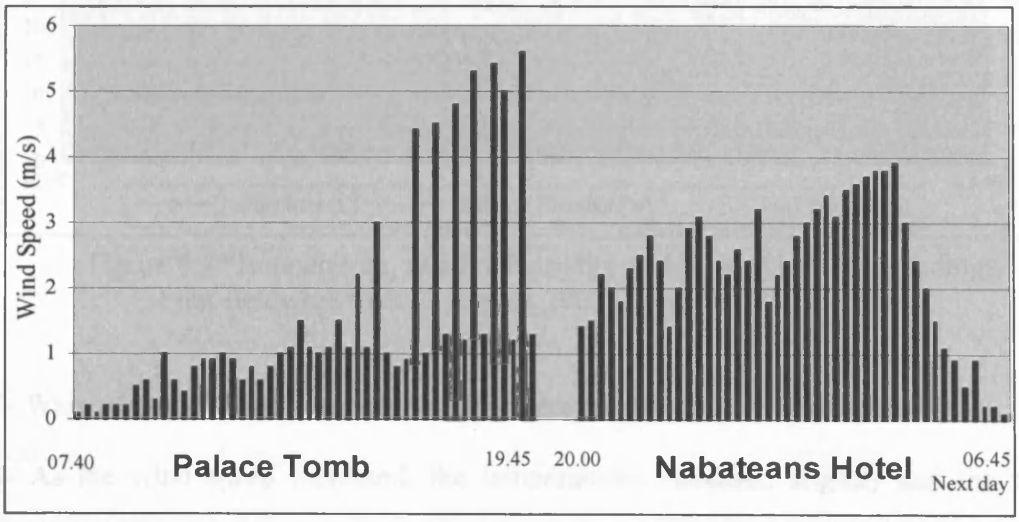

Figure 8.5: Wind speed spot readings. First fieldwork visit (2-3 August 2003). Locations: Palace Tomb and Nabateans Hotel.

8.2.3. Main outcomes from the spot readings of the first fieldwork visit

By comparing all data from the first fieldwork visit, the following points were made:

1- As the temperature increased the relativity humidity decreased and vice versa (figures 8.6 and 8.7).

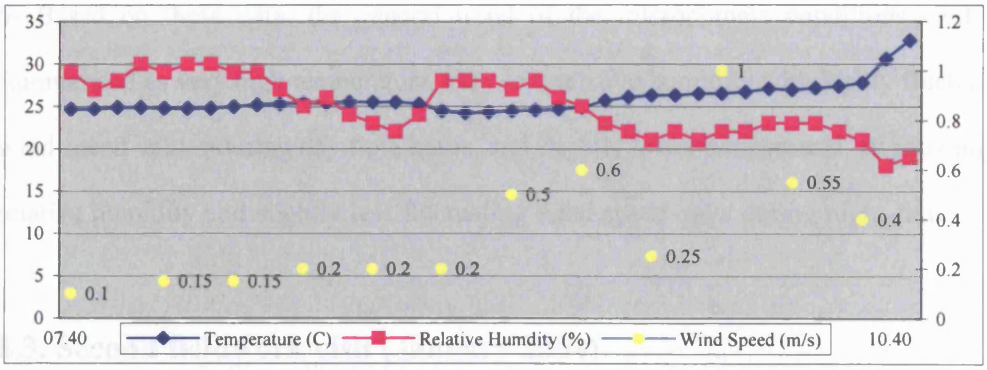

Figure 8.6: Temperature, relative humidity and wind speed spot readings. First fieldwork visit (1 August 2003). Location: Palace Tomb.

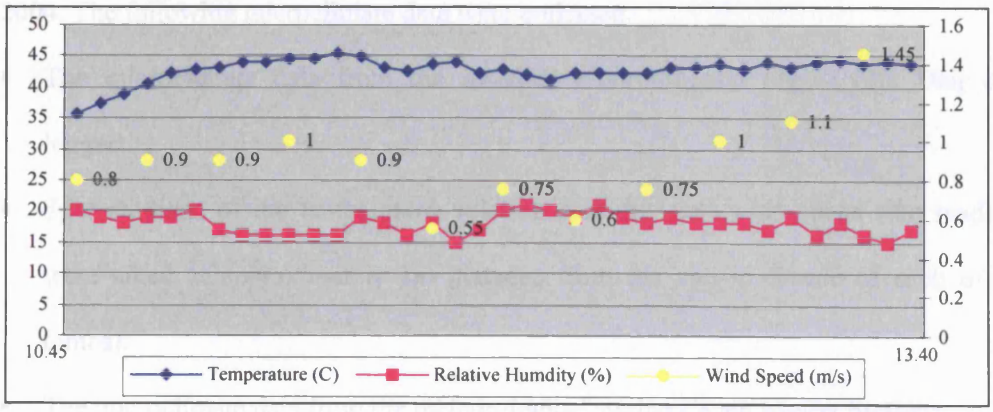

Figure 8.7: Temperature, relative humidity and wind speed spot readings. First fieldwork visit (1 August 2003). Location: Palace Tomb.

2- Wide ranges of wind speed fluctuation were recorded during the same day.

3- As the wind speed increased, the temperatures increased slightly and the relative humidity decreased. (Figures: 8.6 and 8.7).

4- The highest wind speed fluctuation rates were recorded at the Palace Tomb and the lowest at the Bab al Siq Triclinium Tomb.

5- Generally, wind speed fluctuated on a larger scale during the day hours than during the night hours.

6- Based on these data, the general trend of the microclimate conditions could be summarised as very high temperature, very low relative humidity with highly fluctuating wind speed values during day-time hours, and slightly lower temperature, slightly higher relative humidity and slightly less fluctuating wind speed rates during night-time hours.

8.3. Second fieldwork visit (January 2004)

The second fieldwork visit to the site was made between the 10th and 20th of January 2004. The following microclimate data were collected:

- The microclimate data from the installed environmental logger (the Deir data logger).
- Spot readings of the temperature, relative humidity and wind speed (the readings were taken at approximately 1m distance from the carved façade of each of the tombs).
- The microclimate data from the meteorological station (Wadi Mousa Station).

8.3.1. Relative humidity and temperature spot readings

During this visit, both relative humidity and temperature spot readings were taken near each of the three case study tombs: Bab al Siq Tomb, Palace Tomb and Deir Tomb. The measurements were taken every five minutes for 24 hours at each site (Appendix C).

Generally, the relative humidity readings were much higher than those of the first fieldwork visit. The average relative humidity readings were 66.8, 65.2, and 66.1 % near the Bab al Siq Triclinium, Palace and Deir Tomb respectively. Despite the fact that the overall averages at the three locations were very similar, the reading ranges vary slightly from one site to the other (see figures 8.8, 8.9 and 8.10).

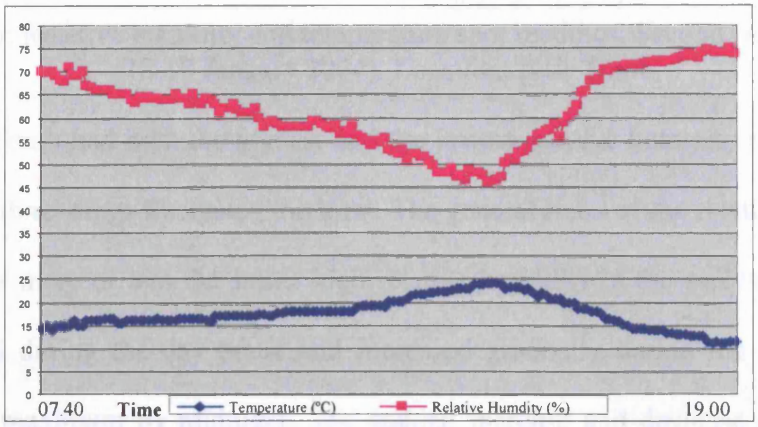

Figure 8.8: Relative humidity and temperature spot readings. Second fieldwork visit (16-17 January 2004). Location: Bab al Siq Triclinium Tomb.

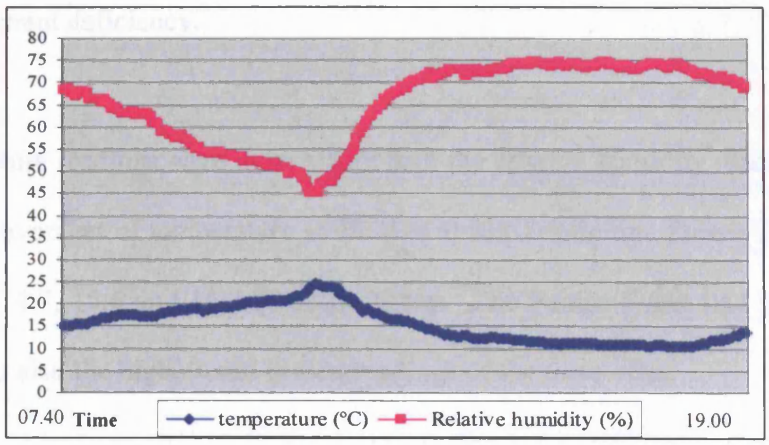

Figure 8.9: Relative humidity and temperature spot readings. Second fieldwork visit (17-18 January 2004). Location: Palace Tomb.

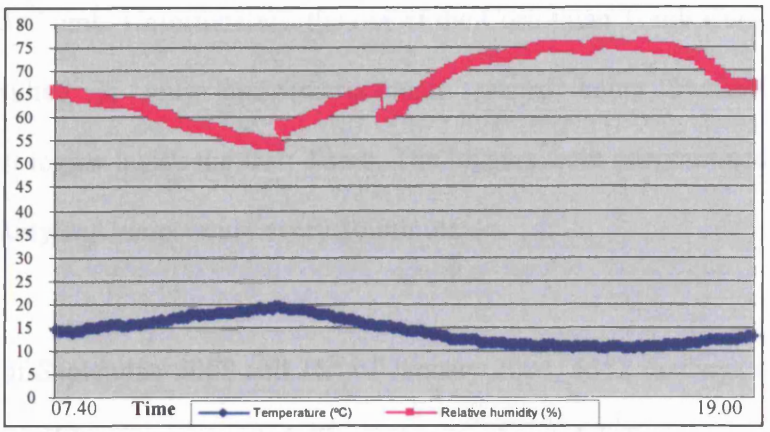

Figure 8.10: Relative humidity and temperature spot readings. Second fieldwork visit (18-19 January 2004). Location: Deir Tomb.

The Palace Tomb had both the highest and the lowest relative humidity readings, while the Deir Tomb readings fluctuated the least. The general trend of the relative humidity at each site was more or less the same: high relative humidity in the early morning hours that declined during the day hours and increased gradually during the evening hours reaching its maximum by midnight. The sudden increase and decrease of the relative humidity during the day in the Deir Tomb readings (figure 8.10) are more likely to be due to equipment deficiency.

The temperature readings were more stable than the relative humidity readings. The day-time overall averages of temperature at the Bab al Siq Triclinium, Palace Tomb and Deir Tomb were 14.7, 15.6 and 14.3 °C respectively. The Palace Tomb had the least stable readings, and also the highest and lowest readings of the three sites.

8.3.2. Relative humidity and temperature readings from the data logger

As mentioned earlier, two environmental loggers were installed to record the relative humidity and temperature on the site: one inside the Corinthian Tomb and the other

inside the Deir Tomb. Unfortunately, the one at the Corinthian Tomb went missing. This situation resulted in only one microclimate record being available, from the environmental logger inside the Deir Tomb. The loggers were programmed to record the relative humidity and temperature every 30 minutes.

Between 4th of September 2003 and 15th of January 2004, 6352 readings of temperature and relative humidity were recorded. The following is a brief discussion on the relative humidity and temperature that were recorded inside the Deir Tomb.

8.3.2.1. Relative humidity

The recorded relative humidity data showed not only significant fluctuation from one month to another, but also wide range of fluctuation within the day (figure 8.11). For example, on 16th September 2003, the relative humidity declined from 65.1 % at midnight to 36.9 % at midday. Generally, the relative humidity readings ranged between 60 % and 30 %. The relative humidity reached its maximum during January due to heavy rain that affected the site in the first half of January 2004. The maximum reading was 85.1 % and was recorded one day before downloading the data from the loggers. The overall average in January was approximately 50 %. It is worth mentioning that during December 2003, before January's heavy rain, the overall average of the relative humidity was less than 35 %.

From the previous data, it can be concluded that the relative humidity is very unstable, with January 2004 as the most humid month and October 2003 the driest month of the recorded period (September 2003-January 2004)

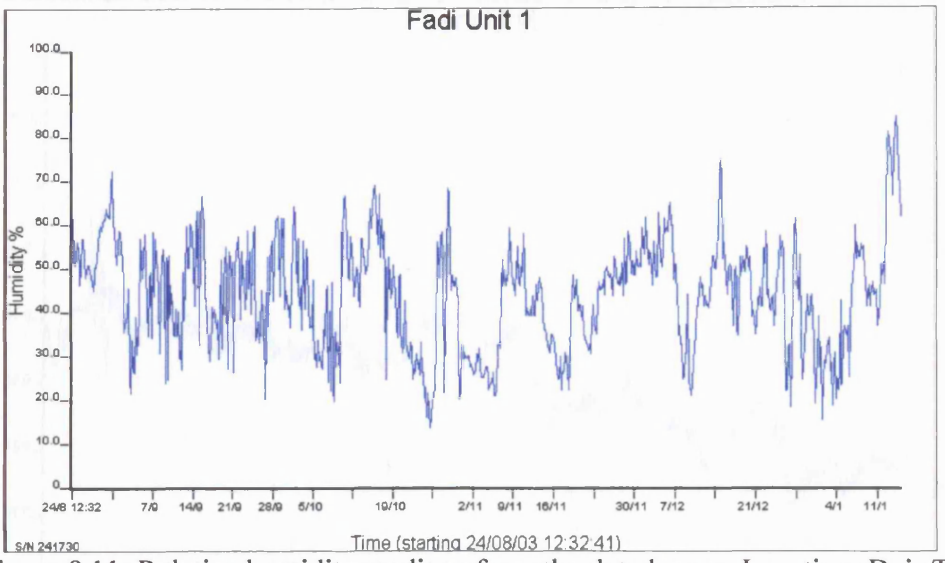

Figure 8.11: Relative humidity readings from the data logger. Location: Deir Tomb (Recorded period: September 2003-January 2004).

8.3.2.2. Temperature

The temperature readings were much more stable than the relative humidity ones (figure 8.12). It should also be noted that, because the logger was installed inside the tomb, the temperature readings were much lower than the outside temperatures.

During September 2003 the temperature readings were stable and ranged between 21.8 °C and 26.9 °C with an overall average of 23.4 °C. During October the temperature readings showed more variation from one day to another, however, the overall average was more or less the same as that of the previous recorded month. During November 2003 huge variations in temperature readings were noticeable. The readings ranged between 25.9 °C and 14.2 °C with an average of 18.6 °C. Temperature reached its minimum during December 2003 and January 2004. The lowest reading was around 9.5 °C on the 13th January 2004 at 07.00.

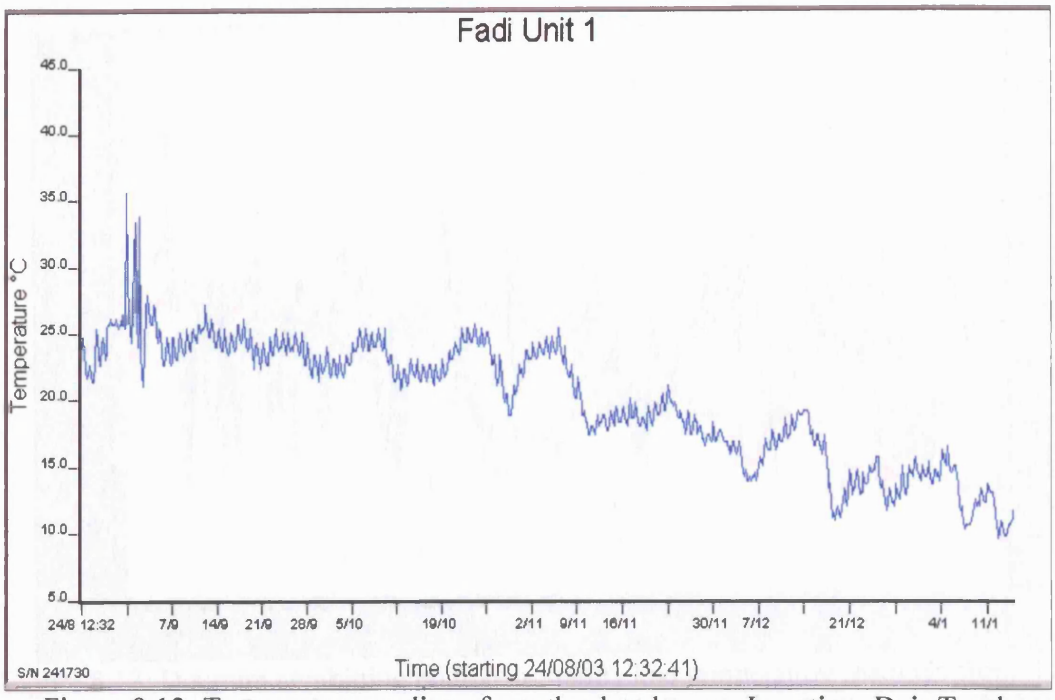

Figure 8:12: Temperature readings from the data logger. Location: Deir Tomb (Recorded period: September 2003-January 2004).

All in all, during the recording period (4 September 2003 - 15 January 2004), the temperature variation was rather low from one day to another and even from one month to another. The main reason behind this is that the logger was located in a sheltered area, inside the tomb.

By combining the relative humidity and temperature readings in one figure (8.13), the relation between these two environmental factors can be easily seen. Generally, as the temperature decreases the relative humidity increases and vice-versa, but the temperature fluctuation rates are much less dramatic than the relative humidity ones.

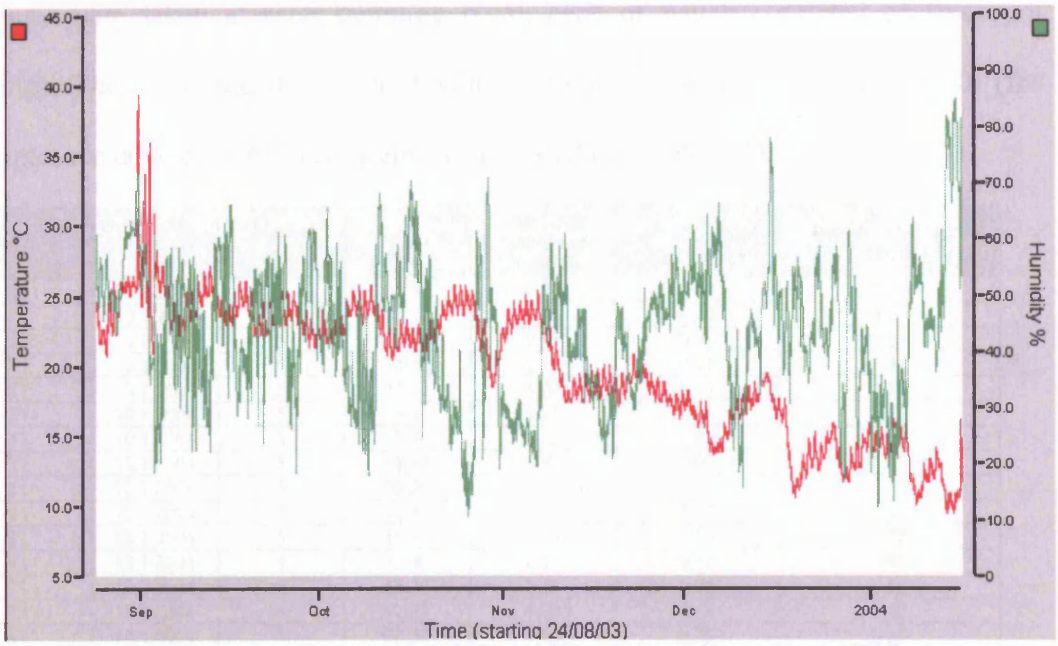

Figure 8.13: Diagram combining relative humidity and temperature readings from the data logger. Location: Deir Tomb (Recorded period: September 2003-January 2004).

8.3.3. Wind speed spot readings

Due to the importance of the wind speed factor in this research, sets of wind speed spot readings were taken during the second fieldwork visit. Unfortunately, there were no loggers or any other instrument available in order to record the wind speed over a long period as in the case of temperature and relative humidity. Therefore, spot reading profiles as well as data from the meteorological station nearest to the site (Wadi Mousa) were used as the main database for the evaluation of the wind speed factor.

- The wind speed spot reading profiles

In order to get a clear indication about wind speed at the studied monuments, wind speed spot readings were taken at different heights at each monument. The readings were taken at approximately 1m distance from the surface of the façades. A total of 21 sets of spot

readings were taken at each sampling point, each of which consisted of five spot readings. These covered the whole daytime period (08.30-17.30 or 09.00-18.00) (for example, see table 8.1). All measurements are listed in appendix D.

Location	Date	Height (cm)	Time	Maximum wind speed (m/s)	Minimum wind speed (m/s)	Average wind speed (m/s)
T1	10.1.2004	5	08.30	0.70	0.00	0.30
T1	10.1.2004	5	09.30	1.10	0.10	0.40
T1	10.1.2004	5	12.30	0.55	0.05	0.25
T1	10.1.2004	5	14.30	1.10	0.25	0.55
T1	10.1.2004	5	15.30	3.00	0.15	1.50
T1	10.1.2004	5	16.30	3.25	0.30	1.75
T1	10.1.2004	5	17.30	2.95	0.05	1.60
T1	12.1.2004	5	08.30	0.80	0.00	0.35
T1	12.1.2004	5	09.30	1.55	0.15	0.50
T1	12.1.2004	5	12.30	0.40	0.00	0.25
T1	12.1.2004	5	14.30	1.30	0.20	0.75
T1	12.1.2004	5	15.30	2.35	0.30	1.45
T1	12.1.2004	5	16.30	3.55	0.25	1.80
T1	12.1.2004	5	17.30	4.00	0.50	2.00
T1	14.1.2004	5	08.30	0.65	0.10	0.35
T1	14.1.2004	5	09.30	2.05	0.25	0.80
T1	14.1.2004	5	12.30	0.40	0.15	0.30
T1	14.1.2004	5	14.30	3.90	0.15	2.05
T1	14.1.2004	5	15.30	4.55	0.35	2.15
T1	14.1.2004	5	16.30	4.20	0.30	2.45
T1	14.1.2004	5	17.30	3.95	0.65	2.50

Table 8.1: Wind speed spot readings. Location: Bab al Siq Triclinium Tomb (January 2004)

Following observation of the wind speed profiles, the following points can be made:

- The wind speed fluctuated significantly at the same sampling point throughout the day (See figure 8.14).
- The wind speed usually started very low in the early morning, then gradually increased and started decreasing again before midday.
- The wind speed started rising again in the afternoon and reached its maximum in the evening.

- In most of the sampling profiles, the wind speed increased generally with the height. For example, the overall average of wind speed varied between 1.10, 1.32 and 1.44 m/s for 5, 205 and 350 cm heights respectively at Bab al Siq Triclinium Tomb. The reason for such a trend is mainly the presence of various natural shelters at low heights, which restricted the wind movement.

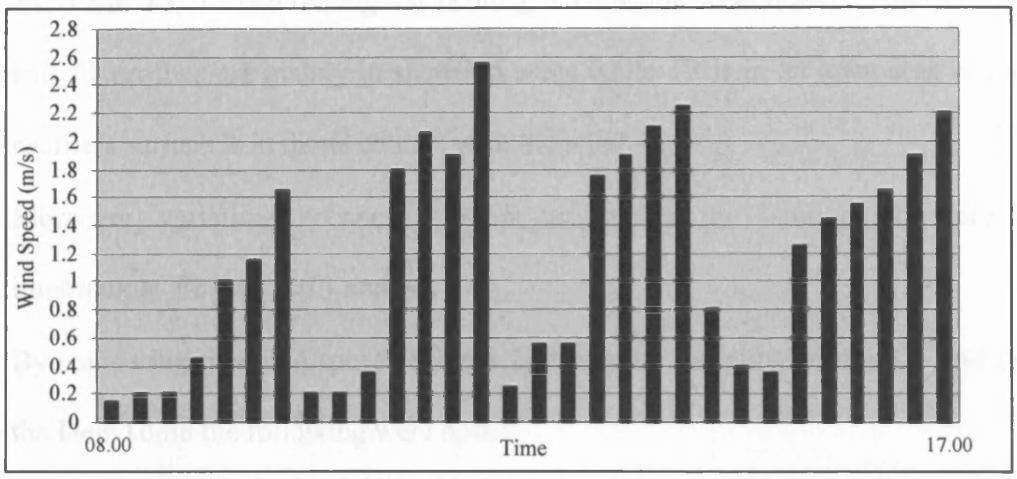

Figure 8.14: Wind speed profile at the Palace Tomb (C2).
Second fieldwork visit (11 January 2004). Height: 350 cm.

- The wind speed varied considerably from one day to another and from one location to another and even from one sampling site to another at the same location.
- The highest measurement and the highest fluctuation rate of wind speed was recorded at C2, which, as shall be seen in chapter 9, were combined with the highest soluble salt content.
- Wind speed readings from the same point were changing considerably within a very short time and large differences were noted between the maximum and minimum readings at each sampling point.
- Dusty windstorms occurred occasionally during the afternoons.

- At the Bab al Siq Triclinium Tomb the highest variations in wind speed were recorded at the second sampling profile T2, at the 350 cm height (see chapter 9 for the sampling profiles location at each monuments). In addition, this point recorded the highest wind speed figure at that location.
- By comparing the wind speeds at the same height (350 cm) of the sampling profiles T1, T2 & T3, T2 had the highest reading, T3 was the second and T1 the lowest. T2 and T1 profiles are mainly in sheltered areas while T3 is in an open area where the profile's surface is in direct contact with the wind.
- Moreover, variations between different readings at the same points were more important at T2 than at T1 and T3.
- By comparing the wind speed readings between the sampling profile D1 and D2, in the Deir Tomb the following were noted:
  - Wind speed readings were higher at D2 than D1.
  - The variations between the wind speed readings are more noticeable above the sampling points in D2 section.
- At the Corinthian Tomb, the average wind speed at the sampling point of 450 cm height is greater than at 350 cm height; however the wind speed variations throughout the day were greater at 350 cm.

8.4. Third fieldwork visit (June 2004)

In order to continue the assessment of the microclimate conditions at the case study monuments, a third fieldwork visit to Petra was held in June 2004. During the 9 days spent in the field, spot readings of the temperature, relative humidity and wind speed were taken at the three sites (Bab al Siq Triclinium, Palace and Deir Tombs), and the microclimate data (temperature and relative humidity) were downloaded from the installed data logger.

8.4.1. Relative humidity and temperature spot readings

Three sets of spot readings for relative humidity and temperature were taken at the Bab al Siq Triclinium, Palace and Deir Tombs. Each set involved a 24-hour monitoring of each site. The readings were taken every five minutes (Appendix F and figures 8.15, 8.16 and 8.17).

These relative humidity readings were lower than the second fieldwork readings (January), but to a large extent higher than the first fieldwork readings (August). The daily averages of the relative humidity were 51.0, 49.2 and 43.1 % at the Bab al Siq Triclinium, Palace and Deir Tombs respectively. In general, the relative humidity readings were less variable, compared to the data from the first and second fieldwork visits. However, the relative humidity figures had a similar general trend to those of the first and second fieldwork visits. A considerable variation between the averages of the day and night readings was noted at the Deir Tomb and on a smaller scale at the Palace and Bab al Siq Tombs (Table 8.2)

Location	RH averages for 24 hours (%)	RH averages for 12 hours (day-time) (%)	RH averages for 12 hours (night -time) (%)	T averages for 24 hours (°C)	T averages for 12 hours (day-time) (°C)	T averages for 12 hours (nigh t-time) (°C)
Bab al Siq Triclinium	51.0	47.7	54.3	22.9	25.6	20.3
Palace Tomb	49.2	45.6	54.9	23.6	26.7	20.7
Deir Tomb	43.1	35.2	50.0	21.6	25.1	18.3

Table 8.2: Day and night overall averages of relative humidity and temperature spot readings. Third fieldwork visit (21-24 June 2005)

The temperature spot readings revealed higher overall averages than January's fieldwork visit, but slightly lower than August's fieldwork visit (figures 8.15, 8.16 and 8.17). The readings from all three locations showed more fluctuation compared to the previous data, with the temperature data being much more stable than the relative humidity data.

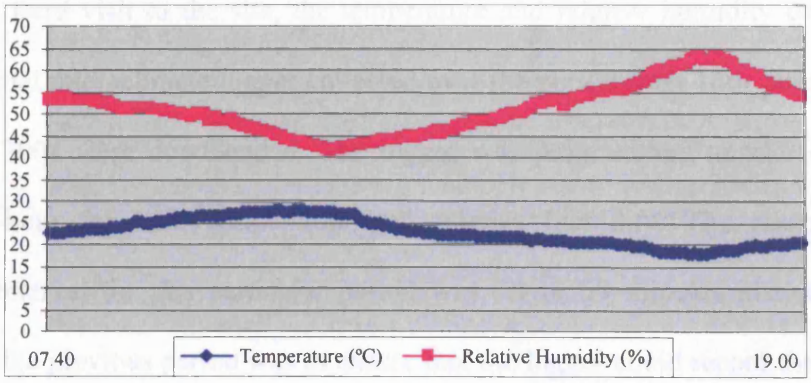

Figure 8.15: Relative humidity and temperature spot readings. Second fieldwork visit (16-17 January 2004). Location: Bab al Siq Tomb.

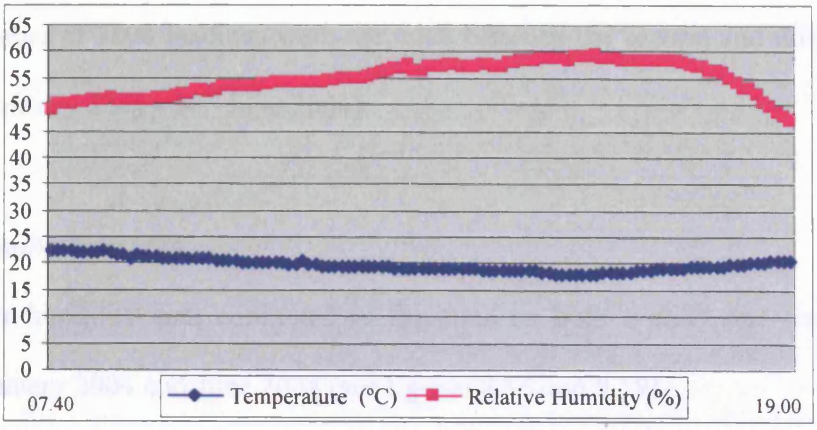

Figure 8.16: Relative humidity and temperature spot readings. Second fieldwork visit (16-17 January 2004). Location: Palace Tomb.

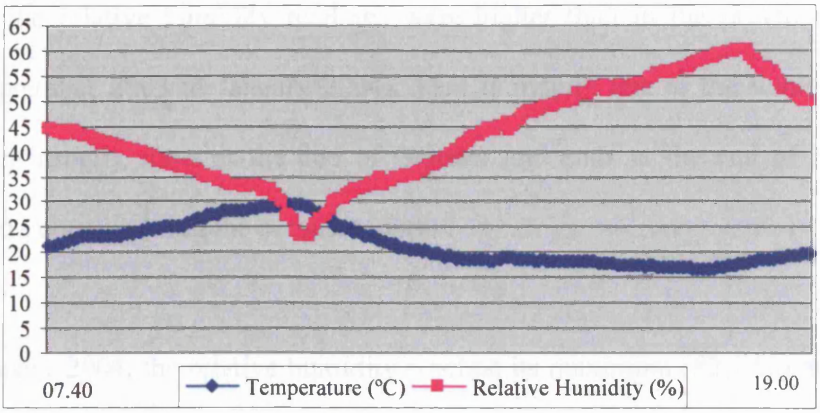

Figure 8.17: Relative humidity and temperature spot readings. Second fieldwork visit (16-17 January 2004). Location: Deir Tomb.

8.4.2. Relative humidity and temperature readings from the data logger

During the third visit to the site, the temperature and relative humidity data from the environmental microclimate logger collected over the period from 16th January 2004 to 20th June 2004 were downloaded. The logger was programmed to take one reading every one-hour for both temperature and relative humidity. The reason why the recording interval for this particular period was set to 60 minutes instead of the 30 minutes of the previous period was to ensure that the logger could record throughout the whole period and would not reach its full capacity before the data could be downloaded. A total number of 3808 readings were recorded between the second and third fieldwork visits (16 January 2004 - 20th June 2004).

8.4.2.1. Relative humidity

The relative humidity data continued to fluctuate on both a daily and monthly basis between January 2004 and June 2004 (see figures 8.18 and 8.19).

Generally, the relative humidity readings were higher than in the previous recording period (September 2003 to January 2004). That is mainly due to the winter season in Petra, which usually starts at the end of October and ends at the end of March with January and February being the coldest months.

During January 2004, the relative humidity reached its maximum (82.1 %) due to heavy rains that affected the area in the second half of the month. The amount of rainfall during this period was the highest in the last 15 years, around 55 mm per day for 5 days (Wadi Mousa meteorological station, personal commun.), which is higher than the average annual rainfall in that area (see chapter 6).

During February 2004, the relative humidity readings were still relatively high with an average of 54.8 %. Moreover, during this month the relative humidity readings showed wide fluctuation between two days and even within a single day. Noticeable falls in the relative humidity were recorded during March 2004. The average relative humidity dropped approximately 10 % from the previous month.

During April 2004, the lowest relative humidity reading of the whole second period of monitoring (January - June 2004) was recorded. However, the relative humidity averages in April were more or less similar to the previous month (approximately 45 %).

The relative humidity continued to drop considerably during May 2004. The average reading was 39.5 %, the lowest monthly average between January and June.

The relative humidity readings for June 2004 showed less fluctuation with an increase in the monthly average (approximately 47 %).

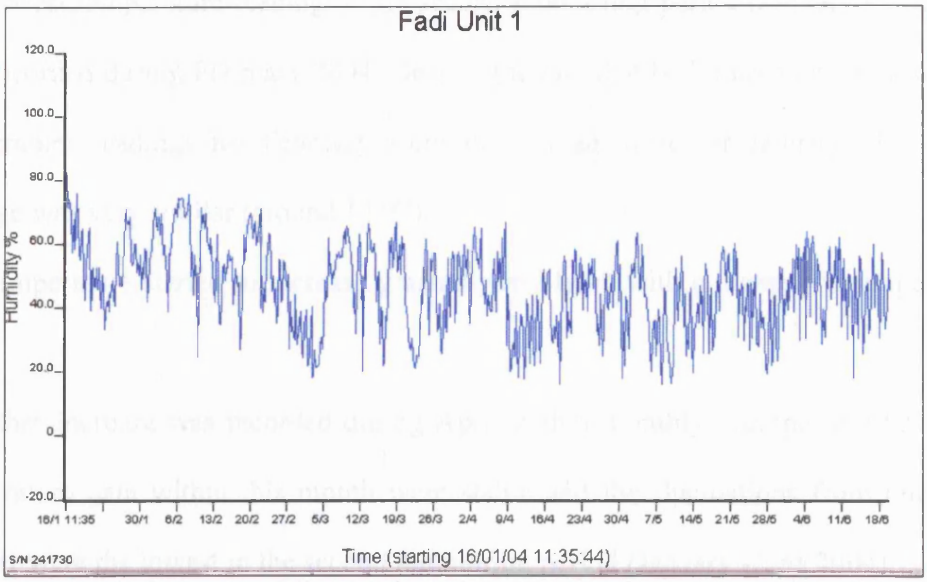

Figure 8.18: Relative humidity readings from the data logger. Location: Deir Tomb. (Recorded period: 16 January-20 June 2004).

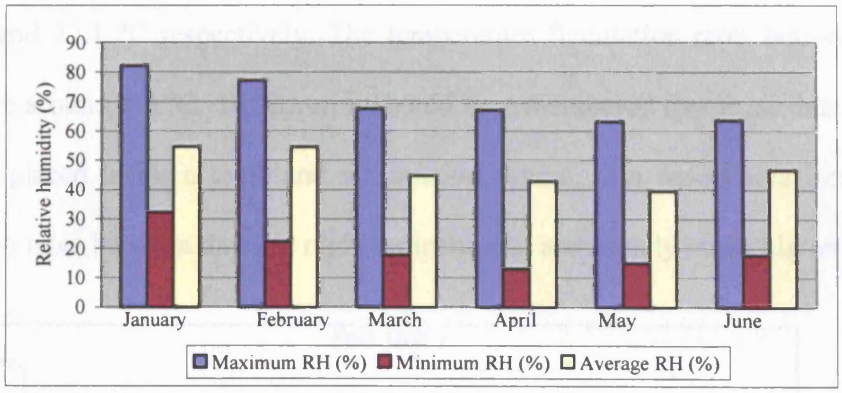

Figure 8.19: Monthly maximum, minimum, and average relative humidity readings. Location: Deir Tomb. (Recorded period: 16 January-20 June 2004).

8.4.2.2. Temperature

The temperature data between January and June 2004 were much more stable than the relative humidity readings (figure 8.20 and 8.21).

In January 2004 the temperature readings ranged between 9.6 and 25.1 °C with an average of 12.5 °C. The fluctuation range within the same day was less than 2 °C during this month.

The lowest temperature reading of the second monitoring period (January - June 2004) was recorded during February 2004. Despite the fact that both maximum and minimum temperature readings for February were lower than those for January, the monthly average was very similar (around 12 °C).

The temperature started to increase gradually in March with a monthly average of 15.8 °C.

A further increase was recorded during April with a monthly average of 17.5 °C. The temperature data within this month were stable and the fluctuations from one day to another were the lowest in the second monitoring period (January -June 2004).

During May and June the temperature continued to increase gradually with an average of 22.6 °C and 22.1 °C respectively. The temperature fluctuation rates between day and night were around 3-4 °C. However, it should be remembered that these data came from a logger, placed inside a tomb and not outside, where, in a desert area like Petra, the fluctuation rates between day and night temperatures are usually much higher.

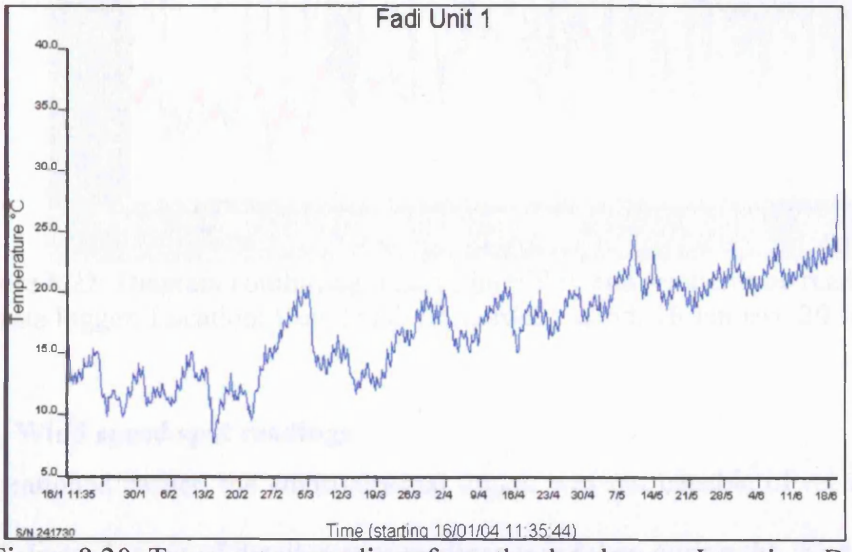

Figure 8.20: Temperature readings from the data logger. Location: Deir Tomb. (Recorded period: 16 January-20 June 2004).

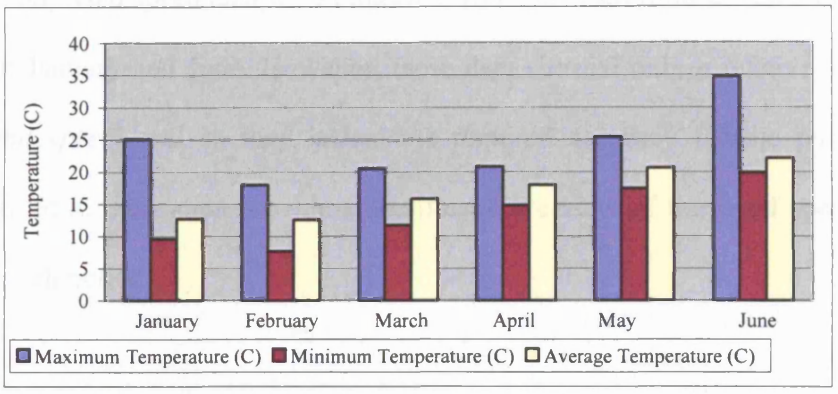

Figure 8.21: Monthly maximum, minimum, and average temperature readings. Location: Deir Tomb. (Recorded period: 16 January-20 June 2004).

The relative humidity and temperature readings were obviously corresponding to each other (Figure 8.22). An increase in temperature was usually combined with a decrease in relative humidity readings and vice-versa.

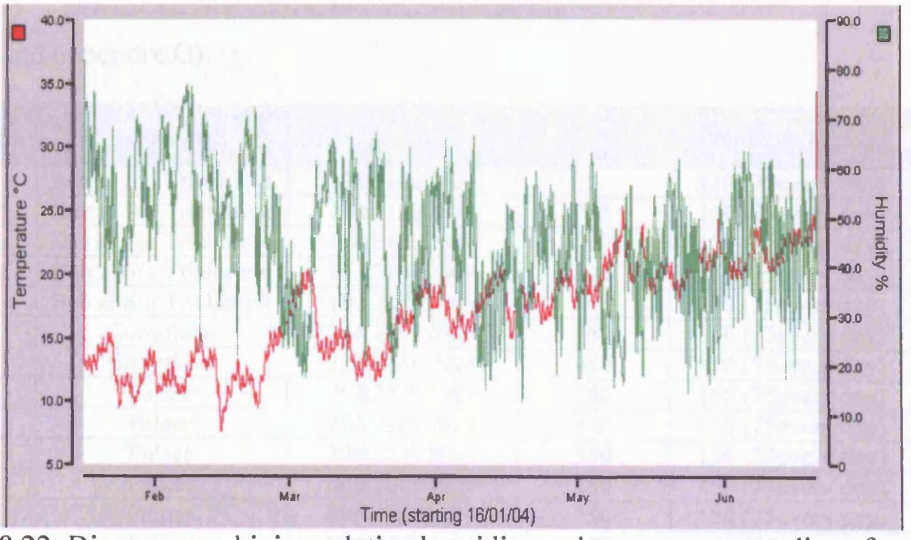

Figure 8.22: Diagram combining relative humidity and temperature readings from the data logger. Location: Deir Tomb (Recorded period: 16 January-20 June 2004).

8.4.3. Wind speed spot readings

As mentioned earlier, the environmental logger was not capable of recording the wind speed. Instead, a set of detailed spot readings was taken during the third fieldwork visit in order to evaluate this important environmental factor (Appendix E).

In addition, wind speed data were collected from the Wadi Mousa meteorological station between January and June. However, these data showed only a relative value (*high or low wind speed*) and so they lacked the required accuracy for the purposes of this research. Still, these data provide a significant overview of the wind speed throughout the research period.

- Wind speed spot reading profiles

Wind speed readings were taken above 17 different sampling points at the four case study monuments. Moreover, during the night hours, a group of wind speed spot readings were taken from a balcony at the Nabateans Hotel near the site. A total of 2685 wind speed spot readings were taken during the third fieldwork visit to the site. (See table 8.3 and appendix G).

Profile Code	Location	Dates	Height (cm)	Number of Reading
T1	Bab al Siq Triclinium	19&21/6/2004	5	150 (75every day)
T1	Bab al Siq Triclinium	19&21/6/2004	205	150 (75every day)
T1	Bab al Siq Triclinium	19&21/6/2004	305	150 (75every day)
T2	Bab al Siq Triclinium	19&21/6/2004	305	150 (75every day)
T3	Bab al Siq Triclinium	19&21/6/2004	305	150 (75every day)
H	Corinthian	20&22/6/2004	350	150 (75every day)
H	Corinthian	20&22/6/2004	450	150 (75every day)
C1	Palace	20&22/6/2004	350	150 (75every day)
C1	Palace	20&22/6/2004	450	150 (75every day)
C2	Palace	20&22/6/2004	350	150 (75every day)
C2	Palace	20&22/6/2004	450	150 (75every day)
C3	Palace	20&22/6/2004	350	150 (75every day)
C3	Palace	20&22/6/2004	450	150 (75every day)
D1	Deir	23&24/6/2004	55	150 (75every day)
D1	Deir	23&24/6/2004	255	150 (75every day)
D2	Deir	23&24/6/2004	55	150 (75every day)
D2	Deir	23&24/6/2004	255	150 (75every day)
NH	Nabateans Hotel	19,21&23/6/2004	500	135(45 every day)

Table 8.3: Wind speed spot readings. Third fieldwork visit (19-24 June 2004)

The main outcomes from the detailed observation of the wind speed during the third fieldwork visit (June 2004) can be summarised in the following points:

- During the daytime hours the wind speed readings above the selected sampling points at the four case-study monuments showed wide fluctuation. This fluctuation appeared not only between two different sampling points, but also at the same sampling point at different times.

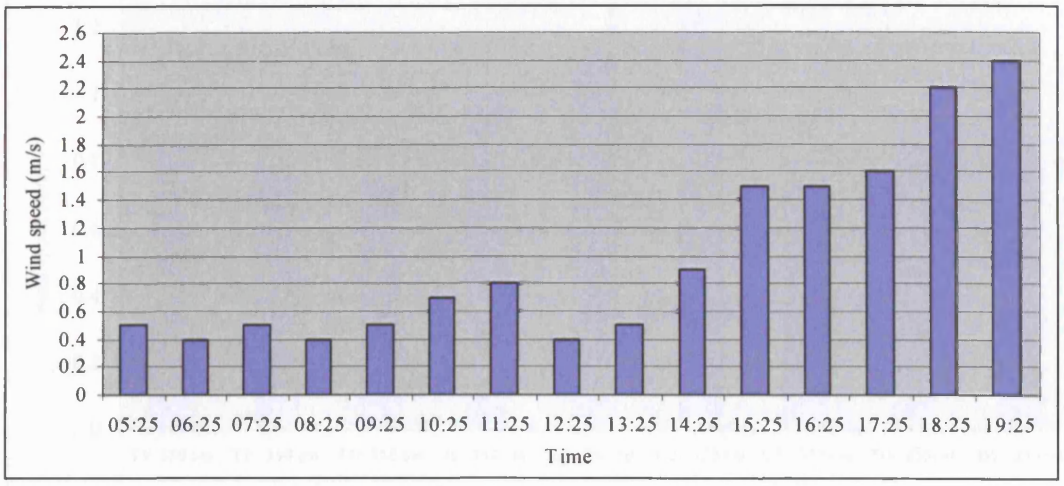

Figure 8.23: Wind speed profile at the Palace Tomb (C2).
Third fieldwork visit (20 June 2004). Height: 350cm.

- During the daytime hours the wind speed readings had a similar trend to the previous fieldwork readings, where the wind speed profile started very low in the early hours of the day, then increased slowly and gradually till the midday hours. Slow wind speed dominated the midday hours, while during the afternoon hours there was again a significant increase in the wind speed (figure 8.23 and appendix E).
- Generally, with some exceptions, the wind speed increased slightly with the increase in the height of the reading level at the profile. For instance, the overall average of the wind speed readings at the Bab al Siq Triclinium increased from 0.43 m/s above the 5 cm sampling point to 0.54 m/s above the 350 cm sampling point.
- The overall weather conditions were mainly stable during the seven days. Thus, the wind speed readings between the monuments could be compared and correlated.

- The highest overall average of the wind speed was recorded at the Palace Tomb, at the middle sampling profile (C2), while the readings at Bab al Siq Triclinium were the lowest. (See figure 8.24).

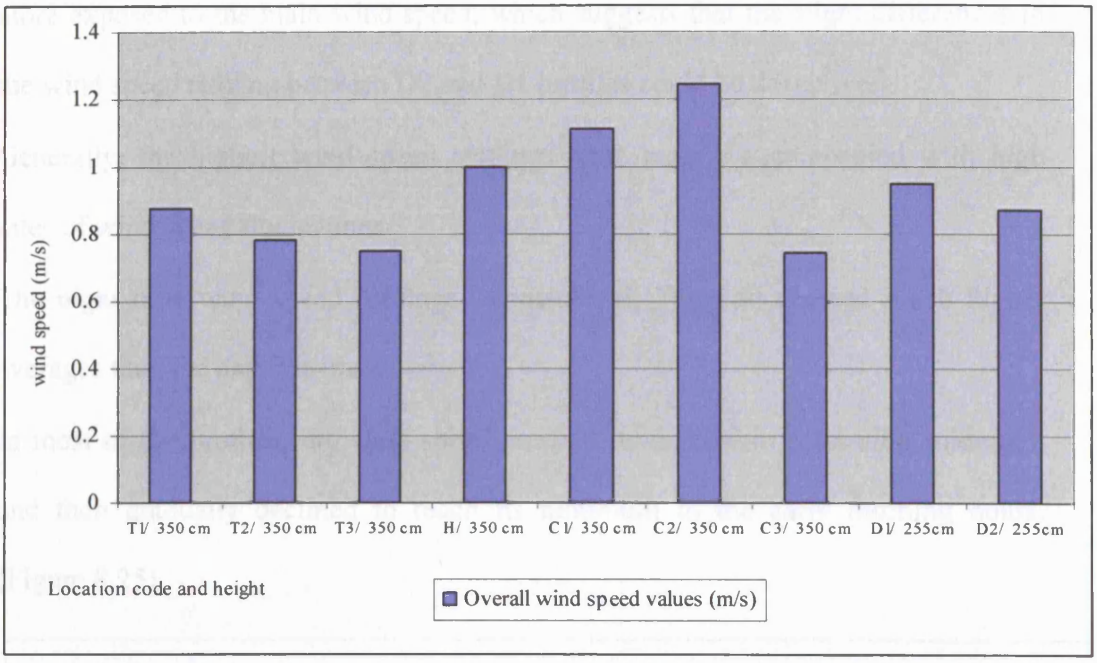

Figure 8.24: The overall averages of wind speed Third fieldwork visit (June 2004). (Above the 350 cm sampling points at the Bab al Siq, Corinthian and Palace Tomb, and above the 255 cm sampling point at the Deir Tomb).

- The readings above T1 and C3 sampling profiles showed the lowest individual wind speed readings. The reason for such low wind speed readings at these profiles is their sheltered location. However, their overall average was higher than T3 due to a few exceptionally high wind speed readings at each of these two profiles.
- At the Palace Tomb, C2 profile revealed not only the highest wind speed readings, but also the highest rate of fluctuations between minimum and maximum wind speed readings.

- At Deir Tomb, the overall average of wind speed readings above D1 profile was higher than that above D2 profile. The fluctuation rate above D1 sampling profile was also higher. However, it must be stated that D2 is located in an area slightly more exposed to the main wind speed, which suggests that the slight differences in the wind speed reading between D2 and D1 profiles could be deceptive.
- Generally, the highest wind speed readings were mainly accompanied with high rates of wind speed fluctuations.
- The night time wind speed readings (Appendix E, Table 9) showed much higher averages than the daytime ones.
- In most of the profiles, the wind speed reached its maximum soon after midnight, and then gradually declined to reach its minimum in the early morning hours. (Figure 8.25).

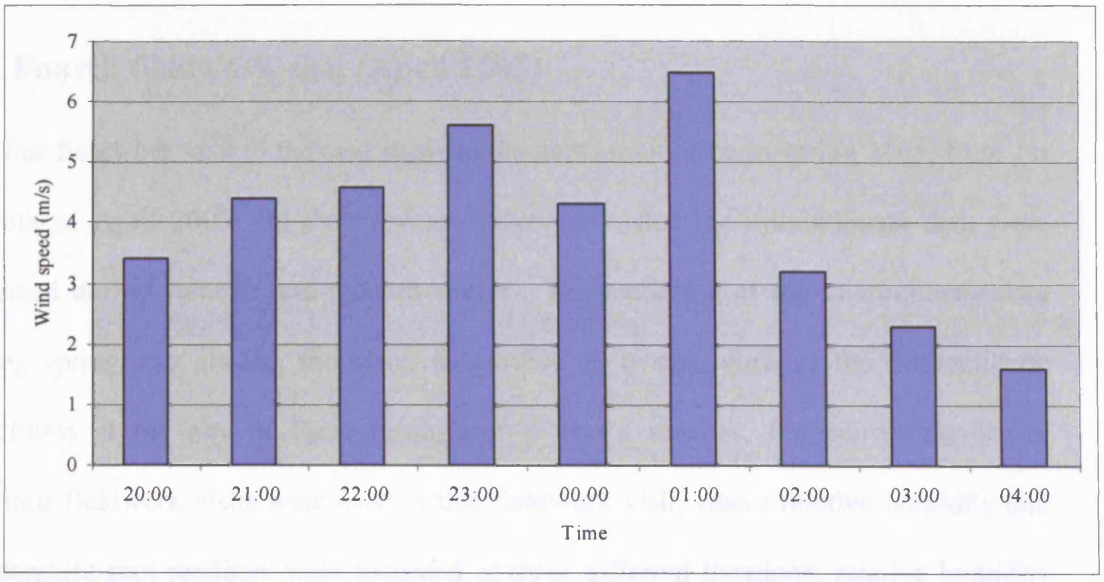

Figure 8.25: Wind speed profile during night time. Third fieldwork visit (19 June 2004). Location: Nabateans Hotel.

In order to create a 24-hour profile of the wind speed the readings from the Bab al Siq Triclinium and the Nabateans Hotel on the 21 June 2004 were combined in the following diagram. (Figure 8.26).

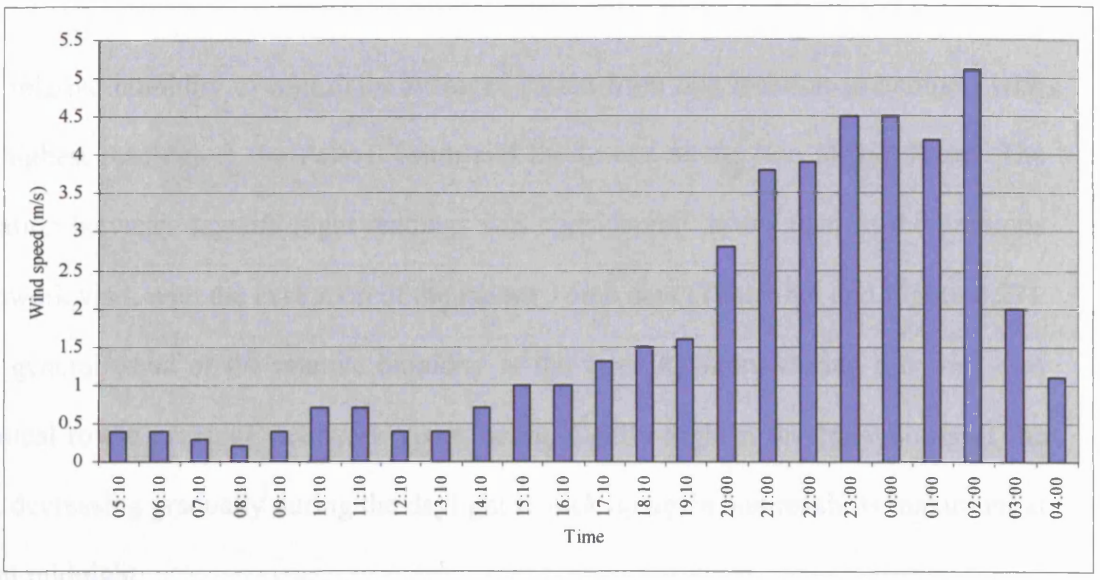

Figure 8.26: 24-hour wind speed profile. Third fieldwork visit (21 June 2004).

8.5. Fourth fieldwork visit (April 2005)

The last fieldwork visit to the case study monuments took place in spring 2005, from 1st to 16th of April 2005. In the previous fieldwork visits, the microclimate data were collected during summer and autumn-winter. The recording of the microclimate data during spring was needed, therefore, to provide an overall view of the microclimate conditions at the city of Petra throughout a year's seasons. Procedures similar to previous fieldwork visits were used in this fieldwork visit, where relative humidity and temperature spot readings were recorded at three different locations, relative humidity and temperature readings were downloaded from the data logger installed on site and detailed wind speed spot readings were taken above the sampling points of each profile.

8.5.1. Relative humidity and temperature spot readings

Three sets of spot readings for temperature and relative humidity were taken at the Bab al Siq Triclinium, Palace and Deir Tombs (Appendix J).

The relative humidity overall daily averages varied from one location to another, with the highest readings at the Palace Tomb and the lowest at the Bab al Siq Tomb. The variation between day and night readings was considerably lower than in the previous fieldwork visit, with the exception of the Palace Tomb data (Table: 8.4 and Figure 8.27). The general trend of the relative humidity at the three locations during this visit was identical to the previous fieldwork visits, being slightly high in the early hours of the day, decreasing gradually during the daylight to pick up again and reach its maximum at about midnight.

Location	RH averages for 24 hours (%)	RH averages for 12 hours (day-time) (%)	RH averages for 12 hours (night-time) (%)	T averages for 24 hours (°C)	T averages for 12 hours (day-time) (°C)	T averages for 12 hours (night-time) (°C)
Bab al Siq Triclinium	48.85	44.83	46.81	17.48	18.73	16.30
Palace Tomb	50.25	42.51	57.61	18.26	22.26	14.46
Deir Tomb	41.81	39.81	43.71	19.09	22.58	15.76

Table 8.4: Day and night overall averages of relative humidity and temperature spot readings. Fourth fieldwork visit (1-3 April 2005)

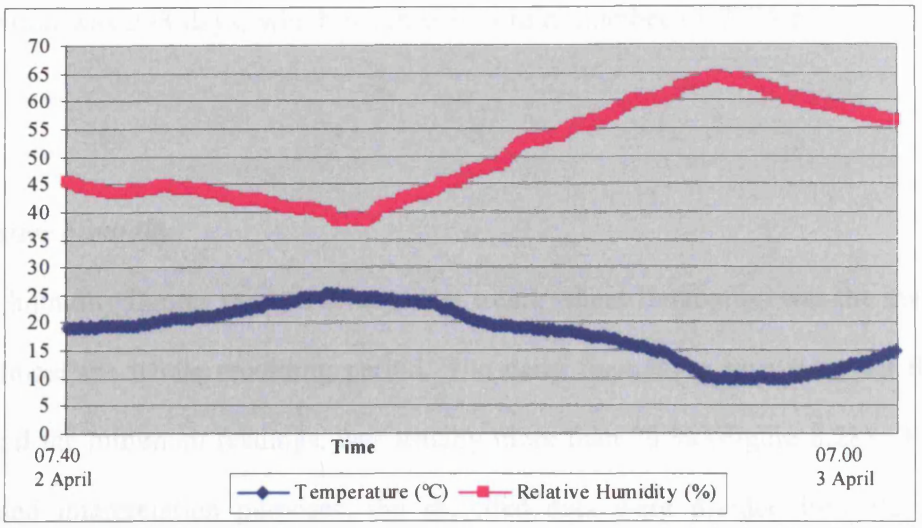

Figure 8.27: Relative humidity and temperature spot readings. Fourth fieldwork visit (2-3 April 2005). Location: Palace Tomb.

On the other hand, temperature readings showed slightly fluctuating figures, which is certainly different from the temperature spot readings of the previous visits (figure; 8.27). The overall daily averages at the three locations are very similar. The variation between the daytime and night-time averages was considerably higher at the Palace and Deir Tombs (Table 8.4). The lowest temperature was recorded at the Palace Tomb, while the highest was recorded at the Bab al Siq Tomb.

8.5.2. Relative humidity and temperature readings from the data logger

As part of the evaluation of the microclimate conditions at Petra, the relative humidity and temperature data from the data logger at the Deir Tomb for the period 20th June 2004 to 15th April 2005 were analysed and assessed.

As for the previous set of data (January-June 2004), the logger was programmed to take one reading for each condition (temperature and relative humidity), every hour. The

logging duration was 298 days, which resulted in a total number of 7294 readings for this period.

8.5.2.1. Relative humidity

The relative humidity figures showed a very clear trend, where fluctuation was the main feature in almost the whole recording period. The daily fluctuation rate, between the maximum and the minimum readings, was usually more than 20 % (Figure 8.28). For evaluation and interpretation purposes, the recorded data were divided into eleven divisions (Table 8.5), each of which represents a certain month. The following is a brief discussion of these data.

The microclimate data recorded in June 2004 showed slightly high relative humidity readings with an overall average of around 46 %.

During July, which is usually a very dry month, relative humidity readings were generally lower than those in June with an overall average of around 41 %. Surprisingly, the relative humidity figures in August, usually the driest month of the year at Petra, were significantly high with a maximum of 67.5 % and an overall average of approximately 47 %. Throughout this month, the relative humidity daily figures were very stable and very slight differences were noted between one day and another. However, the variation rate within the same day was still high.

The relative humidity figures in September were very similar to those recorded in August, with slightly lower readings. These figures showed the lowest readings of the summer period (approximately 12 %).

The relative humidity data for October and November (2005) were very similar, with overall averages of approximately 42 %. During these two months the relative humidity reached higher figures compared to the previous months, however, the overall averages were slightly lower than in August and September.

In the first half of December 2005, the relative humidity readings were unstable with considerable dissimilarities between one day and the next. On the other hand, in the second half of the month, the relative humidity became to some extent more stable. The overall averages of this month were approximately 41 %.

High and relatively stable relative humidity was the main characteristic for the data in January.

The overall averages for February 2005 were the highest for the whole monitored period between June 2004 and April 2005, with an average of approximately 51 %.

In March 2005, the maximum relative humidity reading of all the previous readings was recorded (approximately 82 %), but the overall averages of approximately 44 % were slightly lower than February. With few exceptions, most readings were between 30 % and 60 %.

Finally, the readings in April showed considerably high overall averages of relative humidity (approximately 50 %). Towards the end of this month, the relative humidity started to drop gradually.

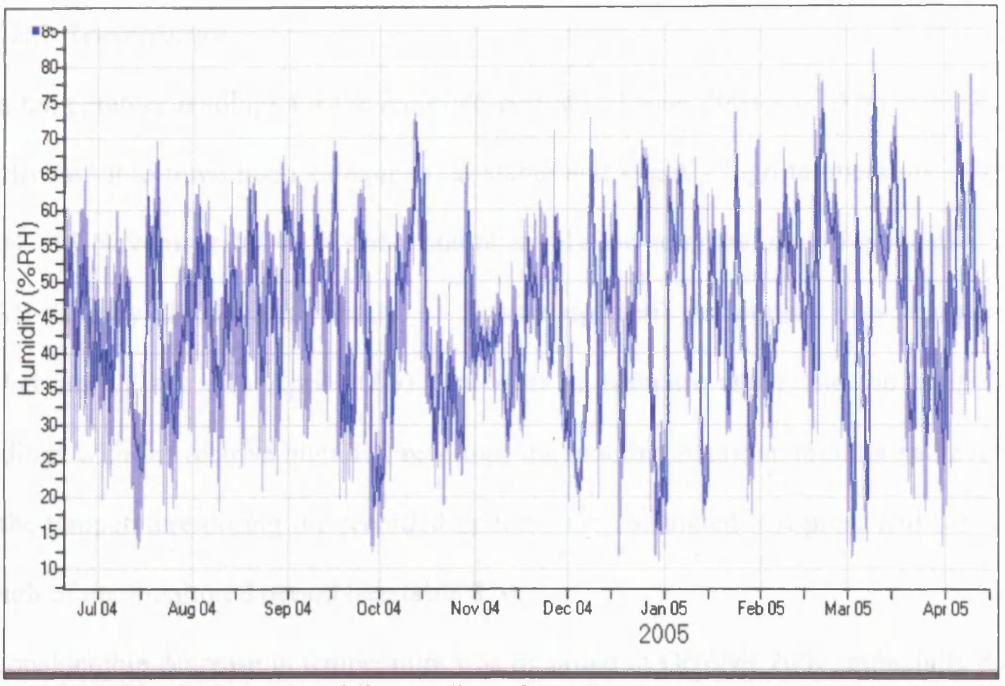

Figure 8.28: The Relative humidity readings from the data logger. Location: Deir Tomb. (Recorded period: 20 June 2004-16 April 2005).

Month	Maximum (%)	Minimum (%)	Average (%)	Number of readings
June 2004 (20-30)	66.06	25.20	45.49	256
July 2004 (1-31)	69.45	12.69	40.74	759
August 2004 (1-31)	67.51	17.78	46.85	755
September 2004 (1-30)	69.45	12.23	44.73	731
October 2004 (1-31)	73.32	16.39	42.94	757
November 2004 (1-30)	70.90	25.20	42.60	731
December 2004 (1-31)	72.83	10.83	41.49	755
January 2005 (1-31)	73.32	12.69	44.65	757
February 2005 (1-28)	78.69	24.74	50.81	683
March 2005 (1-31)	82.12	11.31	44.24	756
April 2005 (1-16)	78.69	18.71	50.31	351

Table 8.5: Monthly maximum, minimum, and average relative humidity readings. Location: Deir Tomb. (Recorded period: 20 June 2004 - 16 April 2005)

8.5.2.2. Temperature

The temperature readings for the recorded period (20 June 2004 - 16 April 2005) could be divided into three main categories: a. stable and slightly high temperature (20 June 2004 - 15 November 2004), b. stable and relatively low temperature (15 November 2004 - 31 January 2005) and finally c. fluctuating and moderately low temperature (1 February 2005 - 16 April 2005). In order to compare and relate the temperature readings with the relative humidity readings, the monthly maxima, minima and averages of the temperature during the recorded period were calculated and presented for every month of the monitored period (see table 8.6).

A considerable decrease in temperature was recorded in October 2004, especially during the second half of this month. The overall averages of the temperature were still very similar to the previous months (July - September 2004), but with slightly lower individual readings.

Temperatures continued to decline significantly during November 2004 and the lowest reading since June 2004 was recorded.

Throughout December 2004 and January 2005 the temperature records illustrate a less stable condition with a daily fluctuation between the maximum and the minimum temperatures of approximately 2 °C.

The lowest temperature readings were recorded during February 2005 (around 7.5 °C). Furthermore, this month's temperature readings show two clear trends: a steady decline during the first half of the month and a constant increase during the second half of the month.

The temperature became more unstable during March 2005, with a daily variation rate of approximately 3-3.5 °C. A regular and slow increase in temperature was recorded in the second half of March 2005 and the first half of April 2005.

All things considered, the temperature readings were still much more stable than the relative humidity readings. Even though only a very slight difference could be seen between the relative humidity monthly overall averages, the individual relative humidity readings varied significantly. June, July, September and October were moderately dry and hot, while January and February were slightly humid and quite cold months. In March and April both temperature and relative humidity were unstable with overall humid and rather cold conditions.

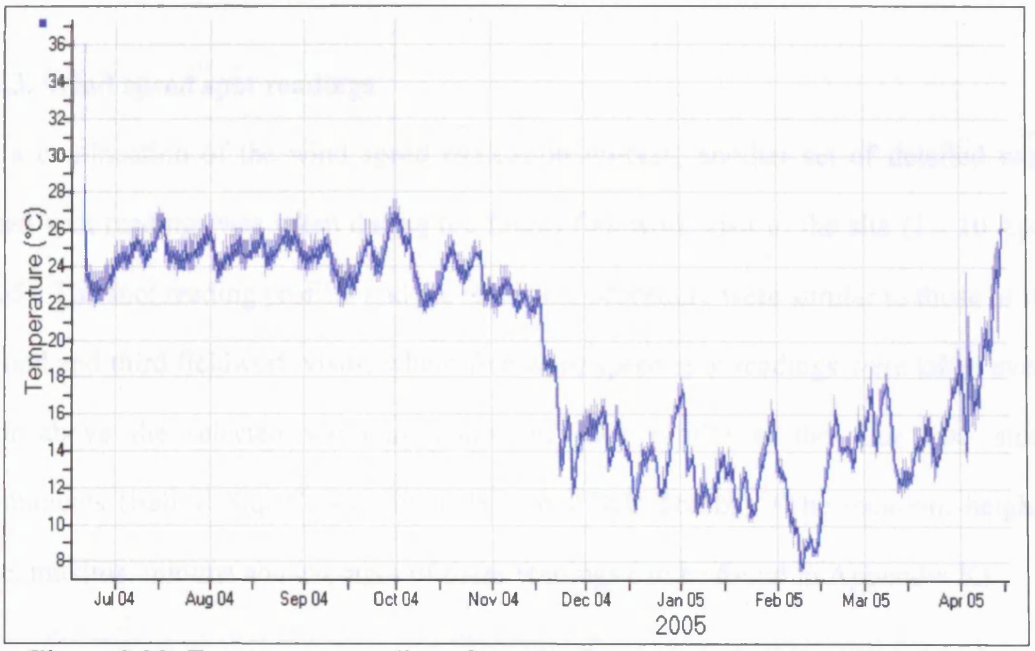

Figure 8.29: Temperature readings from the data logger. Location: Deir Tomb. (Recorded period: 20 June 2004-16 April 2005).

Month	Maximum (°C)	Minimum (°C)	Average (°C)	Number of readings
June 2004 (20-30)	36.10	21.75	23.30	256
July 2004 (1-31)	27.21	23.39	24.90	759
August 2004 (1-31)	26.85	23.06	24.89	755
September 2004 (1-30)	27.85	21.75	24.41	731
October 2004 (1-31)	27.58	21.43	23.87	757
November 2004 (1-30)	24.06	11.46	19.26	731
December 2004 (1-31)	17.72	10.65	14.17	755
January 2005 (1-31)	17.13	10.11	12.57	757
February 2005 (1-28)	17.13	7.47	12.07	683
March 2005 (1-31)	19.54	11.46	14.98	756
April 2005 (1-16)	21.11	19.54	19.79	351

Table (8.6): Monthly maximum, minimum, and average temperature readings. Location: Deir Tomb. Recorded period: 20 June 2004 – 16 April 2005

8.5.3. Wind speed spot readings

As a continuation of the wind speed evaluation process, another set of detailed wind speed spot readings was taken during the fourth fieldwork visit to the site (1 - 10 April 2005). The spot reading profiles and the recording procedure were similar to those of the second and third fieldwork visits, where five wind speed spot readings were taken every hour above the selected sampling points of each profile at the four case study monuments (Bab al Siq, Corinthian, Palace and Deir Tombs). (The location, heights, date, maxima, minima and averages of these readings can be found in Appendix K).

In the main, compared to the previous fieldwork visits, the overall averages of the wind speed readings from this fieldwork trip showed higher wind speed figures. For instance,

the overall average of wind speed readings during the day-time hours above the sampling point 350 cm at the C2 profile of the Palace Tomb were 1.29 and 1.7 m/s for this period, but just above 1 m/s in January. On the other hand, the fluctuation rates within the same sampling point were slightly lower than the previous fieldwork data for all four locations.

- By comparing the wind speed spot readings from the four case-study monuments (Appendix K), the following remarks could be made:
- Fluctuation was still the main characteristic feature of the wind. Fluctuation was noted not only between two monuments, or between two sampling points of the same monument, but also at the same sampling point at different recording times.
- The second profile at the Deir Tomb (D2) had the lowest overall wind speed averages, while the second profile at the Palace Tomb (C2) had the highest overall wind speed figures.
- The readings above the D2 profile had the lowest fluctuation rate and above the C2 profile the highest fluctuation rate.
- The wind speed increased considerably with the height at each monument. For example, the overall averages of the wind speed spot readings at the Bab al Siq Triclinium increased from around 0.85 m/s above the sampling point of the 5 cm height to 1.05 m/s above the sampling point of 350 cm height.
- The Corinthian Tomb readings showed not only high overall averages of wind speed (around 1.1 m/s), but also slightly high fluctuation rates.
- At the Palace Tomb, the data from profile C1 and C2 demonstrated both high wind speeds and high fluctuation rates, compared to profile C3 at the same monument.

- The wind speed readings from the Deir Tomb showed a slight difference between profile D1 and D2, with higher wind speed and higher fluctuation rates at the D1 profile.
- The wind speed spot readings from the Nabateans Hotel during the night-time showed very high wind speed figures. The highest wind speed readings were recorded in the early hours of each day (01.00 and 02.00)
- In summary, one can conclude that the daily wind speed figures from the fourth fieldwork visit are very similar to the previous fieldwork figures, but with higher averages. The Palace and Corinthian Tombs had the highest wind speed readings and the highest fluctuation rates, while the Bab al Siq and Deir Tombs had the lowest wind speed readings and the lowest fluctuation rates.

8.6. Petra microclimate conditions: summary and role in the salt damage process

All things considered, the temperature readings were much more stable than the relative humidity readings. Even though the relative humidity monthly overall averages did not differ greatly from one another, the individual relative humidity readings varied significantly. May, June, July, September and October were moderately dry and hot, while November and December had similar humidity averages but were colder. January and February were slightly humid and quite cold months. In March and April both temperature and relative humidity were unstable with overall humid and rather cold conditions.

Generally, Petra microclimate data demonstrate the domination of the dry, hot and fluctuating wind speed conditions throughout the majority of the year. Besides, the high

rate of fluctuation of the relative humidity and wind speed around the studied monuments was very obvious. The data reveal high fluctuation of these factors not only between one period of the year and another, but even between one location and another within the same period. A considerable variation was also noted between readings that came from the same monument and at the same time, but from different sampling points. Moreover, the wind speed figures showed that the Palace Tomb had the highest wind speed readings and also the highest rates of fluctuation in all the fieldwork visits. By and large, the wind speed fluctuation rates during daytime were higher than during night-time.

By comparing and relating the spot readings for the three environmental factors (temperature, relative humidity and wind speed), the impact of the wind speed on relative humidity was evident. As the wind speed increased, the relative humidity dropped slightly, a condition that could be related to the dry nature of the wind in the Petra area. The fall of the relative humidity was, in effect, accompanied by an increase in the temperature.

8.7. Conclusion

The evaluation of the microclimate conditions at Petra strongly demonstrates the importance of the detailed microclimate monitoring approach in evaluating the salt damage mechanism at that site. As mentioned earlier in chapter 2 and 3, the microclimate conditions are the key factors in activating the salt damage in porous materials. Therefore, there was no doubt that the evaluation of the microclimate

conditions at the site was crucial, but the way of carrying out a monitoring survey at a site of the size of Petra was complicated. Would a general overview of the microclimate conditions be sufficient or would a detailed survey of one of the monuments be representative of the rest? Neither of these methods would have been correct. It is clear, from both the spot reading measurements and the data logger readings, that all monitored environmental conditions varied not only from one site to another and from one day to another, but also from one point to another on the same site and day. Such phenomena indicate that the more detailed the microclimate approach at the site, the more accurate the evaluation of the salt distribution and crystallisation would be. On the other hand, these phenomena elucidate the complexity of understanding the salt damage mechanism at the monuments of Petra, since its main activation factors (the environmental conditions) are highly variable both with time and location.

For these reasons, the research strategy of collecting detailed microclimate data from four different locations at different times of the year was the best that could be achieved within the scope and time available for this study.

Investigation into the interrelation between the substrate, the solution and the surrounding environmental conditions is the key factor for understanding the salt damage process. This chapter has evaluated in great detail the microclimate conditions at the case study monuments. However, this alone, without the consideration of the salt types and distribution, cannot shed adequate light on the mechanism of salt damage at the studied monuments. The following chapter will discuss and evaluate Petra salts and their distribution as analysed from the samples taken during each fieldwork visit.

Chapter 9
Petra: Salt Types and Distributions

9.1. Introduction

The determination of the salt types and their distribution in the case study monuments at Petra has a great importance in understanding and evaluating the weathering process at these monuments. The types of salts, their depth of accumulation, the pore structure and moisture regimes as well as the surrounding microclimate conditions are the main features controlling the decay of stone materials (Nicholson 2001, Winkler 1994, Doehne 1994 and Rossi-Manaresi and Tucci 1991). Moreover, as discussed in detail in chapter 2, different types of salt have different effects on the weathering process of porous building materials. For example, sodium sulfate is well known as a destructive salt, while sodium chloride is one of the least damaging salts, at least in laboratory tests (Doehne 1994, Rodriguez-Navarro, Doehne and Sebastian 2000). In addition, different salts react differently to the surrounding environmental conditions. According to Goudie and Viles (1997), the solubility of some salts, such as sodium sulfate and magnesium sulfate, rapidly decreases when the temperature falls, while the solubility of other salts, such as sodium chloride, is much less affected by changes in temperature. Furthermore, the location where the salt(s) crystallise(s) out of the solution is a dynamic balance between moisture uptake and moisture loss in the porous system. Therefore, the knowledge of the salt types and their distribution at the case study tombs in Petra is a vital aspect not only for the understanding of the thermodynamics of the salt damage process, but also for the understanding of the kinetics of this process.

While chapter 6 introduced the main physical properties of Petra monuments and chapter 8 presented the microclimate monitoring programme at the site, this chapter will examine and evaluate the salt distribution in the case-study monuments in Petra.

The content of soluble salts in porous building materials varies with time; therefore, the evaluation of the ions content in the case study monuments should follow a set procedure. The ions content of the samples collected from the four case study monuments was examined in detail. The samples were collected during 4 fieldwork visits in different seasons, two of which represented the extremes of the area's climate, summer (August 2003: first fieldwork visit) and winter (January 2004: second fieldwork visit), and the other two periods between the extremes (June 2004 and April 2005). One could argue that the outcomes of these fieldwork data might not represent the actual phases of the soluble salts at the site, since phase transitions could happen in very short period of time. However, the author's argument is that the samples were collected during four different seasons when major climatic changes take place in the area and these samples were accompanied by spot readings for the major environmental conditions. By combining the salts content and the microclimate conditions from the same location, the salts distribution in the studied monuments could be evaluated.

In this chapter, the sampling strategy and the sampling profiles of each monument will be presented. Then, the anion and cation content of the samples collected from each monument in the four sampling seasons will be identified and discussed. Finally, the relation between the microclimate conditions and the soluble salts content, types and distribution at the studied monuments will be examined and evaluated.

9.2. Sampling strategy

The first step of the sampling strategy was to select the case study monuments, following the fieldwork observation of the weathering features, the location and the surrounding environment, as discussed in chapter 6. The next step was to select the sampling profiles at each monument. Due to the huge size of the monuments and the fact that different parts of the same monument have different ambient conditions (some are in sheltered areas, others are partly in open spaces), the sampling strategy was extended to more than one sampling profile in each monument. The selection of the sampling points in each sampling profile also proved to be quite difficult. Different scholars used different sampling methods in their studies to evaluate the salt distribution and behaviour in porous materials. Prokos (2005) preferred a spatial sample selecting method based on the extent of salt content fluctuation between the lowest and the highest damage zone of the studied wall painting, while other scholars such as Von Konow (2002) used regular sampling intervals. The scope of this research suggested that since the case study monuments were chosen following a comparative observation, and since the surrounding environmental conditions and especially the wind speed factor varied from one location to another, a system based on regular sampling intervals was more suitable. The samples were collected from the selected profiles with an interval of 50 cm between each sample.

Because of their different solubilities, the salts distribution varies with height, and samples needed to be collected from different heights at each profile. The sampling profiles varied in height from one monument to another, depending not only on accessibility and technical issues, but also on ethical grounds. For example, where the

samples were collected from the carved façades, the heights of the sampling profiles were limited.

Salts at different depths react differently to the surrounding environmental conditions, and therefore have a different effect on the supporting materials. Following the field observations, it was found that these monuments had weathering categories such as granular disintegration, alveolar weathering and contour scaling. All these features suggested not only involvement of soluble salts, but also their crystallisation in the deeper layers of the monuments. As a result, the sampling strategy included collection of samples from different depths at the same sampling point.

All in all, the sampling strategy in this research was not based on regular sampling intervals alone, since the location of the monuments, their weathering features, and the variation of their surrounding environmental conditions were also considered to be key factors.

9.3. Selected monuments and sampling profiles

- The Bab al Siq Triclinium Tomb

Bab al Siq Triclinium Tomb was the first tomb to be chosen as a case study monument at Petra. Its highly deteriorated state, the accessibility of the site for sampling as well as its location (at the edge of the main Wadi on the site) were the main reasons behind its selection. In the first fieldwork visit (late summer fieldwork visit), three sampling profiles were selected on the site (T1, T2 and T3) (Figure 9.1). A total of 23 samples were collected from these profiles (17 from T1, 3 from T2 and 3 from T3). Most

samples were taken from three different depths at each sampling point (0-1, 1-3 and 3-5 cm), but at some sampling points samples were collected from only two depths. The location of these sampling points (near the carved façades) or the difficulty to access the sampling points were the main reasons for reducing the number of sampling intervals at certain places. For the full record of sampling heights[17] and depths see the salts content results in table B1: appendix B.

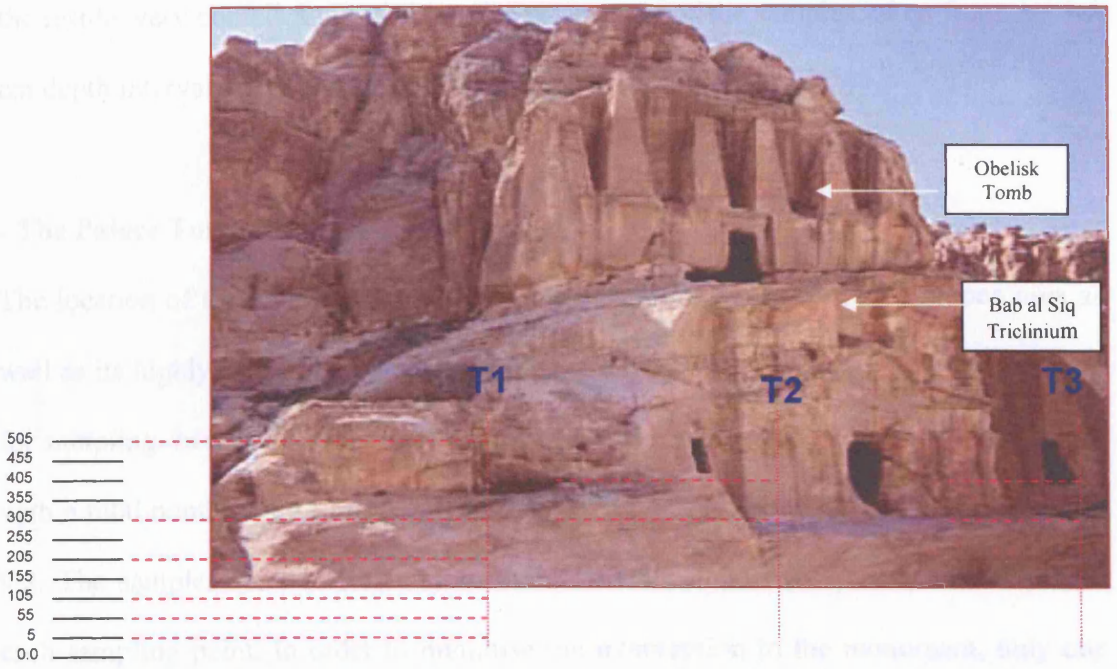

Figure 9.1: The sampling profiles at the Bab al Siq Triclinium Tomb.
(Note: The laboratory samples were collected from the stratum at the left of T1 profile.)

The reason for having three cross-sections on the same site is to get an overview of the salt distribution at the monument and to study the variation between sheltered places, where the impact of the surrounding environmental conditions is minimised (T2), and

[17] Sampling heights are the heights of the sampling points above ground surface in front of the monuments.

open places (T1). In order to ensure minimum intervention to the site, no samples were taken from the carved façades.

During the other fieldwork visits, samples were taken from the same sampling profiles and the number of samples was increased by adding new sampling points to each profile (32-34 samples at each visit). However, the sampling depths were limited to two intervals (0-1 and 1-3 cm). The reason for such a limitation was to reduce the huge amount of data that the first fieldwork sampling provided, making the interpretation of the results very complicated. Besides, the salt content of the samples taken from the 3-5 cm depth interval at the first fieldwork visit was quite low.

- The Palace Tomb

The location of the Palace Tomb on the edge of a mountain and in a very open area as well as its highly deteriorated state were the main reasons for selecting it as a monument for sampling. In the first visit, three sampling profiles were taken from the Palace Tomb with a total number of 42 samples (23 from C1, 11 from C2 and 8 from C3) (see figure 9.2. The samples were collected from three different depths (0-1, 1-3 and 3-5 cm) at each sampling point. In order to minimise the intervention to the monument, only one sampling profile was taken from the carved façade and the samples taken were very small (less than 1 g).

For the rest of the fieldwork visits, samples were taken from the same profiles with between 35-45 samples at each visit, but the sampling depths were limited to two intervals only (0-1 and 1-3 cm) for reasons similar to those mentioned for the Bab al Siq Tomb.

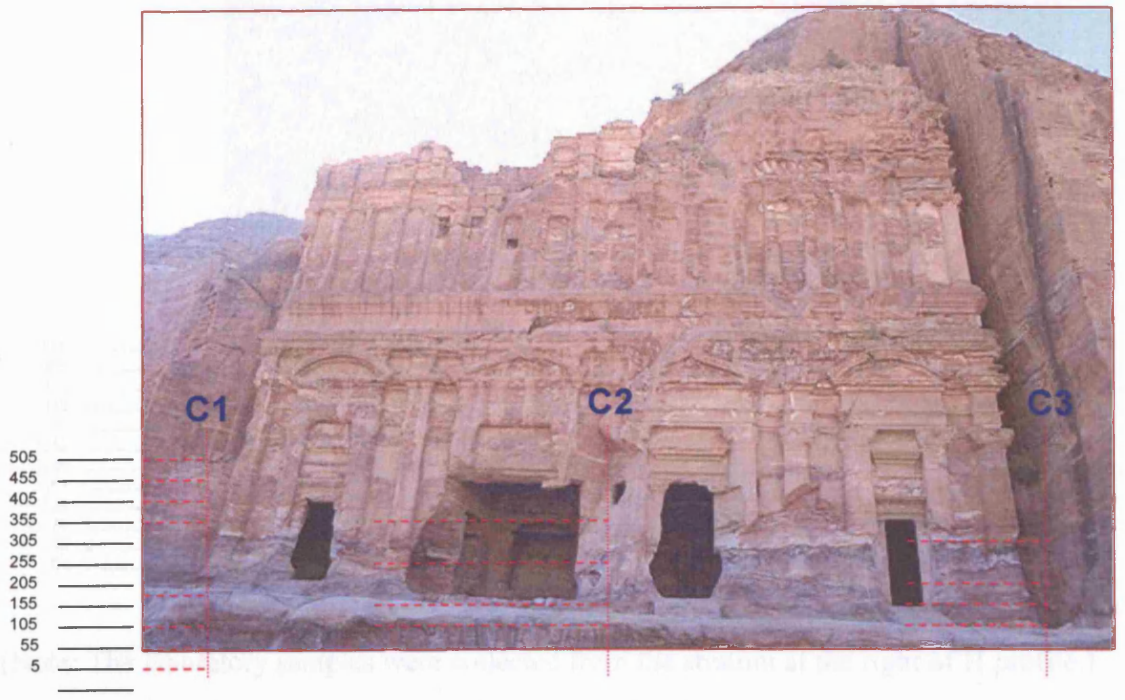

Figure 9.2: The sampling profiles at the Palace Tomb.
(Note: The laboratory samples were collected from the stratum at the left of C1 profile.)

- The Corinthian Tomb

The Corinthian Tomb (figure 9.3) has lost most of its features due to deterioration. The tomb is the most deteriorated carved monument in Petra and, thus, having a sampling profile from this monument is essential for the current research. Only one profile was taken from the monument due to its fragile state. Between 13-18 samples were collected from this profile at each visit. The samples were collected from only two depths (0-1 and 1-3 cm) throughout the sampling campaigns.

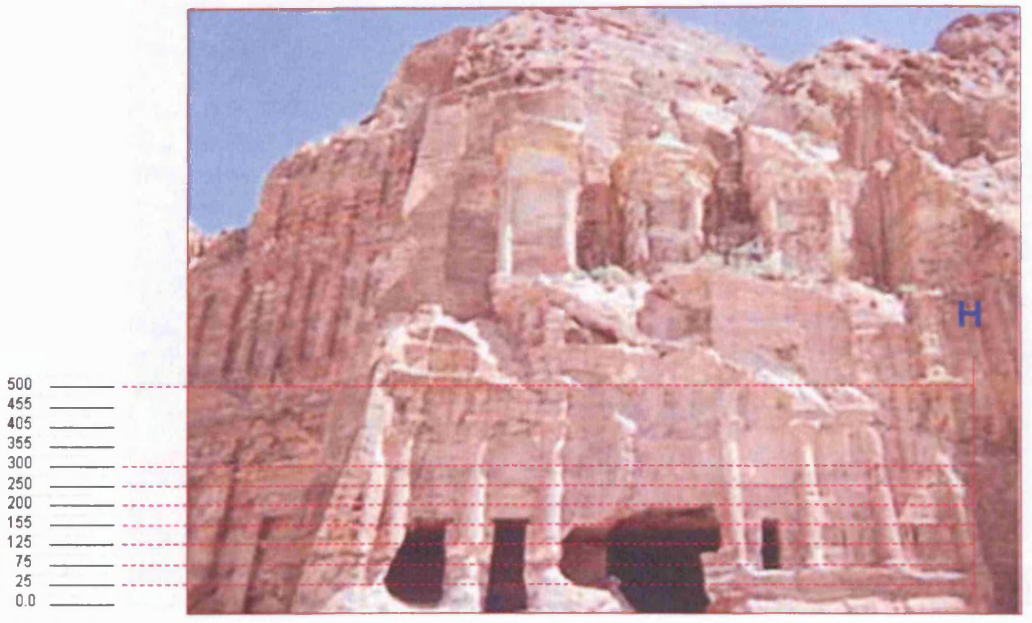

Figure 9.3: The sampling profile at the Corinthian Tomb.
(Note: The laboratory samples were collected from the stratum at the right of H profile.)

- The Deir Tomb

The location of the Deir Tomb on the edge of a high mountain and the presence of two different levels of stone decay between its two storeys were the main reasons for selecting this monument for sampling. Two sampling profiles were taken from the Deir Tomb (figure 9.4); to minimise the level of intervention neither was from the carved façade. 32 samples were collected from this area during the first fieldwork visit. At D1 profile, samples were collected from three different depths (0-1, 1-3 and 3-5 cm), while at D2, samples were collected from only two different depths (0-1 and 1-3 cm). For the rest of the fieldwork visits, between 22-26 samples were collected and the sampling depths were reduced to two intervals only (0-1 and 1-3 cm).

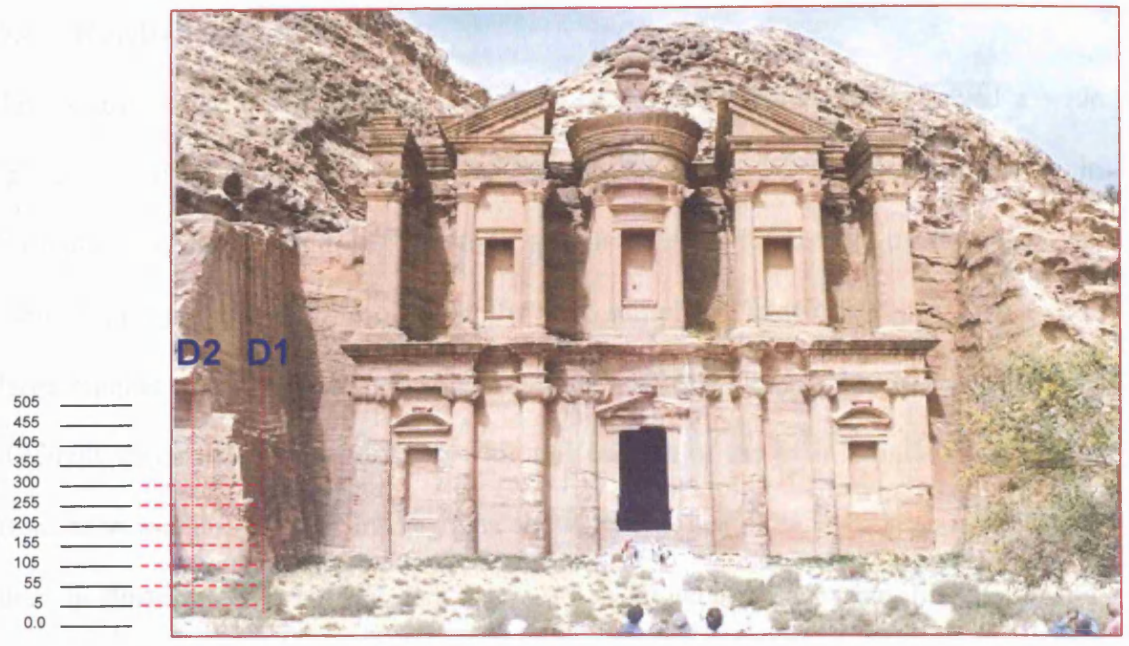

Figure 9.4: The sampling profiles at the Deir Tomb.
(Note: The laboratory samples were collected from the stratum at the left of D2 profile.)

In all monuments, the sampling points on the second, third and fourth fieldwork visits were at the same heights as the first fieldwork visit sampling points, with 2 cm horizontal distance between them from one visit to the next.

9.4. Cation and anion content analysis

In order to identify the total salt content in each of the samples collected from each monument at the four sampling fieldwork visits, the cation and anion content of these samples was measured. The cation content was measured using an inductively coupled plasma atomic emission spectrometer (ICP-AES), while the anion content was measured using ion chromatography (IC). The analytical methods are shown in chapter 7. The total soluble content in all analyses was expressed as the weight % of salt per weight unit of dried stone powder sample (0.2 g).

9.4.1. Results and discussion

The results of the anion and cation analysis of the collected samples showed a wide range of variation. The full results of the ICP-AES and IC analyses are shown in appendices B, E, H, and L. The following is a brief discussion of these results, monument by monument, throughout the four sampling fieldwork visits. Due to the large number of samples and variables from the analysis, the data are presented in four different ways: firstly in a summary with a discussion of the main points of the results from each monument, then in diagrams showing the overall salts content at each site, then in diagrams showing the cation and anion content at each sampling point and, finally, in tables showing the detailed results. The last two presentations are attached in appendices, however, an example of a cation and anion distribution diagram is presented with the results from the first monument (Bab al Siq Triclinium).

9.4.1.1. Bab al Siq Triclinium Tomb results

In the 23 analysed samples from the three sampling profiles at the Bab al Siq Triclinium Tomb taken during the first fieldwork visit (late summer fieldwork visit), sodium and calcium were the major cations, while magnesium, potassium, aluminium and iron were secondary components. On the other hand, chloride, nitrate and sulfate were the main anions. The results of the first fieldwork visit will be discussed in detail since they have been used as a reference point for the salts distribution throughout the following fieldwork visits.

The total soluble salts content at the first profile (T1) ranged between 0.09 and 0.94 % with an average of 0.27 %. By looking at the total soluble salts content from different

heights and depths at this profile (table B1: appendix B, figure 9.9), a general trend of salt distribution can be observed. The total soluble salts content in the two depth intervals (0-1 and 1-3 cm) started very low at low height and increased gradually up to the height of around 105 cm, where it started to drop again.

Moreover, the total soluble salts content usually decreased with height. These figures support the theory that the groundwater is the main source of soluble salts in the area and that salts will rise up to a certain height and crystallise gradually according to each salt's solubility and reaction with the surrounding microclimate. The renewed increase of the soluble salt content in heights over 305 cm might be explained by the presence of wide terraces that can hold water either from the rain or from the damaged water channels creating another possible source of salts solution above that level. Furthermore, the highest concentration of soluble salt was mainly at the 0-1 cm depth interval, however, considerable amounts of salts were found at deeper intervals indicating that the evaporation rate was very high and so salts crystallised underneath the surface (subflorescence). (Figure 9.5).

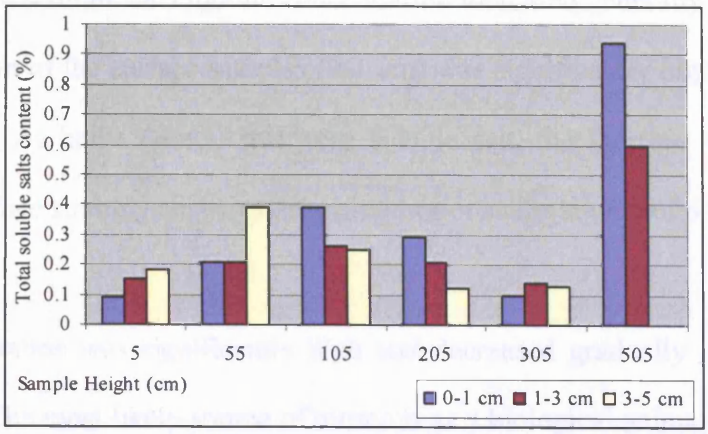

Figure 9.5: The total soluble salts content at Bab al Siq Triclinium Tomb. Location: T1 (Depth intervals: 0-1, 1-3 and 3-5 cm). First fieldwork visit.

Regarding the salt types and salt origins, the results showed a correlation between calcium and sulfate in most of the samples. The calcium and sulfate concentrations mainly increased with height and decreased with depth. Despite the fact that calcium sulfate is a sparingly soluble salt and, therefore, should concentrate in the lower parts of the monuments, its higher concentration at higher levels has two possible explanations. The first reason could be the washout of the calcium sulfate salt by running water in the lower part of the sampling profile during winter, since the sampling profile is just above a valley where rain water accumulates. It is also quite probable that different cations and anions formed very soluble salts that interacted with calcium sulfate and changed its thermodynamic properties (see figures: 1Bb and 2Bb: appendix Bb. Note: these figures are presented below as an example of the cation and anion distribution. The distribution at each site throughout the four different sampling fieldwork visits is presented in appendices Bb, Eb, Hb and Lb).

Another observation was the correlation between sodium and chloride in the majority of the samples. The sodium and chloride concentration increased generally with height and the concentration of the surface samples (0-1 cm) was significantly higher than at other depth intervals. As halite (NaCl) is a very soluble salt, the increase with height and towards the surface strongly suggests the groundwater as the source of origin of this salt.

Nitrate concentration was significantly high and decreased gradually in samples from higher depths. The most likely source of nitrate is as a biological animal by-product (the author has witnessed sheep and goats grazing around the site).

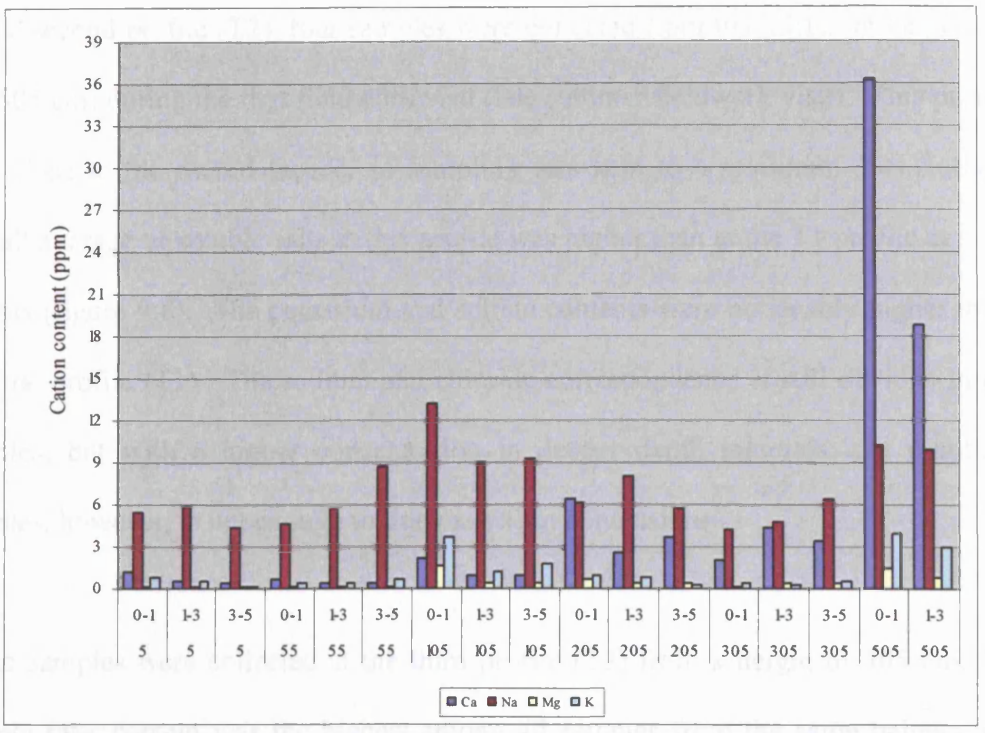

Figure 9.6 (also 1Bb in appendix Bb): The main cation content at the Bab al Siq Triclinium Tomb (T1) (Depth intervals: 0-1, 1-3 and 3-5 cm). First fieldwork visit.

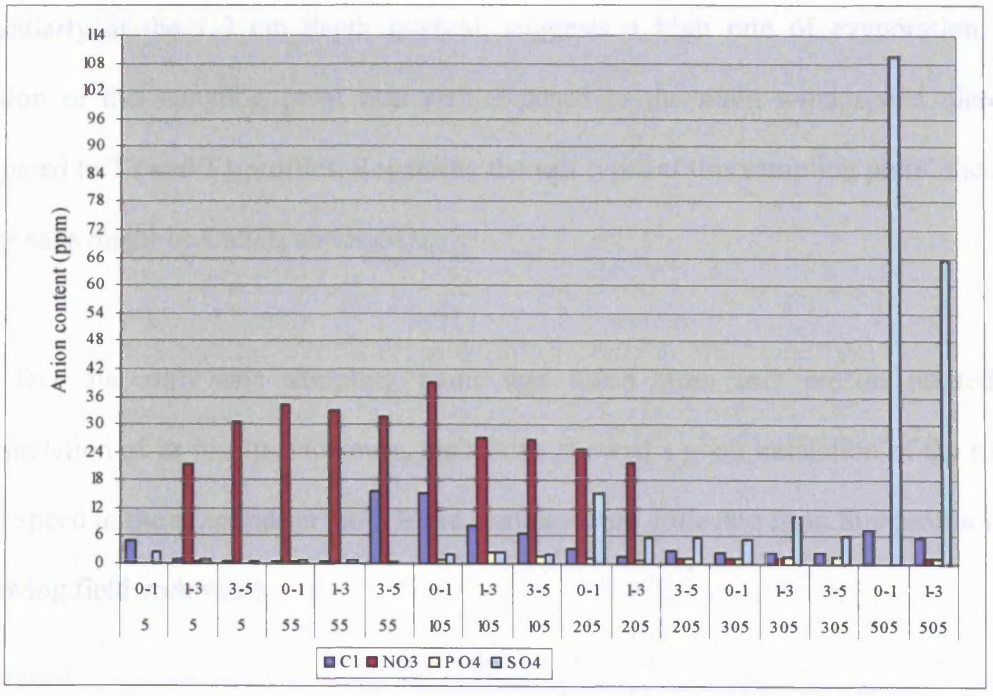

Figure 9.7 (also 2Bb in appendix Bb): The main anion content at the Bab al Siq Triclinium Tomb (T1) (Depth intervals: 0-1, 1-3 and 3-5 cm). First fieldwork visit.

At the second profile (T2), four samples were collected from two different heights (305 and 505 cm) during the first fieldwork visit (late summer fieldwork visit). This profile is very close to the carved façade, so sampling was kept to a minimum. Generally, the overall average of soluble salts at this profile was higher than at the T1 profile at similar heights (figure 9.8). The potassium and sulfate contents were noticeably higher than in the first profile (T1). The sodium and chloride correspondence is still obvious in these samples, but with a higher concentration in deeper depth intervals; the number of samples, however, is not enough to draw any firm conclusions.

Three samples were collected at the third profile (T3) from a height of 305 cm. Their soluble salts content was the highest among all samples from the same heights at the three profiles (figure 9.8). The high concentration of salts at this sampling point, and particularly at the 1-3 cm depth interval, suggests a high rate of evaporation. The location of the sampling point was well exposed to the main wind speed direction compared to T2 and T1 profiles. Regarding the salt types at this sampling point, the most likely salts might be $CaSO_4$ and K_2SO_4.

The fact that only one sampling point was taken from this profile limited the interpretation of its results. However, the results showed a good indication of the role of wind speed in the evaporation rate. More samples were collected from this profile in the following fieldwork visits.

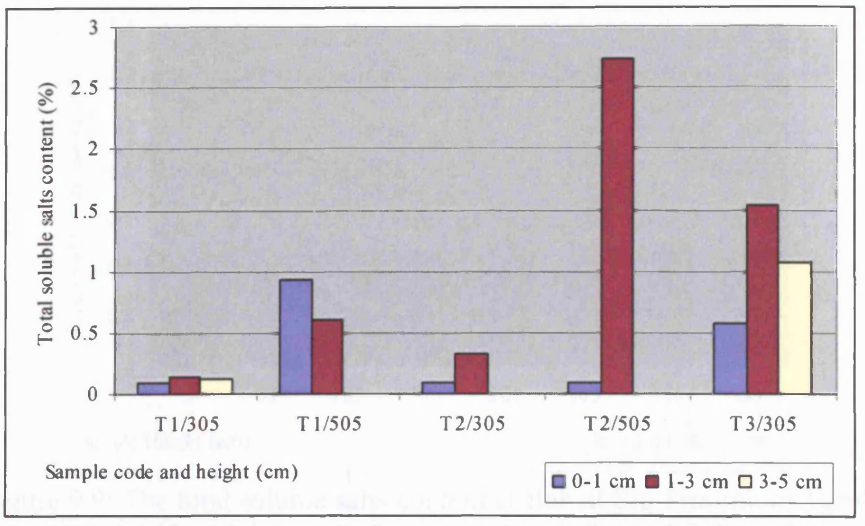

Figure 9.8: The total soluble salts content in five different locations at Bab al Siq Triclinium Tomb. First fieldwork visit.

During the winter fieldwork visit, in January 2004, the cation and anion results of the 27 samples from Bab al Siq Triclinium Tomb (20 from T1, 4 from T2 and 3 from T3) showed that sodium and calcium were the main cations and sulfate and chloride the main anions. Magnesium, nitrate and phosphate existed in low concentrations. The soluble salts content varied largely from one sample to another (see table E1 in appendix E). In the first sampling profile (T1) the overall average of the soluble salts content was 0.37 % and 0.55 % at the 0-1 cm and 1-3 cm depth intervals respectively. Generally, the soluble salts content increased with depth (see figure 9.9).

The presence of wide terraces just below the 305 cm sampling point, where water usually accumulates during the winter season, could explain the significant increase in the total soluble salts content at the 305 and 505 cm height.

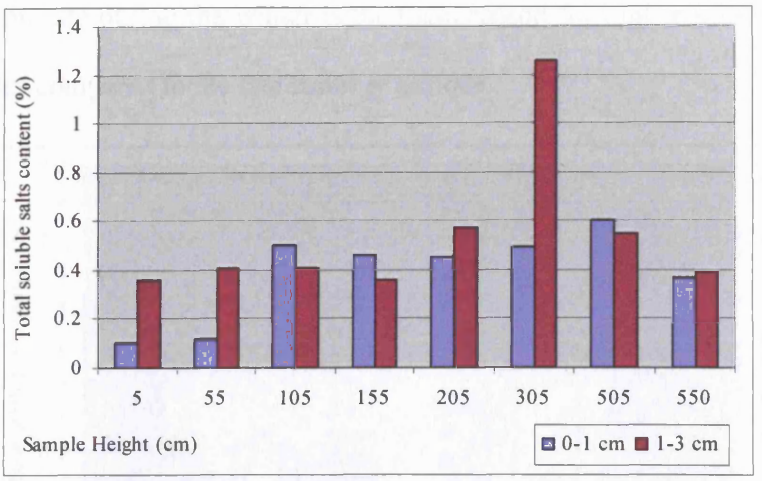

Figure 9.9: The total soluble salts content at Bab al Siq Triclinium Tomb. Location: T1 (Depth intervals: 0-1 and 1-3 cm). Second fieldwork visit.

By and large, the total soluble salts content was much higher during this period. It should also be noted that this could be even higher if all anions had been detected by the analysis. The cation charge was much higher than the anion charge, suggesting a missing anion or a fault in the anion readings. However, a fault in the readings is unlikely since frequent calibration was undertaken during the analysis of the samples. This leaves the undetected carbonate and/or bicarbonate anions as the most likely reason for the high cation charge.

Similar anion and cation contents were found at the other two sampling profiles (T2 and T3) with sodium, calcium and sulfate being dominant (table E1: appendix E). The highest concentration was at T3 at the 1-3 cm depth interval (figure 9.10).

Generally, at these two profiles the soluble salts content was higher at shallow depths and also much higher compared to the salts content of the first fieldwork samples. The

low evaporation rate during the winter is the main reason for higher salts content in the surface samples compared to the late summer periods.

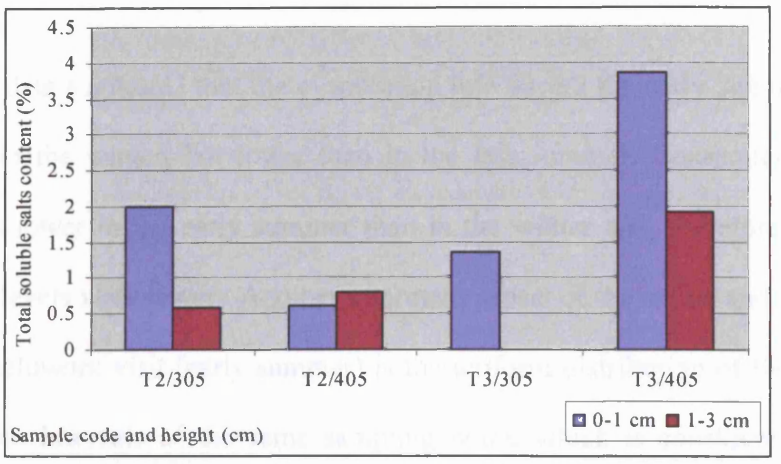

Figure 9.10: The total soluble salts content at Bab al Siq Triclinium Tomb. Location: T2 and T3 (Depth intervals: 0-1 and 1-3 cm). Second fieldwork visit.

By looking at the cation and anion percentages and charges (see table E1: appendix E and figure 1Eb: appendix Eb) it appears that the cation charges were much higher than the anion charges indicating one or more missing anions in the data from the analyses. It is likely that carbonate and/or bicarbonate anions were the undetected ones, causing such unbalanced charges.

The total soluble salts content at the Bab al Siq monument during the third fieldwork visit (June 2004: early summer fieldwork visit) was lower than in the winter fieldwork visit, but considerably higher than in the late summer fieldwork visit (figures 9.11, 9.12 and 9.13 and tables H1 and H2: appendix H) . June, as was shown by the recorded microclimate conditions (chapter 8), is the start of the summer season on the site when relative humidity readings were higher than in the late summer season (August). On the

other hand, the temperature readings in June were much lower than in August, but much higher than in January.

All previous data suggested that the evaporation rate during the early summer visit was higher than in the winter, but lower than in the late summer. Consequently, the salt mobility was lower in the early summer than in the winter and, therefore, the overall soluble salts levels were lower. Another important aspect of the cation and anion results during this fieldwork visit (early summer) is the uniform distribution of the salts in the different depth intervals of the same sampling point, which is considerably different from the results of the winter fieldwork visit. Ca-SO_4 and Ca-NO_3 as well as Na-Cl correspondence trends were dominant in this monument.

Once again, T3 samples had the highest overall average of the soluble salts content and T2 samples the lowest average (see figures: 9.12 and 9.13).

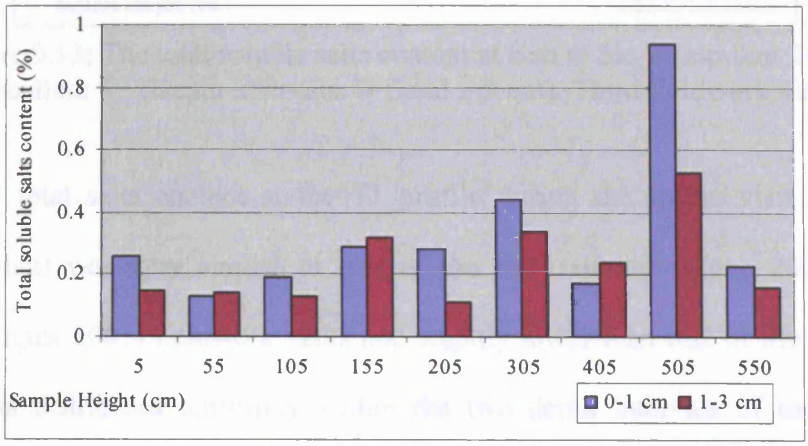

Figure 9.11: The total soluble salts content at Bab al Siq Triclinium Tomb. Location: T1 (Depth intervals: 0-1 and 1-3 cm). Third fieldwork visit.

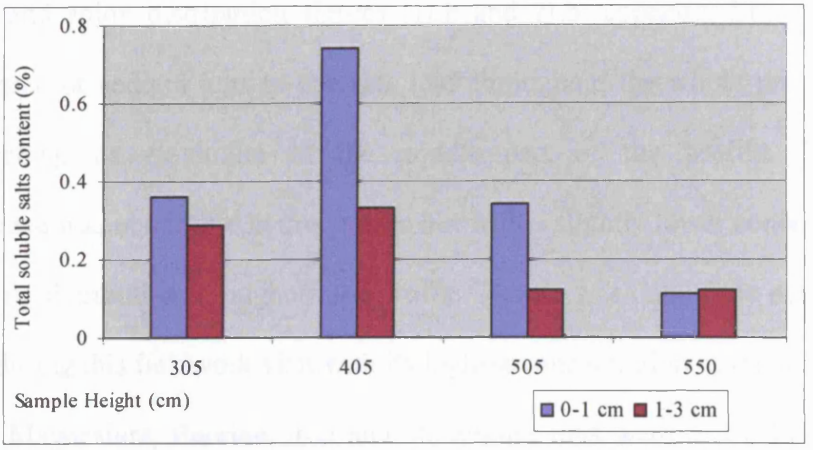

Figure 9.12: The total soluble salts content at Bab al Siq Triclinium Tomb. Location: T2 (Depth intervals: 0-1 and 1-3 cm). Third fieldwork visit.

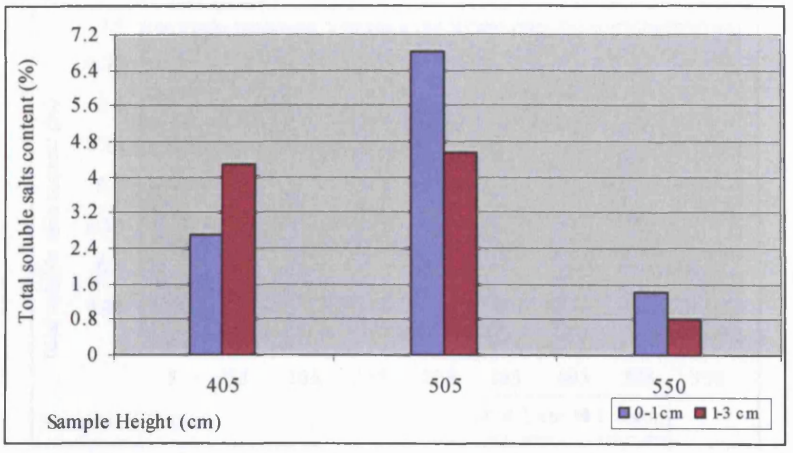

Figure 9.13: The total soluble salts content at Bab al Siq Triclinium Tomb. Location: T3 (Depth intervals: 0-1 and 1-3 cm). Third fieldwork visit.

The overall total salts content at the T1 profile during the spring visit (April 2005 fieldwork visit) was very similar to that of the early summer (June 2004) and late summer (August 2003) fieldwork visits and slightly lower than that of the winter visit. Soluble salts distributed uniformly within the two depth intervals of each sampling point, with slightly higher concentration in the surface samples (0-1 cm) especially at the middle heights of the profile (figure 9.14 and table L1: appendix L).

The cation and anion distribution figures (1Lb and 2Lb: appendix Lb) show a clear correspondence of sodium ions to chloride ions throughout the whole profile with the system reaching its maximum in the middle part of the profile. Ca-SO_4 ion correspondence was noticeable in this profile but with a slightly lower concentration and more uniform distribution throughout the profile. Nitrate was one of the main anions in the profile during this fieldwork visit with its highest concentration in the middle part of the profile. Magnesium, fluorine, iron and aluminium ions were found in most of the samples, but in very low concentrations.

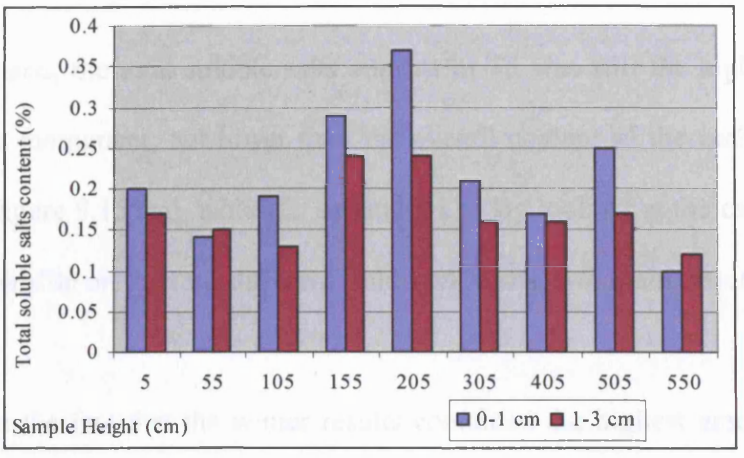

Figure 9.14: The total soluble salts content at Bab al Siq Triclinium Tomb. Location: T1 (Depth intervals: 0-1 and 1-3 cm). Fourth fieldwork visit.

The total soluble salts content at the second profile (T2) was higher than at T1 and very similar to the early summer fieldwork visit (June 2004) with calcium and sodium as the main cations and chloride, nitrate and sulfate as the main anions (see figure 9.15, table L2: appendix L and figures 3Lb and 4Lb: appendix Lb).

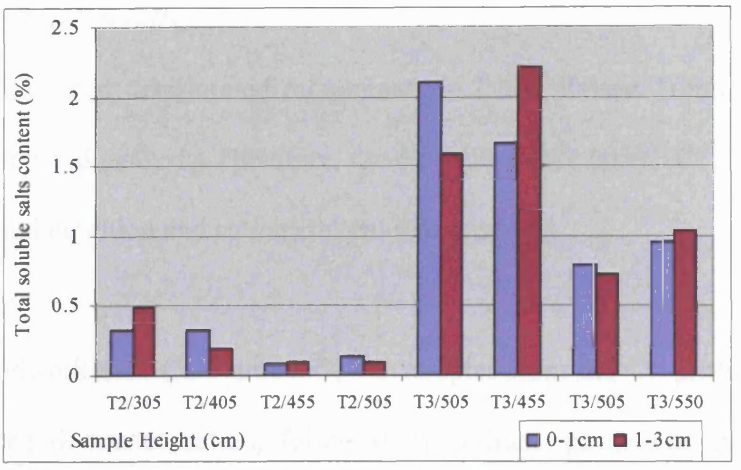

Figure 9.15: The total soluble salts content at Bab al Siq Triclinium Tomb. Location: T2 and T3 (Depth intervals: 0-1 and 1-3 cm). Fourth fieldwork visit.

On the other hand, the total soluble salts content in T3 was still the highest among all profiles of this monument, but lower than the overall content of the early summer and winter visits (figure 9.15 and table L2: appendix L). By looking at the cation and anion figures of the profile on the four different fieldwork visits, two main observations can be made:

- Besides the fact that the winter results contained the highest amount of soluble salts in the monument, they introduced potassium in a very high percentage compared to other profiles.
- Despite the variation of the total soluble salts content at this profile between the seasons, the main cations and anions not only remained unchanged throughout but their distribution at all heights of the profile also followed a very similar trend.

9.4.1.2. Palace Tomb results

Being one of the most deteriorated monuments in Petra, Palace Tomb required more detailed sampling and analysis. Therefore, three profiles were taken (C1, C2 and C3: see section 9.3) and their anion and cation content was analysed.

At the first fieldwork visit (late summer), the samples from the C1 profile showed that calcium was the dominant cation, followed by sodium, potassium, magnesium and aluminium. The samples contained minor amounts of iron. On the other hand, chloride, sulfate and nitrate were the main anions, with a high percentage of bromide in certain samples. Phosphate was found in most of the samples but in a very small amount (see table B1: appendix B).

The total soluble salts content of this section during the late summer visit was generally higher than at the Bab al Siq Tomb in the same period (figure 9.16).

The surface samples from the low height (0-200 cm) had a relatively high percentage of soluble salts, with sulfate and nitrate being the main anions and sodium and calcium the main cations. Animal by-products are the most likely source of nitrate in this area, while groundwater is the main source of the other salts. The samples from the (1-3 cm) depth had lower soluble salts content, while samples from the (3-5 cm) depth had even less. This means that at this profile the soluble salts content generally decreased with depth (figure 9.16).

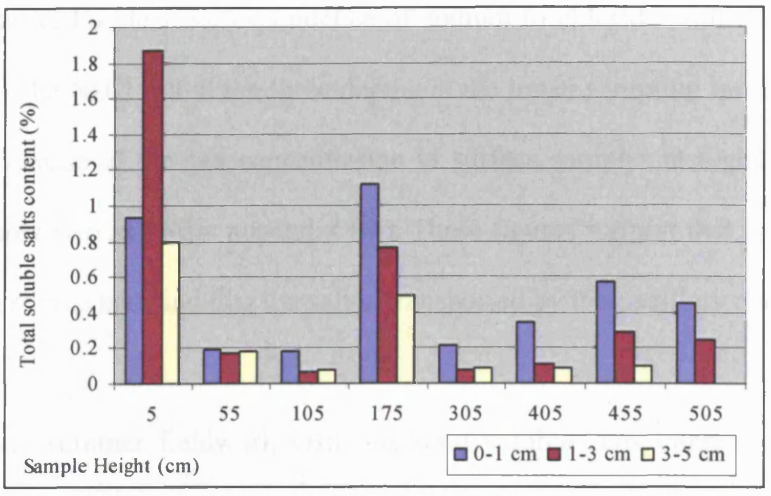

Figure 9.16: The total soluble salts content at Palace Tomb. Location: C1 (Depth intervals: 0-1, 1-3 and 3-5 cm). First fieldwork visit.

Horizontally, namely according to the height of the sample site, the total soluble salts content had a more or less similar trend over all three different depth levels (0-1, 1-3 and 3-5 cm) where the salt content started quite high at the lower height (5 cm), then kept decreasing until it reached its minimum at the 100 cm height, where it started to increase again until the 200 cm height. After that, it started decreasing again until the 350-400 cm height, where it increased slightly. All the previous indications suggest that there are two sources of soluble salts: one external (the nitrate) and one internal (the sulfate). Thus, the high percentage of soluble salts at the low height and surface samples could be correlated to the external source of salts, while the slightly higher soluble salts solution at the higher levels (200 cm) and deeper depths (1-3 and 3-5 cm) could be correlated to the internal source of salts. The increase of soluble salts content at around the 350-400 cm height could be due to the presence of a wide terrace to the left of the profile where rainwater accumulates.

The results showed a clear correspondence of sodium to chloride with slightly uniform distribution of the NaCl salt at the three depths in the lower sampling levels (0-175 cm), and a clear increase of the salt concentration in surface samples at higher levels (175-500 cm) (figures 5Bb and 6Bb: appendix Bb). These figures suggest that the lower levels could act as a source tank and that the salt is transported by the capillary rise.

During the late summer fieldwork visit, the total soluble salts content at the second profile C2 was generally higher than at C1, but the major anions and cations remained the same (table B3: appendix B and figure 9.17). Nitrate was also found in very high percentage at low levels and in very low percentage at higher levels, which supports the theory of its source being mainly animals by-product. At higher levels (250 cm) there was a high percentage of sulfate with a considerable amount of bromide. This high anion content occurred with a considerable increase in calcium. It is most likely that in this case the main salt is calcium sulfate, which is sparingly soluble. The $Ca\text{-}SO_4$ correspondence was obvious in most of the samples in this profile, however, its concentration decreased slightly with height. The sodium ions showed considerable correspondence to chloride ions and a general trend of higher concentration at higher sampling points (figures 7Bb and 8Bb: appendix Bb). It should be remembered that due to the lack of any data for the carbonate and/or bicarbonate ions, the ion pairing could be slightly different to the previous assumptions. The total cation and anion charges of this profile showed considerably higher cation than anion charges, mainly due to the high percentage of calcium, which suggests the possibility of calcium correspondence to carbonate or bicarbonate ions, something the Ion Chromatography (IC) was incapable of

detecting. The carbonate and bicarbonate ions can be determined by titration methods with acid, but this would require large amounts of sample and ethical considerations for this World Heritage Site did not permit such sampling. There was no obvious explanation for the high percentage of bromide in the samples.

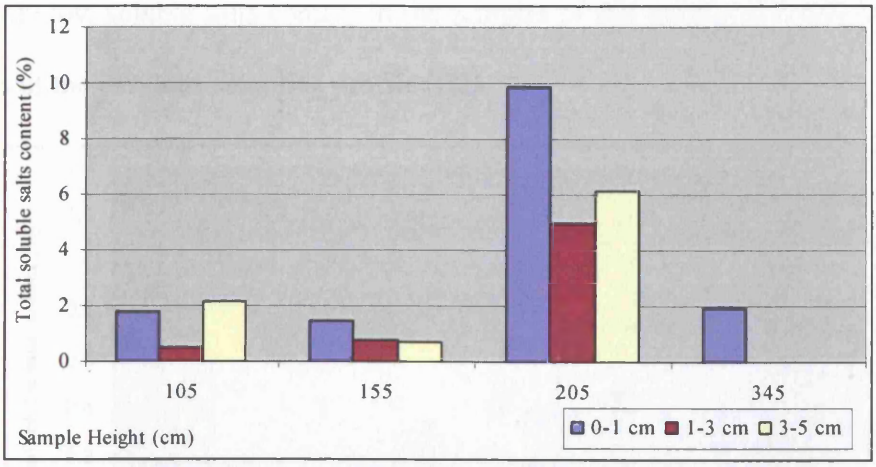

Figure 9.17: The total soluble salts content at Palace Tomb. Location: C2 (Depth intervals: 0-1, 1-3 and 3-5 cm). First fieldwork visit.

At the last sampling profile of this monument during the late summer visit (C3), the total soluble salts content was much lower than C1 and C2 (Appendix B: Table B3 and figure 9.18). In this section nitrate and chloride were the main anions, while sodium and calcium were the main cations. The calcium ions corresponded to chloride ions in some locations, especially in samples from the upper part of the sampling profile (figures 9Bb and 10Bb: appendix Bb). Calcium chloride is a very soluble salt and its high ratio in the upper part reflects the expected thermodynamic properties of a solution of mixed salts, where less soluble salts crystallise at lower parts and salts with high solubility mobilise towards higher levels. The soluble salts content was higher at the 1-3 cm depth than at the 0-1 cm depth, which results mainly from low anion contents in the surface layer. The cation charges were considerably higher than the anion charges, especially in the surface

samples. Considering the high percentage of calcium in these surface layers, this case suggests that the main missing anion is carbonate or bicarbonate.

This sampling profile was in a sheltered area (where the evaporation rate is lower than other sampling profiles of this same monument), which could be an explanation for the significantly low soluble salts content in the samples of this profile (C3) as compared to the values of the previous sampling profile (C2).

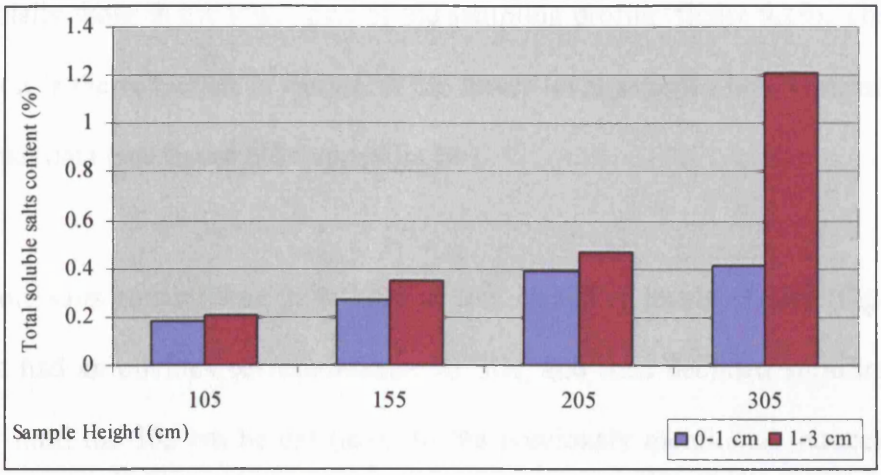

Figure 9.18: The total soluble salts content at Palace Tomb. Location: C3 (Depth intervals: 0-1 and 1-3 cm). First fieldwork visit.

During the winter fieldwork visit, 31 samples were collected from the Palace Tomb (14 from the C1, 10 from C2 and 7 from C3 sampling profiles) and their cation and anion content was analysed (tables E2 and E3: appendix E).

At the first sampling profile (C1), calcium was the main cation, while sodium ions existed in most of the samples but with lower percentages than calcium ions. Potassium and magnesium were found in low concentrations. On the other hand, sulfate was the main anion, and chloride was the second main anion. A high percentage of nitrate was found in a few surface samples. The nitrate concentration was mainly higher in the

samples collected from the 305 cm and 405 cm heights (table E2: appendix E). This high concentration corresponds to fieldwork observations of regular grazing activities on a terrace parallel to these heights.

The total soluble salts content of the C1 samples from the winter visit was generally slightly lower than the soluble salts content of the samples from the late summer visit, and especially those in the lower part of the sampling profile (figure 9.19). The obvious observation is the reduction of nitrate in the lower level samples here compared to the late summer data (see figure 6Eb: appendix Eb).

The soluble salts content was quite high at low sampling levels (5 cm) (figure 9.19), where Ca had an obvious correspondence to SO_4, and then declined significantly and gradually until the 305 cm height (level to the previously mentioned terrace) where a localised increase in soluble salts (mainly nitrate) content was noticed (305-405 cm).

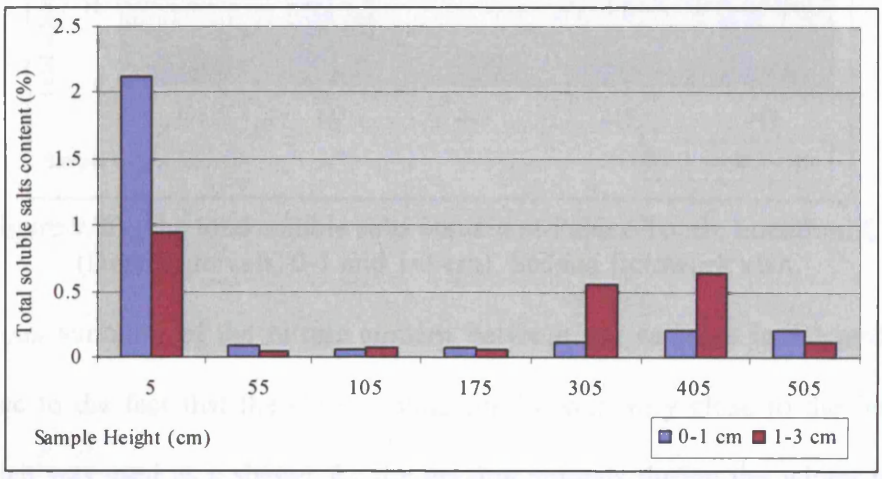

Figure 9.19: The total soluble salts content at Palace Tomb. Location: C1 (Depth intervals: 0-1 and 1-3 cm). Second fieldwork visit.

At the second sampling profile during the winter visit (C2), potassium and calcium were the major cations, while nitrate and sulfate were the major anions (table E3: appendix E).

The soluble salts content was extraordinarily high (table E3: appendix E and figure 9.20), for example, it was around 30 % in a surface sample at the 155 cm height. In addition, the soluble salts content at the surface samples (0-1 cm) was much higher than at the (1-3 cm) depth at the low height sampling points. The soluble salts content increased significantly with height until 155 cm height, where it started decreasing gradually. The total content of soluble salts at shallow depth intervals (0-1 cm) fluctuated much more than at the deeper depth intervals, where the soluble salts content was quite stable (figure 9.20).

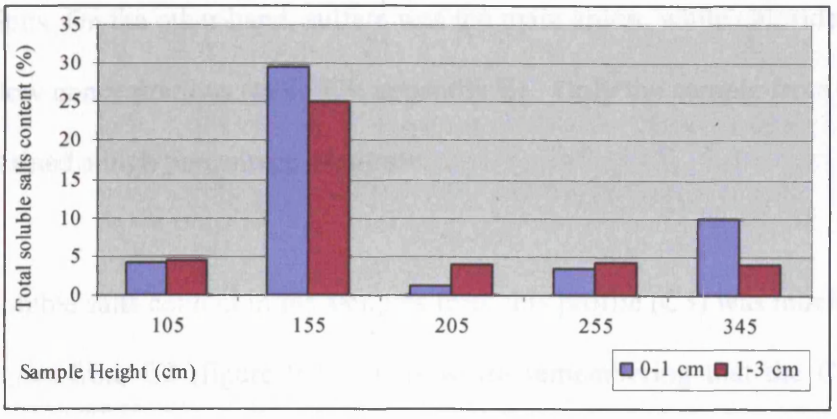

Figure 9.20: The total soluble salts content at Palace Tomb. Location: C1 (Depth intervals: 0-1 and 1-3 cm). Second fieldwork visit.

The obvious variation of the nitrate content between the samples in C1 and C2 was mainly due to the fact that the C2 sampling profile was very close to the inner tomb room which was used as a shelter for the grazing animals during the winter time. The Ca-SO_4 correspondence was obvious in most of the samples in C2 with a gradual decrease with height (see figures 7Eb and 8Eb: appendix Eb). In addition, the samples

showed a high percentage of potassium, with correspondence to nitrate. The K-NO_3 system increased with height. Also, a correspondence was noticed between sodium and chloride in most of the samples with similar trends to the K-NO_3 system. The distribution of the soluble salts in this profile corresponded to the thermodynamic properties of salt solutions in porous building materials where capillary moisture is dominant. The less soluble (Ca-SO_4) crystallised first at lower heights, while the more soluble salts (Na-Cl and K-NO_3) crystallised at later stages in the upper parts of the sampling profile.

At the third sampling profile (C3) in the winter fieldwork visit, calcium was the main cation, sodium the second major cation and potassium and magnesium existed in low concentrations. On the other hand, sulfate was the main anion, while chloride and nitrate existed in low concentrations (table E3: appendix E). Only the sample from the 105 cm height contained a high percentage of nitrate.

The total soluble salts content in the samples from this profile (C3) was much lower than in the samples from C2 (figure 9.21). It is worth remembering that the C3 profile is located in a sheltered area, while C2 is in an open area. The surface samples had higher soluble salts content than the deeper samples at the 105 and 205 cm height, while the samples from the 255 cm height had even lower amounts. This can support the idea of an external source of soluble salts at the low height sampling points.

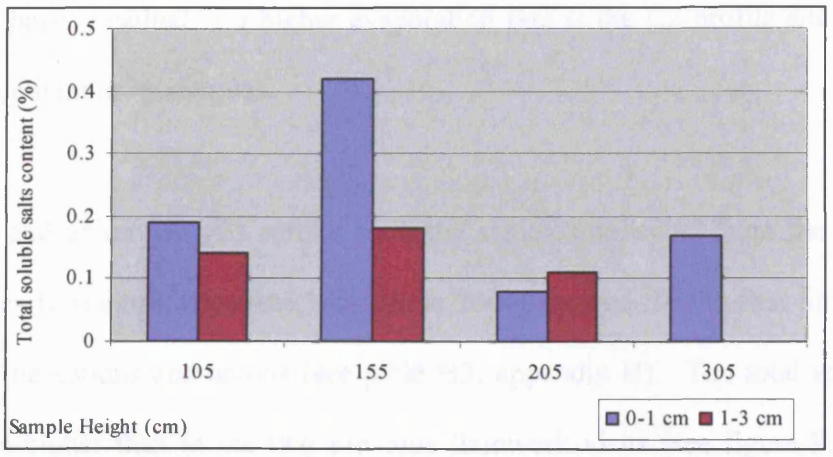

Figure 9.21: The total soluble salts content at Palace Tomb. Location: C3 (Depth intervals: 0-1 and 1-3 cm). Second fieldwork visit.

In summary, the winter fieldwork visit results for the salt distribution in this monument matched, to a large extent, those of the previous late summer fieldwork visit, where the samples from the C2 sampling profile had the highest salts content, C1 less and C3 the least. However, the total soluble salts content in C1 and C3 was slightly lower during the winter fieldwork visit compared to the late summer results, while the total soluble salts content in C2 samples was much higher during the winter fieldwork visit compared to the late summer results. The decrease of soluble salts content in C1 and C3 samples during the winter was the result of higher relative humidity rates during this period that caused less salt movement towards the surface. In other words, due to high relative humidity, soluble salts diffused in greater depth intervals during the winter. On the other hand, the high soluble salts content in C2 during the winter was mainly due to the increase of nitrate, which was generated by an external source (the grazing activities that flourished around this profile during winter). It was also noticed that the wind speed rates were considerably higher near the C2 profile than near the C1 and C3 profiles,

which may have resulted in a higher evaporation rate at the C2 profile and, therefore, higher salt content in its samples.

The cation and anion analysis results from the samples collected from the C1 profile during the early summer fieldwork visit (June 2004) showed for the first time a charge balance of the cations and anions (see table H3: appendix H). The total soluble salts content was higher than in the two previous fieldwork visits (see figure 9.22) with a clear indication of a high percentage of nitrate in the samples from the lower part of the sampling profile. The high percentage of nitrate strongly indicates animals by-product as the source of these ions. This argument is based on the fact that the grazing activities in an open area like C1 were restricted due to the winter season, and the nitrate percentage increased considerably near the inner room of the tomb C2 due to its use as shelter for the animals. The renewed increase of the nitrate concentration in the samples from C1 was mainly due to the return of extensive grazing activities around the open area of the site in the early summer period.

Generally, the total soluble salts content was higher in the samples from greater depth intervals (1-3 cm) compared to the surface samples (0-1 cm), especially towards the upper part of the C1 profile (figure 9.22). Such observations indicate a high evaporation rate. The total soluble salts content was extremely high at the sampling point of 205 cm (figure 9.23), which is just below a wide terrace where a considerable amount of water had been accumulating throughout the winter season. Traces of water were still evident during the June visit.

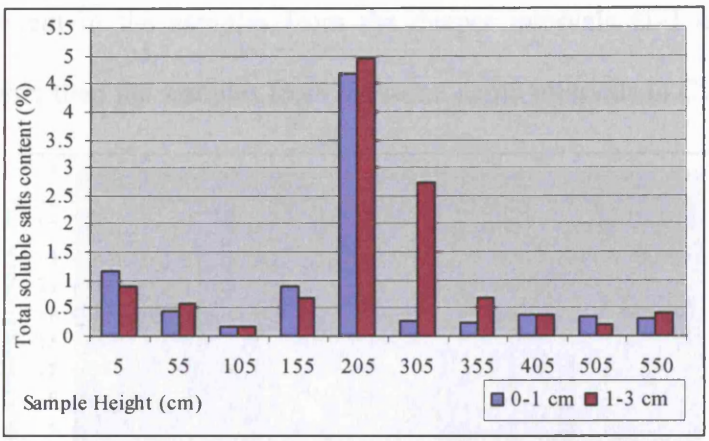

Figure 9.22: The total soluble salts content at Palace Tomb. Location: C1 (Depth intervals: 0-1 and 1-3 cm). Third fieldwork visit.

Regarding the ions distribution, Ca-SO_4 were mainly dominant in the lower part of the profile with relatively high concentrations, while Na-Cl correspondence was uniform throughout the profile.

The analysis of the cations and anions of the samples collected from the C2 profile during the early summer visit (June 2004) showed by far the highest soluble salts content not only among the samples collected from other monuments in the same visit, but also the highest in the same profile compared to previous visits (see figure 9.23 and table H4: appendix H).

The variation in salts distribution between the surface sampling intervals (0-1 cm) and the deeper sampling intervals (1-3 cm) of C2 profile were much higher compared to those of C1 (figures 9.22 and 9.23). The higher wind speed condition near C2 profile may have resulted in higher evaporation rates, and therefore, in a higher rate of soluble salts movement toward the surface of the monument. It should be remembered that the

soluble salts content in the samples from the deeper intervals (1-3 cm) in C2 were considerably higher than the samples from the same depth intervals in C1.

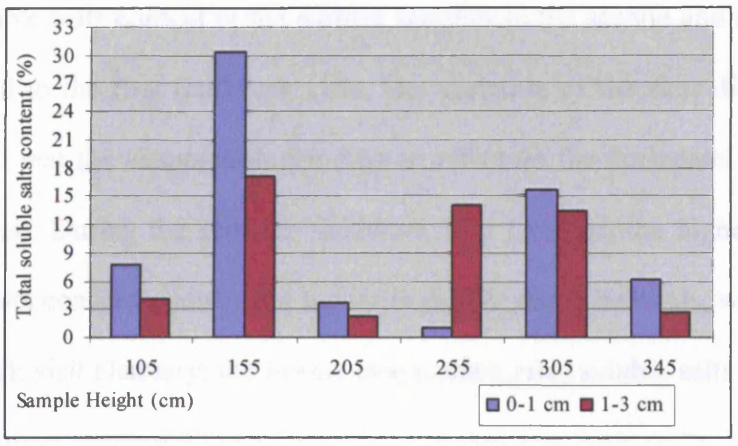

Figure 9.23: The total soluble salts content at Palace Tomb. Location: C2 (Depth intervals: 0-1 and 1-3 cm). Third fieldwork visit.

In relation to the cation and anion distribution at C2 profile in the early summer visit, the calcium ions correspondence to the sulfate ions was dominant in the samples from the lower part of the profile, with a gradual decrease of calcium ions with height. On the other hand, nitrate was in high concentration in the middle part of the profile with a clear correspondence to potassium. The Na-Cl correspondence was obvious throughout the profile and dominant at its upper part. The salts distribution in C2 profile corresponded to a large extent to the thermodynamic properties of such a salt mixture, where the less soluble salt (calcium sulfate) precipitated in the lower part, the more soluble salt (potassium nitrate) in the middle part and the strongly soluble salt (sodium chloride) in the higher levels (see figure 9Hb and 10Hb: appendix Hb).

The results of the total soluble salts content from the C3 samples in the early summer visit continued to be the lowest among the sampling profiles at the Palace Tomb, but

with slightly higher concentration than in the previous two visits (figure 9.24 and table H4: appendix H) . Another obvious observation from the cation and anion analysis was the higher soluble salts content in the surface samples in the second and third fieldwork visits compared to the first fieldwork visit. The variation of the salts distribution with depth indicated that the evaporation rate had an effect on the horizontal distribution of the soluble salts. During the summer fieldwork visit (August: the highest evaporation rate) soluble salts concentrations were higher in deeper depth intervals, while during the winter fieldwork visit (January: the lowest evaporation rate) soluble salts were higher in shallow depths.

Apart from the gradual decrease of calcium with height at C3 profile, the other ions were mainly uniformly distributed, with a trend similar to the ions at C2 in this visit (Ca-SO_4 dominated the lower part, Ca-NO_3 and Na-Cl the middle and upper parts of the profile).

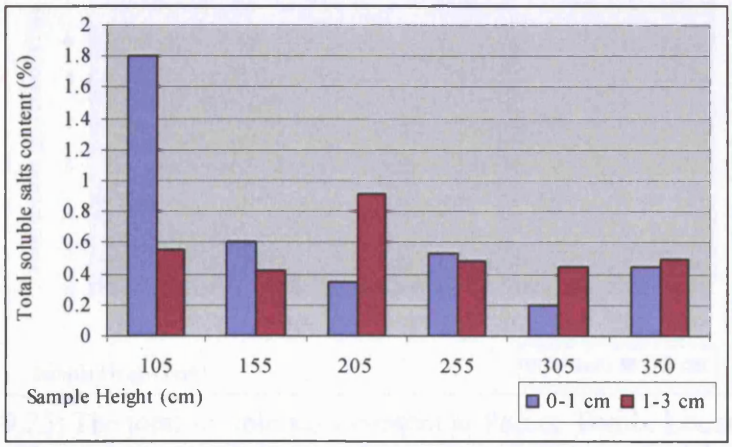

Figure 9.24: The total soluble salts content at Palace Tomb. Location: C3 (Depth intervals: 0-1 and 1-3 cm). Third fieldwork visit.

During the spring fieldwork visit (April 2005), the total soluble salts content at C1 profile reached its highest among all seasons, with the highest concentration in the middle part of the profile (see figure 9.25 and table L3: appendix L). As mentioned in

chapter 8, the wind speed around the profile was considerably high during this visit. This ultimately increased the evaporation rate and resulted in higher soluble salts content in most of the samples. Also, the grazing activities during this period (spring) were much higher than at any other time of the year. One interesting observation was that the highest salts content at the profile was at the sampling point of 205 cm height during the early summer season and at 255 cm during the spring season. This observation suggests that the evaporation rate was much higher in the early summer season resulting in salts crystallisation at lower heights.

Calcium and sulfate correspondence was obvious in the lower part of the profile, sodium and chloride dominated the middle part of the profile, while the total cation and anion content declined significantly towards the upper part of the profile.

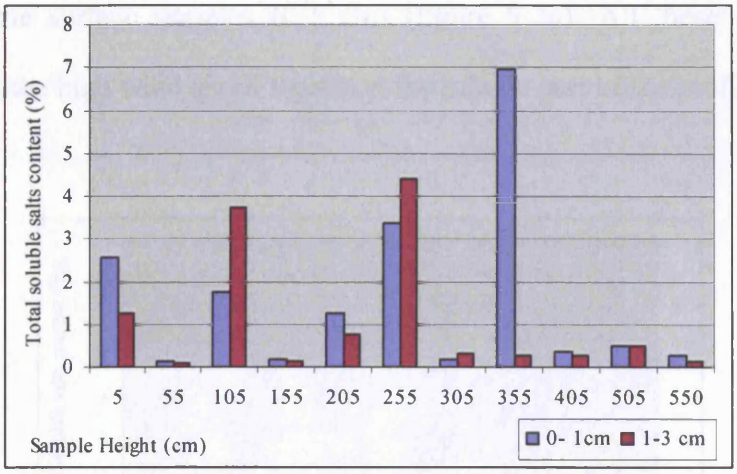

Figure 9.25: The total soluble salts content at Palace Tomb. Location: C1 (Depth intervals: 0-1 and 1-3 cm). Fourth fieldwork visit.

The soluble salts content at C2 profile continued to be the highest among the sampling profiles in the Palace Tomb, but in considerably lower proportion compared to the early summer and winter fieldwork visits and slightly higher than in the late summer fieldwork visit (see figure 9.26 and table L4: appendix L). The main reason for this low

content compared to the winter season fieldwork visit was largely the low nitrate content. As mentioned earlier, during the winter fieldwork visit it was noticed that the inner room of the tomb, which is very close to C2 profile, was being used as a shelter for animals during the winter, while no such use was noticed during the spring fieldwork visit. On the other hand, the surrounding microclimate conditions and mainly the higher relative humidity were the main reason for the lower soluble salts content during this visit compared to the early summer visit where the lower relative humidity conditions resulted in more soluble salts deposition towards the surface of the façade.

The middle part of the C2 profile showed not only the highest soluble salts content, but a higher soluble salts content in the samples from the greater depth intervals (1-3 cm) compared to the surface samples (0-1 cm) (figure 9.26). All these indications are consistent with the high wind speed figures at the middle part of the profile (see chapter: section 8.5.3).

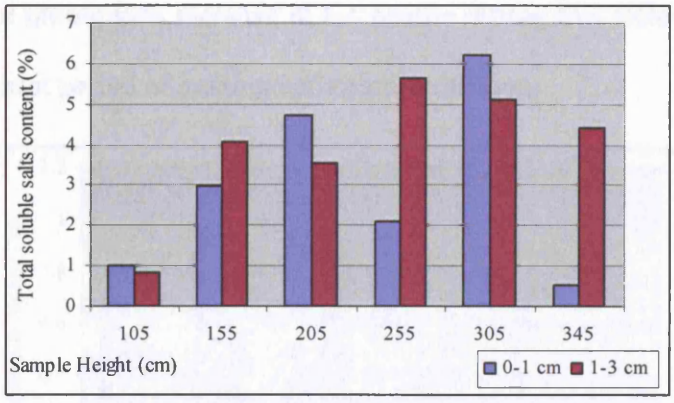

Figure 9.26: The total soluble salts content at Palace Tomb. Location: C2 (Depth intervals: 0-1 and 1-3 cm). Fourth fieldwork visit.

Regarding the cation and anion types in the C2 profile, there was a clear correspondence of calcium and sulfate ions in the lower part of the profile (0-205 cm) and a very clear

association of potassium and nitrate ions in the upper part of the profile (255-345 cm). A proportional quantity of sodium and chloride ions was detected in most of the samples from this profile with a higher concentration towards the middle of this profile (see figure 7Lb and 8Lb: appendix Lb).

Once again, the total soluble salts content in the samples from the C3 profile was the lowest at the Palace Tomb (see figure 8.42 and table L4: appendix L). It needs to be remembered that the wind speed readings from this profile were also the lowest compared to the readings near the other sampling profiles at the Palace Tomb (chapter 8: section 8.3.5). Compared to the previous fieldwork visits, the total soluble salts content of the C3 samples was slightly higher than in the early summer fieldwork visit and much higher than in the winter fieldwork visit. By looking at the cation and anion distribution in this profile (figures 9Lb and 10Lb: appendix Lb) it could be stated that the increase of the total content was mainly due to the increase of nitrate ions. This corresponds to the nitrate ions increase in C1 profile during this fieldwork visit, which represents the highest period of grazing activities in the area.

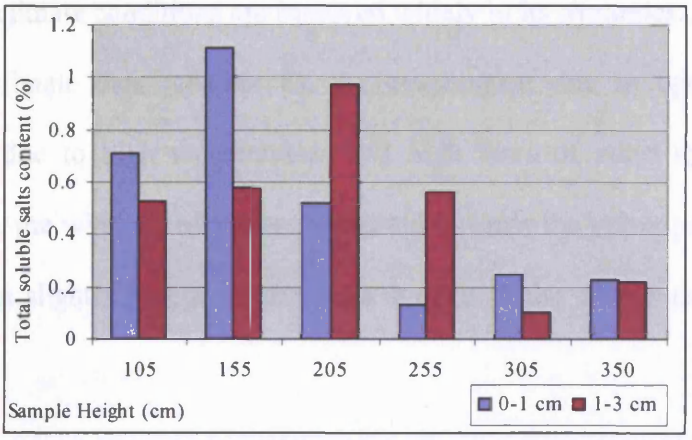

Figure 9.27: The total soluble salts content at Palace Tomb. Location: C3 (Depth intervals: 0-1 and 1-3 cm). Fourth fieldwork visit.

9.4.1.3. Corinthian Tomb results

The Corinthian Tomb is the most deteriorated monument in Petra. It was therefore very important to examine its soluble salts content.

Surprisingly, the soluble salts content in this profile during the first fieldwork visit (late summer) was quite low (See table B4: appendix B and figure 9.28). The average soluble salts content was approximately 0.6 % with a maximum of 4.01 % at the 250 cm height and a minimum of 0.09 % at the 200 cm height.

Calcium and sodium were the main cations, while sulfate, chloride and nitrate were the main anions. At the highest reading of the soluble salt content in this profile (4.01%), the calcium and sulfate content was more than 88%.

Horizontally, namely with depth into the monument, the total soluble salts content showed a very similar trend to that of the Palace Tomb, where higher evaporation rates resulted in a generally uniform distribution of the soluble salts in the two tested depth intervals (0-1 and 1-3 cm). The H profile at the Corinthian Tomb is in an open area, where the microclimate conditions are involved widely in its dynamics. According to the previous microclimate data (chapter 8), the evaporation rate in open areas can be relatively high, due to high temperatures and high rates of wind speed fluctuation. During this visit, the wind speed figures increased towards the upper part of the profile, which resulted in slightly higher soluble salts content in the deeper sampling intervals (figure 9.28).

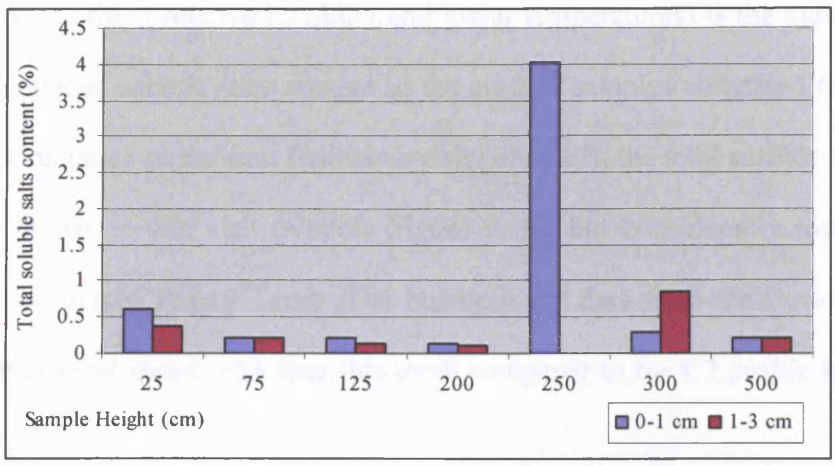

Figure 9.28: The total soluble salts content at Corinthian Tomb. Location: H (Depth intervals: 0-1 and 1-3 cm). First fieldwork visit.

Trends similar to the Palace Tomb samples were noticed, with high calcium content concentrated in the surface samples with no anions to balance it. The dramatic increase of calcium at 250 cm corresponded to the increase of sulfate at this sampling point. The anion and cation charges at this sampling point (250) were more balanced (see table B6: see appendix B).

The results of the sixteen samples taken from the Corinthian Tomb during the winter season visit showed that sodium and calcium were the major cations, while magnesium and potassium were found in much lower concentrations. Sulfate and chloride were the major anions. Nitrate and phosphate existed in very low concentrations (table E4: appendix E).

The total soluble salts content was generally high with an average of 1.1 % and 1.3 % in the 0-1 cm and 1-3 cm depth intervals respectively. Generally, the surface samples from 0-1 cm contained slightly higher concentrations of soluble salts. The relatively low

evaporation rate (high relative humidity and lower temperatures) is the main reason for the slightly higher soluble salts content in the surface samples compared to the deeper samples. Compared to the first fieldwork visit (summer), the total soluble salts content was much higher in this visit (winter) (figure 9.29), but considerably lower than the content of the nearby Palace Tomb. The microclimate data from the Corinthian Tomb showed lower wind speed rates near this tomb compared to the C2 profile in the Palace Tomb data.

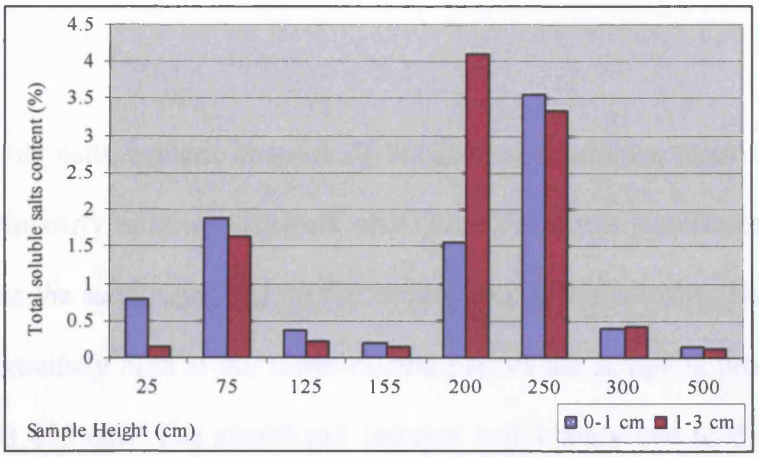

Figure 9.29: The total soluble salts content at Corinthian Tomb. Location: H (Depth intervals: 0-1 and 1-3 cm). Second fieldwork visit.

Cation and anion analysis of the Corinthian Tomb samples showed that the cation charges were much higher than the anion charges (table E4: appendix E). The high cation charges were mainly associated with the high concentration of calcium and sodium, which suggests the presence of calcium carbonate (sparingly soluble salt: 0.016 g in 100 ml at 20 °C, Weast 1974) or sodium carbonate (moderately soluble salt: 10.3 g in 100 ml at 20 °C, Weast 1974) in this profile.

In addition, sodium ions corresponded to chloride ions, especially at the upper part of the profile, while calcium ions decreased significantly towards the upper part of the profile. This decrease was associated with a decrease of sulfate ions (see figures 10Eb and 11Eb). However, the high percentage of sodium and sulfate ions in this profile and the fact that the Corinthian Tomb is the most deteriorated tomb in Petra suggest the presence of sodium sulfate (the most well known damaging salt, see chapter 2) in this monument. Chapter 10 explores the thermodynamic behaviour of the salts solution in more detail.

The total soluble salts content in most of the collected samples from the Corinthian Tomb during the early summer fieldwork visit (June 2004) was significantly higher than the results from the same sampling profile on the two previous visits. The soluble salts content was extremely high at the lower-middle part of the sampling profile (sampling points 125 and 155 cm). The significant increase was mainly due to the considerable increase of nitrate, potassium and calcium as well as the appearance of magnesium in high concentration. The calcium and sulfate concentration decreased gradually with height, while potassium and nitrate dominated the lower middle part. Na-Cl distribution was mainly uniform throughout the profile but with a considerable increase towards the upper middle part of the profile (200-250 cm) (figure 9.30 and table H5: appendix H).
The total soluble salts content horizontally (with depth) varied from one point to another, with high soluble salts content in the surface samples (0-1 cm), where K-NO_3 dominated, and in the deeper intervals (1-3 cm) at higher points of the profile, where Ca-SO_4 dominated. Such observation (the crystallisation of the less soluble salt deep inside

the façade and the more soluble salt towards the external part of the facade) suggests an internal source for the soluble salts.

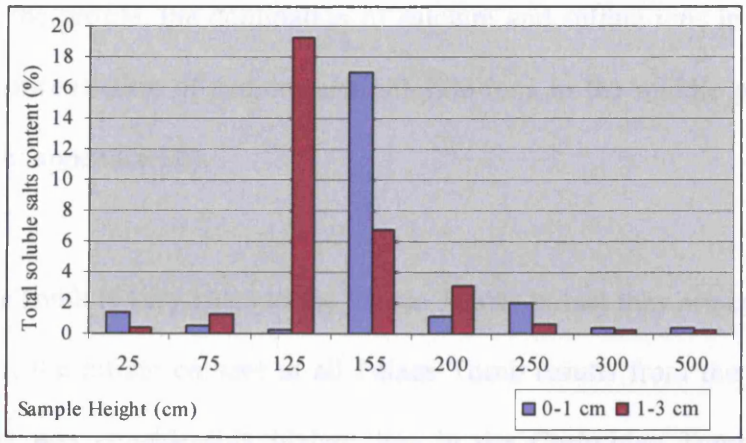

Figure 9.30: The total soluble salts content at Corinthian Tomb. Location: H (Depth intervals: 0-1 and 1-3 cm). Third fieldwork visit.

A significant feature of the cation and anion analysis in the Corinthian Tomb during the spring season is the obvious imbalance between the cation and anion charges, which indicates the presence of undetected anions (presumably carbonate and/or bicarbonate). This imbalance affected the estimated overall soluble salts content in the samples, which appeared to be the lowest among all other results from the same profile in the previous sampling fieldwork visits (see figure 9.31 and table L5: appendix L).

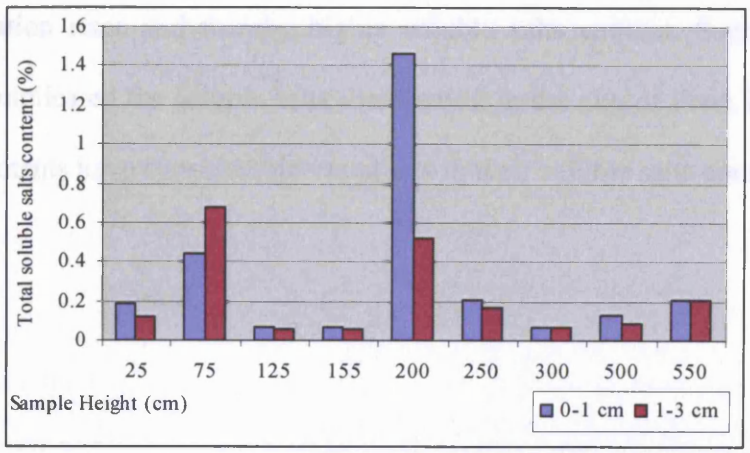

Figure 9.31: The total soluble salts content at Corinthian Tomb. Location: H (Depth intervals: 0-1 and 1-3 cm). Fourth fieldwork visit.

Nevertheless, the trend of the soluble salts distribution on this visit remained similar to the results from the previous fieldwork visits, with the highest concentration towards the middle part of the profile, the domination of calcium and sulfate ions in the lower part and the high concentration of sodium and chloride ions in the middle part (see figure 10Lb and 11 Lb: appendix Lb).

The Corinthian Tomb is very close to the Palace Tomb; in fact they are adjacent to each other. However, the nitrate content in all Palace Tomb results from the four sampling fieldwork visits was considerably higher than in the Corinthian Tomb. No obvious explanation was found for this low concentration of nitrate in the Corinthian Tomb, apart from the limited access of animals to the inner room of the tomb due to its broken entrance (see figure 6.4: chapter 6) . It is also important to mention the presence of a pool of water on the left side of the Palace Tomb throughout most of the fieldwork visits (mainly the spring and winter visits), which must have been attracting the grazing animals to the Palace Tomb side of the area. In addition, the wind speed rates were generally higher at the Palace Tomb, especially near the C2 profile, which resulted in higher evaporation rates and thereby higher soluble salts content. Such observations reflect how complicated the soluble salts distribution in the city of Petra is, where even adjacent monuments have considerable variations in their soluble salts content.

9.4.1.4. Deir Tomb results

The total soluble salts content at the Deir Tomb was generally low. It is worth remembering that the two sampling profiles were taken from the cut façades next to the monument and not from the carved façade itself.

At the D1 profile during the first sampling season (August 2003), calcium and sodium were the main cations, while sulfate, chloride and nitrate were the main anions. Potassium and phosphate were minor components (table B5: appendix B). There was an obvious general trend of the total content of soluble salts in the three sampling depth intervals (figure 9.32). The salt content started very low at 5 cm and increased gradually until it reached its maximum at 105 cm, after which it started to decline again at 155 cm. Thereafter, the salt content increased gradually with height. The significant increase of the total soluble salts content at 105 cm is mainly related to the presence of a small terrace (40 cm wide x 250 cm long) at the height of about 95 cm. This terrace could be the main source of water accumulation and, therefore, an additional source of soluble salts. The increase of total soluble salts content was accompanied by a noticeable increase of bromide content in the samples. The origin of bromide is unknown.

Three samples from the surface were analysed and all showed a much lower salts content than the samples from the 0-1 cm depth intervals. The salts content generally decreased with depth after the 0-1 cm depth interval. The relatively high evaporation rate could be the main reason for such distributions. Still, the microclimate conditions

suggest that the evaporation rates in this monument were generally lower than in the Palace Tomb.

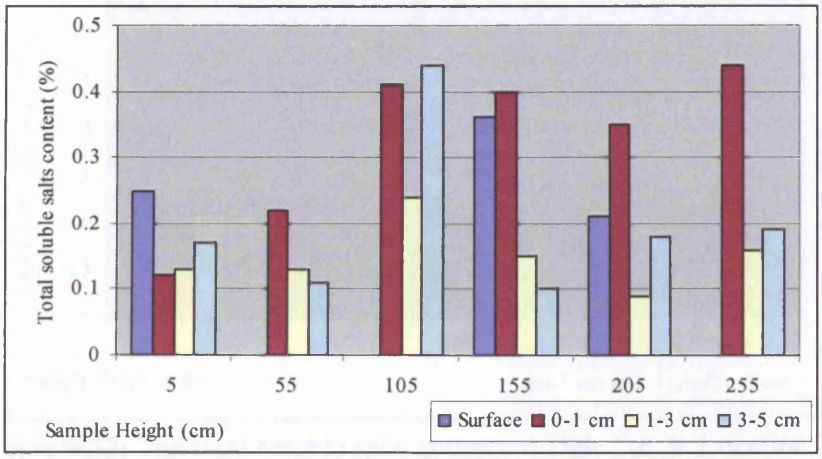

Figure 9.32: The total soluble salts content at Deir Tomb. Location D1 (Depth intervals: surface, 0-1, 1-3 and 3-5 cm). First fieldwork visit.

The total soluble salts content at the second sampling profile (D2) was much higher than at D1. (Table B6: appendix B and figure 9.33). The average soluble salts content of the D2 samples was around 1.5 %, which is eight times higher than the average of the D1 samples. This could be related to the fact that, contrary to the D1 profile, this sampling profile is in an open area,. Moreover, the D2 profile was facing towards the main wind speed direction and gave higher wind speed readings compared to the D1 profile. However, the salt content decreased with depth and recorded its highest at the 0-1 cm depth, which suggests that the rate of evaporation was lower than at the Palace and Corinthian Tombs, resulting in higher salt content near the surface areas.

Calcium was the main cation and sulfate the main anion. However, the sodium and chloride ions were obvious in most of the samples and increased towards the upper part

of the sampling profile, while calcium ions decreased slightly towards the upper end of the profile.

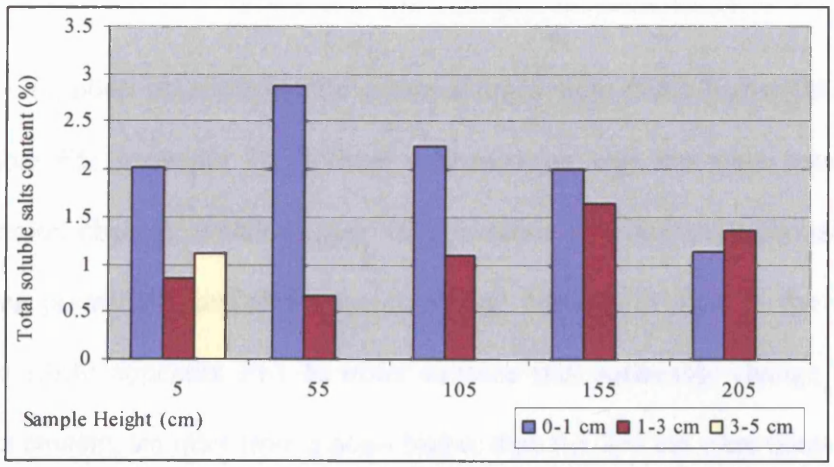

Figure 9.33: The total soluble salts content at Deir Tomb. Location D2 (Depth intervals: 0-1 and 1-3 cm). First fieldwork visit.

During the winter season, two sets of samples were analysed from the D1 and D2 profiles (The cation and anion content results of these samples can be seen in table E5 in appendix E). At the first sampling profile (D1), sodium and calcium were the main cations, while potassium and magnesium were present in low concentrations. Sulfate and chloride were the main anions. A high concentration of nitrate was found in a few samples that came mainly from the lowest level of the sampling profile (5 cm height).

In general, the samples from the D1 profile had very low soluble salts content compared to the rest of the samples from this monument. The average soluble salts content was 0.65 % and 0.22 % at the 0-1 and 1-3 cm sampling depth intervals respectively. The surface samples (0-1 cm) had higher soluble salts content than the samples from deeper sampling points (1-3 cm) (figure 9.34). The soluble salts types and distribution were

generally similar to the previous fieldwork visit with a general decrease of the nitrate content and a general increase of the sodium and sulfate ions.

Similarly to the other monuments, the cation charges were much higher than the anion charges (table E5: appendix E). Sodium concentration was the main reason for this excess of cation charges, which suggests the presence of a sodium carbonate salt. The last sampling point (255 cm) showed a surprising increase in most of the cations and ions (figure 13Eb: appendix Eb). In order to trace this noticeable change in the total soluble salts content, samples from a point higher than the 255 cm were taken in the next fieldwork visit.

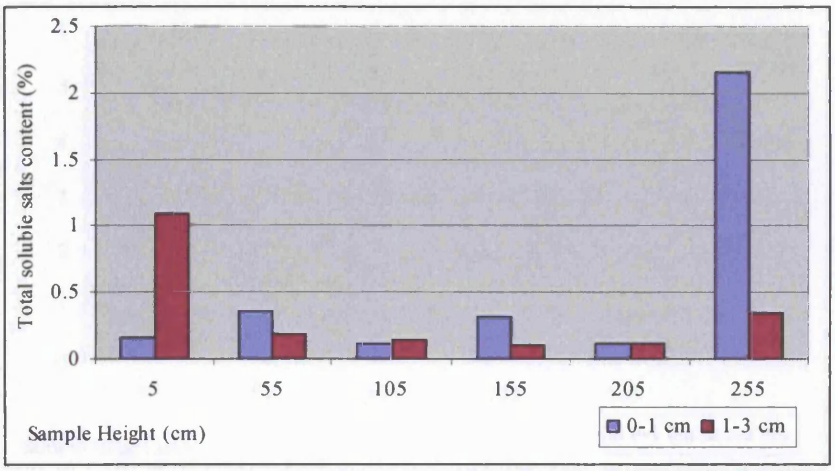

Figure 9.34: The total soluble salts content at Deir Tomb. Location D1 (Depth intervals: 0-1 and 1-3 cm). Second fieldwork visit.

In the second sampling profile (D2), calcium was the dominant cation, and sulfate the dominant anion (see table D5). Sodium and chloride existed in rather high quantities in most of the samples. The samples from this profile (D2) had a much higher concentration of soluble salts than the samples from the previous profile (D1). The average soluble salts content in D2 samples was 2.08 % and 0.89 % at the 0-1 and 1-3

cm depth intervals respectively. In general, the surface samples had a higher concentration of soluble salts compared to the samples from deeper depth intervals (1-3 cm) (figure 9.35). This trend matched the results of the first late summer visit, where the soluble salts content was much higher in samples from the D2 than from the D1 profile. Regarding the total soluble salts content, the second fieldwork samples had higher soluble salts content in the shallow depth intervals (0-1 cm), and lower content in the deeper intervals (1-3 cm). The low evaporation rate during winter is the main reason for the low soluble salts content at the deeper intervals. In other words, higher relative humidity conditions resulted in the diffusion of the soluble salts deep inside the monument and salt crystallisation took place only near the surface of the monument.

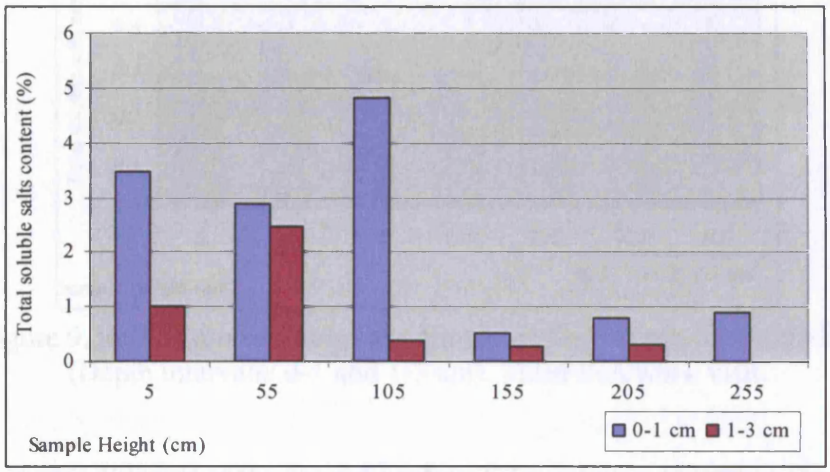

Figure 9.35: The total soluble salts content at Deir Tomb. Location D2 (Depth intervals: 0-1 and 1-3 cm). Second fieldwork visit.

During the early summer fieldwork visit (June 2004), the total soluble salt content in the D1 profile at the Deir Tomb was slightly higher than in the previous two visits, with a more uniform distribution of the salts throughout the profile (figure 9.36 and table H6: appendix H). The total soluble salts content was relatively high in the surface samples,

especially at the upper part of the sampling profile. However, a more uniform distribution and with slightly higher soluble salts content in the surface samples (0-1 cm) was observed in the June fieldwork visit results. The uniform distributions appear not only with regard to the overall soluble salts content but also to the individual ions (see figure 15Hb and 16Hb: appendix Hb). Generally, the higher evaporation rates during this period resulted in higher soluble salts content in the deeper intervals, creating a more uniform distribution of the soluble salts between the surface and the deeper intervals (0-1 and 1-3 cm).

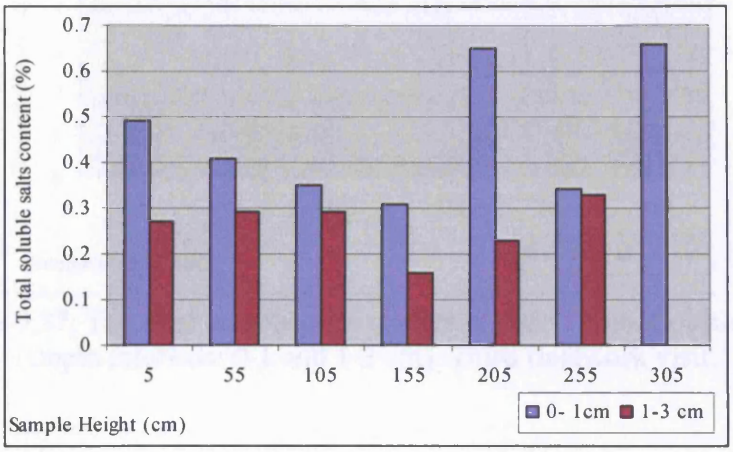

Figure 9.36: The total soluble salts content at Deir Tomb. Location D1 (Depth intervals: 0-1 and 1-3 cm). Third fieldwork visit.

The situation was different at the second profile (D2), not only regarding the overall salt content which was much higher than in the D1 samples, but also regarding the variation in the ions concentration with height and depth. The soluble salts content in the surface samples (0-1 cm), especially in the middle part of the profile, was considerably higher than in the samples from deeper depth intervals (1-3 cm). The only obvious explanation for such variations from the D1 results was the location of this profile at an open area, exposed to the direction of the main wind speed trend.

An obvious correspondence between calcium and sulfate and between sodium and chloride was noted throughout the profile. Nitrate content was much higher than in the two previous visits (figure 9.37, table H6: appendix H, figure 17Hb and 18Hb: appendix Hb). This increase was also observed in the other monuments during this time of the year, when extensive grazing activities take place in Petra.

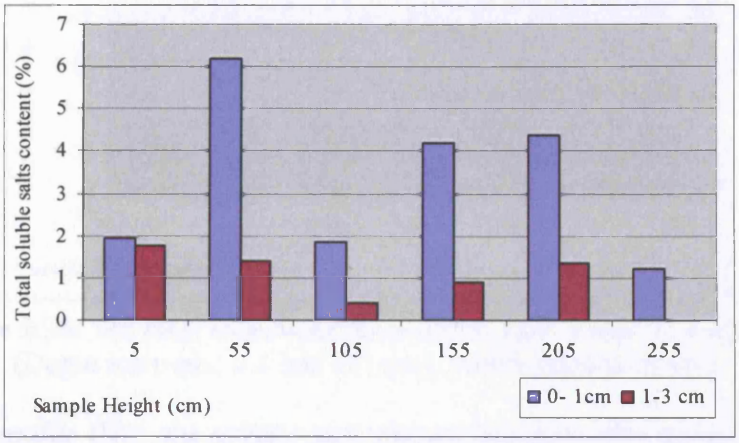

Figure 9.37: The total soluble salts content at Deir Tomb. Location D2 (Depth intervals: 0-1 and 1-3 cm). Third fieldwork visit.

The cation and anion analysis of the samples from the first profile (D1) at the Deir Tomb during the spring sampling fieldwork visit showed the lowest overall soluble salts content from all fieldwork visits (figure 9.38). The excess of cation charges compared to anion charges in these samples was one of the main features in these results. This excess was noticed in most of the samples from the previous fieldwork visits, but was higher in the samples from the spring and winter fieldwork visits. The winter and spring seasons were the most humid ones compared to the early and late summer periods causing higher groundwater level inside the monuments. This situation strongly supports the author's arguments regarding the presence of carbonate or bicarbonate anions in the samples

from the Deir Tomb that originated mainly from groundwater inside the monument. However, despite the non-proportional distribution of the cations and anions, a correspondence of calcium and sulfate and of sodium and chloride ions existed throughout the profile (see figure 13Lb and 14Lb: appendix Lb).

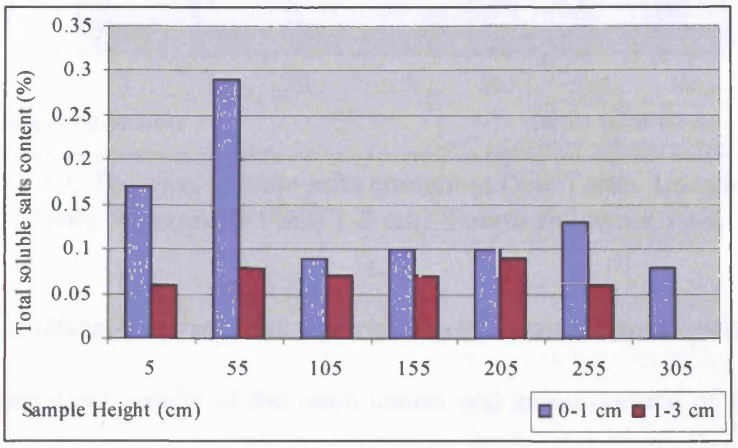

Figure 9.38: The total soluble salts content at Deir Tomb. Location D1 (Depth intervals: 0-1 and 1-3 cm). Fourth fieldwork visit.

At the second profile (D2), the soluble salts content was generally higher than in the D1 samples, but was the lowest among all D2 samples from all sampling campaigns (figure 9.39). Despite the fact that the microclimate data (chapter 8) showed lower wind speed near the D2 profile compared to the readings near the D1 profile at the same monument, the location of D2 profile in an open area, exposed to main wind speed trend, could justify the higher rate of soluble salt content in D2 profile compared to D1 profile. The excess of cation concentration was the highest among all results. In some samples, the cation charges were 30 times more than the anion charges (see table L6: appendix L). Generally, most cation concentrations and particularly the calcium and potassium concentration increased in the D2 profile (see figure 15 Lb and 16 Lb: appendix Lb). The suggested explanation for the unbalanced charges between the cations and the anions is the same as with D1 samples.

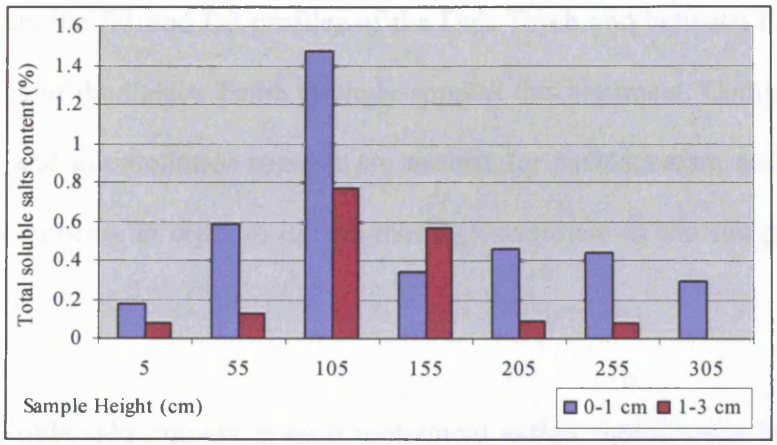

Figure 9.39: The total soluble salts content at Deir Tomb. Location D2 (Depth intervals: 0-1 and 1-3 cm). Fourth fieldwork visit.

9.5. Petra salt distribution and microclimate conditions: general discussion

Based on the analytical results of the main cation and anion content of the samples from the four case study monuments, the role of the microclimate conditions in the distribution of soluble salts has become evident. The following points summarise the main observations regarding the microclimate conditions and the soluble salts distribution:

- The total soluble salts content varied not only from one season to another, but from one monument to another within the same season, and even from one profile to another at the same monument within the same season. These variations reveal not only the complexity of the salt distribution in Petra, but more importantly the significant role of the microclimate conditions, and, in particular, the role of wind speed in salt distribution. This was observed in situations where changes in the wind speed conditions alone resulted in considerable variations in the total soluble salts content. Generally, the total soluble salts content was higher at the profiles where high wind speed readings were recorded. The variations in the total soluble salts

content between the D1 and D2 profiles of the Deir Tomb and between the C1, C2 and C3 profiles of the Palace Tomb strongly support this argument. Comprehensive salts analysis and microclimate surveys are needed for each location and for each part of the monuments in order to have a thorough overview of the salt problem at Petra.

- The total soluble salts content at each monument varied significantly in different seasons. Table 9.1 summarises the fluctuations of the total soluble salts content at each monument during the four fieldwork visits. It shows that both the Corinthian and the Deir Tomb have similar trends with the early summer samples having the highest total soluble salts content and the spring samples the lowest. The evaporation rate during the early summer season was high enough to cause crystallisation of highly soluble salts in both the surface and the deeper sampling intervals. However, according to this theory, the total soluble salts content in the late summer results should be even higher than the early summer ones. This was not the case, as the total soluble salts content was lower in the late summer period. Considering that the groundwater is the main source of soluble salts in these monuments, then by the end of the summer, when the water table reaches its lowest point, the salt supply is reduced. During spring, when the water table was lower than in the winter season and the evaporation rates were lower than in the early and late summer period, the total soluble salts content at the Corinthian and Deir Tombs was the lowest compared to the other seasons. In summary, the total soluble salts content in these tombs was controlled by two factors: the level of the water table (salt supplier) and the surrounding environmental conditions. On the other hand, the Palace Tomb had

the highest soluble salts content during spring, mainly due to the increase of the external source of soluble salts in this period (the nitrate, by-product of grazing animals). Meanwhile, both the Palace and the Bab al Siq Triclinium Tomb had a high content of highly soluble salts during the early summer period, which strongly supports the hypothesis regarding the soluble salts distribution at the Corinthian and Deir Tombs. The high concentration of soluble salts at the Bab al Siq Triclinium during winter can be explained by the fact that the tomb is located above a valley where water accumulates during winter. Therefore, the water table in that area may rise considerably during the winter and, despite the relatively low evaporation rates during this season, the higher rates of accumulation of soluble salts from the groundwater source result in higher soluble salts content. In summary, at the Corinthian and Deir Tombs the high rate of evaporation and the relatively high water table resulted in high soluble salts content during the early summer season, at the Palace Tomb the increase of the external supply resulted in higher soluble salts content during the spring season and at the Bab al Siq Triclinium Tomb the high rate of accumulation of soluble salts from the groundwater resulted in high soluble salts content during the winter season.

Monument	**Season of the highest soluble salts content**	**Season of the second highest soluble salts content**	**Season of the third highest soluble salts content**	**Season of the lowest soluble salts content**
Bab al Siq Triclinium	winter	early summer	spring	late summer
Palace Tomb	spring	early summer	Late summer in C1 and C3 and winter in C2	winter in C1 and C3 and late summer in C2
Corinthian Tomb	early summer	winter	late summer	spring
Deir Tomb	early summer	winter	late summer	spring

Table 9.1: The variations in soluble salts content in the four case study monuments at the four sampling seasons

- During the summer fieldwork visits (August 2003 and June 2004), the total soluble salts content was generally higher at the deeper depth intervals (1-3 cm) than in the surface samples. The high evaporation rates in these periods, attributable to high temperature, low relative humidity and high wind speed, were the main reason behind this distribution of the soluble salts.

- Ca-SO_4 and Na-Cl correspondence was observed in most of the profiles at the four different seasons, with the former at the lower parts of the profiles and the latter towards the middle and the upper parts. The Ca-SO_4 concentration at the lower parts of the sampling profiles increased towards the upper part during winter due to the rise in the water table.

- Despite the variations of the total soluble salts content at the four monuments during the different seasons, the tombs classification according to their overall content of soluble salts was more or less the same, with the Palace Tomb, and particularly its C2 profile, being the highest, and T1 at the Bab al Siq Triclinium and D1 at the Deir Tomb being the lowest. The samples from the Corinthian Tomb mainly contained the second highest soluble salts content.

- Regarding the cation and anions charge, the winter samples in most monuments had by far the highest rates of unbalanced charges, mainly with the cation charges being considerably higher than the anion charges. This observation strongly supports the argument for the presence of undetected carbonate and/or bicarbonate anions, which originated from the groundwater during this season. Since the water table rises during

winter, the carbonate and bicarbonate anions increase, resulting in cation charges higher than those of the anions. The variation between the cation and the anion charges at the C2 profile was the lowest among all profiles during the winter, which suggests that the external source of the soluble salts at this location (the nitrate, by-products of grazing activities) was dominant and that there was less carbonate and/or bicarbonate content from the groundwater.

- In regards to the thermodynamic properties of the salt solution and its relation to the surrounding microclimate conditions, it was noticed that in most of the monuments the sparingly soluble salts were mainly concentrated at the lower parts of the sampling profiles and the more highly soluble salts towards the middle and upper parts of the profiles. As the microclimate data showed higher evaporation rates towards the upper parts of the sampling profiles (mainly due to the increase of the wind speed), it can be concluded that the variations of the microclimate conditions resulted in the fractionation of the salts within the tomb according to each salt's solubility.

Even with the clear correspondence between the anions and cations in most of the results from the four monuments at the four different seasons, it should be remembered that this may not reflect the original salt type, since, as discussed in chapter 2, the presence of a salt mixture may change the thermodynamic properties of individual salts. In other words, the exact types of salts in these monuments can not be concluded from the cation and anion content analysis by the techniques used. Chapter 10 discusses the use of an expert chemical model for determining the exact salt types in Petra monuments during different seasons. The computer program (ECOS) (Price 2000) is capable of predicting

the behaviour of a salt solution under different environmental conditions. Based on the detailed microclimate data from the studied monuments and the detailed cation and anion content analysis, the ECOS program can assist in the study and evaluation of the behaviour of the salt solutions. Due to the large number of samples and the microclimate variations from one site to another, it was decided that only selected sampling points from one sampling profile (C2) would be examined in this way (see chapter 10 for more details).

Besides the use of the ECOS program for the understanding of the solution behaviour under different environmental conditions, the role of environmental conditions and especially the wind speed, in the salt damage in porous materials also needs examination. To this end, a laboratory simulation test for the salt damage process with a particular interest in the wind speed effect was designed and is presented in chapter 11.

Chapter 10
Thermodynamic Consideration of the Soluble Salts in Petra using the ECOS program

10.1. Introduction

The evaluation of the soluble salts content, types and distribution at the studied monuments in Petra (chapter 9) showed not only fractionation of these salts with heights and depths at each sampling profile, but also considerable variations of the salt content, types and distribution over time. The mobility of the soluble salts over time is mainly associated with the changing environmental conditions around the sites.

Despite the fact that the analysis of cations and anions of samples collected from different monuments at different depths and heights and in four different sampling seasons (chapter 9) has revealed very useful information about the salts content and distribution at Petra monuments, the understanding of the dynamics of these soluble salts was limited. In other words, the relationship between soluble salts content, types and distribution and the surrounding environmental conditions was not adequately explained. Therefore, a more specific study of the thermodynamic behaviour of the soluble salts in relation to the surrounding environmental conditions is needed.

As discussed in chapter 2, the determination of the hygrothermal conditions that control the behaviour of single salts is a straightforward process. Each single salt has its specific equilibrium relative humidity (ERH) at a certain temperature and remains in solution when the surrounding relative humidity is higher than this ERH, but crystallises when the surrounding relative humidity is lower than this ERH.

Following these observations, it might be assumed that salt damage could be avoided in a very straightforward way by controlling the surrounding relative humidity and temperature. Unfortunately, the reality is more complicated, mainly because contamination with single salts in porous materials is rare (Price 2000b), while predicting the behaviour of a salt mixture is much more complicated. Many models have been presented in the attempt to understand the behaviour of mixed salt solutions. Pitzer's thermodynamic model (1973) is one of the most widely accepted and applied models in many areas in the chemistry of the natural environment (Clegg and Whitfield 1991). Price and Brimblecombe (1994) used a new version of Pitzer's model, PITZ93, (Clegg 1993) to predict the behaviour of two salt solutions that are commonly found in cultural heritage monuments and objects (the sodium nitrate - sodium chloride solution and the calcium sulfate - sodium chloride solution). The study examined the interaction of the salts in these solutions and their effect on each other's solubility. The study also determined the 'safe' levels of relative humidity, where salt damage in monuments or objects contaminated with these salts can be minimised.

The use of the Pitzer model in preventive conservation studies (Steiger and Dannecker 1995 and Steiger and Zeunet 1996) led to the creation of an expert chemical model (ECOS) for determining the environmental conditions needed to prevent salt damage in porous materials (Price 2000a). This program will be used to study the salt composition and behaviour of a selected sampling profile from the studied monuments in Petra.

10.2. ECOS: the program, its limitations and applications

ECOS (Environmental Control of Salts) is a computer-based program that provides valuable information on the composition and behaviour of salt solution mixtures. The program requires the user's input of data regarding the ionic composition of the samples and an average temperature or relative humidity of the surrounding environments. ECOS can then predict the types, quantities and volumes of salt species present in any specific ion mixture. It can also define the ranges of relative humidity or temperature, accordingly, where no change in the volume will happen. By keeping the mixture of salts away from the critical levels of relative humidity or temperature, where the phase transitions of the salts take place, the salt damage from these salts can be minimised. In other words, by keeping the salts in solution, or even allowing all the salts to crystallise once, the salt damage from these salts can be considerably reduced. The most recommended method in evaluating the salt composition and behaviour using the ECOS program is to run the program using three parameters: the ion content of a salt mixture, the periodic average temperatures of the site and the whole scale of relatively humidity available in the program (15-98 %). This is mainly because it has been proved that the relative humidity variations have more impact on the salts composition and behaviour than the temperature variations (Sawdy 2001 and Bionda and Storemyr 2002).

The limitations of this program were clearly stated by its developers (Price 2000b) and can be summarised as follows:

- The model assumes that the whole salt system is in equilibrium with its surroundings at all times, which is not necessarily the case in practice (for more details see Price 2000b and Steiger, Beyer, Dorn and Zeunert 2000).

- The model also assumes that the exact composition of the solution is known, which is not the usual case, as is obvious from the analytical data in chapter 9.
- The model considers only a limited number of ions in its calculations (calcium, potassium, sodium, magnesium, chloride, nitrate and sulfate), while other ions may also exist at the site or monuments in question. For instance, phosphate is not included in the calculations of this model but existed in most of the samples from the studied monuments in Petra.
- The model demands an ionic balance in the sample (a balance between the sum of the cation and anion charges). However, the sum of the cation and anion charges in a large number of the collected samples showed imbalanced charges. This restricted the use of the ECOS program for these data.
- The ECOS results are based on the cation and anion content from the collected sample, and therefore there is no assurance that the results are representative of salt solution remains in the site or the monument. It is logical to say that the higher the number of samples, the better the behaviour and composition of the salts in the monuments can be understood. But how many samples are needed from a monument like those in Petra? In this study, and despite the large number of samples taken from different depths and heights at each monument and at four seasons, the number of analysed samples is relatively small considering the size of the monuments.

In addition to the above limitations, the ECOS model does not consider any other environmental conditions apart from temperature and relative humidity. Therefore, the evaluation of the Petra salts composition and behaviour using the ECOS program will not contribute directly to the evaluation of the wind speed effect on the salts distribution

and crystallisation. However, it will assist in predicting the salts' composition and behaviour with regards to the surrounding temperature and relative humidity conditions. As discussed in chapter 3, wind speed can have a direct influence on both temperature and relative humidity, and therefore, by evaluating the relationship between the salts system and relative humidity and temperature, the role of wind speed in this process can be evaluated indirectly.

Despite the potential outcomes from the use of ECOS in preventive conservation studies, few scholars have yet used the program in the evaluation of salts solution composition and behaviour in cultural heritage monuments and objects.

Sawdy (2001) used the ECOS program to understand the dynamic behaviour of soluble salts in the Sacristy at Cleeve Abbey, Somerset, England. In this study, the salt content taken from each area with respect to time and depth did not yield a good ionic balance to allow computation using ECOS and, therefore, only one sample from each sampling period, where the ionic balance was the highest, was studied using the ECOS program. The thermodynamic calculations made by ECOS showed some extraordinary results, where none of the salt mixtures present in the surface samples (0-1 cm) should have crystallised under the conditions recorded in the Sacristy. The results showed how different the theoretical conclusions could be compared to a real situation. However, the modification of the cation and anion content of the surface samples based on the results from samples from deeper intervals, before applying ECOS, resulted in more realistic outcomes.

All in all, the study concluded that the salt system in this site was extremely sensitive to changes in relative humidity and less affected by temperature. The 'safe' relative humidity in this site was above 90 %, where salts appeared to remain in solution. With the relative humidity below 90 % RH it was apparent that even a small change, as little as 5 %, was sufficient to affect the salt distribution significantly.

Bionda and Storemyr (2002) used the thermodynamic model of ECOS and the computer program RUNSALT[18] to simulate the response to changing environmental conditions (relative humidity and temperature) of the salts in the test room of the Tenaille von Fersen building, Suomenlinna, Finland. The outcomes of this study reached similar conclusions to Sawdy's (2001), where temperature changes had little influence on the salts' behaviour, while the largest variations in the amount of solid salt minerals occurred when relative humidity ranged between 60-75 %. A limitation in this study was the inability of the ECOS model to handle carbonate ions, which were abundant in the tested building.

Storemyr and Franz (2002) carried out a similar simulation study at the Regalia room in the north wing of the Archbishop's Palace in Trondheim, Norway. The results of the study corresponded roughly with the observations made at the Regalia room. The thermodynamic calculation made by ECOS suggested that all the salt types should be in solution at a relative humidity above 70 % in all seasons, while in 2001 the climate control program established for the room caused the relative humidity to range between

[18] RUNSALT: a MS windows computer programe developed by Bionda 2002 to act as a user friendly front end to the MS-DOS application (SALT) responsible for thermodynamic calculation in the ECOS program (Bionda and Storemyr 2002).

60-65 %. The study recommended that the lowest limit of relative humidity should be 70 % instead of 60 % to prevent salt crystallisation.

Bionda (2004a and 2004b) applied the concept of salt system and microclimate modelling to a pilot study on the church of S. Pietro, Gnosca, Switzerland. In this study, the behaviour of sodium sulfate was examined in detail due to its widespread presence in the case study monument and especially in the youngest repair mortars at the lower part of the church's walls. The theoretical behaviour of sodium sulfate under the environmental conditions actually measured in the building was evaluated from a pure phase stability diagram and then compared with a more complex model for salt mixture using the ECOS program. For pure salt, the recorded microclimate conditions (temperature and relative humidity) were plotted in the phase diagram of sodium sulfate and showed that both mirabilite and thenardite were in stable phase at certain times and, hence, that phase transition must have occurred. In addition, the behaviour of the salt mixtures in the studied mortars was also examined using the ECOS program. The ECOS values of the mirabilite - thenardite transition limits were in agreement with those of pure sodium sulfate.

Prokos (2005) carried out an extensive work on wall paintings in Delos, Greece, using the ECOS application and discussed the potential of the ECOS results focusing on three main points: the ionic composition in response to salts sources and contaminants, the weathering mechanism and the weathering rate in response to daily or annual transitions. Analysis of the samples showed that the cations charges were higher than anions

charges, indicating that ECOS could not operate properly since it requires a high ionic balance. Prokos found through trial and error that by extracting a larger or smaller amount of calcium the samples reached ionic balance without any other manipulation. This alteration was based on the assumption that the anion excess was due to carbonate or bicarbonate ions. Faced with this problem, Prokos deducted the amount of calcium that was necessary to achieve charge balance. The other common problem his research faced with the ECOS program was its inability to calculate the results in samples that contained both calcium and sulfate. In such situations, the ECOS program gives the option to remove the gypsum from the salt system and rerun the rest of the ions. It could be assumed that the removal of gypsum will not significantly affect the results since it is a sparingly soluble salt and precipitates out from the solution at early stages. However, Prokos (2005) found that gypsum was one of the abundant minerals in the salt efflorescence. It was therefore assumed that the gypsum found in the solution represented only a small fraction of the total gypsum content and that the gypsum content should be included in the discussion. Considering the fact that it was impossible to run the ECOS program on samples with too much gypsum, the calculation of these samples was made after the gypsum was removed. The removed gypsum content was recorded separately and was included in the discussion of the research results.

From all previous work on the ECOS program, it is evident that this can be a significantly useful tool in understanding the composition and behaviour of salt solutions and a very practical means for determining preventive conservation measures. However it should be used consciously, considering the phenomenological observations and any

particular conditions of each individual case. The blind use of ECOS calculations without the consideration of the special circumstances of each site could not only be misleading, but could also result in enhancing rather than minimising the salt damage. Experimenting with different ways of adjusting the cation and anion content (by adding or subtracting certain ions) to match the phenomenological observations before applying the ECOS program has proved to be a useful tool.

Because of its potential usefulness, the thermodynamic behaviour of samples from one of the studied profiles at Petra was evaluated using the ECOS program.

10.3. Thermodynamic consideration of soluble salts in Petra

10.3.1. Samples selection and consideration

As mentioned earlier, the ECOS program demands high ionic balance between the cations and the anions and cannot operate where a high amount of gypsum exists in the salts solution. Unfortunately, the cation and anion results from the Petra monuments (chapter 9) did not always give a good ionic balance and showed considerable amounts of calcium and sulfate ions (gypsum). Therefore, evaluating the salts content and behaviour in all samples using the thermodynamic model of ECOS was considered to be an ineffective method for evaluating the dynamics of the Petra salt solutions. Instead, representative samples from one sampling profile (C1, Palace Tomb) were evaluated using the ECOS program. Two main reasons lay behind the selection of this profile as a case study for the thermodynamic assessment of Petra salt solutions:

- The results from this profile (C1) showed the highest ionic balance among the other sampling profiles in three of the four sampling campaigns (late summer, early summer and spring). It was decided that ECOS would not be used on the winter campaign results that showed a high ionic imbalance.
- The cation and anion results from the Palace Tomb revealed the highest total soluble salts content. It is also important to point out that the solution mixture used for the laboratory simulation test (see chapter 7) was based on the cation and anion results from this tomb.

Since this study would be mainly a representative study rather than a detailed one, the thermodynamic calculations were made on the cation and anion content of samples from four sampling points at the C1 profile (5 cm, 105 cm, 355 cm and 505 cm).

In order for the results to be representative of the salt solution in the profile, the sampling points were selected at different heights and, at each sampling point, the samples used for the thermodynamic calculations were taken from different depth intervals.

10.3.2. Results and discussion

As mentioned earlier, in order to run, the ECOS program requires the input of three types of data, a cation and anion content with the average of one environmental parameter (temperature or relative humidity) and the range of fluctuation of the other parameter (temperature or relative humidity). Also, as was previously discussed, the literature review of the ECOS applications showed that temperature did not significantly

affect the salt solution's behaviour, while relative humidity had the greatest impact. Therefore, the current research has used ECOS with the average temperature of each sampling period as the fixed parameter, and with the entire available range of relative humidity (15-98 %). The overall temperatures were 30 °C, 15 °C, 23 °C and 20 °C for the late summer, winter, early summer and spring sampling campaigns respectively.

10.3.2.1. First fieldwork visit: late summer campaign results

During the late summer sampling campaign, the sum of the cations charge at the lower part of the profile was significantly higher than the anions charge, which prohibited the usage of the ECOS program. The excess of the cations charge was mainly due to a high percentage of calcium ions. As discussed earlier, removing the gypsum from the samples dose not affect the thermodynamic behaviour of the salt solution substantially, since gypsum is a sparingly soluble salt and leaves the salt system at early stages. It was found that, due to the high content of calcium and sulfate together in these samples, the ECOS program could not operate. However, after removing the gypsum from the solution, the program operated normally. The removal of gypsum was indicated and performed by the program itself.

- **Results from the lower part** (sampling point: 5 cm) (figures 10.1, 10.2 below and 1N, 2N, 3N and 4N: appendix N)

The ionic imbalance of the surface sample from this sampling point was too great for the requirements of the ECOS program (see table B2: appendix B). Therefore, no calculations were done on the surface sample.

In the sample from 1-3 cm depth interval, aphthitalite ($Na_2SO_4.3K_2SO_4$) was the first salt to precipitate out of the system at approximately 82 % relative humidity, while above this point all salts were in solution. Thenardite was the next salt to leave the system at a relative humidity of approximately 76 %, which is considerably lower than its equilibrium relative humidity as a single salt at a similar temperature (84.4 %) (Arnold and Zehnder 1990). Bloedite ($Na_2SO_4.MgSO_4.4H_2O$), an evaporite mineral which is usually formed in arid regions by the evaporation of water, followed at a relative humidity of about 73.7 %. Halite (NaCl) and darapskite ($NaNO_3.Na_2SO_4.H_2O$) precipitated next at a relative humidity of 62.7 %. The ERH of halite as a single salt at the tested temperature (30 °C) is 75.1 % (Arnold and Zehnder 1990), which means that the crystallisation point of halite from this salt mixture was significantly lower than its ERH as a single salt. Nitre (KNO_3) left the solution at a relative humidity of 59.6 %, which is much lower than its ERH as a single salt (92.3 %) (Arnold and Zehnder 1990). Nitratine ($NaNO_3$) precipitated at 58.6 %RH, while kieserite ($MgSO_4.1H_2O$) precipitated last at a relative humidity of 17.3 %.

The ECOS program has a function that enables the user to change the molar quantities of minerals to volumes, and therefore, the changes in the volume of salts can be tracked (Price 2000c). By applying this function to the solution mixture it was found that some of the salts reached their highest volume at approximately 40 % RH (see figure 2N: appendix N). Considering the microclimate conditions during the sampling period, when the relative humidity fluctuated between 22 % and 60 %, the calculation made by ECOS suggests that at such conditions (22-60 %RH) all salts should be in solid states apart from nitratine, which crystallises out at 37 %RH, and kieserite that remains in solution.

From a preventive conservation point of view, these results indicate that the surrounding relative humidity should be kept either below 17 % or above 82 % in order to prevent the damage from such salt mixtures. Controlling the relative humidity to between 45-55 % or between 21-38 % could also provide relatively 'safe' environments, where salt damage can be contained, since with relative humidity between these two ranges no transition or salt volume change took place in this sample.

In regards to the preventive conservation issues, the ECOS results from the deeper sampling interval (3-5 cm), were very promising since the 'dangerous' relative humidity range was between 53-64 %, which, compared to Petra conditions at this time of the year, could be easily avoided by slight alterations to the microclimate conditions of the site. The highest volume increase of the salts in the salt solution of this sample was recorded between 55-65 %RH (figure 3N and 4N: appendix N). Chapter 13 will discuss the possible recommendations arising from this matter.

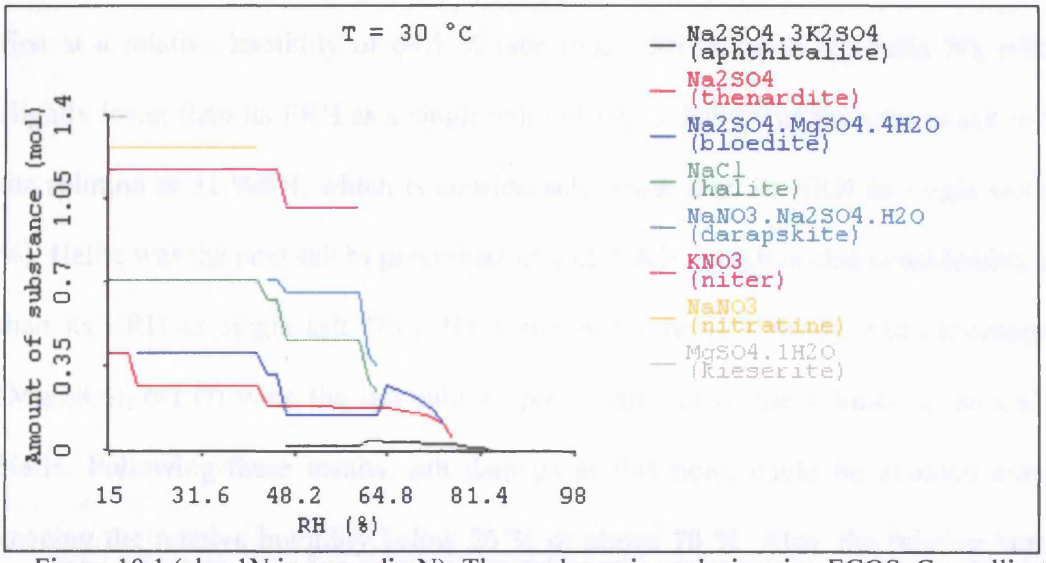

Figure 10.1 (also 1N in appendix N): Thermodynamic analysis using ECOS. Crystallisation sequence of soluble salts: relative humidity against amount of substance (mol). (Sampling height: 5 cm, sampling depth interval: 1-3 cm). First fieldwork visit.

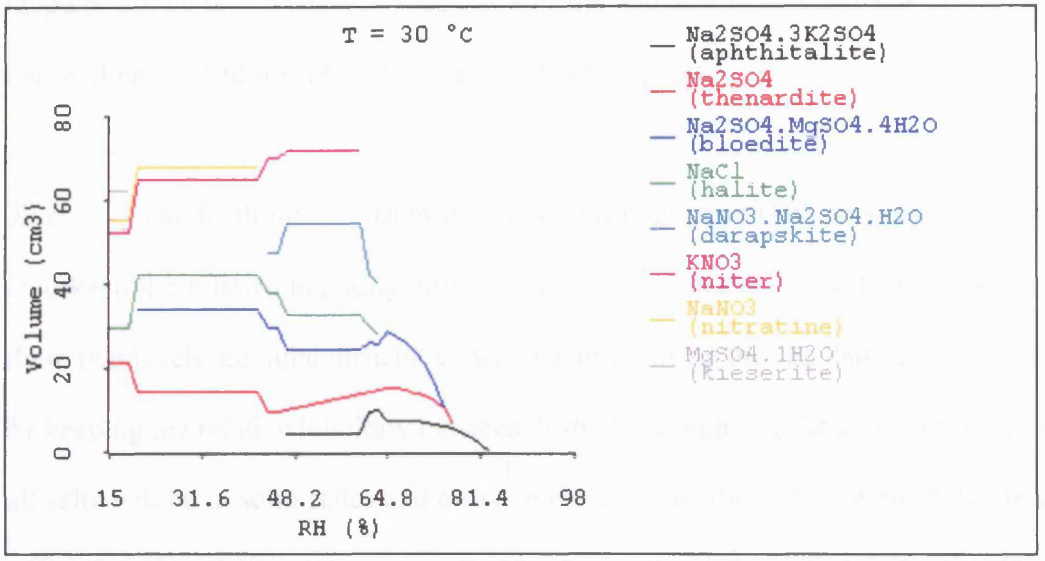

Figure 10.2 (also 2N in appendix N): Thermodynamic analysis using ECOS. Crystallisation sequence of soluble salts: relative humidity against volume of substance (cm^3). Sampling height: 5 cm, sampling depth interval: (1-3 cm). First fieldwork visit.

- **Results from the lower middle part** (sampling point: 105 cm) (figures 5N, 6N, 7N, 8N, 9N, and 10N: appendix N)

After removing the gypsum from its content, the surface sample (0-1 cm) from the sampling point at 105 cm height (lower middle part), showed, that nitratine precipitated first at a relative humidity of 69.5 % (see figure 5N and 6N: appendix N), which is slightly lower than its ERH as a single salt (73.1 %). Nitre was the second salt to leave the solution at 51 %RH, which is considerably lower than its ERH as single salt (92.3 %). Halite was the next salt to precipitate at 45.5 %RH, which is also considerably lower than its ERH as single salt (75.1 %). Calcium nitrate ($Ca(NO_3)_2$) and nitromagnesite ($Mg(NO_3)_2.6H_2O$) were the last salts to precipitate out of the solution at around 26.5 %RH. Following these results, salt damage at this point could be avoided either by keeping the relative humidity below 26 % or above 70 %. Also, the relative humidity

range of 30-44 % is relatively 'safe', as all salts will stay in solution apart from nitratine that will be in solid form but far from its transition point.

At the 1-3 cm depth interval from the same sampling point (105 cm), the ideal situation is to keep the relative humidity either above 98 % or below 37 %. Despite the fact that these two levels are quite difficult to achieve, minimising the salt damage is still possible by keeping the relative humidity between 40-60 %, which is quite a 'stable' range where all salts will be in solid states and away from their transition zone, while calcium nitrate will remain in solution.

At the deeper interval (3-5 cm), gypsum precipitated first at 97.7 % RH, followed by glauberite ($Na_2SO_4.CaSO_4$) at 87 %, thenardite (Na_2SO_4) at 77.9 %, halite at 73 %, bloedite and aphtitalite at 69.5 % and kieserite at 18.6 % (see figure 9N: appendix N). The crystallisation point of all salts in the solution was lower than their ERH as single salts. The ECOS thermodynamic calculations for the salt solution at this point showed that the most 'dangerous' range of relative humidity was between 69-87 %, where the transition states of most salts occurred and where the greatest increase in salt volume the occurred (see figures 9N and 10N: appendix N). Ideally, relative humidity should be kept either above 98 %, which is practically unachievable, or below 18 %, which is also difficult to reach. However, by carefully assessing the ECOS figures, it appears that with the relative humidity between 20 % and 60 %, which is very close to the recorded conditions at the site around the period of sampling, the salts figures were flat and relatively stable with most salts away from their transition points.

- **Results from the upper middle part** (sampling point: 355 cm) (figures 11N, 12N, 13N, 14N, 15N and 16N: appendix N)

The ECOS thermodynamic calculations from the cation and anion content at the surface sample (0-1cm) from the 355 cm sampling point (height), after removing the gypsum from its content, showed precipitation of bloedite at 76 %RH , followed by halite at 65.6 %RH. Nitratine and starkeyite ($MgSO_4.4H_2O$) precipitated at 57.6 %RH. The equilibrium relative humidity of thenardite as single salt at 30 °C (the average temperature of the sampling period) is 84.3 %, while within the solution its crystallisation point dropped massively to around 18.6 %. By taking into account the recorded environmental conditions during late summer around the period of sampling, it seems quite impossible to reach the required relative humidity levels to prevent salt damage. However, the relative humidity range between 35-50 % could be considered to be a 'stable' condition. The relative humidity range of 53-66 % is the most 'dangerous' and should be avoided in order to minimise salt damage at this location (see figures 11N and 12N: appendix N).

At the deeper intervals (1-3 and 3-5 cm) of the same sampling point (355 cm) all salts, after removing gypsum from the solution, were in solution above 62 %RH, and the transition points ranged between 25 % and 61.8 %RH. Considering the microclimate conditions at Petra around the period of sampling, this represents a very 'dangerous' situation as the transition points for most of the salts are within the fluctuation rates of the recorded relative humidity at Petra. Despite that, relative humidity at a range between 36 and 50 %, which is also within the fluctuation rate of the relative humidity at the site, could minimise salt damage (see figures 13N, 14N, 15N and 16N: appendix N).

- **Results from the upper part** (sampling point: 505 cm) (figures 17N, 18N, 19N and 20: appendix N)

From the surface sample (0-1 cm) at this sampling point, gypsum precipitated first at 98%RH, followed by anhydrite ($CaSO_4$) at 74.8 %RH. Halite left the solution system at 71.4 %, while calcium chloride ($CaCl_2.4H_2O$) remained in solution until the relative humidity dropped to around 16.6 %. Therefore, the ECOS theoretically 'safe' relative humidity zones are above 98 %RH and below 16 %RH, neither of which is a practical solution, since these ranges are considerably different from the actual relative humidity levels at the site. However, the ECOS calculations showed that the relative humidity range between 40-55 % could provide a 'stable' condition. On the other hand, the ranges of 58-75 %RH and 15-40 %RH should be avoided, since most salt transitions took place at these relative humidity levels (see figures 17N and 18N: appendix N).

At the sample from the deeper interval (1-3 cm), gypsum was removed prior to the ECOS calculations due to its high content in the solution, and halite was the first salt to precipitate out of the solution at 64.5 %RH. Controlling the relative humidity between 28 % and 55 %, which is within the fluctuation rate of the actual relative humidity during the sampling period in Petra, is the most practical solution in order to minimise salt damage from the salt solution at this sampling point.

10.3.2.2. Second fieldwork visit: winter campaign results

Unfortunately, the sum of cation and anion charges from the winter campaign samples were far from balanced, mainly because of the expected increase of carbonate or bicarbonate ions in the salt solution during this season, which the IC was unable to detect. Therefore, no thermodynamic calculations were made with samples from this visit, as the highly imbalanced ionic charge could result in data very different from the original salts solution and lead to suggestions that could enhance rather than contain the salt damage.

10.3.2.3. Third fieldwork visit: early summer campaign results

Unlike the winter campaign's results, the cation and anion analysis of the samples from the early summer campaign showed very good ionic balance (see table H3: appendix H). This suggests that the undetected carbonate or bicarbonate ions in this monument during early summer were in considerably lower concentrations than in winter. Considering that the most likely origin of these ions is from groundwater, these results seem understandable, since the rise in the groundwater level during winter will result in increased supply of carbonate and bicarbonate ions. The overall temperature averages for the sampling period was approximately 23 °C.

- **Results from the lower part** (sampling point: 5 cm) (figures 21N, 22N, 23N and 24N: appendix N)

The thermodynamic calculations from both sampling intervals (0-1 and 1-3 cm) of the lower part (5 cm: height) showed very similar trends (see figure 21N and 23N: appendix P). Gypsum precipitated out of the salt solution at around 97.7 %RH, followed by halite

at around 69.5 %RH. The crystallisation point of both salts was lower than their ERH as single salts. Anhydrite precipitated out later at 64.5 %RH, followed by nitratine at 56.3 %RH and finally calcium nitrate ($Ca(NO_3)_2$) at 37.6 %RH. Considering that the conditions at Petra around the period of sampling, as shown in figure 10.3, showed fluctuation of the relative humidity between 18 % and 64 %, with most readings above 40 %, it could be stated that the relative humidity range between 45-55 % is relatively 'safe' (no transition points or changes in salt volumes) and salt damage from the salt solution at this sampling point could be minimised by keeping the relative humidity within these limits. The relative humidity fluctuation between 56-68 % is the most 'dangerous' condition as it is at these levels that most salts will crystallise out of the solution and the highest change in salts volumes will occur partly due to dehydration of gypsum. (See figure 22N and 24N: appendix N).

- **Results from the lower middle part** (sampling point: 105 cm) (figures 25N, 26N, 27N and 28N: appendix N)

Once again, the thermodynamic calculations from the early summer campaign samples showed similarity between the samples from the two depth intervals (0-1 and 1-3 cm) at the same sampling point (105 cm height). In both samples, gypsum precipitated out first at 97.7 %RH, followed by halite at around 65 %RH, anhydrite at 63.9 %RH and finally calcium nitrate at 37.6 %RH. These were very similar to the results of the samples from the lower part (5 cm height). The 56-67 % relative humidity range appears to be the most 'unsafe', while the relatively 'safe' conditions are between 40-55 %RH.

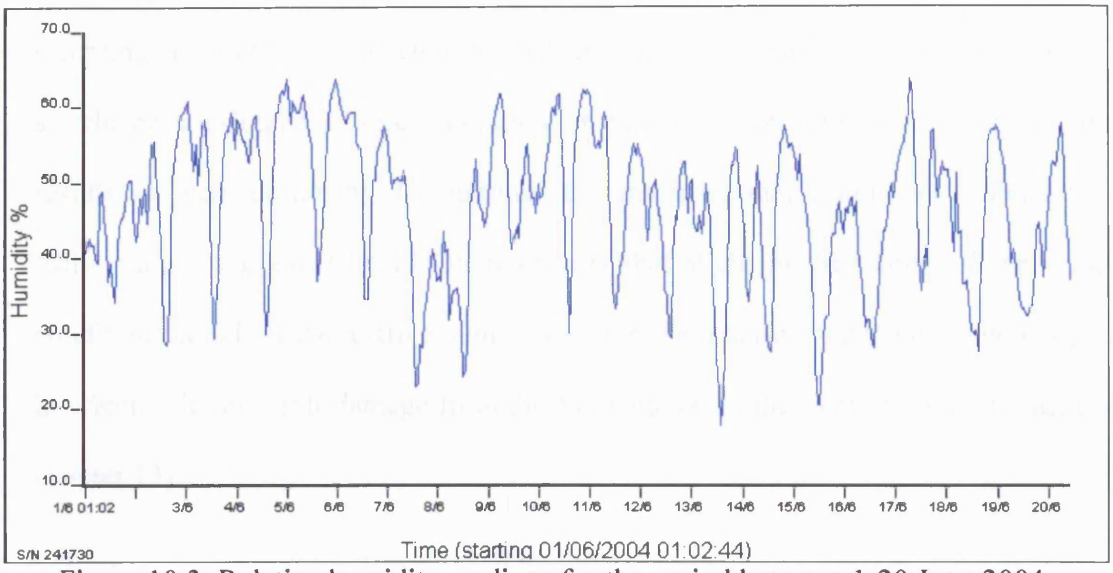

Figure 10.3: Relative humidity readings for the period between 1-20 June 2004. Source: data logger at the Deir Tomb.

- **Results from the upper middle part** (sampling point: 355 cm) (figures 29N, 30N, 31N and 32N: appendix N)

The thermodynamic calculations from the surface samples (0-1 cm) of the upper middle part of the profile (355 cm, height), showed a similar trend to the previous results from both the 5 cm and 105 cm sampling points with the relative humidity range between 55-65 % being the most 'hazardous' condition. Considering the salts volume changes and the points of salts transition, the relative humidity range between 40-55 % seems to be a 'harmless' condition where salt damage from the salt mixture at this point is likely to be minimal.

Despite a considerable variation in the amount of salt content at the deeper intervals (1-3 cm) compared to the surface sample (0-1 cm) from this sampling point, the behaviour of the salt solution showed rather similar figures, with the relative humidity between 63-65 % being the most 'unsafe' range. The thermodynamic calculation for this

sampling interval (1-3 cm) showed that any relative humidity readings below 60 % should be considered a 'safe' condition. In regards to preventive conservation, these results are very promising. Comparing the environmental conditions at Petra to the 'safe' ranges suggested by ECOS it appears that slight modifications of the existing conditions could set the relative humidity within the required 'safe' limits, which could, in effect, minimise salt damage from the salt solution in this part of the monument (see chapter 13).

- **Results from the upper part** (sampling point: 505 cm) (figures 33N, 34N, 35N and 36N: appendix N)

The ECOS thermodynamic calculations for the ions content in the samples from both sampling intervals (0-1 and 1-3 cm) of this sampling point were in agreement with the general trend of the previous sampling points at the Palace Tomb, with relative humidity between 55-66 % being one of the 'unsafe' conditions in regards to salt damage activity. It was within this relative humidity range that halite precipitated out of the solution and a slight change in the total volume of salts occurred, attributed mainly to the loss of water from the hydrated salt (gypsum) at around 65 %. Moreover, the ECOS calculations for this sampling point showed that the relative humidity range between 20-35 % should also be avoided in order to minimise the potential salt damage from the salt solution at this location. The relative humidity range between 38-54 % appears to be relatively 'safe'.

10.3.2.4. Fourth fieldwork visit: spring campaign results

The cation and anion content of the samples collected from C1 profile during the spring fieldwork campaign revealed a high percentage of calcium and sulfate ions. Also, the results showed less ionic balance than in the early summer. As a result, ECOS required the removal of gypsum before presenting the final figures of salt behaviour and composition of the samples. The relative humidity around the period of sampling fluctuated between 19 % and 78 %, with most readings between 40 % and 60 % (see figure 10.4). The average temperature was around 20 °C.

- **Results from the lower part** (sampling point: 5 cm) (figures 37N, 38N, 39N and 40N: appendix N)

After the program removed the gypsum from the cation and anion content of the samples from both the surface (0-1 cm) and the deeper (1-3 cm) sampling intervals, the thermodynamic calculations made by ECOS showed that all soluble salts should remain in solution when the relative humidity is above 66 %. Halite was the first salt to precipitate out of the solution at 65.9 %RH in both sampling intervals. Nitromagnesite was the last salt to leave the solution in the surface sample (0-1cm) at a relative humidity of 25.9 %RH, while kieserite was the last salt to precipitate out from the salt solution of the sampling interval (1-3 cm) at a relative humidity of 26.5 %. Based on the ECOS results, the 40-55 % relative humidity range could be considered to be the most 'safe' as regards to salt damage from this solution. Two relative humidity ranges, 55-65 % and 25-35 %, should be avoided in order to minimise salt damage from the salt solution at the lower part of this profile. It was within these ranges that the highest volume change

of halite and nitre took place, accompanied by the precipitation of other salts (see figure 38N and 40N: appendix N).

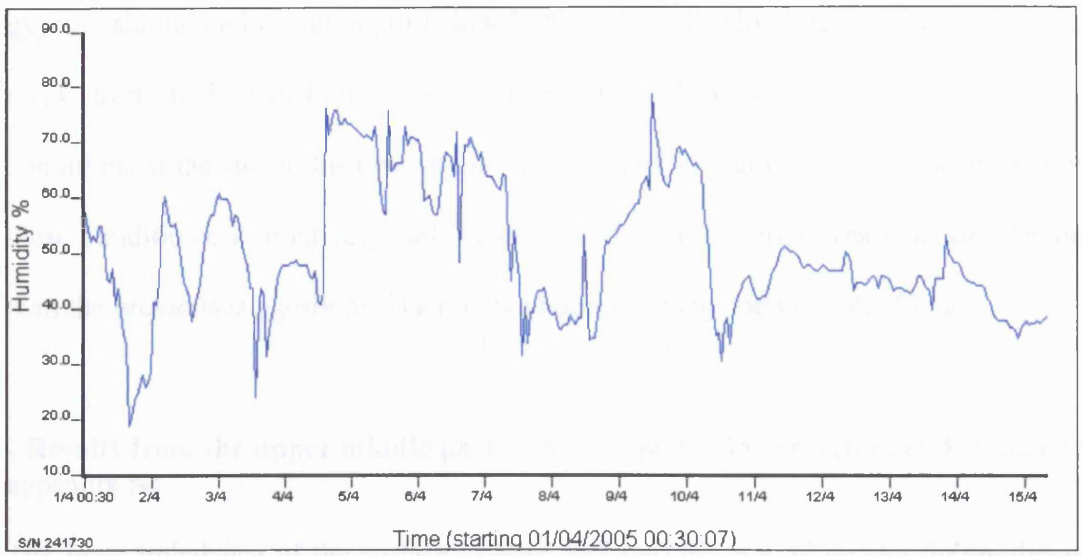

Figure 10.4: Relative humidity readings for the period between 1-15 April 2005. (Source: data logger at the Deir Tomb[19])

- **Results from the lower middle part** (sampling point: 105 cm) (figures 41N, 42N, 43N and 44N: appendix N)

Despite the slight variations in the salt composition between the surface samples (0-1 cm) and the deeper interval samples (1-3 cm) at the lower middle part of this profile (C1), the ECOS calculations for both salt solutions revealed a very similar behaviour regarding their response to changes in relative humidity. Halite precipitated out from both solutions at 73 %RH. Sylvite, a very soluble salt (21.91 g/100 ml at 25 °C, Perry and Phillips 1995, 302), appeared for the first time in this profile at the deeper sample intervals (1-3 cm) at a relative humidity of 64.5 %. The crystallisation point of this salt (sylvite) in the salt solution was 64.5 %, which is considerably lower than its ERH as single salt (85.1 %, Arnold and Zehnder 1990) at the same temperature. Regarding the

[19] The relative humidity readings were from the Deir tomb data logger, since the data logger in the Palace tomb went missing.

'safe' relative humidity conditions that could minimise salt damage at this point, ECOS suggested two ranges: a relative humidity above 73 %, where all salts apart from gypsum should be in solution, or below 26 %, where all salts should be in solid state and away from their transition to solution points. However, given the microclimate conditions at the site at this time of the year (spring), it is quit difficult to achieve any of these conditions. A relatively 'safe' condition, and also a more realistic aim for Petra than the previous suggestions, is a relative humidity range between 42-55 %.

- **Results from the upper middle part** (sampling point: 355 cm) (figures 45N and 46N: appendix N)

The ionic imbalance of the surface sample (0-1 cm) did not allow any thermodynamic calculations. The sample from the deeper interval (1-3 cm) showed a much better ionic balance, especially after removing the gypsum from its content. Halite, as in most of the previous samples, was the first salt to precipitate out of the solution at a relative humidity of 62.9 %. Nitratine was the second salt to leave the solution at a relative humidity of 61.3 %. Nitre was the last salt to precipitate out from the solution at 25.8 %RH, which is very much lower than its ERH as single salt (94.6 %, Arnold and Zehnder 1990). According to ECOS calculations, salt damage from the salt solution at this point can be avoided by keeping the surrounding relative humidity either above 63 % or below 25 %. Moreover, ECOS showed that the relative humidity range between 35-54 % could be considered as relatively 'safe'.

- **Results from the upper part** (sampling point: 505 cm) (figures 47N, 48N 49N and 50N: appendix N)

The salt solutions of the samples from the surface and deeper intervals of the upper part showed a trend very similar to the salt solutions from other sampling points of this profile during the spring sampling season. Halite, after excluding gypsum, precipitated out of the solution first at 65.9 %RH, followed by nitratine at 57.8 %. The precipitation of the rest of salts from the solution took place with the relative humidity between 25-30 %. Consequently, the most 'unsafe' relative humidity ranges regarding the potential salt damage in this part of the profile were 26-30 % and 55-66 %. Considering the volume change and the amount of salts, the ECOS program identified the relative humidity range between 35-52 % to be a relatively 'safe' condition (see figures 47N and 48N: appendix P).

10.4. The soluble salt types and distribution in the Palace Tomb according to the ECOS thermodynamic results: general discussion

Even though the analysis and evaluation of the cation and anion contents of samples from Petra monuments (chapter 9) had revealed significant information regarding the salt types and distribution in the monuments, the ECOS thermodynamic results showed the ultimate importance of including the surrounding environmental conditions not only in the evaluation of the salt types and distribution, but even when determining the salt amounts, types, volumes and distribution.

In addition to this, the evaluation of three sets of samples from the C1 profile, each from different sampling seasons depth intervals and sampling levels, also revealed the

importance of considering the effect from the interaction of different salts in the same solution. Generally, the crystallisation points of most salts within the solution were lower than their ERH as single salts. For example, in most of the samples from the late summer campaign, the crystallisation point of halite was below 65 %, which is significantly below its ERH as a single salt at the same temperature (75.1 %). Also, the presence of very soluble salts in certain samples affects the thermodynamic behaviour of other less soluble salts in the solution. For example, gypsum is a sparingly soluble salt and is expected to accumulate at the lower parts of the monument, but its presence alongside very soluble salts, such as calcium chloride ($CaCl_2.4H_2O$), resulted in its accumulation at higher levels.

The correlation of ECOS results from different sampling intervals at the same sampling point shows that the late summer samples had the highest variations in salts behaviour. The high rate of evaporation during the late summer, accompanied with considerably higher rates of fluctuation in the relative humidity could be the main reason for such variations. However, the crystallisation sequence of common salts in the different sampling intervals did not vary significantly. On the other hand, the results from the early summer and spring sampling seasons showed very slight variations in salts composition and behaviour in samples from different depth intervals at the same sampling point. In fact, the results from these two sampling seasons show very similar trends in salt composition and crystallisation sequences throughout the sampling profile. Such observations could suggest that the chances of minimising salt damage at Petra by

controlling the surrounding climate conditions are higher during the early summer and spring seasons than in late summer.

Moreover, the ECOS thermodynamic calculations confirmed the observations from the cation and anions analysis (chapter 9), where the more soluble salts crystallised at higher levels of the profile than the less soluble ones. For example, calcium chloride, a very soluble salt (73 g in 100 ml of water at 20 °C: Cerny and Rovnanikova 2002, p56), appears for the first time at the upper part of C1 profile during late summer, and calcium nitrate, also a very soluble salt, in the spring sampling season (122 g in 100 ml of water at 20 °C: Cerny and Rovnanikova 2002, p56). As was mentioned earlier, groundwater is the most probable source of salts and moisture in Petra monuments, therefore, the moisture content will decrease towards the upper level of the monuments resulting in only the most soluble of the salts remaining in solution.

All in all, the ECOS results from selected samples at the Palace Tomb revealed the importance of including the thermodynamic considerations in the evaluation of the salt composition and behaviour of a certain salt solution. Therefore, the evaluation of the salt composition and behaviour should consider not only the types of cations and anions but also the interaction between different anions as well as their interaction with the surrounding conditions. In addition, the variations in salt composition and behaviour from one sampling point to another and from one sampling season to another, showed how important it is to apply the calculations to as many samples as possible for a site the

size of Petra. Further research is needed in order to study and compare the thermodynamic behaviour of salts in other monuments.

10.5. Palace Tomb and the optimal conditions for preservation

As was introduced earlier in this chapter, the ultimate purpose of applying the ECOS program to the cation and anion content of a porous material is to predict the environmental conditions needed to prevent salt damage of this material. In order to prevent the damage from a salt solution, the surrounding relative humidity conditions should be kept either above or below the transition points of the different salts in the solution. Relative humidities within these ranges, where no change in the volume or phase took place, could provide relatively 'safe' conditions.

Table 10.1 summarises the results of ECOS applications on the selected samples from the Palace Tomb, identifying the most 'dangerous', 'safe' and achievable relatively 'safe' ranges of relative humidity, in regards to the salt damage from the salt solution at each location. Giving the existing microclimate conditions at Petra, the ideal preventive conservation conditions would be impossible to achieve as it would require controlling the relative humidity around the Palace Tomb either to above 98 % or below 18 %. It would be more realistic to aim to avoid the most 'dangerous' relative humidity levels.

Late summer results showed more than one 'dangerous' relative humidity range, with the 55-87 % appearing as the most common 'dangerous' range in the studied salt solutions. The ECOS thermodynamic calculations presented the relative humidity range of 55-66 % as the most dangerous relative humidity range during the early summer and spring seasons.

Sampling season	Sample location in the profile	Sample interval (cm)	Dangerous relative humidity ranges (%)	Safe relative humidity ranges (%)	Achievable safe relative humidity ranges (%)	Season achievable relative humidity range (%)
Late summer	Lower part (5 cm)	1-3	59-81 39-45	above 83 45-55 21-38 below 17	45-55 21-38	40-45 in all samples expect one sample
		3-5	69-87	above 98 20-60 below 18	20-60	
Late summer	Lower-middle part (105 cm)	0-1	24-29 45-70	above 70 45-30 below 26	45-30	
		1-3	36-40 55-75	above 98 40-60 below 37	40-60	
		3-5	69-87	above 98 20-60 below 18	20-60	
Late summer	Upper-middle part (335 cm)	0-1	53-66	above 76 30-50 below 18	30-50	
		1-3	25-37 51-61	above 62 36-50 below 26	36-50	
		3-5	25-37 51-61	above 62 36-50 below 26	36-50	
Late summer	Upper part (5 05 cm)	0-1	15-40 57-75	above 98 40-55 below 16	40-55	
		1-3	16-25 55-65	above 65 28-55 below 16	28-55	
Early summer	Lower part (5 cm)	0-1	56-68	above 98 45-55 below 37	45-55 below 37	45-54 in all samples
		1-3	56-68	above 98 45-55 below 37	45-55 below 37	
Early summer	Lower-middle part (105 cm)	0-1	56-67	above 98 40-55 below 37	40-55 below 37	
		1-3	56-68	above 98 40-55 below 37	40-55 below 37	
Early summer	Upper-middle part (335 cm)	0-1	55-65	above 98 40-55 below 29	40-55	
		1-3	63-65	above 98 Below 60	40-60	
Early summer	Upper part (5 05 cm)	0-1	26-35 55-66	above 98 38-54 below 38	38-54 below 38	
		1-3	20-35 55-66	above 98 38-54 below 38	38-54 below 38	
Spring	Lower part (5 cm)	0-1	25-35 55-65	above 66 40-55 below 25	40-55	40-52 in all samples
		1-3	25-35 55-65	above 66 40-55 below 26	40-55	
Spring	Lower-middle part (105 cm)	0-1	26-41 60-73	above 37 42-55 below 26	42-55	
		1-3	26-41 60-73	above 37 42-55 below 26	42-55	
Spring	Upper-middle part (335 cm)	1-3	25-30 53-63	above 63 35-54 below 25	35-54	
Spring	Upper part (5 05 cm)	0-1	26-30 55-66	above 66 35-52 below 25	35-52	
		1-3	26-30 55-66	above 66 35-52 below 25	35-52	

Table 10.1: Summary of the samples from the Palace Tomb analysed by ECOS: their location and depth intervals with the dangerous, safe and achievable safe RH ranges.

Based on these results, it could be concluded that in order to minimise salt damage in the Palace Tomb, the relative humidity should be kept below 55% throughout the year. However, as this study did not include samples from the winter sampling campaign, this suggestion may not be valid and should not be assumed to apply for the winter period.

As explained above, the ideal 'safe' relative humidity conditions are unachievable in reality. The term 'safe' in this study is used to refer to the relative humidity ranges in between the transition phase limits of the soluble salts in the solution, where no transition or volume change happens but the salts remain either in solid form or in solution. For example, the samples from the lower part of the Palace Tomb during the early summer season showed that the ideal conditions for preventing salt damage at that sampling point are to be had by keeping the surrounding relative humidity either above 98 % or below 37 %, both very difficult to achieve, since the actual relative humidity at Petra fluctuated between 18 % and 64 % during the early summer period. The relative humidity range of 40-55 %, however, also appears to be 'safe', since equally this range does not have any salt transition or volume change points.

By comparing Petra conditions with the results of the ECOS program, the achievable relative humidity ranges have been identified. These are relatively 'safe' ranges that are not far from the existing ambient conditions at Petra, and, therefore, represent a more realistic approach to the problem.

After identifying the achievable relatively 'safe' conditions for each sample, a common relatively 'safe' environment for each fieldwork visit has been specified. In other words, a relative humidity zone, relatively 'safe' for all salt solutions at the C1 profile, has been identified for each sampling season (see table 10.1). These common relatively 'safe' relative humidity ranges are: 40-45 %, 45-54 % and 40-52 % for the late summer, early summer and spring sampling campaigns respectively.

It should be stated that these results do not suggest that preventing or even minimising the salt damage around Petra monuments by controlling the ambient conditions (relative humidity) is a straightforward process. Nevertheless, these results have shed light on the way towards identifying possible preventive conservation measures for the site.

Thus far, the current research has shown how complicated the salt damage mechanisms are at a site like Petra, where the microclimate conditions, the salt content and the thermodynamic interactions between different salts and their surrounding environment vary significantly from one season to another. Therefore, any attempt to apply any of the suggested relatively 'safe' conditions, if of course possible to do so, should consider the following factors:

- Petra has greatly fluctuating and relatively high wind speed rates throughout the year, which probably affect the salt damage at the site. The same applies for Petra's high solar radiation. Therefore, before any preventive conservation measures are put in place in the entire monument, the ECOS results should be applied on a small area first, in

order to test the effectiveness of the program's suggestions in the actual environment, where other factors could have a great influence on the salt damage mechanism.

- Before modifying the existing relative humidity, the potential impact on any other weathering mechanisms, such as biological weathering, that may also be active at the site, must be assessed.

- Any applications based on the ECOS results should work in parallel with any other conservation measures. As was discussed in previous chapters, the grazing activities around the site are hypothesised to be the main source of nitrate, one of the most common ions in Petra monuments. As the grazing activities are seasonal, the nitrate content is unpredictable and fluctuates greatly, affecting, as a result, the thermodynamic behaviour of the salt solutions in the monument. Therefore, if the grazing activities were to be controlled, the ECOS calculations would have to be repeated with the new data, as the salts composition and behaviour would have changed.

- Despite the relatively large number of samples collected from the Palace Tomb and the detailed microclimate survey that took place during this study, the evaluation of salt compositions and behaviour in a monument like the Palace Tomb and any other monuments in Petra by the ECOS program requires a further detailed study of the salt contents and a more detailed microclimate survey.

All in all, the ECOS program proved to be a useful tool in understanding Petra's Palace Tomb salt compositions and behaviour. It demonstrated the effect of the surrounding environmental conditions on the thermodynamic behaviour of the salts in the tested samples. Also, it showed how the interactions between different salts could significantly

change the salt solution's behaviour. The evaluation of the program's results has led to the identification of the most 'dangerous', 'safe', relatively 'safe' and achievable relatively 'safe' environments, which is an important step towards minimising salt damage. However, the application of ECOS results to a cultural heritage site, like Petra, should take into consideration the nature of the site and all the surrounding environmental conditions, as well as any other weathering mechanism.

Considering the fact that wind speed could have an important role in the salt damage, a simulation test for salt crystallisation, particularly designed for this study, will examine the effect of wind speed on the salt distribution and crystallisation.

Chapter 11
Wind Speed and Salt Crystallisation and Distribution: Simulation Tests

11.1. Introduction

Laboratory simulation tests, where salt damage is accelerated within a short period of time through different procedures, yield vital information regarding salt crystallisation and distribution processes. However, due to the uncertainty of the actual salt damage process at the site and the wide range of variables involved in this process, the results of salt simulation tests vary significantly from one study to another. Chapter 2 introduced some of the commonly used salt damage simulation tests, their procedures, advantages and disadvantages. These tests vary not only in their procedures and materials, but also in the environmental conditions used. Goudie (1993) and Goudie and Viles (1995), for example, preferred to use environmental conditions similar to those found in the field, while the majority of tests preferred overstated environmental conditions to maximise salt damage within a short period of time.

Each of these procedures, the use of the field observations or the overstated environmental conditions, has its strong argument. The use of the field environmental conditions will provide more representative results, but it will not show the long-term results of the salt damage unless the duration of the test is extended significantly. On the other hand, the application of overstated conditions in the simulation tests will provide an important overview of the long-term salt damage. But will it simulate the actual salt damage mechanism in the field? The variations between the different simulation tests

extend to other factors, such as the rock type, the salt type and concentration, the simulating procedure and the interpretation of the results. As a result of these variations, the evaluation and comparison of the test results is quite difficult and may be misleading. Lubelli (2006) showed that the use of different procedures in simulating the damage caused by sodium chloride could considerably affect the simulation results.

Consequently, the selection of a simulation procedure to evaluate the wind speed factor in salt damage generally and in salt damage at Petra monuments particularly was a challenging task. Is it preferable to use one type of salt, which is highly regarded as dangerous in porous building materials, or to include other salts in the test? Which is more representative, a saturated or an unsaturated salt solution? What type of rocks should the test use, sandstone, limestone or brick? Would an accurate representation of the field environmental conditions offer significant results in simulating the salt damage or should these be overstated instead for the test purposes? Is the total immersion test too far from what actually happens in the field, or is the partial immersion test impractical? All these questions were considered when designing the simulation tests for this research.

The simulation test of the wind speed effect on salt crystallisation and distribution started with a salt crystallisation test in an environmentally controlled chamber. Due to the technical failure of the chamber, a modified salt crystallisation test based on the BRE simulation test was used as an alternative. The two simulation tests are described below.

11.2. Microclimate generator test

The first simulation test aimed to evaluate the effect of different wind speed conditions using a controlled environmental chamber to provide the required environmental conditions (the simulation procedure and conditions are presented in chapter 7). Unfortunately, the chamber broke down during a preliminary testing procedure and before the start of the actual test on the selected stone materials (Locharbriggs and Petra stone). Nevertheless, the results of the preliminary tests on two random sandstone specimens were recorded and evaluated.

11.2.1. Accuracy of experimental chamber

Prior to the start of the laboratory experiment, the accuracy of the chamber was tested. The chamber was operated using many different environmental conditions with a Hanwell telemetry unit (a radio telemetry system for monitoring the environmental conditions such as relative humidity and temperature) installed in the chamber. By comparing the results of the Hanwell telemetry unit readings with the chamber readings it was obvious that the chamber was not very accurate at very high or very low relative humidity conditions. In particular, when the chamber was operated in relative humidity conditions above 80 % or below 30 %, there was quite a big difference between the readings of the telemetry unit and the chamber (in an average of $\pm$ 5-7 %). However, the chamber showed high accuracy when it was operated at relative humidity levels above 30 % and below 80 % (in average of $\pm$ 1-2 %) Controlling the temperature inside the chamber was another problem. The temperature control unit used in the chamber is only capable of increasing but not reducing the temperature. Therefore, the lower temperature

conditions were achieved by cooling the air sources of the chamber (namely, the input air) with a cold water vessel placed in front of the input air fan and by using a small air-conditioning unit (see figure 7.1).

11.2.2. Materials

As mentioned earlier, the experiment was only conducted on two random sandstone samples, and not on the laboratory test specimens. Therefore, this section will only briefly present the characterisation of these random sandstone specimens as well as the properties of the sodium sulfate solution used.

- The tested specimens

Sixteen specimens from two British sandstones of unknown origin (supplied by Price) were tested in this experiment. The following is a brief description of these types:

Specimen (1): Gray sandstone specimens (called G sandstone in this study).

Hand specimen: Fine grained, dark grey, non-calcareous sandstone.

Thin section: The principal framework grains were ragged, monocrystalline quartz with quite a high percentage of biotite. Dolomite crystals formed approximately 10 % of the total composition. There were no coarse pores in the sample, but pores with 0-1 μm radius were found. The total porosity was around 10 % (calculated from the thin section and not by mercury intrusion experiment). The pores were mainly connected to each other.

Specimen (2): Red sandstone specimens (called R sandstone in this study).

Hand specimen: medium to coarse, red, non-calcareous sandstone.

Thin section: a mixture of quartz, orthoclase feldspar (pink) and rock fragments were the principal framework grains. The sand grains stood out in high relief (there was little matrix), placing this in a sand category. Few coarse pores (10-100 μm) were evident making an average of 4 %. The percentage of fine pores was around 8 %. This means that the total porosity of the sample was approximately 12 %. Pores were mainly connected to each other, with a few dead-end pores.

- Salt solution

A saturated sodium sulfate solution was used in the four preliminary runs of this experiment (see chapter 7 for the solution properties and preparation methodology).

11.2.3. Simulation cycle

Only four runs were performed in this preliminary test, each run with two samples from each sandstone specimen (G sandstone and R sandstone). The test was carried out under fixed temperature and relative humidity (20±2 °C and 75±2 %RH), but with a different wind speed condition in each run. The four conditions in the experiment runs were as follows:

- First run: no wind speed.
- Second run: low wind speed with an average rate of 0.5 m/s.
- Third run: high wind speed with an average rate of 4 m/s.

- Fourth run: fluctuating wind speed. The experiment in this run started with low wind speed for three hours, then changed to high wind speed for another three hours, and the same process was repeated throughout the duration of the drying cycle.

In each run, the specimens were first dried to a constant weight and then immersed in saturated sodium sulfate solution for two hours. After that they were placed in the environmentally-controlled chamber for 24 hours in the above mentioned conditions. Then the samples were removed from the chamber and the amount of stone decay, salt efflorescence, and subflorescence of each sample was calculated according to the test procedure (see chapter 7).

11.2.4. Results and discussion

Despite the fact that only four runs were performed and with random sandstone samples, the results of the test showed that the wind speed conditions have significant impact on the sodium sulfate crystallisation process. The test results are listed in table 11.1.

Generally, the amount of stone decay in both sandstone types was higher at high wind speed conditions and reached its maximum in fluctuating wind speed conditions (table 11.1 and figure 11.1).

Sample No.	Dry weight (W_0) (g)	Wind speed (m/s)	The loose weight (W_L) (g)	Dry weight (W) after removing the samples from the chamber (g)	The amount of decay (W_s) (g)	Efflorescence (W_E) = (W_L) - (W_s) (g)	Subflorescence (W_{Sb}) = (W) + (W_s)- (W_0) (g)
G1	141.924	-	1.403	142.114	0.503	0.900	0.793
G2	141.534	-	1.168	141.878	0.478	0.690	0.922
R1	135.838	-	1.332	136.214	0.624	0.708	1.100
R2	135.759	-	1.344	136.247	0.679	0.665	1.367
G3	140.978	0.5	1.558	141.547	0.702	0.856	1.271
G4	141.235	0.5	1.601	141.786	0.774	0.827	1.325
R3	136.100	0.5	1.704	136.601	0.889	0.815	1.590
R4	136.882	0.5	1.626	137.542	0.791	0.835	1.451
G5	139.878	4.0	1.568	140.421	0.901	0.667	1.444
G6	141.147	4.0	1.481	141.642	1.008	0.473	1.503
R5	137.001	4.0	1.545	137.454	0.980	0.565	1.433
R6	136.587	4.0	1.645	137.184	0.993	0.652	1.590
G7	139.878	0.5-4.0	1.791	140.556	1.105	0.686	1.556
G8	141.147	0.5-4.0	1.885	142.003	0.978	0.907	1.640
R7	137.001	0.5-4.0	1.863	137.859	1.121	0.742	1.758
R8	136.587	0.5-4.0	1.788	137.469	1.087	0.701	1.805
G7	139.878	0.5-4.0	1.791	140.556	1.105	0.686	1.556

Table 11.1: Results of the sodium sulfate crystallisation test on sixteen random sandstone samples

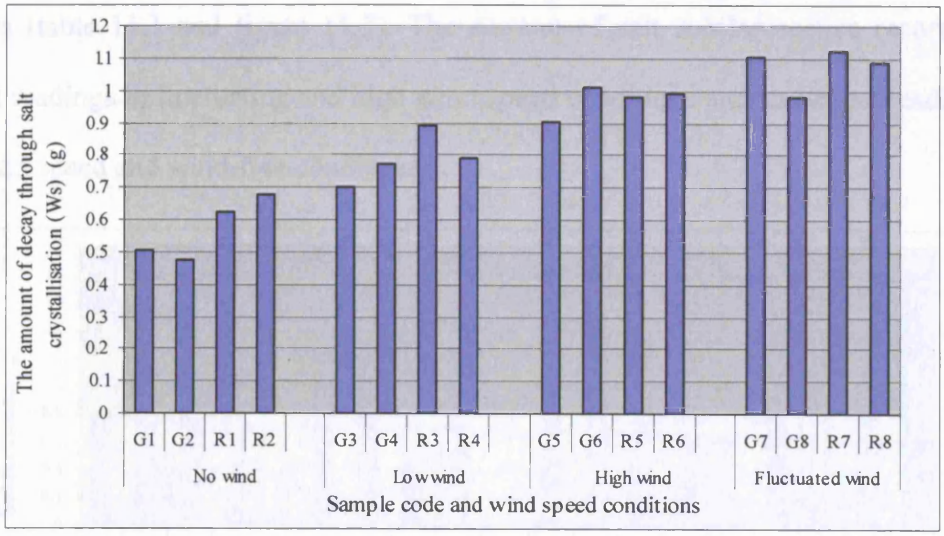

Figure 11.1: The amount of decay through salt crystallisation (W_s) (g) for the sixteen samples tested using sodium sulfate solution.

The amount of salt efflorescence was slightly higher in low wind speed and fluctuated wind speed conditions. The salt efflorescence recorded its lowest reading in high wind speed conditions (table 1.1 and figure 11.2).

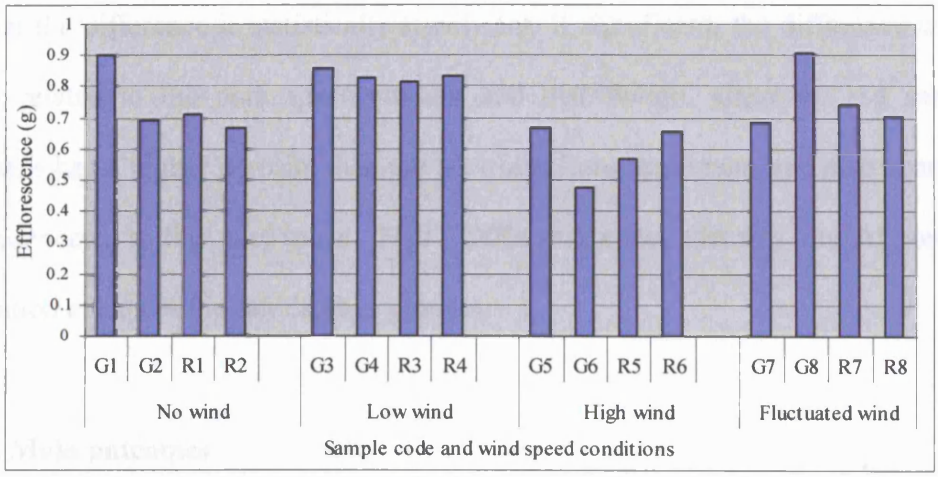

Figure 11.2: The amount of salt efflorescence (g) for the sixteen samples tested using sodium sulfate solution.

Furthermore, wind speed affected the total amount of salt subflorescence in the tested samples (table 11.1 and figure 11.3). The amount of salt subflorescence recorded its highest readings in fluctuating and high wind speed conditions and its lowest readings in low wind speed and wind-free conditions.

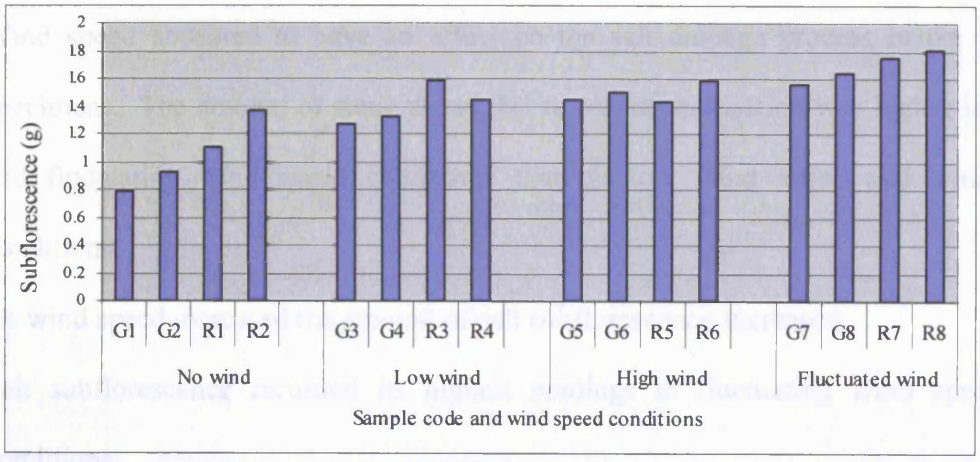

Figure 11.3: The amount of salt subflorescence (g) for the sixteen samples tested using sodium sulfate solution.

In addition, it was observed that the amounts of stone decay due to salt crystallisation as well as the amounts of salt subflorescence were generally higher in the arkosic sandstone specimens (Red sandstone: group 1), although too few samples were tested for one to be sure that the difference is statistically significant. If significant, the difference could be mainly related to the pore space amount and distribution, since the red sandstone specimens had a higher porosity than the grey sandstone specimens and also coarse pore space connected to fine pore space. Flatt (2002a) has stated that this kind of pore space distribution enhances the salt damage process.

11.2.5. Main outcomes

The small number of specimens and the low porosity of the specimens made it very hard to reach a general conclusion on the role of wind speed in the crystallisation process of sodium sulfate. Also, the chamber broke down when the test experiment was being run and before the planned experiments with Petra-like stone could take place. Nevertheless, the laboratory test revealed significant information and its main outcomes can be summarised as follows:

- Wind speed appeared to have an effect on the salt damage process in the tested specimens. The amount of stone decay due to salt crystallisation was higher in high and fluctuating wind speed conditions than in low wind speed and wind-free conditions.
- As wind speed increased the amount of salt subflorescence increased.
- Salt subflorescence recorded its highest readings in fluctuating wind speed conditions.

- The total porosity as well as the pore space distribution appeared to have a role in the salt crystallisation process. In the specimens with high porosity and macropores connected to micropores, the stone damage was accelerated.

11.3. Modified salt crystallisation test

As an alternative to the microclimate controlled chamber test, a modified salt crystallisation test based on the BRE salt crystallisation test was developed to continue the experimental part of the research. The test consisted of six different runs, each run consisting of 16 day cycles. In each cycle, the specimens were immersed in a salt solution (two salt solutions were used: saturated sodium sulfate solution and saturated Petra salts solution) for two hours and then subjected to a 24-hour cycle of drying at certain environmental conditions (see chapter 7 for details of the experiment conditions and procedures). The evaluation of each run was carried out by measuring the weight gain or loss of the tested specimens. The salt distribution was also evaluated at the end of each run, in order to assess the impact of the different environmental conditions on the distribution of different types of salts. The salts distribution was evaluated by two means: analysis of the main cations and anions of drilled samples using IC and ICP-AES, and thin section study using the ESEM. The weight change (gain or loss) was correlated with the salts distribution.

11.3.1. Simulation test conditions

As mentioned earlier, the simulation test used in this research was a modified BRE salt crystallisation test designed to suit the research aims and purposes. The main

modifications to the BRE test were the introduction of the wind speed factor, the use of saturated sodium sulfate solution, the introduction of Petra salts solution as the second salt solution, the control of the relative humidity conditions during the test, and the reduction of the drying temperature to 60 °C. The following table (11.2) summarises the conditions of each run of the test.

Experiment run number	Relative humidity %	Temperature °C	Wind speed condition
1	Low	60	low
2	Low	60	high
3	Low	60	fluctuated
4	High	60	low
5	High	60	high
6	High	60	fluctuated

Table 11.2: The different environmental conditions for the six runs of the modified salt crystallisation test.

11.3.2. Materials

11.3.2.1. Stone

Five different types of stone were used in each run of this experiment and these were:

- Locharbriggs sandstone (S): This stone was chosen because its chemical composition and open porosity content are similar to Petra stone. Unlike Petra stone though, this stone has no clay minerals.
- Monks Park limestone (L): This stone was used in this test because it is the most common tested stone in many salt crystallisation tests, including the BRE test.
- Disi sandstone (D): This stone was selected because the Bab al Siq Triclinium Tomb is carved from this stone.
- Upper Umm Ishrin sandstone (U): This stone was selected because the Deir Tomb is carved from this stone.

- Middle Umm Ishrin sandstone (M): This stone was selected because the Palace and Corinthian Tombs are carved from this stone.

11.3.2.2. Salt solution

Saturated sodium sulfate and saturated 'Petra' salt solution were the two salt solutions used in the test. The specification and preparation procedure of these two salt solutions are presented in detail in chapter 7.

As a result, the test was composed of twelve runs, six with the sodium sulfate salt solution and six with the Petra salt solution. Each run consisted of sixteen cycles of two-hour immersion and 24-hour exposure to certain environmental conditions. The five different stone types mentioned above were used in each run.

11.3.3. Pre-simulation tests

Prior to the start of the salt simulation test, a range of tests were carried out to determine the main properties of the tested stone specimens. These included thin-section petrographic study, XRD and XRF analysis, and open porosity, water absorption capacity and wetting and drying measurements.

11.3.3.1. Petrography

A petrographic study of the main stone properties was carried out on two thin sections from each tested stone. The 30 μm thin section slides were prepared using a kerosene-based technique, in order to avoid any alteration to the physical properties of the stones,

especially the Petra specimens, which contain soluble salts and clay minerals (see chapter 7). The following is a brief description of the properties of the tested stones as determined by the microscopic study of their thin-sections.

Locharbriggs sandstone (Locharbriggs, UK)

Locharbriggs sandstone is red, fine grained Permian sandstone extracted from the New Red Sandstone formation near the village of Locharbriggs, Dumfries, Scotland (Historical Scotland: 12 Technical advice Note 1997).

Thin section description: a medium to fine-grained sandstone consisting of well-sorted, sub-angular to well rounded quartz grains, coated in iron oxide and cemented by silica. K-feldspar grains make up approximately 5 % of the total rock content. Porosity: very high total porosity around 22 %, with mainly coarse (10-100 μm radii) to very coarse (100-1000 μm radii) pores.

Monks Park limestone (Bath, UK)

Monks Park limestone is an oolitic limestone from the Great Oolite of middle Jurassic age (The BRE/ British Stone Stone List 1997 and Leary 1983).

Thin section description: a fine-grained, homogeneous, buff-coloured oolitic limestone. The ooliths comprise approximately 70 % of the rock, range in size from 300 to 600 μm and are cemented by sparite matrix. The pore spaces (coloured with blue resin) are mainly very fine and difficult to distinguish and appear only within the ooliths rather than the cement (figure 11.5).

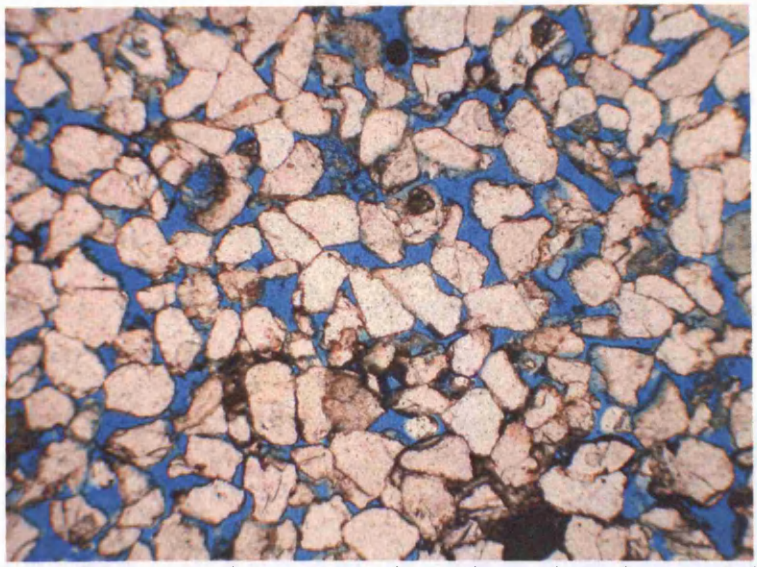

Figure 11.4: Photomicrograph of the petrological thin section of Locharbriggs sandstone specimen. Field of view 2.5 mm. Magnification: 40x. (Plain polarized light) (ppl).

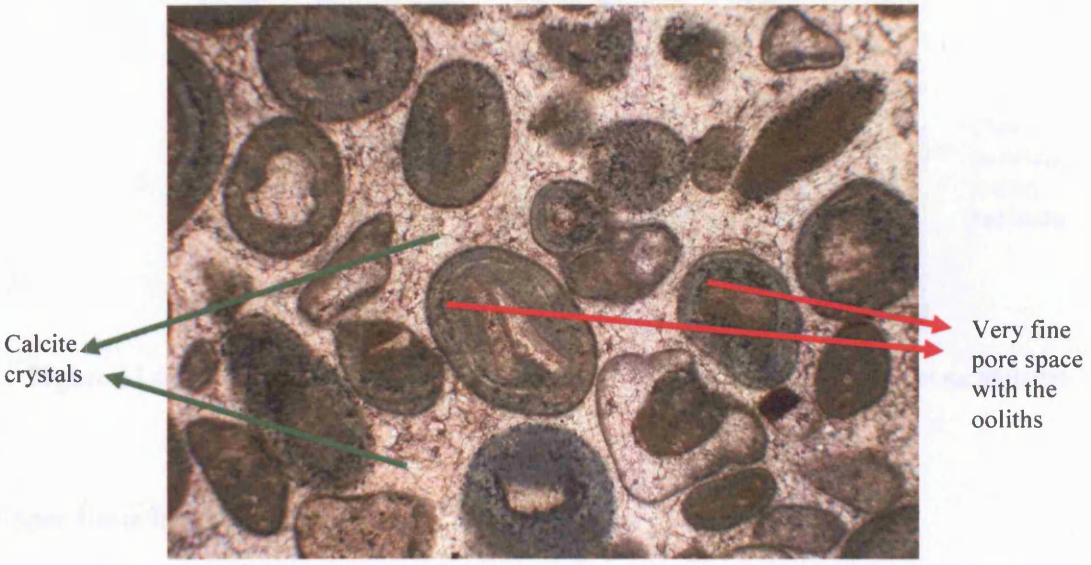

Figure 11.5: Photomicrograph of the petrological thin section of the Monks Park limestone specimen. Field of view 2.5 mm. Magnification: 40x. (ppl)

Disi Sandstone (Petra, Jordan)

Disi sandstone is white, medium grained, massive sandstone from the late Cambrian to early Ordovician age. The Bab al Siq Tomb is carved out of this sandstone formation.

Thin section description: a white to grey, medium to coarse grained sandstone with quartz making up more than 85 % of its content. The sample is bimodal and shows a significant variation of grain size compared to Locharbriggs sandstone. Clay minerals (mainly kaolinite) are the main matrix. Calcite is the secondary matrix. Porosity: very high total porosity, approximately 22 %, with mainly coarse (10-100 μm radii) to very coarse pores (100-1000 μm radii). (Figure 11.6).

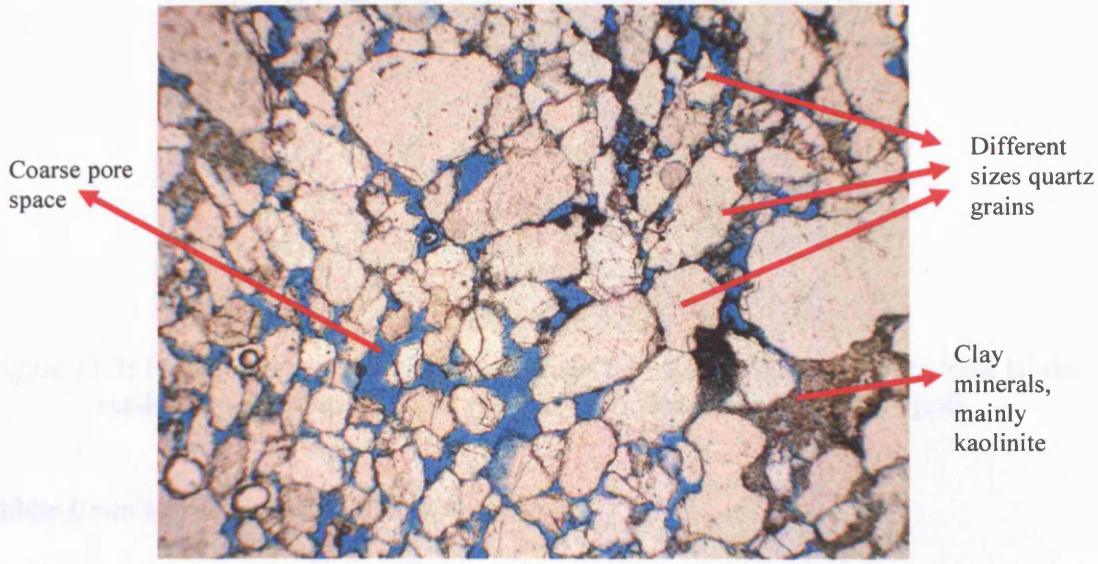

Figure 11.6: Photomicrograph of the petrological thin section of the Disi sandstone specimen. Field of view 2.5 mm. Magnification: 40x. (ppl).

Upper Umm Ishrin Sandstone (Petra, Jordan)

Upper Umm Ishrin sandstone is a multicoloured sandstone from the subarkosic Umm Ishrin formation of the middle to late Cambrian age. The Deir Tomb is carved out of this formation.

Thin section description: a multicoloured, fine to medium, sub-angular to sub-rounded grained sandstone. Iron oxides and kaolinite are the main matrix. Quartz grains make up

above 80 % of the stone content. Porosity: moderate total porosity (around 15 %) with mainly medium (1-10 μm) to coarse pores (10-100 μm radii).

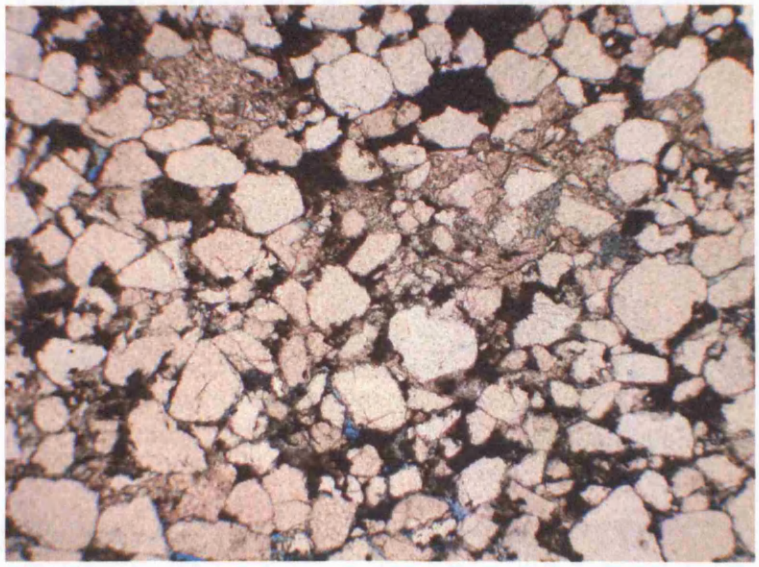

Figure 11.7: Photomicrograph of the petrological thin section of the Upper Umm Ishrin sandstone specimen. Field of view 2.5 mm. Magnification: 40x. (ppl)

Middle Umm Ishrin Sandstone (Petra, Jordan)

Middle Umm Ishrin sandstone is a multicoloured, mainly fine grained, massive sandstone from the sub-arkosic Umm Ishrin formation of the middle to late Cambrian age. Both the Corinthian and the Palace Tombs are carved out of this formation.

Thin section description: a multicoloured, fine to medium grained, sub-angular to sub-rounded, well sorted sandstone. Similarly to the Upper Umm Ishrin sandstone, iron oxide (hematite) and clay minerals are the main cementing materials.

Porosity: high total porosity (approximately 20 %) with medium (1-10 μm) to coarse pores (10-100 μm radii) (figure 11.8).

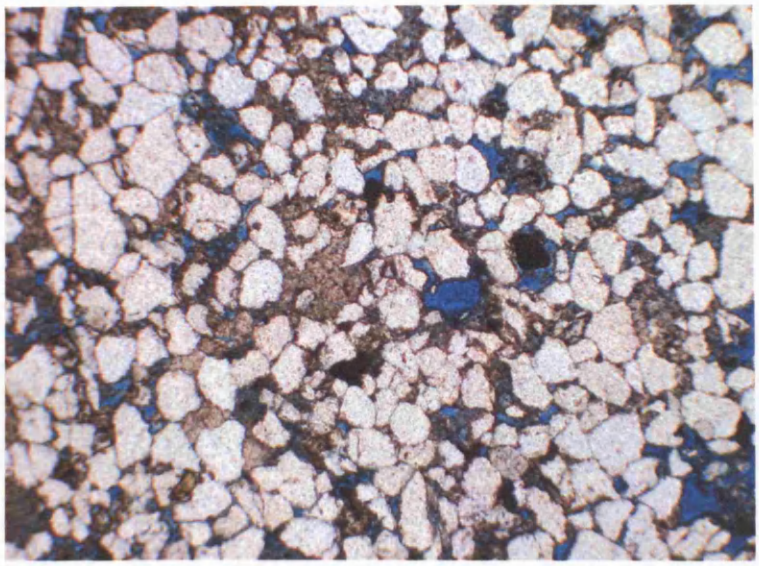

Figure 11.8: Photomicrograph of the petrological thin section of the middle Umm Ishrin sandstone specimen. Field of view 2.5 mm. Magnification: 40x. (ppl).

11.3.3.2. X-ray Fluorescence (XRF) and X-ray Diffraction (XRD)

In addition to the petrographic studies, both XRF and XRD tests were carried out on the tested stones to verify the chemical composition of the specimens. (The XRD and XRF testing methodologies are discussed in chapter 7).

The XRF results for the tested samples are presented in appendix O and the average readings of each specimen are summarised in table 11.3.

The results (all expressed as weight percentage of the oxides) show that silicon is the main component of all sandstone samples, with the highest percentage in Locharbriggs sandstone specimens (approximately 92 %), and the lowest in Middle Umm Ishrin sandstone specimens (approximately 85 %). Aluminium is the second major component, with the highest readings in Petra stones. Middle Umm Ishrin sandstone specimens have the highest amount of aluminium among Petra stones, at approximately 9 %. Following the petrographic study, it can be stated that the higher aluminium content is found in the

specimens with higher clay mineral content. Approximately 3 % hematite was found in Middle Umm Ishrin sandstone specimens. Locharbriggs sandstone has the highest potassium (approximately 2 %).

In the limestone specimens, calcium is the main component, with silicon as a minor component (approximately1 %) and traces of aluminium (less than 0.5 %).

Sample Code	Na_2O %	MgO %	Al_2O_3 %	SiO_2 %	K_2O %	CaO %	Fe_2O_3 %	TiO_2 %
U	0.51	0.02	6.17	88.19	0.10	0.05	0.19	0.22
M	0.46	0.06	9.32	86.03	0.11	0.17	2.88	0.22
D	0.87	0.11	7.10	86.69	0.08	0.08	0.47	0.36
S	0.59	0.17	4.73	91.71	1.90	0.16	0.82	0.09
L	0.09	0.36	0.40	2.20	0.01	50.29	0.00	0.00

Table 11.3: Summary of the averages of the main oxides in the simulation test stone specimens. U: Upper Umm Ishrin sandstone. M: Middle Umm Ishrin sandstone D: Disi sandstone. S: Locharbriggs sandstone. L: Monks Park limestone.

The petrographic studies indicate the presence of a relatively high percentage of clay minerals in Petra stone samples and this was confirmed by the high amount of aluminium in these stones. XRD analysis was, therefore, performed on the Petra stone samples to identify the mineral phases and especially the clay mineral types. The XRD analysis was carried out in two stages: firstly, a mineral phase identification without any preparation or treatment of the samples, and, secondly an analysis of preferred oriented samples (see chapter 7 for more details). The XRD spectra[19] of both stages are presented in appendix P.

[19] The evaluation of these spectra and the identification of the minerals phases were carried out with help of Steve Hirons from the Department of Earth Science at the University College London.

It was found that kaolinite was the main clay mineral in all the Petra specimens. Hematite was identified in the Middle Umm Ishrin sandstone specimens. Calcite was found in Upper Umm Ishrin and Disi sandstone specimens, but not in the Middle Umm Ishrin specimen.

As discussed in chapter 4, the identification of the clay mineral types is a crucial factor in the evaluation of the salt damage in stone. The clay mineral contents in the tested specimens are included in the discussion of the simulation test of this research.

11.3.3.3. Open porosity

The determination of the total open porosity as well as the type of pore space is essential in the evaluation of salt damage in porous building materials (Benavente *et al.* 2004 and Flatt 2000a). The current study carried out a total open porosity test on the five stone specimens mentioned earlier. The procedure, commonly used in the Earth Science Department at University College London (Woodman 2004, personal commun.), is presented in chapter 7. The test results are in appendix R and are also summarised in table 11.4.

Generally, all tested specimens showed very similar percentages of total open porosity, with Monks Park limestone specimens having the highest averages, approximately 22 % and Upper Umm Ishrin specimens the lowest averages, approximately 19 %. Even though the petrographic studies showed that each stone of the laboratory simulation test has different pore space sizes, the total open porosity tests indicated that the total porosity of all tested stone was within very similar ranges. This shows the importance

of including the total open porosity and pore sizes in any evaluation of the pore system. This point will be discussed further in the evaluation of the simulation test results.

11.3.3.4. Water absorption capacity

The water absorption capacity test (WAC) is one of the most commonly used tests to evaluate stone materials before applying any simulation tests to them (Goudie 1974, Goudie and Viles 1995 and Goudie 1999a and b).

In general, the higher the water absorption capacity in specimens, the more susceptible to salt damage these will be. In this study, the ASTM C 642-97 (American Society of Testing and Materials Standard) was used to measure the water absorption capacity after immersion and the water absorption capacity after immersion and boiling (Annual Book of ASTM Standards 2004) (see chapter 7 for more details). The full results are in appendix R and the main outcomes are summarised in table 11.4.

Sample Code	Average Total open porosity %	Average WAC after immersion %	Average WAC after immersion and boiling %	ΔW (weight loss or gain) after the drying - wetting test %
U	19. 08	5.77	7.20	-1.66
M	20.40	5.50	5.80	-1.49
D	20.98	6.51	6.83	-5.63
S	20.87	7.57	10.18	-0.40
L	21.92	9.93	10.73	-0.19

Table 11.4: Summary of the main characteristics of the tested stone specimens: total open porosity, water absorption capacity and weight loss from the wetting and drying test

The results showed that Monks Park limestone has the highest WAC percentage (approximately 10 %), while Petra stones have very similar WAC ratios of about 5-6 %. It also important to note that, during the test, some Petra stone specimens, especially the Disi sandstone sample, lost some of their original weight by immersion in water, which

means that the actual WAC of these samples could be slightly higher than what was shown in the final results. (For a more complete documentation of the water absorption test, and the dry and wet weights recorded at regular intervals, see appendix R). It was observed that the wet weight of specimens with fine pores (such as Monks Park limestone) increased with time to greater degree compared to specimens with larger pore spaces (such as Locharbriggs sandstone and Disi sandstone). On the other hand, the Disi sandstone specimens showed the lowest increase in the WAC after immersion and boiling, while the Upper Umm Ishrin sandstone showed high WAC after boiling. By comparing these results to the pore sizes of these stones, it can be said that pore space sizes can significantly affect the WAC ratios. The coarser the pore space of the specimen, the lower the difference between its WAC with and without boiling.

11.3.3.5. Wetting and drying

Due to the large percentage of clay minerals in Petra stone, it was considered essential to measure the weight loss of the tested specimens with a wetting and drying test using de-ionised water. This can reveal how much the clay minerals on their own can cause damage to the tested stone. But due to the existence of soluble salts in the original tested Petra stones, the effect of the soluble salt in this test cannot be eliminated. Nevertheless, this can still be used to compare the behaviour of different stones under wetting and drying conditions before the introduction of the salt solutions in the simulation test.

The Building Research Establishment (BRE) procedure for the wetting and drying test was used in this study (see chapter 7). The full results of this test are presented in tables S1, S2 and S3: appendix S and summarised in table 11.4.

Generally, Petra specimens suffered the highest weight loss in this test, with Disi sandstone having the highest weight loss among them. Considering the fact that all XRD diffraction analyses showed that the mineral phases in these specimens were very similar, including the clay mineral phases, their weight loss should be correlated with their pore geometry. Disi sandstone specimens had the highest porosity percentage (both in the petrography and the open total porosity tests) and also the highest WAC. Disi specimens also have coarser pore spaces compared to the other two Petra stones. Therefore, it seems likely that the coarse pore spaces together with the high open porosity are the main reasons for the considerable weight loss of Disi sandstone specimens. The Monks Park limestone and Locharbriggs sandstone specimens were very sound in this test with insignificant weight loss compared to Petra specimens. The absence of clay minerals seems the most obvious reason for such behaviour.

11.3.3.6. Soluble salts

The soluble salts content of the specimens was measured prior to the start of the test and at the end of every run of the test. Two methods for evaluating the soluble salts content were used: the measurement of the main cations and anions using the IC and ICP-AES techniques respectively, and the measurement of the main cations and anions from the thin sections using the ESEM. In the IC and ICP-AES technique, four powder samples were taken from the samples at four depth intervals (0.0-0.5, 0.5-1, 1-1.5 and 1.5-2 cm) and analysed using the same procedure as that of the fieldwork samples (see chapter 7). In the ESEM technique, an average of 10 measurements was taken from the surface of each sample to its centre, each covering an area 2 mm x 2 mm (see sketch below). The

same methods will be used again in the evaluation of salt distribution at the end of the simulation test.

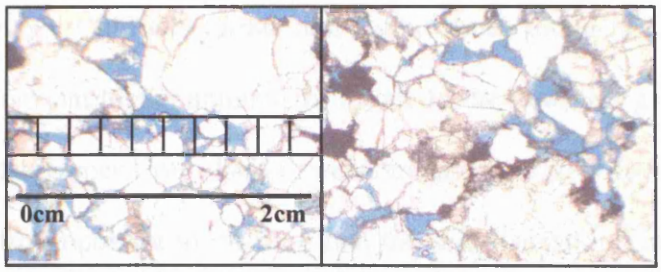

Figure 11.9: Measurement of the main cations and anions from thin sections using the ESEM.

Each method has its advantage and by combining the results the salt distribution before and after the simulation test can be evaluated in more detail. The main advantage of the IC and ICP techniques is that they measure only the soluble cations and anions, while the ESEM measures all the cations and anions in the tested area. However, the ESEM can provide a more detailed analysis including some information about the salt morphology and the changes to the stone structure. The last point applies particularly for the evaluation of the specimens at the end of the simulation test.

The IC and ICP results are presented in table Q1: appendix Q, while the ESEM results are presented in table V1 and V2: appendix V.

Both tests showed that, in general, the tested specimens had low soluble salts content. Most of the samples had less than 0.5 weight percent of soluble salts. More importantly, all specimens had a very similar soluble salts content, which is much better for the correlation and evaluation of the test results at the end of the test. Slight variations were noted in regards to the types of soluble cations and anions in the samples before the start

of the simulation test. All Petra stones had sodium and calcium as the main cations, while Locharbriggs sandstone had potassium and calcium and Monks Park limestone calcium and sodium. Chloride, nitrate and sulfate were found in similar ratios in all samples, with somewhat higher amounts of nitrate in the Locharbriggs sandstone, lower chloride ratio in the Upper Umm Ishrin sandstone and relatively low nitrate in the Disi sandstone. It is also important to mention that the salt distribution in Locharbriggs and Monks Park specimens was more uniform with depth, while calcium was slightly higher at the surface samples and sodium was higher at the deeper intervals in Petra samples.

11.3.4. Simulation procedures

As discussed earlier, the simulation test was based on the BRE salt crystallisation test with modifications to suit the research purposes. The test consisted of six runs, each of which was for sixteen days. Each cycle included two hours immersion in saturated solution and then drying in certain conditions for 24 hours. The original dry weight, the wet weight after each immersion cycle and the dry weight at the end of each drying cycle were recorded in each run (see appendix T). At the end of the sixteenth cycle, the weight loss or gain was calculated as follows:

$$\Delta W\ (\%) = 100\ (W_f - W_o)/W_o$$

where:
ΔW: weight loss or gain ratio
W_f: the final dry weight
W_o: the original dry weight

11.3.5. Simulation results and discussion

The simulation test consisted of eighteen different runs: six runs using saturated sodium sulfate solution, six using saturated Petra salt solution and six using de-ionised water. De-ionised water was used to examine the effect of clay minerals to see whether the specimens decay without introducing the salt solutions. The following is a brief discussion of the main outcomes of these tests. The results of each salt solution are discussed separately, and are then correlated. The evaluation of the results is based on:

- Material loss during the different cycles of each run, and more importantly, at end of each run.
- Salt distribution at the end of each run.
- Petrographic evaluation of the tested specimens at the end of each run.

11.3.5.1. Sodium sulfate simulation test

First Run: Low relative humidity and low wind speed conditions

The results of the sixteen cycles of immersion and drying at low relative humidity and low wind speed conditions (0.6 $\pm$0.2 m/s) showed that by the end of the test most of specimens had disintegrated considerably (tables T1 and T2: appendix T and figure 11.10).

All Petra specimens were completely destroyed after the eighth cycle. Disi sandstone was the first to break down after the fifth cycle of immersion. On the other hand, Locharbriggs sandstone was the most resistant to salt crystallisation damage under these conditions. Generally, the weight loss intensity increased as the test progressed (see figure 11.10). It should be stated that most of the weight loss occurred during the

immersion cycles and not during the drying cycles. This can be explained by the fact that the salt crystallisation pressure during the drying stage weakens the stone structure and, during the next immersion cycle, as the new salt solution tries to find its way in the specimen, the weak particles of the stone come off.

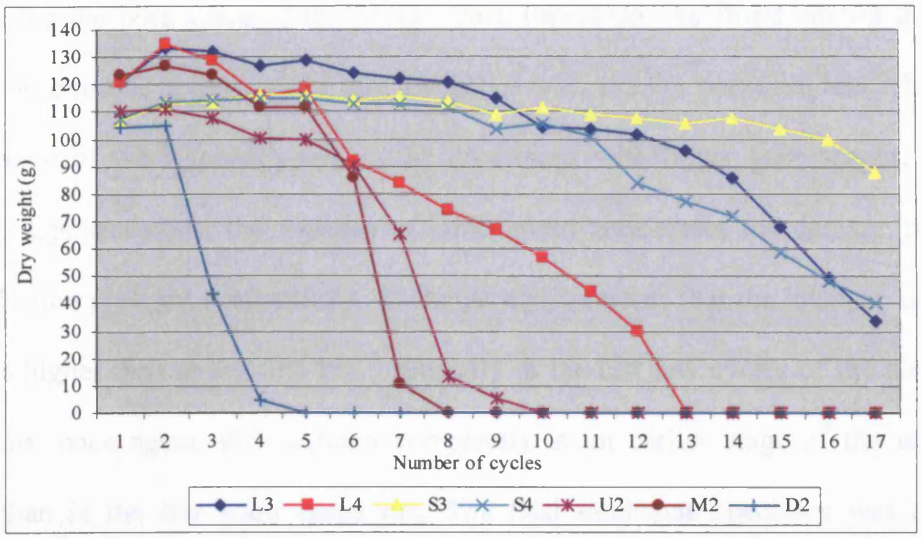

Figure 11.10: The change in dry weight after each immersion cycle. Solution: saturated sodium sulfate. First run.[20]

The environmental conditions (temperature and relative humidity) inside the drying chamber were monitored throughout the test using a Tinytag Extra Logger (TXG 3580) and are presented in appendix U.

Second Run: Low relative humidity and high wind speed conditions

The procedure used in the first run was repeated in this run, but with introduction of the high wind speed factor (3.6 $\pm$ 0.2 m/s) that replaced the low wind speed of the first run.

[20] Note: the original dry weight is represented as cycle number 1 in all weight loss figures and therefore the first cycle will be numbered as cycle number 2 and so on.

The results from this run showed a general increase in the weight loss percentage of the tested specimens, except those of the Monks Park limestone specimens where a lower percentage of weight loss occurred (see tables T1 and T2: appendix T and figure 11.11). Particularly, the weight loss of Locharbriggs sandstone was increased massively. Considering the pore space of the Monks Park limestone, the finest among the tested stones, these results could suggest that the stones with smaller pores are less affected by the increase of wind speed, while in the specimens with larger pore spaces, such as Locharbriggs sandstone, the increase of wind speed accelerates the damage from salt crystallisation pressure substantially. It should also be noted that the intensity of weight loss was higher than in the first run, especially in the last few cycles of the test. Petra specimens, once again, disintegrated completely at an earlier stage of the test, even earlier than in the low wind speed run. The Disi sandstone specimen was the least resistant to weathering and the Upper Umm Ishrin sandstone specimen was the most resistant among the Petra specimens. These results emphasise the observation made for Locharbriggs sandstone specimens, that higher wind speed seemingly accelerates the damage of specimens with large pores. The damage was higher in Disi than Locharbriggs sandstone, as Disi sandstone has not only micro and coarse pore spaces, but also soluble salts and clay minerals in its original composition. For the role of clay minerals, see the de-ionised water simulation test (section 11.3.6).

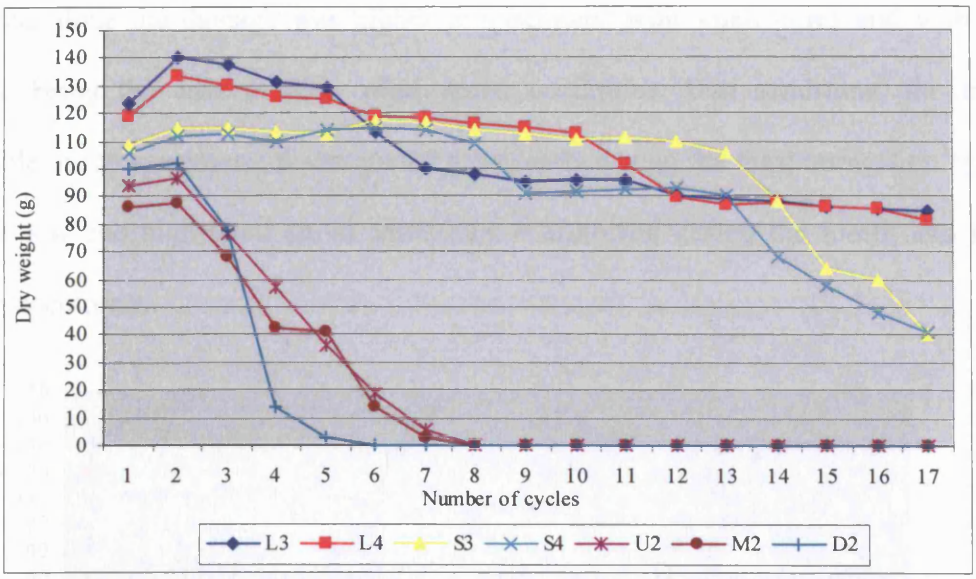

Figure 11.11: The change in dry weight after each immersion cycle.
Solution: saturated odium sulfate. Second run.

Third Run: Low relative humidity and fluctuating wind speed conditions

The third run was carried out under fluctuating wind speed conditions and with similar relative humidity ranges as in the first and second runs (low relative humidity). The wind speed was controlled using two two-way general-purpose solenoid valves connected to two multifunction time delay relays (see chapter 7 and appendix Za for more details). Fluctuation was produced with three hours of low wind speed conditions, followed by three hours of high wind speed throughout the drying period of each cycle (24 hours). The results of weight changes are presented in tables T5 and T6: appendix T and figure 11.12.

In general, the weight loss at the end of this run was the highest among all previous runs. The most notable observation was that under fluctuating wind speed conditions, all stone types showed a very high percentage of weight loss, while under low wind speed

conditions alone the damage was higher in specimens with small pores and with the opposite being the case in high wind speed conditions. Disi sandstone, the most vulnerable of the specimens, disintegrated completely during the third immersion cycle, while at low and high wind speed conditions it dissolved during the fourth and fifth cycles respectively.

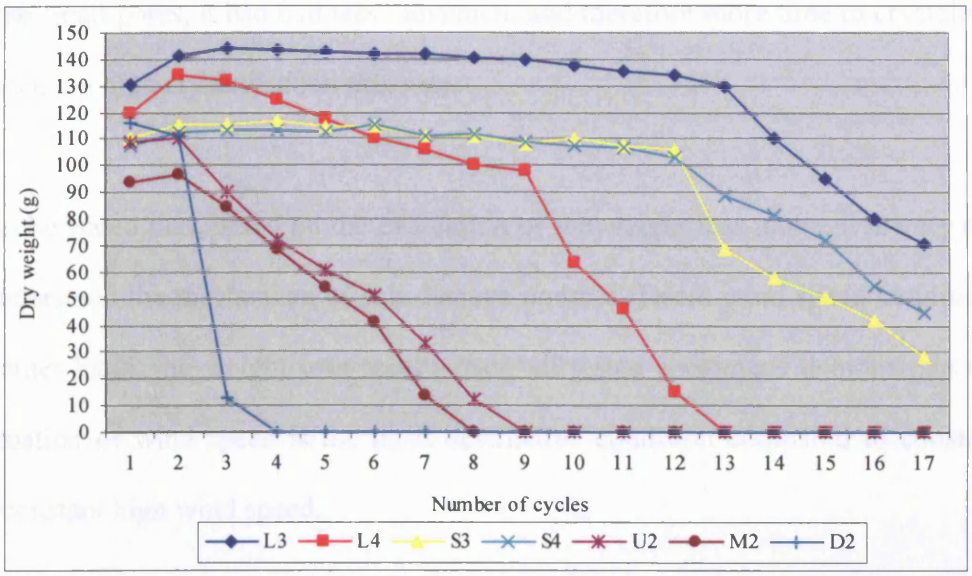

Figure 11.12: The change in dry weight after each immersion cycle.
Solution: saturated sodium sulfate. Third run.

It can be suggested that the higher weight loss at fluctuating wind speed conditions, was mainly due to a combination of two processes:

1- Some of the salts that were formed under high wind speed conditions may have dissolved during low wind speed and then re-crystallised during the following high wind speed conditions. The sequence of dissolving and re-crystallising resulted in weakened internal structures and ultimately more weight loss. This process is more possible in specimens with large pores than with fine ones, since wind speed affects less the behaviour of salts in the small pores, see chapter 12.

2- The second explanation is related to the different pore sizes of the tested specimens and their interaction with the wind speed conditions. During the high wind speed intervals, the evaporation rate at larger pores increased resulting in more salts crystallising out from the solution compared to the lower evaporation rate during low wind speed conditions. At low wind speed intervals, once the salt solution entered the small pores, it had had less movement and therefore more time to crystallise thus creating high crystallisation pressure.

It can be stated that, based on the evaluation of the weight loss alone, it is very difficult to understand the mechanism of salt damage under different wind speed conditions. On the other hand, the weight loss results from all tested specimens demonstrate that the fluctuation of wind speed is the most destructive condition compared to constant low and constant high wind speed.

Fourth Run: High relative humidity and low wind speed conditions

The weight change during low wind speed and high relative humidity conditions, was generally lower than in all previous tests under low relative humidity conditions (see table T7 and T8: appendix T and figure 11.13). The limestone specimens, in particular, recorded their lowest weight loss in one sample, while in another sample a weight gain was recorded at the end of the test. The average weight loss in Locharbriggs sandstone was 25%.

In regards to Petra specimens, despite the fact that all specimens disintegrated completely by the end of the test, the samples showed higher resistance than in similar

wind speed conditions with lower relative humidity. It should be noted that the Middle Umm Ishrin sample, and not Disi sandstone, was the first sample to disintegrate in this run. However, the difference in the original weights of the sample is the most likely reason for this rather than the surrounding conditions, since Disi sandstone sample was almost twice the weight of the Middle Umm Ishrin sample.

On the other hand, the intensity of weight changes during this simulation test cycle was much lower than at low relative humidity conditions (see figure 11.13). The incomplete drying of these samples at high relative humidity conditions is the main reason for the low rate of weight loss, reducing the amount of salt solution able to enter the specimens after the first cycle of immersion. These results are in correspondence with Price's observations while evaluating three salt simulation test procedures (Price 1978).

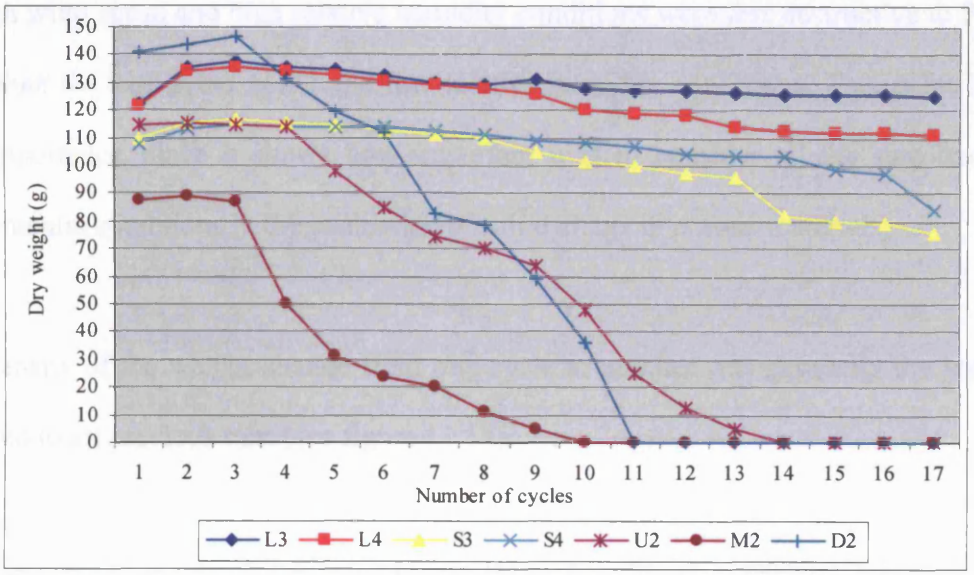

Figure 11.13: The change in dry weight after each immersion cycle. Solution: saturated sodium sulfate. Fourth run.

Fifth Run: High relative humidity and high wind speed conditions

The results of the simulation test at high relative humidity and high wind speed conditions (table T9 and T10: appendix T and figure 11.14) showed considerable weight gain in the limestone specimens. The samples gained an average of 9 % weight by the end of the test, while Locharbriggs sandstone showed an average weight loss of approximately 26 %. These results confirmed the previous observations, that high wind speed conditions have less impact on the evaporation process of the salt solution in stone specimens with small pore spaces. The weight loss of the Locharbriggs sandstone was slightly higher than in the fourth run.

Once again, all Petra specimens disintegrated completely by the end of the test, with Disi sandstone being the first specimen to disintegrate during the tenth immersion cycle. The high wind speed and high relative humidity conditions were less destructive to Petra stones than the high wind speed and low relative humidity conditions. This point is of great importance, since it shows how important it is to consider all the surrounding environmental conditions in the evaluation of salt damage in porous materials.

The intensity of the weight change from one cycle to another was generally the lowest compared to all previous runs (see figure 11.14).

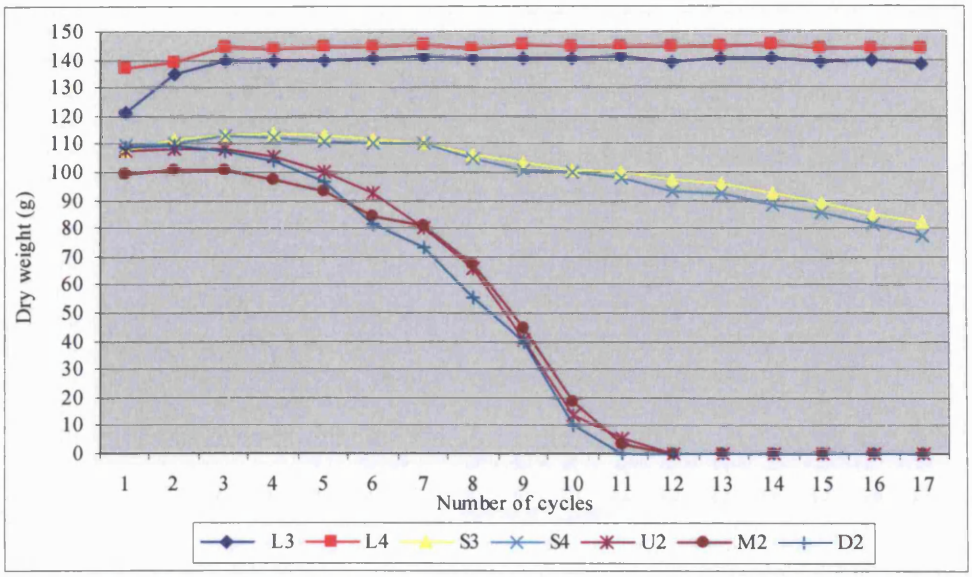

Figure 11.14: The change in dry weight after each immersion cycle.
Solution: saturated sodium sulfate. Fifth run.

Sixth Run: High relative humidity and fluctuated wind speed conditions

The fluctuating wind speed at high relative humidity conditions changed the weight loss ratio of the tested specimens considerably compared to the low and high wind speed conditions (table T11 and T12: appendix T and figure 11.15).

In this run, Monks Park limestone showed its lowest weight lost at high relative humidity conditions at an average of around 19 %, while the average weight loss of Locharbriggs sandstone was slightly lower than at low and high wind speed conditions.

All Petra samples showed 100 % weight loss at the end of the test and generally disintegrated at earlier stages compared to the fourth and fifth runs. Disi sandstone fragmented after just three cycles of immersing and drying.

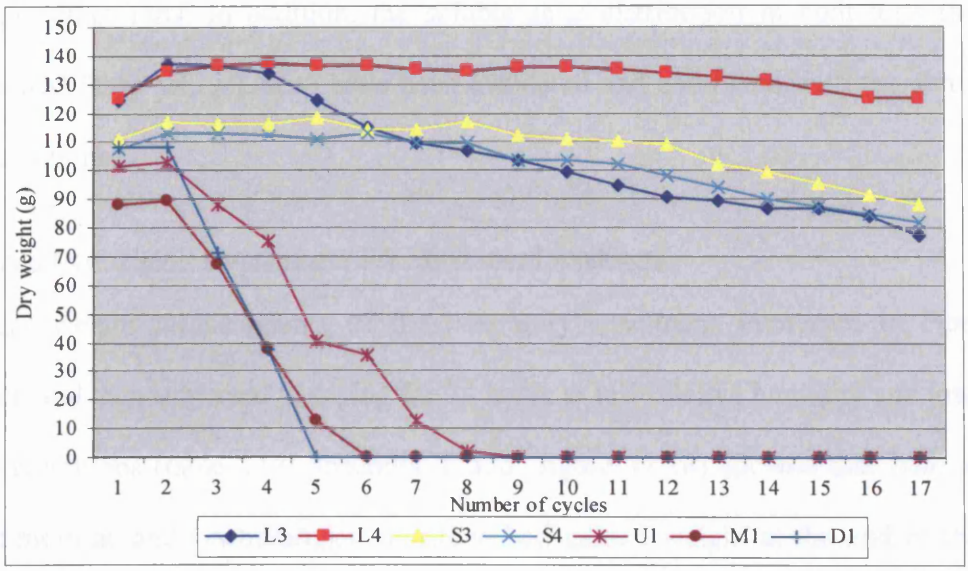

Figure 11.15: The change in dry weight after each immersion cycle.
Solution: saturated sodium sulfate. Sixth run.

11.3.5.2. Petra salt solution simulation test

The second part of the modified salt crystallisation test was carried out with similar specimens and with the same conditions used for the sodium sulfate test, but with Petra saturated salt solution instead of the saturated sodium sulfate salt solution. It is important to state that both tests as well as the de-ionised water controlling test (presented in the next section), were carried out simultaneously. In other words each drying run was carried out with specimens from all three categories: specimens immersed in saturated sodium sulfate, in saturated Petra salt solution and in de-ionised water. This was intended mainly to eliminate any differences from resetting the different test conditions. The following is a brief discussion of the six runs of the Petra salt solution test (for the specification and preparation procedure of this salt solution, see chapter 7). The evaluation of the results of this test is presented in the same way as was done for the sodium sulfate test, where weight change during and at the end of each run is compared

with the other runs. In addition, the soluble salts distribution in both tests (sodium sulfate and Petra salt solution) have been evaluated and correlated with the simulation test conditions.

First Run: Low relative humidity and low wind speed conditions

The dry weight measurements of the laboratory specimens immersed in Petra salt solution and then subjected to drying for 24 hours at low relative humidity and low wind speed conditions (table T13: appendix T and figure 11.16) showed that both Monks Park limestone and Locharbriggs sandstone had gained weight at the end of the test. The weight gain at these conditions does not suggest that there was no weight loss in these specimens during the test, as the test has recorded detachment of small particles from the original tested stone specimens. It mainly suggests that the weight of crystallised salts inside and at the surface of the specimens at the end of the drying cycles was much higher than the loss of their original weight from the crystallisation pressure of the salts.

On the other hand, all Petra specimens showed some weight loss at the end of the test, but the percentage of the weight loss was considerably lower than in the sodium sulfate test at the same drying conditions. The highest weight loss was recorded in the Disi sandstone specimens.

All tested samples showed much higher salt efflorescence compared to the sodium sulfate test at the same conditions. Also, the intensity of the weight change from one cycle to another was significantly lower than in the sodium sulfate test.

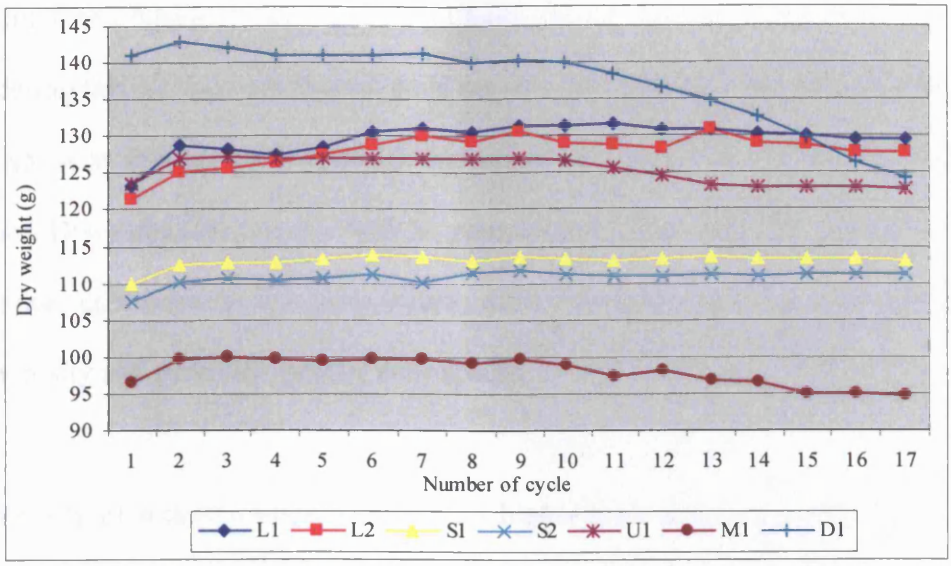

Figure 11.16: The change in dry weight after each immersion cycle. Solution: saturated Petra salt solution. First run.

Second Run: Low relative humidity and high wind speed conditions

At low relative humidity and high wind speed conditions, the weight gain in Monks Park and Locharbriggs specimens was slightly lower than at low wind speed conditions (table T15 and T16: appendix T and figure 11.17). As explained in the results of the low wind speed run, the weight gain does not suggest the absence of stone loss during the immersion and drying cycles. Considering that the amount of salt uptake was very similar in both tests (low and high wind speed), the lower weight gain percentage at the low wind speed run suggests higher loss of the original weight of the specimens compared to the high wind speed test. This weight loss was more noticeable in the Locharbriggs sandstone, confirming the previous test results, where high wind speed conditions had higher impact in specimens with coarse pore spaces.

Petra specimens also showed higher weight loss percentages at high wind speed compared to the low wind speed conditions of the same salt solution test (T15 and T16:

appendix T and figure 11.16). The weight loss in these samples ranged between 2-8 %. Considering that all these specimens have very similar composition and their salt uptake was also very similar, the variations in weight loss could be related to their pore structure. Disi sandstone has the highest percentage of open porosity, alongside coarse pore spaces connected to fine pore spaces, while the other two types have slightly less open porosity and generally smaller pore spaces.

The intensity of weight change was slightly higher than at the low wind speed of this test, but was considerably lower than at the low wind speed conditions of the sodium sulfate test. Moreover, the amount of salt efflorescence was slightly lower than at the low wind speed conditions of this test.

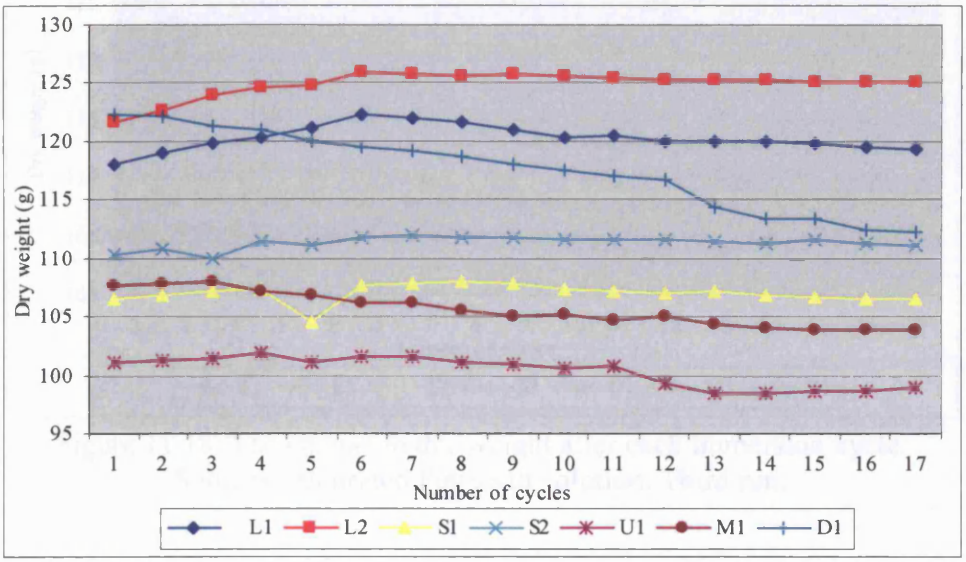

Figure 11.17: The change in dry weight after each immersion cycle.
Solution: saturated Petra salt solution. Second run.

Third Run: Low relative humidity and fluctuating wind speed conditions

The weight loss of the specimens, following their immersion in Petra salt solution and drying at low relative humidity and fluctuating wind speed conditions, recorded its

highest figures (see table T17 and T18: appendix T and figure 11.18). The results from this test showed, for the first time, weight loss of Locharbriggs sandstone in the Petra salt solution tests. Moreover, Monks Park specimens had the lowest weight gain in all low relative humidity tests using Petra salt solution. Regarding Petra samples, the weight loss was also generally higher than in the previous Petra salt solution tests.

In general, after the tenth cycle, all specimens showed a gradual loss of their weight, with more intensity in the Petra specimens and especially the Disi sandstone sample (see figure 11.18).

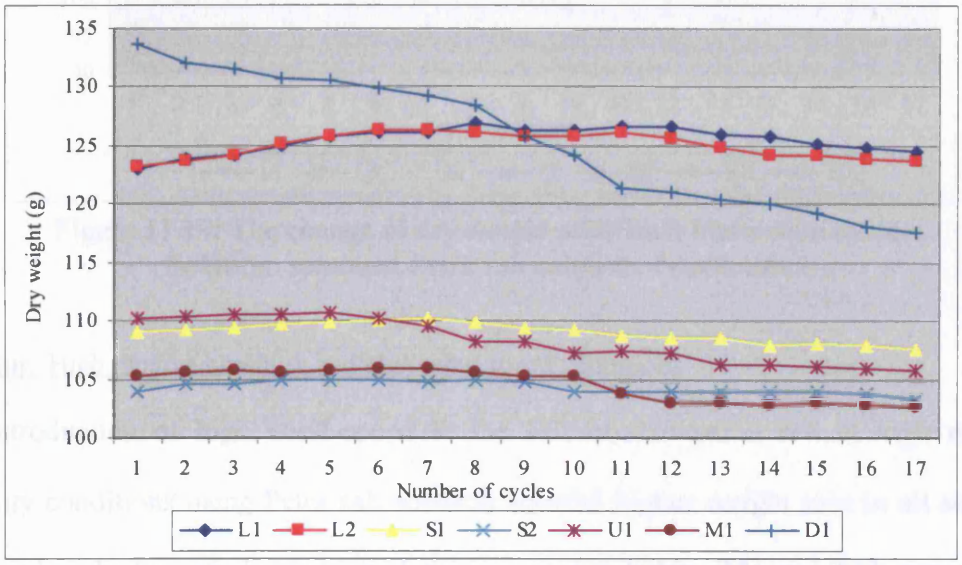

Figure 11.18: The change in dry weight after each immersion cycle.
Solution: saturated Petra salt solution. Third run.

Fourth Run: High relative humidity and low wind speed conditions

Apart from the Disi sandstone specimens, the results showed less weight loss in specimens, compared to the low relative humidity results (run 1: Petra solution test) (tables T19 and T20: appendix T and figure 11.19). Monks Park limestone and Locharbriggs sandstone specimens showed an increase in weight at the end of test,

which, as was explained earlier, does not rule out the loss of some of their original content. Petra specimens showed less weight loss than in the low wind speed and low relative humidity conditions. The only exception was the Disi sandstone specimens where the weight loss was higher in this run.

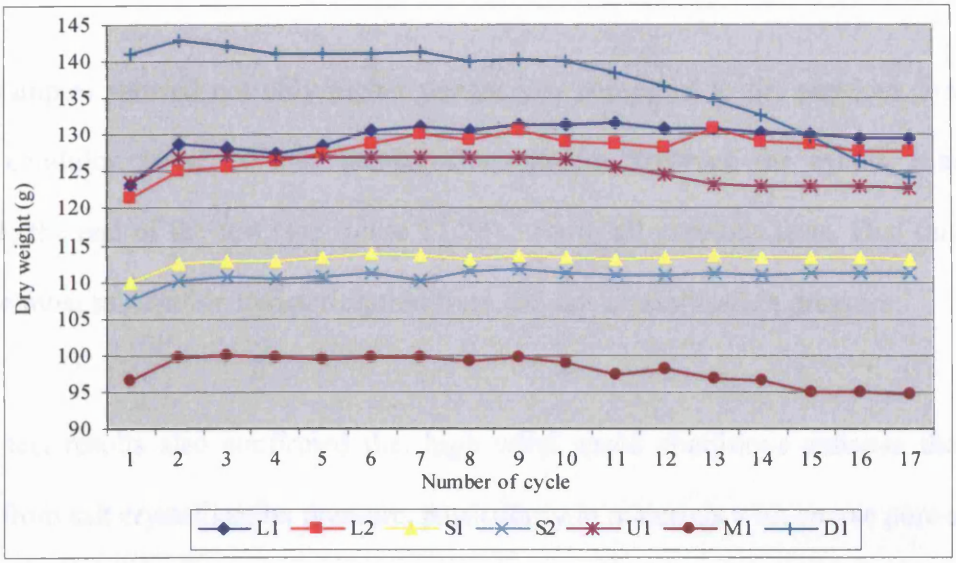

Figure 11.19: The change in dry weight after each immersion cycle.
Solution: saturated Petra salt solution. Fourth run.

Fifth Run: High relative humidity and high wind speed conditions

The introduction of high wind speed in the salt crystallisation test at high relative humidity conditions using Petra salt solution showed higher weight loss in all samples compared to the low wind speed simulation test results (tables T21 and T22: appendix T and figure 11.20). Even though Monks Park limestone and Locharbriggs sandstone showed a small weight gain percentage, these specimens lost a certain amount of their original content, but their incomplete drying during the drying cycle as well as the high percentage of salt efflorescence resulted in weight gain rather than weight loss. This point is important for the methodology of assessing the damage in salt crystallisation tests, as it indicates that, if the evaluation of the damage is based only on the final weight

loss or gain, the results could be misleading. The evaluation should be carried out with detailed monitoring of the damage throughout the test. In addition, as will be seen later in this chapter, post-test analyses, such as petrographic study of the tested samples, could provide further significant information about the weathering behaviour of stone.

Petra samples showed not only higher weight loss compared to the previous low wind speed condition tests, but also intense disintegration between the cycles, especially towards the end of the test (see figure 11.20). As in all previous tests, Disi sandstone was the most susceptible to deterioration from the salt crystallisation pressure.

These test results also confirmed that high wind speed conditions enhance the stone decay from salt crystallisation pressure, particularly in materials with coarse pore spaces.

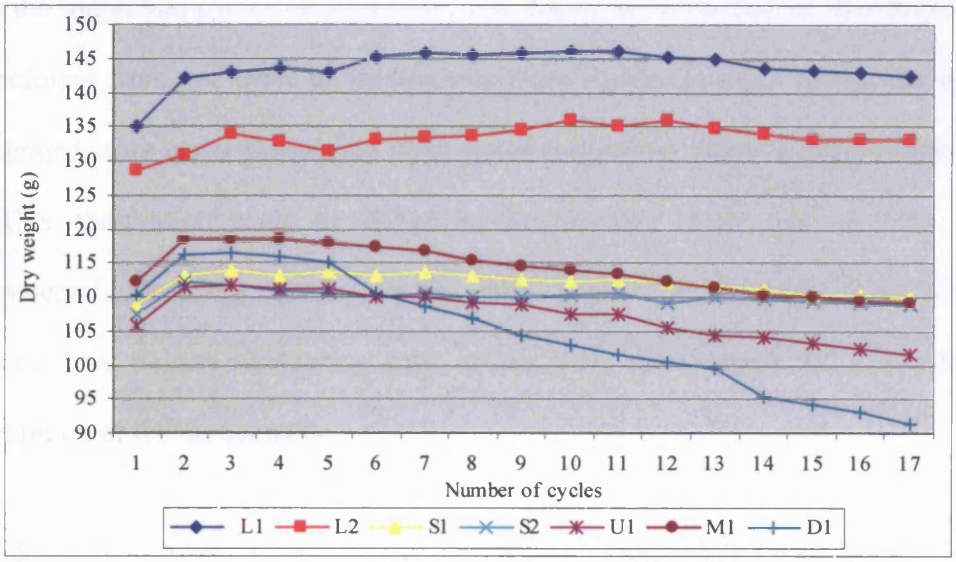

Figure 11.20: The change in dry weight after each immersion cycle. Solution: saturated Petra salt solution. Fifth run.

Sixth Run: High relative humidity and fluctuating wind speed conditions

The average weight loss at fluctuating wind speed and high relative humidity conditions, was generally lower than at the previous high and low wind speed and high relative humidity conditions (tables T23 and T24: appendix T and figure 11.21). Considering that the salt uptake for each of the specimens was very similar in all runs, the less the gained weight at the end of each run, the higher was the stone disintegration. Both Monks Park limestone and Locharbriggs sandstone recorded their lowest weight gain under high relative humidity conditions, while Petra specimens in general recorded their highest weight loss.

Despite the fact that at the end of the test the total weight loss under fluctuating wind speed was higher than under low and high wind speed conditions, the weight changes during the individual cycles of immersion and drying showed that the disintegration of the specimens from one cycle to another was more steady. In other words, the samples disintegrated more under fluctuating wind speed conditions, but in a gradual and erratic way. This observation could be linked to the situation at the site of Petra, where environmental conditions similar to the ones applied in this run were recorded, indicating that a low weathering rate could, with time, result in a considerable disintegration of the monuments.

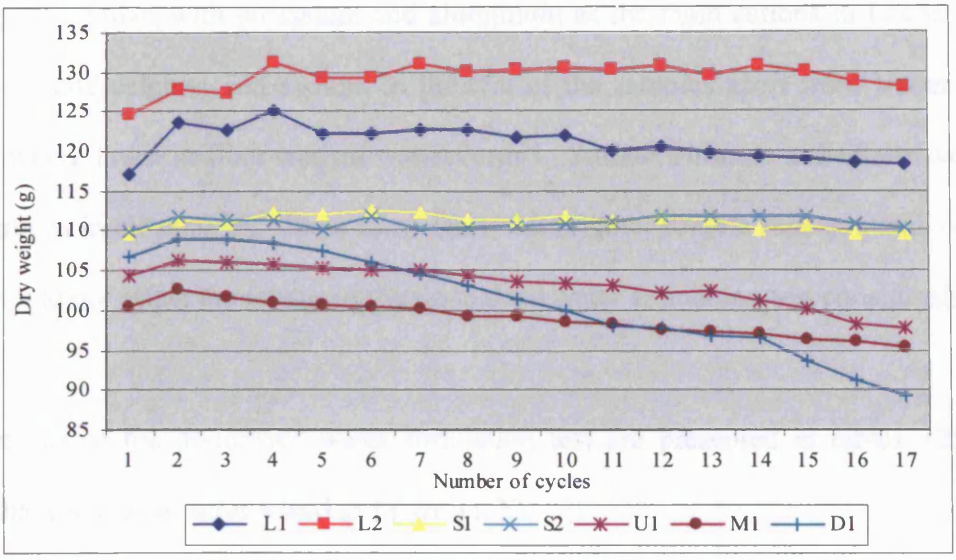

Figure 11.21: The change in dry weight after each immersion cycle.
Solution: saturated Petra salt solution. Sixth run.

11.3.5.3. De-ionised water simulation test

In the control test, the runs were carried out using de-ionised water instead of a salt solution. One sample from each of the stone specimens was immersed in de-ionised water for two hours and then dried for 24 hours under the same drying conditions used in the previous sodium sulfate and Petra salt solution tests. The main aim of this test was to evaluate the role of clay minerals in the stone decay and the role of the soluble salts originally present in the tested samples and also to identify the relation between soluble salts and clay minerals in the mechanism of stone decay.

As mentioned earlier in this chapter, prior to the start of the simulation test, the soluble salts content of the laboratory tested specimens was identified using the IC and ICP-AES techniques. The total original soluble salts contents of the tested samples ranged between 0.3 % and 0.65 % (see table V1: appendix V and figure 11.22). Their cations and anions

were quite similar, with potassium and aluminium as the main cations in Locharbriggs sandstone and calcium and sodium in the rest of the samples apart from Upper Umm Ishrin, where lower sodium content was recorded. Sulfate, chloride and nitrate were the main anions in all samples. Given these facts, the original soluble salts contents on their own should not affect the results of the de-ionised water simulation test considerably.

The results of the de-ionised water simulation test are presented in tables T25-T36: appendix T and also summarised in figure 11.22.

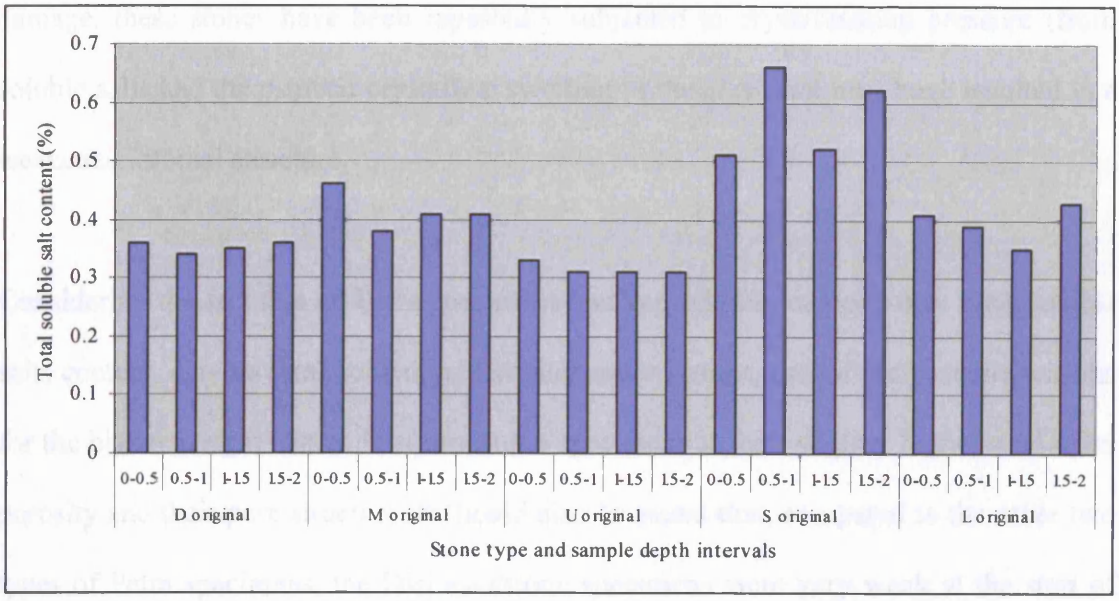

Figure 11.22: The original total soluble salts content in the laboratory tested specimens prior to the start of the simulation test.

Under all the different drying conditions applied in the test, Locharbriggs sandstone and Monks Park limestone specimens were very sound. Their weight loss or gain through the six runs of the test was generally less than 1 %. On the other hand, Petra specimens, and particularly the Disi sandstone sample, were more vulnerable (see figure 11.23). The clay mineral content is the main difference between the Petra specimens and the Monks

Park limestone and Locharbriggs sandstone specimens, used in the test. While all Petra samples contain a high percentage of kaolinite, the other specimens have no clay minerals. As discussed earlier in chapter 4, the osmotic swelling of the otherwise non-swelling clay plays a vital role in the decay of porous materials with high clay mineral contents, especially when these materials interact with the soluble salts of the host rock. In addition to the role of clay minerals, the other possible reason for the high weight loss in Petra specimens during immersion in de-ionised water is that these specimens were weak at the start of test. Coming from a site with long and on-going salt and clay damage, these stones have been repeatedly subjected to crystallisation pressure (from soluble salts and the osmotic crystalline swelling of the clay) that may have resulted in a weakened internal structure.

Considering the fact that all Petra specimens had very similar composition, total soluble salts content, clay mineral content and similar water uptake, one of the possible reasons for the higher weight loss in Disi sandstone specimens is their slightly higher total open porosity and their pore structure. It should also be stated that, compared to the other two types of Petra specimens, the Disi sandstone specimens were very weak at the start of the tests. This might suggest that this stone has been subjected to different pressures, mainly salt crystallisation pressure, which resulted in a weak and less durable structure. The Upper Umm Ishrin sandstone specimens were the most durable among Petra specimens.

Regarding the specimens' behaviour at different environmental conditions, the weight changes in Monks Parks limestone and Locharbriggs sandstone were too small to draw any conclusions, but most of Petra specimens showed higher weight loss at fluctuating wind speed and high wind speed conditions than at low wind speed condition both at the low and at the high relative humidity environments (see figure 11.23). The higher evaporation rates under fluctuating wind speed and high wind speed conditions in these environments may have caused faster drying of the osmotic swelling clay minerals and therefore higher rate of contraction and ultimately more weaken structure.

All in all, Petra specimens, with their high clay mineral contents, showed higher weight loss compared to Locharbriggs and Monks Park specimens. The osmotic swelling of Petra specimens and their original weak structure are the main obvious reasons for their decay from immersion in de-ionised water. The weight loss ratio in Petra samples during the de-ionised water test was less than a tenth of the weight loss during the sodium sulfate solution test, but was as high as the weight loss ratio during the Petra salt solution test. Further studies are needed to examine the clay minerals swelling pressure.

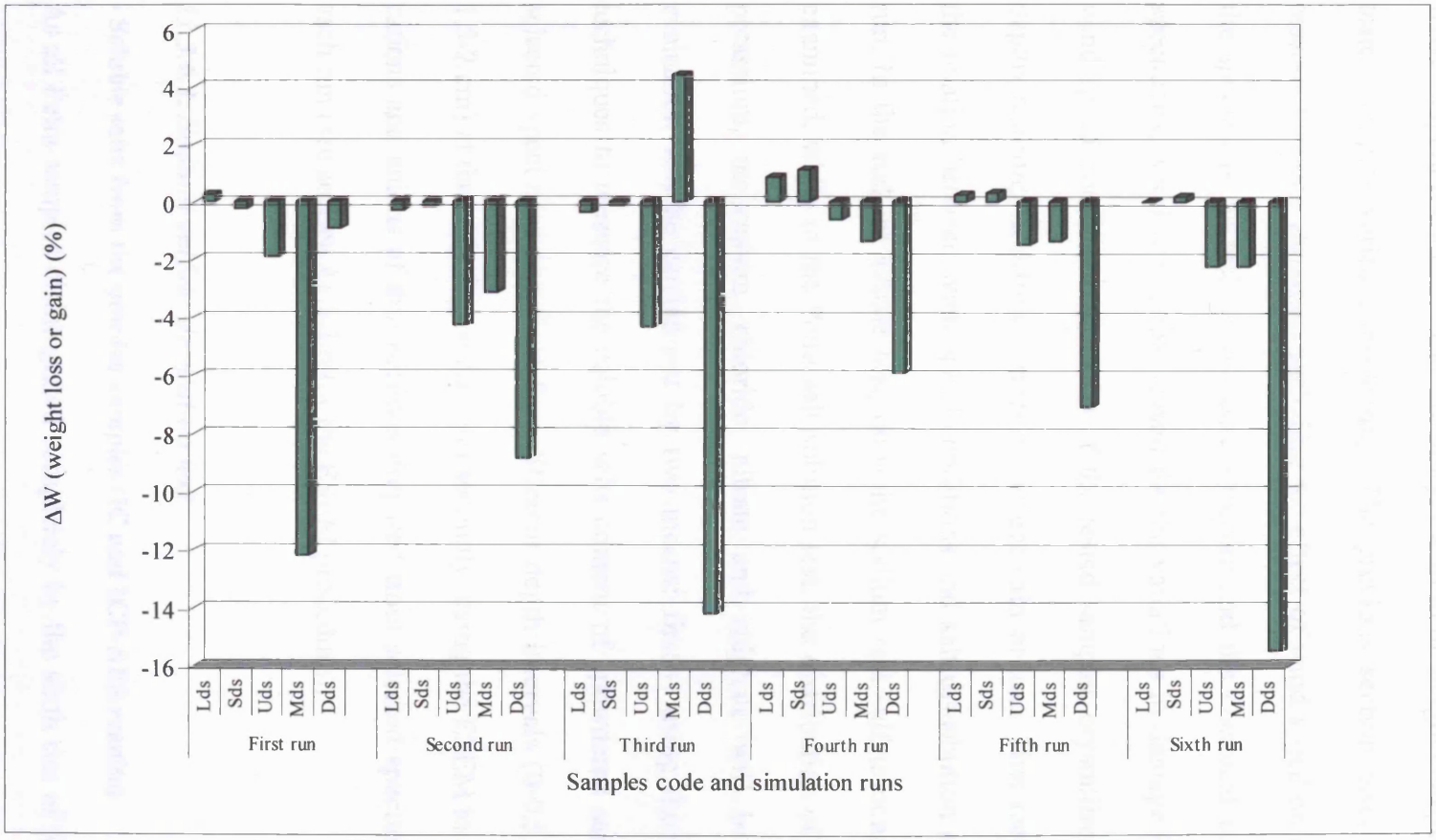

Figure 11.23: Percentage (%) of specimens weight loss or gain from the immersion in de-ionised water and drying at different environmental conditions.

Figure key legend: Lds: Monks Park limestone in the de-ionised water simulation test
Sds: Locharbriggs sandstone in the de-ionised water simulation test
Uds: Upper Umm Ishrin sandstone in the de-ionised water simulation test
Mds: Upper Umm Ishrin sandstone in the de-ionised water simulation test
Dds: Disi sandstone in the de-ionised water simulation test

11.3.6. Wind speed and salt distribution

The simulation test results showed that under different wind speed conditions and at fixed temperature and relative humidity, the ratio of weight change in the laboratory tested samples varied considerably. The previous section discussed the possible reasons for such variations including the effect of wind speed on the drying rate of the specimens, as well as the pore structure and the chemical composition of the specimens. Another possible reason for the variations in damage is that at different wind speed conditions, the salts of the tested samples crystallised out at different depths resulting in different rates of weight gain or loss. This section will examine the relation between wind speed conditions and salt distribution at the end of each run. In the sodium sulfate test, only the sodium and sulfate concentration will be examined, while in the Petra salt solution test, the distribution of calcium, sodium, potassium, magnesium, chloride, nitrate and sulphate will be evaluated. This evaluation will be carried out by two means: firstly, using the IC and ICP-AES techniques to measure the soluble salts content of powdered samples taken from selected specimens and from four different depth intervals (0-0.5, 0.5-1, 1-1.5 and 1.5-2 cm) at the end of each run, and secondly, using the ESEM to measure the main cations and anions of thin sections prepared from selected specimens at the end of each run (see section 11.3.3.6 for the ESEM procedure).

11.3.6.1. Sodium sulfate simulation test

- Soluble salts from the powder samples (IC and ICP-AES results)

As all Petra samples disintegrated completely by the sixth run of the sodium sulfate simulation test, it was not possible to carry out any further tests on them. Instead, the sodium and sulfate content was evaluated in the Locharbriggs sandstone specimens,

which are rather similar to the Petra stone specimens. The evaluation also includes comments about the salt distribution in the Monks Park limestone specimens.

The full results of the soluble salts content of the tested samples at the end of each run are presented in appendix V. In general, the results show that the sodium and sulfate concentration at different depths varied significantly from one simulation run to another.

In the Locharbriggs sandstone specimens at low relative humidity conditions (runs 1-3), the concentration of both ions (sodium and sulfate) was higher in the surface samples at the low wind speed conditions, while at high wind speed conditions the highest concentration was at deeper intervals (0.5-1 cm). At fluctuating wind speed with low relative humidity conditions, the Locharbriggs specimens disintegrated massively to less than 2 cubic centimetres and the ions content from the two intervals tested after this run showed uniform distribution. (See figures 11.24 and 11.25). Similar results were observed for the Monks Park limestone specimens, where at low relative humidity conditions the sodium and sulfate concentrations were higher in deeper intervals at high and fluctuating wind speeds. At fluctuating wind speed conditions, in particular, the highest sodium and sulfate concentration in Monks Park limestone was near the centre of the sample (1.5-2 cm) (see table V4:appendix V).

At high relative humidity conditions (runs 4-6), the sodium and sulfate distribution in Locharbriggs sandstone was higher in the surface samples in all runs, with higher

values during the high wind speed conditions run (run 5) (see figures 11.24 and 11.25).

The evaluation of the results for the sodium and sulfate distribution in the laboratory tested samples at the end of the simulation test runs leads to the following observations:

- At low relative humidity, the wind speed conditions affected the sodium and sulfate distribution considerably.

- At high wind speed and low relative humidity, both sodium and sulfate had higher concentrations in the deeper intervals, compared to low wind speed and low relative humidity.

- The sodium and sulfate content in Locharbriggs sandstone specimens at the end of run 3 (fluctuating wind speed and low RH) was uniformly distributed in the two depth intervals. It should be remembered, however, that because this stone had disintegrated massively, its salt distribution results could not be compared with other Locharbriggs sandstone specimens exposed to different wind speed conditions.

- The low evaporation rate at the high relative humidity runs resulted in a higher concentration of sodium and sulfate at the surface samples in all runs, with higher content in high wind speed than low wind speed conditions. These results are in correspondence with what was anticipated at the start of the test, since at low wind speed conditions the drying rate will be slower resulting in higher crystallisation near the surface of the sample, while at high wind speed conditions the drying rate is faster and therefore the salt will crystallise before reaching the surface of the sample. Once again, at fluctuating wind speed the stone disintegrated and most of the

crystallised sodium - sulfate became detached along with broken parts of the stone (see figures 11.24 and 11.25).

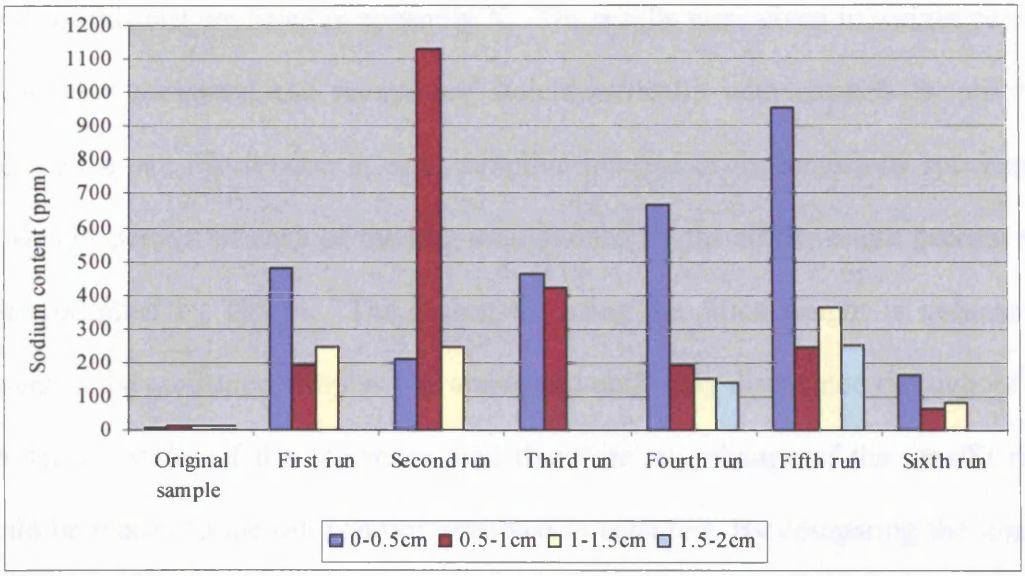

Figure 11.24: Sodium concentration, as weight %, in the Locharbriggs sandstone powder samples collected from different depth intervals at the end of the modified sodium sulfate simulation test.

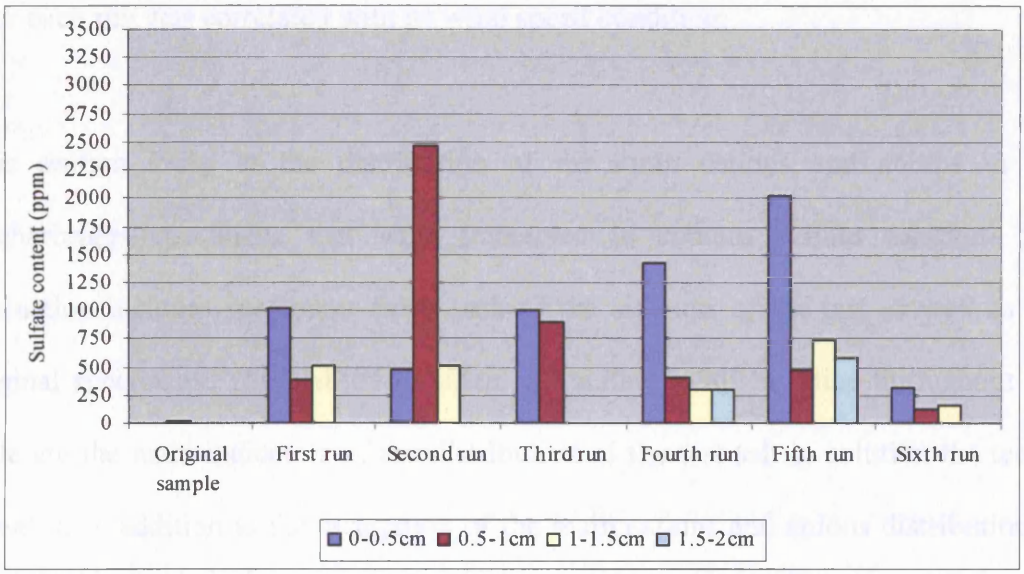

Figure 11.25: Sulfate concentration, as weight %, in the Locharbriggs sandstone powder samples collected from different depth intervals at the end of the modified sodium sulfate simulation test.

- Main cations and anions from the thin section analysis (ESEM results)

A more detailed analysis of the distribution of the main cations and anions in the tested specimens was carried out using the ESEM. The measurements were taken

from thin sections of the specimens prepared at the end of each run as well as from thin sections of the original samples prepared before the start of the test. The full results of this test are listed in appendix X. The results were given in weight percent of each ion measured and normalised stoichimetrically with oxygen. In order to evaluate the salt distribution in each sampling interval of the sandstone specimens, the weight percent of each of the ions was divided by the silica weight percent and then multiplied by 100 %. The reason for using the silica weight is because its content in the sandstone samples was stable and uniformly distributed throughout the thin section slides of the specimens and therefore any change of the ions/Si ratio would be related to the salt solution involved in each test. By comparing the ions/Si ratio after each run to the original ions/Si ratio (of the samples before the test), the salt distribution in each of the specimens was evaluated. In addition, the ions/Si ratio after each run was correlated with its wind speed condition.

This section looks at the distribution of the main cations and anions in the Locharbriggs specimens that were immersed in sodium sulfate solution. The evaluation includes specimens from each of the six runs of the test as well as the original specimens. The sodium to silica and sulfate to silica ratios throughout the slide are the main indicators of the distribution of the test salt in solution the tested samples. In addition to the evaluation of the main cations and anions distribution in the Locharbriggs specimens, the main outcomes of the cations and anions distribution analysis in Petra and Monks Park specimens are summarised.

Even though the thin sections were prepared carefully and without the use of water, it should be stated that it was not possible to keep all salt crystals in their location and

some may have been lost in the grinding stage of the thin section preperation. However, since the main aim of the test was to evaluate the distribution of the salt ions rather than their exact quantities and as all thin sections were prepared using the same technique, the results of the salt ions distribution in each run of the tested samples can be compared and correlated with environmental conditions in each run.

The original Locharbriggs specimen was clear of sodium and sulfate ions, and therefore, the content of these ions at the end of each run is a direct result of the testing salt solution. Potassium and aluminium as well as traces of chloride were distributed uniformly in the original specimens.

The thin section from the Locharbriggs specimen at the end of the first run showed wide distribution of sodium and sulfate ions throughout the slide, with relatively higher content towards the surface of the sample (see figure 11.26). Potassium, aluminium and chloride distributions were very similar to the original sample.

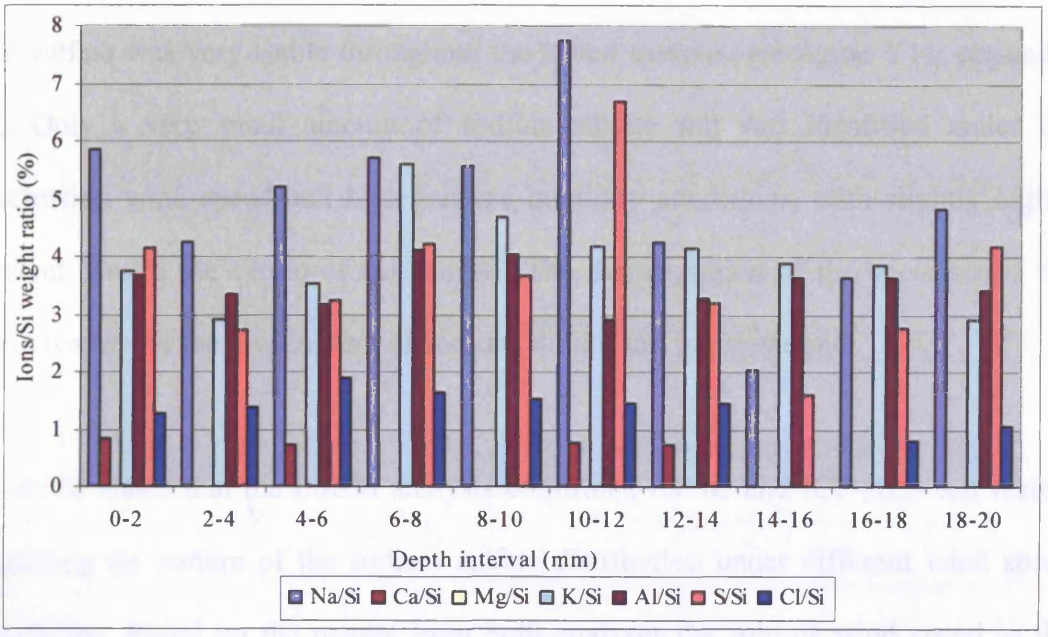

Figure 11.26: The main ions/Si ratio in the Locharbriggs sandstone at the end of the first run. Solution: saturated sodium sulfate.

At high wind speed and low relative humidity conditions (second run), the concentration of sodium and sulfate ions was generally lower than in the first run and distributed more uniformly (see figure Y4: appendix Y). Chloride ion content and distribution was similar to the previous run.

The ESEM investigation of the Locharbriggs specimen after the third run showed very small traces of sodium and sulfate (see table 10X: appendix X and figure Y6: appendix Y). It should be stated that this specimen showed a high rate of disintegration during this run, which suggests that most of the crystallised salts had fallen off together with disintegrated stone particles.

The sodium and sulfate analysis during the high relative humidity runs (4-6), showed more uniform distribution throughout the tested samples compared to the low relative humidity runs (1-3). The highest uniformity of the distribution of these ions was recorded under the high wind speed conditions, where the concentration of sodium and sulfate was very stable throughout the tested sample (see figure Y11: appendix Y). Only a very small amount of sodium sulfate salt was identified under the fluctuating wind speed and high relative humidity conditions, with slightly higher content toward the centre of the sample. The disintegration of the specimen is the main reason for the low amount of sodium sulfate salt in the sample.

It can be stated that the ESEM analysis confirmed the IC and ICP-AES test results regarding the pattern of the sodium sulfate distribution under different wind speed conditions. Based on the results from both analyses the role of wind speed in the distribution of sodium sulfate salt can be summarised as follows:

- Generally, at low wind speed conditions, sodium and sulfate ions were in higher concentrations towards the surface of the samples, with higher amounts under low relative humidity conditions.
- At high wind speed and low relative humidity conditions, higher concentrations of sodium and sulfate ions were recorded at deeper intervals, while the salts were distributed uniformly at high wind speed and high relative humidity conditions.
- The high disintegration rates of the tested specimens under fluctuating wind speed conditions prevented the evaluation of the sodium sulfate distribution under these conditions. However, the ESEM analysis showed that the sodium sulfate content was slightly higher at deeper intervals under high relative humidity and fluctuating wind speed conditions.
- The complete disintegration of all Petra samples made the evaluation of the role of wind speed in the sodium sulfate distribution in these specimens impossible.

11.3.6.2. Petra salt solution simulation test

- Soluble salts from the powder samples (IC and ICP-AES results)

In order to evaluate the role of wind speed in the distribution of Petra salts, the content of the main cations and anions of this salt solution (Ca, Na, K, Cl, NO_3 and SO_4) were examined from powder samples collected from different depth intervals of selected specimens at the end of each simulation run.

The salt distribution results (appendix V) showed that all tested specimens had a very similar pattern in most of the simulation runs. This section will look at the salt distribution in the Locharbriggs samples as representative of all tested samples.

The salt distribution in each run was evaluated by comparing the ion concentration of each cation and anion in each run to the ion concentration in the original sample (before the test) and to the ion concentration in other runs. The ion concentration of the main cations and anions in the six simulation runs of the test are presented in Appendix W. (see figure 11.27 for calcium distribution as an example).

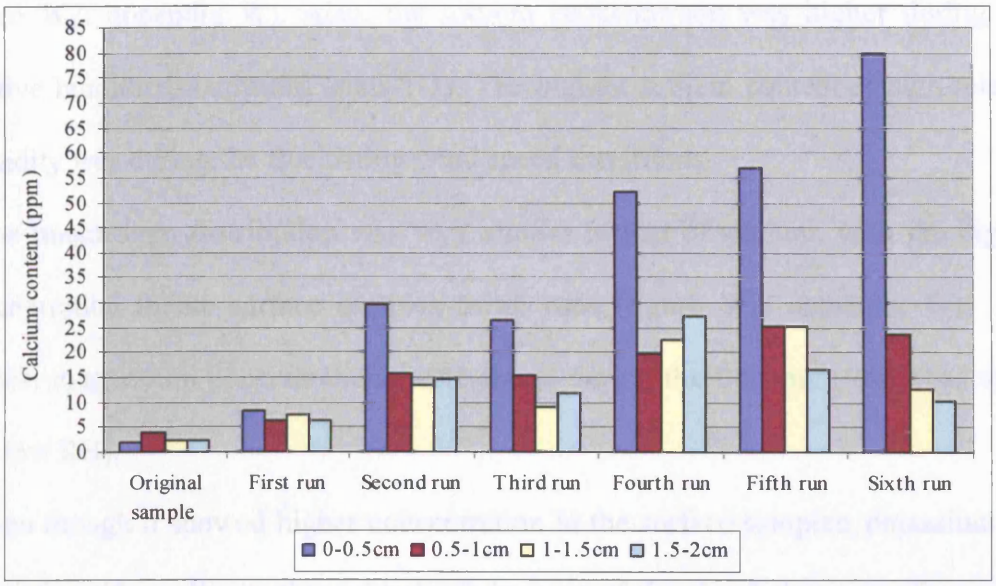

Figure 11.27: Calcium concentration, as weight %, in the Locharbriggs sandstone powder samples collected from different depth intervals at the end of the modified salt crystallisation test.

The main observations from the evaluation of the cations and anions distribution in the Locharbriggs sandstone specimens can be summarised as follows:

- In all runs, and for most cations and anions, the surface samples contained the highest concentration.
- Apart from the surface depth intervals, the results for the rest of the sampling intervals showed a more uniform distribution of their ions content.
- Most of the calcium content was concentrated in the surface samples, and the highest surface concentration occurred during high relative humidity and fluctuating

wind speed conditions (run 6, see figure 11.24). Generally the calcium content was much higher in the high relative humidity runs (4-6).

- Sodium concentration was also higher in the surface sampling intervals, but the variation in sodium content between the surface samples and the samples from the other sampling intervals was much lower than the variation in calcium content (see figure W2: appendix W). Also, the sodium concentration was higher during low relative humidity conditions (runs 1-3). The highest sodium content at high relative humidity was during the fluctuating wind speed conditions.
- The magnesium distribution was very similar to that of sodium, with the highest concentration in the surface samples in all runs (figure W3: appendix W). The highest magnesium concentrations were found during the first run (low wind speed and low RH).
- Even though it showed higher concentration in the surface samples, potassium had the most uniform distribution with depth in most of the simulation runs (figure W4: appendix W).
- Chloride and nitrate had the highest concentration in the surface samples in all runs, with higher content at low relative humidity conditions. At high relative humidity conditions, the highest content of these ions was observed during the fluctuating wind speed conditions (see figures W5 and W6: appendix W).
- As with all other ions, sulfate showed higher concentration in the surface samples in all runs (figure W7: appendix W). The fluctuating wind speed, at both high and low relative humidity conditions, resulted in a higher sulfate concentration in the surface sample intervals, compared to high wind speed conditions.

Considering all previous results, it is very difficult to draw any conclusions about the role of different wind speed conditions in the distribution of different cations and anions, since the highest percentage of these ions was concentrated in the surface samples and then distributed uniformly in the deeper depth intervals. However, the measured soluble salts content was slightly higher at low relative humidity conditions (runs 1-3). At high relative humidity, the highest content of all the ions was recorded under fluctuating wind speed conditions.

- Main cations and anions from the thin sections (ESEM results)

An ESEM analysis similar to that of the sodium sulfate solution test was carried out on tested specimens that were immersed in Petra salt solution. The results of the distribution of the main cations and anions in these samples are presented in appendix X and appendix Y. In this section, the Petra salt ions distribution in the Locharbriggs sandstone specimens at different simulation conditions is evaluated.

Generally, the sodium content corresponded strongly with chloride in all runs, while the sulfate content corresponded with a major increase in the potassium concentration.

At low wind speed and low relative humidity conditions (run 1), sodium and chloride content was higher near the surface samples, while both ions were distributed more uniformly at high and fluctuating wind speed conditions (runs 2 and 3). At all different wind speed conditions under high relative humidity, the sodium and chloride distributions were very alike and uniform. However, a slightly higher

content of these ions was found at deeper intervals under high wind speed conditions (see figure 11.28 and appendix Y).

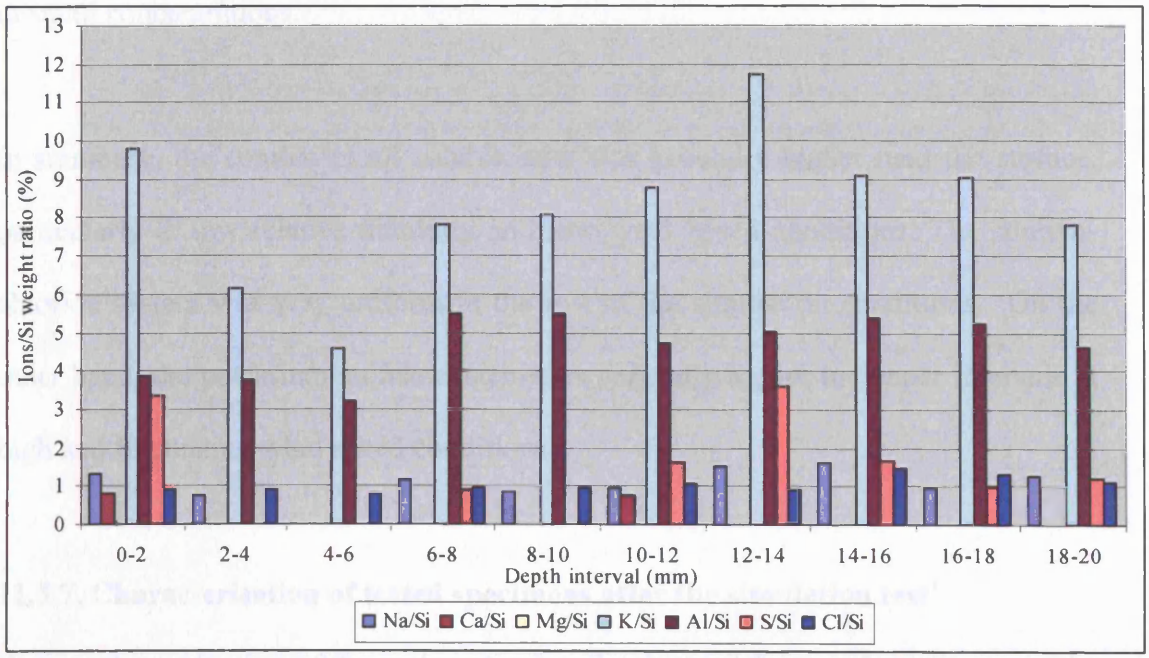

Figure 11.28: The main ions/Si ratio in the Locharbriggs sandstone at the end of the fifth run. Solution: saturated Petra salt solution.

On the other hand, at low wind speed and low relative humidity conditions (run 1), potassium concentration reached its maximum just below the surface, namely in the 2-4 mm depth interval (see figure Y3: appendix Y). At high and fluctuating wind speed and low relative humidity conditions (runs 2 and 3) the sulfate concentration was very low, while the potassium content was uniform throughout the tested intervals with slightly higher concentration in the deeper ones. During high relative humidity and high wind speed conditions (run 5), the sulfate and potassium contents were generally higher in the deeper intervals of the tested specimens, while at fluctuating wind speed (run 6) both ions were distributed uniformly (see figure Y9, Y11 and Y13: appendix Y).

In the first four runs, traces of calcium ions were found mainly near the surface, while in the fifth and sixth run, the calcium ions were also found at deeper intervals in small concentrations.

In summary, the content of all soluble salts was generally higher near the surface, particularly at low relative humidity and low wind speed conditions. The sodium-chloride system was very uniform in the rest of the simulation conditions. On the other hand, the potassium-sulfate system was generally higher in deeper intervals at high and fluctuating wind speed conditions.

11.3.7. Characterisation of tested specimens after the simulation test

Besides the evaluation of the main cations and anions of the tested specimens at the end of the simulation tests, a petrographic study and an ESEM investigation were carried out to evaluate the main changes in the tested specimens. The following are the main observations from these post-simulation studies:

- The porosity and pore space sizes increased massively in all samples at the end of sodium sulfate simulation test. The highest increase in pore spaces was observed in Monks Park specimens during low relative humidity and fluctuating wind speed conditions, where the micropore spaces of the stone became very coarse (see figure 11.29).

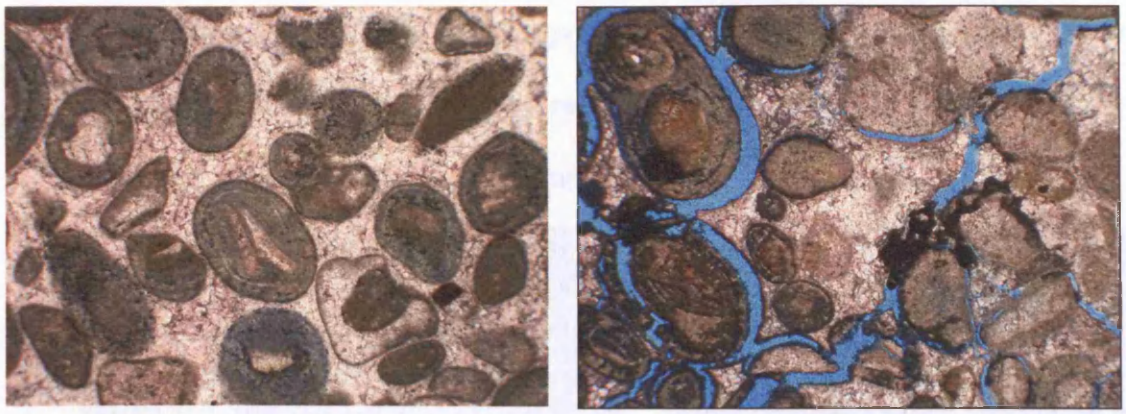

A B

Figure 11.29: Photomicrograph of the petrological thin section of the Monks Park limestone specimen before the start of the test (A) and at the end of the third run (B). Field of view 2.5mm. Magnification: 40x.

- The quartz grains showed different types of fractures and a concave-convex contact as a result of the crystallisation pressure in the Locharbriggs sandstone specimens at the end of the first three runs, and especially the third run, of the simulation test (see figure 11.30).

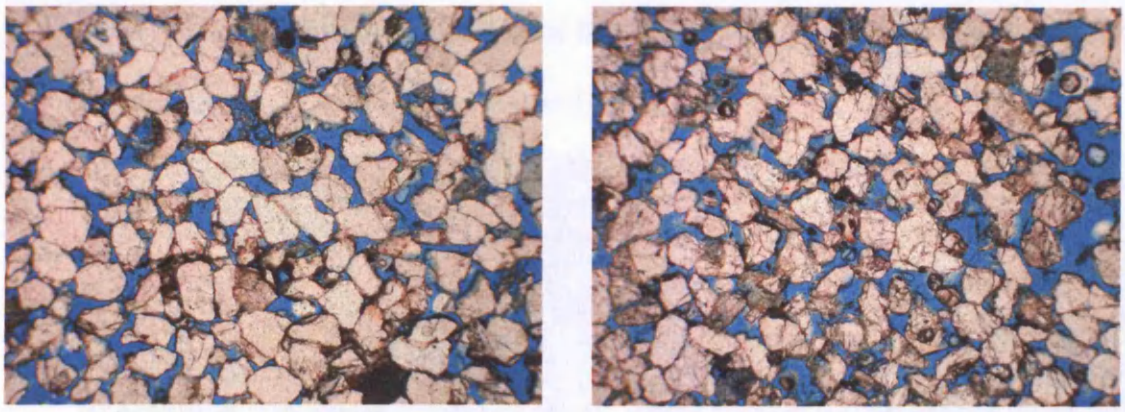

A B

Figure 11.30: Photomicrograph of the petrological thin section of the Locharbriggs sandstone specimen before the start of the test (A) and at the end of the third run (B). Field of view 2.5mm. Magnification: 40x.

Petra specimens lost a high percentage of their clay minerals during the Petra salt simulation test, especially under high relative humidity conditions. The highest loss was noted during the sixth run (see figure 11.31).

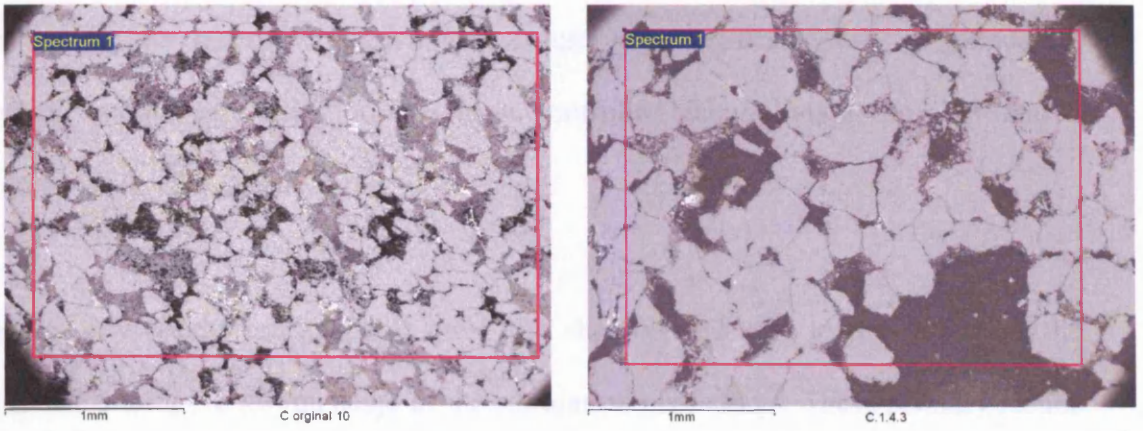

A **B**

Figure 11.31: Scanning electron micrograph showing the clay minerals distribution in Middle Umm Ishrin sandstone specimen before the start of the test (A) and at the end of the fourth run (B).

- Despite the fact that different salt crystals were identified during the ESEM investigations, the study was not able to correlate the salt crystals morphology with the wind speed conditions since the salt crystals were in more than one form within some thin sections (see figure 11.32).

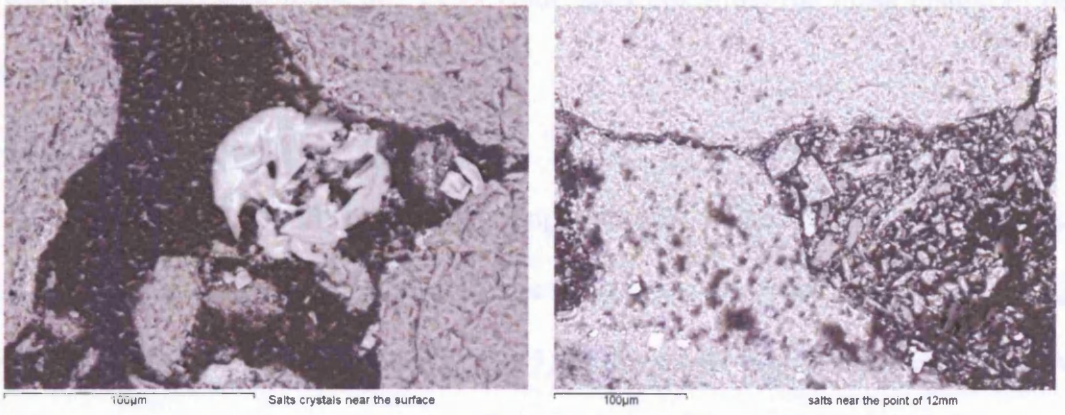

Figure 11.32: Scanning electron micrograph showing different morphologies of sodium chlorine salts in the same specimens (Disi sandstone: fifth run).

11.4. Summary

The overall aim of this chapter was to evaluate the role of wind speed, as well as relative humidity and temperature conditions, in the crystallisation and distribution of salts in porous materials. Two simulation tests were performed for this purpose: a sodium sulfate crystallisation test in a controlled microclimate chamber and a modified salt crystallisation test.

Only a few results are available from the chamber test due to the failure of the chamber during the testing stage of the simulation procedures. These primary results showed that stone decay and the salt efflorescence and subflorescence of salts were different under different wind speed conditions, with the highest stone decay occurring under fluctuating wind speed conditions. The amount of salt efflorescence was higher at low wind speed and wind-free conditions, while the amount of salt subflorescence was generally higher in high and fluctuating wind speeds. However, the limited number of tested samples as well as the different rock characterisations between the tested specimens and Petra stone does not allow the these results to be generalised.

In the modified salt crystallisation test using saturated sodium sulfate solution, the highest disintegration rate in all tested specimens was recorded under fluctuating wind speed and low relative humidity (run 3), followed by high wind speed and low relative humidity (run 2). Also, it was observed that the weight loss was generally higher at low relative humidity (runs 1-3) compared to high relative humidity (runs 4-6). In the high relative humidity runs, the weight loss was higher in high and

fluctuating wind speed conditions compared to the low wind speed conditions, with the highest in fluctuating wind speed conditions (see table 11. 5).

Experiment conditions	Sample type	ΔM (weight loss or gain) sodium sulfate salt solution %	ΔM (weight loss or gain) Petra salt solution %	ΔM (weight loss or gain) de-ionised water %
low RH-low wind speed	Monks Park limestone	-66.34	4.79	0.24
	Monks Park limestone	-100.00	4.90	-----
	Locharbriggs sandstone	-12.11	0.50	-0.25
	Locharbriggs sandstone	-59.59	1.17	-----
	Upper Umm Ishrin sandstone	-100.00	-0.87	-1.88
	Middle Umm Ishrin sandstone	-100.00	-3.85	-12.16
	Disi Sandstone	-100.00	-7.85	-0.89
low RH-high wind speed	Monks Park limestone	-15.43	1.23	-0.31
	Monks Park limestone	-18.46	2.88	-----
	Locharbriggs sandstone	-59.40	0.03	-0.15
	Locharbriggs sandstone	-61.40	0.79	-----
	Upper Umm Ishrin sandstone	-100.00	-2.11	-4.29
	Middle Umm Ishrin sandstone	-100.00	-3.57	-3.13
	Disi Sandstone	-100.00	-8.10	-8.83
low RH-fluctuated wind speed	Monks Park limestone	-29.45	1.28	-0.39
	Monks Park limestone	-100.00	0.48	-----
	Locharbriggs sandstone	-74.70	-1.32	-0.13
	Locharbriggs sandstone	-58.15	- 0.66	-----
	Upper Umm Ishrin sandstone	-100.00	-4.16	-4.32
	Middle Umm Ishrin sandstone	-100.00	-2.80	4.41
	Disi Sandstone	-100.00	-12.11	-14.16
high RH-low wind speed	Monks Park limestone	2.31	4.96	0.86
	Monks Park limestone	-8.14	5.10	-----
	Locharbriggs sandstone	-31.35	3.01	1.12
	Locharbriggs sandstone	-21.84	3.27	-----
	Upper Umm Ishrin sandstone	-100	- 0.48	-0.61
	Middle Umm Ishrin sandstone	-100	-2.09	-1.35
	Disi Sandstone	-100	-12.02	-5.89
high RH-high wind speed	Monks Park limestone	13.87	5.32	0.24
	Monks Park limestone	4.73	3.49	-----
	Locharbriggs sandstone	-23.65	1.83	0.30
	Locharbriggs sandstone	-29.32	1.38	-----
	Upper Umm Ishrin sandstone	-100	-3.91	-1.45
	Middle Umm Ishrin sandstone	-100	-2.87	-1.37
	Disi Sandstone	-100	-17.20	-7.05
high RH-fluctuated wind speed	Monks Park limestone	-37.73	0.95	-0.02
	Monks Park limestone	-0.25	3.11	-----
	Locharbriggs sandstone	-20.50	0.01	0.19
	Locharbriggs sandstone	-23.56	0.28	-----
	Upper Umm Ishrin sandstone	-100	-6.07	-2.24
	Middle Umm Ishrin sandstone	-100	-5.18	-2.22
	Disi Sandstone	-100	-16.33	-15.94

Table 11.5: Summary of the weight gain or loss (%) of specimens in the modified salt crystallisation test

In the second part of the modified salt crystallisation test, where the Petra saturated salt solution was used instead of the sodium sulfate solution, the rate of disintegration was much lower. But as regards the role of wind speed conditions in the weight loss or gain of the samples, similar results to the sodium sulfate solution test were observed. The highest weight loss in both low and high relative humidity

conditions was recorded under fluctuating wind speed conditions. It should be stated that, apart from the Petra specimens, most of the specimens showed weight gain rather than weight loss in most of the simulation runs. Based on the laboratory observation, this weight gain does not suggest that there has been no weight loss from the original specimens, but that the amount of the crystallised salts was higher than the amount of the lost particles of stones. In order to evaluate the durability of the specimens that showed weight gain rather than loss, the stone with the highest weight gain was regarded as the most durable one. This was based on the fact that the amount of salt uptake in all runs was very similar and, therefore, it seems logical that the specimen with the lowest salt content was the stone with the highest disintegration rate.

The last part of the modified salt crystallisation test was to evaluate the role of clay minerals as well as the original salt content of the samples in the specimens behaviour. The same procedure as in the previous modified salt crystallisation test was used, with de-ionised water instead of a salt solution. The specimens without clay minerals (Locharbriggs and Monks Park limestone) were very sound at the end of this test, while Petra specimens showed a certain degree of disintegration confirming the role of clay minerals in the decay mechanism of these stones.
Disi sandstone specimens were the most vulnerable in all tests. The high clay content, the pore space geometry (small and coarse pore spaces) and the high porosity of this stone are the most likely explanations for such vulnerability.

The correlation between the water and salts uptake of the different specimens showed that all sandstone specimens (Petra and Locharbriggs) had a very similar

capacity, while the limestone specimen (Monks Park) had a much higher capacity for water and salts uptake (see figure 11.33). Generally, the salt uptake was higher in the sodium sulfate solution test than in the Petra salt solution test. However, the weight loss was higher in the sandstone specimens and not in the limestone specimens that had the highest water and salt uptake. The small pore size and the lack of clay minerals in the Monks Park limestone are the most likely reasons for such behaviour.

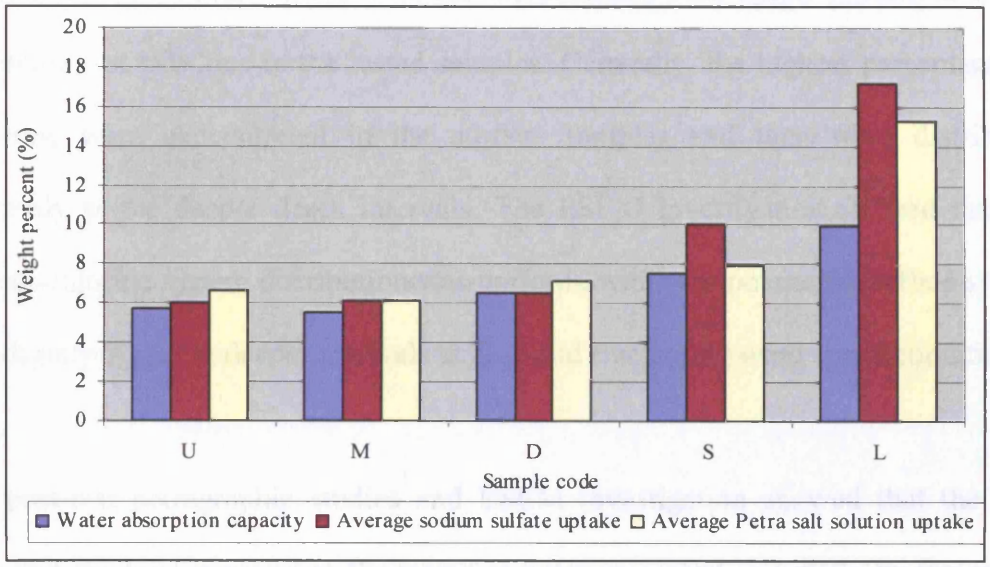

Figure 11.33: Water and salts uptake from the tested specimens

In addition to the evaluation of the weight loss or gain of the samples, the research studied the distribution of soluble salts at the end of each run in both modified salt crystallisation tests (sodium sulfate and Petra salt solution tests). The results of the test using saturated sodium sulfate showed that sodium and sulfate ions were distributed differently under different wind speed conditions, with generally higher amounts in the surface intervals at low wind speed conditions and higher contents in deeper intervals under high wind speed conditions. These variations were more obvious under low relative humidity conditions. At fluctuating wind speed, sodium and sulfate were distributed uniformly throughout the tested specimens, but it should

be remembered that under these conditions the specimens suffered a massive loss of material and therefore lost most of their salt content. At high relative humidity conditions, sodium and sulfate were in higher concentration near the surface of the specimens, with generally higher amounts in high and fluctuating wind speed conditions.

In the modified salt crystallisation test using Petra salt solution, the salt distribution analysis did not reveal a major role for the different wind speed conditions in the distribution of salt ions in the tested samples. Generally, the highest percentages of salt ions were concentrated in the surface samples and then were distributed uniformly at the deeper depth intervals. The ESEM investigation showed that the sodium-chloride system distribution was uniform, while the potassium-sulfate system was slightly higher at deeper intervals at high and fluctuating wind speed conditions.

The post-test petrographic studies and ESEM investigation showed that the pore sizes and the total porosity of the tested samples increased massively by the end of sodium sulfate test, with the highest increase under fluctuating wind speed and low relative humidity conditions. In addition, at the end of the modified salt crystallisation test using Petra salt solution, the Petra samples suffered a considerable loss of their clay minerals matrix. The loss was observed mainly at high relative humidity conditions.

Considering all results, it can be concluded that the simulation tests were mainly in agreement with the research's hypothesis that the fluctuation in wind speed enhances the salt damage behaviour in porous materials. However, the exact mechanism of this process has not been identified. The evaluation of the test results points towards three

possible mechanisms that can lead to salt damage under fluctuating wind speed. One is the crystallisation of a high percentage of salt ions during high wind speed conditions and the dissolution of some of these ions during low wind speed conditions. The succession of high and low wind speed results in a succession of crystallisation and dissolution cycles causing higher damage than a steady rate of crystallisation would cause. The other mechanism is based on the relationship between different wind speed conditions, pore structure and type of salt solution. The fluctuating wind speed can enhance the salt damage by creating a combined pressure during high and low wind speed cycles. During high wind speed, the evaporation rate at larger pores will increase resulting in higher crystallisation pressure than in the smaller pores compared to a low evaporation rate during low wind speed. During low wind speed, however, once the salt solution enters the small pores of the stone, it will be capable of less movement and will therefore have more time to crystallise within the small pores, thereby creating higher crystallisation pressure there. As a result, at fluctuating wind speed conditions, the porous materials will be subjected to a continuous pressure at both high and low wind speed intervals, which will result in more damage. In addition, another explanation for the higher weight loss ratio at fluctuating wind speed conditions could be the way salt distributes inside the pores, since the relatively sound samples showed higher sodium sulfate content at deeper depth intervals during fluctuating wind speed than at low and high wind speed conditions.

These findings would be correlated with the fieldwork investigation in Petra in order to draw a general conclusion about the role of wind speed in the salt crystallisation and distribution in porous materials which is undertaken in the next chapter.

Chapter 12
Discussion

12.1. Introduction

The complexity of the salt damage process in porous materials is very much related to the many variables involved and the way these variables interact with host materials and with each other. The results of different studies in salt damage add confusion to this complexity. Doehne (2002, 60) reported more than 1800 references in the scientific literature on the topic of salt weathering in porous materials, most of which, however, are studies for individual sites and their results are difficult to interpret or apply to other case studies. Viles (2005a, 15) illustrated that the way forward in stone decay research is to provide as much information as possible regarding the input and output in this process in order to identify the nonlinear behaviour of the stone decay process, which could be the key factor in interpreting such a complex system.

The overall aim of this research has been to contribute to the scientific knowledge of salt damage by exploring a factor in this process not thoroughly explored thus far. The role of wind speed in salt crystallisation and distribution in porous materials generally, and in Petra monuments particularly, has been evaluated in this study through fieldwork and laboratory investigations. This chapter summarises and evaluates the main limitations and outcomes of this research. It also discusses aspects of salt damage based on the observations from this research and presents proposals for conservation measures at the case study site.

12.2. Limitations of the current research

12.2.1. Fieldwork observation and data collection

Producing a valid investigation of the salt deterioration problem in a huge site like Petra presented a number of challenges. Petra has more than 2000 monuments, each of which has different composition, stratigraphy, location, salt content and environment. Carrying out a detailed survey in each of the monuments was beyond the time scale of this research. Therefore, four different monuments were chosen as representative case study sites, each of which has certain features that could help reveal further information about the salt damage problem in Petra.

Dealing with a cultural heritage site raised a further ethical challenge. Sampling had to be kept to a minimum and away from the carved façades as much as possible. Consequently, the sampling profiles were mainly taken from un-carved sections near the carved façades. Also due to the huge size of each monument, the sampling profiles were not as many as is usually required in order to obtain a detailed survey of the salt distribution in them. In addition, neither the time scale nor the budget of this research could provide a detailed survey of the salt distribution at the whole site. Regarding the recording of the microclimate conditions around the studied sites, two data loggers were initially installed in two different monuments. Unfortunately, one of them was stolen and the research had to rely on only one data logger for the recording of the temperature and the relative humidity at the site. In addition, no data logger or other alternative equipment was available for the recording of the wind speed over a long period. Spot readings taken during the four fieldwork visits to the site were, therefore, the only option for the evaluation of the wind speed.

Nonetheless, the collection of representative samples and a detailed microclimate survey from four different monuments at four different seasons revealed significant information about the salt distribution in the site and the way different environmental conditions affect the mobility of the salts content in each monument.

12.2.2. Laboratory experiments

Following the breakdown of the microclimate generator, the main challenge in the laboratory experiment was the lack of accurate equipment that could control the different environmental conditions to very specific ranges. However, the equipment that was used in the modified salt crystallisation test produced acceptable ranges of the required conditions.

The selection of the salt solutions was another challenge. Results from fieldwork data showed that the salt content varied from one point to another in the same monument and at the same time of year. Therefore, no single type of salt solution could be representative of the whole site. Consequently, two different salts were used: sodium sulfate (the most well known damaging salt) and a salt solution based on the calculation of the overall averages of the main cations and anions at the Palace Tomb recorded at the four fieldwork visits. The Palace Tomb was chosen mainly because, throughout the fieldwork observation, it had shown the highest salt content and the highest rate of wind speed fluctuation among the four monitored monuments.

The current research work was also limited by the fact that the experiment was carried out on individual stone cubes while the actual salt damage at the studied

monuments is the result of interaction between multiple layers. In other words, the salt movement in the current research was restricted to small specimens, while at Petra it happens in more complicated multi-layered systems, through a series of mountains. Also, the research experiment used a total immersion technique for a certain period before allowing the salts to mobilise under the different experiment conditions, while no fieldwork data has suggested similar mechanisms. Practically, a partial immersion test would be more representative, but the limited time of the research and the need to carry out the test under six different conditions favoured the use of the total immersion technique (see chapter 7). Nevertheless, the current research experiment revealed valuable information regarding the effect of the environmental conditions in salt distribution and, therefore, towards the understanding of salt damage in porous materials.

A further limitation of the current research was the use of sandstone specimens that were slightly different from Petra stone. The main difference was the lack of clay minerals in the laboratory tested specimens. However, the pore space and the total effective porosity were similar. Alongside these laboratory sandstone specimens, three different specimens from Petra and a standard limestone were also used in each set of experiments and the differences in the behaviour of each stone type were evaluated and correlated (see chapter 11). The author strongly believes that the use of stone specimens slightly different from Petra stone (no clay minerals in their components) and a totally different building material (limestone) alongside some Petra specimens offered great assistance in realising the research aims. These test results presented the behaviour of different stone specimens under similar

environmental conditions, and, therefore, offered a wider understanding of the salt damage process.

The research faced a practical limitation in preparing the salt mixture based on the data collected from the sites. This salt solution of various specific salts was prepared according to the overall averages of the main cations and anions of the Palace Tomb. During the solution preparation, due to a high percentage of calcium and sulfate in the mixture, a white residue of calcium sulfate formed at the bottom of the container (see chapter 11). Despite this residue, it was believed that the salt solution should be prepared at a high concentration in order to achieve the highest saturation level.

Another difficulty in the current research was the selection of the drying temperature for the simulation test. As the main purpose was to achieve complete drying after each immersion cycle, a higher drying temperature was needed. On the other hand, the research was in favour of replicating the environmental conditions found at Petra. The simulation test followed a compromise procedure where temperatures were higher than those recorded at the site, but lower than the drying temperature used in other simulation tests.

It must be stated that only very basic statistical analysis was applied to the fieldwork data and the laboratory investigation data. The main reason behind that this was that both the fieldwork and the laboratory analysis had shown some individual readings that did not agree with the general trend of the rest of the data and applying further statistical calculations on such readings could result in manipulation of the data.

12.3. Summary of findings

12.3.1. Microclimate conditions

The microclimate monitoring programmes of this research revealed the following as the main features of the microclimate conditions at the site of Petra:

- Dry, hot and fluctuating wind speed conditions dominated throughout the majority of the year.
- The fluctuation of wind speed was observed not only between one period of the year and another, but even between one location and another within the same period and at each location within a 24-hour period.
- Even though the relative humidity monthly averages did not vary significantly, the individual readings showed a wide range of fluctuation.
- The temperature was very stable compared to the wind speed and relative humidity conditions.

12.3.2. Sampling profiles

The results showed variation in the salt content not only between one profile and another, but also from one sampling point to another at the same sampling profile and in the same sampling period. Despite the large number of sampling profiles and the large number of collected samples, it was impossible to produce a single evaluation of the salt content and behaviour in the tested monuments, since the results from the different sampling profiles of each monument varied so much that any generalisations concerning the salt content and behaviour throughout the whole monument were not viable.

It should be stated that the author is aware of the fact that more work is needed in order to have a better understanding of the salt distribution in monuments of such size. More samples are needed, especially from higher sampling points (above 5m), since the rate of disintegration of the upper and lower parts of these monuments are substantially different and the evaluation of the salt content in both parts could reveal significant information about the salts origin, distribution and thermodynamic behaviour. Nevertheless, the general overview of the salt types and distribution in four monuments during four different seasons that this study has been able to provide has been satisfactory for the purposes of this research.

12.3.3. Sampling periods

The results of the analysis of samples has shown that the soluble salts content varied not only from one season to another, but from one monument to another within the same season and even from one profile to another at the same monument within the same season, indicating the significant impact of the microclimate conditions, wind speed in particular, on the salt crystallisation and distribution. The profiles with a high rate of wind speed fluctuation also had the highest amount of soluble salts. These results suggest that further analysis of the salt content during other periods of the year could be useful. Two further sampling periods especially could be considered: the period between late February to early March and during October, but as has been stated earlier the research budget and time scale as well as the consideration of the integrity of the monuments dictated a limited number of sampling seasons.

In addition, the seasonal variation of nitrate in the tested samples was considerable. As discussed earlier, the obvious source of nitrate is the grazing animals. In view of these results, more studies are needed to examine the seasonal grazing activities and their relation to the salt damage at the monuments. This point will be discussed further in the next chapter.

12.3.4. Wind speed and salt damage: the simulation tests

The use of a microclimate controlled chamber to evaluate the salt damage process had the great advantage of providing very accurate relative humidity and temperature conditions. However the technical failure of the chamber during the preliminary tests prevented completion of an experiment that could have provided the research with valuable information. The short drying period for each cycle of this test (24-hour drying time), as well as the low drying temperature (20 $\pm$ 2 °C), resulted in incomplete drying of the samples. As a result and in order to achieve complete drying of the samples, an additional drying cycle was carried out in an oven at 105 °C at the end of each monitored cycle. It could be argued that in this case the salt crystallisation was achieved under completely different drying conditions than those initially proposed for the simulation test. However, as complete drying was carried out mainly in order to calculate the amount of subflorescence rather than the amount of stone decay, the use of complete drying could be justified. In addition, the complete drying cycle was performed in the same way throughout the simulation test, minimising any impact on the results.

Despite the small number of simulation runs performed in the chamber and the fact that the characterisation of the tested samples did not match with Petra stone, the test

revealed significant information about the role of wind speed in salt damage. The results showed that the amount of stone decay caused by salt crystallisation was higher in high and fluctuating wind speed conditions than in low wind speed and wind-free conditions. The results also revealed that salt subflorescence was higher in fluctuating wind speed conditions.

The second simulation test was a modified salt crystallisation test. The main advantage of this test was the introduction of the wind speed factor into a commonly used standard test for the evaluation of stone durability. This step not only assisted in evaluating the role of wind speed conditions, but it also made the simulation test more representative of the actual salt damage in porous materials. While the use of sodium sulfate solution made the results of this test comparable to other simulation tests, most of which use sodium sulfate as a major testing salt, the use of Petra salt gave results more specific to the salt damage in Petra, and the use of de-ionised water was to test the particular role of clay minerals in the salt damage process.

The modified salt crystallisation test results showed that different wind speed conditions had different impact on the amount of weight loss or gain of the tested specimens, with higher disintegration rates at high and fluctuating wind speed conditions. Also, low relative humidity conditions were more damaging than high relative humidity conditions. In regards to the immersion solutions, the rate of disintegration was higher in the samples immersed in the saturated sodium sulfate solution, while all other tested specimens apart from Petra specimens remained sound in the de-ionised water tests. Evaluation of the salt distribution in the specimens showed that in the sodium sulfate test, sodium and sulfate ions were

distributed differently at different wind speed conditions, with generally higher content in the surface intervals at low wind speed conditions and in the deeper intervals at high wind speed conditions. At fluctuating wind speed conditions, the sodium and sulfate ions were distributed uniformly throughout the tested specimens, but the samples were too small at the end of the simulation runs under these wind speed conditions to enable elaborate analysis of their salts distribution. On the other hand, in the Petra salt solution test, the salts distribution analysis did not reveal significant differences in the distribution of salt ions at different wind speed conditions. In this test the highest percentages of salt ions were concentrated in the surface samples and then distributed uniformly at the deeper depth intervals.

12.4. General discussion

Considering the results of the fieldwork observations and laboratory analyses, the research outcomes direct the discussion towards four main subjects that could shed light on the understanding of the mechanism of salt damage in porous materials. The following is discussion of these concepts.

12.4.1. Wind speed and salt damage: effects and results

Despite the fact that the relation between salt damage and wind speed has been known for a long time, the actual effect of different wind speed conditions has not been previously examined. Most of the studies that discuss the wind speed effect have mainly been a comparison between high and low or wind-free conditions (Mossotti and Castainer 1990 and Rodriguez-Navarro and Doehne 1999b) and none has investigated fluctuating wind speed conditions. Considering the fact that fluctuating wind speed is more common than a steady high or low wind speed, the evaluation of the impact of fluctuation seems crucial. The results of the simulation tests carried out for the current research have shown not only that the rate of salt damage is higher under fluctuating wind speed conditions, but also that these are the only conditions under which secondary coarse pore space was formed as a result of salt crystallisation. This was particularly obvious in the thin sections of the stone samples with fine pores (Monks Park limestone), where the formation of secondary coarse pore space was noted under fluctuating wind speed, while no such pores were generated by low or high wind speed conditions (see figure 12.1.a, b and c). Another interesting observation with the Monks Park limestone samples was that the main decay occurred in the matrix where coarse secondary porosity was formed rather than in the fine pores within the ooliths, as expected.

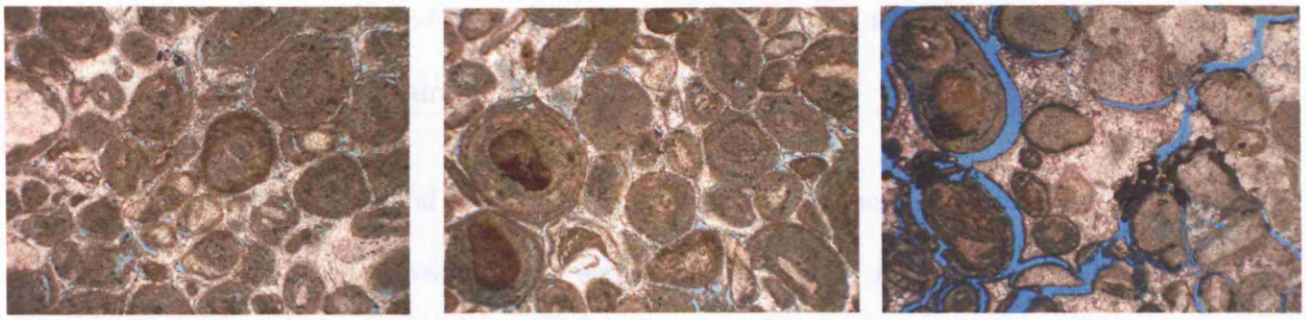

A B C

Figure 12.1: Photomicrographs of the petrological thin sections of the Monks Park limestone specimen at the end of the simulation test.
A: first run (low wind speed). B: second run (high wind speed). C: third run (fluctuated wind speed) Field of view 2.5 mm. Microscope Magnification: 40x. (ppl).

On the contrary, the ooliths remained sound and, once the secondary porosity was formed in the Monks Park limestone matrix, damage was at a higher rate in these coarse pores than in the fine pores within the ooliths, as expected. These results are very interesting, as they suggest that the higher rate of damage took place in the coarse pores that were fed with solution from the fine pores, which contradicts previous theoretical and experimental models, such as Rodriguez-Navarro and Doehne 1999b and Scherer 1999 that suggested that growth pressure is more likely to happen in fine than coarser pores. On the other hand, the results of the current research are in agreement with the observations of Wellman and Wilson (1965) and Fitzner and Snethlage (1982), who suggested that crystal growth will take place preferentially in large pores by solution supply from the smaller pores. It must be stated that the small number of tested samples limits the generalisation of these results, but at the same time these put forward a question concerning the validity of applying theoretical models to evaluate the salt damage process in porous materials. The understanding of what type of pore spaces the salt solution is more likely to crystallise in and continue to grow in, is a fundamental issue in the salt damage process. The next chapter will put forward some suggestions for further research in

this area that could enhance the understanding of the relationship between salt solution and pore structure of the host material.

The high weight loss and the formation of coarse pore space during fluctuating wind speed compared to a lower rate of weight loss and much smaller size of secondary pore space in high and low wind speed conditions indicated a more aggressive rate of decay in unstable and fluctuating wind speed conditions. But what mechanism could be responsible for this high rate of decay? Unfortunately, the current research has not been able to answer this question fully. However, some possible mechanisms can be suggested.

The first suggested mechanism is related to salt distribution at different wind speed conditions. In the sodium sulfate simulation test, the highest rate of damage occurred under fluctuating wind speed when the salt content was generally higher, deep inside the tested stone. Even though it seems that salts were distributed uniformly under the fluctuating wind speed, it could still be argued that the way this distribution happened may have contributed to the high rate of damage. Most of the tested samples deteriorated substantially under these conditions and underwent a major loss of their original material, while the remaining specimens still contained a high ratio of salts. The relatively high ratio of salts in the remaining small samples suggests that the salts content was higher in the deeper intervals of the original samples. On the other hand, comparing these to the results of the sodium sulfate distribution under low and high wind speed, it could be noted that the salt content was generally higher at greater depths in high wind speed conditions. Considering the fact that all other factors that could influence the way the salt distributed were controlled throughout

the test, the results show that wind speed may have a major impact in the salt distribution within porous materials and ultimately in the rate of decay, since a higher ratio of salt at greater depths means higher crystallisation pressure and therefore higher rate of deterioration.

The second possible mechanism is related to pore size and will be discussed separately in the next section.

The third possible mechanism is related to phase change of salt crystals during fluctuating wind speed conditions. This process can be described as follows. During a high wind speed interval, a high percentage of salt ions crystallise due to the high rate of evaporation, while some of these salts can then re-dissolve during the next low wind speed interval. The succession of high and low wind speed results in a succession of crystallisation and dissolution, which weakens the internal structure of the porous material and, as a result, causes greater damage than a steady rate of crystallisation would cause.

It must be stated that the above discussed concepts need further testing to be fully evaluated. Chapter 13 will introduce some recommendations for future research that could contribute to a better understanding of the wind speed effect on the salt damage mechanism.

12.4.2. Wind speed and salt damage: the possible role of pore structure

One of the most interesting findings of this research was that the effect of different wind speed conditions on salt damage varies according to the pore structure of porous materials. While previous studies (such as Rossi-Manaresi and Tucci 1991

and Honeyborne and Harris 1958) have pointed out that salt damage is mainly higher in materials with fine rather than coarse pores, the current research has shown that there are significant variations in this depending on the environmental conditions. It was observed that, while at low wind speed conditions the salt damage rate was higher in stones with fine pores, at high wind speed conditions the salt damage rate was higher in stones with coarse pore structure. Despite the fact that the numbers of samples were limited and only represented two types of UK stones, the relationship between wind speed and pore structure is evident. The possible reason for this can be explained as follows. At high wind speed, the evaporation rate is higher and thus the rate of crystallisation will be higher in the coarse pores than the fine ones, since their surface area is greater. On the other hand, at low wind speed conditions the lower rate of evaporation will cause salts in the fine pores to crystallise more quickly than salts in the coarse pores. This is because, despite the fact that the surface area is lower, the volume of the solution in the fine pores is less and will therefore crystallise faster resulting in more damage.

This could also be linked to the observations made by many scientists (such as Rodriguez-Navarro and Doehne 1999b and Flatt 2000a) who report that the higher rate of damage is largely higher in stones with micropores connected to macropores. The higher rate of disintegration in these types of stone could be explained in the light of the current findings, which show that different pores react differently to their surrounding conditions. As this research has shown, the higher rates of disintegration occurred under fluctuating wind speed conditions in the stones that had micropores connected to macropores. Considering that fluctuating wind speed is the most common feature in wind speed conditions in nature, the high rate of damage in

porous materials with macropores connected to micropores could be explained by the fact that during fluctuating wind speed conditions these materials are subjected to a combined crystallisation pressure, with a high rate of crystallisation pressure in the fine pores under low wind speed conditions and a high rate of crystallisation pressure in the coarse pores under high wind speed conditions. The surface area is greater in the coarse compared to the fine pores, which means higher crystallisation pressure in these pores during the high wind speed cycle. On the other hand, during the low wind speed cycle the salt solution in the fine pores will crystallise earlier as the fine pores are lower in volume with low solution flow which results in higher crystallisation pressure. This suggests that a combination of high rate of damage in the coarse pores during high wind speed intervals and high rate of damage in the fine pores during low wind speed conditions may take place in stones with co-existing micropores and macropores that ultimately results in more damage than in stones with either fine or coarse pores alone.

In other words, it seems that different pore structures have an impact on the way salt solutions react to their surrounding conditions and that there is not a general rule that controls the interaction between salt solutions in porous materials and pore structure. This undoubtedly needs more investigation, since, if proved, the present understanding of the role of pore structure in salt damage could be enhanced.

12.4.3. Wind speed and salt distribution

Another significant observation was that the salt distribution within the tested samples varied under different wind speed conditions in the case of the sodium sulfate test, while no such variations were noted in the case of the Petra salt solution

test. The question arises as to whether it is only sodium sulfate that responds to surrounding environmental conditions, which may account for it being considered the most aggressive salt. In their simulation test, Rodriguez-Navarro and Doehne (1999b) concluded that, in general, sodium sulfate tends to crystallise inside the stone samples, while sodium chloride tends to crystallise on the surface. In addition, they reported that the sodium sulfate distribution through the pore system of the stone was not homogenous, while sodium chloride showed a more uniform distribution. The observations made in the current research, as well as the findings by Rodriguez-Navarro and Doehne (1999b), indicate that different salt types respond differently to surrounding conditions. More research is needed to test the behaviour of sodium sulfate and to compare it with other salt solutions in the context of interacting with surrounding environmental conditions.

12.4.4. Salt damage and simulation tests: what is really needed?

In the current research, discussion of the different simulation tests for salt damage has shown the diversity and complexity of the used tests and the confusion caused by the correlation of their results. Also, it has been demonstrated that each test, including that applied here, was formed according to the particular needs of each study. The author believes that it is time to establish one standard salt damage simulation test procedure that will include all possible factors with more realistic testing conditions and will thus have a wider applicability. The idea behind this suggestion is to minimise the impact of the simulation test procedure on the overall results making results more easily comparable and also to provide a salt simulation test that is able to evaluate the effect of all factors involved in salt damage. The identification of these factors should be based on a comparative evaluation of salt

damage as it happens in nature. For instance, despite the fact that many scholars have pointed out the role of wind speed in salt damage, none of the commonly used standards, such as the BRE and ASTM standards, have included this factor in their simulation procedures. In addition, many studies that have developed simulation tests with environmental conditions based on fieldwork observations, such as the simulation test of this research, have not attempted to make their tests applicable to other environmental conditions. In this respect, a test with one standard procedure but also with a certain flexibility that would simulate the salt behaviour in porous materials under different environmental conditions would be ideal. This could be achieved if a single procedure were designed to operate under three or more test environments, each representing a particular climate type. The simulation test of the current research, which has been designed to include possible factors relating salt damage to its environments, was based on a field survey at the site of Petra and represented a typical dry, arid climate. It could however be made more applicable for other sites with different climates by introducing two or three more test phases, each simulating the environmental conditions of a particular climate.

All in all, the current research has been able not only to demonstrate the role of wind speed conditions in salt crystallisation and distribution in porous materials, but also, to point out some important aspects that could enhance the overall understanding of the salt damage problem.

12.5. Preventive conservation measures

The ultimate objective of a research on salt damage is to understand the mechanism of this process in order to minimise its effect on porous materials, in this case the World Heritage Site of Petra. The current research has explored the role of wind speed in salt crystallisation and distribution through fieldwork surveys, laboratory analyses and laboratory simulation tests. This section will look at what the fieldwork observations combined with the results of the laboratory work indicate in regards to preventive conservation measures that might help minimise the salt damage in Petra monuments.

Based on the outcomes of both the fieldwork analysis and the simulation test, fluctuating wind speed accelerates the salt crystallisation process, and thereby increases the potential for higher stone decay rates, compared to steady flows of high or low wind speed. This suggests that an important preventive conservation measure would be to try to contain the high rates of wind speed fluctuation. This could be achieved, firstly, by providing shelters for the most vulnerable monuments, such as the Corinthian and Palace tombs and, secondly, by planting trees around the monuments to act as wind breaks. Even though many scholars are concerned about the impact of shelters on the integrity of heritage sites, the presence of shelters could ultimately minimise the impact of the surrounding environmental conditions on the monuments and provide a more stable environment. The construction of shelters should be reversible, flexible, fit the context of the monuments and have a minimal impact on them. It must be stated that even though a shelter could offer relatively stable environments that might help in reducing the rate of decay in Petra monuments, the construction of a shelter over the major tourist attractions in Petra,

such as the Palace, Deir or Corinthian Tomb, would be challenging in regards to practicality and finance and could also have a negative impact on tourism. Instead, this solution could be applied and tested first on one of the monuments near the back entrance to Petra, where salt damage is equally evident but visitor figures are much lower. In the case that the shelter solution there shows significant reduction in the rate of decay, the thought of extending it to other monuments would be more convincing. It should also be noted that the shelter design should be aesthetically compatible with the environment of Petra. The shelter of the Byzantine Church in Petra is a good example of how much impact shelters can have on archaeological sites. Despite having been constructed with minimum intervention and great flexibility, this shelter with its modern metal frames and reflecting covering is totally incompatible with the surrounding environment and is visible from a great distance. The site of Petra cannot afford to have more shelters like this and it is essential that any new shelter designs take into consideration the aesthetic values of the site.

The salt distribution figures showed that nitrate is a major soluble salt in the tested monuments. As mentioned before, the grazing animals around the site are the most obvious source of this salt, and, thus, control of the grazing activities is a critical need for the protection of the site. The grazing animals should not be allowed anywhere near the tombs and the use of the tombs as shelters for animals should be completely banned. In some cases, this may mean that small wire fences need to be installed around some of the tombs to restrict animal activities. It must be stressed once again that any intervention should be aesthetically compatible with the site.

The thermodynamic evaluation of the salt behaviour in one of the sampling profiles showed that it may be possible to minimise the salt damage by controlling the surrounding relative humidity conditions. This study was able to determine the 'dangerous', 'safe' and achievable 'safe' relative humidity conditions. The suggested safe relative humidity conditions though cannot be achieved without the application of the first suggested measure, namely sheltering the monuments. Realistically, the modification of the environments around monuments of the size of those in Petra will be very difficult even if shelters were constructed. Therefore, it may be worth focusing on exploring the feasibility of developing the means to revise the relative humidity so as to avoid the most 'dangerous' ranges. Any measures that are based on the results of such thermodynamic evaluations should work in parallel with any other conservation measures. For example, if the grazing activities were to be controlled, the current thermodynamic calculations that consider nitrate in their system will not give the same results without the nitrate and would therefore have to be repeated.

The presence of trees, apart from minimising the direct impact of wind speed, could also reduce the temperature around the monuments and, thereby, slow down the evaporation rates. On the other hand, the trees should be located as far as possible away from the carved façades in order not to weaken the infrastructure of these monuments or cause disruption of the archaeological layers. It might even be a better idea if the trees were placed in tubs rather than planted in the ground directly in front of the monuments. This would not only reduce the impact on the infrastructure of the monuments, but could also provide a more flexible and reversible conservation measure. However, it is vitally important that the efficiency and possible impact of

such measures are tested prior to their application. This can be achieved by putting these measures into practice at one monument for a prescribed period of time and under a close monitoring programme.

Furthermore, it has been noted that most Nabatean water channels, which run along the carved façades, are broken, allowing water to leak into the carved façades. This water not only provides a source of moisture that can mobilise the salts present in these monuments, but it also washes the salts down from different heights and concentrates them at lower levels, thus, causing more damage. The repair of these water channels using appropriate materials should help to reduce the salt damage decay in Petra monuments. The author is aware of the fact that the repair of these water channels would be challenging both in practical and financial terms. However, this could be a long-term project that is carried out in different stages incorporating the knowledge and experience of local people.

All in all, the first step towards the conservation of the site is the identification of a single monument with evident salt damage, where the conservation measures presented above should be put into practice in order to test their efficiency. It should be stated that the salt damage problem is far from being solved by the outcomes of this research. Salt damage is generally a very complicated process, one that becomes even more complicated at a site of Petra's size and condition. The next chapter addresses some proposals for further research on the salt damage problem in Petra monuments.

Chapter 13
Proposals for Further Research

13.1. Introduction

The current research has contributed to the understanding of the effect of the surrounding environmental conditions, and wind speed in particular, on the salt crystallisation and distribution in porous building materials. Also, it has produced an overview of the salt damage in four monuments in Petra. However, further research is still needed for a greater overall understanding of the role of environmental conditions, and especially wind speed, in the salt damage mechanism in porous materials. In addition further investigations are needed to establish a more complete and firm perspective of stone decay from soluble salts in Petra.

13.2. Further research in salt damage studies

As was stated earlier, despite the large number of studies in the field of salt damage in porous materials, more research continues to be needed since neither the causes nor the mechanism of salt damage are fully understood. In this section, the proposals for further research will focus on three areas:

- Environmental conditions, particularly wind speed, and salt damage.
- Stone characterisation and salt damage.
- Salt damage simulation tests.

13.2.1. Environmental conditions and salt damage

The current research has demonstrated the rate of stone decay due to salt crystallisation pressure under fixed relative humidity and temperature conditions and

under different wind speed conditions. However, the mechanisms of how different wind speed rates have resulted in different rates of decay have not been identified. The next step in salt damage research should be directed towards the understanding of this mechanism under different wind speed conditions. The use of new techniques that are capable of producing three-dimensional images of the salt distribution rather than surface images could prove to be a significant tool for such research. Computer-aided tomography (CAT-Scan) could be one such possible technique that could provide three-dimensional images of the salts distribution within porous materials and thus aid in the understanding of the role of wind speed in the salt damage mechanism. The main purpose of this non-destructive technique would be to evaluate in three-dimensions the way salts distribute within porous materials at regular intervals during the drying process rather than just at the end of this process. This could be done by saturating different porous materials with different salts and drying them under fixed temperature and relative humidity and under different wind speeds in a chamber similar to the one used in this research, while carrying out interval monitoring of the salt distribution in the materials with the CAT-Scanning technology. Such a technique could provide a better understanding of the way salts distribute within porous materials under different environmental conditions and, as a result, enhance the understanding of the relationship between different rates of decay and salt distribution within porous materials. As this research has shown, the evaluation of the way salts have been distributed at the end of the simulation test could be misleading, since by that stage the original materials have deteriorated substantially and, therefore, the results of their salts content might not reflect the original pattern of distribution.

Moreover, nuclear magnetic resonance (NMR) could be another useful technique in the understanding of the role of wind speed in salt damage behaviour, since it can provide further information about the moisture and salt ion distribution inside porous materials. The proposal is to introduce the wind speed factor to this technique and to record how salt ions and moisture are distributed under different wind speed conditions. Rijniers (2004) considered the control of temperature during the evaluation of salt ions and moisture distribution in porous materials using the NMR technique, but no studies have considered the role of wind speed in the salt ions transport process. Therefore further studies using the NMR, where the wind speed factor is introduced and controlled, could reveal significant information regarding the effect of wind speed in salt ions transport in porous materials. (For more information about CAT-scanning technology see Mossoti and Castainer 1990 and Jacobs, Sevens and Kunnen 1994. For the NMR technology see Slichter 1990, Pel *et al.* 2003 and Rijiners 2004).

In addition, the simulation tests showed that the sodium sulfate concentration at the end of the drying cycles varied with depth under different wind speed conditions, while wind speed conditions had less impact on the distribution of salts from the Petra salt solution. These results suggest that the effect of wind speed on the salt distribution in porous materials should be tested further using different types of salts, both in individual form and in mixtures, as well as different types of porous materials.

13.2.2. Stone characterisation and salt damage

The current study has shown that different stones have different rates of decay from salt crystallisation pressure under different wind speed conditions. However, the

limited number of stone types used and the relatively small number of samples tested prevent generalisation of the results of this research. Thus, its outcomes should be explored further by applying the same modified salt crystallisation test to other stones of different composition, porosity and pore structure. In particular, the relationship between different pore structure and the possible different interaction with surrounding conditions that could result in different salt crystallisation pressure needs more investigation.

Equally, the role of clay minerals in the salt damage process should be examined further. The research should be focused on identifying the conditions that modify the non-swelling clay minerals into swelling minerals (osmotic swelling). The role of clay minerals in the salt ions and moisture distribution within porous materials could be studied using the previously mentioned techniques (CAT scanning technology and NMR) and the results of salt ions transport and distribution in samples with similar composition and pore structure, but with different clay mineral content, could then be compared.

13.2.3. Salt damage simulation tests

The evaluation of the salt damage process through various simulation tests, each of which has used different materials, conditions and procedures, has produced an enormous amount of information that does not necessarily reflect the actual salt damage process and has produced results that can be contradictory. A study that would standardise the simulation tests in salt damage research and put forward a simulation test that includes all possible factors involved should be considered as a priority.

13.3. Petra and salt damage: the unanswered questions

As was mentioned earlier, the current research has established a detailed overview of the microclimate conditions, salt distribution and behaviour in selected monuments in Petra. However, further research is still needed to answer some significant, yet unanswered, questions relating to salt damage at this site.

Firstly and most importantly, a detailed study of the hydrology of the area, and especially of the archaeological site of Petra is essential for the full understanding of the salt damage mechanism. The importance of such a study is due to the fact that groundwater is the obvious main source of the soluble salts in Petra monuments, and therefore, the determination of the hydrological features of the area, such as the water table levels throughout the year, will greatly assist in determining the ways salt is mobilised and distributed in the monuments.

Secondly, the geochemistry of groundwater in the Petra area needs to be studied in detail. Such a study will help to determine the origins of the soluble salts in the monuments and to identify the groundwater properties and how these may affect the salt behaviour in the monuments.

Regarding the site's microclimate monitoring programme, a more detailed evaluation of the wind speed around the monuments designed to cover a longer period of time than the current research, should be carried out. Further research should also include more detailed recording of temperature and relative humidity conditions in and around each monument, since this study has shown that it is difficult to generalise outcomes for the whole site of Petra based on monitoring data collected from one

monument. In brief, it would be more realistic and accurate to evaluate the environmental conditions for each monument individually rather than having fixed environmental data for the whole site of Petra as an entity.

In the subject of salt distribution analysis, further studies should be carried out to include more monuments and more sampling points at each of the tested monuments. In particular, sampling is needed from the upper and middle parts of the monuments and the analytical results should be correlated with those of the lower part, especially at monuments like the Deir Tomb, where the stone decay is prominent in the lower part, while the upper parts are in a far better condition. In addition, thermodynamic evaluations similar to the one carried out for one of the sampling profiles in the Palace Tomb should be applied to other sampling profiles and correlated with the results of the current research.

The animal grazing activities seem to have a major impact on the salt content and distribution in Petra monuments, as explained earlier. Further research is needed in order to examine these activities, their peak times throughout the year, the animals' paths and distribution around the monuments, their impact on the content and behaviour of salts within the monuments and what potential changes in the salts content and behaviour might occur if these activities were contained.

In addition, the monitoring of the salt distribution and damage rates during the application of the preventive conservation measures recommended by the current study is a matter that further studies must tackle.

In summary, while the current study has revealed significant information about the role of wind speed and other environmental conditions in salt crystallisation and distribution in porous building materials generally, and in Petra monuments in particular, there are still many aspects of the salt damage mechanism that need to be addressed. One of the main areas for further examination is the part played by different wind speed conditions in this mechanism. In addition, the size of Petra monuments, the variation of the microclimate conditions and salt content from one site to another, the lack of a definitive account of the origins of salts and moisture in these monuments, as well as the uncontrolled activities around the site, indicate the complexity of salt damage at the site of Petra. On the other hand, the different proposals set out by this research point to the need for an interdisciplinary approach which can address the various aspects of this complex mechanism and put forward an effective conservation plan for the World Heritage Site of Petra.

Chapter 14
Conclusions

14.1. Wind speed and salt damage

Fieldwork observation and data analysis as well as laboratory experiments in this research have shown that wind speed conditions have a major impact on the salt crystallisation and distribution in porous building materials. While the fieldwork data and samples analysis have revealed a strong relationship between salt content in the collected samples and wind speed at the sampling locations, the simulation test has indicated that wind speed affects the rate of stone decay, with the fluctuating wind speed conditions causing the highest damage. In addition, the depth of salt distribution in the samples varied under different wind speed conditions, especially in the experiment that used a single salt solution (sodium sulfate). This research has also shown that stones with different pore structures have different levels of interaction with wind speed, with the stones with coarser pore spaces being more affected by wind speed than those with fine pores. Considering all these factors it could be concluded that wind speed has a significant and multilateral role in the salt damage process and controlling it could help to minimise salt damage in archaeological sites and monuments greatly. Based on the findings of this research it can be argued that the lower and less fluctuating the wind speed conditions are, the less is the potential for salt damage to occur.

Furthermore, the results of the current research have pointed towards some mechanisms that could be responsible for the high rate of damage under fluctuating wind speed conditions. One is the succession of high and low wind speed that results

in cycles of crystallisation and dissolution causing higher damage than a steady rate of crystallisation would cause. The second mechanism is based on the relation between different wind speed conditions, pore structure and salt solution. The research results have shown that, at low wind speed, the rate of decay is higher in porous materials with fine pores, while, at high wind speed conditions, a higher rate of decay was noted in porous materials with coarse pores. Considering the fact that most porous materials have a combination of coarse and fine pores in their structure, fluctuating wind speed conditions could result in combined pressures: in the fine pores during low wind speed and in the coarse pores during high wind speed conditions, ultimately resulting in a higher rate of decay than a steady low or high wind speed could cause. The third possible mechanism in regards to the high rate of decay under fluctuating wind speed conditions is related to salt distribution within porous materials under such conditions. Despite the fact that salts were mainly distributed uniformly under these conditions, the high salt content in the remaining small samples at the end of the simulation test suggests that the salt content was generally higher at greater depths.

All in all, the results of the current research have not only answered the main research questions in regards to the role of wind speed in salt crystallisation and distribution, but have also pointed towards new directions for the overall understanding of salt damage in porous materials. In particular, the relationship between pore structure and salt crystallisation under different environmental conditions is one of the most exciting aspects revealed by this research that deserves more thorough investigation.

14.2. Clay minerals and salt damage

The current research has demonstrated that clay minerals have a major role in the process of decay in Petra monuments. It has also shown that the rate of decay from salt damage was much higher when the tested materials had clay minerals in their composition. The high rate of decay of the Petra samples during the de-ionised water test indicates the possibility of osmotic swelling of the otherwise non-swelling clay minerals. The fact that Petra stones contain a high percentage of clay (kaolinite) and soluble salts means that the two, as individual and interrelated factors, contribute towards a higher rate of decay. In other words, the swelling pressure generally increases due to the high content of soluble salts that enhances the osmotic swelling of the otherwise non-swelling clay minerals, while at the same time the high percentage of clay minerals enhances salt damage by providing an extra source of moisture and by weakening the internal structure of the host materials. The combination of these factors, the clay minerals swelling pressure and the salt crystallisation pressure, increases the rate of deterioration in these stones. Considering the fact that these two mechanisms are interrelated, controlling one could also be effective in minimising the impact of the other. In particular, the reduction of the amount of soluble salts in Petra monuments may also lead to the reduction of the swelling pressure, resulting in a more effective control of the rate of stone decay. The current research was able to suggest a number of ways of minimising the soluble salts content in the Petra monuments.

14.3. Petra: the microclimate conditions

The results of the microclimate monitoring programme at Petra showed variation in all monitored conditions (wind speed, relative humidity and temperature) not only

from one site to another and from one day to another, but also from one point to another at the same site and on the same day. This indicates the importance of the detailed microclimate monitoring approach in evaluating the salt damage mechanism. The more detailed monitoring approach could lead to better understanding of the salt solution behaviour in porous materials, but at the same time could produce a huge amount of data that could complicate or even impede interpretation. The current research followed a balanced approach to these aspects by carrying out a comparative but detailed survey in a limited but representative number of monuments at its case study site. In addition, the research has demonstrated the importance of considering all factors when monitoring the environmental conditions at a site. In particular, the results of this research have pointed out the significant role of wind speed in salt crystallisation and distribution and, thus, emphasised the importance of including this environmental factor when evaluating salt damage in porous materials, which previous monitoring programmes have not included.

14.4. Petra: the soluble salts distribution and behaviour

The results of this research have shown the complexity of salt distribution in the Petra monuments and how much this can be affected by the particular microclimate conditions, and especially wind speed. In general, the total soluble salts content was higher at the profiles where fluctuating and high wind speed was recorded. Furthermore, the total soluble salts content at each monument varied significantly in different seasons, mainly due to variations in the water table level as well as the seasonal animal grazing activities in the area. These results demonstrate the importance of carrying out a seasonal evaluation of the salt content and distribution in the studied monuments, as this research has done, as well as the need for a detailed

hydrological survey of the Petra area and a monitoring programme for the grazing activities at the site.

Equally, the way salts were distributed within the monuments, with the less soluble salts mainly concentrated in the lower parts of the sampling profiles and the more soluble salts towards the middle and upper parts of the profiles, indicates that different salts fractionate within the porous materials according to their solubility and that the surrounding environmental conditions can have a significant impact on this fractionation process. The higher wind speed at the higher sampling points resulted in crystallisation of more soluble salts, which, at lower parts of the monuments, remained in solution. This observation is very interesting, as it indicates that controlling the surrounding environmental conditions, such as minimising wind speed, could result in minimising the salt damage by keeping the more soluble salts in their solution state.

Moreover, the research results have shown that the behaviour of a soluble salt when mixed with other salts varies significantly from its behaviour as a single salt, demonstrating the importance of using the thermodynamic calculation method in the evaluation of the salt distribution and behaviour. Generally, salts in the Petra salts solution had a lower crystallisation point compared to their equilibrium relative humidity as single salts. The current research has emphasised that the modification of current environmental conditions based on the thermodynamic calculations should consider other factors that are involved in salt damage at the site. For instance, controlling the wind speed conditions could affect the other microclimate conditions around the site, namely the temperature and relative humidity, and as a result affect

the thermodynamic calculation. In a wider context, this clearly demonstrates that salt damage in an archaeological site should be dealt with using a comprehensive approach that considers all possible factors in this process.

14.5. Wind speed and salt simulation tests

The results of the present research have shown the importance of including the wind speed factor in the salt weathering simulation tests, since both the salt decay rate and the salt distribution were found to vary significantly at different wind speed conditions. The research has also emphasised the need for standard procedures in the salt weathering simulation tests that will incorporate all factors involved in the salt damage process and will have wider applicability by including conditions that represent more than one climate type.

14.6. Petra: some preventive conservation measures

Based on the findings that fluctuation of wind speed normally accelerates the salt crystallisation process and, thereby, the potential for higher stone decay rates, compared to the steady flow of high or low wind speed, it is clear that fluctuation of this factor should be contained in order to minimise salt damage at Petra monuments. Natural shelters, such as trees, or built shelters appear to be the priority in preventive measures. Although the author is totally aware that these measures could be difficult to implement, both for practical and aesthetic reasons, they still seem vital for the long-term conservation plan of the site.

In addition, control of the grazing activities is undoubtedly an essential preventive conservation measure for the site, since nitrate concentration, mainly a result of these activities, has a major role in the salt distribution and behaviour in the monuments.

This study has also highlighted the problem with the Nabatean water system and its broken channels. Repair of these channels would undoubtedly minimise water leakage on the monument façades and limit salt mobility within the monuments.

The thermodynamic calculations carried out by this research have also shown that salt damage could be minimised by controlling the surrounding relative humidity conditions. This measure is undoubtedly the most challenging of all, and its application, if deemed feasible, should be carried out in parallel with other conservation measures.

14.7. Concluding statement

This research has succeeded in demonstrating the role of an important environmental factor, wind speed, in salt crystallisation and distribution. It has established methods for carrying out a microclimate monitoring programme and a salt distribution survey in a huge and complex site such as Petra. It has also shown how important it is to combine fieldwork investigation with laboratory analysis and simulation tests for the evaluation of the salt damage process. In addition, the research has designed and applied a practical salt crystallisation test that included wind speed as well as other environmental conditions in its procedure. Moreover, it has indicated a large number of factors that need to be considered before any conservation measures are applied.

All in all, the results of this research represent a significant step forward in our attempts to understand the process of salt damage in porous materials and to contain the problem of salt damage at the World Heritage Site of Petra.

Bibliography

Al Naddaf, M., 2002. *Weathering Mechanisms: Technical Investigation in Relation to the Conservation of the Sandstone Monuments in Petra, Jordan.* Berlin: Mensch and Buch Verlag. 126p.

American Centre of Oriental Research (ACOR), 1999. *Petra, Jordan: Conservation in an Ancient City.* Amman: ACOR Publications.
Available from: http://student.rwu.edu/users/ah1826/ah1826/Petra/PPPETRA.htm . Accessed on 3 December 2001.pp: 1-15.

Arnold, A., 1996. Origin and behaviour of some salts in context of weathering on monuments. In Zezza, F., (ed.), 1996. *Origin, Mechanisms and Effects of Salts on Degradation of Monuments in Marine and Continental Environments.* Bari: European Commission Research Report. pp: 133-139.

Arnold, A. and Zehnder, K., 1991. Monitoring wall paintings affected by soluble salts. In Cather, S., (ed.), 1991. *The conservation of Wall Paintings.* Proceedings of a Symposium organized by the Courtauld Institute of Art, University of London, and the Getty Conservation Institute, London. July 13-16, 1987. Los Angeles: Getty Conservation Institute. pp: 103-135.

Arnold, A. and Zehnder, K., 1990. Salt weathering on monuments. In Zezza, F., (ed.), 1990. *1st International Symposium on the Conservation of Monuments in the Mediterranean Basin.* Bresica: Garfo Publication. pp: 31-38.

ASTM, 2004. ASTM C 642-97, Standard test methods for density, absorption and voids in hardened concrete. In *Annual Book of ASTM Standar*ds. Vol.04.02. Philadelphia: American Society for Testing and Materials. pp: 334-335.

ASTM, 2004. ASTM C-88, Standard test methods for soundness of aggregates by use of sodium sulfate or magnesium sulfate. In *Annual Book of ASTM Standar*ds. Vol.04.02. Philadelphia: American Society for Testing and Materials. pp: 42-46.

ASTM, 1990. ASTM C-88, Standard test methods for soundness of aggregates by use of sodium sulfate or magnesium sulfate. In *Annual Book of ASTM Standar*ds. Vol.04.02. Philadelphia: American Society for Testing and Materials. pp: 39-43.

Atlas Tours Net, 2004. Petra map and monuments. [On-line]. Available from: http://www.atlastours.net/jordan/petra_map.html .Accessed on 29 April 2004.12p.

Bailey, S., 1980. Structure of layer silicates. In Brindley, G. and Brown, G., (eds.), 1980. *Crystal Structure of Clay Minerals and their X-Ray Identifications.* London: Mineralogical society. pp: 1-115.

Bala'awi, F., 2002. *Conservation Work at Petra: A Critical Review.* Unpublished MA Dissertation. London: University College London. 105p.

Bates, R. L. and Jackson, J. A., 1980. *Glossary of Geology*, 2nd Edition. Falls Church, Virginia: American Geological Institute. 751p.

Bear, J., 1988. *Dynamic of Fluids in Porous Media.* New York: Courier Dover Publications. 784p.

Beggan, J., Long, A. and Basheer, P., 1996. The permeability testing of masonry materials. In Smith, B. and Warke, P., (eds.), 1996. *Processes of Urban Stone Decay.* Proceedings of SWAPNET 95 Stone Weathering and Atmospheric Pollution Network Conference held in Belfast 19-25 May 1995. London: Donhead Publishing Limited. pp: 205-211.

Benavente, D., García del Cura, M., Bernabèu, A. and Ordóñez, S., 2001. Quantification of salt weathering in porous stones using an experimental continuous partial immersion method. *Engineering Geology.* Vol. **59** (3-4). pp: 313-325.

Benavente, D., García del Cura, M. and Fort, R., 1999. Thermodynamic modelling of changes induced by salt pressure crystallization in porous media of stone. *Journal of Crystal Growth.* Vol. **204**. pp: 168- 178.

Bender, F., 1974. *Geology of Jordan.* Berlin: Gebrüder Borntrager. 102p.

Bionda, D., 2004a. *Salt Deterioration and Microclimate in Historical Buildings*: Intermediary report of the project "Sustained Care of Sensitive Historical Monuments". E-collection: available from: http://www.ethbib.ethz.ch. Accessed on 25 December 2005. 10p.

Bionda, D., 2004b. Methodology for the preventive conservation of sensitive monuments: microclimate and salt activity in a church. In Kwiatkowski, D. and Löfendahl, R., (eds.), 2004. *10th International Congress on Deterioration and Conservation of Stone.* Vol. 2. Stockholm June 27- July 2, 2004. Sweden: ICOMOS Publication. pp: 627-634.

Bionda, D., 2002. RUNSALT computer program. Unpublished.

Bionda, D. and Storemyr, P., 2002. Modelling the behaviour of salt mixture in walls: A case study from Tenaille Von Fersen building. In Von Know, T., (ed.), 2002. *The Study of Salt Deterioration Mechanisms. Decay of Brick Walls Influenced by Interior Climate Changes.* Suomenlinna, Finland: Suomenlinna hitookunta. pp: 95-98.

Bird, R., Stewart, W. and Lightfoot, E., 1960. *Transport Phenomena.* New York: John Wiley & Sons Publication. 780p.

Bonnell, D., 1965. The crystallization of salts in natural building stone. Building Research Report: *a Discussion of a Series of Experiment Carried out in the 1930s Explaining the Mechanism of Failure of Building Stone in Crystallization Test.* Garston: Building Research Station. 18p.

Bourbon, F., 1999. *Petra: Art, History and Itineraries in the Nabateans Capital.* Italy: White Star S.R.I. Publication. 59p.

Brattlie, B. and Broch, E., 1995. Stability problems in water tunnels caused by expandable minerals: Swelling pressure measurements and mineralogical analysis. *Engineering Geology.* Vol. **39**. pp: 151-169.

British Standards, 2005. *British - European Standard BS EN14617-1:2005 Agglomerated Stone Test Methods. Part 1: Determination of Apparent Density and Water Absorption.* English version. Brussels: European Committee for Standardization. 8p.

British Standards, 1999. *British - European Standard BS EN 12370, Natural Stone Test Methods - Determination of Resistance to Salt crystallisation.* English version. Brussels: European Committee for Standardization. 4p.

Brown, G. and Brindley, G., 1980. X-ray diffraction techniques. In Brindley, G. and Brown, G., (eds.) 1980. *Crystal Structure of Clay Minerals and their X-Ray Identifications.* London: Mineralogical Society. pp: 305-356.

Browning, I., 1989. *Petra.* Third Edition. Amman: Jordan Distribution Agency in association with Chatto and Windus, London. 256p.

Burgen, D., 2000. Petra: *Match me such a marvel, save in Eastern clime A rose-red city, half as old time* [On-line]. Available from: http://www.raingod.com/angus/Gallery/Photos/MiddleEast/Jordan/Petra. Accessed on 12 March 2002. 10p.

Camuffo, D., 1998. *Microclimate for Cultural Heritage.* Amsterdam and New York: Elsevier Publication. 415p.

Camuffo, D. and Bernarai, A., 1995. The microclimate of Sistine Chapel. *European Cultural Heritage Newsletter on Research.* Vol. **9**. pp: 7-32.

Cerny, R. and Rovnanikova, P., 2002. *Transport Processes in Concrete.* London: Spon Press. 560p.

Charola, A.E., 2004. Stone deterioration in historic buildings and monuments. In Kwiatkowski, D. and Löfendahl, R., (eds.), 2004. *10th International Congress on Deterioration and Conservation of Stone.* Vol. 1. Stockholm June 27 - July 2, 2004. Sweden: ICOMOS Publication. pp: 3-14.

Charola, A.E., 2000. Salt in the deterioration of porous material: An overview. *JAIC (Journal of American Institute for Conservation).*Vol. **39**. pp: 327-343.

Clegg, S, L., 1993. *PITZ93*: a FORTRAN program for determining activity in electrolyte solutions available from S. L. Clegg or P. Brimblecombe at the school of Environmental sciences of the University of East Anglia, Norwich: UK.

Clegg, S, L. and Whitefield, M., 1991. Activity coefficient in natural waters. In Pitzer, K.S., (ed.), 1991. *In Activity Coefficient in Electrolyte Solutions*. Baca Raton: CRC Press. pp: 279-434.

Cooke, R., 1979. Laboratory simulation of salt weathering in arid environment. *Earth Surface Processes*. Vol. **4**. pp: 347-359.

Cooke, R. and Gibbs, G., 1993. *Crumbling Heritage?* Studies of Stone Weathering in Polluted Atmosphere. Swindon: National Power. 68p.

Cooke, R. and Smalley, I., 1969. Salt weathering in deserts. *Nature*. Vol. **220**. pp: 1226-1227.

Cooke, R., Warren, A. and Goudie, A., 1993. *Desert Geomorphology*. London: UCL Press. 526p.

Cooke, R., 1974. Salt weathering and the urban water table in deserts. In Robinson, D. and Williams, B., 1974. Rock Weathering and Landform Evolution. Chichester: John Wiley and sons Publication. pp: 193-205.

Cooling, F., 1930. Contributions to the study of fluorescence. The evaporation of water from brick. *Transactions of British Ceramic Society*. Vol. **29**. pp: 39-34.

Correns, C., 1949. Growth and dissolution of crystal under liner pressure. *Discussion of the Faraday Society*. Vol. **5**. pp: 267-271.

Delgado-Rodrigues, J., 1976. Estimation of the cement of clay content minerals and its significance in stone decay. *In Deterioration of Building Stone, Second International Symposium*. Athens: National Technical University. pp: 105-108.

de Thury, H., 1828. On the method proposed by Mr. Brard for immediate detection of stones unable to resist the action of frost. *Annales de Chimie et de Physique*. Vol. **38**. pp: 160-192.

Doehne, E., 2002. Salt weathering: a selective review. In Siegesmund, S., Weiss, T. and Vollbrecht, A., 2002. *Natural Stone, Weathering, Phenomena, Conservation Strategies and Case Studies*. London: The Geological Society. pp: 51-64.

Doehne, E., 1994. In situ dynamic of sodium sulfate hydration and dehydration in stone pores: observation of high magnification using the environmental scanning electron microscope. In Fassina, V. and Zezza, F., (eds.), 1994. *3rd International Symposium on the Conservation of Monuments in the Mediterranean Base*. pp: 143-150.

Doehne, E., Selwitz, C. and Carson, D., 2002. The damage mechanism of sodium sulfate in porous stone. *Paper in the SALTeXPERT Salt Damage and Desalination - A Combined Short Course/Workshop organised by The Getty Conservation Institute and ACRCCHIP, 2002*, Prague- Czech Republic. 22p.

Dunn, J. and Hudec, P., 1996. Water, clay, and rock soundness. *Ohio Journal of Science*. Vol. **66**. pp: 153-168.

Duoung, D., 1998. *Absorption Analysis*. London: Imperial College Press. 899p.

Duttlinger, W. and Knöfel, D., (1993). Salzkristallisation und Salzchadensmechanism. In Snethlage, R., (ed.), 1993. *Jahresberichte Steinzerfall: Steinkonsservierug 1991*. Berlin: Ernst & Sohn. pp: 197-213.

Evans, I. S., 1970. Salt crystallization and rock weathering: A review. *Revue de Geomorphologie Dynamique*. Vol. **19**. pp: 153-177.

Everett, D., 1961. The thermodynamic of frost damage to porous materials. *Transactions of the Faraday Society*. Vol. **1541**. pp: 1541-1551.

Fischer, H., 1997. Petra's Melting. In American Centre of Oriental Research (ACOR) Report, 1999. *Petra, Jordan: Conservation in an Ancient City*. Amman: ACOR Publications. pp: 1-15.

Fitzner, B., and Heinrichs, K., 2004. *Photo Atlas of Weathering Forms on Stone Monuments*. [On-line]. Available from: http://www.stone.rwthaachen.de/atlas1.htm. Accessed on 20 March 2005.

Fitzner, B. and Heinrichs, K., 2002. Damage diagnosis on stone monuments - weathering forms, damage categories and damage indices. In Přikryl, R. and Viles, H., (eds.), 2002. *Understanding and Managing Stone Decay: Proceeding of the International Conference Stone Weathering and Atmospheric Pollution Network (SWAPNET 2001)*. Prague: Charles University and the Karolinum Press. pp:11-56.

Fitzner, B. and Heinrichs, K., 1998. Evaluation of weathering damages on monuments carved from rocks in Petra/Jordan - research project 1996-1999. *ADAJ (Annual of the Department of Antiquities, Amman - Jordan)*. Vol. **42**. pp: 341-360.

Fitzner, B. and Heinrichs, K., 1991. Weathering forms and rock characteristics of historical monuments carved from bedrocks in Petra/Jordan. In Baer, S., Sabbioni, C. and Sors, A., (eds.) 1991. *Science, Technology and European Cultural Heritage. Proceeding of the European Symp.* Bologna, Italy: Butterworth-Heinemann Ltd. pp: 908-911.

Fitzner, B., Heinrichs, K. and Kownataki, R., 1995.Weathering forms - classification and mapping. In Denkmalpflege und Naturwissenschaft, 1995. *.Natursteinkonservierung.* I. Berlin: Ernst and Sohn. pp: 41-88.

Fitzner, B. and Snethlage, R., 1982. Zum Einfluß der Porenradienverteilung auf das verwitterungasverhalten asugewälter sandsteine. *Bautenschutz und Bausanierung*. Vol. **5**. No. 3. pp: 97-103.

Flatt, R., 2002a. Hydration pressure: A bad case of crystallization pressure. *Paper in the SALTeXPERT Salt Damage and Desalination - A Combined Short Course/Workshop organized by The Getty Conservation Institute and ACRCCHIP, 2002*, Prague- Czech Republic. 16p.

Flatt, R., 2002b. Salt damage in porous materials: How high supersaturation is generated. *Journal of Crystal growth.* Vol. **242.** Issues 3-4, July 2002. pp: 435-454.

Fookes, P. and Poole, A., 1981. Some preliminary consideration on the selection and durability of rocks and concrete materials for breakwaters and coastal protection works. *Quarterly Journal of Engineering Geology*. Vol. **14**. pp: 97-128.

Franchi, R. and Pallecchip, P., 1996. The sandstone of Petra: petrography and problems in conservation. In Panacella, P., (ed.), 1996. *Preservation and Restoration of Cultural Heritage*. Proceedings of the 1995 LCP congress. Montreux, 1995. pp: 679-689.

Franks, L. and Schumann, I., 1998. *Damage Atlas*: *Classification and Analysis of Damage Patterns Found in Brick Masonry.* Expert system for the evaluation of the deterioration of ancient brick masonry structural. Stuttgart: Fraunhofer IRB Verlag. 165p.

Gabriel, G. and Inkpen, R., 1996. The nature of decay of Monk's Park limestone under simulated salt weathering. In Reiderer, J., (ed.), 1996. *Proceedings of the 8th International Congress on the Deterioration and Conservation of Stone*. Berlin, 30 September - 4 October 1996. Berlin: Möller Druck und Verlag gmbh. pp: 573-578.

Gemini Data Loggers, 2005. [On-line]. Available from: http://www.geminidataloggers.com. Accessed on April 2005.

Ginza Marketing, 2005. [On-line]. Available from: http://www.ginza.com.ph/lutron.htm. Accessed on April 2005.

Goudie, A., 1999a. Experimental salt weathering of limestone on relation to rock properties. *Earth Surface Processes and Landforms*. Vol. **24**. pp: 715-724.

Goudie, A., 1999b. A comparison of the relative resistance of limestone to frost and salt weathering. *Permafrost Periglac*. Vol. **10**. pp: 309-316.

Goudie, A., 1993. Salt weathering simulation using a single-immersion technique. *Earth Surface Processes and Landforms*. Vol. **18**. pp: 369-376.

Goudie, A., 1986. Laboratory simulation of the 'wick effect' in salt weathering of rock. *Earth Surface Processes and Landforms*. Vol. **11**. pp: 275-285.

Goudie, A., 1974. Further experimental investigation of rock weathering by salt and other mechanical processes. *Zeitschrift für Geomorphologie*. Vol. **21**. pp: 1-12.

Goudie, A. and Viles, H., 1997. *Salt Weathering Hazards*. Chichester: John Wiley & Sons Ltd. 241p.

Goudie, A. and Viles, H., 1995. The nature and pattern of debris liberation by salt weathering: a laboratory study. *Earth Surface Processes and Landforms*. Vol. **20**. pp: 437-449.

Grassegger, G., 1999. Decay mechanisms of natural building stones on monuments - A review of the latest theories. In Stumpp, S., Krüger, M. and Grosse, C.U., (eds.), 1999. *Werkstoffe und Werkstoffprüfung im Bauwesen*. Festschrift zum 60 Geburtstag von Prof. Dr. Ing.H.W. Reinhardt-Hamburg: Libri BOD, 1999. Stuttgart: IWP publication. pp: 54-81.

Greenspan, L., 1977. Humidity fixed points of binary saturated aqueous solutions. *J. Research of National Bureau of Standards - A. Physics and Chemistry*. Vol. **81A**. pp: 89-96.

Griffin, P., Indictor, N. and Koestler, R. J., 1991. The biodeterioration of stone: A review of deterioration mechanisms, conservation case histories, and treatments. *International Biodeterioration*. Vol. **28**. pp: 187-207.

Grimshaw, R., 1971. *The Chemistry and Physics of Clays and Allied Ceramic Materials*. New York: John Wiley & Sons. 1024p.

Gummerson, R., Hall, C., Hoff, W., Hawkes, R., Holland, G. and Moore, W., 1979. Unsaturated water flow within porous materials observed by NMR imaging. *Nature*. Vol. **218**. pp: 56-57.

Heinrichs, K. and Fitzner, B., 2000. Lithotypes of rock-carved monuments in Petra/ Jordan - classification and petrographical properties. *ADAJ (Annual of the Department of Antiquities, Amman - Jordan)*. Vol. **44**. pp: 283-312.

Heinrichs, K. and Fitzner, B., 1999. Comprehensive characterization and rating of the weathering state of the rock carved monuments in Petra/Jordan - weathering forms, damage categories and damage index. *ADAJ (Annual of the Department of Antiquities, Amman - Jordan)*. Vol. **43**. pp: 321-351.

Hobbs, W. H., 1917. The erosional degradational processes of deserts, with special reference to the origin of desert depressions. *Annals of the Association of American Geographers*. Vol. **7**. pp: 25-60.

Honeyborne, B., 1990. Weathering and decay of masonry. In Ashurst, J. and Dimes, F., (eds.), 1990. *Conservation of Building and Decorative Stone*. Vol.1. London: Butterworth-Heinemann. pp: 153-178.

Honeyborne, B. and Harris, B., 1958. The structure of porous building stone and its relation to weathering behaviour. *Proceedings of the 10th Symposium of the Colston Research Society*. London: Bitterworths Scientific Publications. pp: 343-359.

I.A.E.G. 1979. Semiquantitative classification. Classification of rocks and soils for engineering geological mapping, Part I: Rock and Soil Materials. *Bulletin of. International. Association of Engineering Geology.* Vol. **19**. pp: 364-371.

Jacobs, P., Sevens, E. and Kunnen, M., 1994. Principles of computerised tomography and application in geology related topics. *In Proceedings of the EC Workshop, Research on the Conservation of Brick Masonry Monuments*. Leuven, October 1994. 8p.

Jaser, D. and Barjous, M., 1992. Geotechnical studies and geological mapping of ancient Petra city. *Town Mapping Project, Bulletin* **1**. Amman: Hashemite Kingdom of Jordan - Ministry of Energy and Mineral Resources - Natural Resources Authority - Geological Directorate - Geological Mapping Division. 60p.

Johannessen, C., Feiereisen, J. and Wells, A., 1982. Weathering of ocean cliffs by salts expansion in mid-latitude coastal environment. *Shore and Beach*. Vol. **50**. pp: 26-34.

Jordan Meteorological Department Annual Report, 2003. Amman: Jordan Meteorological Department Press. 54p.

Kaufmann, W., 1971. *Sodium Chloride - The Production and Properties of Salt and Brine*. New York: Hafner Publication. 743p.

Keighin, C., 1980. Characterisation of pores in some Upper Cretaceous nonmarine sandstone, Uinta Basin, Utah. In Johari, O., (ed.), 1980. *Scanning Electron Microscope*. Chicago: A.M.F.O Hare. pp: 559-564.

Kenkel, J. 2002. *Analytical Chemistry for Technicians*. Third Edition. Florida: CRC Press. 584p.

Kennedy, A, 1925. *Petra: Its History and Monuments*. London: Country Life Publication. 88p.

Khouri, R., 1986. *Petra: A Guide to the Capital of Nabateans*. London: Longman Publication. 160p.

Koestler, R. Warscheid, T. and Nieto, F., 1997. Biodeterioration: risk factors and their management. In Baer, N. and Snethlage, R., (eds.), 1997. *Saving Our Architectural Heritage*: *The Conservation of Historic Stone Structural.* Chichester: John Wiley & Sons Ltd. pp: 25-36.

Kühlenthal, M., 2000, The Restoration of Tomb 825, a case study. In Kühlenthal, M. and Fisher, H., (eds.), 2000. *Petra: The Restoration of the Rock Cut Tomb Façades*. Müchen: Bayerisches Landesamt für Denkmalpfleg Publication. pp: 217-230.

Laudelout, H., 1987. Cation exchange equilibria in clays. In Newman, A., 1987. *Chemistry of Clay and Clay Minerals*. London: Longman Scientific & Technical and Mineralogical Society. pp: 225-236.

Lavalle, M., 1853. Recherches sur la formation de cristaur á la temperature ordinaire. *Compt. Rend. Sci.* Vol. **34**. pp: 493-495.

Leary, E., 1983. *The building limestone of the British Isles.* Department of Environment, Building Research Establishment. London: Her Majesty's Stationery Office (HMSO). 91p.

Lewin, S., 1982. The Mechanism of masonry decay through crystallization. In the report of The Committee on conservation of historic Stone Buildings and Monuments, 1982. *Conservation of Historic stone Buildings and Monuments*. Washington, D. C.: National Academy Press. pp: 120-144.

Lloyd, J., 1969. The hydrology of the southern desert of Jordan. NDP/FAO 212. Unpublished Technical Report No.**1**.

Lonely Planet, 2004. Map of Jordan. [On-line] Available from: http://www.lonelyplanet.com/mapshells/middle_east/jordan/jordan.htm. Accessed on 23 April 2004. 1p.

Lott, G., 2004. *Petrographic Description, and Matching of Two Stone Samples from Petra, Jordan.* Unpublished report. Keyworth, Nottingham: British Geological Survey. 13p.

Lubelli, B., 2006. *Sodium Chloride Damage to Porous Building Materials*. Published PhD thesis. Politecnico di Milano: Italy. 164p.

Luquer, L.M., 1895. The relative effects of frost and sulfates of soda efflorescence test on building stones. *Transactions, American Society of Civil Engineers.* Vol. **33**. pp: 235-256.

Mahan, B., 1964. *Elementary Chemical Thermodynamics*. Amsterdam: Benjamin Publication. 155p.

Maqsood, R., 1994. *Petra: a Travellers' Guide*. Glasgow: Garnet Publishing Limited. 224p.

Markoe, G., 2003. *Petra Rediscovered: The Lost City of the Nabataeans*. New York: Thames and Hudson Publication. 288p.

Martini, I., 1978. Tafoni weathering with examples from Tuscany, Italy. *Zeitschrift für Geomorphologie.* Vol. **22**. pp: 44-67.

Massari, G. and Massari, I., 1993. *Damp Building Old and New*. Rome: ICCROM, International Center for the Study of Preservation and Restoration of Cultural Property publication. 305p.

Matsukura, Y. and Matstuoka, N., 1991. Rates of tafoni weathering on uplifted shore platforms in Nomi-Zaki, Boso Peninsula, Japan. *Earth Surface and Landforms*. Vol. **16**. pp: 51-56.

McBride, E. and Picard, M., 2004. Origin of Honeycomb and related weathering forms on Oligocene Macigno sandstone, Tuscan coast near Livorno, Italy. *Earth Surface Processes and Landforms*. Vol. **29**. pp: 713-735.

McEwan, D. and Wilson, J., 1981. Interlayer and interaction complex of clay minerals. In Brindley, G., and Brown, G., 1980. *Crystal Structure of Clay Minerals and their X-Ray Identifications.* London: Mineralogical society. pp: 197-249.

McGreevy, J. and Smith, B., 1984. The possible role of clay minerals in salt weathering. *Catena.* Vol. **11**. pp: 169-175.

McKenzie, J., 1990. *The Architecture of Petra.* Oxford: Oxford University Press. 454p.

McMillan, A., 1997. *Quarries of Scotland.* Historical Scotland: 12 Technical advice Note. Edinburgh: Historical Scotland. 84p.

Miglio, B., Richardson, T., Yates, T. and West, D., 2000. Assessment of the durability of porous limestone: specification and interpretation of test data in UK practice. In Hoigart, K., 2000. Dimension Stone Cladding. ASTM international. pp: 57-71.

Mortensen, H., 1933. Die "Salzprengung" und ihre Bedeutung für die Regionalklimatische Gliederung der Wüsten. Dr.A. *Petermanns mitteilungen*. Gotha: Justus Prethes, Vol. **79**. pp. 35-130.

Mohmoud, S., 2000. The ECOS program. Price, C.A., (ed.), 2000a. *An Expert Chemical Model for Determining the Environmental Conditions Needed to Prevent Salt Damage in Porous Materials.* European Commission Report 11, Protection and Conservation of European Cultural Heritage. London: Archetype Publications. pp: 125-128.

Mossotti, V. and Castanier, L., 1990. The measurement of water transport in Salem limestone by X-ray computer aided tomography. In Marinos, P. and Koukis, G., (eds.), 1990. *The Engineering Geology of Ancient Works, Monuments and Historical Sites; Preservation and Protection.* Rotterdam: Balkema publications. pp: 2079-2082.

Mullin, J., 1961. *Crystallization.* London: Butterworth Publication. 286p.

Nabataea net 2005. Petra Water Works. [On-line]. Available from: http://nabataea.net/waterw.html. Accessed on 14 March 2005.

Nelson, S., 2004. *Weathering and Clay Minerals.* [On-line]. Available from: http://www.tulane.edu/~sanelson/eens211/weathering&claymineralS.htm. Accessed on 19 February 2004.

Newman, A. and Brown, G., 1987. The chemical constitution of clay. In Newman, A., (ed.), 1987. *Chemistry of Clay and Clay Minerals.* London: Longman Scientific & Technical and Mineralogical Society. pp: 1-129.

Newitt, D., Nagara, P. and Papadopoulos, A., 1960. The deposition of solute material in porous beds during convection and conduction drying. *Transactions of the Institute of Chemical Engineers.* Vol. **38**. pp: 273-288.

Nicholson, D., 2001. Pore properties as indicators of breakdown mechanisms in experimentally weathered limestone. *Earth Surface Processes and Landforms.* Vol. **26**. pp: 819-838.

Ordóñez, S., Frot, R. and García del Cura, A., 1997. Pore size distribution and the durability of a porous limestone. *Quarterly Journal of Engineering Geology.* Vol. **30**. pp: 221.230.

Paradise, T., 2005. Petra revisited: An examination of sandstone weathering research in Petra, Jordan. In Turkington, A., 2005. *Stone Decay in the Architectural Environment.* Boulder: The Geological Society of America. Special Paper 390. pp: 39-49.

Paradise, T., 1999. Analysis of sandstone weathering of the Roman Theatre in Petra, Jordan. *ADAJ* (*Annual of the Department of Antiquities, Amman - Jordan*). Vol. **43**. pp: 353-368.

Pauling, L., 1970. *General Chemistry.* Third edition. San Francisco: W.H. Freeman. 959p.

Pauly, J., 1976. Maladie alveolaire: conditions de formation et de l'evolution. In Rossi-Manresi, R., (ed.), 1976. *The Conservation of Stone.* Bologna: Centre per Conservazione Delle sculture all Aperto. pp: 55-80.

Pavía S., and Bolton, J., 2000. *Stone, Brick and Mortar: Historical Use, Decay and Conservation of Building Materials in Ireland.* Wicklow: Wordwell Ltd. 296p.

Pel, L., Huinink, H. and Kopinga, K., 2003. Salt transport and crystallization in porous building materials. *Magnetic Resonance Imaging*. Vol. **21**. pp: 317-320.

Pel, L., Huinink, H., Kopinga, K., Rijniers, L. and Kaasschieter, E., 2001. Ion transport in porous media studied by NMR. *Magnetic Resonance Imaging*. Vol. **19**. pp: 549-550.

Pel, L., Kopinga, K. and Kaasschieter, E., 2000. Saline absorption in calcium-silicate brick observed by NMR scanning. *Journal of Applied Physics*. Vol. **33**. pp: 1380-1385.

Pender, R., 2000. *The Behaviour of Moisture in the Porous Support Materials of Wall Paintings*: An Investigation of Some Environmental Parameters. Unpublished PhD Thesis, London: Courtauld Institute of Art, University of London. 328p.

Perry, D. and Phillips, S., 1995. *Handbook of Inorganic Compounds*. Florida: CRC Press. 464p.

Pflüger, F., 1995. Archaeo-Geology in Petra Jordan. *ADAJ (Annual of the Department of Antiquities, Amman - Jordan)*. Vol. **29**. pp: 281-295.

Philip, R. and de Vries, A., 1957. Moisture movement in porous materials under temperature gradient. *Transactions, American Geophysical Union*. Vol. **38** (2). pp: 222-232.

Pitzer, K, S., 1973. Thermodynamics of electrolytes, I. Theoretical basis and equations. *J.Phys.Chem*. Vol.**77**. pp: 268-277.

Powers, M. C., 1953. A new roundness scale for sedimentary particles. *Journal of Sedimentary Petrology*. Vol. **23**. pp: 117-119.

Price, C. A., 2002. An expert chemical model for determining the environmental conditions needed to prevent salt damage in historic porous materials. In Brandt-Grau, A., Péres-Vitoria, S., Chapuis, M. and Leissner, J., (eds.), (2002). *Research for Protection, Conservation and Enhancement of Cultural Heritage: Opportunities for European Enterprises*. Luxembourg: European Commission. pp: 159-168.

Price, C.A., (ed.) 2000a. *An Expert Chemical Model for Determining the Environmental Conditions Needed to Prevent Salt Damage in Porous Materials*. European Commission Report 11, Protection and Conservation of European Cultural Heritage. London: Archetype Publications. 136p.

Price, C. A., 2000b. Salt damage in porous materials. In Price, C. A., (ed.), 2000. *An Expert Chemical Model for Determining the Environmental Conditions Needed to Prevent Salt Damage in Porous Materials*. European Commission Report 11, Protection and Conservation of European Cultural Heritage. London: Archetype Publications. pp:3-12.

Price, C. A., 2000c. Using ECOS. In Price, C. A., (ed.), 2000. *An Expert Chemical Model for Determining the Environmental Conditions Needed to Prevent Salt Damage in Porous Materials.* European Commission Report 11, Protection and Conservation of European Cultural Heritage. London: Archetype Publications. pp: 129-136.

Price, C.A., 1996. *Stone Conservation: An Overview of Current Research.* Los Angeles: The Getty Conservation Institute. 73p.

Price, C.A. and Brimblecombe, P., 1994. Preventing salt damage in porous materials. In Roy, A. and Smith, P., (eds.), 1994. *Preventive Conservation, Practice, Theory and Research.* London: International Institute for Conservation of Historic and Artistic Works. pp: 90-93.

Price, C.A., 1991. Causes and mechanisms of deterioration in porous materials. In Proceedings of the EEC China Workshop on the Preservation of Cultural Heritage. Xian, Shaanxi, 1991. Naples: Teti. pp: 177-182.

Price, C.A., 1978. The use of sodium sulphate crystallisation test for the determining the weathering resistance of untreated stone. *Alteration et Protection des Monuments en Pierre: Colloque International.* Paris du 5 au 9 juin 1978. Unesco-Relim, Paris. pp: 1-23.

Prokos, P., 2005. *Salt Weathering in the Coastal Environment: The Deterioration of Wall Painting at Delos, Greece.* Unpublished PhD Thesis. London: Institute of Archaeology, University College London. 258p (text only).

Pye, K. and Mottershead, D., 1995. Honeycomb weathering of Carboniferous sandstone in sea wall at Weston-super-Mare, UK. *Quarterly Journal of Engineering Geology.* Vol. **28**. pp: 333-347.

Reitz, J. 2005. ODLIS: *Online Dictionary for Library and Information Science.* Portsmouth: Library limited. [On-line].
Available from: http://lu.com.odlis/odlis_h.cfm. Accessed on 22 June 2005.

Putnis, A., Prieto, M. and Fernandez-Diaz, L., 1995. Fluid supersaturation and crystallization in porous media. *Geological Magazine.* Vol. **132** (1). pp: 1-13.

Reynolds, R., 1980. Interstratified clay minerals. In Brindley, G. and Brown, G., (eds.), 1980. *Crystal Structure of Clay Minerals and their X-Ray Identifications.* London: Mineralogical Society. pp: 1-115.

Rijiniers, L., 2004. *Salt Crystallization in Porous Materials: An NMR Study.* PhD Thesis. Eindhoven: Technische Uinversiteit Eindhoven, 2004. 112p.

RILEM, 1980. Recommendation provisoires /Tentative Recommendations. (RILEM) Commission 25-PEM. Protection et érosion des monuments: Essais recomandès pour mesurer láltèration des pierres et évaluer leèfficacitè des méthodes de traitement. *Matèriaux et Constructions.* Vol. **13** (75). pp: 175-253.

Robertson, E., 1982. Physical properties of building stone. In the report of the Committee on Conservation of Historic Stone Buildings and Monuments, 1982. *Conservation of Historic Stone Buildings and Monuments.* Washington, D. C.: National Academy Press. pp: 62-86.

Rodriguez-Navarro, C., 1994. *Causas y Mecanismos de Alteración de Los Materials Calcareous de Las Catedrales de Granada y Jaèn.* PhD Thesis. Spain: University of Granada.

Rodriguez-Navarro, C., Doehne, E. and Sebastian, E., 2000. How does sodium sulfate crystallize? Impactions for the decay and testing of building materials. *Cement and Concrete Research.* Vol. **30** (10). pp: 1527-1534.

Rodriguez-Navarro, C. and Doehne, E., 1999a. Origins of honeycomb weathering: The role of salts and wind. *Geological Society of America Bulletin.* Vol. **111**. pp: 1250-1255.

Rodriguez-Navarro, C. and Doehne, E., 1999b. Salt weathering: influence of evaporation rate, supersaturation and crystallization pressure. *Earth Surface Processes and Landforms.* Vol. **24**. pp: 191-209.

Rodriguez-Navarro, C., Hansen, E., Sebastian, E. and Ginell, W., 1997. The role of clays in the decay of ancient Egyptian limestone sculptures. *Journal of American Institute for Conservation.* Vol. **36**, Number 2, article 5. pp: 151-163.

Ross, K. and Butlin, R., 1989. Durability test for building stone. *Building Research Establishment Report.* Watford: Building Research Establishment. 8p.

Rossi-Manaresi, R. and Tucci, A., 1991. Pore structure and the disruptive or cementing effect of salt crystallization in various types of stone. *Studies in Conservation.* Vol. **36**. pp: 53-58.

Sabbioni, C., 2003. Mechanisms of air pollution damage to stone. In Brimblecombe, P., (ed.), 2003. *The Effects of Air Pollution on the Built Environment.* Vol. 2. London: Imperial College Press. pp: 63-106.

Salt research project, Getty Conservation Institute, 2005. Mechanisms of salt decay and methods of migration. [On-line]. Available from: http://www.getty.edu/conservation/science/salt/index.html. Accessed on 10 July 2005.

Sawdy, A., 2001. *The Kinetics of Salt Weathering of Porous Materials: Stone Monuments and Wall Paintings.* Unpublished PhD Thesis, University College London. 325p.

Sawdy, A. and Price, C.A., 2002. Environmental control: recent research and future prospects. *Paper in the SALTeXPERT Salt Damage and Desalination - A Combined Short Course/Workshop organized by The Getty Conservation Institute and ACRCCHIP, 2002,* Prague-Czech Republic. 17p.

Scherer, G., 2004. Stresses from crystallization of salt. *Cement and Concrete Research*. Vol. **34**.(9). pp: 1613-1624.

Scherer, G., 2000. Stress from crystallization of salt in pores. In Fassina, V., (ed.), 2000. *9th International Congress on Deterioration and Conservation of Stone*. Venice June 19-24, 2000. Amsterdam: Elsevier. pp: 187-194.

Scherer, G., 1999. Crystallization in pores. *Cement and Concrete Research*, Vol. **29**. pp: 1347-1358.

Scherer, G. and Gonzalez, I., 2005. Characterization of swelling in clay-bearing stone. In Turkington, A., 2005. *Stone Decay in the Architectural Environment*. Boulder: The Geological Society of America. Special Paper 390. pp: 51-61.

Shaer, M. and Aslan, Z., 2000, Nabataean building techniques with special reference to the architecture of tomb 825. In Kühlenthal, M. and Fisher, H., (eds.), 2000. *Petra: The Restoration of the Rockcut Tomb Façades*. Müchen: Bayerisches Landesamt für Denkmalpfleg publication. pp: 89-109.

Skaling, J. and Hearn, N., 2000. Surface area measurements. In Ramachandran, V. and Beaudoin, J., 2000. *Handbook of Analytical Techniques in Concrete Science and Technology*. New York: William Andrew publishing. pp: 505-524.

Slichter, C., 1996. *Principles of Magnetic Resonance*. Third and updated edition. Berlin: Springer. 655p.

Smith, B. and McAlister, J., 1986. Observation on the occurrence and origins of salt weathering phenomena near lake Merged, southern Kenya. *Zeitschrift für Geomorphologie*. Vol. **30**. pp: 445-460.

Smith, B. McGreevy, J., 2004. *Urban Stone Decay and Acid Deposition: An Introduction to the Problem and Causes*. School of Geography, Queen's University Belfast, Belfast + Conservation Laboratory, The Ulster Museum, Belfast. [On-line].
Available from: http://www.qub.ac.uk/geog/documents/research/weathering/usd.html. Accessed on 3 March 2004. 12p.

Smith, S. and McGreevy, J., 1983. A simulation study of salt weathering in hot deserts. *Geografiska Annaler*. Vol. **65** A. pp: 127-133.

Snethlage, R. and Wendler, E., 1997. Moisture cycles and sandstone degradation. In Baer, N. and Snethlage, R., (eds.), 1997. *Saving Our Architectural Heritage: The Conservation of Historic Stone Structural*. Chichester: John Wiley & Sons Ltd. pp: 7-24.

Steiger, M., 2005. Crystal growth in porous materials-I: The crystallization pressure of large crystals. *Journal of Crystal Growth*. Vol. **282**, Issue 3-4, September 2005. pp: 455-469.

Steiger, M., 2003. Salts and crusts. In Brimblecombe, P., (ed.), 2003. *The Effects of Air Pollution on the Built Environment.* Vol.2. London: Imperial College Press. pp: 133-181.

Steiger, M., 2002. Properties of salt mixtures: Theory and modelling. *Paper in the SALTeXPERT Salt Damage and Desalination - A Combined Short Course/Workshop organized by The Getty Conservation Institute and ACRCCHIP, 2002*, Prague-Czech Republic. 14p.

Steiger, M., 1994. Crystallization properties of mixed salt system containing chloride and nitrate. In *preprints of the EC workshop: Research on the conservation of brick-masonry monuments*. Levuven, Belgium. 9p.

Steiger, M. and Dannecker, W., 1995. Hygroskopishe eigenschaften und kristallisationsverhalten von salzgemischen. In Snethlage, R., (ed.), 1995. Jahresberichte Steinzerfall: Servierung 1993. Berlin: Ernst & Sohn Publication. pp: 115-128.

Steiger, M., Beyer, R., Dorn, J. and Zeunert, A., 2002. Data compilation and experimental determinations. In Price, C. A., (ed.), 2000. *An Expert Chemical Model for Determining the Environmental Conditions Needed to Prevent Salt Damage in Porous Materials.* European Commission Report 11, Protection and Conservation of European Cultural Heritage. London: Archetype Publications. pp: 19-43.

Steiger, M. and Zeunert, A., 1996. Crystallization properties of salt mixtures: comparison of experimental results and model calculation. In Riederer, J., (ed.), 1996. Proceedings of the *8th International Congress on the Deterioration and Conservation of Stone*. Berlin, 30 September - 4 October 1996. Berlin: Möller druck und verlag gmbh. pp: 535-544.

Storemyr, P. and Franz, A., (eds.), 2002. The Regalia Room Mural Paintings Conservation Project, Trondheim, Norway: *Conservation Measures and Monitoring of Salt weathering 2001-2002.* [On-line]. Available from: http://www.ecd.ethz.ch/regalia. Accessed on 23 December 2005. 43p

Taber, S., 1916. The growth of crystal under external pressure. *American Journal of Science,* Vol. **41.** pp: 532-556.

Taylor, J., 2000. *Petra and the Lost Kingdom of the Nabataeans*. London: I.B. Tauris Publishers. 224p.

The Building Research Establishment (BRE), 2000. *British Stone Stone List.* [On-line]. Available from: http://projects.bre.co.uk/ConDiv/stonelist/lochabriggs.html. Accessed on 9 October 2005.

Torraca, G., 1988. *Porous Building Materials*. Third Edition. Rome: ICROM publication. 149p.

Tricio, V. and Viloria, R., 2002. Microclimatic study of a historical building. In Galaán, E. and Zezza, F., (eds.), 2002. *Protection and Conservation of the Cultural Heritage of the Mediterranean Cites*. Lisse: Sweets and Zeitlinger. pp: 67-70.

Turkington, A. and Phillips, J., 2004. Cavernous weathering, dynamical instability and self-organization. *Earth Surface Processes and Landforms*. Vol. **29**. pp: 665-675.

Turkington, A. and Smith, J., 2000. Observation of three-dimensional salt distribution in building sandstone. *Earth Surface Processes and Landforms*. Vol. **25**. pp: 1317-1332.

Ulama, M., 1997. *All Petra: A Wonderland of the Past*. Amman - Jordan: Al-Ulama Publishing Centre. 184p.

UNESCO Report, 1992. *Petra National Park Management Plan*, Unpublished report. Coordinators: Lane, B., and Bousquet, B. pp: 1-176.

VanOlphen, H., 1977. *An Introduction to Clay Colloid Chemistry*. New York: John Wiley & Sons Publication. 301p.

Velde, B, 1992. *Introduction to Clay Minerals: Chemistry, Origins, Uses and Environmental Significance*. London: Chapman & Hall Publications. 198p.

Velde, B., 1995. Composition and mineralogy of clay minerals. In Velde, B., (ed.), 1995. *Origin and Mineralogy of Clays*. New York: Springer-Verlag. pp: 8-42.

Viles, H., 2005a. Can stone decay be chaotic? In Turkington, A., 2005. *Stone Decay in the Architectural Environment*. Boulder: The Geological Society of America. Special Paper 390. pp: 11-16.

Viles, H., 2005b. Self-organized or disorganized? Towards a general explanation of cavernous weathering. *Earth Surface Processes and Landforms*. Vol. **30**. pp: 1471-1473.

Viles, H., *et al.* 1997. Group report. What is the state of our knowledge of the mechanisms of deterioration and how good are estimates of rates of deterioration? In Baer, N. and Snethlage, R., (eds.), 1997. *Saving Our Architectural Heritage-The Conservation of Historic Stone Structure*. Report of the Dahlem Workshop. Berlin, 3-8 March 1996: John Wiley & Sons Ltd. pp: 95-112.

Visualization and analysis system project glossary. 1996. [On-line]. Available from: http://sedac.ciesin.org/mva/shared.htmls/glossary.html. Accessed on 20 March 2005.

Vivekanand, P., 1995. *Petra*. Amman: Arabesque International publication. 126p.

Von Konow, T., 2002. Testing methods. In Von Konow, T., (ed.) 2002. *The Study of Salt Deterioration Mechanisms. Decay of Brick Walls Influenced by Interior Climate Changes.* Suomenlinna, Finland: Suomenlinna hitookunta. pp: 43-53.

Wadell, H., 1932. Volume, shape and roundness of rock particles. *Journal of Geology.* Vol. **40**. pp: 443-451.

Warke, P. and Smith, B., 2000. Salt distribution in clay-rich weathered sandstone. *Earth Surface Processes and Landforms.* Vol. **25**. pp: 1333-1342.

Washburn, W., 1921. Notes on method of determining the distribution of pore sizes in a porous material. *Proceedings, National Academy of Science.* Vol. **7**. pp: 115-116.

Wendler, E., Klemm, D. and Snethlage, R., 1991. Contour scale on building façades: Dependence on stone type and conditions. In Vandiver, B., *et al.* (eds.), 1991. *Materials Issues in Art and Archaeology*, II, Materials Research Society symposium proceeding. Pittsburgh: Materials Research Society. pp: 265-271.

Wellman, H. and Wilson, A., 1965. Salt weathering: A neglected geological erosive agent in coastal and arid environments. *Nature.* Vol. **205**. pp: 1097-1098.

Wendler, E. and Snethlage, R., 1989. Der wassereindringprüfer nach karsten anwendung und Interpretation der messwerte. *Bautenschutz und Bausanierung.* Vol. **12**. pp: 110-115.

Weast, C., 1974. *Handbook of Chemistry and Physics.* 54 Ed. Ohio: CRC press.

Weyl, P., 1959. Pressure solution and the force of crystallization: a phenomenological theory. *Journal of Geophysical Research,* Vol. **64.** No. 11. pp: 2001-2025.

White, W., 1988. *Geomorphology and Hydrology of Karst Terrains.* Oxford: Oxford University Press. 447p.

Winkler, E., 1994. *Stone in Architecture: Properties, Durability.* Third Edition. Berlin: Springer-Verlag Publications. 313p.

Winkler, E. and Singer, P., 1972. Crystallization pressure of salts in stone and concrete. *Geological Society of America Bulletin.* Vol. **83**. pp: 3509-3514.

Winkler, E. and Wilhelm, E., 1970. Salt burst by hydration pressure in architectural stone in urban atmosphere. *Geological Society of America Bulletin.* Vol. **81**. pp: 567-572.

Woodman, N., 2004. personal commun. London: Earth Science Department at University College London.

Salt Damage at Petra, Jordan: A Study of the Effects of Wind on Salt Distribution and Crystallisation

F. Bala'awi

PhD Thesis

A thesis submitted for the degree of Doctor of Philosophy in Archaeology (Conservation)

APPENDICES

Institute of Archaeology
University College London

May 2006

Volume II

Appendices

Appendix A: Temperature, relative humidity and wind speed spot readings. First fieldwork visit: August 2003.

Time	T (°C)	RH %	Wind Speed (m/s)	Time	T (°C)	RH %	Wind Speed (m/s)	Time	T (°C)	RH %	Wind Speed (m/s)	Time	T (°C)	RH %	Wind Speed (m/s)	Time	T (°C)	RH %	Wind Speed (m/s)	Time	T (°C)	RH %	Wind Speed (m/s)
07.40	23.8	31.0	0.1	09.50	25.8	24.0		12.00	37.2	18.0	0.4	14.10	42.5	15.0		16.20	36.1	21.0		18.30	25.0	28.0	2.1
07.45	23.9	31.0		09.55	26.0	23.0		12.05	37.3	17.0		14.15	42.1	15.0	1.0	16.25	35.8	21.0		18.35	25.1	28.0	
07.50	23.8	31.0		10.00	26.1	22.0	0.7	12.10	37.9	17.0		14.20	39.9	17.0		16.30	35.1	21.0	1.7	18.40	25.0	28.0	
07.55	23.9	31.0		10.05	26.2	22.0		12.15	38.1	17.0	0.5	14.25	38.7	17.0		16.35	34.7	22.0		18.45	24.9	29.0	1.8
08.00	24.0	30.0	0.1	10.10	26.4	22.0		12.20	38.3	17.0		14.30	39.8	17.0	1.1	16.40	34.8	22.0		18.50	24.7	29.0	
08.05	24.0	30.0		10.15	26.4	21.0	0.6	12.25	39.0	17.0		14.35	39.7	17.0		16.45	34.0	22.0	1.5	18.55	24.7	29.0	
08.10	24.2	30.0		10.20	26.2	21.0		12.30	39.5	17.0	0.4	14.40	40.0	17.0		16.50	33.4	23.0		19.00	24.7	29.0	2.0
08.15	24.2	30.0	0.1	10.25	26.3	21.0		12.35	40.1	16.0		14.45	39.8	17.0	1.2	16.55	33.3	23.0		19.05	24.5	29.0	
08.20	24.3	30.0		10.30	26.7	21.0	0.3	12.40	39.7	16.0		14.50	39.7	17.0		17.00	33.2	23.0	2.2	19.10	24.5	29.0	
08.25	24.6	29.0		10.35	27.0	21.0		12.45	39.7	16.0	0.7	14.55	38.7	18.0		17.05	31.9	24.0		19.15	24.1	29.0	1.6
08.30	24.7	29.0	0.1	10.40	27.1	21.0		12.50	39.8	16.0		15.00	39.0	17.0	1.3	17.10	31.8	24.0		19.20	24.0	29.0	
08.35	25.0	29.0		10.45	28.1	20.0	0.6	12.55	40.0	16.0		15.05	38.0	18.0		17.15	31.4	24.0	2.2	19.25	23.9	30.0	
08.40	25.0	29.0		10.50	28.0	20.0		13.00	40.0	16.0	0.7	15.10	38.1	18.0		17.20	31.2	24.0		19.30	23.7	30.0	2.3
08.45	25.0	28.0	0.1	10.55	28.1	20.0		13.05	40.5	16.0		15.15	37.9	18.0	1.3	17.25	31.1	24.0		19.35	24.0	29.0	
08.50	25.2	28.0		11.00	30.3	19.0	0.7	13.10	42.0	15.0		15.20	37.5	19.0		17.30	30.7	25.0	2.4	19.40	24.0	29.0	
08.55	25.1	28.0		11.05	31.2	19.0		13.15	41.7	15.0	0.8	15.25	37.1	19.0		17.35	30.1	25.0		19.45	23.8	29.0	2.4
09.00	24.8	29.0	0.2	11.10	31.8	19.0		13.20	41.2	15.0		15.30	37.2	19.0	1.5	17.40	30.0	25.0		19.50	23.7	30.0	
09.05	24.6	29.0		11.15	32.0	19.0	0.7	13.25	41.0	15.0		15.35	37.5	19.0		17.45	30.0	25.0	1.2	19.55	23.4	30.0	
09.10	24.5	29.0		11.20	32.5	19.0		13.30	41.0	15.0	0.8	15.40	36.5	20.0		17.50	28.9	27.0		20.00	23.3	31.0	
09.15	24.1	30.0	0.2	11.25	33.5	18.0		13.35	41.8	15.0		15.45	36.4	20.0	1.5	17.55	28.9	27.0		20.05	23.3	31.0	
09.20	24.5	30.0		11.30	34.6	18.0	0.8	13.40	42.0	15.0		15.50	36.4	20.0		18.00	28.4	27.0	2.3	20.10	23.2	31.0	
09.25	24.4	30.0		11.35	34.5	18.0		13.45	42.1	15.0	0.9	15.55	36.2	20.0		18.05	27.6	27.0		20.15	23.0	32.0	
09.30	24.4	29.0	0.5	11.40	35.4	18.0		13.50	42.3	15.0		16.00	35.6	20.0	1.8	18.10	26.9	27.0		20.20	22.9	32.0	
09.35	25.0	28.0		11.45	35.9	18.0	0.8	13.55	42.4	15.0		16.05	35.7	21.0		18.15	26.7	27.0	1.5	20.25	23.0	32.0	
09.40	25.1	27.0		11.50	36.0	18.0		14:00	42.8	15.0	0.9	16.10	36.0	20.0		18.20	26.1	27.0		20.30	22.9	32.0	
09.45	25.3	26.0	0.3	11.55	36.2	18.0		14.05	40.8	15.0		16.15	36.5	20.0	1.9	18.25	26.0	27.0		20.35	22.5	33.0	

Table (A1): Temperature, relative humidity and wind speed spot readings. Location: Bab al Siq Triclinium Tomb.
First fieldwork visit: 1-2 August 2003, between 07.40-20.35.

Appendix A: Temperature, relative humidity and wind speed spot readings. First fieldwork visit: August 2003.

Time	T (°C)	RH%	Time	T (°C)	RH%	Time	T (°C)	RH%	Time	T (°C)	RH%	Time	T (°C)	RH%	RH%
20.40	22.5	33.0	22.50	19.0	35.0	01.00	17.6	36.0	03.10	16.5	37.0	05.20	16.3	36.0	36.0
20.45	22.4	33.0	22.55	19.0	35.0	01.05	17.5	36.0	03.15	16.4	37.0	05.25	16.8	36.0	36.0
20.50	22.4	33.0	23.00	18.8	35.0	01.10	17.5	36.0	03.20	16.4	37.0	05.30	16.9	36.0	36.0
20.55	22.1	33.0	23.05	18.7	36.0	01.15	17.5	36.0	03.25	16.4	37.0	05.35	17.2	36.0	36.0
21.00	22.1	33.0	23.10	18.7	36.0	01.20	17.6	36.0	03.30	16.4	37.0	05.40	17.3	36.0	36.0
21.05	22.0	33.0	23.15	18.7	36.0	01.25	17.6	36.0	03.35	16.4	37.0	05.45	18.0	35.0	36.0
21.10	21.7	33.0	23.20	18.7	35.0	01.30	17.5	36.0	03.40	16.4	37.0	05.50	18.4	35.0	36.0
21.15	21.9	33.0	23.25	18.2	36.0	01.35	17.4	36.0	03.45	16.1	37.0	05.55	18.6	35.0	36.0
21.20	21.3	34.0	23.30	18.2	34.0	01.40	17.4	36.0	03.50	16.0	38.0	06.00	18.7	34.0	36.0
21.25	21.2	34.0	23.35	18.1	35.0	01.45	17.3	36.0	03.55	16.0	38.0	06.05	19.7	34.0	36.0
21.30	21.0	34.0	23.40	18.2	35.0	01.50	17.3	36.0	04.00	15.8	37.0	06.10	20.1	33.0	36.0
21.35	21.1	34.0	23.45	18.2	35.0	01.55	17.3	36.0	04.05	15.8	38.0	06.15	20.9	32.0	36.0
21.40	20.8	34.0	23.50	18.1	35.0	02.00	17.3	36.0	04.10	15.9	38.0	06.20	21.4	32.0	36.0
21.45	20.7	34.0	23.55	18.1	36.0	02.05	17.0	36.0	04.15	15.9	37.0	06.25	21.9	31.0	36.0
21.50	20.7	34.0	00.00	18.3	35.0	02.10	16.9	36.0	04.20	15.9	38.0	06.30	22.0	30.0	36.0
21.55	20.6	34.0	00.05	18.3	35.0	02.15	16.9	36.0	04.25	15.8	38.0	06.35	22.0	30.0	36.0
22.00	20.0	33.0	00.10	18.2	35.0	02.20	16.9	36.0	04.30	15.7	38.0	06.40	22.6	29.0	36.0
22.05	19.8	34.0	00.15	18.2	35.0	02.25	17.0	36.0	04.35	15.7	38.0	06.45	22.9	29.0	36.0
22.10	19.9	33.0	00.20	18.2	35.0	02.30	17.0	36.0	04.40	15.4	38.0	06.50	23.3	28.0	36.0
22.15	19.8	33.0	00.25	18.1	34.0	02.35	16.9	37.0	04.45	15.4	38.0	06.55	23.4	28.0	37.0
22.20	19.4	34.0	00.30	18.1	35.0	02.40	16.9	37.0	04.50	15.3	38.0	07.00	23.5	27.0	37.0
22.25	19.5	33.0	00.35	17.9	36.0	02.45	16.8	37.0	04.55	15.4	37.0				
22.30	19.4	33.0	00.40	17.8	36.0	02.50	16.8	37.0	05.00	15.6	37.0				
22.35	19.3	34.0	00.45	17.8	35.0	02.55	16.8	37.0	05.05	16.0	37.0				
22.40	19.3	35.0	00.50	17.9	35.0	03.00	16.9	36.0	05.10	16.2	36.0				
22.45	19.1	35.0	00.55	17.6	35.0	03.05	16.8	37.0	05.15	16.3	36.0				

Table (A2): Temperature, relative humidity and wind speed spot readings. Location: Bab al Siq Triclinium Tomb. First fieldwork visit: 1-2 August 2003, between 20.40-07.00.

Appendix A: Temperature, relative humidity and wind speed spot readings. First fieldwork visit: August 2003.

Time	Wind Speed m/s	Time	Wind Speed m/s	Time	Wind Speed m/s	Time	Wind Speed m/s	Time	Wind Speed m/s
20.00	1.5	22.10		00.20		02.30	3.2	04.40	
20.05		22.15	2.0	00.25		02.35		04.45	2.7
20.10		22.20		00.30	2.4	02.40		04.50	
20.15	1.5	22.25		00.35		02.45	3.0	04.55	
20.20		22.30	2.1	00.40		02.50		05.00	2.0
20.25		22.35		00.45	2.8	02.55		05.05	
20.30	2.0	22.40		00.50		03.00	3.3	05.10	
20.35		22.45	2.6	00.55		03.05		05.15	1.4
20.40		22.50		01.00	3.0	03.10		05.20	
20.45	2.1	22.55		01.05		03.15	3.5	05.25	
20.50		23.00	2.7	01.10		03.20		05.30	1.3
20.55		23.05		01.15	2.4	03.25		05.35	
21.00	1.7	23.10		01.20		03.30	3.5	05.40	
21.05		23.15	2.7	01.25		03.35		05.45	0.7
21.10		23.20		01.30	2.4	03.40		05.50	
21.15	2.2	23.25		01.35		03.45	3.6	05.55	
21.20		23.30	2.3	01.40		03.50		06.00	0.4
21.25		23.35		01.45	2.6	03.55		06.05	
21.30	2.3	23.40		01.50		04.00	3.7	06.10	
21.35		23.45	2.0	01.55		04.05		06.15	0.1
21.40		23.50		02.00	2.8	04.10		06.20	
21.45	2.5	23.55		02.05		04.15	3.9	06.25	
21.50		00.00	2.0	02.10		04.20		06.30	0.1
21.55		00.05		02.15	2.9	04.25		06.35	
22.00	2.4	00.10		02.20		04.30	2.9	06.40	
22.05		00.15	2.2	02.25		04.35		06.45	0.1

Table (A3): Wind speed spot readings. Location: Nabateans Hotel (10 minutes walking distance from the archaeological site). First fieldwork visit: 1-2 August 2003, between 20.00-07.00.

Appendix A: Temperature, relative humidity and wind speed spot readings. First fieldwork visit: August 2003

Time	T (°C)	RH%	Wind Speed(m/s)	Time	T (°C)	RH%	Wind Speed(m/s)	Time	T (°C)	RH%	Wind Speed(m/s)	Time	T (°C)	RH%	Wind Speed(m/s)	Time	T (°C)	RH%	Wind Speed(m/s)	Time	T (°C)	RH%	Wind Speed(m/s)
07.40	24.7	29.0	0.1	09.50	26.3	22.0		12.00	43.6	18.0	0.6	14.10	44.1	16.0		16.20	40.10	18.0		18.30	33.80	24.00	1.3
07.45	24.7	27.0		09.55	26.5	21.0		12.05	44.1	15.0		14.15	44.20	18.0		16.25	41.60	19.0		18.35	33.20	23.00	
07.50	24.9	28.0		10.00	26.5	22.0	1	12.10	42.2	17.0		14.20	43.60	16.0	1.5	16.30	43.2	19.0	0.9	18.40	33.60	24.00	
07.55	24.9	30.0		10.05	26.7	22.0		12.15	42.8	20.0	0.8	14.25	44.00	15.0		16.35	41.8	21.0		18.45	33.00	23.00	5.4
08.00	24.8	29.0	0.2	10.10	27.1	23.0		12.20	41.9	21.0		14.30	43.80	17.0	1.1	16.40	40.80	20.0		18.50	33.00	24.00	
08.05	24.8	30.0		10.15	27	23.0	0.6	12.25	41.2	20.0		14.35	42.60	20.0		16.45	40.60	19.0	4.4	18.55	33.00	22.00	
08.10	24.8	30.0		10.20	27.2	23.0		12.30	42.1	19.0	0.6	14.40	41.60	22.0		16.50	41.90	21.0		19.00	32.80	21.00	5.0
08.15	25	29.0	0.1	10.25	27.4	22.0		12.35	42.2	21.0		14.45	41.80	22.0	2.2	16.55	39.60	22.0		19.05	33.00	23.00	
08.20	25.2	29.0		10.30	27.8	21.0	0.4	12.40	42.2	19.0		14.50	41.00	20.0		17.00	42.60	19.0	1.0	19.10	33.10	24.00	
08.25	25.3	27.0		10.35	30.6	18.0		12.45	42.3	18.0	0.8	14.55	41.20	22.0		17.05	42.40	20.0		19.15	32.60	25.00	1.2
08.30	25.4	25.0	0.2	10.40	32.8	19.0		12.50	43	19.0		15.00	41.00	21.0	1.1	17.10	41.40	22.0		19.20	31.80	25.00	
08.35	25.4	26.0		10.45	35.6	20.0	0.8	12.55	43.1	18.0		15.05	41.20	22.0		17.15	40.00	22.0	4.5	19.25	31.10	25.00	
08.40	25.5	24.0		10.50	37.5	19.0		13.00	43.6	18.0	1.0	15.10	41.00	21.0		17.20	40.20	23.0		19.30	30.20	26.00	5.6
08.45	25.5	23.0	0.2	10.55	38.9	18.0		13.05	42.9	18.0		15.15	40.90	22.0	3.0	17.25	38.60	24.0		19.35	29.90	26.00	
08.50	25.5	22.0		11.00	40.6	1900	0.9	13.10	44	17.0		15.20	40.90	22.0		17.30	38.20	23.0	1.3	19.40	29.80	26.00	
08.55	25.3	24.0		11.05	42.3	19.0		13.15	43	19.0	1.1	15.25	41.30	22.0		17.35	37.90	23.0		19.45	29.00	25.00	1.3
09.00	24.5	28.0	0.2	11.10	42.9	18.0		13.20	44.1	16.0		15.30	40.10	22.0	1.0	17.40	37.80	24.0		19.50	29.30	26.00	
09.05	24.2	28.0		11.15	43.2	17.0	0.9	13.25	44.20	18.0		15.35	41.50	22.0		17.45	37.80	22.0	4.8	19.55	29.10	24.00	
09.10	24.3	28.0		11.20	44	16.0		13.30	43.60	16.0	1.5	15.40	40.70	21.0		17.50	36.50	24.0		20.00	28.60	26.00	
09.15	24.5	27.0	0.5	11.25	44.1	16.0		13.35	44.00	15.0		15.45	40.30	22.0	0.8	17.55	36.50	24.0		20.05	28.60	26.00	
09.20	24.6	28.0		11.30	44.5	16.0	1.0	13.40	43.80	17.0		15.50	40.00	22.0		18.00	36.60	24.0	1.20	20.10	27.80	26.00	
09.25	24.7	26.0		11.35	44.6	16.0		13.45	42.60	20.0	1.1	15.55	41.00	21.0		18.05	36.40	24.0		20.15	27.60	25.00	
09.30	24.9	25.0	0.6	11.40	45.3	1600		13.50	43.6	18.0	1.0	16.00	40.80	21.0	3.7	18.10	35.80	24.0		20.20	27.60	25.00	
09.35	25.7	23.0		11.45	44.8	19.00	0.9	13.55	42.9	18.0		16.05	39.90	20.0		18.15	35.00	24.0	5.3	20.25	26.50	27.00	
09.40	26.1	22.0		11.50	43.1	18.0		14:00	44	17.0		16.10	39.90	21.0		18.20	35.20	24.0		20.30	26.40	28.00	
09.45	26.3	21.0	0.3	11.55	42.5	16.0		14.05	43	19.0	1.1	16.15	40.10	18.0	1.40	18.25	34.90	23.0		20.35	26.40	28.00	

Table (A4): Temperature, relative humidity and wind speed spot readings Location: Palace Tomb.
First fieldwork visit: 2-3 August 2003, between 07.40-20.35.

Appendix A: Temperature, relative humidity and wind speed spot readings. First fieldwork visit: August 2003.

Time	T (°C)	RH%	Time	T (°C)	RH%	Time	T (°C)	RH%	Time	T (°C)	RH%	Time	T (°C)	RH%
20.40	26.0	28.0	22.50	23.9	33.0	01.00	22.8	28.0	03.10	21.6	32.0	05.20	20.6	32.0
20.45	25.6	28.0	22.55	24.2	30.0	01.05	22.8	27.0	03.15	21.8	33.0	05.25	20.6	32.0
20.50	25.4	29.0	23.00	24.0	32.0	01.10	22.4	28.0	03.20	21.5	33.0	05.30	20.4	32.0
20.55	25.4	28.0	23.05	24.2	30.0	01.15	22.6	28.0	03.25	21.5	32.0	05.35	20.4	31.0
21.00	25.0	29.0	23.10	24.1	29.0	01.20	22.5	27.0	03.30	21.6	33.0	05.40	20.4	33.0
21.05	25.1	29.0	23.15	24.2	30.0	01.25	22.7	30.0	03.35	21.6	33.0	05.45	20.3	33.0
21.10	25.0	30.0	23.20	24.3	29.0	01.30	22.6	31.0	03.40	21.5	34.0	05.50	20.4	32.0
21.15	25.0	31.0	23.25	24.2	29.0	01.35	22.6	31.0	03.45	21.3	32.0	05.55	20.1	33.0
21.20	24.9	32.0	23.30	24.0	29.0	01.40	22.6	32.0	03.50	21.3	33.0	06.00	20.0	33.0
21.25	24.8	33.0	23.35	24.1	29.0	01.45	22.1	31.0	03.55	21.4	32.0	06.05	19.7	33.0
21.30	24.8	32.0	23.40	24.1	29.0	01.50	22.4	29.0	04.00	21.3	33.0	06.10	20.0	32.0
21.35	24.5	32.0	23.45	24.0	28.0	01.55	22.3	29.0	04.05	21.3	32.0	06.15	20.9	32.0
21.40	24.6	31.0	23.50	23.9	30.0	02.00	22.3	30.0	04.10	21.3	33.0	06.20	21.8	33.0
21.45	24.4	31.0	23.55	24.1	29.0	02.05	22.3	31.0	04.15	21.4	32.0	06.25	22.6	33.0
21.50	24.2	32.0	00.00	24.0	28.0	02.10	22.0	32.0	04.20	21.5	33.0	06.30	22.5	31.0
21.55	24.0	31.0	00.05	23.9	27.0	02.15	22.5	31.0	04.25	21.4	32.0	06.35	22.5	33.0
22.00	24.4	30.0	00.10	23.6	28.0	02.20	22.3	32.0	04.30	21.2	32.0	06.40	23.9	32.0
22.05	24.3	31.0	00.15	23.5	27.0	02.25	22.5	33.0	04.35	21.2	32.0	06.45	24.6	33.0
22.10	24.3	31.0	00.20	23.1	28.0	02.30	22.1	33.0	04.40	21.0	32.3	06.50	24.6	33.0
22.15	24.1	32.0	00.25	23.3	29.0	02.35	22.0	33.0	04.45	21.1	32.0	06.55	23.8	32.0
22.20	24.2	32.0	00.30	23.3	30.0	02.40	22.0	33.0	04.50	21.0	32.0	07.00	22.4	33.0
22.25	24.5	31.0	00.35	23.2	27.0	02.45	22.0	32.0	04.55	21.0	33.0			
22.30	24.0	33.0	00.40	23.0	28.0	02.50	21.8	33.0	05.00	21.0	33.0			
22.35	24.3	31.0	00.45	23.0	28.0	02.55	21.8	33.0	05.05	20.9	32.0			
22.40	24.4	32.0	00.50	22.8	28.0	03.00	22.9	33.0	05.10	20.7	33.0			
22.45	24.1	32.0	00.55	22.9	27.0	03.05	21.8	33.0	05.15	20.7	33.0			

Table (A5): Temperature and relative humidity spot readings. Location: Palace Tomb.
First fieldwork visit: 2-3 August 2003, between 19.50-07.00.

Appendix A: Temperature, relative humidity and wind speed spot readings. First fieldwork visit: August 2003.

Time	Wind Speed m/s	Time	Wind Speed m/s	Time	Wind Speed m/s	Time	Wind Speed m/s	Time	Wind Speed m/s
20.00	1.4	22.10		00.20		02.30	3.4	04.40	
20.05		22.15	1.4	00.25		02.35		04.45	2.4
20.10		22.20		00.30	3.2	02.40		04.50	
20.15	1.5	22.25		00.35		02.45	3.1	04.55	
20.20		22.30	2.0	00.40		02.50		05.00	2.0
20.25		22.35		00.45	1.8	02.55		05.05	
20.30	2.2	22.40		00.50		03.00	3.5	05.10	
20.35		22.45	2.9	00.55		03.05		05.15	1.5
20.40		22.50		01.00	2.2	03.10		05.20	
20.45	2.0	22.55		01.05		03.15	3.6	05.25	
20.50		23.00	3.1	01.10		03.20		05.30	1.1
20.55		23.05		01.15	2.5	03.25		05.35	
21.00	1.8	23.10		01.20		03.30	3.7	05.40	
21.05		23.15	2.8	01.25		03.35		05.45	0.9
21.10		23.20		01.30	2.4	03.40		05.50	
21.15	2.3	23.25		01.35		03.45	3.8	05.55	
21.20		23.30	2.4	01.40		03.50		06.00	0..5
21.25		23.35		01.45	2.8	03.55		06.05	
21.30	2.5	23.40		01.50		04.00	3.8	06.10	
21.35		23.45	2.2	01.55		04.05		06.15	0.2
21.40		23.50		02.00	3.0	04.10		06.20	
21.45	2.8	23.55		02.05		04.15	3.9	06.25	
21.50		00.00	2.6	02.10		04.20		06.30	0.2
21.55		00.05		02.15	3.2	04.25		06.35	
22.00	2.4	00.10		02.20		04.30	3.0	06.40	
22.05		00.15	2.4	02.25		04.35		06.45	0.1

Table (A6): Wind speed spot readings. Location: Nabateans Hotel (10 minutes walking distance from the archaeological site). First fieldwork visit: 2-3 August 2003, between 20.00-07.00.

Appendix A: Temperature, relative humidity and wind speed spot readings. First fieldwork visit: August 2003.

Time	T (°C)	RH%	Wind Speed (m/s)	Time	T (°C)	RH%	Wind Speed(m/s)	Time	T (°C)	RH%	Wind Speed (m/s)	Time	T (°C)	RH%	Wind Speed(m/s)	Time	T (°C)	RH%	Wind Speed(m/s)	Time	T (°C)	RH%	Wind Speed(m/s)
07.40	22.3	32.0		09.50	25.4	28.0		12.00	35.4	21.0	0.7	14.10	41.5	16.0		16.20	38.8	18.0		18.30	32.7	21.0	2.3
07.45	22.4	32.0	0.1	09.55	25.4	28.0		12.05	35.4	20.0		14.15	42.0	15.0	0.9	16.25	38.8	18.0		18.35	32.6	21.0	
07.50	22.8	32.0		10.00	25.7	28.0	0.4	12.10	35.5	20.0		14.20	42.0	15.0		16.30	38.8	18.0	1.9	18.40	32.7	21.0	
07.55	23.0	31.0		10.05	25.8	27.0		12.15	35.5	20.0	0.8	14.25	42.0	15.0		16.35	38.7	18.0		18.45	32.6	20.0	3.0
08.00	23.0	31.0	0.1	10.10	25.9	27.0		12.20	35.0	20.0		14.30	42.1	15.0	1.1	16.40	38.7	17.0		18.50	33.0	20.0	
08.05	23.1	31.0		10.15	25.9	27.0	0.3	12.25	36.0	19.0		14.35	42.6	15.0		16.45	37.9	17.0	2.3	18.55	32.5	20.0	
08.10	23.2	30.0		10.20	26.3	27.0		12.30	37.0	19.0	0.9	14.40	42.1	16.0		16.50	37.8	17.0		19.00	32.5	20.0	3.1
08.15	24.2	30.0	0.1	10.25	26.4	27.0		12.35	37.0	19.0		14.45	42.1	16.0	1.3	16.55	37.8	17.0		19.05	31.9	21.0	
08.20	24.2	30.0		10.30	27.0	27.0	0.3	12.40	37.5	19.0		14.50	42.3	16.0		17.00	36.4	18.0	2.4	19.10	31.8	21.0	
08.25	24.5	29.0		10.35	27.1	26.0		12.45	37.6	18.0	0.5	14.55	42.6	16.0		17.05	36.1	17.0		19.15	31.8	21.0	2.2
08.30	24.9	29.0	0.2	10.40	27.0	26.0		12.50	38.0	18.0		15.00	42.5	15.0	1.9	17.10	35.1	17.0		19.20	31.8	21.0	
08.35	25.0	29.0		10.45	27.2	26.0	0.4	12.55	38.5	18.0		15.05	42.5	15.0		17.15	35.5	16.0	2.4	19.25	30.0	21.0	
08.40	25.0	29.0		10.50	27.3	26.0		13.00	39.0	18.0	0.4	15.10	42.4	15.0		17.20	35.1	17.0		19.30	30.0	21.0	2.7
08.45	25.1	29.0	0.2	10.55	27.5	26.0		13.05	39.2	17.0		15.15	42.6	15.0	1.9	17.25	35.1	17.0		19.35	30.0	21.0	
08.50	25.5	28.0		11.00	27.8	26.0	0.4	13.10	39.3	17.0		15.20	42.8	15.0		17.30	35.1	17.0	2.0	19.40	29.8	22.0	
08.55	25.5	28.0		11.05	28.9	25.0		13.15	40.0	17.0	0.3	15.25	43.0	15.0		17.35	35.2	18.0		19.45	29.0	22.0	2.5
09.00	25.0	28.0	0.2	11.10	29.0	25.0		13.20	40.2	17.0		15.30	42.3	16.0	1.8	17.40	34.6	18.0		19.50	29.0	22.0	
09.05	25.0	28.0		11.15	29.1	25.0	0.5	13.25	40.2	17.0		15.35	42.3	16.0		17.45	34.6	18.0	1.8	19.55	28.7	22.0	
09.10	24.5	28.0		11.20	29.8	25.0		13.30	39.8	17.0	0.4	15.40	42.0	17.0		17.50	34.4	18.0		20.00	28.1	22.0	1.3
09.15	24.5	28.0	0.1	11.25	30.1	24.0		13.35	40.2	16.0		15.45	42.0	17.0	1.8	17.55	34.5	19.0		20.05	27.6	22.0	
09.20	24.5	29.0		11.30	31.2	24.0	0.6	13.40	40.0	17.0		15.50	41.3	17.0		18.00	34.3	19.0	2.5	20.10	27.6	22.0	
09.25	24.0	30.0		11.35	33.0	22.0		13.45	40.1	17.0	0.6	15.55	41.1	17.0		18.05	34.5	19.0		20.15	27.6	23.0	1.4
09.30	24.0	30.0	0.2	11.40	34.0	22.0		13.50	40.1	16.0		16.00	41.5	18.0	1.7	18.10	33.8	19.0		20.20	26.5	23.0	
09.35	24.5	29.0		11.45	34.0	22.0	0.6	13.55	41.0	16.0		16.05	40.0	18.0		18.15	33.0	19.0	2.6	20.25	26.4	23.0	
09.40	25.0	29.0		11.50	34.5	21.0		14:00	41.1	16.0	0.7	16.10	39.8	18.0		18.20	33.0	20.0		20.30	26.4	23.0	2.8
09.45	25.3	28.0	0.3	11.55	35.0	21.0		14.05	41.2	16.0		16.15	39.7	18.0	1.1	18.25	32.8	20.0		20.35	26.1	23.0	

Table (A7): Temperature, relative humidity and wind speed spot readings. Location: Deir Tomb.
First fieldwork visit: 3-4 August 2003, between 07.40-20.35.

Appendix A: Temperature, relative humidity and wind speed spot readings. First fieldwork visit: August 2003.

Time	T (°C)	RH%	Time	T (°C)	RH%	Time	T (°C)	RH%	Time	T (°C)	RH%	Time	T (°C)	RH%
20.40	24.4	27.0	22.50	20.8	31.0	01.00	19.4	33.0	03.10	17.5	35.0	05.20	16.8	32.0
20.45	24.3	27.0	22.55	20.8	31.0	01.05	19.4	33.0	03.15	17.3	35.0	05.25	16.9	33.0
20.50	24.0	28.0	23.00	20.8	32.0	01.10	19.1	34.0	03.20	17.3	36.0	05.30	16.9	33.0
20.55	24.0	28.0	23.05	20.4	32.0	01.15	19.1	34.0	03.25	17.3	365.0	05.35	17.4	32.0
21.00	23.9	28.0	23.10	20.7	32.0	01.20	19.2	33.0	03.30	17.4	36.0	05.40	17.8	32.0
21.05	23.9	29.0	23.15	20.7	32.0	01.25	19.2	33.0	03.35	17.3	36.0	05.45	17.9	32.0
21.10	23.9	29.0	23.20	20.7	32.0	01.30	19.0	34.0	03.40	17.0	36.0	05.50	18.6	31.0
21.15	23.8	29.0	23.25	20.4	32.0	01.35	19.0	34.0	03.45	17.0	36.0	05.55	18.5	31.0
21.20	22.8	29.0	23.30	20.0	33.0	01.40	19.0	34.0	03.50	16.9	36.0	06.00	18.5	31.0
21.25	22.5	29.0	23.35	20.1	33.0	01.45	18.8	35.0	03.55	16.9	36.0	06.05	19.1	31.0
21.30	22.1	29.0	23.40	20.1	33.0	01.50	18.8	35.0	04.00	16.4	37.0	06.10	19.3	31.0
21.35	22.0	29.0	23.45	19.8	33.0	01.55	18.8	34.0	04.05	16.4	37.0	06.15	19.8	31.0
21.40	22.0	29.0	23.50	19.8	33.0	02.00	18.7	34.0	04.10	16.1	37.0	06.20	19.9	30.0
21.45	22.0	29.0	23.55	19.9	32.0	02.05	18.6	34.0	04.15	15.8	37.0	06.25	20.3	30.0
21.50	21.9	30.0	00.00	19.8	32.0	02.10	18.6	34.0	04.20	15.7	37.0	06.30	20.4	30.0
21.55	22.0	30.0	00.05	19.8	33.0	02.15	18.5	35.0	04.25	15.5	38.0	06.35	20.6	30.0
22.00	21.4	29.0	00.10	19.7	33.0	02.20	18.5	34.0	04.30	15.5	38.0	06.40	20.8	30.0
22.05	21.4	29.0	00.15	19.7	33.0	02.25	18.2	34.0	04.35	15.4	37.0	06.45	20.9	29.0
22.10	21.4	29.0	00.20	19.7	33.0	02.30	18.2	35.0	04.40	15.4	37.0	06.50	21.0	29.0
22.15	21.5	29.0	00.25	19.7	33.0	02.35	18.2	35.0	04.45	15.5	36.0	06.55	21.5	29.0
22.20	21.3	30.0	00.30	19.7	33.0	02.40	18.0	35.0	04.50	15.8	36.0	07.00	21.8	29.0
22.25	21.3	30.0	00.35	19.6	34.0	02.45	18.1	35.0	04.55	15.9	35.0			
22.30	21.3	30.0	00.40	19.6	34.0	02.50	17.8	35.0	05.00	16.1	35.0			
22.35	21.0	31.0	00.45	19.4	34.0	02.55	17.8	34.0	05.05	16.3	35.0			
22.40	21.0	31.0	00.50	19.3	34.0	03.00	17.8	34.0	05.10	16.4	33.0			
22.45	21.0	31.0	00.55	19.4	34.0	03.05	17.6	35.0	05.15	16.4	33.0			

Table (A8): Temperature, relative humidity and wind speed spot readings. Location: Deir Tomb.
First fieldwork visit: 3-4 August 2003, between 19.50-07.00.

Appendix A: Temperature, relative humidity and wind speed spot readings. First fieldwork visit: August 2003.

Time	Wind Speed m/s	Time	Wind Speed m/s	Time	Wind Speed m/s	Time	Wind Speed m/s	Time	Wind Speed m/s
20.00	2.7	22.10		00.20		02.30	3.0	04.40	
20.05		22.15	3.0	00.25		02.35		04.45	1.8
20.10		22.20		00.30	3.5	02.40		04.50	
20.15	2.1	22.25		00.35		02.45	3.1	04.55	
20.20		22.30	3.1	00.40		02.50		05.00	1.4
20.25		22.35		00.45	3.4	02.55		05.05	
20.30	2.0	22.40		00.50		03.00	3.0	05.10	
20.35		22.45	2.9	00.55		03.05		05.15	1.3
20.40		22.50		01.00	3.4	03.10		05.20	
20.45	2.3	22.55		01.05		03.15	3.7	05.25	
20.50		23.00	2.6	01.10		03.20		05.30	0.9
20.55		23.05		01.15	3.3	03.25		05.35	
21.00	3.0	23.10		01.20		03.30	3.8	05.40	
21.05		23.15	2.2	01.25		03.35		05.45	0.7
21.10		23.20		01.30	3.0	03.40		05.50	
21.15	3.1	23.25		01.35		03.45	4.0	05.55	
21.20		23.30	2.8	01.40		03.50		06.00	0.5
21.25		23.35		01.45	3.6	03.55		06.05	
21.30	3.1	23.40		01.50		04.00	3.1	06.10	
21.35		23.45	2.4	01.55		04.05		06.15	0.3
21.40		23.50		02.00	4.0	04.10		06.20	
21.45	3.3	23.55		02.05		04.15	2.9	06.25	
21.50		00.00	2.8	02.10		04.20		06.30	0.3
21.55		00.05		02.15	3.0	04.25		06.35	
22.00	2.8	00.10		02.20		04.30	2.8	06.40	
22.05		00.15	3.1	02.25		04.35		06.45	0.2

Table (A9): Wind speed spot readings. Location: Nabateans Hotel (10 minutes walking distance from the archaeological site). First fieldwork visit: 3-4 August 2003, between 20.00-06.45.

Appendix B: The anion and cation content of the drilled samples. First fieldwork visit: August 2003.

Sample Number	Location	Height (cm)	Depth (cm)	Ca (ppm)	Na (ppm)	Mg (ppm)	K (ppm)	Fe (ppm)	Al (ppm)	Tl (ppm)	Zn (ppm)	F (ppm)	Br (ppm)	Cl (ppm)	NO_3 (ppm)	PO_4 (ppm)	SO_4 (ppm)	Cation charge with Al	Cation charge without Al	Anion charge	Sum of cations & anions (ppm)	Soluble salt content in the sample (%) of dry weight
1	T1	5	0-1	1.19	5.47	0.17	0.85	0.00	0.09	0.00	0.01	0.00	2.40	4.78	0.00	0.00	2.41	0.34	0.33	0.22	17.38	0.09
2	T1	5	1-3	0.58	5.81	0.10	0.60	0.00	0.28	0.01	0.06	0.00	0.06	0.87	21.54	0.40	0.66	0.34	0.31	0.40	30.98	0.15
3	T1	5	3-5	0.42	4.30	0.08	0.08	0.00	0.15	0.01	0.08	0.00	0.07	0.32	30.59	0.00	0.57	0.24	0.22	0.52	36.67	0.18
4	T1	55	0-1	0.63	4.66	0.11	0.41	0.00	0.61	0.14	0.01	0.00	0.08	0.52	34.24	0.44	0.93	0.32	0.25	0.60	42.76	0.21
5	T1	55	1-3	0.36	5.68	0.07	0.42	0.00	0.09	0.01	0.01	0.00	0.07	0.59	33.11	0.00	0.93	0.29	0.28	0.57	41.34	0.21
6	T1	55	3-5	0.42	8.77	0.09	0.65	0.00	0.22	0.06	0.03	19.48	0.74	15.77	31.51	0.25	0.00	0.45	0.43	2.00	77.98	0.39
7	T1	105	0-1	2.18	13.27	1.61	3.71	0.00	0.36	0.03	0.01	0.00	0.00	15.12	39.07	0.62	2.14	0.95	0.91	1.12	78.13	0.39
8	T1	105	1-3	0.96	9.02	0.43	1.23	0.00	0.11	0.00	0.00	0.00	0.00	8.31	27.34	2.46	2.66	0.52	0.51	0.81	52.52	0.26
9	T1	105	3-5	0.91	9.27	0.36	1.74	0.00	0.15	0.01	0.01	0.00	0.00	6.52	26.73	1.48	1.94	0.54	0.52	0.70	49.12	0.25
10	T1	205	0-1	6.38	6.13	0.67	0.89	0.00	0.04	0.00	0.00	0.00	0.00	3.12	24.78	1.19	15.40	0.67	0.67	0.85	58.60	0.29
11	T1	205	1-3	2.55	8.02	0.35	0.80	0.00	0.13	0.01	0.00	0.00	0.00	1.66	21.97	0.66	5.57	0.54	0.53	0.54	41.72	0.21
12	T1	205	3-5	3.68	5.67	0.35	0.33	0.00	0.09	0.01	0.01	0.61	2.63	2.96	1.08	1.41	5.59	0.48	0.47	0.33	24.42	0.12
13	T1	305	0-1	2.03	4.28	0.19	0.40	0.00	0.02	0.00	0.00	0.00	2.50	2.44	1.07	1.40	5.46	0.32	0.32	0.28	19.79	0.10
14	T1	305	1-3	4.41	4.83	0.41	0.34	0.00	0.08	0.00	0.00	0.59	2.82	2.30	1.09	1.52	10.27	0.48	0.47	0.41	28.66	0.14
15	T1	305	3-5	3.45	6.37	0.38	0.49	0.00	0.11	0.00	0.00	0.93	3.15	2.48	0.00	1.46	6.26	0.51	0.50	0.33	25.09	0.13
16	T1	505	0-1	36.24	10.28	1.52	3.94	0.00	0.02	0.00	0.02	0.74	18.82	7.46	0.00	0.00	109.28	2.48	2.48	2.76	188.31	0.94
17	T1	505	1-3	18.87	9.97	0.88	3.05	0.00	0.09	0.01	0.05	0.77	12.41	5.78	1.08	1.42	65.32	1.54	1.53	1.78	119.69	0.60
18	T3	305	0-1	15.84	6.89	0.63	12.53	0.00	0.19	0.01	0.00	0.70	13.27	6.22	1.53	1.20	55.37	1.48	1.46	1.59	114.38	0.57
19	T3	305	1-3	30.63	6.85	0.62	62.84	0.00	0.02	0.00	0.00	2.76	8.95	8.09	0.00	4.57	181.91	3.49	3.49	4.42	307.23	1.54
20	T3	305	3-5	15.22	8.72	0.96	36.82	0.00	0.03	0.00	0.00	0.70	13.84	12.18	0.00	0.00	127.18	2.16	2.16	3.20	215.64	1.08
21	T2	305	0-1	2.81	6.06	0.27	1.30	0.00	0.17	0.01	0.00	0.64	1.95	1.86	0.00	1.56	2.63	0.48	0.46	0.21	19.26	0.10
22	T2	305	1-3	12.74	8.34	0.73	1.50	0.00	0.34	0.06	0.01	0.77	5.73	4.59	0.00	1.42	28.17	1.14	1.10	0.87	64.40	0.32
23	T2	505	0-1	1.50	5.63	0.12	0.91	0.00	0.27	0.01	0.00	0.00	2.29	1.78	1.08	1.55	1.86	0.38	0.35	0.18	17.01	0.09
24	T2	505	1-3	50.50	12.21	1.57	131.34	0.00	0.06	0.00	0.01	3.29	18.28	15.71	5.39	7.08	301.71	6.55	6.54	7.44	547.14	2.74

Table (B1): The anion and cation content of drilled samples from the Bib al Siq Triclinium Tomb, locations (T1, T2 and T3). First fieldwork visit: August 2003.

Appendix B: The anion and cation content of the drilled samples. First fieldwork visit: August 2003.

Sample Number	Location	Height (cm)	Depth (cm)	Ca (ppm)	Na (ppm)	Mg (ppm)	K (ppm)	Fe (ppm)	Al (ppm)	Tl (ppm)	Zn (ppm)	F (ppm)	Br (ppm)	Cl (ppm)	NO_3 (ppm)	PO_4 (ppm)	SO_4 (ppm)	Cation charge with Al	Cation charge without Al	Anion charge	Sum of cations & anions (ppm)	Soluble salt content in the sample (%) of dry weight
25	C1	5	0-1	82.33	14.94	2.30	12.27	0.00	0.08	0.01	0.02	0.00	0.00	23.79	52.00	0.00	0.00	5.27	5.26	1.51	187.75	0.94
26	C1	5	1-3	37.10	11.27	1.31	7.45	0.00	0.15	0.02	0.01	0.00	0.00	10.90	34.33	1.27	269.50	2.66	2.64	6.52	373.31	1.87
27	C1	5	3-5	22.52	9.92	0.89	6.09	0.00	0.25	0.02	0.05	0.00	0.00	9.69	29.13	0.00	80.69	1.81	1.78	2.42	159.24	0.80
28	C1	55	0-1	0.95	6.90	0.13	0.85	0.00	0.34	0.04	0.00	0.00	0.00	0.85	19.14	0.71	7.27	0.42	0.38	0.51	37.17	0.19
29	C1	55	1-3	1.26	7.61	0.17	0.88	0.00	0.41	0.07	0.00	0.00	0.00	1.05	20.05	0.63	0.96	0.48	0.43	0.39	33.08	0.17
30	C1	55	3-5	1.17	7.32	0.26	1.23	0.00	0.25	0.07	0.01	0.00	0.00	2.19	21.26	0.61	0.66	0.46	0.43	0.44	35.02	0.18
31	C1	105	0-1	1.74	7.79	0.20	1.24	0.25	0.62	0.05	0.00	0.00	0.00	0.59	19.76	0.67	2.33	0.55	0.48	0.40	35.23	0.18
32	C1	105	1-3	0.31	6.43	0.05	0.44	0.24	0.55	0.04	0.00	0.60	1.15	0.97	0.00	0.90	0.74	0.38	0.32	0.12	12.42	0.06
33	C1	105	3-5	0.58	7.39	0.08	0.78	0.19	0.57	0.05	0.00	0.70	1.28	1.06	0.00	0.00	1.16	0.45	0.39	0.11	13.84	0.07
34	C1	175	0-1	11.72	41.31	3.91	39.55	0.00	0.12	0.01	0.01	0.56	60.73	56.51	0.00	0.84	8.58	3.73	3.72	2.59	223.86	1.12
35	C1	175	1-3	5.73	23.81	2.34	20.50	0.00	0.06	0.00	0.01	0.41	47.60	44.59	0.00	0.87	5.21	2.05	2.04	2.01	151.12	0.76
36	C1	175	3-5	2.83	16.78	1.31	14.56	0.00	0.03	0.00	0.06	0.58	30.59	28.15	0.00	0.00	2.46	1.36	1.36	1.26	97.36	0.49
37	C1	305	0-1	11.57	5.87	0.94	0.24	1.03	1.47	0.00	0.06	12.08	0.00	1.31	0.00	0.00	8.47	1.12	0.96	0.85	43.03	0.22
38	C1	305	1-3	4.54	3.97	0.31	0.18	1.21	1.28	0.00	0.19	0.24	0.86	0.73	0.00	1.29	0.56	0.62	0.48	0.10	15.37	0.08
39	C1	305	3-5	6.69	5.45	0.41	0.12	0.50	0.63	0.00	0.20	0.00	0.87	0.69	1.07	1.20	0.31	0.70	0.63	0.09	18.13	0.09
40	C1	405	0-1	19.36	5.83	1.88	0.66	0.80	1.04	0.01	0.02	0.15	0.87	3.01	2.77	1.35	29.88	1.54	1.42	0.81	67.62	0.34
41	C1	405	1-3	7.31	6.72	0.66	0.23	1.48	1.12	0.00	0.01	0.00	0.87	0.22	1.12	1.27	0.31	0.90	0.78	0.08	21.32	0.11
42	C1	405	3-5	4.75	4.83	0.38	0.21	1.36	1.11	0.00	0.13	0.06	1.11	0.65	1.25	1.28	0.31	0.66	0.54	0.10	17.42	0.09
43	C1	455	0-1	25.11	12.40	3.47	2.05	0.50	1.13	0.01	0.05	0.24	3.18	4.42	0.00	0.00	62.12	2.28	2.15	1.47	114.67	0.57
44	C1	455	1-3	15.80	5.59	1.70	0.27	0.25	1.45	0.01	0.07	0.15	0.87	1.02	1.05	1.13	28.21	1.35	1.19	0.69	57.57	0.29
45	C1	455	3-5	6.88	3.64	0.69	0.13	0.46	2.60	0.00	0.28	0.18	0.99	0.67	0.00	1.23	2.36	0.88	0.59	0.13	20.11	0.10
46	C1	505	0-1	17.93	11.19	2.21	1.00	1.50	1.16	0.07	0.04	0.21	8.11	21.68	0.00	1.24	23.23	1.77	1.64	1.25	89.56	0.45
47	C1	505	1-3	20.21	9.65	1.98	0.55	1.16	1.01	0.05	0.06	0.00	0.97	9.79	3.39	1.25	0.32	1.76	1.65	0.39	50.39	0.25

Table (B2): The anion and cation content of drilled samples from the Palace Tomb, location (C1). First fieldwork visit: August 2003.

Appendix B: The anion and cation content of the drilled samples. First fieldwork visit: August 2003.

Sample Number	Location	Height (cm)	Depth (cm)	Ca (ppm)	Na (ppm)	Mg (ppm)	K (ppm)	Fe (ppm)	Al (ppm)	Tl (ppm)	Zn (ppm)	F (ppm)	Br (ppm)	Cl (ppm)	NO_3 (ppm)	PO_4 (ppm)	SO_4 (ppm)	Cation charge with Al	Cation charge without Al	Anion charge	Sum of cations & anions (ppm)	Soluble salt content in the sample (%) of dry weight
48	C2	105	0-1	175.57	23.99	5.75	13.86	0.07	0.34	0.01	0.06	0.00	0.90	22.17	107.01	1.16	0.82	10.67	10.63	2.42	351.71	1.76
49	C2	105	1-3	43.62	9.83	2.40	3.90	0.28	1.54	0.07	0.02	0.00	0.87	0.20	27.05	0.00	0.37	3.08	2.91	0.46	90.14	0.45
50	C2	105	3-5	107.27	14.96	4.14	8.91	0.18	0.67	0.02	0.04	0.00	55.04	10.82	0.00	1.50	217.67	6.65	6.58	5.58	421.21	2.11
51	C2	155	0-1	191.78	11.10	2.53	8.85	0.27	0.33	0.01	0.07	0.85	46.55	19.55	0.00	3.02	0.00	10.54	10.50	1.27	284.91	1.42
52	C2	155	1-3	32.98	10.45	1.06	3.55	0.95	1.09	0.05	0.22	0.48	10.57	6.23	0.00	0.00	81.81	2.44	2.32	2.04	149.43	0.75
53	C2	155	3-5	26.46	8.80	0.66	4.48	0.00	0.05	0.00	0.14	0.44	7.57	3.74	0.00	0.83	82.79	1.88	1.87	1.97	135.96	0.68
54	C2	205	0-1	305.49	53.36	7.88	63.79	0.00	0.05	0.01	0.45	0.43	160.56	80.23	0.00	1.65	1300.65	19.86	19.85	31.44	1,974.55	9.87
55	C2	205	1-3	153.45	40.17	6.41	35.49	0.00	0.02	0.00	1.01	5.17	109.08	64.70	0.00	8.29	563.85	10.87	10.87	15.47	987.64	4.94
56	C2	205	3-5	89.92	43.57	5.13	64.90	0.00	0.03	0.00	1.00	2.04	183.68	95.88	10.91	8.48	726.34	8.50	8.50	20.68	1,231.88	6.16
57	C2	345	0-1	47.56	20.08	4.22	18.17	0.00	0.19	0.01	0.01	0.49	53.47	42.54	0.00	0.00	200.85	4.08	4.06	6.08	387.59	1.94
58	C3	105	0-1	16.72	5.35	1.62	1.28	0.30	0.00	0.16	0.01	0.00	1.00	2.41	4.91	1.15	0.42	1.25	1.25	0.20	35.33	0.18
59	C3	105	1-3	22.32	6.03	1.89	1.42	0.30	1.79	0.06	0.03	0.00	0.92	1.91	3.40	1.12	0.32	1.78	1.58	0.16	41.52	0.21
60	C3	155	0-1	15.84	11.58	1.87	1.68	0.42	1.64	0.12	0.01	0.00	0.87	0.18	18.38	1.15	0.32	1.69	1.51	0.36	54.06	0.27
61	C3	155	1-3	16.67	11.53	1.90	1.84	0.62	2.29	0.15	0.02	0.00	16.06	14.79	0.00	1.40	3.00	1.82	1.57	0.73	70.28	0.35
62	C3	205	0-1	17.40	17.31	2.61	2.00	0.48	1.97	0.10	0.01	0.00	34.37	0.21	0.00	1.33	0.31	2.13	1.91	0.48	78.10	0.39
63	C3	205	1-3	17.07	14.72	2.17	1.45	0.52	2.40	0.15	0.02	0.00	0.95	27.93	25.28	1.12	0.44	2.00	1.73	1.25	94.23	0.47
64	C3	305	0-1	21.05	14.30	3.48	1.69	1.43	2.90	0.14	0.01	0.00	0.92	0.21	33.82	1.29	0.33	2.38	2.06	0.61	81.58	0.41
65	C3	305	1-3	42.49	36.85	4.89	2.85	5.01	5.63	0.20	0.08	0.00	0.87	83.42	58.61	1.23	0.33	5.01	4.38	3.35	242.46	1.21

Table (B3): The anion and cation content from drilled samples from the Palace Tomb, locations (C2 and C3).
First fieldwork visit: August 2003.

Appendix B: The anion and cation content of the drilled samples. First fieldwork visit: August 2003.

Sample Number	Location	Height (cm)	Depth (cm)	Ca (ppm)	Na (ppm)	Mg (ppm)	K (ppm)	Fe (ppm)	Al (ppm)	Tl (ppm)	Zn (ppm)	F (ppm)	Br (ppm)	Cl (ppm)	NO_3 (ppm)	PO_4 (ppm)	SO_4 (ppm)	Cation charge with Al	Cation charge without Al	Anion charge	Sum of cations & anions (ppm)	Soluble salt content in the sample (%) of dry weight
66	H	25	0-1	21.11	60.97	3.84	8.43	3.21	0.52	0.04	0.01	0.00	0.00	3.76	9.61	0.00	8.88	4.41	4.35	0.45	120.38	0.60
67	H	25	1-3	14.52	9.02	1.28	2.57	32.73	3.96	0.25	0.06	0.00	0.00	2.51	3.14	1.00	2.98	2.91	2.47	0.21	74.02	0.37
68	H	75	0-1	15.24	12.44	2.40	1.27	0.83	2.13	0.09	0.11	0.00	0.00	0.47	0.91	2.03	1.32	1.80	1.56	0.12	39.25	0.20
69	H	75	1-3	13.21	10.80	1.97	3.00	0.42	2.07	0.08	0.16	0.00	0.00	1.49	4.01	0.67	3.79	1.62	1.39	0.21	41.66	0.21
70	H	125	0-1	19.27	9.89	1.49	1.51	0.33	0.56	0.07	0.01	0.16	0.00	1.56	1.94	0.00	2.31	1.63	1.57	0.13	39.10	0.20
71	H	125	1-3	9.56	6.12	1.06	0.47	1.29	2.59	0.18	0.01	0.00	0.00	0.19	1.07	0.71	0.87	1.18	0.89	0.06	24.12	0.12
72	H	200	0-1	12.11	8.55	1.07	0.41	0.53	2.46	0.16	0.01	0.00	0.00	0.38	0.79	0.69	1.34	1.37	1.10	0.07	28.50	0.14
73	H	200	1-3	6.81	6.53	0.71	0.38	0.42	1.88	0.11	0.01	0.00	0.00	0.03	0.54	0.69	0.89	0.92	0.71	0.05	19.01	0.10
74	H	250	0-1	189.45	14.57	1.60	1.92	0.16	1.68	0.09	0.06	0.00	30.09	20.86	20.37	0.63	520.42	10.46	10.27	12.15	801.90	4.01
75	H	300	0-1	13.82	8.41	1.88	0.86	0.87	5.42	0.77	0.13	0.00	0.00	1.56	1.38	0.00	20.39	1.89	1.29	0.49	55.48	0.28
76	H	300	1-3	39.51	9.52	1.38	1.10	0.25	1.36	0.00	0.06	0.11	3.37	5.21	1.07	1.16	103.51	2.69	2.54	2.41	167.61	0.84
77	H	500	0-1	8.82	7.79	1.39	2.11	1.70	5.14	0.01	0.02	0.15	4.68	5.73	0.00	1.15	2.48	1.58	1.01	0.32	41.17	0.21
78	H	500	1-3	7.05	7.07	1.42	1.76	1.83	8.39	0.01	0.01	0.11	6.38	5.08	1.09	1.15	2.61	1.82	0.89	0.34	43.97	0.22

Table (B4): The anion and cation content of drilled samples from the Corinthian Tomb, location (H).
First fieldwork visit: August 2003.

Appendix B: The anion and cation content of the drilled samples. First fieldwork visit: August 2003.

Sample Number	Location	Height (cm)	Depth (cm)	Ca (ppm)	Na (ppm)	Mg (ppm)	K (ppm)	Fe (ppm)	Al (ppm)	Ti (ppm)	Zn (ppm)	F (ppm)	Br (ppm)	Cl (ppm)	NO_3 (ppm)	PO_4 (ppm)	SO_4 (ppm)	Cation charge with Al	Cation charge without Al	Anion charge	Sum of cations & anions (ppm)	Soluble salt content in the sample (%) of dry weight
79	D1	5	surface	24.45	17.10	2.55	3.10	0.00	0.00	0.06	0.03	0.00	0.00	0.00	0.96	1.99	0.21	2.26	2.26	0.08	50.44	0.25
80	D1	5	1	3.01	9.66	0.33	0.82	0.00	0.00	0.01	0.02	0.00	0.00	5.37	3.22	0.52	0.50	0.62	0.62	0.23	23.46	0.12
81	D1	5	1-3	4.91	10.52	0.39	0.57	0.02	0.39	0.03	0.02	0.00	0.00	5.26	0.71	0.48	2.78	0.79	0.75	0.23	26.08	0.13
82	D1	5	3-5	4.58	11.52	0.41	0.96	0.00	0.00	0.00	0.01	0.00	0.00	1.91	8.78	0.40	4.44	0.79	0.79	0.30	33.00	0.17
83	D1	55	0-1	8.70	15.27	2.22	1.15	0.00	0.05	0.15	0.02	0.00	0.00	1.15	11.84	3.52	0.15	1.32	1.31	0.34	44.21	0.22
84	D1	55	1-3	3.33	8.47	0.33	0.57	0.00	0.00	0.04	0.01	0.00	0.00	1.60	10.83	0.34	0.06	0.58	0.58	0.23	25.59	0.13
85	D1	55	3-5	3.15	6.86	0.26	0.35	0.42	0.10	0.00	0.00	0.00	0.00	0.95	10.00	0.39	0.00	0.51	0.50	0.20	22.47	0.11
86	D1	105	0-1	15.29	15.84	1.91	1.42	0.00	0.00	0.07	0.01	0.60	1.15	0.00	0.00	0.00	45.16	1.65	1.65	0.99	81.44	0.41
87	D1	105	1-3	6.16	16.53	0.50	1.72	0.00	0.06	0.02	0.01	0.70	1.28	4.65	7.73	0.35	9.09	1.12	1.11	0.51	48.80	0.24
88	D1	105	3-5	3.57	6.85	0.24	0.19	0.00	0.74	0.01	0.00	0.56	60.73	5.61	8.25	0.34	1.54	0.58	0.50	1.12	88.62	0.44
89	D1	155	Surface	3.22	6.43	0.42	1.53	0.78	1.87	0.03	0.00	0.41	47.60	2.18	1.08	0.92	4.68	0.75	0.54	0.82	71.12	0.36
90	D1	155	0-1	4.44	8.18	0.67	0.61	0.00	0.00	0.01	0.00	0.58	30.59	0.96	29.85	0.00	4.06	0.65	0.65	1.01	79.96	0.40
91	D1	155	1-3	1.36	7.05	0.20	0.20	0.81	1.33	0.01	0.00	12.08	0.00	2.15	1.08	0.87	2.11	0.57	0.42	0.79	29.25	0.15
92	D1	155	3-5	3.73	6.69	0.24	0.11	0.25	0.96	0.02	0.00	0.24	0.86	2.36	1.07	0.89	2.25	0.62	0.51	0.18	19.67	0.10
93	D1	205	Surface	2.95	7.15	0.26	0.54	0.78	3.00	0.00	0.00	0.00	0.87	6.59	1.10	0.92	17.77	0.85	0.52	0.61	41.93	0.21
94	D1	205	0-1	7.03	7.75	0.87	0.52	0.00	0.09	0.03	0.00	0.15	0.87	6.41	33.37	0.36	11.87	0.78	0.77	1.00	69.32	0.35
95	D1	205	1-3	2.29	4.86	0.20	0.47	0.00	1.59	0.01	0.00	0.00	0.87	3.28	0.00	0.84	4.09	0.53	0.35	0.21	18.49	0.09
96	D1	205	3-5	2.29	4.86	0.20	0.47	0.78	1.66	0.01	0.00	0.06	1.11	3.23	1.07	0.96	19.52	0.57	0.39	0.56	36.21	0.18
97	D1	255	0-1	9.12	11.03	1.43	1.23	0.00	0.05	0.02	0.00	0.24	3.18	16.13	39.10	0.00	6.19	1.09	1.08	1.27	87.71	0.44
98	D1	255	1-3	3.46	6.72	0.53	0.36	0.55	5.78	0.00	0.00	0.15	0.87	9.02	0.00	0.87	4.07	1.18	0.54	0.39	32.38	0.16
99	D1	255	3-5	3.65	6.61	0.45	0.42	0.70	5.95	0.02	0.00	0.18	0.99	8.60	0.00	0.90	9.43	1.20	0.54	0.49	37.89	0.19

Table (B5): The anion and cation content of drilled samples from the Deir Tomb, location (D1). First fieldwork visit: August 2003.

Appendix B: The anion and cation content of the drilled samples. First fieldwork visit: August 2003.

Sample Number	Location	Height (cm)	Depth (cm)	Ca (ppm)	Na (ppm)	Mg (ppm)	K (ppm)	Fe (ppm)	Al (ppm)	Tl (ppm)	Zn (ppm)	F (ppm)	Br (ppm)	Cl (ppm)	NO_3 (ppm)	PO_4 (ppm)	SO_4 (ppm)	Cation charge with Al	Cation charge without Al	Anion charge	Sum of cations & anions (ppm)	Soluble salt content in the sample (%) of dry weight
100	D2	5	0-1	44.59	10.22	0.82	2.28	0.00	0.04	0.00	0.01	2.83	17.72	14.44	10.98	11.12	290.11	2.80	2.80	7.35	405.16	2.03
101	D2	5	1-3	27.03	6.51	0.47	1.50	0.00	0.07	0.00	0.00	1.80	7.74	6.76	4.36	3.40	108.34	1.72	1.71	2.82	167.97	0.84
102	D2	5	3-5	53.50	8.66	0.63	1.89	0.00	0.22	0.01	0.01	0.93	6.83	5.25	0.00	2.58	144.33	3.17	3.15	3.37	224.84	1.12
103	D2	55	0-1	138.38	24.70	2.81	0.82	0.00	0.11	0.00	0.02	1.65	8.98	5.93	0.00	2.49	390.27	8.24	8.23	8.57	576.15	2.88
104	D2	55	1-3	30.22	6.52	1.65	0.49	0.00	1.25	0.06	0.00	1.27	5.00	4.90	3.26	2.80	76.05	2.08	1.94	1.99	133.46	0.67
105	D2	105	0-1	105.16	22.28	2.77	6.02	0.00	0.10	0.00	0.02	1.23	15.56	15.23	0.00	2.64	277.01	6.61	6.60	6.54	448.03	2.24
106	D2	105	1-3	21.43	7.50	0.95	0.43	0.00	0.12	0.00	0.00	0.84	5.72	5.15	0.00	1.51	175.39	1.50	1.49	3.96	219.05	1.10
107	D2	155	0-1	55.49	16.27	6.13	17.66	0.26	1.04	0.05	0.01	2.30	27.08	17.44	0.00	6.04	251.86	4.56	4.44	6.39	401.62	2.01
108	D2	155	1-3	25.87	32.66	2.62	14.63	0.00	0.02	0.00	0.01	0.00	36.61	59.33	0.00	0.00	156.01	3.30	3.30	5.38	327.77	1.64
109	D2	205	0-1	30.69	6.30	3.12	2.77	0.29	0.89	0.05	0.01	0.57	8.77	6.81	0.00	4.58	161.36	2.24	2.14	3.84	226.21	1.13
110	D2	205	1-3	21.70	15.06	2.94	4.94	0.00	0.45	0.01	0.00	0.52	12.24	10.25	0.00	2.36	200.19	2.16	2.11	4.71	270.66	1.35

Table (B6): The anion and cation content of drilled samples from the Deir Tomb, location (D2).
First fieldwork visit: August 2003.

Appendix Bb: The anion and cation content and distribution in the drilled samples. First fieldwork: August 2003.

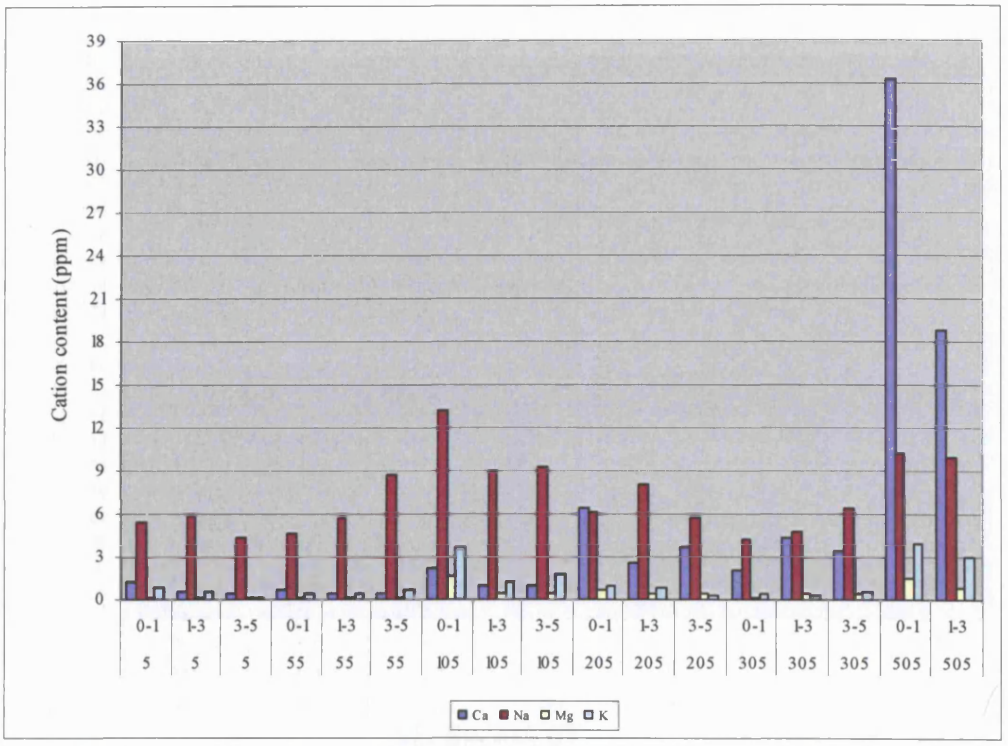

Figure (1Bb): The main cation content of drilled samples from the Bab al Siq Triclinium Tomb, location (T1) (Depth intervals: 0-1, 1-3 and 3-5 cm).
First fieldwork visit: August 2003.

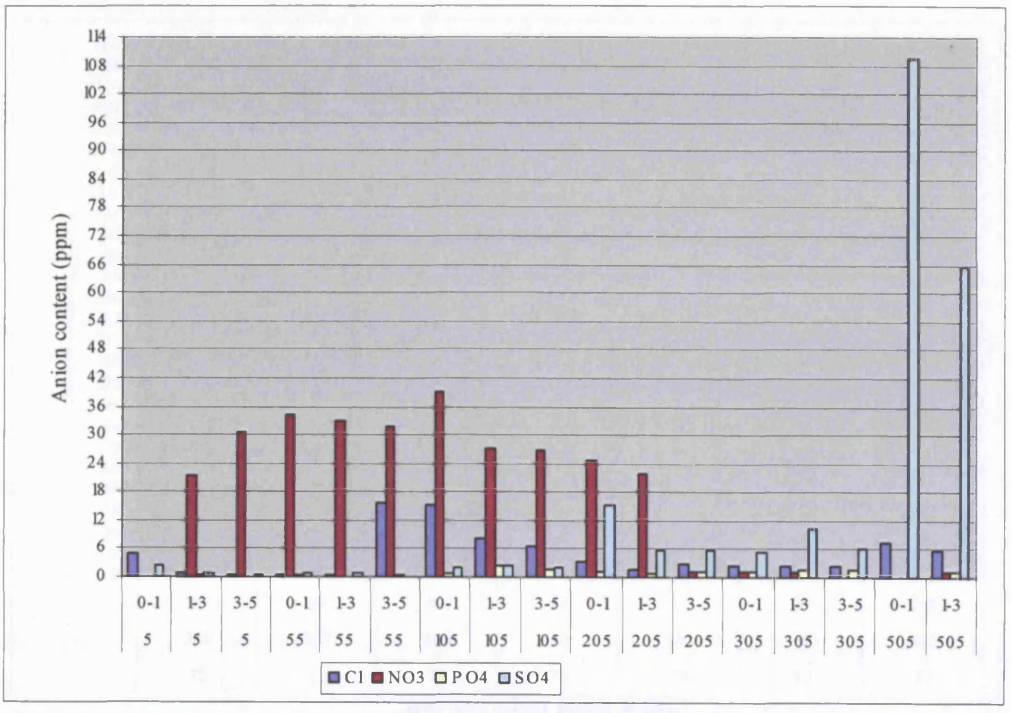

Figure (2Bb): The main anion content of drilled samples from the Bab al Siq Triclinium Tomb, location (T1) (Depth intervals: 0-1, 1-3 and 3-5 cm).
First fieldwork visit: August 2003.

Appendix Bb: The anion and cation content and distribution in the drilled samples. First fieldwork: August 2003.

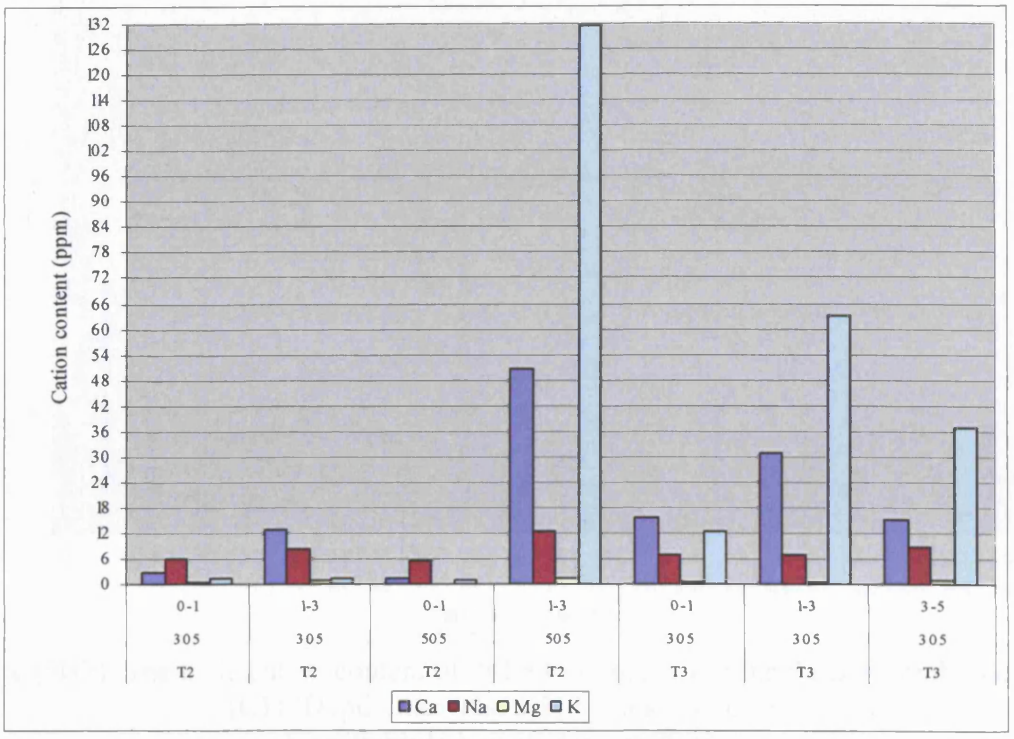

Figure (3Bb): The main cation content of drilled samples from the Bab al Siq Triclinium Tomb, locations (T2 and T3) (Depth intervals: 0-1, 1-3 and 3-5 cm).
First fieldwork visit: August 2003.

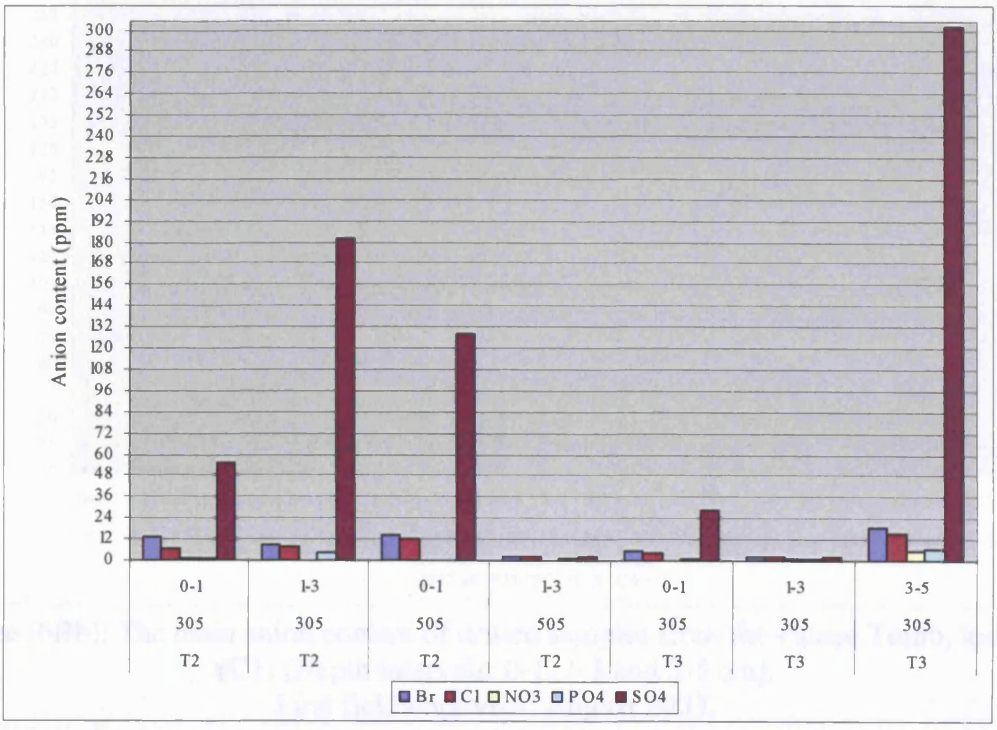

Figure (4Bb): The main anion content of drilled samples from the Bab al Siq Triclinium Tomb, locations (T2 and T3) (Depth intervals: 0-1, 1-3 and 3-5 cm).
First fieldwork visit: August 2003.

Appendix Bb: The anion and cation content and distribution in the drilled samples. First fieldwork: August 2003.

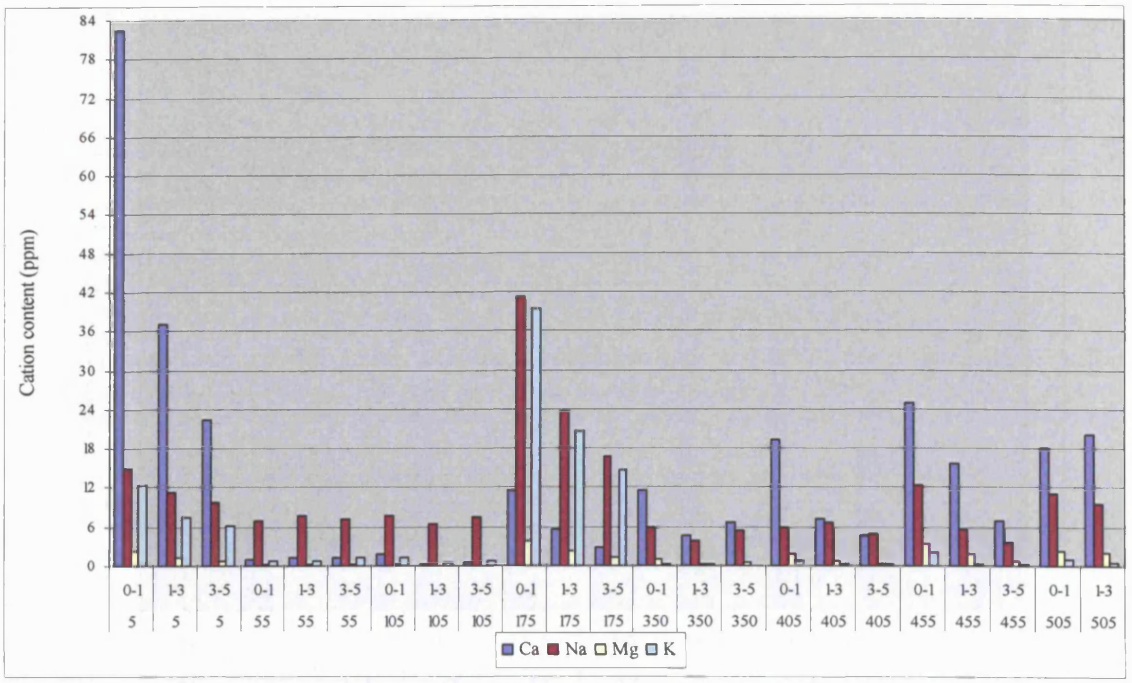

Figure (5Bb): The main cation content of drilled samples from the Palace Tomb, location (C1) (Depth intervals: 0-1, 1-3 and 3-5 cm).
First fieldwork visit: August 2003.

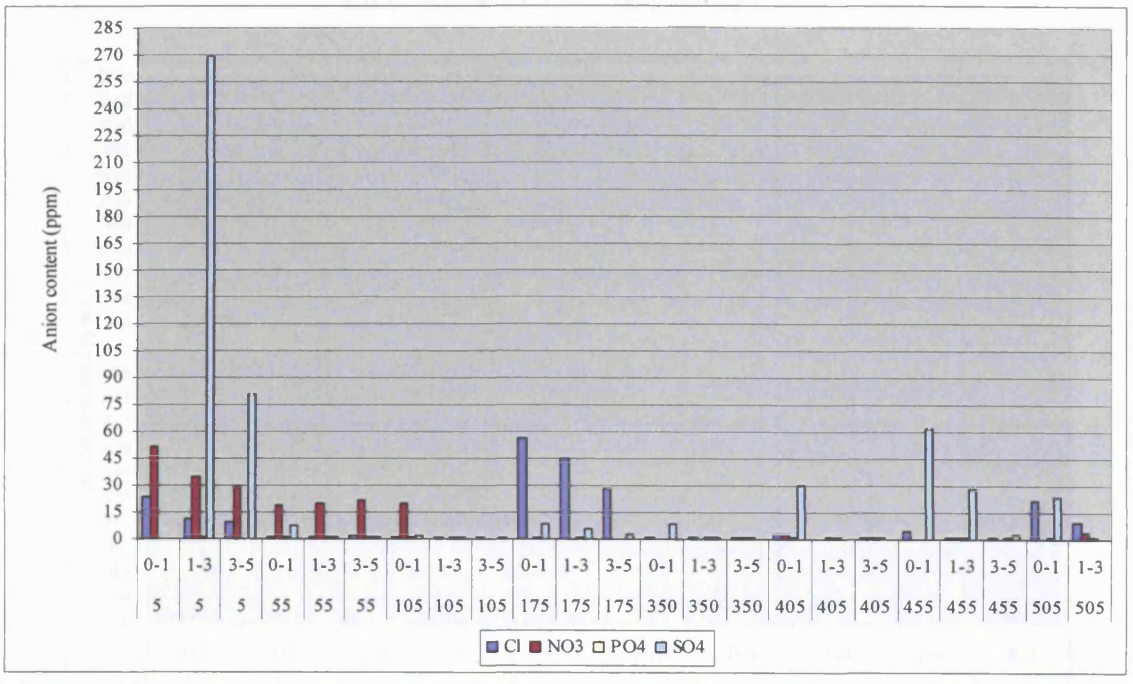

Figure (6Bb): The main anion content of drilled samples from the Palace Tomb, location (C1) (Depth intervals: 0-1, 1-3 and 3-5 cm).
First fieldwork visit: August 2003.

Appendix Bb: The anion and cation content and distribution in the drilled samples. First fieldwork: August 2003.

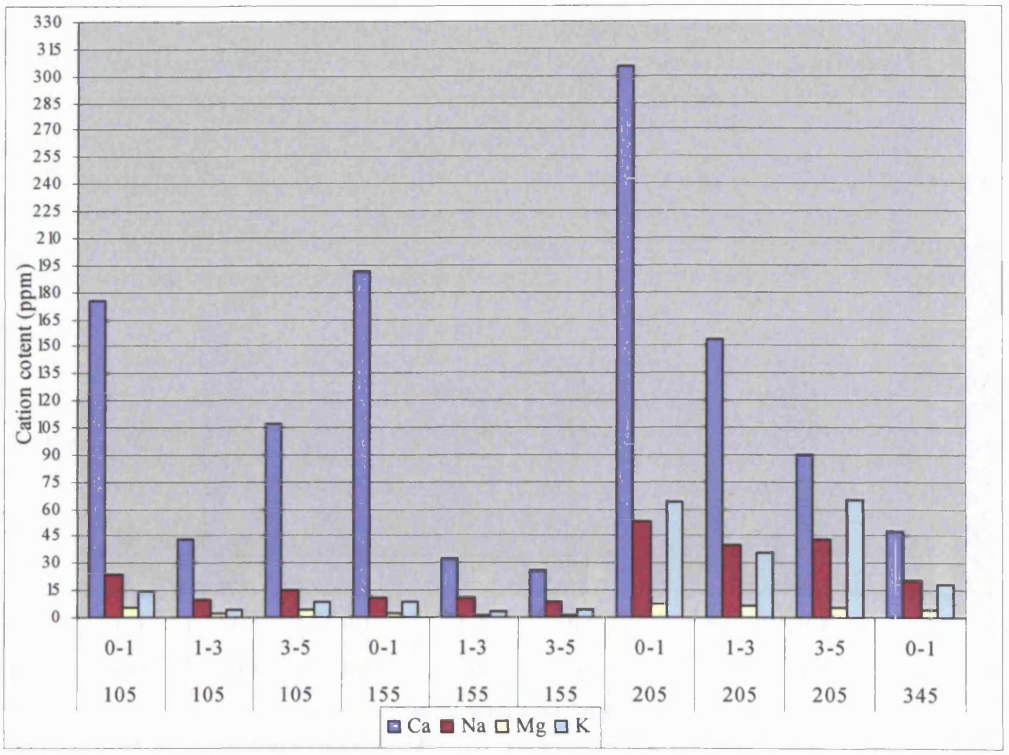

Figure (7Bb): The main cation content of drilled samples from the Palace Tomb, location (C2) (Depth intervals: 0-1, 1-3 and 3-5 cm).
First fieldwork visit: August 2003.

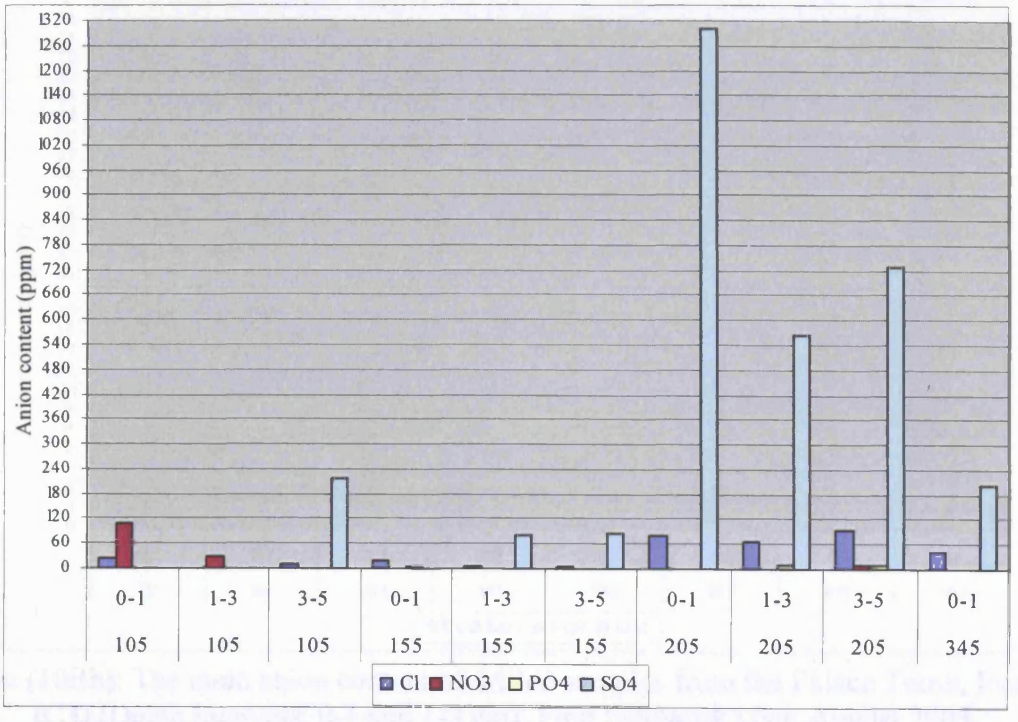

Figure (8Bb): The main anion content of drilled samples from the Palace Tomb, location (C2) (Depth intervals: 0-1, 1-3 and 3-5 cm).
First fieldwork visit: August 2003.

Appendix Bb: The anion and cation content and distribution in the drilled samples. First fieldwork: August 2003.

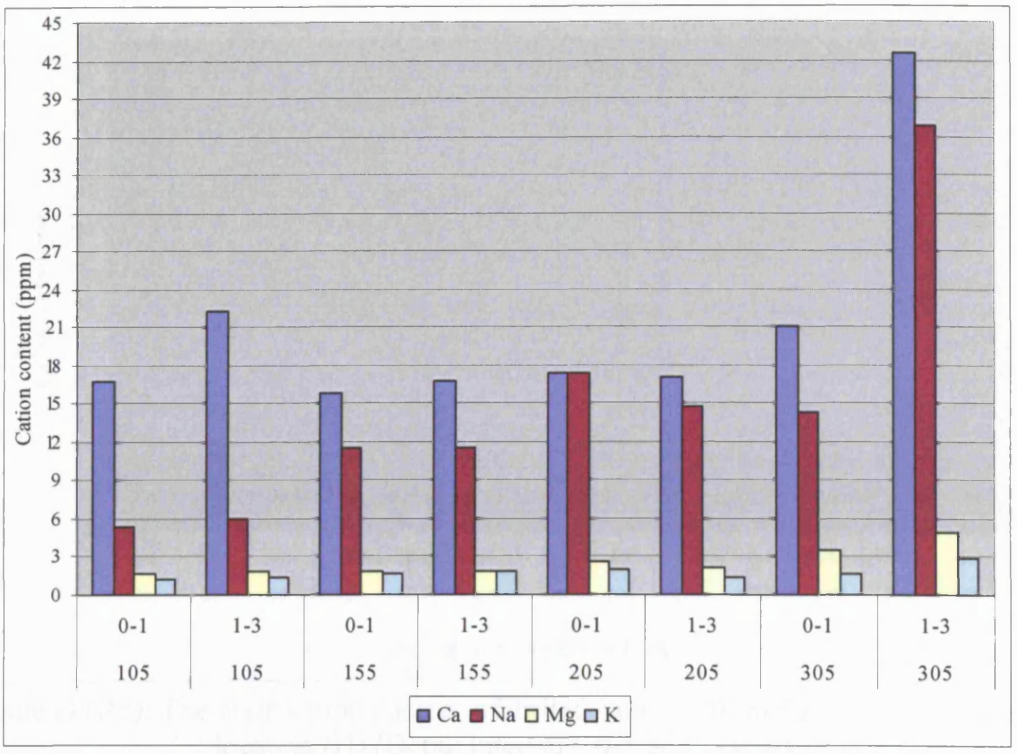

Figure (9Bb): The main cation content of drilled samples from the Palace Tomb, location (C3) (Depth intervals: 0-1 and 1-3cm). First fieldwork visit: August 2003.

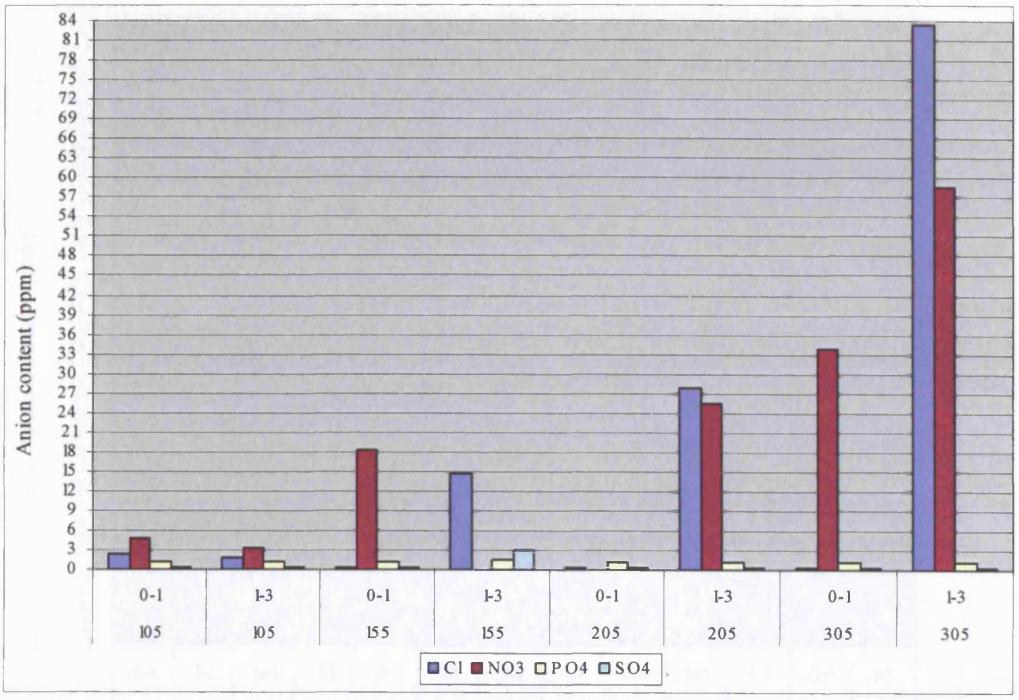

Figure (10Bb): The main anion content of drilled samples from the Palace Tomb, location (C3) (Depth intervals: 0-1 and 1-3 cm). First fieldwork visit: August 2003.

Appendix Bb: The anion and cation content and distribution in the drilled samples. First fieldwork: August 2003.

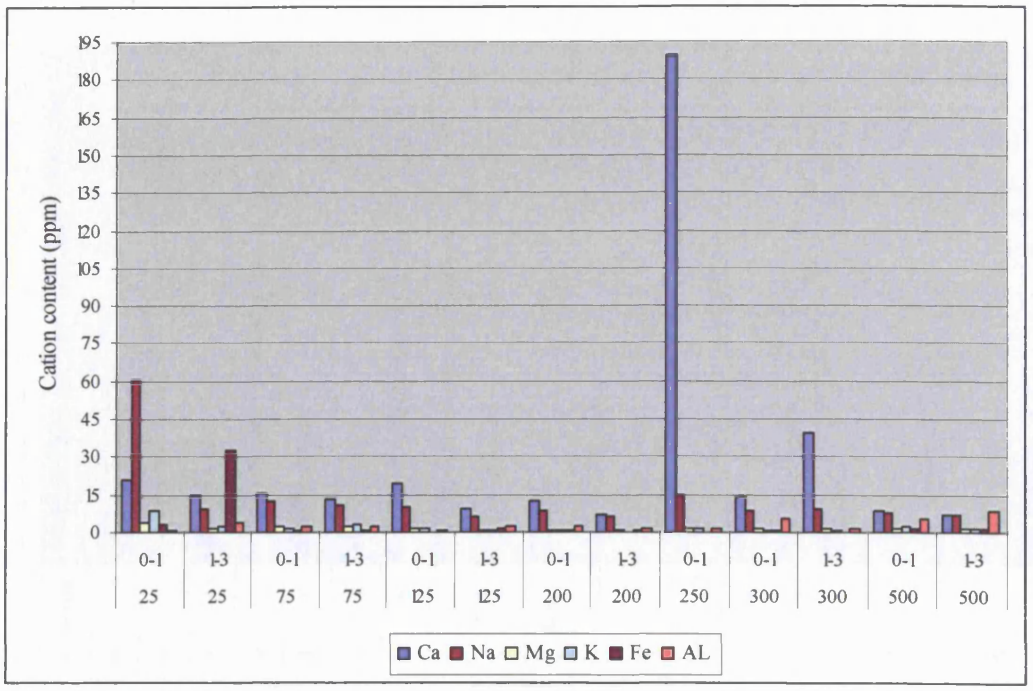

Figure (11Bb): The main cation content of drilled samples from the Corinthian Tomb, location (H) (Depth intervals: 0-1 and 1-3cm).
First fieldwork visit: August 2003.

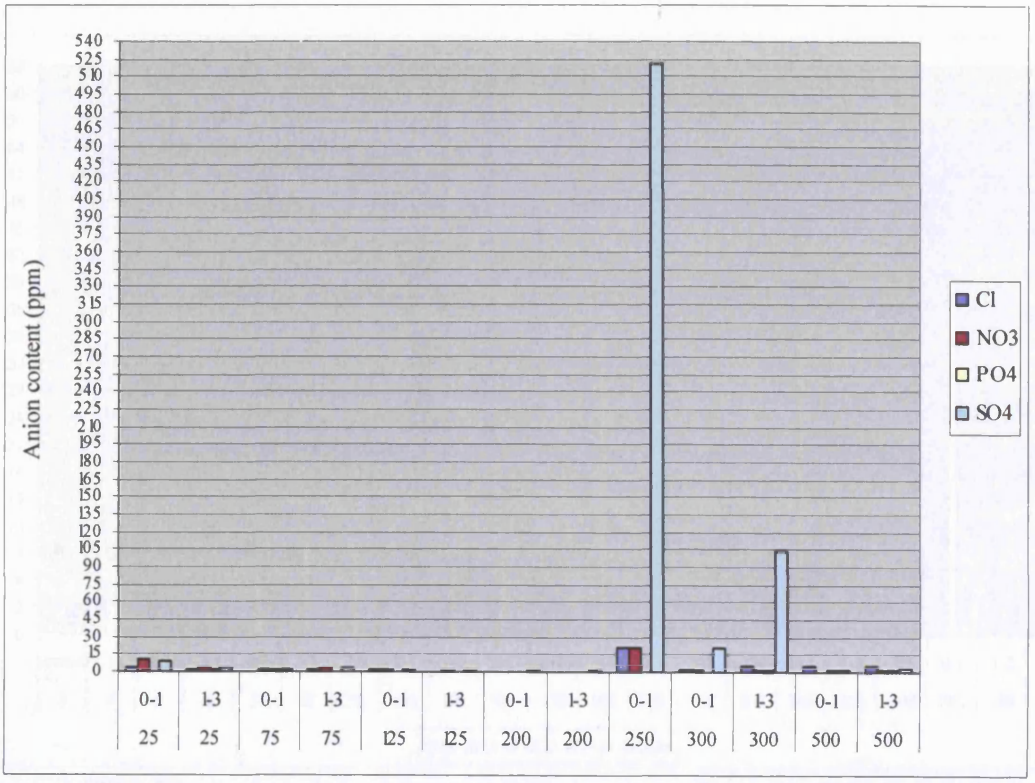

Figure (12Bb): The main anion content of drilled samples from the Corinthian Tomb, location (H) (Depth intervals: 0-1 and 1-3cm). First fieldwork visit: August 2003.

Appendix Bb: The anion and cation content and distribution in the drilled samples. First fieldwork: August 2003.

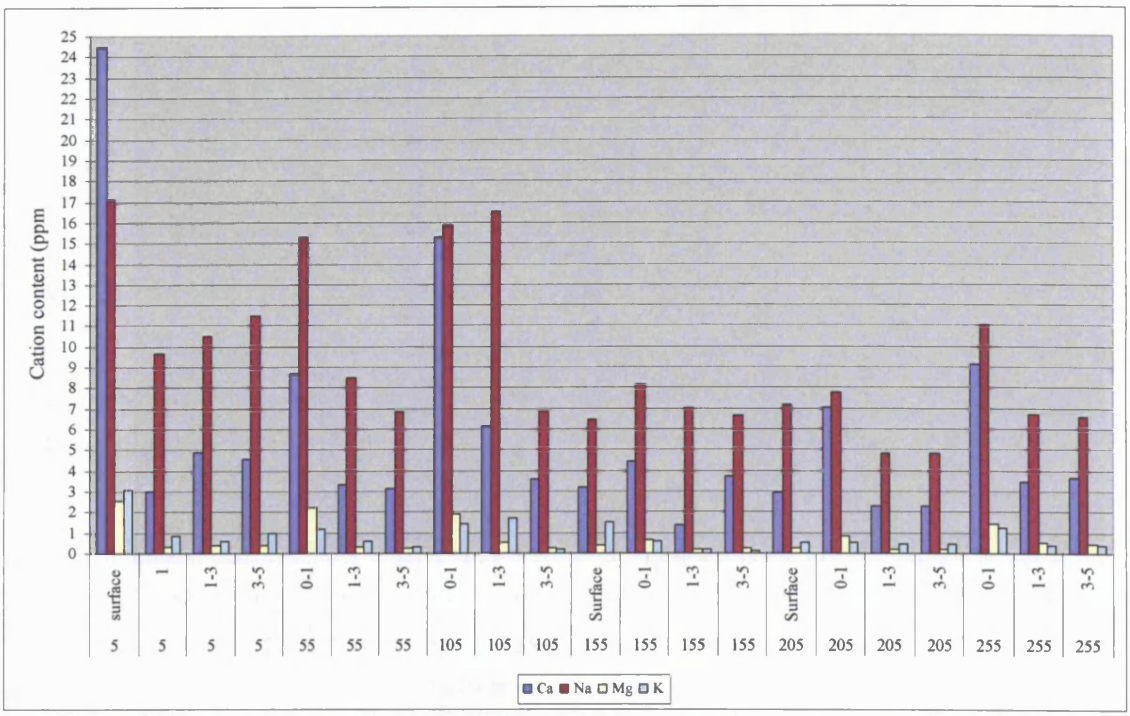

Figure (13Bb): The main cation content of drilled samples from the Deir Tomb, location (D1) (Depth intervals: surface, 0-1, 1-3 and 3-5cm).
First fieldwork visit: August 2003.

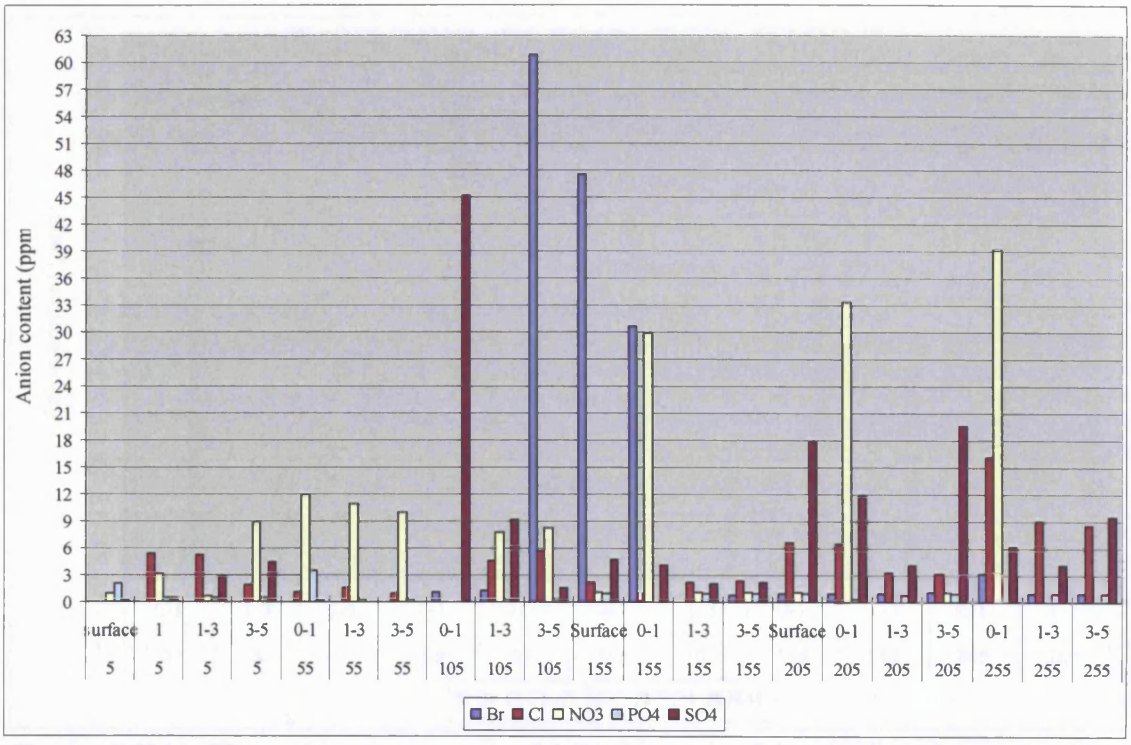

Figure (14Bb): The main anion content of drilled samples from the Deir Tomb, location (D1) (Depth intervals: surface, 0-1, 1-3 and 3-5cm).
First fieldwork visit: August 2003.

Appendix Bb: The anion and cation content and distribution in the drilled samples. First fieldwork: August 2003.

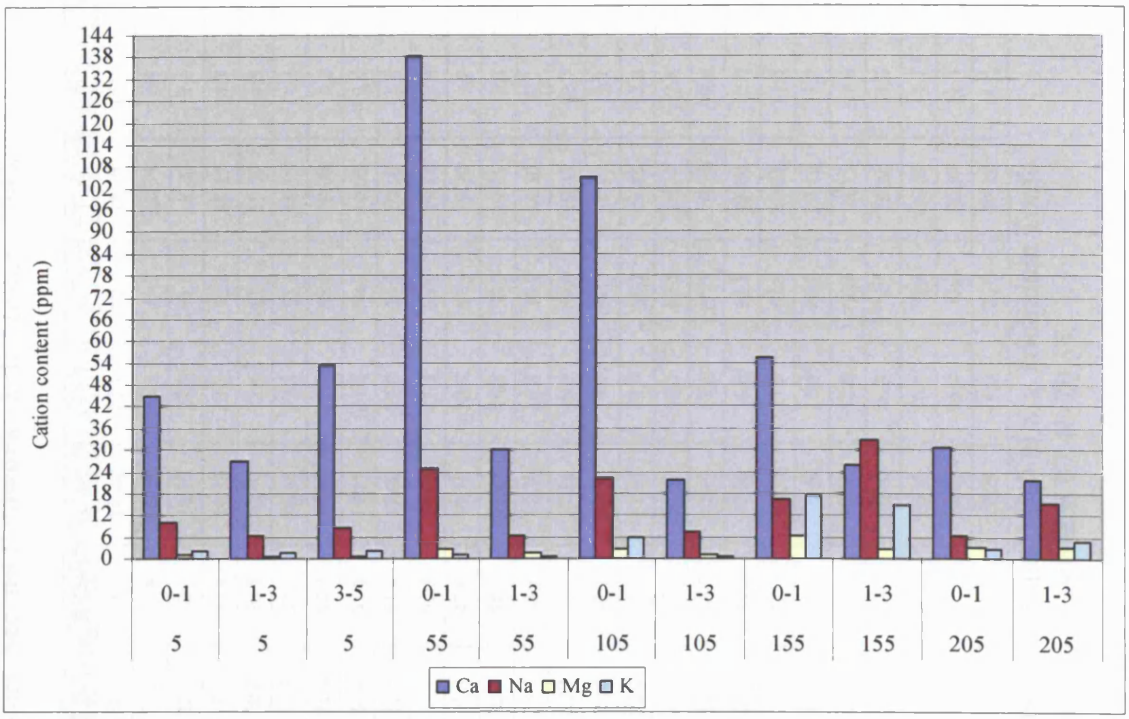

Figure (15Bb): The main cation content of drilled samples from the Deir Tomb, location (D2) (Depth intervals: 0-1, 1-3 and 3-5cm).
First fieldwork visit: August 2003.

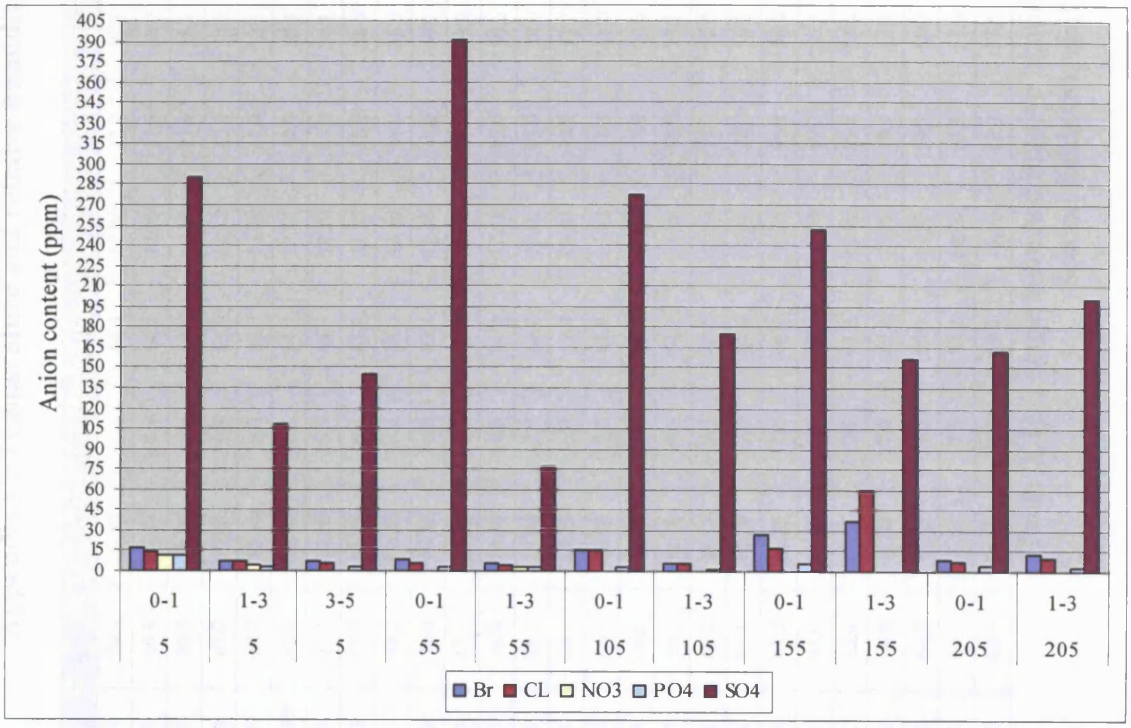

Figure (16Bb): The main anion content of drilled samples from the Deir Tomb, location (D2) (Depth intervals: 0-1, 1-3 and 3-5cm).
First fieldwork visit: August 2003.

Appendix C: Temperature and relative humidity spot readings. Second fieldwork visit: January 2004.

Time	T (°C)	RH%	Time	T (°C)	RH%	Time	T (°C)	RH%	Time	T (°C)	RH%	Time	T (°C)	RH%	Time	T (°C)	RH%
07.40	14.3	70.0	09.50	16.3	64.3	12.00	17.2	59.1	14.10	20.1	53.0	16.20	23.1	50.1	18.30	15.1	71.0
07.45	14.9	69.8	09.55	16.1	64.0	12.05	17.8	58.7	14.15	20.2	52.8	16.25	23.2	51.2	18.35	14.8	71.2
07.50	14.0	70.0	10.00	16.0	64.0	12.10	17.6	58.1	14.20	20.2	52.1	16.30	23.2	51.0	18.40	14.3	71.3
07.55	15.0	69.0	10.05	16.0	63.9	12.15	17.9	58.0	14.25	20.3	53.1	16.35	23.3	52.3	18.45	14.3	71.2
08.00	15.0	68.2	10.10	16.0	65.0	12.20	17.9	58.1	14.30	20.8	50.8	16.40	22.6	52.6	18.50	14.3	71.4
08.05	15.0	68.0	10.15	16.5	64.3	12.25	17.9	58.1	14.35	21.3	52.0	16.45	22.8	53.3	18.55	14.3	71.6
08.10	15.0	71.1	10.20	16.5	64.3	12.30	17.9	58.1	14.40	21.6	52.0	16.50	22.0	55.0	19.00	14.1	71.9
08.15	16.0	69.3	10.25	16.4	63.0	12.35	18.0	58.0	14.45	21.8	51.6	16.55	21.0	56.2	19.05	13.9	71.9
08.20	15.0	69.2	10.30	16.4	65.0	12.40	18.0	58.0	14.50	21.6	51.4	17.00	22.0	56.3	19.10	13.8	72.3
08.25	15.0	70.0	10.35	16.3	63.4	12.45	18.0	59.1	14.55	21.9	50.4	17.05	21.4	56.9	19.15	13.8	71.8
08.30	16.0	67.1	10.40	16.5	63.1	12.50	18.0	59.2	15.00	21.9	49.6	17.10	20.9	57.3	19.20	13.2	72.1
08.35	16.1	66.6	10.45	16.0	64.2	12.55	18.0	58.6	15.05	22.4	48.1	17.15	20.8	58.6	19.25	13.2	72.3
08.40	16.0	66.2	10.50	15.9	64.0	13.00	18.0	58.0	15.10	22.4	48.1	17.20	20.8	55.9	19.30	13.1	72.6
08.45	16.0	66.0	10.55	16.9	62.9	13.05	18.1	57.7	15.15	22.3	48.1	17.25	19.9	59.0	19.35	13.1	73.0
08.50	16.3	66.0	11.00	17.0	61.0	13.10	18.1	58.2	15.20	22.5	49.1	17.30	19.9	60.3	19.40	13.1	73.1
08.55	16.3	66.0	11.05	17.0	62.1	13.15	18.1	56.3	15.25	23.0	47.1	17.35	19.9	61.2	19.45	12.8	73.7
09.00	16.3	65.0	11.10	17.0	62.1	13.20	18.0	57.2	15.30	23.1	47.3	17.40	18.5	62.5	19.50	12.8	73.2
09.05	15.6	65.0	11.15	17.0	63.1	13.25	18.0	56.3	15.35	23.1	46.5	17.45	18.6	65.3	19.55	12.8	73.0
09.10	15.6	65.1	11.20	17.0	61.8	13.30	18.0	58.2	15.40	23.1	48.6	17.50	18.6	65.8	20.00	12.8	74.0
09.15	16.1	65.2	11.25	17.1	61.1	13.35	19.0	56.0	15.45	23.8	48.2	17.55	17.9	67.9	20.05	11.4	74.6
09.20	16.0	64.0	11.30	17.1	61.1	13.40	19.2	55.6	15.50	23.8	48.0	18.00	17.9	68.0	20.10	11.3	74.5
09.25	16.2	63.4	11.35	17.0	61.2	13.45	19.1	55.0	15.55	23.8	47.5	18.05	17.8	68.1	20.15	11.6	74.1
09.30	16.2	64.5	11.40	17.0	62.0	13.50	19.1	53.9	16.00	24.1	46.0	18.10	16.3	70.3	20.20	11.1	74.2
09.35	16.2	64.2	11.45	17.3	59.9	13.55	19.3	55.0	16.05	24.1	46.1	18.15	16.4	70.2	20.25	11.1	74.2
09.40	16.2	64.5	11.50	17.5	58.0	14:00	19.3	54.6	16.10	24.1	46.5	18.20	16.0	70.6	20.30	11.4	74.9
09.45	16.2	64.3	11.55	17.2	59.0	14.05	19.0	55.5	16.15	24.0	47.0	18.25	15.8	70.9	20.35	11.4	73.8

Table (C1): Temperature and relative humidity spot readings. Location: Bab al Siq Triclinium Tomb.
Second fieldwork visit: 16-17 January 2004, between 07.40-20.35.

Appendix C: Temperature and relative humidity spot readings. Second fieldwork visit: January 2004.

Time	T (°C)	RH%	Time	T (°C)	RH%	Time	T (°C)	RH%	Time	T (°C)	RH%	Time	T (°C)	RH%
20.40	11.3	73.0	22.50	11.1	74.0	01.00	10.6	74.2	03.10	10.8	74.2	05.20	11.0	72.9
20.45	11.3	73.2	22.55	11.0	74.0	01.05	10.6	73.9	03.15	10.8	74.3	05.25	11.0	72.5
20.50	11.4	73.0	23.00	11.0	73.6	01.10	10.6	73.6	03.20	10.8	74.1	05.30	11.2	72.3
20.55	11.4	72.8	23.05	11.0	73.2	01.15	10.6	74.1	03.25	10.4	74.3	05.35	11.3	73.0
21.00	11.4	73.1	23.10	11.0	73.0	01.20	10.6	74.3	03.30	101.4	74.6	05.40	11.6	72.1
21.05	11.3	73.2	23.15	10.9	74.1	01.25	10.3	74.6	03.35	10.5	74.9	05.45	11.7	72.5
21.10	11.3	73.0	23.20	10.9	74.5	01.30	10.3	74.5	03.40	10.5	74.1	05.50	11.7	72.3
21.15	11.4	73.3	23.25	11.0	73.4	01.35	10.3	74.6	03.45	10.5	74.6	05.55	11.9	73.0
21.20	11.4	73.2	23.30	10.8	74.0	01.40	10.0	75.1	03.50	10.5	74.6	06.00	12.1	72.0
21.25	11.4	73.3	23.35	10.8	74.1	01.45	10.2	75.0	03.55	10.6	74.9	06.05	12.3	71.8
21.30	11.3	73.3	23.40	10.8	74.2	01.50	10.1	75.1	04.00	10.6	74.8	06.10	12.3	71.6
21.35	11.6	72.3	23.45	10.8	73.9	01.55	10.1	75.1	04.05	10.6	74.9	06.15	12.3	71.6
21.40	11.6	72.1	23.50	11.0	73.2	02.00	10.1	75.1	04.10	10.6	74.5	06.20	12.4	71.3
21.45	11.5	72.3	23.55	11.0	73.4	02.05	10.1	75.0	04.15	10.6	73.3	06.25	12.6	71.4
21.50	11.5	72.5	00.00	10.8	74.1	02.10	10.0	75.0	04.20	10.5	73.1	06.30	12.8	71.3
21.55	11.5	72.5	00.05	10.8	74.6	02.15	10.1	74.8	04.25	10.5	73.0	06.35	12.8	71.0
22.00	11.5	72.6	00.10	10.8	74.5	02.20	9.9	75.9	04.30	10.5	73.0	06.40	13.0	71.0
22.05	11.3	73.0	00.15	10.7	74.0	02.25	9.9	75.9	04.35	10.5	73.0	06.45	13.0	70.8
22.10	11.4	72.8	00.20	10.9	73.5	02.30	10.3	75.4	04.40	10.6	73.2	06.50	13.1	70.5
22.15	11.3	72.8	00.25	11.0	73.0	02.35	10.3	75.3	04.45	10.6	73.0	06.55	13.3	70.3
22.20	11.2	73.1	00.30	10.8	73.1	02.40	10.3	75.2	04.50	10.1	73.0	07.00	13.6	70.2
22.25	11.2	73.0	00.35	10.4	74.6	02.45	10.4	75.3	04.55	10.1	72.8			
22.30	11.2	73.6	00.40	10.6	74.5	02.50	10.4	75.5	05.00	10.1	72.9			
22.35	11.2	73.6	00.45	10.6	74.3	02.55	10.6	75.3	05.05	10.6	72.5			
22.40	11.3	73.2	00.50	10.5	74.6	03.00	10.6	74.3	05.10	10.7	72.1			
22.45	11.3	73.4	00.55	10.5	74.6	03.05	10.7	75.1	05.15	10.8	72.1			

Table (C2): Temperature and relative humidity spot readings. Location: Bab al Siq Triclinium Tomb.
Second fieldwork visit: 16-17 January 2004, between 20.40-07.00.

Appendix C: Temperature and relative humidity spot readings. Second fieldwork visit: January 2004.

Time	T (°C)	RH%	Time	T (°C)	RH%	Time	T (°C)	RH%	Time	T (°C)	RH%	Time	T (°C)	RH%	Time	T (°C)	RH%
07.40	15.0	68.5	09.50	17.6	63.1	12.00	18.9	56.4	14.10	20.3	52.1	16.20	24.3	45.0	18.30	17.3	65.0
07.45	15.1	68.4	09.55	17.5	63.0	12.05	18.9	55.9	14.15	20.4	52.2	16.25	24.3	46.8	18.35	17.0	66.2
07.50	15.2	68.6	10.00	17.5	63.3	12.10	19.0	55.0	14.20	20.4	52.0	16.30	24.0	47.2	18.40	17.0	66.0
07.55	15.2	68.0	10.05	17.5	63.4	12.15	19.0	55.5	14.25	20.6	51.9	16.35	24.0	47.6	18.45	16.5	67.1
08.00	15.2	67.5	10.10	17.5	62.8	12.20	19.0	55.3	14.30	20.6	51.8	16.40	23.8	48.1	18.50	16.5	67.3
08.05	15.6	67.0	10.15	17.4	62.9	12.25	18.5	54.2	14.35	20.8	51.3	16.45	23.8	48.8	18.55	16.5	67.5
08.10	15.6	67.4	10.20	17.4	63.0	12.30	18.6	54.2	14.40	20.8	51.2	16.50	23.8	47.6	19.00	16.4	68.0
08.15	15.5	68.1	10.25	17.4	62.8	12.35	18.6	54.2	14.45	20.8	51.0	16.55	23.6	49.1	19.05	16.4	68.0
08.20	15.5	68.0	10.30	17.4	63.0	12.40	19.1	54.0	14.50	20.8	51.9	17.00	23.6	50.1	19.10	16.1	69.0
08.25	15.5	67.8	10.35	17.3	63.2	12.45	19.1	54.0	14.55	20.8	51.8	17.05	22.3	50.5	19.15	16.3	69.0
08.30	15.5	67.5	10.40	17.2	62.5	12.50	19.1	53.8	15.00	20.9	51.0	17.10	22.3	51.1	19.20	16.3	68.8
08.35	16.0	66.3	10.45	17.1	60.9	12.55	19.1	54.3	15.05	20.9	50.8	17.15	22.0	52.1	19.25	16.0	69.9
08.40	16.3	66.4	10.50	17.1	61.1	13.00	19.3	54.2	15.10	20.9	50.6	17.20	21.6	52.9	19.30	15.8	70.0
08.45	16.3	66.3	10.55	17.5	60.5	13.05	19.3	53.9	15.15	20.9	50.6	17.25	21.6	53.6	19.35	15.4	70.5
08.50	16.3	66.3	11.00	18.1	59.0	13.10	19.3	53.6	15.20	21.3	49.2	17.30	21.0	54.6	19.40	15.1	70.4
08.55	16.6	66.1	11.05	18.0	59.1	13.15	19.4	53.7	15.25	21.3	49.6	17.35	20.3	55.5	19.45	15.0	70.6
09.00	16.8	65.4	11.10	18.1	58.9	13.20	19.5	53.6	15.30	21.4	50.0	17.40	19.6	57.3	19.50	15.0	70.7
09.05	16.8	66.2	11.15	18.2	58.8	13.25	19.5	53.6	15.35	21.8	49.8	17.45	19.4	58.4	19.55	14.5	71.2
09.10	16.8	65.4	11.20	18.2	58.3	13.30	19.7	53.2	15.40	21.8	49.6	17.50	18.3	59.7	20.00	14.6	71.6
09.15	16.9	65.3	11.25	18.3	58.0	13.35	19.8	53.2	15.45	21.8	49.4	17.55	18.8	60.3	20.05	14.3	72.2
09.20	17.1	64.2	11.30	18.5	57.5	13.40	19.8	53.0	15.50	22.2	48.2	18.00	18.9	61.2	20.10	14.3	71.0
09.25	17.2	64.4	11.35	18.6	57.6	13.45	20.1	53.1	15.55	22.6	47.6	18.05	18.4	62.3	20.15	14.0	71.0
09.30	17.2	64.0	11.40	18.8	57.8	13.50	20.1	52.0	16.00	23.3	46.2	18.10	18.1	62.9	20.20	14.1	72.0
09.35	17.5	63.8	11.45	18.8	58.0	13.55	20.3	52.1	16.05	24.1	45.0	18.15	17.9	63.8	20.25	13.8	71.6
09.40	17.6	63.1	11.50	18.8	57.2	14:00	20.4	52.0	16.10	24.3	45.3	18.20	18.0	63.9	20.30	13.4	71.8
09.45	17.6	63.2	11.55	18.8	57.0	14.05	20.4	52.3	16.15	24.6	45.1	18.25	17.7	64.8	20.35	13.2	72.2

Table (C3): Temperature and relative humidity spot readings. Location: Palace Tomb.
Second fieldwork visit: 17-18 January 2004, between 07.40-20.35.

Appendix C: Temperature and relative humidity spot readings. Second fieldwork visit: January 2004.

Time	T (°C)	RH%	Time	T (°C)	RH%	Time	T (°C)	RH%	Time	T (°C)	RH%	Time	T (°C)	RH%
20.40	13.4	72.1	22.50	12.2	73.4	01.00	11.2	74.3	03.10	10.8	73.0	05.20	10.8	72.3
20.45	13.2	72.8	22.55	12.1	74.5	01.05	11.2	74.3	03.15	10.9	73.1	05.25	11.0	72.0
20.50	13.2	72.9	23.00	12.1	74.0	01.10	11.2	74.5	03.20	10.9	73.4	05.30	11.2	72.1
20.55	13.0	73.0	23.05	12.1	74.2	01.15	11.3	74.0	03.25	10.8	73.6	05.35	11.2	72.3
21.00	12.8	73.1	23.10	12.1	74.0	01.20	11.3	73.8	03.30	10.8	73.7	05.40	11.3	71.9
21.05	12.8	73.1	23.15	12.0	74.3	01.25	11.2	73.7	03.35	10.7	74.0	05.45	11.6	71.8
21.10	12.9	72.8	23.20	12.0	73.9	01.30	11.3	73.4	03.40	10.6	74.1	05.50	11.9	71.6
21.15	13.0	72.0	23.25	11.8	74.2	01.35	11.2	73.9	03.45	10.6	74.2	05.55	11.9	71.3
21.20	13.1	71.5	23.30	11.8	74.1	01.40	11.2	74.0	03.50	10.8	74.5	06.00	12.0	71.0
21.25	12.8	72.1	23.35	11.6	74.6	01.45	11.3	73.5	03.55	10.8	74.3	06.05	12.0	71.3
21.30	12.2	72.9	23.40	11.5	74.5	01.50	11.0	73.9	04.00	10.8	74.5	06.10	12.3	71.0
21.35	12.5	72.4	23.45	11.5	74.8	01.55	10.9	74.3	04.05	10.9	74.0	06.15	12.1	71.4
21.40	12.5	72.9	23.50	11.6	74.4	02.00	10.9	74.6	04.10	10.9	73.9	06.20	12.4	70.8
21.45	12.5	72.6	23.55	11.5	74.5	02.05	10.8	74.7	04.15	10.5	73.5	06.25	12.4	70.6
21.50	12.5	72.6	00.00	11.4	74.4	02.10	10.8	74.6	04.20	10.5	73.2	06.30	12.6	70.7
21.55	12.5	72.4	00.05	11.4	74.0	02.15	10.9	74.1	04.25	10.5	74.0	06.35	13.0	70.5
22.00	12.5	72.3	00.10	11.4	73.87	02.20	10.9	74.3	04.30	10.6	74.2	06.40	13.2	69.9
22.05	12.6	72.2	00.15	11.3	73.5	02.25	11.0	74.0	04.35	10.5	74.3	06.45	13.2	70.0
22.10	12.6	72.8	00.20	11.2	74.2	02.30	11.0	74.0	04.40	10.5	74.3	06.50	13.6	69.7
22.15	12.6	72.9	00.25	11.2	74.06	02.35	11.0	73.7	04.45	10.4	73.6	06.55	13.8	68.7
22.20	12.4	73.1	00.30	11.1	74.8	02.40	11.1	73.2	04.50	10.4	73.8	07.00	13.9	68.9
22.25	12.4	73.3	00.35	11.2	74.1	02.45	10.9	74.1	04.55	10.5	73.2			
22.30	12.3	73.4	00.40	11.2	74.0	02.50	11.0	73.5	05.00	10.5	73.0			
22.35	12.3	73.0	00.45	11.3	73.8	02.55	11.0	73.6	05.05	10.6	72.8			
22.40	12.2	73.5	00.50	11.2	74.1	03.00	11.0	73.2	05.10	10.6	72.6			

Table (C4): Temperature and relative humidity spot readings. Location: Palace Tomb.
Second fieldwork visit: 17-18 January 2004, between 20.40-07.00.

Appendix C: Temperature and relative humidity spot readings. Second fieldwork visit: January 2004.

Time	T (°C)	RH%	Time	T (°C)	RH%	Time	T (°C)	RH%	Time	T (°C)	RH%	Time	T (°C)	RH%	Time	T (°C)	RH%
07.40	14.6	65.8	09.50	15.8	63.0	12.00	17.2	58.5	14.10	18.6	55.3	16.20	18.5	59.6	18.30	15.4	65.8
07.45	14.3	65.1	09.55	15.4	63.1	12.05	17.2	58.2	14.15	18.9	55.0	16.25	18.1	60.2	18.35	15.3	65.9
07.50	14.3	65.0	10.00	15.4	62.8	12.10	17.6	58.0	14.20	18.9	55.1	16.30	17.9	60.3	18.40	15.3	59.9
07.55	14.1	65.3	10.05	15.3	63.1	12.15	17.6	58.0	14.25	19.0	54.8	16.35	17.9	60.4	18.45	15.3	60.3
08.00	14.1	65.2	10.10	15.5	63.3	12.20	17.6	57.9	14.30	19.1	54.3	16.40	17.8	60.6	18.50	15.2	60.5
08.05	14.1	65.0	10.15	15.5	62.8	12.25	17.8	57.6	14.35	19.1	54.2	16.45	17.6	61.2	18.55	15.2	60.6
08.10	14.1	65.2	10.20	15.5	62.7	12.30	17.5	58.0	14.40	19.0	54.3	16.50	17.6	61.3	19.00	15.0	61.2
08.15	14.0	65.0	10.25	15.5	62.8	12.35	17.7	57.9	14.45	19.0	54.4	16.55	17.5	62.0	19.05	15.0	61.3
08.20	14.3	64.2	10.30	15.6	62.4	12.40	17.7	57.8	14.50	19.3	54.0	17.00	17.5	62.3	19.10	15.0	61.3
08.25	14.3	65.0	10.35	15.7	62.4	12.45	17.7	57.7	14.55	19.3	54.1	17.05	17.1	62.8	19.15	15.0	61.4
08.30	14.3	64.2	10.40	15.9	62.9	12.50	17.8	57.6	15.00	19.0	54.3	17.10	17.2	62.9	19.20	14.6	62.3
08.35	14.3	64.0	10.45	15.9	61.5	12.55	17.8	57.3	15.05	19.4	53.8	17.15	17.2	63.0	19.25	14.6	63.4
08.40	14.8	64.0	10.50	15.9	61.3	13.00	17.7	57.5	15.10	19.4	53.7	17.20	17.0	62.5	19.30	14.4	63.7
08.45	14.8	63.9	10.55	15.9	61.2	13.05	18.0	57.0	15.15	19.3	57.9	17.25	16.8	63.4	19.35	14.4	63.9
08.50	14.8	64.0	11.00	16.2	60.3	13.10	18.0	56.9	15.20	19.3	57.4	17.30	16.8	63.4	19.40	14.3	63.8
08.55	14.9	63.9	11.05	16.2	60.6	13.15	18.0	56.8	15.25	19.1	57.0	17.35	16.8	63.9	19.45	14.3	64.0
09.00	14.9	63.4	11.10	16.3	60.0	13.20	18.0	56.5	15.30	19.0	57.8	17.40	16.7	63.8	19.50	14.2	64.3
09.05	14.9	64.0	11.15	16.6	60.1	13.25	18.1	56.5	15.35	19.0	57.9	17.45	16.2	64.2	19.55	14.2	65.0
09.10	15.2	64.1	11.20	16.4	60.1	13.30	18.1	56.0	15.40	19.0	58.2	17.50	16.2	64.2	20.00	14.2	65.1
09.15	15.3	63.8	11.25	16.3	60.3	13.35	18.2	55.8	15.45	19.0	58.3	17.55	16.0	64.6	20.05	14.0	65.3
09.20	15.3	63.8	11.30	16.6	59.8	13.40	18.2	55.4	15.50	19.0	58.6	18.00	16.0	65.0	20.10	13.9	66.6
09.25	15.4	63.4	11.35	16.8	59.7	13.45	18.4	55.4	15.55	19.0	58.8	18.05	15.8	65.1	20.15	13.8	66.9
09.30	15.6	63.1	11.40	16.9	58.9	13.50	18.4	55.5	16.00	18.7	59.0	18.10	15.8	65.3	20.20	13.5	67.1
09.35	15.7	63.0	11.45	17.0	58.8	13.55	18.5	55.0	16.05	18.7	59.2	18.15	15.8	65.3	20.25	13.5	67.3
09.40	15.8	62.8	11.50	17.2	58.8	14:00	18.5	55.6	16.10	18.5	59.3	18.20	15.8	65.4	20.30	13.4	67.8
09.45	15.8	63.0	11.55	17.3	58.6	14.05	18.5	55.3	16.15	18.5	59.5	18.25	15.4	65.2	20.35	13.4	68.2

Table (C5): Temperature and relative humidity spot readings. Location: The Deir Tomb.
Second fieldwork visit: 18-19 January 2004, between 07.40-20.35.

Appendix C: Temperature and relative humidity spot readings. Second fieldwork visit: January 2004.

Time	T (°C)	RH%	Time	T (°C)	RH%	Time	T (°C)	RH%	Time	T (°C)	RH%	Time	T (°C)	RH%
20.40	13.0	69.0	22.50	11.5	73.0	01.00	10.8	74.9	03.10	11.0	75.0	05.20	12.0	71.9
20.45	13.1	69.1	22.55	11.5	73.2	01.05	11.0	74.9	03.15	10.9	75.2	05.25	12.0	71.0
20.50	13.0	69.3	23.00	11.5	73.3	01.10	11.0	74.5	03.20	10.8	75.9	05.30	12.0	71.0
20.55	12.5	70.1	23.05	11.4	73.1	01.15	11.0	74.4	03.25	11.0	75.1	05.35	12.3	71.1
21.00	12.3	70.2	23.10	11.4	73.5	01.20	11.0	74.4	03.30	11.0	74.8	05.40	12.3	69.7
21.05	12.3	70.4	23.15	11.4	73.4	01.25	11.0	74.3	03.35	11.1	74.7	05.45	12.4	69.7
21.10	12.3	70.5	23.20	11.4	73.6	01.30	11.1	74.0	03.40	11.1	74.6	05.50	12.4	68.5
21.15	12.4	70.6	23.25	11.4	73.5	01.35	11.0	74.2	03.45	11.1	74.8	05.55	12.4	68.9
21.20	12.4	71.2	23.30	11.4	73.7	01.40	10.9	75.0	03.50	11.2	74.6	06.00	12.4	68.4
21.25	12.4	71.6	23.35	11.4	73.3	01.45	10.9	75.1	03.55	11.2	74.3	06.05	12.4	68.0
21.30	12.4	71.8	23.40	11.2	74.0	01.50	10.9	75.3	04.00	11.2	74.5	06.10	12.6	67.0
21.35	12.4	71.9	23.45	11.2	74.2	01.55	10.8	75.6	04.05	11.3	74.3	06.15	12.6	66.9
21.40	12.3	71.9	23.50	11.2	74.6	02.00	10.8	75.8	04.10	11.3	74.6	06.20	12.6	66.8
21.45	12.3	72.0	23.55	11.2	74.5	02.05	10.8	75.9	04.15	11.3	74.6	06.25	12.5	66.6
21.50	12.3	72.1	00.00	11.2	74.8	02.10	10.8	75.8	04.20	11.4	74.2	06.30	12.6	66.5
21.55	11.9	72.1	00.05	11.3	75.0	02.15	10.9	75.8	04.25	11.4	74.0	06.35	12.8	66.5
22.00	11.9	72.3	00.10	11.2	75.0	02.20	10.9	75.4	04.30	11.4	73.8	06.40	12.9	66.7
22.05	11.8	72.5	00.15	11.5	75.0	02.25	10.9	75.4	04.35	11.5	73.6	06.45	12.9	66.5
22.10	11.8	72.3	00.20	11.4	75.1	02.30	10.9	75.3	04.40	11.5	73.5	06.50	13.0	66.4
22.15	11.8	72.6	00.25	11.2	74.9	02.35	10.9	75.3	04.45	11.5	73.2	06.55	13.1	66.4
22.20	11.8	72.8	00.30	11.0	74.6	02.40	10.8	75.2	04.50	11.6	73.1	07.00	13.1	66.5
22.25	11.9	72.6	00.35	11.0	75.0	02.45	10.8	75.2	04.55	11.7	73.1			
22.30	11.8	72.6	00.40	11.0	75.1	02.50	10.8	75.0	05.00	11.8	73.0			
22.35	11.8	72.5	00.45	11.0	74.8	02.55	10.8	75.1	05.05	11.9	73.0			
22.40	11.8	72.6	00.50	11.0	74.6	03.00	10.8	74.9	05.10	11.8	72.8			
22.45	11.6	72.7	00.55	10.9	74.5	03.00	10.8	75.0	05.10	11.9	72.8			

Table (C6): Temperature and relative humidity spot readings. Location: The Deir Tomb.
Second fieldwork visit: 18-19 January 2004, between 20.40-07.00.

Appendix D: Wind speed spot readings. Second fieldwork visit: January 2004.

Location	Date	Height (cm)	Time	Maximum wind speed (m/s)	Minimum wind speed (m/s)	Average wind speed (m/s)	Location	Date	Height (cm)	Time	Maximum wind speed (m/s)	Minimum wind speed (m/s)	Average wind speed (m/s)
T1	10.1.2004	5	08.30	0.7	0.0	0.3	T1	10.1.2004	205	08.35	0.9	0.0	0.5
T1	10.1.2004	5	09.30	1.1	0.1	0.4	T1	10.1.2004	205	09.35	1.2	0.0	0.6
T1	10.1.2004	5	12.30	0.6	0.1	0.3	T1	10.1.2004	205	12.35	0.5	0.1	0.3
T1	10.1.2004	5	14.30	1.1	0.3	0.6	T1	10.1.2004	205	14.35	1.0	0.2	0.6
T1	10.1.2004	5	15.30	3.0	0.2	1.5	T1	10.1.2004	205	15.35	3.6	0.5	1.7
T1	10.1.2004	5	16.30	3.3	0.3	1.8	T1	10.1.2004	205	16.35	4.0	0.3	1.6
T1	10.1.2004	5	17.30	3.0	0.1	1.6	T1	10.1.2004	205	17.35	4.1	0.3	1.9
T1	12.1.2004	5	08.30	0.8	0.0	0.4	T1	12.1.2004	205	08.35	1.1	0.2	0.5
T1	12.1.2004	5	09.30	1.6	0.2	0.5	T1	12.1.2004	205	09.35	1.8	0.3	0.9
T1	12.1.2004	5	12.30	0.4	0.0	0.3	T1	12.1.2004	205	12.35	0.6	0.2	0.5
T1	12.1.2004	5	14.30	1.3	0.2	0.8	T1	12.1.2004	205	14.35	3.7	0.4	2.1
T1	12.1.2004	5	15.30	2.4	0.3	1.5	T1	12.1.2004	205	15.35	4.2	0.4	2.3
T1	12.1.2004	5	16.30	3.6	0.3	1.8	T1	12.1.2004	205	16.35	4.3	0.4	2.3
T1	12.1.2004	5	17.30	4.0	0.5	2.0	T1	12.1.2004	205	17.35	4.1	0.5	2.5
T1	14.1.2004	5	08.30	0.7	0.1	0.4	T1	14.1.2004	205	08.35	0.6	0.1	0.3
T1	14.1.2004	5	09.30	2.1	0.3	0.8	T1	14.1.2004	205	09.35	1.9	0.2	0.9
T1	14.1.2004	5	12.30	0.4	0.2	0.3	T1	14.1.2004	205	12.35	0.7	0.2	0.4
T1	14.1.2004	5	14.30	3.9	0.2	2.1	T1	14.1.2004	205	14.35	3.5	0.2	1.9
T1	14.1.2004	5	15.30	4.6	0.4	2.2	T1	14.1.2004	205	15.35	4.3	0.5	2.1
T1	14.1.2004	5	16.30	4.2	0.3	2.5	T1	14.1.2004	205	16.35	4.0	0.6	2.2
T1	14.1.2004	5	17.30	4.0	0.7	2.5	T1	14.1.2004	205	17.35	4.4	0.4	2.2

Table (D1): Wind speed spot readings. Location: Bab al Siq Triclinium Tomb (T1). Second fieldwork visit: January 2004.

Appendix D: Wind speed spot readings. Second fieldwork visit: January 2004.

Location	Date	Height (cm)	Time	Maximum wind speed (m/s)	Minimum wind speed (m/s)	Average wind speed (m/s)	Location	Date	Height (cm)	Time	Maximum wind speed (m/s)	Minimum wind speed (m/s)	Average wind speed (m/s)
T1	10.1.2004	305	08.40	0.8	0.1	0.5	T2	10.1.2004	305	08.45	0.8	0.1	0.4
T1	10.1.2004	305	09.40	1.1	0.1	0.6	T2	10.1.2004	305	09.45	1.2	0.2	0.7
T1	10.1.2004	305	12.40	0.8	0.1	0.3	T2	10.1.2004	305	12.45	0.6	0.1	0.3
T1	10.1.2004	305	14.40	0.8	0.2	0.5	T2	10.1.2004	305	14.45	1.1	0.2	0.6
T1	10.1.2004	305	15.40	3.0	0.7	1.8	T2	10.1.2004	305	15.45	3.2	0.5	1.8
T1	10.1.2004	305	16.40	3.3	0.3	1.7	T2	10.1.2004	305	16.45	3.6	0.4	2.1
T1	10.1.2004	305	17.40	4.7	0.5	2.1	T2	10.1.2004	305	17.45	4.7	0.5	2.2
T1	12.1.2004	305	08.40	0.6	0.1	0.3	T2	12.1.2004	305	08.45	0.7	0.2	0.4
T1	12.1.2004	305	09.40	2.1	0.4	1.2	T2	12.1.2004	305	09.45	2.0	0.6	1.1
T1	12.1.2004	305	12.40	0.7	0.3	0.4	T2	12.1.2004	305	12.45	0.5	0.3	0.5
T1	12.1.2004	305	14.40	4.0	0.5	2.2	T2	12.1.2004	305	14.45	4.1	0.7	2.3
T1	12.1.2004	305	15.40	4.4	0.4	2.4	T2	12.1.2004	305	15.45	4.7	0.7	2.6
T1	12.1.2004	305	16.40	4.3	0.6	2.6	T2	12.1.2004	305	16.45	4.1	0.4	2.3
T1	12.1.2004	305	17.40	3.9	0.4	2.7	T2	12.1.2004	305	17.45	4.2	1.0	2.7
T1	14.1.2004	305	08.40	0.5	0.1	0.3	T2	14.1.2004	305	08.45	0.5	0.2	0.3
T1	14.1.2004	305	09.40	2.6	0.3	1.3	T2	14.1.2004	305	09.45	2.3	0.3	1.2
T1	14.1.2004	305	12.40	0.6	0.2	0.3	T2	14.1.2004	305	12.45	1.1	0.2	0.5
T1	14.1.2004	305	14.40	2.9	0.4	2.0	T2	14.1.2004	305	14.45	3.1	0.5	2.1
T1	14.1.2004	305	15.40	4.6	0.4	2.5	T2	14.1.2004	305	15.45	4.5	0.4	2.6
T1	14.1.2004	305	16.40	4.2	0.6	2.4	T2	14.1.2004	305	16.45	4.1	0.7	2.5
T1	14.1.2004	305	17.40	4.8	0.6	2.7	T2	14.1.2004	305	17.45	4.6	1.1	2.9

Table (D2): Wind speed spot readings. Location: Bab al Siq Triclinium Tomb (T1 and T2). Second fieldwork visit: January 2004.

Appendix D: Wind speed spot readings. Second fieldwork visit: January 2004.

Location	Date	Height (cm)	Time	Maximum wind speed (m/s)	Minimum wind speed (m/s)	Average wind speed (m/s)
T3	10.1.2004	305	08.50	0.7	0.0	0.3
T3	10.1.2004	305	09.50	1.1	0.1	0.6
T3	10.1.2004	305	12.50	0.5	0.0	0.3
T3	10.1.2004	305	14.50	1.0	0.1	0.5
T3	10.1.2004	305	15.50	2.8	0.3	1.6
T3	10.1.2004	305	16.50	2.9	0.2	1.8
T3	10.1.2004	305	17.50	4.1	0.3	2.0
T3	12.1.2004	305	08.50	0.6	0.1	0.3
T3	12.1.2004	305	09.50	1.8	0.5	1.0
T3	12.1.2004	305	12.50	0.6	0.2	0.4
T3	12.1.2004	305	14.50	3.8	0.5	2.2
T3	12.1.2004	305	15.50	4.3	0.6	2.5
T3	12.1.2004	305	16.50	4.1	0.4	2.3
T3	12.1.2004	305	17.50	3.8	0.7	2.6
T3	14.1.2004	305	08.50	0.6	0.1	0.3
T3	14.1.2004	305	09.50	2.3	0.3	1.3
T3	14.1.2004	305	12.50	1.3	0.2	0.6
T3	14.1.2004	305	14.50	3.3	0.5	1.8
T3	14.1.2004	305	15.50	4.1	0.4	2.3
T3	14.1.2004	305	16.50	4.3	0.5	2.4
T3	14.1.2004	305	17.50	4.5	0.8	2.8

Table (D3): Wind speed spot readings. Location: Bab al Siq Triclinium Tomb (T3)
Second fieldwork visit: January 2004.

Appendix D: Wind speed spot readings. Second fieldwork visit: January 2004.

Location	Date	Height (cm)	Time	Maximum wind speed (m/s)	Minimum wind speed (m/s)	Average wind speed (m/s)	Location	Date	Height (cm)	Time	Maximum wind speed (m/s)	Minimum wind speed (m/s)	Average wind speed (m/s)
H	11.1.2004	350	08.35	0.7	0.1	0.3	H	11.1.2004	450	08.40	0.8	0.1	0.5
H	11.1.2004	350	09.35	0.7	0.2	0.3	H	11.1.2004	450	09.40	0.8	0.2	0.6
H	11.1.2004	350	12.35	0.6	0.1	0.3	H	11.1.2004	450	12.40	0.5	0.1	0.4
H	11.1.2004	350	14.35	1.0	0.3	0.7	H	11.1.2004	450	14.40	1.5	0.2	0.9
H	11.1.2004	350	15.35	1.6	0.3	1.2	H	11.1.2004	450	15.40	1.9	0.5	1.3
H	11.1.2004	350	16.35	2.5	0.4	1.4	H	11.1.2004	450	16.40	2.6	0.8	1.6
H	11.1.2004	350	17.35	2.7	0.4	1.5	H	11.1.2004	450	17.40	2.8	0.5	1.6
H	13.1.2004	350	08.35	0.9	0.1	0.5	H	13.1.2004	450	08.40	1.1	0.1	0.7
H	13.1.2004	350	09.35	1.0	0.2	0.6	H	13.1.2004	450	09.40	1.2	0.3	0.8
H	13.1.2004	350	12.35	0.9	0.2	0.5	H	13.1.2004	450	12.40	1.5	0.1	0.7
H	13.1.2004	350	14.35	1.6	0.1	1.0	H	13.1.2004	450	14.40	2.0	0.4	1.3
H	13.1.2004	350	15.35	2.4	0.4	1.5	H	13.1.2004	450	15.40	2.8	0.5	1.8
H	13.1.2004	350	16.35	2.5	0.4	1.3	H	13.1.2004	450	16.40	3.1	0.6	2.0
H	13.1.2004	350	17.35	2.7	0.3	1.6	H	13.1.2004	450	17.40	3.7	0.6	2.3
H	15.1.2004	350	08.35	0.6	0.1	0.3	H	15.1.2004	450	08.40	0.7	0.2	0.4
H	15.1.2004	350	09.35	0.4	0.1	0.3	H	15.1.2004	450	09.40	0.3	0.0	0.2
H	15.1.2004	350	12.35	0.3	0.0	0.2	H	15.1.2004	450	12.40	0.2	0.1	0.2
H	15.1.2004	350	14.35	1.0	0.2	0.6	H	15.1.2004	450	14.40	1.1	0.2	0.5
H	15.1.2004	350	15.35	1.8	0.2	1.1	H	15.1.2004	450	15.40	1.5	0.3	1.0
H	15.1.2004	350	16.35	3.0	0.5	1.6	H	15.1.2004	450	16.40	2.5	0.6	1.3
H	15.1.2004	350	17.35	3.2	0.5	1.7	H	15.1.2004	450	17.40	3.0	0.5	1.8

Table (D4): Wind speed spot readings. Location: Corinthian Tomb (H). Second fieldwork visit: January 2004.

Appendix D: Wind speed spot readings. Second fieldwork visit: January 2004.

Location	Date	Height (cm)	Time	Maximum wind speed (m/s)	Minimum wind speed (m/s)	Average wind speed (m/s)	Location	Date	Height (cm)	Time	Maximum wind speed (m/s)	Minimum wind speed (m/s)	Average wind speed (m/s)
C1	11.1.2004	350	08.00	0.3	0.0	0.2	C1	11.1.2004	450	08.15	0.5	0.0	0.2
C1	11.1.2004	350	09.00	0.4	0.1	0.2	C1	11.1.2004	450	09.15	0.4	0.2	0.3
C1	11.1.2004	350	12.00	0.3	0.1	0.2	C1	11.1.2004	450	12.15	0.5	0.0	0.3
C1	11.1.2004	350	14.00	0.7	0.3	0.5	C1	11.1.2004	450	14.15	0.9	0.3	0.6
C1	11.1.2004	350	15.00	1.8	0.3	1.0	C1	11.1.2004	450	15.15	1.4	0.4	1.0
C1	11.1.2004	350	16.00	2.0	0.2	1.2	C1	11.1.2004	450	16.15	2.0	0.3	1.2
C1	11.1.2004	350	17.00	3.3	0.4	1.7	C1	11.1.2004	450	17.15	2.5	0.6	1.3
C1	13.1.2004	350	08.00	0.3	0.1	0.2	C1	13.1.2004	450	08.15	0.4	0.1	0.3
C1	13.1.2004	350	09.00	0.3	0.2	0.2	C1	13.1.2004	450	09.15	0.7	0.2	0.4
C1	13.1.2004	350	12.00	0.4	0.2	0.4	C1	13.1.2004	450	12.15	0.5	0.1	0.3
C1	13.1.2004	350	14.00	3.0	0.5	1.8	C1	13.1.2004	450	14.15	1.2	0.4	0.8
C1	13.1.2004	350	15.00	3.1	0.6	2.1	C1	13.1.2004	450	15.15	2.1	0.5	1.4
C1	13.1.2004	350	16.00	2.8	0.7	1.9	C1	13.1.2004	450	16.15	3.2	0.5	1.6
C1	13.1.2004	350	17.00	3.8	0.7	2.6	C1	13.1.2004	450	17.15	4.0	0.5	2.1
C1	13.1.2004	350	08.00	0.5	0.1	0.3	C1	15.1.2004	450	08.15	0.6	0.0	0.3
C1	15.1.2004	350	09.00	1.1	0.3	0.6	C1	15.1.2004	450	09.15	0.5	0.1	0.3
C1	15.1.2004	350	12.00	1.0	0.1	0.6	C1	15.1.2004	450	12.15	0.4	0.1	0.2
C1	15.1.2004	350	14.00	2.7	0.4	1.8	C1	15.1.2004	450	14.15	1.4	0.3	0.8
C1	15.1.2004	350	15.00	3.2	0.5	1.9	C1	15.1.2004	450	15.15	1.7	0.1	1.1
C1	15.1.2004	350	16.00	3.5	0.4	2.1	C1	15.1.2004	450	16.15	2.7	0.5	1.5
C1	15.1.2004	350	17.00	3.8	0.6	2.3	C1	15.1.2004	450	17.15	3.5	0.6	1.9

Table (D5): Wind speed spot readings. Location: Palace Tomb (C1). Second fieldwork visit: January 2004.

Appendix D: Wind speed spot readings. Second fieldwork visit: January 2004.

Location	Date	Height (cm)	Time	Maximum wind speed (m/s)	Minimum wind speed (m/s)	Average wind speed (m/s)	Location	Date	Height (cm)	Time	Maximum wind speed (m/s)	Minimum wind speed (m/s)	Average wind speed (m/s)
C2	11.1.2004	350	08.05	0.6	0.0	0.3	C2	11.1.2004	450	08.20	0.6	0.0	0.3
C2	11.1.2004	350	09.05	1.0	0.1	0.5	C2	11.1.2004	450	09.20	0.7	0.1	0.4
C2	11.1.2004	350	12.05	0.6	0.2	0.3	C2	11.1.2004	450	12.20	0.6	0.0	0.3
C2	11.1.2004	350	14.05	1.1	0.1	0.6	C2	11.1.2004	450	14.20	1.1	0.1	0.7
C2	11.1.2004	350	15.05	3.1	0.2	1.6	C2	11.1.2004	450	15.20	1.8	0.3	1.1
C2	11.1.2004	350	16.05	3.2	0.2	1.6	C2	11.1.2004	450	16.20	2.2	0.3	1.4
C2	11.1.2004	350	17.05	3.6	0.4	1.9	C2	11.1.2004	450	17.20	2.9	0.4	1.6
C2	13.1.2004	350	08.05	0.6	0.1	0.3	C2	13.1.2004	450	08.20	0.8	0.2	0.5
C2	13.1.2004	350	09.05	1.4	0.4	0.9	C2	13.1.2004	450	09.20	1.2	0.3	0.8
C2	13.1.2004	350	12.05	0.7	0.2	0.4	C2	13.1.2004	450	12.20	0.9	0.2	0.6
C2	13.1.2004	350	14.05	3.3	0.4	1.8	C2	13.1.2004	450	14.20	2.0	0.4	1.3
C2	13.1.2004	350	15.05	4.6	0.6	2.5	C2	13.1.2004	450	15.20	2.9	0.6	2.0
C2	13.1.2004	350	16.05	4.3	0.4	2.3	C2	13.1.2004	450	16.20	3.1	0.4	1.9
C2	13.1.2004	350	17.05	4.5	0.6	2.3	C2	13.1.2004	450	17.20	4.1	0.6	2.3
C2	13.1.2004	350	08.05	0.4	0.1	0.3	C2	15.1.2004	450	08.20	0.6	0.1	0.2
C2	15.1.2004	350	09.05	1.8	0.3	1.1	C2	15.1.2004	450	09.20	0.5	0.1	0.4
C2	15.1.2004	350	12.05	1.1	0.3	0.7	C2	15.1.2004	450	12.20	0.3	0.1	0.2
C2	15.1.2004	350	14.05	3.1	0.4	1.7	C2	15.1.2004	450	14.20	1.5	0.3	0.9
C2	15.1.2004	350	15.05	4.0	0.4	2.1	C2	15.1.2004	450	15.20	1.6	0.2	1.0
C2	15.1.2004	350	16.05	4.7	0.6	2.4	C2	15.1.2004	450	16.20	2.1	0.4	1.2
C2	15.1.2004	350	17.05	4.6	0.7	2.5	C2	15.1.2004	450	17.20	3.0	0.5	1.7

Table (D6): Wind speed spot readings. Location: Palace Tomb (C2). Second fieldwork visit: January 2004.

Appendix D: Wind speed spot readings. Second fieldwork visit: January 2004.

Location	Date	Height (cm)	Time	Maximum wind speed (m/s)	Minimum wind speed (m/s)	Average wind speed (m/s)	Location	Date	Height (cm)	Time	Maximum wind speed (m/s)	Minimum wind speed (m/s)	Average wind speed (m/s)
C3	11.1.2004	350	08.10	0.5	0.1	0.2	C3	11.1.2004	450	08.25	0.5	0.1	0.3
C3	11.1.2004	350	09.10	0.9	0.2	0.6	C3	11.1.2004	450	09.25	0.6	0.1	0.4
C3	11.1.2004	350	12.10	0.8	0.3	0.5	C3	11.1.2004	450	12.25	0.5	0.2	0.3
C3	11.1.2004	350	14.10	1.3	0.3	0.7	C3	11.1.2004	450	14.25	0.9	0.2	0.6
C3	11.1.2004	350	15.10	2.3	0.2	1.3	C3	11.1.2004	450	15.25	1.2	0.4	0.8
C3	11.1.2004	350	16.10	2.2	0.4	1.4	C3	11.1.2004	450	16.25	1.9	0.5	1.2
C3	11.1.2004	350	17.10	3.4	0.5	1.7	C3	11.1.2004	450	17.25	2.6	0.5	1.4
C3	13.1.2004	350	08.10	0.6	0.3	0.4	C3	13.1.2004	450	08.25	0.7	0.1	0.4
C3	13.1.2004	350	09.10	1.5	0.6	0.9	C3	13.1.2004	450	09.25	1.1	0.5	0.7
C3	13.1.2004	350	12.10	1.2	0.3	0.7	C3	13.1.2004	450	12.25	1.2	0.1	0.6
C3	13.1.2004	350	14.10	3.5	0.5	1.9	C3	13.1.2004	450	14.25	1.7	0.4	1.1
C3	13.1.2004	350	15.10	4.7	0.7	2.4	C3	13.1.2004	450	15.25	2.6	0.4	1.6
C3	13.1.2004	350	16.10	4.5	0.4	2.3	C3	13.1.2004	450	16.25	3.2	0.3	1.7
C3	13.1.2004	350	17.10	3.7	0.5	2.2	C3	13.1.2004	450	17.25	3.7	0.4	0.5
C3	15.1.2004	350	08.10	0.3	0.1	0.2	C3	15.1.2004	450	08.25	0.5	0.2	0.3
C3	15.1.2004	350	09.10	1.7	0.3	0.9	C3	15.1.2004	450	09.25	0.8	0.3	0.4
C3	15.1.2004	350	12.10	1.4	0.3	0.8	C3	15.1.2004	450	12.25	0.6	0.2	0.4
C3	15.1.2004	350	14.10	3.0	0.6	1.8	C3	15.1.2004	450	14.25	1.2	0.4	0.7
C3	15.1.2004	350	15.10	3.9	0.7	2.2	C3	15.1.2004	450	15.25	1.6	0.3	0.9
C3	15.1.2004	350	16.10	3.8	0.8	2.2	C3	15.1.2004	450	16.25	2.5	0.6	1.2
C3	15.1.2004	350	17.10	4.3	0.6	2.3	C3	15.1.2004	450	17.25	2.8	0.4	1.7

Table (D7): Wind speed spot readings. Location: Palace Tomb (C3). Second fieldwork visit: January 2004.

Appendix D: Wind speed spot readings. Second fieldwork visit: January 2004.

Location	Date	Height (cm)	Time	Maximum wind speed (m/s)	Minimum wind speed (m/s)	Average wind speed (m/s)	Location	Date	Height (cm)	Time	Maximum wind speed (m/s)	Minimum wind speed (m/s)	Average wind speed(m/s)
D1	16.1.2004	55	08.00	0.4	0.2	0.3	D1	16.1.2004	255	08.05	0.7	0.2	0.5
D1	16.1.2004	55	09.00	0.5	0.2	0.3	D1	16.1.2004	255	09.05	0.5	0.2	0.3
D1	16.1.2004	55	12.00	0.3	0.2	0.2	D1	16.1.2004	255	12.05	0.4	0.2	0.4
D1	16.1.2004	55	14.00	1.5	0.6	1.2	D1	16.1.2004	255	14.05	2.0	0.8	1.4
D1	16.1.2004	55	15.00	1.7	0.5	1.4	D1	16.1.2004	255	15.05	2.3	0.5	1.3
D1	16.1.2004	55	16.00	2.5	0.6	1.8	D1	16.1.2004	255	16.05	2.8	0.7	1.9
D1	16.1.2004	55	17.00	3.2	0.5	2.0	D1	16.1.2004	255	17.05	3.6	0.6	2.2
D1	17.1.2004	55	08.00	0.2	0.0	0.1	D1	17.1.2004	255	08.05	0.3	0.2	0.2
D1	17.1.2004	55	09.00	0.3	0.3	0.3	D1	17.1.2004	255	09.05	0.5	0.3	0.4
D1	17.1.2004	55	12.00	0.4	0.1	0.2	D1	17.1.2004	255	12.05	0.3	0.0	0.2
D1	17.1.2004	55	14.00	1.2	0.5	0.9	D1	17.1.2004	255	14.05	1.3	0.5	1.0
D1	17.1.2004	55	15.00	1.3	0.6	1.0	D1	17.1.2004	255	15.05	1.7	0.5	1.2
D1	17.1.2004	55	16.00	2.7	0.6	1.7	D1	17.1.2004	255	16.05	1.8	0.8	1.2
D1	17.1.2004	55	17.00	3.3	0.7	2.1	D1	17.1.2004	255	17.05	2.8	0.5	1.6
D1	18.1.2004	55	08.00	0.4	0.3	0.4	D1	18.1.2004	255	08.05	0.5	0.2	0.4
D1	18.1.2004	55	09.00	1.1	0.5	0.7	D1	18.1.2004	255	09.05	1.3	0.4	0.8
D1	18.1.2004	55	12.00	0.5	0.3	0.4	D1	18.1.2004	255	12.05	0.7	0.4	0.5
D1	18.1.2004	55	14.00	2.2	0.7	1.3	D1	18.1.2004	255	14.05	2.5	0.6	1.6
D1	18.1.2004	55	15.00	2.0	0.5	1.3	D1	18.1.2004	255	15.05	2.9	0.7	1.7
D1	18.1.2004	55	16.00	3.3	0.6	1.9	D1	18.1.2004	255	16.05	3.1	0.7	1.8
D1	18.1.2004	55	17.00	3.5	0.7	2.0	D1	18.1.2004	255	17.05	4.0	0.5	2.2

Table (D8): Wind speed spot readings. Location: Deir Tomb (D1). Second fieldwork visit: January 2004.

Appendix D: Wind speed spot readings. Second fieldwork visit: January 2004.

Location	Date	Height (cm)	Time	Maximum wind speed (m/s)	Minimum wind speed (m/s)	Average wind speed (m/s)	Location	Date	Height (cm)	Time	Maximum wind speed (m/s)	Minimum wind speed (m/s)	Average wind speed (m/s)
D2	16.1.2004	55	08.10	0.5	0.1	0.4	D2	16.1.2004	255	08.15	1.0	0.0	0.5
D2	16.1.2004	55	09.10	0.7	0.2	0.3	D2	16.1.2004	255	09.15	0.8	0.3	0.5
D2	16.1.2004	55	12.10	0.5	0.1	0.3	D2	16.1.2004	255	12.15	0.6	0.2	0.4
D2	16.1.2004	55	14.10	2.2	0.6	1.4	D2	16.1.2004	255	14.15	2.5	0.5	1.4
D2	16.1.2004	55	15.10	2.0	0.5	1.5	D2	16.1.2004	255	15.15	2.2	0.7	1.6
D2	16.1.2004	55	16.10	2.4	0.4	1.5	D2	16.1.2004	255	16.15	2.3	0.5	1.4
D2	16.1.2004	55	17.10	4.3	0.5	2.2	D2	16.1.2004	255	17.15	4.7	0.8	2.4
D2	17.1.2004	55	08.10	0.4	0.2	0.3	D2	17.1.2004	255	08.15	0.5	0.2	0.4
D2	17.1.2004	55	09.10	0.3	0.3	0.3	D2	17.1.2004	255	09.15	0.3	0.2	0.3
D2	17.1.2004	55	12.10	0.7	0.2	0.4	D2	17.1.2004	255	12.15	0.7	0.0	0.3
D2	17.1.2004	55	14.10	2.1	0.6	1.2	D2	17.1.2004	255	14.15	1.8	0.5	1.2
D2	17.1.2004	55	15.10	2.2	0.5	1.3	D2	17.1.2004	255	15.15	3.0	0.6	1.7
D2	17.1.2004	55	16.10	3.2	0.5	1.6	D2	17.1.2004	255	16.15	3.6	0.7	1.9
D2	17.1.2004	55	17.10	3.7	0.6	2.3	D2	17.1.2004	255	17.15	3.8	0.7	2.1
D2	18.1.2004	55	08.10	0.4	0.0	0.2	D2	18.1.2004	255	08.15	0.5	0.1	0.3
D2	18.1.2004	55	09.10	0.9	0.3	0.7	D2	18.1.2004	255	09.15	1.2	0.3	0.8
D2	18.1.2004	55	12.10	0.6	0.3	0.4	D2	18.1.2004	255	12.15	0.8	0.2	0.4
D2	18.1.2004	55	14.10	1.9	0.6	1.2	D2	18.1.2004	255	14.15	2.1	0.7	1.1
D2	18.1.2004	55	15.10	2.7	0.7	1.8	D2	18.1.2004	255	15.15	3.2	0.6	1.7
D2	18.1.2004	55	16.10	3.6	0.7	2.4	D2	18.1.2004	255	16.15	4.4	0.7	2.4
D2	18.1.2004	55	17.10	4.3	0.7	2.2	D2	18.1.2004	255	17.15	4.7	0.6	2.3

Table (D9): Wind speed spot readings. Location: Deir Tomb (D2). Second fieldwork visit: January 2004.

Appendix E: The anion and cation content of the drilled samples. Second fieldwork visit: January 2004.

Sample Number	Location	Height (cm)	Depth (cm)	Ca (ppm)	Na (ppm)	Mg (ppm)	K (ppm)	Fe (ppm)	Al (ppm)	Tl (ppm)	Zn (ppm)	F (ppm)	Br (ppm)	Cl (ppm)	NO_3 (ppm)	PO_4 (ppm)	SO_4 (ppm)	Cation charge with Al	Cation charge without Al	Anion charge	Sum of cations & anions (ppm)	Soluble salt content in the sample (%) of dray weight
1	T1	5	0-1	2.92	12.92	0.41	1.16	0.00	0.16	0.01	0.10	0.00	0.00	1.46	0.00	0.00	1.26	0.79	0.77	0.07	20.40	0.10
2	T1	5	1-3	1.35	59.50	0.30	3.70	0.55	3.55	0.35	0.75	0.00	0.00	0.34	0.13	0.00	0.70	3.22	2.83	0.03	71.22	0.36
3	T1	55	0-1	6.59	12.54	0.58	1.22	0.19	1.37	0.10	0.05	0.00	0.00	0.28	0.10	0.00	0.64	1.12	0.97	0.02	23.66	0.12
4	T1	55	1-3	1.50	68.25	0.30	5.30	0.35	3.80	0.30	0.25	0.00	0.00	0.28	0.09	0.00	0.61	3.65	3.23	0.02	81.02	0.41
5	T1	105	0-1	7.15	76.30	1.00	5.85	1.40	6.40	0.85	0.20	0.00	0.00	0.30	0.17	0.00	0.54	4.69	3.98	0.02	100.17	0.50
6	T1	105	1-3	4.05	62.30	0.60	4.15	1.80	7.50	1.10	0.25	0.00	0.00	0.30	0.13	0.00	0.56	4.00	3.17	0.02	82.73	0.41
7	T1	155	0-1	6.35	61.40	1.15	4.55	1.90	13.20	1.65	0.15	0.00	0.00	0.79	0.09	0.00	1.27	4.77	3.30	0.05	92.49	0.46
8	T1	155	1-3	1.75	56.10	0.65	4.90	0.80	4.60	0.30	0.20	0.17	0.00	0.93	0.10	0.00	1.19	3.26	2.75	0.06	71.69	0.36
9	T1	205	0-1	8.00	70.00	2.05	3.90	0.25	1.85	0.15	0.15	0.00	0.00	0.32	0.16	0.51	2.43	3.93	3.72	0.08	89.77	0.45
10	T1	205	1-3	36.50	62.30	3.35	4.70	0.25	4.20	0.25	0.15	0.02	0.00	0.45	0.08	0.51	1.12	5.41	4.94	0.05	113.89	0.57
11	T1	305	0-1	25.95	46.70	4.60	4.20	0.00	0.90	0.05	0.15	0.02	0.00	0.72	0.58	0.49	13.50	3.92	3.82	0.33	97.86	0.49
12	T1	305	1-3	46.80	108.90	4.00	7.00	0.00	1.25	0.05	0.15	0.00	0.00	3.89	0.75	0.25	79.80	7.73	7.59	1.79	252.84	1.26
13	T1	505	0-1	31.40	49.30	3.40	4.80	0.00	7.20	0.40	0.15	0.00	0.00	1.18	1.05	0.27	21.12	4.93	4.13	0.50	120.27	0.60
14	T1	505	1-3	11.15	76.05	2.00	4.30	0.05	6.00	0.40	0.15	0.10	0.00	1.31	0.95	0.22	7.51	4.82	4.15	0.22	110.19	0.55
15	T1	550	0-1	14.25	48.10	0.85	3.85	0.00	4.05	0.75	0.10	0.00	0.00	0.33	0.10	0.27	0.87	3.44	2.99	0.04	73.52	0.37
16	T1	550	1-3	0.60	58.95	0.15	2.90	0.80	11.62	1.80	0.10	0.14	0.00	0.57	0.00	0.00	0.58	4.04	2.75	0.04	78.20	0.39
17	T2	305	0-1	64.80	232.20	10.20	10.80	0.00	6.00	1.20	0.20	0.23	0.00	1.35	0.47	0.00	74.28	15.15	14.48	1.60	401.72	2.01
18	T2	305	1-3	16.10	84.60	1.10	4.70	0.00	2.15	0.30	0.10	0.12	0.00	0.60	0.14	0.00	5.83	4.94	4.70	0.15	115.73	0.58
19	T2	405	0-1	19.35	90.10	2.30	8.40	0.00	1.85	0.05	0.40	0.00	0.00	0.18	0.14	0.24	0.57	5.51	5.30	0.03	123.58	0.62
20	T2	405	1-3	2.38	136.25	0.38	7.13	0.00	13.88	0.38	0.25	0.17	0.00	0.63	0.07	0.26	0.70	7.82	6.28	0.05	162.45	0.81
21	T3	305	0-1	45.30	57.65	8.75	6.75	0.00	0.70	0.05	0.05	0.16	0.00	13.17	17.57	6.87	116.22	5.74	5.66	3.30	273.24	1.37
22	T3	405	0-1	107.97	17.74	5.05	226.30	0.00	0.02	0.00	0.02	14.49	0.00	56.37	36.57	1.24	304.17	12.37	12.37	9.32	769.94	3.85
23	T3	405	1-3	30.60	93.70	3.45	78.90	0.00	1.50	0.10	0.20	0.81	0.00	15.83	11.52	1.25	144.48	8.08	7.91	3.72	382.34	1.91

Table (E1): The anion and cation content of drilled samples from the Bib al Siq Triclinium Tomb, locations (T1, T2 and T3). Second fieldwork visit: January 2004.

Appendix E: The anion and cation content of the drilled samples. Second fieldwork visit: January 2004.

Sample Number	Location	Height (cm)	Depth (cm)	Ca (ppm)	Na (ppm)	Mg (ppm)	K (ppm)	Fe (ppm)	Al (ppm)	Tl (ppm)	Zn (ppm)	F (ppm)	Br (ppm)	Cl (ppm)	NO_3 (ppm)	PO_4 (ppm)	SO_4 (ppm)	Cation charge with Al	Cation charge without Al	Anion charge	Sum of cations & anions (ppm)	Soluble salt content in the sample (%) of dray weight
24	C1	5	0-1	191.80	6.95	1.10	1.78	0.00	0.04	0.01	0.03	0.00	0.12	1.64	0.49	0.22	219.24	10.01	10.01	4.63	423.43	2.12
25	C1	5	1-3	175.29	6.07	1.10	1.77	0.00	0.03	0.01	0.03	0.00	0.00	0.98	0.62	0.00	4.00	9.15	9.15	0.12	189.90	0.95
26	C1	55	0-1	5.72	5.43	0.31	0.52	0.00	0.09	0.01	0.00	0.00	0.15	0.43	0.91	0.00	2.52	0.57	0.56	0.08	16.09	0.08
27	C1	55	1-3	3.10	5.95	0.25	0.33	0.00	0.08	0.01	0.00	0.00	0.00	0.17	0.03	0.11	0.60	0.45	0.44	0.02	10.64	0.05
28	C1	105	0-1	3.94	6.25	0.23	0.51	0.02	0.19	0.02	0.02	0.00	0.12	0.00	0.00	0.00	0.26	0.52	0.50	0.01	11.56	0.06
29	C1	105	1-3	4.94	6.97	0.26	0.86	0.05	0.23	0.02	0.01	0.00	0.00	0.42	0.04	0.15	0.28	0.62	0.59	0.02	14.23	0.07
30	C1	175	0-1	4.95	6.49	0.40	0.67	0.00	0.06	0.00	0.01	0.00	0.00	0.51	0.03	0.12	0.97	0.59	0.58	0.04	14.21	0.07
31	C1	175	1-3	2.54	7.86	0.27	0.50	0.00	0.01	0.00	0.01	0.00	0.00	0.53	0.04	0.00	0.28	0.51	0.51	0.02	12.04	0.06
32	C1	305	0-1	9.88	7.57	0.82	1.83	0.00	0.02	0.00	0.00	0.00	0.00	0.37	0.32	0.17	0.76	0.94	0.94	0.04	21.74	0.11
33	C1	305	1-3	34.72	7.08	1.59	0.80	0.00	0.05	0.00	0.01	0.00	0.00	0.58	0.12	0.22	65.36	2.20	2.19	1.39	110.53	0.55
34	C1	405	0-1	16.05	6.70	2.43	0.39	0.00	0.10	0.00	0.00	0.00	0.00	3.66	2.39	0.00	10.05	1.31	1.30	0.35	41.77	0.21
35	C1	405	1-3	39.18	6.31	3.86	0.53	0.00	0.06	0.00	0.01	0.00	0.00	2.62	0.62	0.00	74.96	2.57	2.56	1.65	128.15	0.64
36	C1	505	0-1	12.20	7.73	1.33	1.28	0.18	0.29	0.02	0.01	0.00	0.00	2.22	9.13	0.29	5.27	1.13	1.10	0.33	39.95	0.20
37	C1	505	1-3	8.16	7.98	1.00	0.82	0.00	0.02	0.00	0.01	0.00	0.00	1.71	1.45	0.71	2.37	0.86	0.86	0.14	24.23	0.12

Table (E2): The anion and cation content of drilled samples from the Palace Tomb, location (C1).
Second fieldwork visit: January 2004.

Appendix E: The anion and cation content of the drilled samples. Second fieldwork visit: January 2004.

Sample Number	Location	Height (cm)	Depth (cm)	Ca (ppm)	Na (ppm)	Mg (ppm)	K (ppm)	Fe (ppm)	Al (ppm)	Ti (ppm)	Zn (ppm)	F (ppm)	Br (ppm)	Cl (ppm)	NO_3 (ppm)	PO_4 (ppm)	SO_4 (ppm)	Cation charge with Al	Cation charge without Al	Anion charge	Sum of cations & anions (ppm)	Soluble salt content in the sample (%) of dray weight
38	C2	105	0-1	281.62	6.00	1.20	15.54	0.00	0.02	0.01	0.05	0.08	0.01	6.30	159.48	4.83	357.39	14.81	14.81	10.35	832.53	4.16
39	C2	105	1-3	320.54	7.87	2.72	11.98	0.00	0.02	0.01	0.05	0.07	0.30	2.74	9.10	0.13	526.26	16.87	16.87	11.20	881.79	4.41
40	C2	155	0-1	93.51	11.06	15.49	513.35	0.00	0.02	0.00	0.02	4.01	1.23	41.46	4181.10	0.00	1064.40	19.55	19.55	91.00	5,925.65	29.63
41	C2	155	1-3	304.84	33.03	42.97	1378.71	0.00	0.11	0.02	0.05	1.61	0.96	34.50	2454.00	0.00	749.55	55.46	55.45	56.26	5,000.35	25.00
42	C2	205	0-1	11.05	31.94	1.27	50.34	0.00	0.00	0.00	0.01	0.00	0.01	34.80	81.00	6.90	19.26	3.33	3.33	2.91	236.58	1.18
43	C2	205	1-3	57.63	76.37	1.60	221.59	0.00	0.04	0.00	0.02	1.16	0.23	79.32	273.48	4.88	83.36	12.00	12.00	8.60	799.68	4.00
44	C2	255	0-1	22.37	45.55	1.38	246.82	0.00	0.62	0.04	0.01	1.02	1.26	78.48	292.00	0.02	26.12	9.59	9.52	7.54	715.69	3.58
45	C2	255	1-3	21.84	41.88	1.40	211.32	0.00	0.07	0.00	0.03	5.68	2.02	106.94	436.11	0.00	41.64	8.44	8.43	11.24	868.93	4.34
45	C2	345	0-1	24.53	23.30	1.14	516.27	0.00	0.05	0.00	0.01	1.03	1.69	35.58	1318.50	0.00	52.48	15.54	15.53	23.44	1,974.58	9.87
47	C2	345	1-3	13.25	31.23	0.91	221.54	0.00	0.13	0.00	0.00	15.36	1.25	65.48	409.48	4.20	20.64	7.77	7.76	9.84	783.47	3.92
48	C3	105	0-1	10.32	6.59	0.56	2.12	0.00	0.02	0.00	0.00	1.25	0.85	1.08	0.98	3.33	10.47	0.90	0.90	0.45	37.57	0.19
49	C3	105	1-3	10.92	5.80	0.40	0.83	0.00	0.05	0.00	0.00	0.00	0.01	0.69	0.24	0.14	8.89	0.86	0.85	0.21	27.97	0.14
50	C3	155	0-1	25.08	7.34	1.26	1.66	0.00	0.09	0.00	0.01	0.69	0.14	2.15	1.44	0.13	43.96	1.73	1.72	1.04	83.93	0.42
51	C3	155	1-3	10.60	6.35	1.86	1.13	0.08	0.22	0.02	0.00	0.00	0.00	2.90	9.86	0.48	2.04	1.01	0.99	0.30	35.54	0.18
52	C3	205	0-1	8.26	5.77	0.56	0.58	0.00	0.04	0.00	0.00	0.00	0.00	0.33	0.18	0.14	0.75	0.73	0.73	0.03	16.60	0.08
53	C3	205	1-3	10.76	5.87	0.63	0.79	0.01	0.38	0.02	0.00	0.03	0.00	0.91	0.67	0.18	0.93	0.91	0.87	0.06	21.18	0.11
54	C3	305	0-1	14.39	5.58	0.52	0.75	0.00	0.04	0.00	0.00	0.00	0.00	0.30	0.53	0.12	11.93	1.03	1.03	0.27	34.16	0.17

Table (E3): The anion and cation content of drilled samples from the Palace Tomb, locations (C2 and C3).
Second fieldwork visit: January 2004.

Appendix E: The anion and cation content of the drilled samples. Second fieldwork visit: January 2004.

Sample Number	Location	Height (cm)	Depth (cm)	Ca (ppm)	Na (ppm)	Mg (ppm)	K (ppm)	Fe (ppm)	Al (ppm)	Tl (ppm)	Zn (ppm)	F (ppm)	Br (ppm)	Cl (ppm)	NO_3 (ppm)	PO_4 (ppm)	SO_4 (ppm)	Cation charge with Al	Cation charge without Al	Anion charge	Sum of cations & anions (ppm)	Soluble salt content in the sample (%) of dray weight
55	H	25	0-1	43.05	84.05	4.30	6.15	0.00	2.20	0.10	0.10	0.27	0.00	0.59	0.27	0.33	15.71	6.57	6.33	0.37	157.13	0.79
56	H	25	1-3	10.83	9.38	0.27	0.55	0.00	0.08	0.00	0.05	0.08	0.00	0.63	0.18	0.28	5.16	1.00	0.99	0.14	27.48	0.14
57	H	75	0-1	175.40	80.45	5.85	5.20	0.00	1.40	0.28	0.10	0.11	0.00	2.14	4.70	0.29	99.71	13.03	12.87	2.23	375.63	1.88
58	H	75	1-3	75.60	36.75	1.40	3.10	0.00	0.05	0.01	0.10	0.13	0.00	5.96	0.87	0.00	200.10	5.57	5.56	4.36	324.07	1.62
59	H	125	0-1	20.85	46.95	1.50	2.45	0.00	0.90	0.18	0.00	0.00	0.00	0.25	1.65	0.33	0.97	3.37	3.27	0.06	76.02	0.38
60	H	125	1-3	14.65	22.29	1.44	1.55	0.43	1.30	0.13	0.13	0.00	0.00	0.38	0.24	0.23	0.96	2.03	1.89	0.04	43.72	0.22
61	H	155	0-1	17.46	16.53	0.75	1.48	0.00	0.10	0.01	0.02	0.09	0.00	0.45	1.34	0.27	1.11	1.70	1.69	0.07	39.60	0.20
62	H	155	1-3	10.61	17.65	0.88	1.00	0.00	0.13	0.01	0.02	0.00	0.00	0.34	0.00	0.33	1.03	1.41	1.40	0.04	31.99	0.16
63	H	200	0-1	55.10	96.65	1.50	3.05	0.00	0.00	0.00	0.10	1.42	0.00	64.30	2.16	0.24	87.30	7.16	7.16	3.75	311.82	1.56
64	H	200	0-1	46.40	269.05	1.65	3.65	0.00	0.40	0.00	0.10	0.99	0.00	338.40	26.40	0.00	132.32	14.30	14.26	12.78	819.36	4.10
64	H	250	0-1	188.45	109.00	1.55	4.00	0.00	0.20	0.00	0.15	0.05	0.00	79.92	6.00	0.24	319.68	14.40	14.38	9.02	709.24	3.55
66	H	250	1-3	31.85	212.05	0.73	1.66	0.00	0.03	0.00	0.03	0.01	0.00	337.44	1.20	0.35	81.42	10.92	10.92	11.25	666.78	3.33
67	H	300	0-1	6.72	15.19	0.43	0.64	0.00	0.05	0.00	0.01	0.33	0.00	12.10	6.80	11.20	25.05	1.05	1.04	1.34	78.52	0.39
68	H	300	1-3	14.45	63.35	0.50	2.90	0.00	0.10	0.00	0.06	0.00	0.00	0.47	0.10	0.60	0.74	3.60	3.59	0.05	83.26	0.42
69	H	500	0-1	9.18	13.51	0.65	1.21	0.07	0.60	0.04	0.01	0.00	0.00	1.89	3.22	0.00	1.19	1.20	1.13	0.13	31.57	0.16
70	H	500	1-3	1.33	14.94	0.21	0.90	0.18	2.91	0.22	0.01	0.00	0.00	0.68	0.94	0.24	0.82	1.09	0.77	0.06	23.38	0.12

Table (E4): The anion and cation content of drilled samples from the Corinthian Tomb, location (H).
Second fieldwork visit: January 2004.

Appendix E: The anion and cation content of the drilled samples. Second fieldwork visit: January 2004.

Sample Number	Location	Height (cm)	Depth (cm)	Ca (ppm)	Na (ppm)	Mg (ppm)	K (ppm)	Fe (ppm)	Al (ppm)	Ti (ppm)	Zn (ppm)	F (ppm)	Br (ppm)	Cl (ppm)	NO_3 (ppm)	PO_4 (ppm)	SO_4 (ppm)	Cation charge with Al	Cation charge without Al	Anion charge	Sum of cations & anions (ppm)	Soluble salt content in the sample (%) of dray weight
71	D1	5	0-1	9.18	13.51	0.65	1.21	0.07	0.60	0.04	0.01	0.00	0.00	1.89	3.22	0.00	1.19	1.20	1.13	0.13	31.57	0.16
72	D1	5	1-3	7.70	100.30	1.40	6.40	0.00	5.70	0.50	0.10	0.38	0.00	11.96	3.72	0.00	79.60	5.67	5.04	2.08	217.76	1.09
73	D1	55	0-1	10.44	18.18	0.81	1.72	0.00	0.08	0.00	0.01	0.15	0.00	12.28	5.00	0.00	23.72	1.43	1.42	0.93	72.39	0.36
74	D1	55	1-3	7.24	15.89	1.14	0.81	0.00	0.18	0.01	0.01	0.18	0.00	4.05	0.87	0.00	7.42	1.19	1.17	0.29	37.80	0.19
75	D1	105	0-1	0.55	16.42	0.06	0.91	0.00	0.75	0.05	0.00	0.00	0.00	1.70	0.11	0.00	0.85	0.85	0.77	0.07	21.40	0.11
76	D1	105	1-3	9.16	13.47	2.29	0.91	0.00	0.17	0.00	0.01	0.03	0.00	0.52	0.29	0.00	3.28	1.27	1.25	0.09	30.13	0.15
77	D1	155	0-1	7.80	51.90	0.75	1.85	0.00	0.10	0.00	0.00	0.00	0.00	0.60	0.00	0.00	0.76	2.77	2.76	0.03	63.76	0.32
78	D1	155	1-3	11.30	6.06	0.50	0.65	0.00	0.51	0.02	0.01	0.11	0.00	0.92	0.10	0.00	0.71	0.94	0.88	0.05	20.89	0.10
79	D1	205	0-1	6.36	11.51	0.43	0.88	0.00	1.40	0.08	0.01	0.07	0.00	0.75	0.08	0.00	0.85	1.03	0.87	0.04	22.43	0.11
80	D1	205	1-3	9.96	7.37	0.80	0.58	0.00	0.23	0.00	0.00	0.00	0.00	0.96	0.20	0.00	1.54	0.92	0.89	0.06	21.64	0.11
81	D1	255	0-1	122.30	137.10	11.85	10.65	0.00	0.25	0.00	0.75	4.69	0.00	31.45	6.42	1.58	103.71	13.36	13.33	3.45	430.74	2.15
82	D1	255	1-3	14.65	28.70	0.95	2.45	0.00	0.00	0.00	0.00	0.06	0.00	1.57	0.19	0.00	18.48	2.12	2.12	0.44	67.06	0.34
83	D2	5	0-1	71.01	22.55	2.29	11.52	0.00	0.07	0.00	0.43	0.04	0.00	6.10	2.64	4.78	572.42	5.03	5.02	12.29	693.85	3.47
84	D2	5	1-3	26.45	25.95	1.05	2.75	0.00	0.00	0.00	0.15	0.52	0.00	4.62	3.46	97.58	39.04	2.61	2.61	4.11	201.57	1.01
85	D2	55	0-1	160.00	28.65	4.25	3.55	0.00	0.00	0.00	0.10	0.14	0.00	4.72	1.58	0.00	370.50	9.67	9.67	7.88	573.49	2.87
86	D2	55	1-3	342.95	92.35	10.60	9.35	0.00	0.15	0.00	0.30	0.00	0.00	2.34	1.30	0.00	33.44	22.27	22.25	0.78	492.78	2.46
87	D2	105	0-1	293.45	45.90	7.35	3.65	0.00	3.05	0.10	0.10	0.16	0.00	24.40	10.36	0.00	575.48	17.68	17.34	12.85	964.00	4.82
88	D2	105	1-3	5.82	7.70	0.30	0.48	0.00	0.00	0.00	0.00	0.14	0.00	7.08	1.01	0.00	51.72	0.66	0.66	1.30	74.25	0.37
89	D2	155	0-1	59.32	10.99	3.67	2.86	0.00	0.10	0.03	0.01	0.03	0.00	2.10	1.75	0.00	21.02	3.83	3.82	0.53	101.88	0.51
90	D2	155	1-3	17.66	9.87	1.28	1.87	0.00	0.03	0.00	0.00	0.02	0.00	4.89	1.98	0.00	20.08	1.47	1.47	0.59	57.68	0.29
91	D2	205	0-1	36.44	12.13	4.52	3.60	0.00	0.00	0.00	0.01	0.17	0.00	17.69	14.32	0.00	74.00	2.81	2.81	2.28	162.88	0.81
92	D2	205	1-3	17.58	7.01	1.20	0.89	0.00	0.27	0.08	0.02	0.01	0.00	2.64	1.03	0.00	29.94	1.34	1.31	0.72	60.67	0.30
93	D2	255	0-1	68.59	11.41	4.27	4.35	0.00	0.03	0.00	0.01	0.02	0.00	4.91	4.37	0.00	82.29	4.39	4.39	1.92	180.25	0.90

Table (E5): The anion and cation content of drilled samples from the Deir Tomb, locations (D1 and D2). Second fieldwork visit: January 2004.

Appendix Eb: The anion and cation content and distribution in the drilled samples. Second fieldwork visit: January 2004.

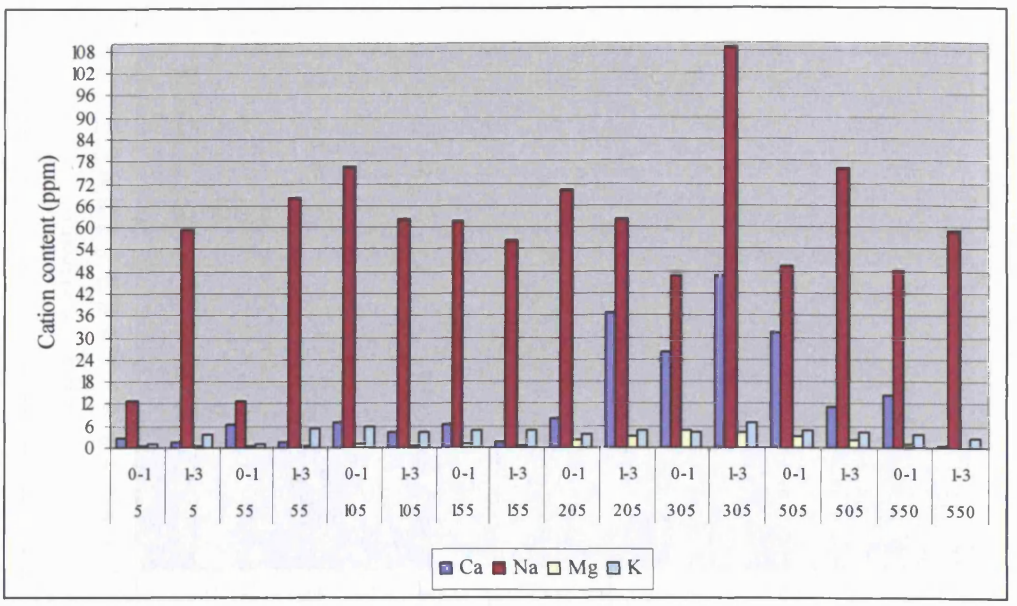

Figure (1Eb): The main cation content in drilled samples from the Bab al Siq Triclinium Tomb, location (T1) (Depth intervals: 0-1 and 1-3 cm).
Second fieldwork visit: January 2004.

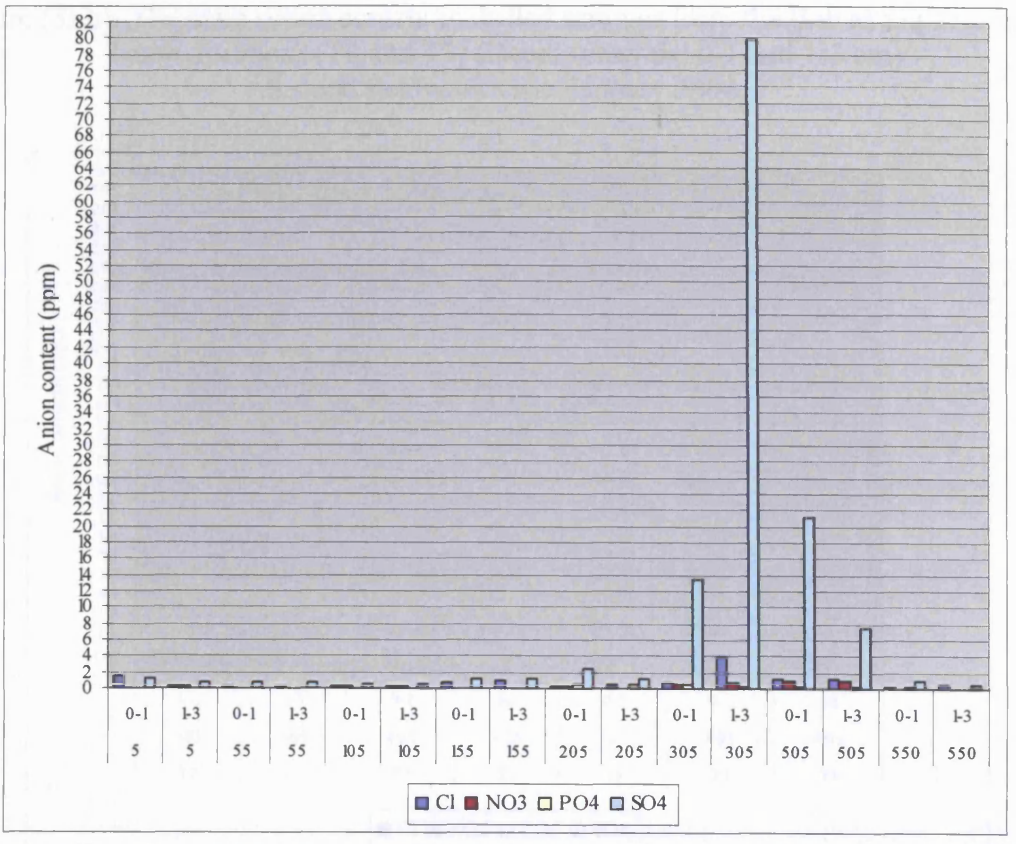

Figure (2Eb): The main anion content in drilled samples from the Bab al Siq Triclinium Tomb, location (T1) (Depth intervals: 0-1 and 1-3 cm).
Second fieldwork visit: January 2004.

Appendix Eb: The anion and cation content and distribution in the drilled samples. Second fieldwork visit: January 2004.

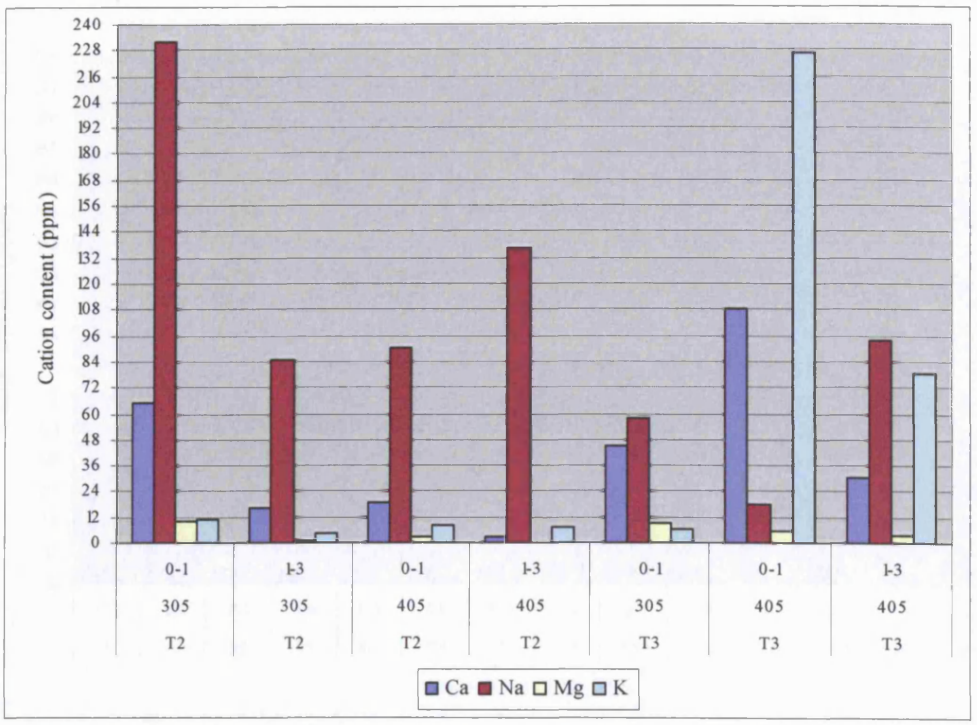

Figure (3Eb): The main cation content in drilled samples from the Bab al Siq Triclinium Tomb, locations (T2 and T3) (Depth intervals: 0-1 and 1-3 cm).
Second fieldwork visit: January 2004.

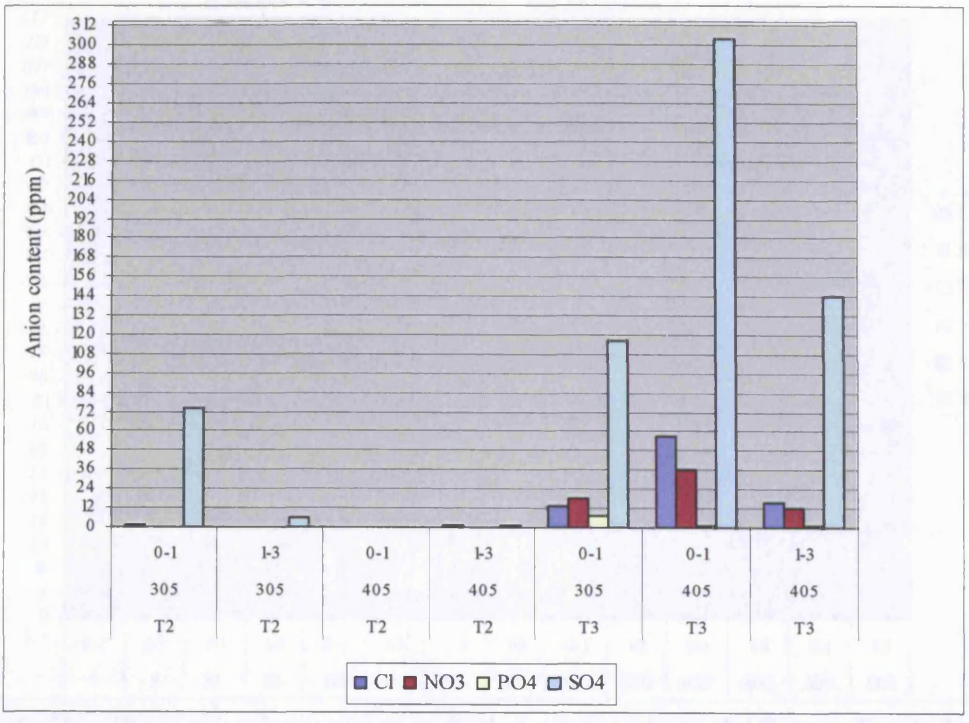

Figure (4Eb): The main anion content in drilled samples from the Bab al Siq Triclinium Tomb, locations (T2 and T3) (Depth intervals: 0-1 and 1-3 cm).
Second fieldwork visit: January 2004.

Appendix Eb: The anion and cation content and distribution in the drilled samples. Second fieldwork visit: January 2004.

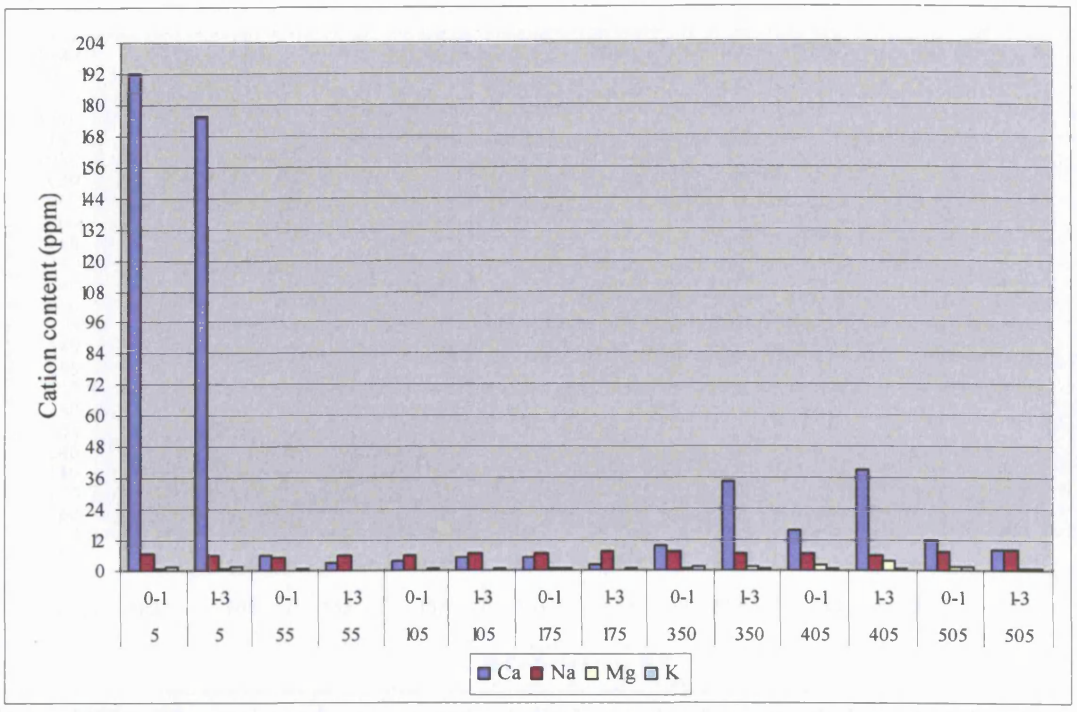

Figure (5Eb): The main cation content in drilled samples from the Palace Tomb, location (C1) (Depth intervals: 0-1 and 1-3 cm).
Second fieldwork visit: January 2004.

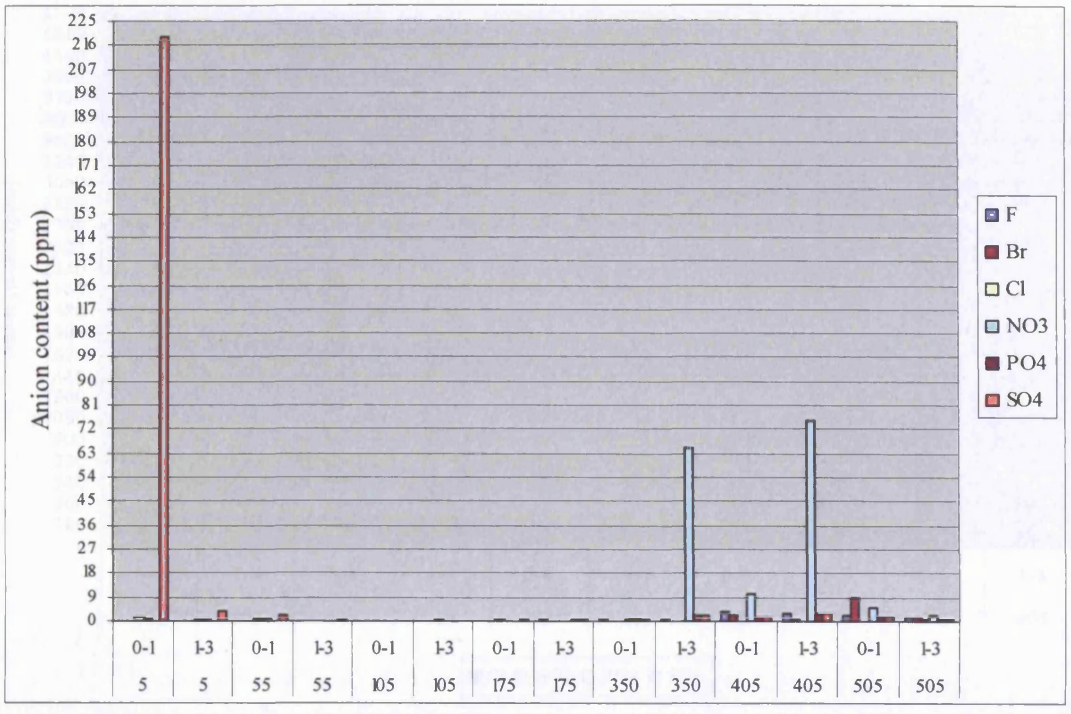

Figure (6Eb): The main anion content in drilled samples from the Palace Tomb, location (C1) (Depth intervals: 0-1 and 1-3 cm).
Second fieldwork visit: January 2004.

Appendix Eb: The anion and cation content and distribution in the drilled samples. Second fieldwork visit: January 2004.

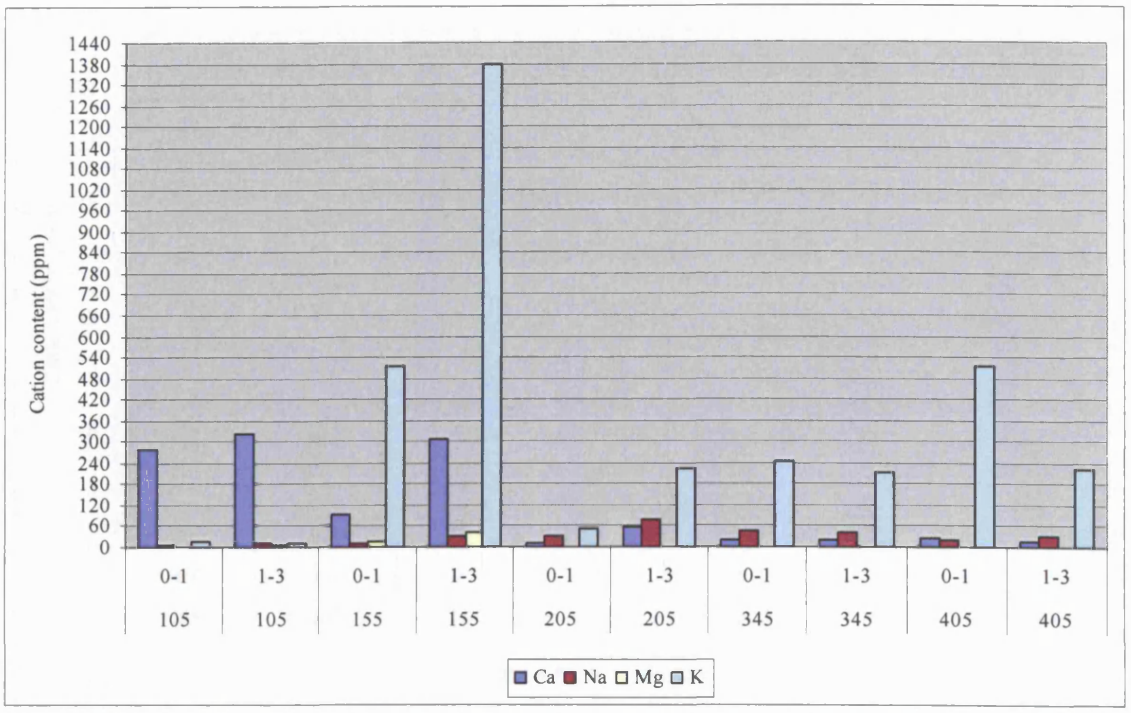

Figure (7Eb): The main cation content in drilled samples from the Palace Tomb, location (C2) (Depth intervals: 0-1 and 1-3 cm).
Second fieldwork visit: January 2004.

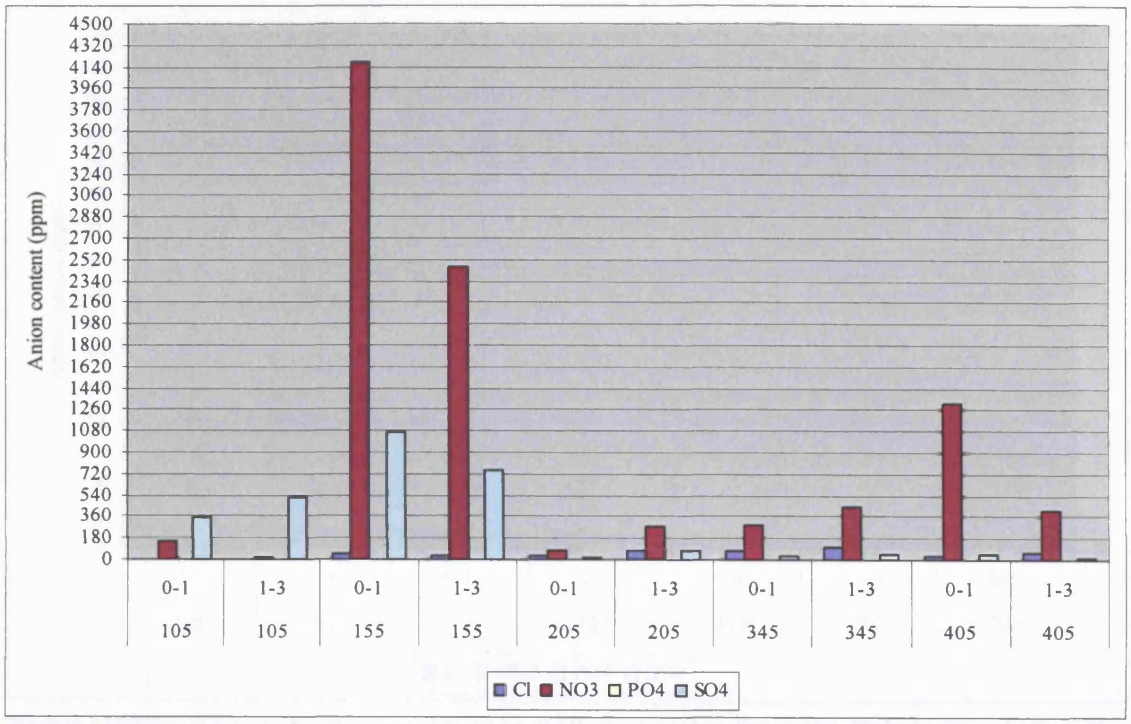

Figure (8Eb): The main anion content in drilled samples from the Palace Tomb, location (C2) (Depth intervals: 0-1 and 1-3 cm).
Second fieldwork visit: January 2004.

Appendix Eb: The anion and cation content and distribution in the drilled samples. Second fieldwork visit: January 2004.

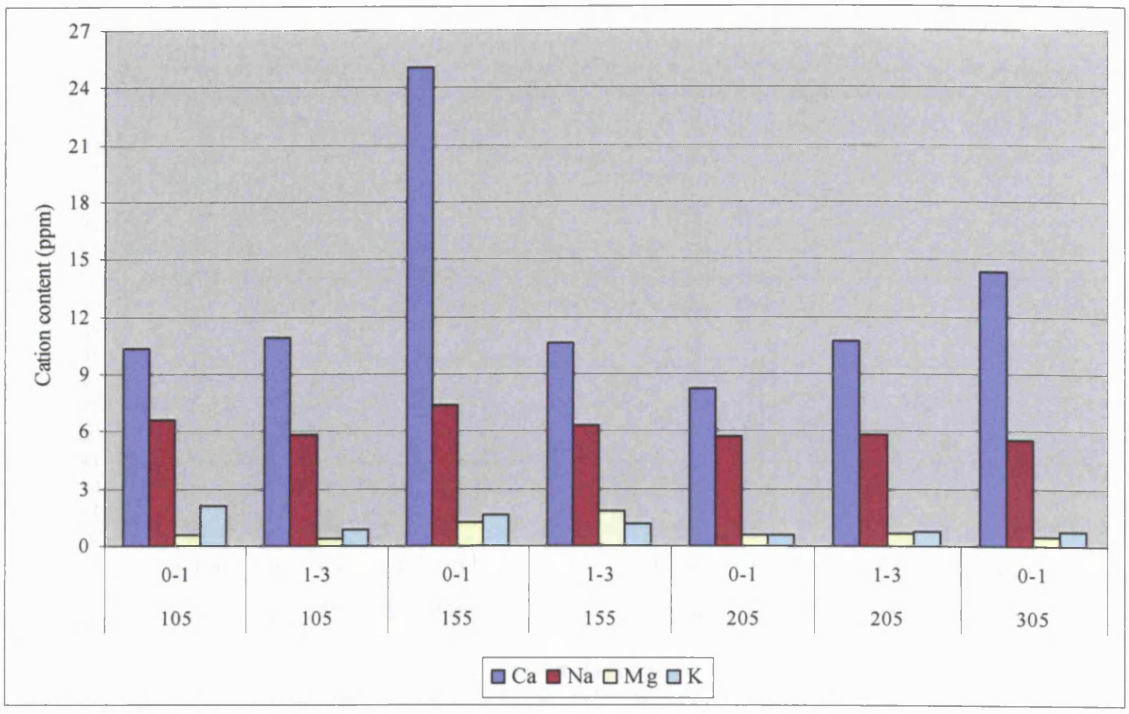

Figure (9Eb): The main cation content in drilled samples from the Palace Tomb, location (C3) (Depth intervals: 0-1 and 1-3 cm).
Second fieldwork visit: January 2004.

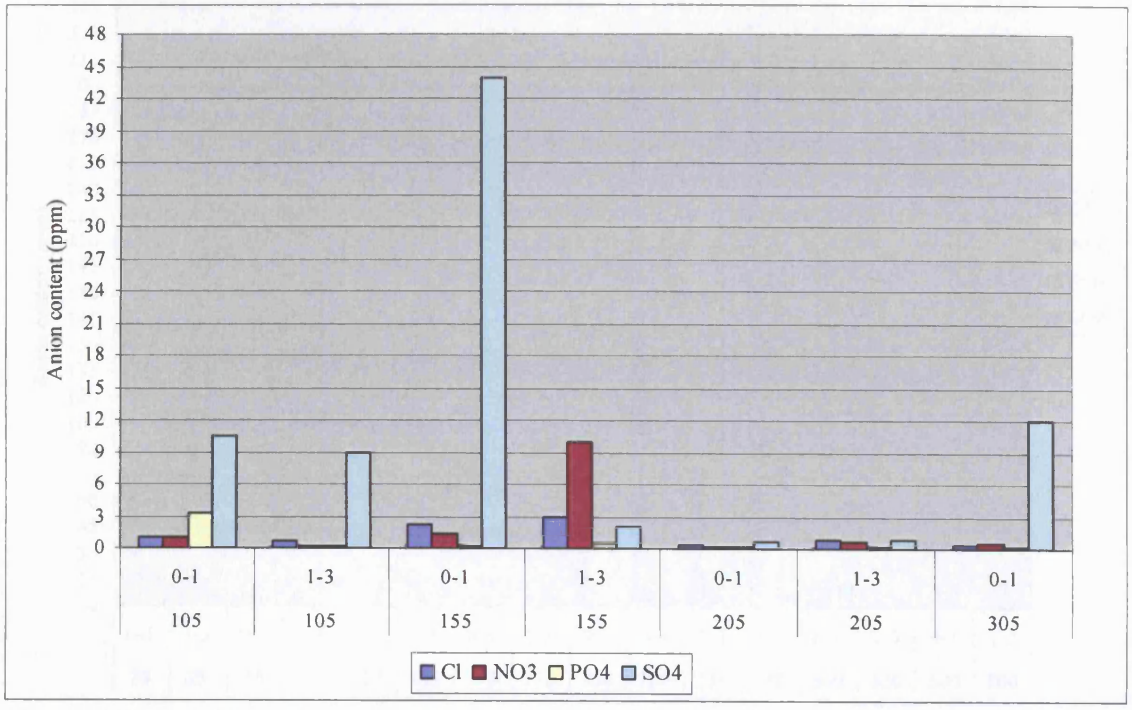

Figure (10Eb): The main anion content in drilled samples from the Palace Tomb, location (C3) (Depth intervals: 0-1 and 1-3 cm).
Second fieldwork visit: January 2004.

Appendix Eb: The anion and cation content and distribution in the drilled samples. Second fieldwork visit: January 2004.

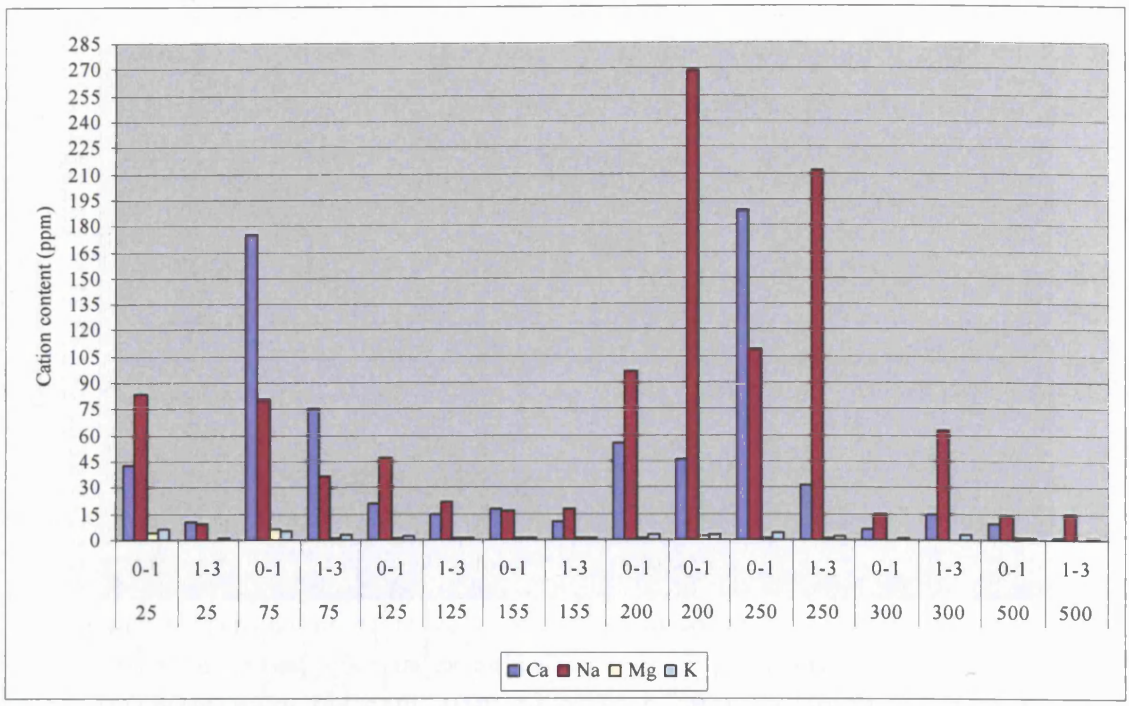

Figure (11Eb): The main cation content in drilled samples from the Corinthian Tomb, location (H) (Depth intervals: 0-1 and 1-3 cm). Second fieldwork visit: January 2004.

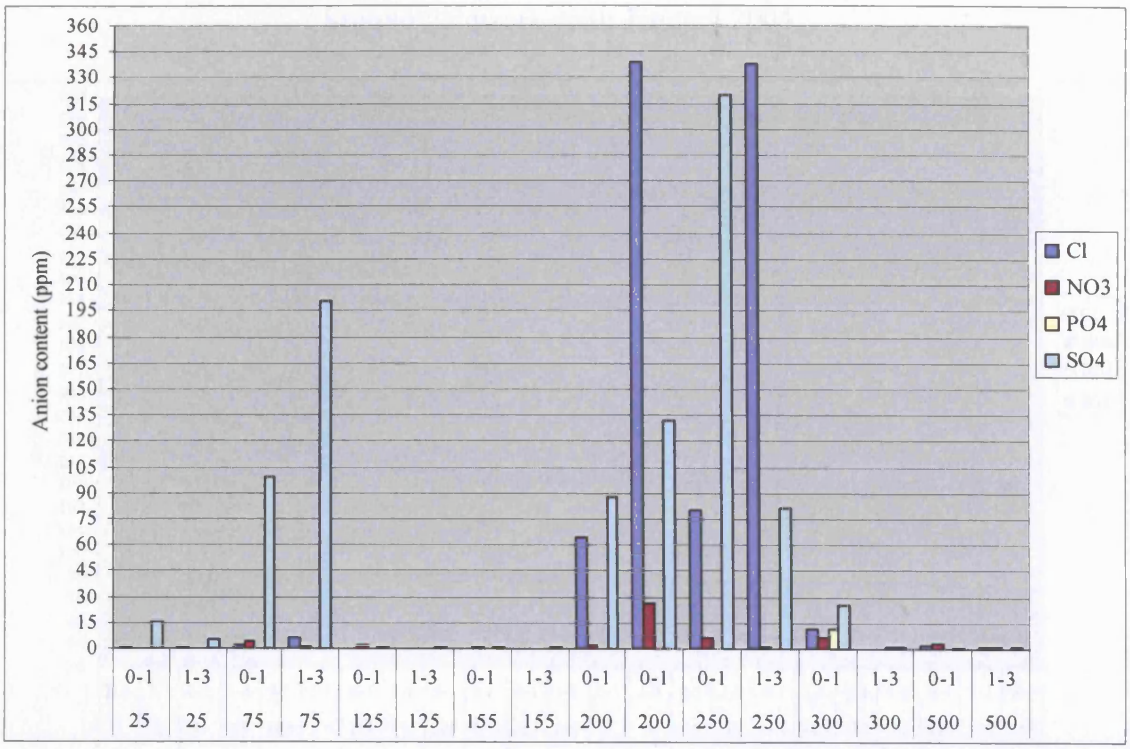

Figure (11Eb): The main anion content in drilled samples from the Corinthian Tomb, location (H) (Depth intervals: 0-1 and 1-3 cm). Second fieldwork visit: January 2004.

Appendix Eb: The anion and cation content and distribution in the drilled samples. Second fieldwork visit: January 2004.

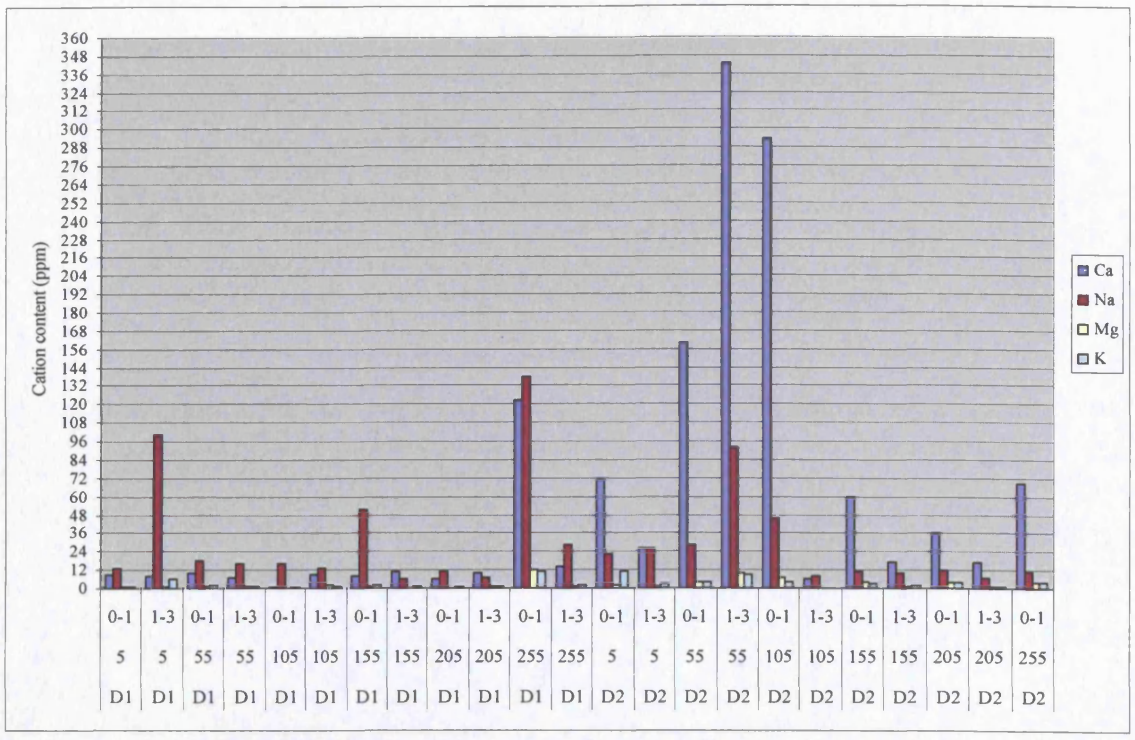

Figure (12Eb): The main cation content in drilled samples from the Deir Tomb, locations (D1 and D2) (Depth intervals: 0-1 and 1-3 cm).
Second fieldwork visit: January 2004.

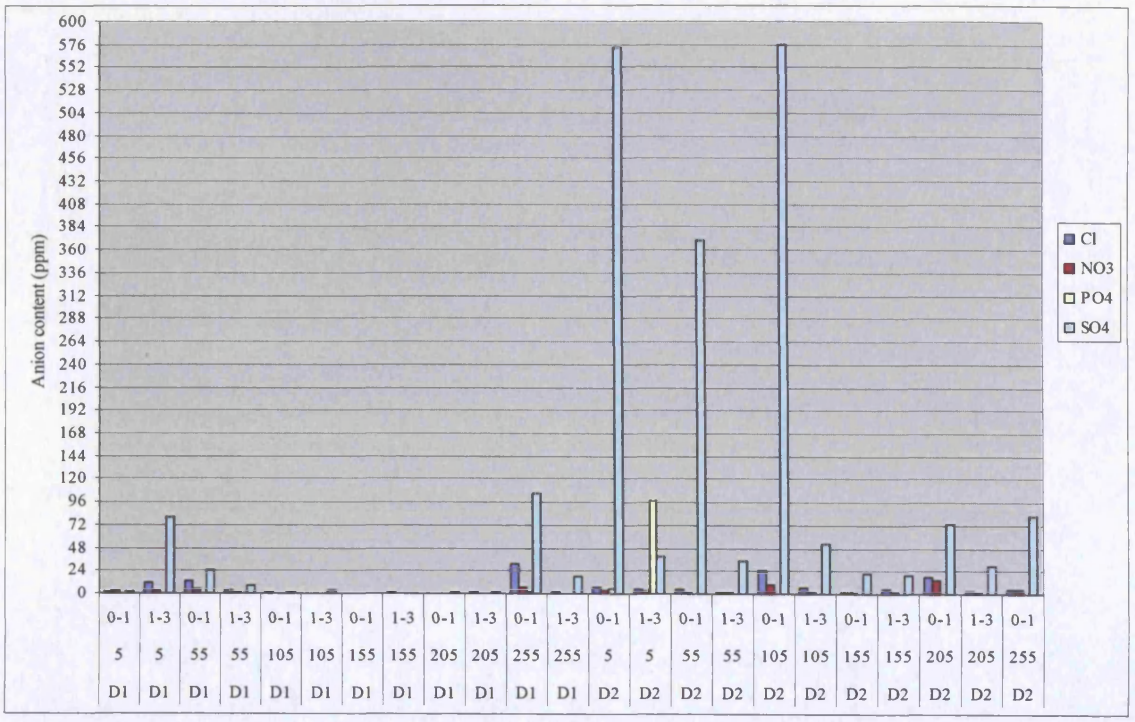

Figure (12Eb): The main anion content in drilled samples from the Deir Tomb, locations (D1 and D2) (Depth intervals: 0-1 and 1-3 cm).
Second fieldwork visit: January 2004.

Appendix F: Temperature and relative humidity spot readings. Third fieldwork visit: June 2004

Time	T (°C)	RH%	Time	T (°C)	RH%	Time	T (°C)	RH%	Time	T (°C)	RH%	Time	T (°C)	RH%	Time	T (°C)	RH%
07.40	22.7	53.2	09.50	24.1	51.4	12.00	25.9	49.4	14.10	27.5	46.5	16.20	27.3	41.8	18.30	23.6	44.0
07.45	22.7	53.6	09.55	24.1	51.4	12.05	25.9	49.4	14.15	27.6	46.3	16.25	27.3	41.6	18.35	23.6	44.1
07.50	22.8	53.4	10.00	24.3	51.0	12.10	26.0	49.3	14.20	27.6	45.9	16.30	27.3	41.5	18.40	23.6	44.3
07.55	22.8	53.6	10.05	24.3	51.2	12.15	26.3	49.6	14.25	27.6	45.9	16.35	27.3	41.7	18.45	23.6	44.5
08.00	22.8	53.0	10.10	24.3	51.2	12.20	26.4	49.8	14.30	27.5	45.7	16.40	27.0	41.9	18.50	23.2	44.5
08.05	22.8	54.1	10.15	24.3	51.0	12.25	26.4	49.7	14.35	7.6	45.7	16.45	27.0	41.9	18.55	23.2	44.6
08.10	22.8	54.0	10.20	25.1	51.1	12.30	26.4	49.6	14.40	7.6	45.6	16.50	27.0	42.0	19.00	23.2	44.5
08.15	23.0	53.5	10.25	25.2	51.3	12.35	26.5	49.8	14.45	27.7	45.1	16.55	26.8	42.0	19.05	23.2	44.6
08.20	23.0	53.1	10.30	25.2	51.2	12.40	26.5	48.2	14.50	27.8	45.0	17.00	26.8	42.3	19.10	23.0	44.5
08.25	23.0	53.0	10.35	25.2	51.1	12.45	26.5	48.6	14.55	27.8	44.6	17.05	26.8	42.3	19.15	23.0	44.9
08.30	23.0	52.9	10.40	25.0	51.2	12.50	26.5	49.0	15.00	27.6	44.6	17.10	26.8	42.5	19.20	22.8	45.0
08.35	23.0	53.0	10.45	25.0	51.3	12.55	26.5	49.1	15.05	27.6	44.1	17.15	26.8	42.6	19.25	22.8	45.1
08.40	22.9	53.0	10.50	25.0	51.2	13.00	26.5	48.4	15.10	27.6	44.1	17.20	26.0	42.7	19.30	22.8	45.3
08.45	22.9	53.1	10.55	25.0	51.0	13.05	26.7	48.4	15.15	27.6	44.0	17.25	25.4	42.7	19.35	22.4	45.1
08.50	23.4	52.9	11.00	25.3	50.8	13.10	26.7	48.2	15.20	27.8	43.5	17.30	25.4	42.9	19.40	22.4	45.6
08.55	23.4	52.9	11.05	25.3	51.0	13.15	26.8	48.1	15.25	27.8	43.4	17.35	25.4	43.1	19.45	22.4	45.2
09.00	23.4	52.9	11.10	25.3	50.8	13.20	26.8	48.3	15.30	27.9	43.6	17.40	25.0	43.1	19.50	22.1	45.9
09.05	23.4	52.7	11.15	25.3	50.7	13.25	26.8	48.5	15.35	27.9	43.5	17.45	24.7	43.0	19.55	22.0	45.1
09.10	23.5	53.0	11.20	25.3	50.6	13.30	26.8	48.0	15.40	27.9	43.1	17.50	24.8	43.1	20.00	22.0	45.8
09.15	23.5	52.4	11.25	25.5	50.3	13.35	27.0	47.6	15.45	27.6	43.0	17.55	24.6	43.6	20.05	22.0	46.0
09.20	23.5	52.0	11.30	25.5	50.3	13.40	27.1	47.5	15.50	27.6	42.8	18.00	24.6	43.6	20.10	22.0	46.1
09.25	23.5	52.6	11.35	25.5	50.0	13.45	27.3	47.1	15.55	27.6	42.7	18.05	24.5	43.7	20.15	22.0	46.2
09.30	23.5	52.6	11.40	26.0	50.1	13.50	27.6	47.1	16.00	27.5	42.5	18.10	24.5	43.9	20.20	22.0	46.3
09.35	24.0	52.0	11.45	26.0	50.0	13.55	27.5	47.0	16.05	27.5	42.3	18.15	24.5	43.9	20.25	22.1	46.9
09.40	24.1	51.9	11.50	26.1	49.9	14:00	27.5	46.4	16.10	27.5	42.1	18.20	24.1	43.9	20.30	22.3	47.0
09.45	24.1	51.9	11.55	26.4	49.6	14.05	27.4	46.4	16.15	27.4	42.0	18.25	24.1	43.9	20.35	22.0	47.2

Table (F1): Temperature and relative humidity spot readings. Location: Bab al Siq Triclinium Tomb.
Third fieldwork visit: 21-22 June 2004, between 07.40-20.35.

Appendix F: Temperature and relative humidity spot readings. Third fieldwork visit: June 2004.

Time	T (°C)	RH%	Time	T (°C)	RH%	Time	T (°C)	RH%	Time	T (°C)	RH%	Time	T (°C)	RH%
20.40	22.1	47.3	22.50	21.1	52.2	01.00	20.3	55.1	03.10	18.2	60.9	05.20	19.6	59.0
20.45	22.0	47.6	22.55	21.2	52.2	01.05	20.3	55.2	03.15	18.2	60.8	05.25	19.6	59.0
20.50	22.0	47.6	23.00	21.1	52.2	01.10	20.3	55.2	03.20	18.2	61.2	05.30	19.6	58.8
20.55	22.0	48.2	23.05	21.0	52.8	01.15	20.1	55.6	03.25	18.3	61.4	05.35	19.8	58.8
21.00	21.9	48.2	23.10	21.0	52.7	01.20	20.1	55.6	03.30	18.0	61.3	05.40	19.5	58.6
21.05	21.9	48.3	23.15	21.0	52.7	01.25	20.0	55.5	03.35	18.0	62.2	05.45	19.6	57.4
21.10	21.9	48.1	23.20	20.8	52.9	01.30	20.1	55.4	03.40	18.1	62.4	05.50	19.6	57.1
21.15	21.8	48.3	23.25	21.0	52.9	01.35	20.1	55.6	03.45	17.9	63.0	05.55	19.6	56.9
21.20	21.8	48.2	23.30	20.8	53.0	01.40	20.0	56.0	03.50	17.9	63.0	06.00	19.8	56.8
21.25	21.8	48.4	23.35	20.8	53.1	01.45	19.7	56.3	03.55	18.0	62.8	06.05	19.8	56.0
21.30	21.8	48.1	23.40	20.8	51.9	01.50	19.7	56.5	04.00	18.0	62.1	06.10	19.8	56.2
21.35	21.8	48.5	23.45	20.7	51.8	01.55	19.7	56.6	04.05	18.0	62.2	06.15	19.9	55.6
21.40	21.6	48.5	23.50	20.6	52.8	02.00	19.5	56.8	04.10	18.1	62.1	06.20	19.9	55.5
21.45	21.7	48.9	23.55	20.6	53.1	02.05	19.5	57.0	04.15	18.2	62.0	06.25	20.0	55.7
21.50	21.6	49.3	00.00	20.6	53.6	02.10	19.5	57.3	04.20	18.4	62.9	06.30	20.0	55.9
21.55	21.7	49.6	00.05	20.6	53.6	02.15	19.0	58.1	04.25	18.5	63.0	06.35	20.2	55.3
22.00	21.7	49.7	00.10	20.6	53.6	02.20	19.0	58.2	04.30	18.5	62.5	06.40	20.3	55.0
22.05	21.7	50.1	00.15	20.6	53.9	02.25	18.6	59.3	04.35	18.5	62.1	06.45	20.3	54.3
22.10	21.6	50.2	00.20	20.6	54.0	02.30	18.6	59.4	04.40	18.6	62.0	06.50	20.3	54.3
22.15	21.6	50.2	00.25	20.6	54.0	02.35	18.4	59.5	04.45	18.7	61.8	06.55	20.3	54.1
22.20	21.6	50.1	00.30	20.6	54.3	02.40	18.4	59.8	04.50	18.8	61.7	07.00	20.4	53.9
22.25	21.6	50.2	00.35	20.4	54.6	02.45	18.4	59.3	04.55	18.8	61.2			
22.30	21.5	50.3	00.40	20.4	54.8	02.50	18.3	60.0	05.00	18.9	60.1			
22.35	21.5	50.7	00.45	20.3	54.8	02.55	18.3	60.2	05.05	19.3	60.2			
22.40	21.0	51.2	00.50	20.4	54.9	03.00	18.4	60.5	05.10	19.3	60.0			
22.45	21.0	51.1	00.55	20.4	54.9	03.05	18.2	60.9	05.15	19.4	59.8			

Table (F2): Temperature and relative humidity spot readings. Location: Bab al Siq Triclinium Tomb.
Third fieldwork visit: 21-22 June 2004, between 20.40-07.00.

Appendix F: Temperature and relative humidity spot readings. Third fieldwork visit: June 2004.

Time	T (°C)	RH%	Time	T (°C)	RH%	Time	T (°C)	RH%	Time	T (°C)	RH%	Time	T (°C)	RH%	Time	T (°C)	RH%
07.40	20.6	53.8	09.50	24.3	50.6	12.00	26.6	48.4	14.10	28.3	46.4	16.20	30.0	39.5	18.30	27.4	36.8
07.45	20.6	53.4	09.55	24.3	50.7	12.05	26.7	48.5	14.15	28.3	46.3	16.25	29.8	39.4	18.35	27.4	37.6
07.50	20.7	53.2	10.00	24.5	50.7	12.10	26.7	48.5	14.20	28.3	46.1	16.30	29.8	38.8	18.40	27.3	37.8
07.55	20.7	53.0	10.05	24.6	50.5	12.15	27.0	48.3	14.25	28.4	46.0	16.35	29.7	38.6	18.45	27.3	37.9
08.00	20.7	53.2	10.10	24.8	50.5	12.20	27.0	48.3	14.30	28.4	46.0	16.40	29.7	38.4	18.50	27.3	38.8
08.05	20.8	53.2	10.15	24.7	50.3	12.25	27.0	48.1	14.35	28.5	45.8	16.45	29.6	38.1	18.55	27.1	38.8
08.10	20.9	53.1	10.20	24.7	50.3	12.30	27.0	48.0	14.40	28.5	45.4	16.50	29.1	37.5	19.00	27.1	39.2
08.15	20.9	52.08	10.25	24.7	50.1	12.35	27.3	48.2	14.45	28.5	45.1	16.55	29.3	37.2	19.05	26.6	39.3
08.20	22.0	52.8	10.30	24.7	50.1	12.40	27.3	48.3	14.50	28.5	45.0	17.00	29.3	37.3	19.10	26.6	40.1
08.25	22.0	52.4	10.35	25.0	50.0	12.45	27.4	48.1	14.55	28.6	44.9	17.05	29.3	37.1	19.15	26.6	40.2
08.30	22.1	52.4	10.40	25.2	49.8	12.50	27.5	48.0	15.00	29.0	44.8	17.10	29.3	37.0	19.20	26.1	40.3
08.35	22.1	52.1	10.45	25.3	49.4	12.55	27.6	47.6	15.05	29.1	44.2	17.15	29.0	36.8	19.25	26.0	40.4
08.40	22.0	52.1	10.50	25.3	49.1	13.00	27.6	47.5	15.10	29.1	44.1	17.20	28.8	36.7	19.30	26.0	40.6
08.45	22.3	51.9	10.55	25.3	49.2	13.05	28.0	47.4	15.15	29.1	44.0	17.25	28.8	36.6	19.35	25.8	40.7
08.50	22.4	51.9	11.00	25.6	49.3	13.10	28.0	47.2	15.20	29.4	43.8	17.30	28.8	36.5	19.40	25.4	41.0
08.55	22.6	51.9	11.05	25.6	49.3	13.15	28.0	47.3	15.25	29.6	43.6	17.35	28.5	36.4	19.45	25.4	41.3
09.00	22.6	51.6	11.10	25.6	49.2	13.20	28.1	47.3	15.30	29.7	42.9	17.40	28.5	36.4	19.50	25.4	42.5
09.05	22.6	51.6	11.15	25.7	49.2	13.25	28.1	47.1	15.35	30.0	42.9	17.45	28.5	36.1	19.55	25.0	42.6
09.10	22.9	51.6	11.20	25.7	49.1	13.30	28.1	47.1	15.40	30.1	42.1	17.50	28.5	36.0	20.00	24.4	43.8
09.15	23.0	51.5	11.25	25.9	48.6	13.35	28.2	47.2	15.45	30.1	41.7	17.55	28.5	35.8	20.05	24.4	44.4
09.20	23.5	51.0	11.30	25.9	48.6	13.40	28.3	47.0	15.50	30.1	41.5	18.00	28.1	35.3	20.10	24.1	44.6
09.25	23.5	51.0	11.35	26.3	48.7	13.45	28.3	47.0	15.55	30.0	41.3	18.05	28.1	35.6	20.15	24.0	44.9
09.30	24.1	51.1	11.40	26.3	48.5	13.50	28.2	46.8	16.00	30.3	41.1	18.10	28.0	35.9	20.20	24.0	45.7
09.35	24.2	50.8	11.45	26.5	48.5	13.55	28.0	46.8	16.05	30.4	40.8	18.15	28.0	36.2	20.25	23.6	45.8
09.40	24.3	50.6	11.50	26.5	48.4	14:00	28.0	46.4	16.10	30.1	40.1	18.20	27.7	36.7	20.30	23.6	45.9
09.45	24.2	50.6	11.55	26.5	48.4	14.05	28.2	46.4	16.15	30.0	39.9	18.25	27.5	36.9	20.35	23.6	46.0

Table (F3): Temperature and relative humidity spot readings. Location: Palace Tomb.
Third fieldwork visit: 22-23 June 2004, between 7.40-20.35.

Appendix F: Temperature and relative humidity spot readings. Third fieldwork visit: June 2004.

Time	T (°C)	RH%	Time	T (°C)	RH%	Time	T (°C)	RH%	Time	T (°C)	RH%	Time	T (°C)	RH%
20.40	23.1	46.3	22.50	21.6	50.8	01.00	19.8	54.3	03.10	18.8	57.6	05.20	18.9	58.3
20.45	23.1	46.4	22.55	21.4	50.9	01.05	19.7	54.3	03.15	18.8	57.4	05.25	19.0	58.4
20.50	23.0	46.5	23.00	21.4	50.9	01.10	19.6	54.3	03.20	18.8	57.3	05.30	19.1	58.3
20.55	23.0	46.8	23.05	21.4	51.2	01.15	19.6	54.5	03.25	18.8	57.2	05.35	19.2	58.1
21.00	23.0	46.9	23.10	21.1	51.2	01.20	19.5	54.5	03.30	18.6	57.9	05.40	19.2	57.8
21.05	22.8	47.6	23.15	21.1	51.3	01.25	19.4	55.0	03.35	18.6	58.0	05.45	19.3	57.6
21.10	22.8	47.8	23.20	21.1	51.6	01.30	19.4	55.1	03.40	18.6	58.3	05.50	19.3	57.0
21.15	22.8	48.2	23.25	20.9	51.9	01.35	19.4	55.1	03.45	18.5	58.2	05.55	19.4	57.1
21.20	22.8	48.2	23.30	20.9	52.0	01.40	19.4	55.1	03.50	18.5	58.2	06.00	19.4	56.4
21.25	22.4	48.2	23.35	20.9	52.6	01.45	19.3	55.3	03.55	18.3	58.8	06.05	19.4	56.3
21.30	22.5	48.2	23.40	20.8	52.6	01.50	19.3	55.8	04.00	18.3	58.8	06.10	19.6	56.1
21.35	22.4	48.9	23.45	20.8	52.4	01.55	19.3	56.2	04.05	18.1	58.7	06.15	19.8	55.0
21.40	22.3	48..9	23.50	20.7	52.8	02.00	19.3	56.4	04.10	18.1	58.6	06.20	19.9	54.2
21.45	22.3	48.9	23.55	20.4	53.3	02.05	19.2	56.7	04.15	18.0	58.3	06.25	19.9	53.2
21.50	22.3	50.1	00.00	20.4	53.3	02.10	19.0	56.8	04.20	18.0	59.0	06.30	20.1	53.1
21.55	22.3	50.2	00.05	20.4	53.3	02.15	19.0	57.4	04.25	17.8	59.2	06.35	20.3	52.1
22.00	22.3	50.2	00.10	20.2	53.6	02.20	19.0	56.5	04.30	18.0	59.2	06.40	20.3	50.3
22.05	22.0	50.3	00.15	20.1	53.5	02.25	19.0	56.5	04.35	18.1	59.3	06.45	20.4	49.8
22.10	22.0	50.6	00.20	20.1	53.6	02.30	18.9	57.0	04.40	18.3	58.8	06.50	20.4	48.6
22.15	22.0	50.9	00.25	20.1	53.7	02.35	18.9	57.0	04.45	18.3	58.6	06.55	20.5	47.8
22.20	22.0	50.9	00.30	20.0	53.8	02.40	18.9	57.3	04.50	18.3	58.6	07.00	20.5	47.2
22.25	22.4	50.9	00.35	20.0	54.0	02.45	18.9	57.4	04.55	18.3	58.4			
22.30	22.0	51.0	00.40	20.0	54.0	02.50	18.9	57.4	05.00	18.4	58.4			
22.35	21.8	50.8	00.45	19.9	54.1	02.55	18.9	57.1	05.05	18.6	58.4			
22.40	21.8	50.8	00.50	19.8	54.2	03.00	18.9	57.2	05.10	18.6	58.1			
22.45	21.0	50.7	00.55	20.4	54.3	03.05	18.9	57.1	05.15	18.8	58.2			

Table (F4): Temperature and relative humidity spot readings. Location: Palace Tomb.
Third fieldwork visit: 22-23 June 2004, between 20.40-07.00.

Appendix F: Temperature and relative humidity spot readings. Third fieldwork visit: June 2004.

Time	T (°C)	RH%	Time	T (°C)	RH%	Time	T (°C)	RH%	Time	T (°C)	RH%	Time	T (°C)	RH%	Time	T (°C)	RH%
07.40	21.1	46.2	09.50	23.2	42.0	12.00	25.0	37.5	14.10	28.3	33.1	16.20	28.4	24.4	18.30	22.0	34.0
07.45	21.0	46.5	09.55	23.1	42.1	12.05	25.1	37.2	14.15	28.3	33.0	16.25	28.0	25.6	18.35	21.5	34.2
07.50	21.0	46.1	10.00	23.4	41.5	12.10	25.1	37.2	14.20	28.3	33.0	16.30	28.0	26.7	18.40	21.6	34.2
07.55	21.0	46.0	10.05	23.4	41.5	12.15	25.1	37.3	14.25	28.6	33.1	16.35	27.6	26.7	18.45	21.6	34.8
08.00	21.0	45.7	10.10	23.4	41.6	12.20	25.2	36.9	14.30	28.6	33.2	16.40	27.6	27.1	18.50	21.0	34.7
08.05	21.0	45.1	10.15	23.4	41.5	12.25	25.2	36.8	14.35	28.6	33.1	16.45	27.6	27.6	18.55	21.0	35.0
08.10	21.1	45.2	10.20	23.4	41.3	12.30	25.6	37.2	14.40	28.7	33.1	16.50	26.5	28.4	19.00	21.0	35.0
08.15	21.2	45.0	10.25	23.4	41.0	12.35	25.9	36.7	14.45	28.9	33.0	16.55	26.5	29.7	19.05	21.0	35.4
08.20	21.2	44..3	10.30	23.4	41.1	12.40	26.1	36.5	14.50	28.9	32.2	17.00	25.1	30.1	19.10	20.6	35.3
08.25	21.21	44.5	10.35	23.4	40.7	12.45	26.4	36.4	14.55	29.0	32.5	17.05	25.2	30.4	19.15	20.6	35.1
08.30	21.2	44.4	10.40	23.5	40.7	12.50	26.7	36.4	15.00	29.0	32.5	17.10	25.0	30.4	19.20	20.6	35.4
08.35	21.3	44.3	10.45	23.6	40.5	12.55	26.8	36.1	15.05	29.0	32.5	17.15	25.0	30.6	19.25	20.4	35.6
08.40	21.4	44.1	10.50	23.8	40.4	13.00	26.8	35.1	15.10	29.1	31.0	17.20	24.7	31.4	19.30	20.5	36.0
08.45	21.5	43.8	10.55	23.6	40.0	13.05	26.8	35.1	15.15	29.1	31.3	17.25	24.7	31.9	19.35	20.3	36.0
08.50	21.5	44.0	11.00	23.8	40.1	13.10	27.4	35.0	15.20	29.1	30.1	17.30	23.9	31.8	19.40	20.5	36.4
08.55	21.9	43.4	11.05	24.1	39.8	13.15	27.5	34.7	15.25	29.3	29.8	17.35	23.9	32.4	19.45	20.0	37.1
09.00	22.2	44.1	11.10	24.1	39.8	13.20	27.5	34.7	15.30	29.4	27.1	17.40	23.9	32.5	19.50	19.8	37.1
09.05	22.3	44.1	11.15	24.3	39.8	13.25	27.5	34.7	15.35	29.4	27.4	17.45	23.9	32.5	19.55	19.8	37.2
09.10	22.6	44.0	11.20	24.5	39.4	13.30	27.6	34.0	15.40	29.4	27.1	17.50	23.4	32.7	20.00	19.7	37.6
09.15	22.8	43.8	11.25	24.6	39.4	13.35	28.1	34.1	15.45	29.4	26.5	17.55	23.4	32.9	20.05	19.6	37.8
09.20	22.9	43.4	11.30	24.5	39.1	13.40	28.2	34.0	15.50	29.5	24.1	18.00	23.1	33.1	20.10	19.4	38.1
09.25	23.1	43.2	11.35	24.8	38.8	13.45	28.2	33.6	15.55	29.3	23.1	18.05	23.3	33.6	20.15	19.1	38.5
09.30	23.1	42.9	11.40	24.9	38.1	13.50	28.2	33.4	16.00	29.4	23.1	18.10	23.2	33.4	20.20	19.5	38.6
09.35	23.1	42.9	11.45	24.9	38.2	13.55	28.2	33.3	16.05	29.2	23.1	18.15	22.4	33.9	20.25	19.2	39.4
09.40	23.1	42.8	11.50	25.0	38.0	14:00	28.4	33.4	16.10	29.1	23.3	18.20	22.4	34.8	20.30	19.0	39.4
09.45	23.1	42.4	11.55	25.0	37.7	14.05	28.4	33.1	16.15	29.1	23.4	18.25	22.0	33.3	20.35	18.7	40.2

Table (F5): Temperature and relative humidity spot readings.Location: The Deir Tomb.
Third fieldwork visit: 23-24 June 2004, between 07.40-20.35.

Appendix F: Temperature and relative humidity spot readings. Third fieldwork visit: June 2004.

Time	T (°C)	RH%	Time	T (°C)	RH%	Time	T (°C)	RH%	Time	T (°C)	RH%	Time	T (°C)	RH%
20.40	18.8	40.0	22.50	18.4	47.6	01.00	17.9	52.0	03.10	17.1	56.2	05.20	18.2	58.1
20.45	18.7	41.2	22.55	18.3	48.0	01.05	17.8	52.3	03.15	17.0	56.4	05.25	18.3	58.0
20.50	18.7	41.3	23.00	18.3	18.4	01.10	17.8	52.4	03.20	17.0	56.4	05.30	18.4	57.1
20.55	18.7	41.6	23.05	18.4	48.3	01.15	17.8	52.6	03.25	16.9	56.4	05.35	18.4	56.4
21.00	18.7	42.6	23.10	18.4	48.6	01.20	17.4	52.8	03.30	16.9	57.0	05.40	18.5	56.1
21.05	18.7	42.8	23.15	18.2	48.7	01.25	17.4	52.9	03.35	16.8	57.2	05.45	18.6	56.4
21.10	18.7	42.8	23.20	18.2	48.9	01.30	17.4	52.4	03.40	16.8	57.8	05.50	18.7	55.4
21.15	18.6	42.9	23.25	18.2	48.9	01.35	17.4	52.0	03.45	16.8	57.8	05.55	18.7	55.9
21.20	18.6	43.6	23.30	18.2	49.3	01.40	17.5	52.4	03.50	16.8	58.0	06.00	18.8	55.1
21.25	18.5	43.6	23.35	18.2	49.4	01.45	17.5	52.5	03.55	16.7	58.2	06.05	18.9	53.6
21.30	18.5	44.5	23.40	18.0	49.4	01.50	17.5	52.9	04.00	16.7	58.3	06.10	19.0	53.1
21.35	18.3	44.5	23.45	18.0	49.8	01.55	17.4	53.0	04.05	16.8	58.4	06.15	19.1	52.2
21.40	18.3	44.5	23.50	18.3	49.7	02.00	17.4	53.4	04.10	16.8	58.6	06.20	19.3	52.4
21.45	18.4	44.1	23.55	18.3	50.1	02.05	17.3	53.5	04.15	16.9	59.0	06.25	19.4	52.1
21.50	18.6	44.9	00.00	18.3	50.1	02.10	17.2	53.4	04.20	17.0	59.1	06.30	19.4	52.0
21.55	18.6	45.0	00.05	18.2	50.1	02.15	17.3	54.0	04.25	17.1	59.2	06.35	19.5	51.4
22.00	18.9	45.0	00.10	18.2	51.3	02.20	17.3	54.5	04.30	17.2	59.3	06.40	19.5	50.8
22.05	18.9	45.6	00.15	18.0	51.3	02.25	17.3	54.6	04.35	17.3	59.4	06.45	19.6	50.4
22.10	18.9	44.3	00.20	18.0	51.0	02.30	17.1	55.3	04.40	17.4	59.5	06.50	19.7	49.9
22.15	19.0	44.8	00.25	18.0	51.4	02.35	17.0	55.4	04.45	17.5	59.4	06.55	19.8	49.8
22.20	18.7	45.1	00.30	18.0	51.0	02.40	17.1	55.4	04.50	17.6	60.0	07.00	19.7	49.8
22.25	18.6	46.2	00.35	18.0	51.9	02.45	17.1	55.8	04.55	17.8	59.8			
22.30	18.6	46.3	00.40	18.1	52.8	02.50	17.1	55.4	05.00	17.8	60.1			
22.35	18.5	47.2	00.45	17.8	52.6	02.55	17.2	55.2	05.05	17.9	60.0			
22.40	18.5	47.6	00.50	17.8	52.7	03.00	17.0	55.8	05.10	17.9	59.8			
22.45	18.4	48.0	00.55	17.7	52.9	03.05	17.0	56.2	05.15	18.0	58.7			

Table (F6): Temperature and relative humidity spot readings. Location: The Deir Tomb.
Third fieldwork visit: 23-24 June 2004, between 20.40-07.00.

Appendix G: Wind speeds spot readings profiles. Third fieldwork visit: June 2004.

Location	Date	Height (cm)	Time	Maximum wind speed (m/s)	Minimum wind speed (m/s)	Average wind speed (m/s)	Location	Date	Height (cm)	Time	Maximum wind speed (m/s)	Minimum wind speed (m/s)	Average wind speed (m/s)
T1	19.6.2004	5	05.00	0.9	0.1	0.5	T1	19.6.2004	205	05.05	0.8	0.2	0.4
T1	19.6.2004	5	06.00	0.7	0.1	0.4	T1	19.6.2004	205	06.05	0.7	0.1	0.4
T1	19.6.2004	5	07.00	0.5	0.1	0.4	T1	19.6.2004	205	07.05	0.6	0.1	0.4
T1	19.6.2004	5	08.00	0.3	0.0	0.2	T1	19.6.2004	205	08.05	0.4	0.1	0.3
T1	19.6.2004	5	09.00	0.6	0.2	0.3	T1	19.6.2004	205	09.05	0.7	0.0	0.3
T1	19.6.2004	5	10.00	0.7	0.2	0.5	T1	19.6.2004	205	10.05	0.9	0.4	0.6
T1	19.6.2004	5	11.00	0.7	0.3	0.5	T1	19.6.2004	205	11.05	0.8	0.2	0.5
T1	19.6.2004	5	12.00	0.5	0.0	0.3	T1	19.6.2004	205	12.05	0.3	0.3	0.3
T1	19.6.2004	5	13.00	0.4	0.1	0.3	T1	19.6.2004	205	13.05	0.5	0.1	0.4
T1	19.6.2004	5	14.00	0.8	0.2	0.6	T1	19.6.2004	205	14.05	1.0	0.4	0.7
T1	19.6.2004	5	15.00	0.8	0.2	0.5	T1	19.6.2004	205	15.05	1.5	0.6	0.9
T1	19.6.2004	5	16.00	1.7	0.3	1.0	T1	19.6.2004	205	16.05	1.8	0.6	1.1
T1	21.6.2004	5	17.00	1.6	0.4	1.1	T1	19.6.2004	205	17.05	2.1	0.7	1.4
T1	19.6.2004	5	18.00	2.1	0.5	1.3	T1	19.6.2004	205	18.05	2.4	0.6	1.6
T1	19.6.2004	5	19.00	2.7	0.6	1.6	T1	19.6.2004	205	19.05	2.7	0.9	1.9
T1	21.6.2004	5	05.00	0.6	0.2	0.4	T1	21.6.2004	205	05.05	0.5	0.2	0.4
T1	21.6.2004	5	06.00	0.6	0.2	0.3	T1	21.6.2004	205	06.05	0.6	0.0	0.4
T1	21.6.2004	5	07.00	0.6	0.2	0.4	T1	21.6.2004	205	07.05	0.7	0.0	0.4
T1	21.6.2004	5	08.00	0.2	0.0	0.1	T1	21.6.2004	205	08.05	0.4	0.1	0.3
T1	21.6.2004	5	09.00	0.3	0.2	0.3	T1	21.6.2004	205	09.05	0.4	0.1	0.3
T1	21.6.2004	5	10.00	0.7	0.2	0.4	T1	21.6.2004	205	10.05	0.9	0.2	0.5
T1	21.6.2004	5	11.00	0.7	0.3	0.5	T1	21.6.2004	205	11.05	1.0	0.1	0.6
T1	21.6.2004	5	12.00	0.4	0.1	0.2	T1	21.6.2004	205	12.05	0.6	0.1	0.4
T1	21.6.2004	5	13.00	0.4	0.1	0.3	T1	21.6.2004	205	13.05	0.6	0.0	0.3
T1	21.6.2004	5	14.00	0.8	0.3	0.5	T1	21.6.2004	205	14.05	1.0	0.4	0.6
T1	21.6.2004	5	15.00	1.2	0.4	0.7	T1	21.6.2004	205	15.05	1.3	0.5	0.9
T1	21.6.2004	5	16.00	1.3	0.4	0.9	T1	21.6.2004	205	16.05	1.3	0.4	0.9
T1	21.6.2004	5	17.00	2.0	0.5	1.3	T1	21.6.2004	205	17.05	1.8	0.5	1.1
T1	21.6.2004	5	18.00	1.9	0.7	1.4	T1	21.6.2004	205	18.05	2.4	1.0	1.5
T1	21.6.2004	5	19.00	2.5	0.6	1.5	T1	21.6.2004	205	19.05	2.7	0.9	1.7

Table (G1): Wind speed spot readings. Location: Bab al Siq Triclinium Tomb (T1). Third fieldwork visit: June 2004.

Appendix G: Wind speed spot readings. Third fieldwork visit: June 2004.

Location	Date	Height (cm)	Time	Maximum wind speed (m/s)	Minimum wind speed (m/s)	Average wind speed (m/s)	Location	Date	Height (cm)	Time	Maximum wind speed (m/s)	Minimum wind speed (m/s)	Average wind speed (m/s)
T1	19.6.2004	350	05.10	0.8	0.2	0.5	T2	19.6.2004	350	05.15	0.7	0.1	0.4
T1	19.6.2004	350	06.10	0.8	0.2	0.4	T2	19.6.2004	350	06.15	0.7	0.3	0.5
T1	19.6.2004	350	07.10	0.7	0.2	0.4	T2	19.6.2004	350	07.15	0.6	0.1	0.3
T1	19.6.2004	350	08.10	0.5	0.1	0.3	T2	19.6.2004	350	08.15	0.5	0.1	0.3
T1	19.6.2004	350	09.10	0.6	0.1	0.4	T2	19.6.2004	350	09.15	0.6	0.1	0.3
T1	19.6.2004	350	10.10	0.9	0.4	0.6	T2	19.6.2004	350	10.15	0.7	0.2	0.5
T1	19.6.2004	350	11.10	0.8	0.3	0.6	T2	19.6.2004	350	11.15	0.8	0.2	0.5
T1	19.6.2004	350	12.10	0.4	0.2	0.3	T2	19.6.2004	350	12.15	0.5	0.1	0.3
T1	19.6.2004	350	13.10	0.6	0.0	0.4	T2	19.6.2004	350	13.15	0.6	0.1	0.4
T1	19.6.2004	350	14.10	1.2	0.5	0.7	T2	19.6.2004	350	14.15	1.1	0.4	0.7
T1	19.6.2004	350	15.10	1.7	0.7	1.0	T2	19.6.2004	350	15.15	1.1	0.5	0.9
T1	19.6.2004	350	16.10	1.8	0.6	1.1	T2	19.6.2004	350	16.15	1.4	0.6	1.0
T1	21.6.2004	350	17.10	2.2	0.5	1.5	T2	19.6.2004	350	17.15	1.9	0.7	1.3
T1	19.6.2004	350	18.10	2.8	0.8	1.7	T2	19.6.2004	350	18.15	2.0	0.9	1.6
T1	19.6.2004	350	19.10	2.8	0.9	2.0	T2	19.6.2004	350	19.15	2.6	1.1	1.7
T1	21.6.2004	350	05.10	0.8	0.1	0.4	T2	21.6.2004	350	05.15	0.5	0.2	0.3
T1	21.6.2004	350	06.10	0.7	0.2	0.4	T2	21.6.2004	350	06.15	0.5	0.1	0.3
T1	21.6.2004	350	07.10	0.5	0.2	0.3	T2	21.6.2004	350	07.15	0.6	0.1	0.4
T1	21.6.2004	350	08.10	0.2	0.1	0.2	T2	21.6.2004	350	08.15	0.4	0.1	0.2
T1	21.6.2004	350	09.10	0.6	0.2	0.4	T2	21.6.2004	350	09.15	0.5	0.2	0.2
T1	21.6.2004	350	10.10	1.0	0.3	0.7	T2	21.6.2004	350	10.15	0.7	0.2	0.5
T1	21.6.2004	350	11.10	0.9	0.3	0.7	T2	21.6.2004	350	11.15	0.9	0.2	0.5
T1	21.6.2004	350	12.10	0.7	0.1	0.4	T2	21.6.2004	350	12.15	0.5	0.0	0.3
T1	21.6.2004	350	13.10	0.6	0.2	0.4	T2	21.6.2004	350	13.15	0.5	0.1	0.3
T1	21.6.2004	350	14.10	1.0	0.4	0.7	T2	21.6.2004	350	14.15	1.0	0.4	0.7
T1	21.6.2004	350	15.10	1.3	0.5	1.0	T2	21.6.2004	350	15.15	1.4	0.4	1.0
T1	21.6.2004	350	16.10	1.6	0.4	1.0	T2	21.6.2004	350	16.15	1.5	0.4	1.0
T1	21.6.2004	350	17.10	1.7	0.5	1.3	T2	21.6.2004	350	17.15	1.6	0.6	1.1
T1	21.6.2004	350	18.10	2.1	0.6	1.5	T2	21.6.2004	350	18.15	2.3	0.7	1.4
T1	21.6.2004	350	19.10	2.8	0.8	1.6	T2	21.6.2004	350	19.15	2.5	0.8	1.5

Table (G2): Wind speed spot readings. Location: Bab al Siq Triclinium Tomb (T1 and T2). Third fieldwork visit: June 2004.

Appendix G: Wind speed spot readings. Third fieldwork visit: June 2004.

Location	Date	Height (cm)	Time	Maximum wind speed (m/s)	Minimum wind speed (m/s)	Average wind speed (m/s)
T3	19.6.2004	350	05.20	0.6	0.1	0.3
T3	19.6.2004	350	06. 20	0.6	0.3	0.4
T3	19.6.2004	350	07. 20	0.4	0.2	0.3
T3	19.6.2004	350	08. 20	0.6	0.2	0.3
T3	19.6.2004	350	09. 20	0.5	0.2	0.3
T3	19.6.2004	350	10. 20	0.7	0.2	0.4
T3	19.6.2004	350	11. 20	0.7	0.3	0.5
T3	19.6.2004	350	12. 20	0.5	0.1	0.3
T3	19.6.2004	350	13. 20	0.5	0.1	0.3
T3	19.6.2004	350	14. 20	0.9	0.4	0.6
T3	19.6.2004	350	15. 20	1.0	0.5	0.9
T3	19.6.2004	350	16. 20	1.5	0.7	1.0
T3	21.6.2004	350	17. 20	1.8	0.7	1.3
T3	19.6.2004	350	18. 20	1.9	0.9	1.4
T3	19.6.2004	350	19. 20	2.4	1.0	1.5
T3	21.6.2004	350	05.20	0.5	0.2	0.3
T3	21.6.2004	350	06. 20	0.6	0.3	0.4
T3	21.6.2004	350	07. 20	0.5	0.2	0.3
T3	21.6.2004	350	08. 20	0.5	0.2	0.3
T3	21.6.2004	350	09. 20	0.4	0.2	0.3
T3	21.6.2004	350	10. 20	0.6	0.3	0.4
T3	21.6.2004	350	11. 20	0.8	0.3	0.5
T3	21.6.2004	350	12. 20	0.4	0.1	0.3
T3	21.6.2004	350	13. 20	0.5	0.1	0.3
T3	21.6.2004	350	14. 20	0.9	0.4	0.6
T3	21.6.2004	350	15. 20	1.1	0.7	0.8
T3	21.6.2004	350	16. 20	1.6	0.6	1.1
T3	21.6.2004	350	17. 20	1.5	0.6	1.1
T3	21.6.2004	350	18. 20	1.9	0.8	1.4
T3	21.6.2004	350	19. 20	2.3	0.9	1.5

Table (G3): Wind speed spot readings. Location: Bab al Siq Triclinium Tomb (T3). Third fieldwork visit: June 2004.

Appendix G: Wind speed spot readings. Third fieldwork visit: June 2004.

Location	Date	Height (cm)	Time	Maximum wind speed (m/s)	Minimum wind speed (m/s)	Average wind speed (m/s)	Location	Date	Height (cm)	Time	Maximum wind speed (m/s)	Minimum wind speed (m/s)	Average wind speed (m/s)
H	20.6.2004	350	05.00	0.7	0.2	0.5	H	20.6.2004	450	05.05	0.8	0.3	0.5
H	20.6.2004	350	06.00	0.7	0.2	0.4	H	20.6.2004	450	06.05	0.7	0.3	0.5
H	20.6.2004	350	07.00	0.6	0.1	0.4	H	20.6.2004	450	07.05	0.7	0.2	0.5
H	20.6.2004	350	08.00	0.4	0.1	0.3	H	20.6.2004	450	08.05	0.5	0.0	0.3
H	20.6.2004	350	09.00	0.8	0.2	0.4	H	20.6.2004	450	09.05	0.7	0.3	0.5
H	20.6.2004	350	10.00	0.7	0.4	0.5	H	20.6.2004	450	10.05	0.9	0.4	0.7
H	20.6.2004	350	11.00	0.8	0.3	0.6	H	20.6.2004	450	11.05	1.0	0.3	0.7
H	20.6.2004	350	12.00	0.5	0.2	0.4	H	20.6.2004	450	12.05	0.7	0.2	0.5
H	20.6.2004	350	13.00	0.7	0.1	0.5	H	20.6.2004	450	13.05	0.5	0.1	0.4
H	20.6.2004	350	14.00	1.3	0.4	0.8	H	20.6.2004	450	14.05	1.4	0.4	0.9
H	20.6.2004	350	15.00	2.0	0.7	1.2	H	20.6.2004	450	15.05	1.9	0.7	1.3
H	20.6.2004	350	16.00	1.9	0.7	1.3	H	20.6.2004	450	16.05	2.0	0.7	1.3
H	20.6.2004	350	17.00	2.2	0.5	1.3	H	20.6.2004	450	17.05	2.1	0.5	1.3
H	20.6.2004	350	18.00	2.7	0.7	1.7	H	20.6.2004	450	18.05	3.0	1.0	1.9
H	20.6.2004	350	19.00	3.0	1.1	2.1	H	20.6.2004	450	19.05	3.2	1.1	2.1
H	22.6.2004	350	05.00	0.8	0.2	0.5	H	22.6.2004	450	05.05	0.8	0.2	0.5
H	22.6.2004	350	06.00	0.9	0.2	0.5	H	22.6.2004	450	06.05	0.9	0.2	0.6
H	22.6.2004	350	07.00	0.7	0.2	0.4	H	22.6.2004	450	07.05	0.8	0.2	0.5
H	22.6.2004	350	08.00	0.5	0.0	0.3	H	22.6.2004	450	08.05	0.6	0.1	0.4
H	22.6.2004	350	09.00	0.8	0.1	0.5	H	22.6.2004	450	09.05	0.9	0.2	0.5
H	22.6.2004	350	10.00	0.9	0.4	0.6	H	22.6.2004	450	10.05	1.0	0.4	0.7
H	22.6.2004	350	11.00	1.1	0.3	0.7	H	22.6.2004	450	11.05	1.2	0.4	0.8
H	22.6.2004	350	12.00	0.7	0.1	0.4	H	22.6.2004	450	12.05	0.6	0.1	0.4
H	22.6.2004	350	13.00	0.6	0.1	0.4	H	22.6.2004	450	13.05	0.5	0.1	0.4
H	22.6.2004	350	14.00	1.6	0.5	1.0	H	22.6.2004	450	14.05	1.5	0.6	1.0
H	22.6.2004	350	15.00	2.1	0.8	1.3	H	22.6.2004	450	15.05	2.2	0.9	1.4
H	22.6.2004	350	16.00	2.0	0.9	1.3	H	22.6.2004	450	16.05	2.2	0.9	1.3
H	22.6.2004	350	17.00	2.1	0.6	1.4	H	22.6.2004	450	17.05	2.3	0.8	1.6
H	22.6.2004	350	18.00	3.0	0.7	1.8	H	22.6.2004	450	18.05	2.8	0.8	1.8
H	22.6.2004	350	19.00	2.9	1.2	2.1	H	22.6.2004	450	19.05	3.2	1.0	2.0

Table (G4): Wind speed spot readings. Location: Corinthian Tomb (H). Third fieldwork visit: June 2004.

Appendix G: Wind speed spot readings. Third fieldwork visit: June 2004.

Location	Date	Height (cm)	Time	Maximum wind speed (m/s)	Minimum wind speed (m/s)	Average wind speed (m/s)	Location	Date	Height (cm)	Time	Maximum wind speed (m/s)	Minimum wind speed (m/s)	Average wind speed (m/s)
C1	20.6.2004	350	05.15	0.7	0.2	0.5	C1	20.6.2004	450	05.20	0.8	0.2	0.5
C1	20.6.2004	350	06.15	0.7	0.1	0.4	C1	20.6.2004	450	06. 20	0.8	0.1	0.5
C1	20.6.2004	350	07.15	0.7	0.1	0.4	C1	20.6.2004	450	07. 20	0.8	0.2	0.4
C1	20.6.2004	350	08.15	0.5	0.1	0.3	C1	20.6.2004	450	08. 20	0.7	0.1	0.4
C1	20.6.2004	350	09.15	0.8	0.2	0.5	C1	20.6.2004	450	09. 20	1.0	0.2	0.6
C1	20.6.2004	350	10.15	0.8	0.3	0.6	C1	20.6.2004	450	10. 20	0.9	0.3	0.6
C1	20.6.2004	350	11.15	0.9	0.2	0.6	C1	20.6.2004	450	11. 20	1.1	0.2	0.7
C1	20.6.2004	350	12.15	0.6	0.1	0.4	C1	20.6.2004	450	12. 20	0.6	0.1	0.4
C1	20.6.2004	350	13.15	0.9	0.1	0.5	C1	20.6.2004	450	13. 20	1.1	0.1	0.6
C1	20.6.2004	350	14.15	1.5	0.4	0.9	C1	20.6.2004	450	14. 20	1.7	0.6	1.1
C1	20.6.2004	350	15.15	2.0	0.8	1.3	C1	20.6.2004	450	15. 20	2.2	0.7	1.4
C1	20.6.2004	350	16.15	2.2	0.6	1.4	C1	20.6.2004	450	16. 20	2.5	0.7	1.5
C1	20.6.2004	350	17.15	2.2	0.5	1.4	C1	20.6.2004	450	17. 20	2.7	0.8	1.5
C1	20.6.2004	350	18.15	3.1	1.0	1.9	C1	20.6.2004	450	18. 20	3.5	1.0	2.1
C1	20.6.2004	350	19.15	3.2	1.1	2.2	C1	20.6.2004	450	19. 20	3.8	1.2	2.5
C1	22.6.2004	350	05.15	1.0	0.3	0.6	C1	22.6.2004	450	05.20	1.0	0.2	0.6
C1	22.6.2004	350	06.15	1.0	0.3	0.5	C1	22.6.2004	450	06. 20	1.1	0.2	0.6
C1	22.6.2004	350	07.15	0.8	0.2	0.5	C1	22.6.2004	450	07. 20	0.8	0.2	0.5
C1	22.6.2004	350	08.15	0.8	0.1	0.4	C1	22.6.2004	450	08. 20	0.9	0.2	0.5
C1	22.6.2004	350	09.15	1.0	0.1	0.5	C1	22.6.2004	450	09. 20	1.0	0.1	0.5
C1	22.6.2004	350	10.15	1.2	0.3	0.7	C1	22.6.2004	450	10. 20	1.3	0.4	0.8
C1	22.6.2004	350	11.15	1.3	0.3	0.8	C1	22.6.2004	450	11. 20	1.3	0.5	0.9
C1	22.6.2004	350	12.15	0.8	0.1	0.4	C1	22.6.2004	450	12. 20	0.8	0.1	0.5
C1	22.6.2004	350	13.15	0.7	0.0	0.4	C1	22.6.2004	450	13. 20	0.6	0.1	0.4
C1	22.6.2004	350	14.15	1.8	0.6	1.3	C1	22.6.2004	450	14. 20	2.1	0.7	1.3
C1	22.6.2004	350	15.15	2.3	0.9	1.5	C1	22.6.2004	450	15. 20	2.3	0.9	1.5
C1	22.6.2004	350	16.15	2.5	1.0	1.6	C1	22.6.2004	450	16. 20	2.8	1.2	1.8
C1	22.6.2004	350	17.15	2.8	0.5	1.7	C1	22.6.2004	450	17. 20	3.1	1.3	2.1
C1	22.6.2004	350	18.15	3.2	1.0	1.9	C1	22.6.2004	450	18. 20	3.5	1.1	2.3
C1	22.6.2004	350	19.15	3.4	1.1	2.2	C1	22.6.2004	450	19. 20	4.0	1.2	2.4

Table (G5): Wind speed spot readings. Location: Palace Tomb (C1). Third fieldwork visit: June 2004.

Appendix G: Wind speed spot readings. Third fieldwork visit: June 2004.

Location	Date	Height (cm)	Time	Maximum wind speed (m/s)	Minimum wind speed (m/s)	Average wind speed (m/s)	Location	Date	Height (cm)	Time	Maximum wind speed (m/s)	Minimum wind speed (m/s)	Average wind speed (m/s)
C2	20.6.2004	350	05.25	0.8	0.2	0.5	C2	20.6.2004	450	05.30	1.0	0.2	0.6
C2	20.6.2004	350	06.25	0.8	0.1	0.4	C2	20.6.2004	450	06.30	0.8	0.1	0.5
C2	20.6.2004	350	07.25	0.8	0.2	0.5	C2	20.6.2004	450	07.30	1.1	0.2	0.7
C2	20.6.2004	350	08.25	0.7	0.0	0.4	C2	20.6.2004	450	08.30	0.8	0.1	0.4
C2	20.6.2004	350	09.25	0.9	0.2	0.5	C2	20.6.2004	450	09.30	1.1	0.3	0.7
C2	20.6.2004	350	10.25	1.1	0.3	0.7	C2	20.6.2004	450	10.30	1.1	0.3	0.7
C2	20.6.2004	350	11.25	1.3	0.4	0.8	C2	20.6.2004	450	11.30	1.4	0.3	0.8
C2	20.6.2004	350	12.25	0.7	0.2	0.4	C2	20.6.2004	450	12.30	0.8	0.2	0.5
C2	20.6.2004	350	13.25	0.9	0.1	0.5	C2	20.6.2004	450	01.30	1.2	0.2	0.8
C2	20.6.2004	350	14.25	1.3	0.4	0.9	C2	20.6.2004	450	14.30	1.5	0.5	1.0
C2	20.6.2004	350	15.25	2.3	0.9	1.5	C2	20.6.2004	450	15.30	2.2	0.8	1.5
C2	20.6.2004	350	16.25	2.4	0.7	1.5	C2	20.6.2004	450	16.30	2.8	0.8	1.7
C2	20.6.2004	350	17.25	2.6	0.7	1.6	C2	20.6.2004	450	17.30	3.0	1.0	1.9
C2	20.6.2004	350	18.25	3.5	1.1	2.2	C2	20.6.2004	450	18.30	4.1	1.3	2.4
C2	20.6.2004	350	19.25	3.9	1.0	2.4	C2	20.6.2004	450	19.30	4.5	1.2	3.0
C2	22.6.2004	350	05.25	1.1	0.3	0.6	C2	22.6.2004	450	05.30	1.2	0.3	0.8
C2	22.6.2004	350	06.25	1.0	0.3	0.7	C2	22.6.2004	450	06.30	1.2	0.4	0.7
C2	22.6.2004	350	07.25	0.9	0.2	0.5	C2	22.6.2004	450	07.30	1.1	0.2	0.6
C2	22.6.2004	350	08.25	0.9	0.2	0.5	C2	22.6.2004	450	08.30	1.3	0.4	0.7
C2	22.6.2004	350	09.25	1.2	0.2	0.6	C2	22.6.2004	450	09.30	1.4	0.4	0.9
C2	22.6.2004	350	10.25	1.4	0.3	0.8	C2	22.6.2004	450	10.30	1.7	0.5	1.0
C2	22.6.2004	350	11.25	1.5	0.5	0.9	C2	22.6.2004	450	11.30	2.0	0.7	1.2
C2	22.6.2004	350	12.25	0.8	0.2	0.5	C2	22.6.2004	450	12.30	1.0	0.2	0.6
C2	22.6.2004	350	13.25	0.8	0.1	0.5	C2	22.6.2004	450	01.30	1.1	0.2	0.6
C2	22.6.2004	350	14.25	2.1	0.6	1.3	C2	22.6.2004	450	14.30	2.6	0.8	1.6
C2	22.6.2004	350	15.25	2.3	0.9	1.5	C2	22.6.2004	450	15.30	2.5	0.9	1.8
C2	22.6.2004	350	16.25	2.9	1.0	1.7	C2	22.6.2004	450	16.30	3.6	1.1	2.1
C2	22.6.2004	350	17.25	3.1	0.9	2.0	C2	22.6.2004	450	17.30	3.9	1.3	2.5
C2	22.6.2004	350	18.25	3.5	1.0	2.1	C2	22.6.2004	450	18.30	4.2	1.2	2.5
C2	22.6.2004	350	19.25	4.1	1.3	2.8	C2	22.6.2004	450	19.30	4.6	1.4	3.1

Table (G6): Wind speed spot readings. Location: Palace Tomb (C2). Third fieldwork visit: June 2004.

Appendix G: Wind speed spot readings. Third fieldwork visit: June 2004.

Location	Date	Height (cm)	Time	Maximum wind speed (m/s)	Minimum wind speed (m/s)	Average wind speed (m/s)	Location	Date	Height (cm)	Time	Maximum wind speed (m/s)	Minimum wind speed (m/s)	Average wind speed (m/s)
C3	20.6.2004	350	05.35	0.5	0.2	0.4	C3	20.6.2004	450	05.40	0.6	0.2	0.5
C3	20.6.2004	350	06.35	0.6	0.1	0.3	C3	20.6.2004	450	06.40	0.9	0.3	0.6
C3	20.6.2004	350	07.35	0.5	0.1	0.4	C3	20.6.2004	450	07.40	0.6	0.2	0.4
C3	20.6.2004	350	08.35	0.4	0.1	0.2	C3	20.6.2004	450	08.40	0.5	0.2	0.4
C3	20.6.2004	350	09.35	0.6	0.3	0.4	C3	20.6.2004	450	09.40	0.6	0.3	0.4
C3	20.6.2004	350	10.35	0.8	0.3	0.5	C3	20.6.2004	450	10.40	0.9	0.4	0.6
C3	20.6.2004	350	11.35	0.7	0.3	0.5	C3	20.6.2004	450	11.40	0.8	0.3	0.6
C3	20.6.2004	350	12.35	0.4	0.2	0.3	C3	20.6.2004	450	12.40	0.6	0.2	0.4
C3	20.6.2004	350	13.35	0.8	0.3	0.5	C3	20.6.2004	450	13.40	1.0	0.4	0.6
C3	20.6.2004	350	14.35	1.2	0.5	0.8	C3	20.6.2004	450	14.40	1.3	0.5	0.9
C3	20.6.2004	350	15.35	1.5	0.8	1.1	C3	20.6.2004	450	15.40	1.7	0.8	1.3
C3	20.6.2004	350	16.35	1.8	0.6	1.2	C3	20.6.2004	450	16.40	1.7	0.9	1.3
C3	20.6.2004	350	17.35	2.0	0.6	1.2	C3	20.6.2004	450	17.40	2.2	0.6	1.3
C3	20.6.2004	350	18.35	2.1	0.9	1.5	C3	20.6.2004	450	18.40	2.3	1.0	1.6
C3	20.6.2004	350	19.35	2.2	0.9	1.4	C3	20.6.2004	450	19.40	2.5	1.2	1.8
C3	22.6.2004	350	05.35	0.7	0.3	0.5	C3	22.6.2004	450	05.40	0.6	0.3	0.5
C3	22.6.2004	350	06.35	0.8	0.2	0.5	C3	22.6.2004	450	06.40	1.0	0.3	0.7
C3	22.6.2004	350	07.35	0.5	0.2	0.4	C3	22.6.2004	450	07.40	0.6	0.3	0.4
C3	22.6.2004	350	08.35	0.6	0.2	0.3	C3	22.6.2004	450	08.40	0.6	0.2	0.4
C3	22.6.2004	350	09.35	0.5	0.2	0.3	C3	22.6.2004	450	09.40	0.8	0.2	0.5
C3	22.6.2004	350	10.35	0.8	0.3	0.6	C3	22.6.2004	450	10.40	1.1	0.4	0.7
C3	22.6.2004	350	11.35	0.7	0.3	0.5	C3	22.6.2004	450	11.40	0.8	0.4	0.6
C3	22.6.2004	350	12.35	0.5	0.2	0.3	C3	22.6.2004	450	12.40	0.8	0.2	0.5
C3	22.6.2004	350	13.35	0.5	0.0	0.3	C3	22.6.2004	450	13.40	0.7	0.2	0.4
C3	22.6.2004	350	14.35	1.0	0.7	0.9	C3	22.6.2004	450	14.40	1.3	0.7	0.9
C3	22.6.2004	350	15.35	1.3	0.9	1.0	C3	22.6.2004	450	15.40	1.5	0.9	1.2
C3	22.6.2004	350	16.35	2.0	0.9	1.2	C3	22.6.2004	450	16.40	1.8	1.0	1.4
C3	22.6.2004	350	17.35	2.3	0.8	1.5	C3	22.6.2004	450	17.40	2.3	1.0	1.6
C3	22.6.2004	350	18.35	2.2	1.0	1.6	C3	22.6.2004	450	18.40	2.3	1.2	1.8
C3	22.6.2004	350	19.35	2.4	1.2	1.7	C3	22.6.2004	450	19.40	2.3	1.3	1.9

Table (G7): Wind speed spot readings. Location: Palace Tomb (C3). Third fieldwork visit: June 2004.

Appendix G: Wind speed spot readings. Third fieldwork visit: June 2004.

Location	Date	Height (cm)	Time	Maximum wind speed (m/s)	Minimum wind speed (m/s)	Average wind speed (m/s)	Location	Date	Height (cm)	Time	Maximum wind speed (m/s)	Minimum wind speed (m/s)	Average wind speed (m/s)
D1	23.6.2004	55	05.00	0.6	0.3	0.4	D1	23.6.2004	255	05.05	0.7	0.3	0.5
D1	23.6.2004	55	06.00	0.5	0.2	0.4	D1	23.6.2004	255	06.05	0.7	0.2	0.5
D1	23.6.2004	55	07.00	0.6	0.2	0.4	D1	23.6.2004	255	07.05	0.7	0.3	0.4
D1	23.6.2004	55	08.00	0.5	0.2	0.3	D1	23.6.2004	255	08.05	0.8	0.2	0.4
D1	23.6.2004	55	09.00	0.7	0.3	0.5	D1	23.6.2004	255	09.05	0.9	0.4	0.7
D1	23.6.2004	55	10.00	0.8	0.4	0.6	D1	23.6.2004	255	10.05	1.0	0.5	0.7
D1	23.6.2004	55	11.00	0.7	0.3	0.5	D1	23.6.2004	255	11.05	0.8	0.4	0.6
D1	23.6.2004	55	12.00	0.6	0.2	0.4	D1	23.6.2004	255	12.05	0.7	0.3	0.4
D1	23.6.2004	55	13.00	0.9	0.3	0.6	D1	23.6.2004	255	13.05	0.8	0.3	0.6
D1	23.6.2004	55	14.00	1.2	0.5	0.8	D1	23.6.2004	255	14.05	1.4	0.7	0.9
D1	23.6.2004	55	15.00	1.7	0.8	1.2	D1	23.6.2004	255	15.05	1.9	0.9	1.3
D1	23.6.2004	55	16.00	1.8	0.7	1.0	D1	23.6.2004	255	16.05	2.0	0.7	1.5
D1	23.6.2004	55	17.00	2.1	0.7	1.3	D1	23.6.2004	255	17.05	2.0	1.0	1.4
D1	23.6.2004	55	18.00	2.2	1.1	1.6	D1	23.6.2004	255	18.05	2.7	1.0	1.8
D1	23.6.2004	55	19.00	2.6	1.1	1.7	D1	23.6.2004	255	19.05	2.8	1.2	1.9
D1	24.6.2004	55	05.00	0.8	0.4	0.5	D1	24.6.2004	255	05.05	0.9	0.4	0.6
D1	24.6.2004	55	06.00	0.9	0.3	0.6	D1	24.6.2004	255	06.05	1.1	0.3	0.8
D1	24.6.2004	55	07.00	0.7	0.2	0.4	D1	24.6.2004	255	07.05	0.8	0.4	0.6
D1	24.6.2004	55	08.00	0.7	0.3	0.4	D1	24.6.2004	255	08.05	0.7	0.3	0.5
D1	24.6.2004	55	09.00	0.7	0.3	0.5	D1	24.6.2004	255	09.05	0.8	0.4	0.6
D1	24.6.2004	55	10.00	1.0	0.3	0.6	D1	24.6.2004	255	10.05	1.2	0.4	0.8
D1	24.6.2004	55	11.00	0.9	0.4	0.7	D1	24.6.2004	255	11.05	1.0	0.4	0.7
D1	24.6.2004	55	12.00	0.6	0.2	0.4	D1	24.6.2004	255	12.05	0.8	0.3	0.5
D1	24.6.2004	55	13.00	0.6	0.2	0.4	D1	24.6.2004	255	13.05	0.5	0.2	0.4
D1	24.6.2004	55	14.00	1.0	0.8	1.0	D1	24.6.2004	255	14.05	1.3	0.9	1.1
D1	24.6.2004	55	15.00	1.5	0.8	1.1	D1	24.6.2004	255	15.05	1.7	1.0	1.3
D1	24.6.2004	55	16.00	2.2	1.0	1.3	D1	24.6.2004	255	16.05	2.0	1.1	1.5
D1	24.6.2004	55	17.00	2.3	1.0	1.6	D1	24.6.2004	255	17.05	2.5	1.2	1.7
D1	24.6.2004	55	18.00	2.5	1.2	1.8	D1	24.6.2004	255	18.05	2.4	1.1	1.8
D1	24.6.2004	55	19.00	2.5	1.2	1.8	D1	24.6.2004	255	19.05	2.6	1.3	2.0

Table (G8): Wind speed spot readings. Location: Deir Tomb (D1). Third fieldwork visit: June 2004.

Appendix G: Wind speed spot readings. Third fieldwork visit: June 2004.

Location	Date	Height (cm)	Time	Maximum wind speed (m/s)	Minimum wind speed (m/s)	Average wind speed (m/s)	Location	Date	Height (cm)	Time	Maximum wind speed (m/s)	Minimum wind speed (m/s)	Average wind speed (m/s)
D2	23.6.2004	55	05.10	0.5	0.3	0.4	D2	23.6.2004	255	05.15	0.6	0.3	0.4
D2	23.6.2004	55	06.10	0.4	0.2	0.3	D2	23.6.2004	255	06.15	0.5	0.2	0.4
D2	23.6.2004	55	07.10	0.5	0.2	0.4	D2	23.6.2004	255	07.15	0.6	0.3	0.4
D2	23.6.2004	55	08.10	0.4	0.2	0.2	D2	23.6.2004	255	08.15	0.6	0.2	0.3
D2	23.6.2004	55	09.10	0.5	0.3	0.4	D2	23.6.2004	255	09.15	0.7	0.4	0.5
D2	23.6.2004	55	10.10	0.7	0.4	0.6	D2	23.6.2004	255	10.15	0.8	0.5	0.6
D2	23.6.2004	55	11.10	0.5	0.3	0.4	D2	23.6.2004	255	11.15	0.7	0.4	0.6
D2	23.6.2004	55	12.10	0.4	0.2	0.3	D2	23.6.2004	255	12.15	0.7	0.3	0.4
D2	23.6.2004	55	13.10	0.7	0.4	0.5	D2	23.6.2004	255	13.15	1.0	0.4	0.6
D2	23.6.2004	55	14.10	1.0	0.5	0.7	D2	23.6.2004	255	14.15	1.1	0.6	0.9
D2	23.6.2004	55	15.10	1.1	0.7	0.9	D2	23.6.2004	255	15.15	1.4	0.7	1.0
D2	23.6.2004	55	16.10	1.3	0.7	1.1	D2	23.6.2004	255	16.15	1.5	0.8	1.2
D2	23.6.2004	55	17.10	1.7	0.8	1.1	D2	23.6.2004	255	17.15	2.0	1.0	1.4
D2	23.6.2004	55	18.10	2.0	0.9	1.3	D2	23.6.2004	255	18.15	2.1	1.0	1.5
D2	23.6.2004	55	19.10	2.2	1.3	1.5	D2	23.6.2004	255	19.15	2.3	1.3	1.6
D2	24.6.2004	55	05.10	0.6	0.4	0.5	D2	24.6.2004	255	05.15	0.7	0.5	0.6
D2	24.6.2004	55	06.10	0.7	0.4	0.6	D2	24.6.2004	255	06.15	0.8	0.4	0.7
D2	24.6.2004	55	07.10	0.6	0.3	0.4	D2	24.6.2004	255	07.15	0.7	0.3	0.5
D2	24.6.2004	55	08.10	0.5	0.3	0.4	D2	24.6.2004	255	08.15	0.6	0.4	0.5
D2	24.6.2004	55	09.10	0.6	0.4	0.4	D2	24.6.2004	255	09.15	0.7	0.5	0.5
D2	24.6.2004	55	10.10	1.1	0.4	0.7	D2	24.6.2004	255	10.15	1.3	0.5	0.9
D2	24.6.2004	55	11.10	1.1	0.4	0.7	D2	24.6.2004	255	11.15	1.2	0.5	0.9
D2	24.6.2004	55	12.10	0.8	0.3	0.4	D2	24.6.2004	255	12.15	0.9	0.5	0.7
D2	24.6.2004	55	13.10	0.7	0.3	0.4	D2	24.6.2004	255	13.15	0.8	0.4	0.6
D2	24.6.2004	55	14.10	1.0	0.7	0.8	D2	24.6.2004	255	14.15	1.0	0.7	0.7
D2	24.6.2004	55	15.10	1.2	0.8	1.1	D2	24.6.2004	255	15.15	1.4	0.7	1.2
D2	24.6.2004	55	16.10	1.6	1.0	1.2	D2	24.6.2004	255	16.15	1.8	1.1	1.4
D2	24.6.2004	55	17.10	1.8	1.1	1.3	D2	24.6.2004	255	17.15	2.0	1.1	1.5
D2	24.6.2004	55	18.10	2.3	1.0	1.6	D2	24.6.2004	255	18.15	2.3	1.2	1.7
D2	24.6.2004	55	19.10	2.8	1.2	1.7	D2	24.6.2004	255	19.15	2.9	1.3	1.9

Table (G9): Wind speed spot readings. Location: Deir Tomb (D2). Third fieldwork visit: June 2004.

Appendix G: Wind speed spot readings. Third fieldwork visit: June 2004.

Location	Date	Height (cm)	Time	Maximum wind speed (m/s)	Minimum wind speed (m/s)	Average wind speed (m/s)
Nabateans Hotel (10 minutes from the archaeological site).	19.6.2004	500	20.00	3.4	1.3	2.9
	19.6.2004	500	21.00	4.4	1.6	3.4
	19.6.2004	500	22.00	4.6	1.4	3.5
	19.6.2004	500	23.00	5.6	1.5	3.8
	19.6.2004	500	00.00	4.3	1.6	3.6
	20.6.2004	500	01.00	6.5	1.6	4.7
	20.6.2004	500	02.00	3.2	1.3	2.1
	20.6.2004	500	03.00	2.3	1.1	1.5
	20.6.2004	500	04.00	1.6	0.6	0.9
	21.6.2004	500	20.00	2.8	0.7	2.0
	21.6.2004	500	21.00	3.8	1.3	2.6
	21.6.2004	500	22.00	3.9	1.5	3.1
	21.6.2004	500	23.00	4.5	1.6	3.4
	21.6.2004	500	00.00	4.5	1.2	3.3
	22.6.2004	500	01.00	4.2	1.8	3.5
	22.6.2004	500	02.00	5.1	1.5	3.7
	22.6.2004	500	03.00	2.0	1.0	1.3
	22.6.2004	500	04.00	1.1	0.5	0.7
	23.6.2004	500	20.00	3.5	1.1	2.2
	23.6.2004	500	21.00	4.1	1.2	2.9
	23.6.2004	500	22.00	5.4	1.6	3.7
	23.6.2004	500	23.00	5.5	1.3	4.1
	23.6.2004	500	00.00	3.0	1.4	2.2
	24.6.2004	500	01.00	3.3	1.2	2.3
	24.6.2004	500	02.00	4.5	1.6	3.4
	24.6.2004	500	03.00	2.0	0.8	1.1
	24.6.2004	500	04.00	0.9	0.2	0.7

Table (G10): Wind speed spot readings. Location: Nabateans Hotel (10 minutes walking distance from the archaeological site). Third fieldwork visit: June 2004.

Appendix H: The anion and cation content of the drilled samples. Third fieldwork visit: June 2004.

Sample Number	Location	Height (cm)	Depth (cm)	Ca (ppm)	Na (ppm)	Mg (ppm)	K (ppm)	Fe (ppm)	Al (ppm)	Ti (ppm)	Zn (ppm)	F (ppm)	Br (ppm)	Cl (ppm)	NO_3 (ppm)	PO_4 (ppm)	SO_4 (ppm)	Cation charge with Al	Cation charge without Al	Anion charge	Sum of cations & anions (ppm)	Soluble salt content in the sample (%) of dry weight
1	T1	5	0-1	4.30	8.90	0.60	12.10	0.00	0.00	0.00	0.00	0.00	0.00	13.48	0.00	0.00	13.48	0.96	0.96	0.66	52.87	0.26
2	T1	5	1-3	2.40	10.90	0.00	0.00	0.00	0.00	0.00	0.00	0.00	0.00	12.79	0.00	0.00	4.66	0.59	0.59	0.46	30.75	0.15
3	T1	55	0-1	4.70	7.60	0.50	0.00	0.00	0.00	0.00	0.00	0.00	0.00	7.01	0.00	0.00	5.90	0.61	0.61	0.32	25.71	0.13
4	T1	55	1-3	3.30	6.30	0.00	0.00	0.00	0.00	0.00	0.00	0.00	0.00	6.88	6.80	0.00	4.76	0.44	0.44	0.40	28.04	0.14
5	T1	105	0-1	4.10	9.20	0.00	0.00	0.00	0.00	0.00	0.00	0.00	0.00	10.16	8.58	0.00	5.90	0.60	0.60	0.55	37.93	0.19
6	T1	105	1-3	3.80	7.70	0.00	0.00	0.00	0.00	0.00	0.00	0.02	0.00	8.24	0.00	0.00	5.42	0.52	0.52	0.35	25.18	0.13
7	T1	155	0-1	6.30	10.90	0.00	0.00	0.00	0.00	0.00	0.00	0.02	0.00	12.93	22.17	0.00	6.43	0.79	0.79	0.86	58.75	0.29
8	T1	155	1-3	6.50	10.60	1.20	0.00	0.00	0.00	0.00	0.00	0.02	0.00	15.31	25.09	0.00	5.89	0.88	0.88	0.96	64.60	0.32
9	T1	205	0-1	5.70	11.90	0.80	0.00	0.00	0.00	0.00	0.00	0.02	0.00	13.72	15.21	0.00	8.81	0.87	0.87	0.82	56.16	0.28
10	T1	205	1-3	2.80	7.50	0.00	0.00	0.00	0.00	0.00	0.00	0.02	0.00	7.86	0.00	0.00	4.67	0.47	0.47	0.32	22.85	0.11
11	T1	305	0-1	12.50	8.60	1.30	0.00	0.00	0.00	0.00	0.00	0.02	0.00	20.14	18.81	0.00	26.48	1.10	1.10	1.42	87.86	0.44
12	T1	305	1-3	13.90	11.10	1.70	0.00	0.00	0.00	0.00	0.00	0.02	0.00	9.39	14.20	0.00	16.87	1.32	1.32	0.85	67.18	0.34
13	T1	405	0-1	9.50	8.40	0.90	0.00	0.00	0.00	0.00	0.00	0.02	0.00	7.47	0.00	0.00	7.04	0.91	0.91	0.36	33.33	0.17
14	T1	405	1-3	9.40	9.10	0.80	0.00	0.00	0.00	0.00	0.00	0.03	0.00	8.20	12.12	0.00	8.40	0.93	0.93	0.60	48.04	0.24
15	T1	505	0-1	40.50	3.40	1.80	0.00	0.00	0.00	0.00	0.00	2.06	0.00	7.61	26.28	0.00	107.20	2.32	2.32	2.98	188.84	0.94
16	T1	505	1-3	21.40	3.50	1.30	0.00	0.00	0.00	0.00	0.00	0.00	0.00	7.71	22.31	0.00	50.13	1.33	1.33	1.62	106.35	0.53
17	T1	550	0-1	8.10	10.50	0.60	0.00	0.00	0.00	0.00	0.00	0.01	0.00	9.55	11.11	0.00	6.84	0.91	0.91	0.59	46.71	0.23
18	T1	550	1-3	2.80	2.00	0.00	0.00	0.00	0.00	0.00	0.00	2.26	0.00	7.07	17.28	0.00	0.00	0.23	0.23	0.60	31.41	0.16
19	T2	305	0-1	9.80	14.10	0.00	0.00	0.00	0.00	0.00	0.00	0.00	0.00	20.33	17.42	0.00	10.70	1.10	1.10	1.08	72.35	0.36
20	T2	305	1-3	11.10	8.10	0.00	0.00	0.00	0.00	0.00	0.00	0.01	0.00	11.84	18.83	0.00	8.86	0.91	0.91	0.82	58.74	0.29
21	T2	405	0-1	35.90	3.40	1.90	0.00	0.00	0.00	0.00	0.00	0.00	0.00	18.58	28.36	0.00	59.36	2.10	2.10	2.22	147.51	0.74
22	T2	405	1-3	13.70	10.90	0.90	0.00	0.00	0.00	0.00	0.00	0.00	0.00	12.08	12.46	0.00	15.23	1.23	1.23	0.86	65.27	0.33
23	T2	505	0-1	13.80	10.75	0.88	0.00	0.00	0.00	0.00	0.00	0.00	0.00	11.99	12.50	0.00	16.21	1.23	1.23	0.90	65.27	0.34
24	T2	505	1-3	5.80	5.90	0.00	0.00	0.00	0.00	0.00	0.00	0.00	0.00	5.88	0.00	0.00	5.60	0.55	0.55	0.28	23.19	0.12
25	T2	550	0-1	4.10	6.90	0.00	0.00	0.00	0.00	0.00	0.00	0.01	0.00	5.98	0.00	0.00	4.40	0.50	0.50	0.26	21.38	0.11
26	T2	550	1-3	6.00	6.90	0.00	0.00	0.00	0.00	0.00	0.00	0.00	0.00	6.06	0.00	0.00	5.00	0.60	0.60	0.27	23.96	0.12

Table (H1): The anion and cation content of drilled samples from the Bib al Siq Triclinium Tomb, locations (T1 and T2). Third fieldwork visit: June 2004.

Appendix H: The anion and cation content of the drilled samples. Third fieldwork visit: June 2004.

Sample Number	Location	Height (cm)	Depth (cm)	Ca (ppm)	Na (ppm)	Mg (ppm)	K (ppm)	Fe (ppm)	Al (ppm)	Ti (ppm)	Zn (ppm)	F (ppm)	Br (ppm)	Cl (ppm)	NO_3 (ppm)	PO_4 (ppm)	SO_4 (ppm)	Cation charge with Al	Cation charge without Al	Anion charge	Sum of cations & anions (ppm)	Soluble salt content in the sample (%) of dry weight
27	T3	405	0-1	38.20	31.10	11.80	100.40	0.00	0.00	0.00	0.00	0.00	0.00	57.95	186.63	0.00	117.49	6.80	6.80	7.09	543.56	2.72
28	T3	405	1-3	46.40	23.80	0.00	197.00	0.00	0.00	0.00	0.00	0.00	0.00	31.61	283.07	0.00	277.68	8.39	8.39	11.24	859.56	4.30
29	T3	505	0-1	140.90	29.60	0.00	266.20	0.00	0.00	0.00	0.00	3.65	0.00	46.63	56.01	0.00	816.56	15.13	15.13	19.42	1,359.54	6.80
30	T3	505	1-3	77.50	48.70	8.30	174.60	0.00	0.00	0.00	0.00	0.00	0.00	90.42	84.49	0.00	425.34	11.13	11.13	12.77	909.35	4.55
31	T3	550	0-1	9.50	40.80	0.00	50.10	0.00	0.00	0.00	0.00	3.75	0.00	82.54	75.64	0.00	24.39	3.53	3.53	4.25	286.72	1.43
32	T3	550	1-3	4.90	27.50	0.00	27.10	0.00	0.00	0.00	0.00	0.00	0.00	49.48	44.43	0.00	9.47	2.13	2.13	2.31	162.89	0.81

Table (H2): The anion and cation content of drilled samples from the Bib al Siq Triclinium Tomb, location (T3).
Third fieldwork visit: June 2004.

Appendix H: The anion and cation content from the drilled samples. Third fieldwork visit: June 2004.

Sample Number	Location	Height (cm)	Depth (cm)	Ca (ppm)	Na (ppm)	Mg (ppm)	K (ppm)	Fe (ppm)	Al (ppm)	Tl (ppm)	Zn (ppm)	F (ppm)	Br (ppm)	Cl (ppm)	NO_3 (ppm)	PO_4 (ppm)	SO_4 (ppm)	Cation charge with Al	Cation charge without Al	Anion charge	Sum of cations & anions (ppm)	Soluble salt content in the sample (%) of dry weight
33	C1	5	0-1	59.20	10.30	0.00	0.00	0.00	0.00	0.00	0.00	0.00	0.00	15.82	11.46	0.00	133.71	3.40	3.40	3.42	230.49	1.15
34	C1	5	1-3	44.80	8.90	0.00	0.00	0.00	0.00	0.00	0.00	0.00	0.00	10.05	8.94	0.00	107.61	2.62	2.62	2.67	180.30	0.90
35	C1	55	0-1	10.20	12.00	3.10	5.20	0.00	0.00	0.00	0.00	2.83	0.00	23.58	23.46	0.00	6.87	1.42	1.42	1.34	87.24	0.44
36	C1	55	1-3	9.00	12.80	12.90	0.00	0.00	0.00	0.00	0.00	0.00	0.00	54.66	21.44	0.00	5.95	2.07	2.07	2.01	116.75	0.58
37	C1	105	0-1	4.30	8..70	0.00	0.00	0.00	0.00	0.00	0.00	0.00	0.00	8.27	6.41	0.00	5.24	0.59	0.59	0.45	32.92	0.16
38	C1	105	1-3	3.80	8.70	0.00	0.00	0.00	0.00	0.00	0.00	1.40	0.00	9.05	6.68	0.00	6.21	0.57	0.57	0.57	35.84	0.18
39	C1	155	0-1	13.50	27.90	4.50	14.50	0.00	0.00	0.00	0.00	1.52	0.00	51.58	40.08	0.00	21.80	2.63	2.63	2.64	175.38	0.88
40	C1	155	1-3	8.60	23.30	6.50	12.10	0.00	0.00	0.00	0.00	1.43	0.00	43.87	33.29	0.00	10.06	2.29	2.29	2.06	139.14	0.70
41	C1	205	0-1	9.90	95.80	9.70	194.80	0.00	0.00	0.00	0.00	0.00	0.00	180.38	435.88	0.00	10.45	10.44	10.44	12.34	936.91	4.68
42	C1	205	1-3	13.80	238.10	0.00	106.00	0.00	0.00	0.00	0.00	1.55	0.00	417.85	196.80	0.00	19.31	13.76	13.76	15.44	993.41	4.97
43	C1	305	0-1	11.40	9.70	0.70	0.00	0.00	0.00	0.00	0.00	0.01	0.00	13.40	9.73	0.00	13.07	1.05	1.05	0.81	58.01	0.29
44	C1	305	1-3	114.50	17.00	0.00	0.00	0.00	0.00	0.00	0.00	4.33	0.00	16.80	12.63	0.00	378.72	6.45	6.45	8.79	543.98	2.72
45	C1	355	0-1	8.90	8.60	0.90	0.00	0.00	0.00	0.00	0.00	0.02	0.00	8.89	9.55	0.00	10.14	0.89	0.89	0.62	46.99	0.23
46	C1	355	1-3	30.10	9.60	0.00	0.00	0.00	0.00	0.00	0.00	1.49	0.00	7.98	8.09	0.00	76.29	1.92	1.92	2.02	133.56	0.67
47	C1	405	0-1	14.30	13.10	2.00	0.00	0.00	0.00	0.00	0.00	1.60	0.00	18.19	13.73	0.00	13.66	1.45	1.45	1.10	76.58	0.38
48	C1	405	1-3	15.30	11.50	2.50	0.00	0.00	0.00	0.00	0.00	0.00	0.00	16.45	14.70	0.00	14.50	1.47	1.47	1.00	74.95	0.37
49	C1	505	0-1	14.90	10.60	1.70	0.00	0.00	0.00	0.00	0.00	1.40	0.00	14.00	12.95	0.00	13.27	1.34	1.34	0.95	68.81	0.34
50	C1	505	1-3	5.90	9.90	0.00	0.00	0.00	0.00	0.00	0.00	1.65	0.00	9.46	7.72	0.00	7.38	0.73	0.73	0.63	42.00	0.21
51	C1	550	0-1	13.10	11.20	1.70	0.00	0.00	0.00	0.00	0.00	0.00	0.00	15.31	12.58	0.00	10.44	1.28	1.28	0.85	64.33	0.32
52	C1	550	1-3	14.50	12.00	1.40	0.00	0.00	0.00	0.00	0.00	0.00	0.00	15.00	10.54	0.00	30.90	1.36	1.36	1.24	84.33	0.42

Table (H3): The anion and cation content of drilled samples from the Palace Tomb, location (C1).
Third fieldwork visit: June 2004.

Appendix H: The anion and cation content from the drilled samples. Third fieldwork visit: June 2004.

Sample Number	Location	Height (cm)	Depth (cm)	Ca (ppm)	Na (ppm)	Mg (ppm)	K (ppm)	Fe (ppm)	Al (ppm)	Tl (ppm)	Zn (ppm)	F (ppm)	Br (ppm)	Cl (ppm)	NO_3 (ppm)	PO_4 (ppm)	SO_4 (ppm)	Cation charge with Al	Cation charge without Al	Anion charge	Sum of cations & anions (ppm)	Soluble salt content in the sample (%) of dry weight
53	C2	105	0-1	272.90	11.90	3.50	32.60	0.00	0.00	0.00	0.00	0.00	0.00	14.22	20.09	5.23	1172.54	15.26	15.26	25.32	1,532.97	7.66
54	C2	105	1-3	153.10	17.40	0.00	0.00	0.00	0.00	0.00	0.00	2.22	0.00	15.86	30.44	4.18	594.84	8.40	8.40	13.58	818.03	4.09
55	C2	155	0-1	334.60	127.70	68.50	1093.00	0.00	0.00	0.00	0.00	5.43	0.00	108.10	2617.70	4.00	1698.79	55.84	55.84	81.07	6,057.81	30.29
56	C2	155	1-3	292.70	105.40	14.60	523.00	0.00	0.00	0.00	0.00	0.00	0.00	56.10	1238.13	4.74	1204.95	33.77	33.77	46.80	3,439.62	17.20
57	C2	205	0-1	19.10	99.40	5.20	92.50	0.00	0.00	0.00	0.00	0.00	0.00	227.92	219.77	0.00	55.28	8.07	8.07	11.12	719.16	3.60
58	C2	205	1-3	14.60	60.00	0.00	56.10	0.00	0.00	0.00	0.00	1.94	0.00	144.87	131.74	0.00	44.14	4.77	4.77	7.23	453.38	2.27
59	C2	255	0-1	38.10	13.00	0.00	0.00	0.00	0.00	0.00	0.00	0.02	0.00	24.08	14.23	0.00	103.38	2.47	2.47	3.06	192.81	0.96
60	C2	255	1-3	292.90	90.00	38.40	2252.00	0.00	0.00	0.00	0.00	4.13	0.00	134.80	0.00	0.00	0.00	79.28	79.28	4.02	2,812.23	14.06
61	C2	305	0-1	292.70	177.90	30.50	1012.00	0.00	0.00	0.00	0.00	3.45	0.00	140.92	658.45	0.00	834.92	50.73	50.73	32.17	3,150.84	15.75
62	C2	305	1-3	313.90	74.60	0.00	380.90	0.00	0.00	0.00	0.00	4.65	0.00	130.84	866.21	0.00	904.06	28.65	28.65	36.74	2,675.16	13.38
63	C2	345	0-1	301.40	142.00	20.20	468.90	0.00	0.00	0.00	0.00	3.65	0.00	115.04	113.62	0.00	48.21	34.87	34.87	6.27	1,213.02	6.07
64	C2	345	1-3	19.20	42.40	0.00	92.80	0.00	0.00	0.00	0.00	0.00	0.00	133.98	210.89	0.00	46.66	5.18	5.18	8.15	545.92	2.73
65	C3	105	0-1	46.60	41.80	0.00	0.00	0.00	0.00	0.00	0.00	4.40	0.00	87.86	130.04	0.00	48.69	4.14	4.14	5.82	359.39	1.80
66	C3	105	1-3	15.30	15.70	1.30	0.00	0.00	0.00	0.00	0.00	3.27	0.00	29.48	32.75	0.00	11.70	1.55	1.55	1.78	109.50	0.55
67	C3	155	0-1	23.70	14.50	1.80	0.00	0.00	0.00	0.00	0.00	0.00	0.00	29.36	36.37	0.00	16.67	1.96	1.96	1.76	122.39	0.61
68	C3	155	1-3	14.70	10.80	0.00	0.00	0.00	0.00	0.00	0.00	3.39	0.00	15.92	12.45	0.00	26.11	1.20	1.20	1.37	83.37	0.42
69	C3	205	0-1	18.60	10.00	1.20	0.00	0.00	0.00	0.00	0.00	0.00	0.00	12.50	15.56	0.00	11.11	1.46	1.46	0.84	68.98	0.34
70	C3	205	1-3	48.10	9.40	1.50	0.00	0.00	0.00	0.00	0.00	3.07	0.00	12.61	10.74	0.00	96.04	2.93	2.93	2.69	181.46	0.91
71	C3	255	0-1	25.00	9.30	0.00	0.00	0.00	0.00	0.00	0.00	1.26	0.00	8.90	7.27	0.00	53.78	1.65	1.65	1.55	105.50	0.53
72	C3	255	1-3	20.40	10.10	0.00	0.00	0.00	0.00	0.00	0.00	3.67	0.00	10.05	10.53	0.00	40.70	1.46	1.46	1.49	95.45	0.48
73	C3	305	0-1	6.80	8.90	0.00	0.00	0.00	0.00	0.00	0.00	0.01	0.00	11.88	7.04	0.00	5.68	0.73	0.73	0.57	40.32	0.20
74	C3	305	1-3	13.50	14.50	0.00	0.00	0.00	0.00	0.00	0.00	8.54	0.00	18.37	16.65	0.00	17.97	1.30	1.30	1.61	89.53	0.45
75	C3	350	0-1	13.80	14.60	1.80	0.00	0.00	0.00	0.00	0.00	0.01	0.00	30.76	19.78	0.00	7.33	1.47	1.47	1.34	88.09	0.44
76	C3	350	1-3	18.30	12.50	0.00	0.00	0.00	0.00	0.00	0.00	3.37	0.00	17.94	12.50	0.00	32.66	1.46	1.46	1.57	97.27	0.49

Table (H4): The anion and cation content of drilled samples from the Palace Tomb, locations (C2 and C3). Third fieldwork visit: June 2004.

Appendix H: The anion and cation content from the drilled samples. Third fieldwork visit: June 2004.

Sample Number	Location	Height (cm)	Depth (cm)	Ca (ppm)	Na (ppm)	Mg (ppm)	K (ppm)	Fe (ppm)	Al (ppm)	Tl (ppm)	Zn (ppm)	F (ppm)	Br (ppm)	Cl (ppm)	NO_3 (ppm)	PO_4 (ppm)	SO_4 (ppm)	Cation charge with Al	Cation charge without Al	Anion charge	Sum of cations & anions (ppm)	Soluble salt content in the sample (%) of dry weight
77	H	25	0-1	44.60	33.40	0.00	0.00	0.00	0.00	0.00	0.00	0.00	0.00	44.05	74.53	0.00	87.68	3.68	3.68	4.27	284.25	1.42
78	H	25	1-3	14.00	9.50	0.00	0.00	0.00	0.00	0.00	0.00	0.01	0.00	15.19	17.85	0.00	16.82	1.11	1.11	1.07	73.37	0.37
79	H	75	0-1	20.30	9.70	1.50	0.00	0.00	0.00	0.00	0.00	1.31	0.00	11.16	12.91	0.00	43.58	1.56	1.56	1.50	100.46	0.50
80	H	75	1-3	61.10	10.70	1.20	0.00	0.00	0.00	0.00	0.00	3.60	0.00	11.64	12.34	0.00	150.57	3.61	3.61	3.85	251.15	1.26
81	H	125	0-1	7.80	8.70	0.00	0.00	0.00	0.00	0.00	0.00	0.00	0.00	11.47	9.67	0.00	6.88	0.77	0.77	0.62	44.52	0.22
82	H	125	1-3	292.70	30.50	117.90	1012.00	292.70	0.00	0.00	0.00	3.59	0.00	122.42	1985.63	0.00	0.00	62.00	62.00	35.67	3,857.44	19.29
83	H	155	0-1	167.50	19.70	155.30	894.30	278.50	0.00	0.00	0.00	1.99	0.00	114.78	1679.02	0.00	79.32	54.84	54.84	32.07	3,390.40	16.95
84	H	155	1-3	98.00	11.40	101.20	259.10	89.00	0.00	0.00	0.00	1.33	0.00	245.99	459.37	0.00	91.67	23.53	23.53	16.33	1,357.05	6.79
84	H	200	0-1	7.80	8.70	0.00	0.00	7.80	0.00	0.00	0.00	1.40	0.00	82.91	45.80	0.00	81.56	1.05	1.05	4.85	235.98	1.18
85	H	200	1-3	39.20	60.00	0.00	0.00	39.20	0.00	0.00	0.00	1.26	0.00	306.66	60.34	0.00	109.19	5.97	5.97	11.96	615.85	3.08
86	H	250	0-1	46.30	188.20	2.70	9.90	46.30	2.70	0.00	0.00	1.27	0.00	42.18	40.74	0.00	7.80	12.93	12.63	2.08	388.09	1.94
87	H	250	1-3	20.00	15.90	4.00	0.00	20.00	4.00	0.00	0.00	0.02	0.00	27.89	29.41	0.00	4.75	3.18	2.74	1.36	125.96	0.63
88	H	300	0-1	18.30	11.40	2.70	0.00	18.30	2.70	0.00	0.00	2.92	0.00	9.37	8.30	0.00	6.67	2.59	2.29	0.69	80.66	0.40
89	H	300	1-3	5.60	10.80	0.00	0.00	5.60	0.00	0.00	0.00	3.89	0.00	14.16	8.18	0.00	7.45	0.95	0.95	0.89	55.67	0.28
90	H	500	0-1	4.40	13.00	0.00	0.00	4.40	0.00	0.00	0.00	1.43	0.00	18.54	17.54	0.00	7.79	0.94	0.94	1.04	67.10	0.34
91	H	500	1-3	8.30	10.90	0.00	0.00	8.30	0.00	0.00	0.00	0.00	0.00	11.29	13.36	0.00	7.28	1.19	1.19	0.69	59.42	0.30

Table (H5): The anion and cation content of drilled samples from the Corinthian Tomb, location (H).
Third fieldwork visit: June 2004.

Appendix H: The anion and cation content from the drilled samples. Third fieldwork visit: June 2004.

Sample Number	Location	Height (cm)	Depth (cm)	Ca (ppm)	Na (ppm)	Mg (ppm)	K (ppm)	Fe (ppm)	Al (ppm)	Ti (ppm)	Zn (ppm)	F (ppm)	Br (ppm)	Cl (ppm)	NO_3 (ppm)	PO_4 (ppm)	SO_4 (ppm)	Cation charge with Al	Cation charge without Al	Anion charge	Sum of cations & anions (ppm)	Soluble salt content in the sample (%) of dry weight
92	D1	5	0-1	15.90	24.40	1.90	0.00	0.00	0.00	0.00	0.00	2.24	0.00	22.81	7.27	0.00	22.70	2.01	2.01	1.35	97.22	0.49
93	D1	5	1-3	8.90	12.40	0.00	0.00	0.00	0.00	0.00	0.00	0.00	0.00	16.75	5.13	0.00	10.31	0.98	0.98	0.77	53.49	0.27
94	D1	55	0-1	20.30	18.50	0.00	0.00	0.00	0.00	0.00	0.00	2.21	0.00	16.29	5.79	0.00	19.50	1.82	1.82	1.08	82.60	0.41
95	D1	55	1-3	11.10	11.60	0.00	0.00	0.00	0.00	0.00	0.00	1.00	0.00	15.21	5.01	0.00	13.37	1.06	1.06	0.84	57.30	0.29
96	D1	105	0-1	12.70	9.20	1.50	0.00	0.00	0.00	0.00	0.00	4.44	0.00	10.12	10.98	0.00	21.01	1.16	1.16	1.13	69.95	0.35
97	D1	105	1-3	9.00	11.70	0.00	0.00	0.00	0.00	0.00	0.00	5.63	0.00	12.31	10.52	0.00	8.63	0.96	0.96	0.99	57.79	0.29
98	D1	155	0-1	11.30	13.00	0.00	0.00	0.00	0.00	0.00	0.00	1.85	0.00	12.28	11.32	0.00	12.47	1.13	1.13	0.89	62.22	0.31
99	D1	155	1-3	6.60	8.90	0.00	0.00	0.00	0.00	0.00	0.00	5.05	0.00	8.98	0.00	0.00	3.34	0.72	0.72	0.59	32.87	0.16
100	D1	205	0-1	21.60	17.90	1.80	0.00	0.00	0.00	0.00	0.00	1.87	0.00	17.91	11.48	0.00	57.37	2.00	2.00	1.98	129.93	0.65
101	D1	205	1-3	6.50	10.40	0.00	0.00	0.00	0.00	0.00	0.00	0.01	0.00	12.67	8.96	0.00	6.84	0.78	0.78	0.64	45.38	0.23
102	D1	255	0-1	13.60	10.50	0.00	0.00	0.00	0.00	0.00	0.00	0.01	0.00	11.83	10.94	0.00	21.14	1.14	1.14	0.95	68.02	0.34
103	D1	255	1-3	7.70	17.40	0.00	0.00	0.00	0.00	0.00	0.00	1.91	0.00	15.46	11.79	0.00	11.78	1.14	1.14	0.97	66.03	0.33
104	D1	305	0-1	16.50	22.90	1.70	0.00	0.00	0.00	0.00	0.00	0.00	0.00	48.21	15.82	0.00	27.05	1.96	1.96	2.18	132.17	0.66
105	D2	5	0-1	281.20	13.50	1.90	0.00	0.00	0.00	0.00	0.00	0.01	0.00	50.22	15.85	0.00	27.18	14.78	14.78	2.24	389.87	1.95
106	D2	5	1-3	74.90	7.10	0.00	0.00	0.00	0.00	0.00	0.00	0.02	0.00	7.65	6.81	0.00	255.04	4.05	4.05	5.64	351.52	1.76
107	D2	55	0-1	270.50	14.70	3.20	0.00	0.00	0.00	0.00	0.00	5.12	0.00	21.02	20.78	0.00	899.83	14.40	14.40	19.94	1,235.15	6.18
108	D2	55	1-3	54.90	14.10	1.50	0.00	0.00	0.00	0.00	0.00	1.84	0.00	18.66	13.27	0.00	171.09	3.48	3.48	4.40	275.35	1.38
109	D2	105	0-1	72.50	19.40	2.20	0.00	0.00	0.00	0.00	0.00	1.86	0.00	27.01	21.08	0.00	230.06	4.64	4.64	5.99	374.10	1.87
110	D2	105	1-3	13.60	11.50	0.00	0.00	0.00	0.00	0.00	0.00	1.88	0.00	15.62	12.10	0.00	30.01	1.18	1.18	1.36	84.71	0.42
111	D2	155	0-1	233.90	27.50	6.10	9.00	0.00	0.00	0.00	0.00	0.01	0.00	59.93	39.73	0.00	458.98	13.60	13.60	11.89	835.15	4.18
112	D2	155	1-3	31.80	14.60	0.00	0.00	0.00	0.00	0.00	0.00	1.20	0.00	21.65	15.54	0.00	96.41	2.22	2.22	2.93	181.19	0.91
113	D2	205	0-1	240.40	16.30	6.80	5.40	0.00	0.00	0.00	0.00	0.00	0.00	18.92	21.35	0.00	570.07	13.40	13.40	12.75	879.23	4.40
114	D2	205	1-3	53.80	12.50	2.90	0.00	0.00	0.00	0.00	0.00	1.74	0.00	14.87	13.17	0.00	170.00	3.47	3.47	4.26	268.98	1.34
115	D2	255	0-1	43.20	13.30	2.90	5.40	0.00	0.00	0.00	0.00	1.81	0.00	22.68	26.15	0.00	130.13	3.11	3.11	3.87	245.56	1.23

Table (H6): The anion and cation content of drilled samples from the Deir Tomb, locations (D1 and D2).
Third fieldwork visit: June 2004.

Appendix Hb: The anion and cation content and distribution in the drilled samples. Third fieldwork visit: June 2004.

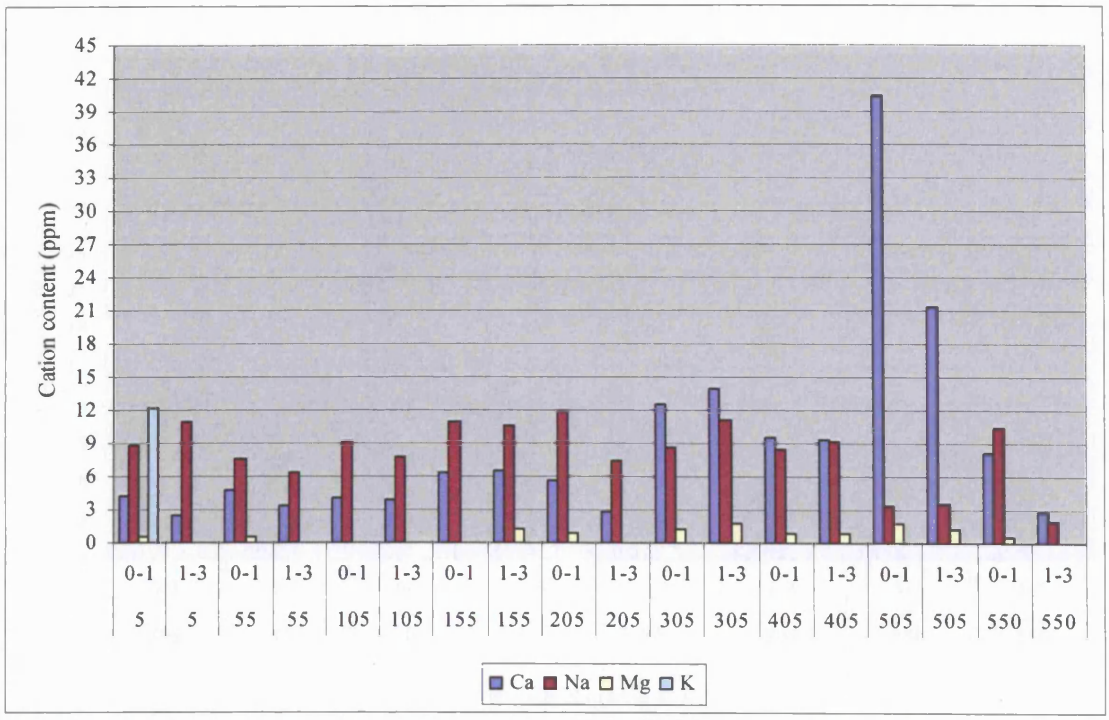

Figure (1Hb): The main cation content of drilled samples from the Bab al Siq Triclinium Tomb, location (T1) (Depth intervals: 0-1 and 1-3 cm).
Third fieldwork visit: June 2004.

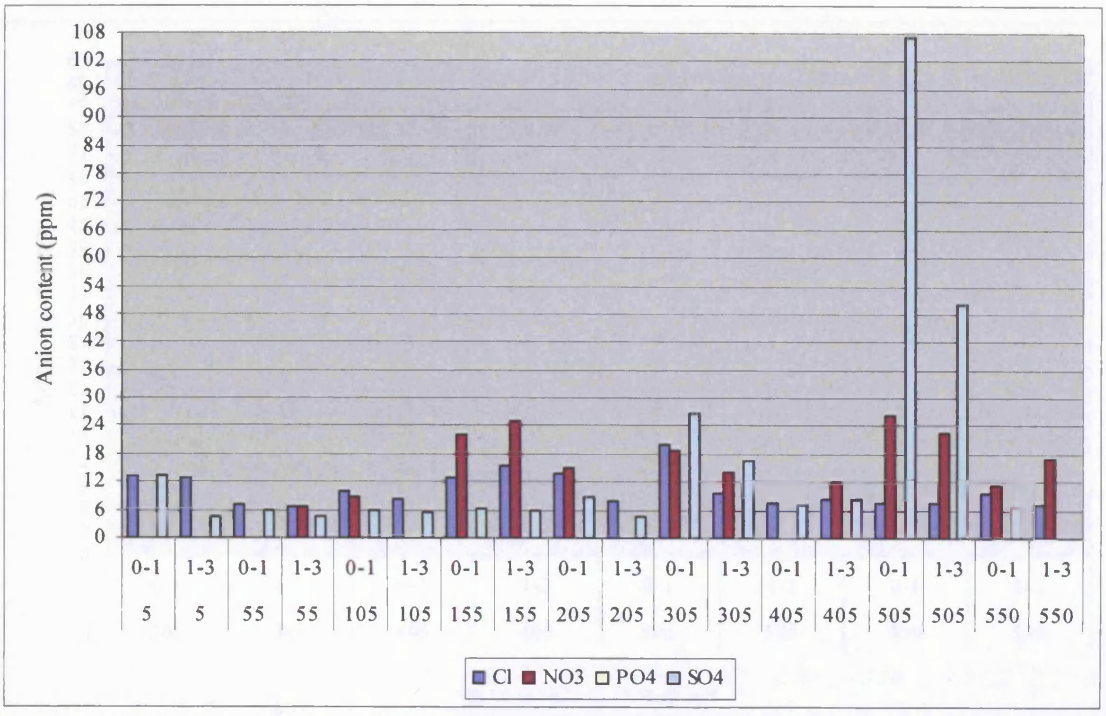

Figure (2Hb): The main anion content of drilled samples from the Bab al Siq Triclinium Tomb, location (T1) (Depth intervals: 0-1 and 1-3 cm).
Third fieldwork visit: June 2004.

Appendix Hb: The anion and cation content and distribution in the drilled samples. Third fieldwork visit: June 2004.

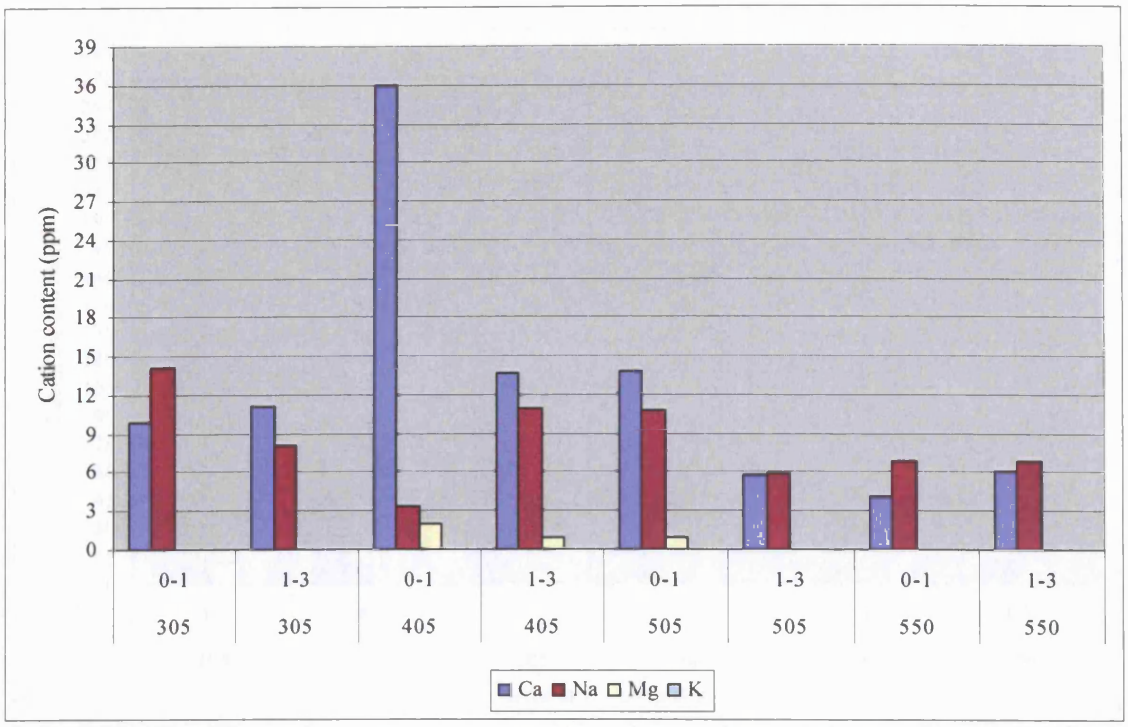

Figure (3Hb): The main cation content of drilled samples from the Bab al Siq Triclinium Tomb, location (T2) (Depth intervals: 0-1 and 1-3 cm).
Third fieldwork visit: June 2004.

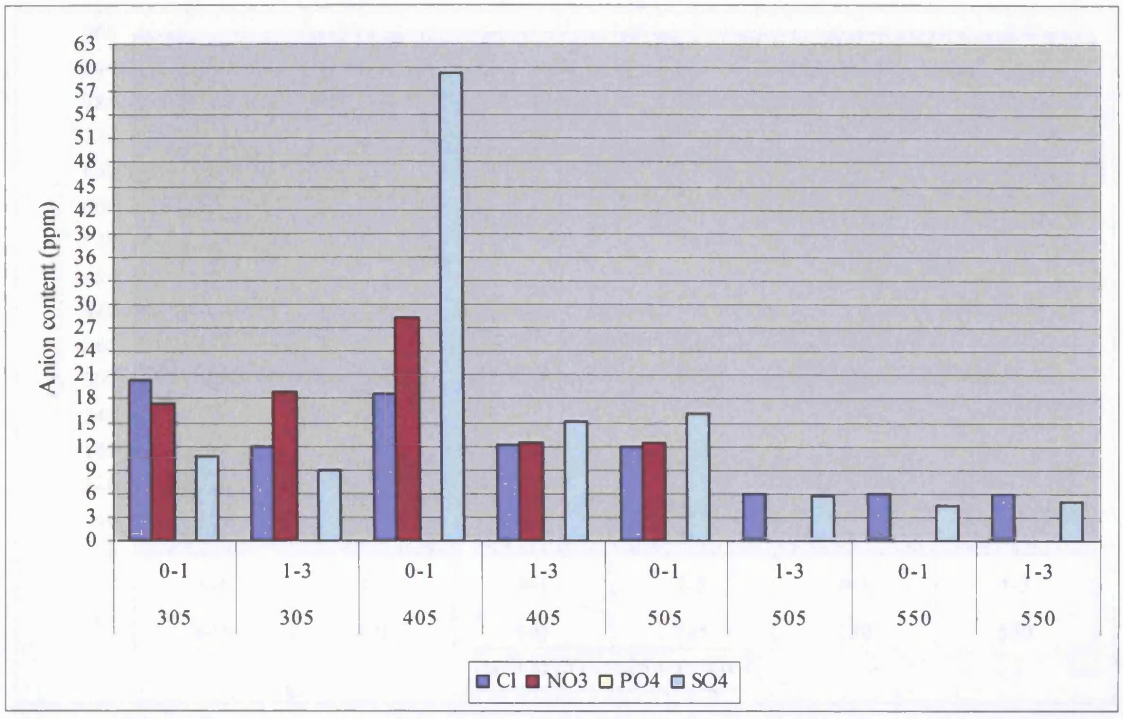

Figure (4Hb): The main anion content of drilled samples from the Bab al Siq Triclinium Tomb, location (T2) (Depth intervals: 0-1 and 1-3 cm).
Third fieldwork visit: June 2004.

Appendix Hb: The anion and cation content and distribution in the drilled samples. Third fieldwork visit: June 2004.

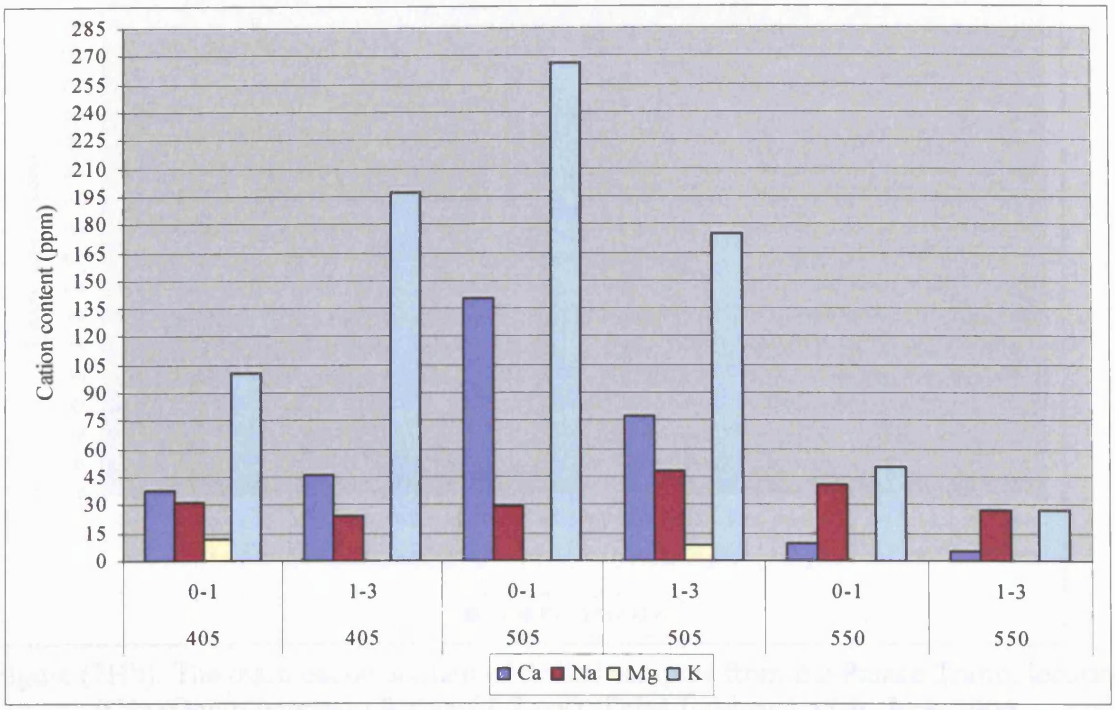

Figure (5Hb): The main cation content of drilled samples from the Bab al Siq Triclinium Tomb, location (T3) (Depth intervals: 0-1 and 1-3 cm).
Third fieldwork visit: June 2004.

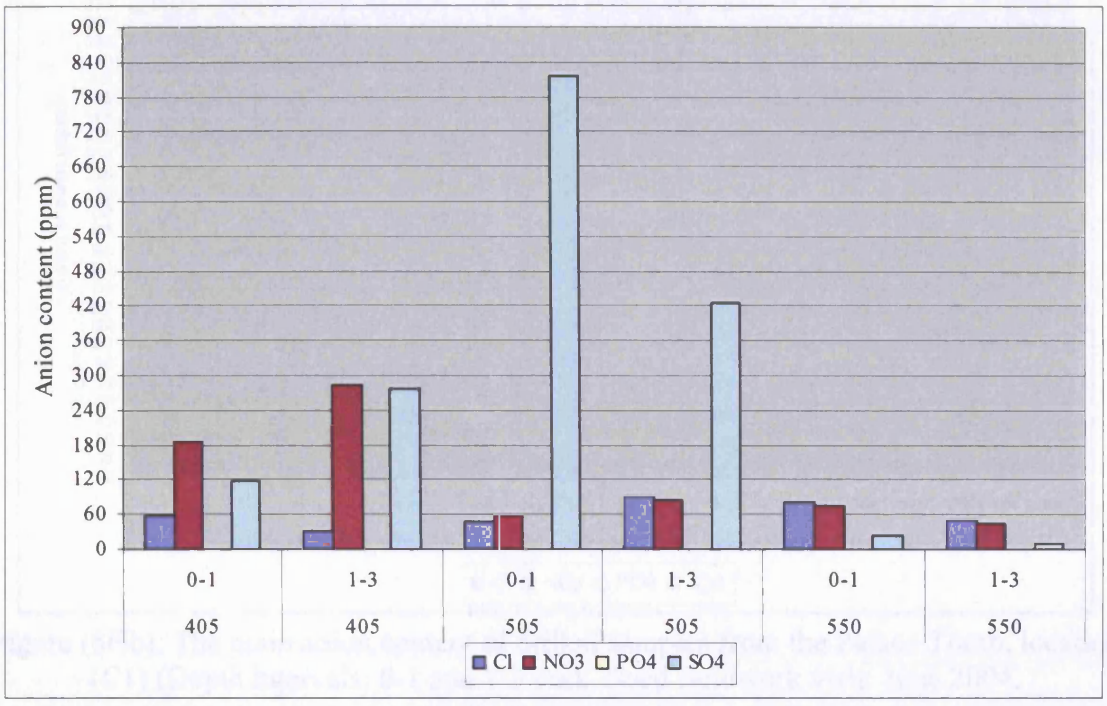

Figure (6Hb): The main anion content of drilled samples from the Bab al Siq Triclinium Tomb, location (T3) (Depth intervals: 0-1 and 1-3 cm).
Third fieldwork visit: June 2004.

Appendix Hb: The anion and cation content and distribution in the drilled samples. Third fieldwork visit: June 2004.

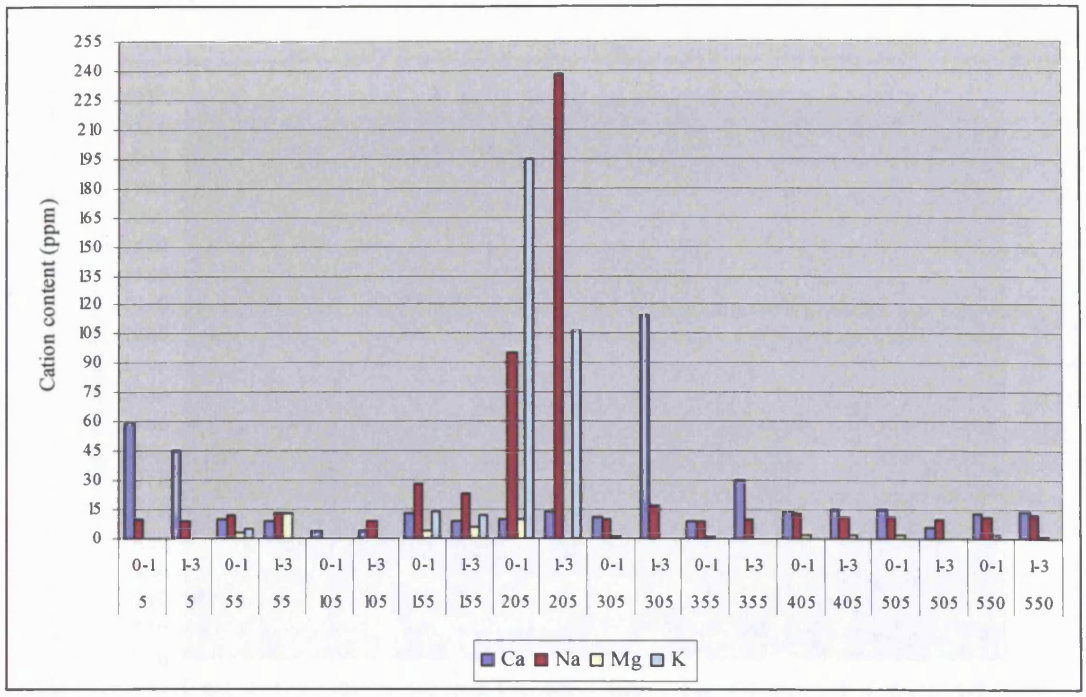

Figure (7Hb): The main cation content of drilled samples from the Palace Tomb, location (C1) (Depth intervals: 0-1 and 1-3 cm). Third fieldwork visit: June 2004.

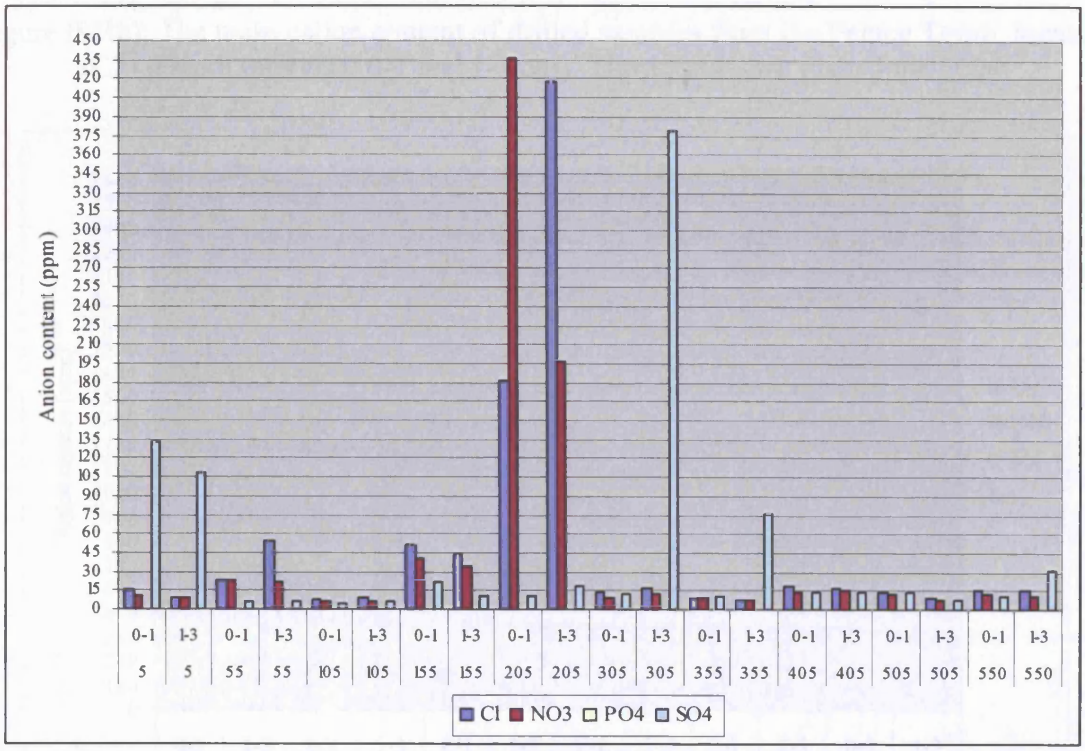

Figure (8Hb): The main anion content of drilled samples from the Palace Tomb, location (C1) (Depth intervals: 0-1 and 1-3 cm). Third fieldwork visit: June 2004.

Appendix Hb: The anion and cation content and distribution in the drilled samples. Third fieldwork visit: June 2004.

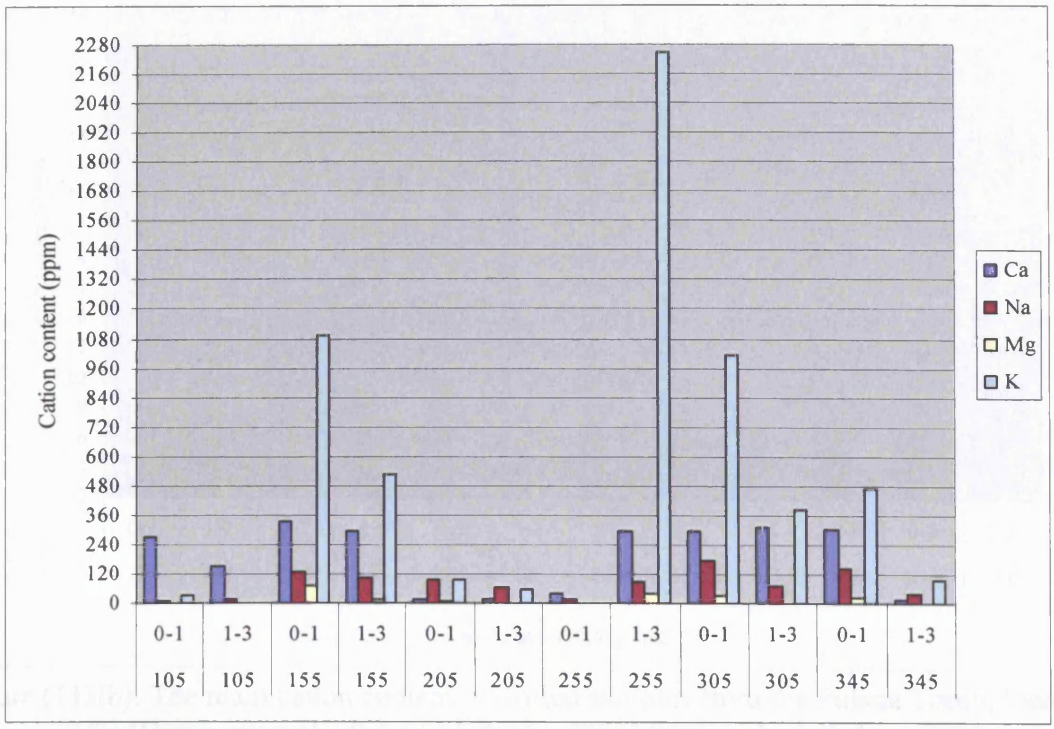

Figure (9Hb): The main cation content of drilled samples from the Palace Tomb, location (C2) (Depth intervals: 0-1 and 1-3 cm). Third fieldwork visit: June 2004.

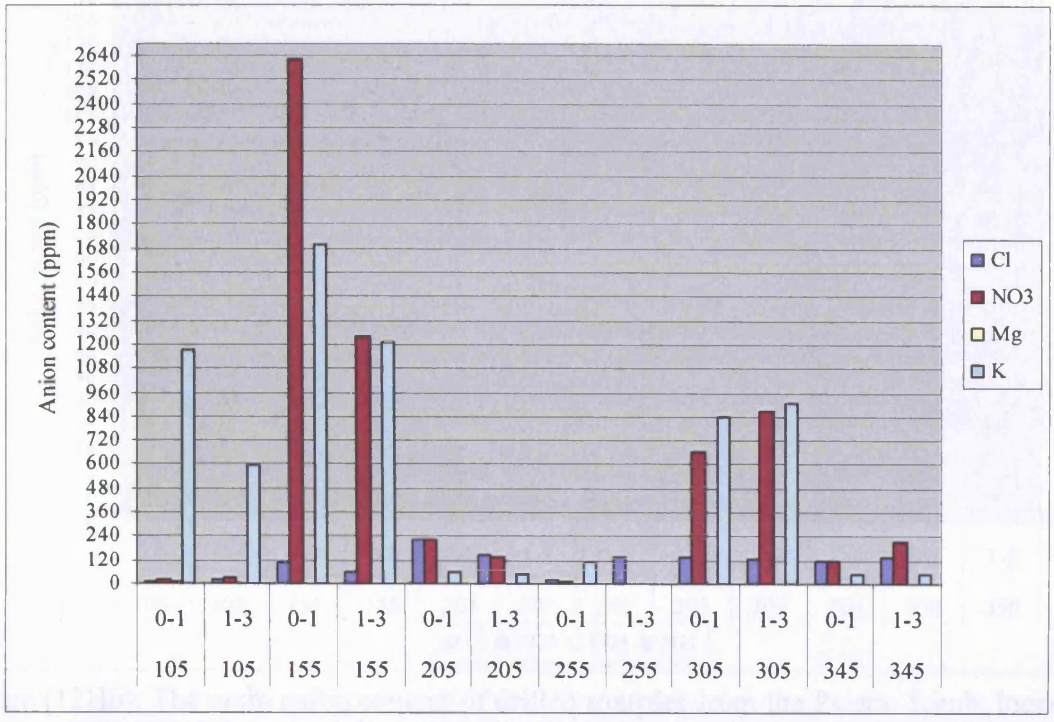

Figure (10Hb): The main anion content of drilled samples from the Palace Tomb, location (C2) (Depth intervals: 0-1 and 1-3 cm). Third fieldwork visit: June 2004.

Appendix Hb: The anion and cation content and distribution in the drilled samples. Third fieldwork visit: June 2004.

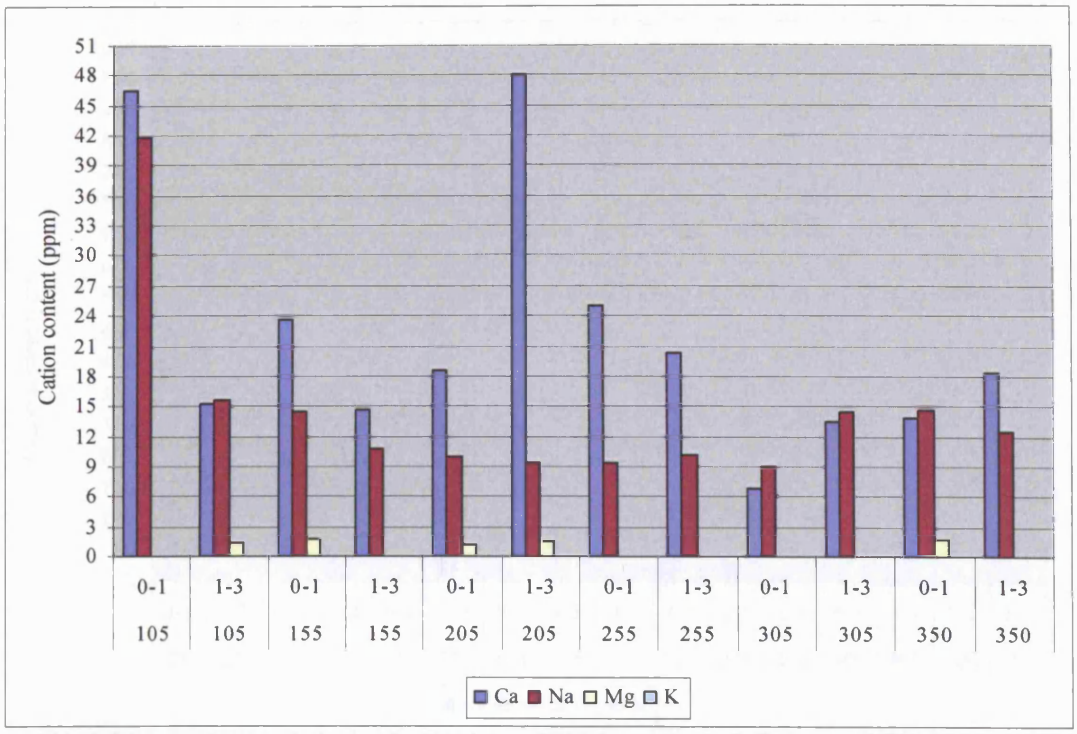

Figure (11Hb): The main cation content of drilled samples from the Palace Tomb, location (C3) (Depth intervals: 0-1 and 1-3 cm). Third fieldwork visit: June 2004.

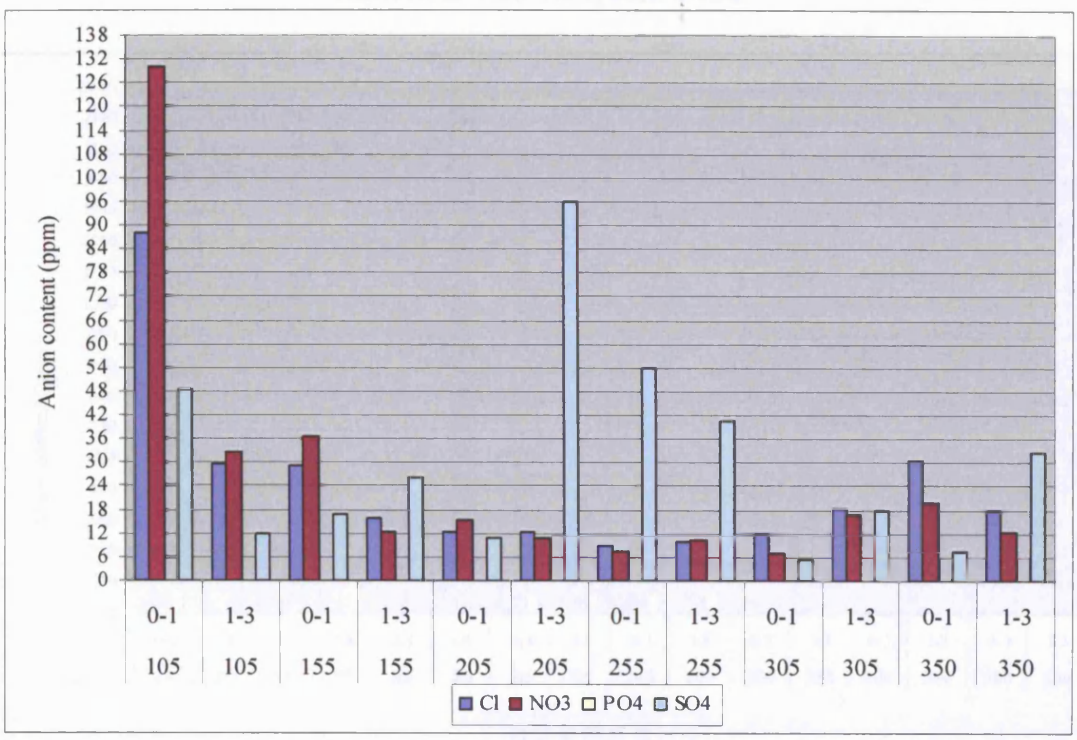

Figure (12Hb): The main anion content of drilled samples from the Palace Tomb, location (C3) (Depth intervals: 0-1 and 1-3 cm). Third fieldwork visit: June 2004.

Appendix Hb: The anion and cation content and distribution in the drilled samples. Third fieldwork visit: June 2004.

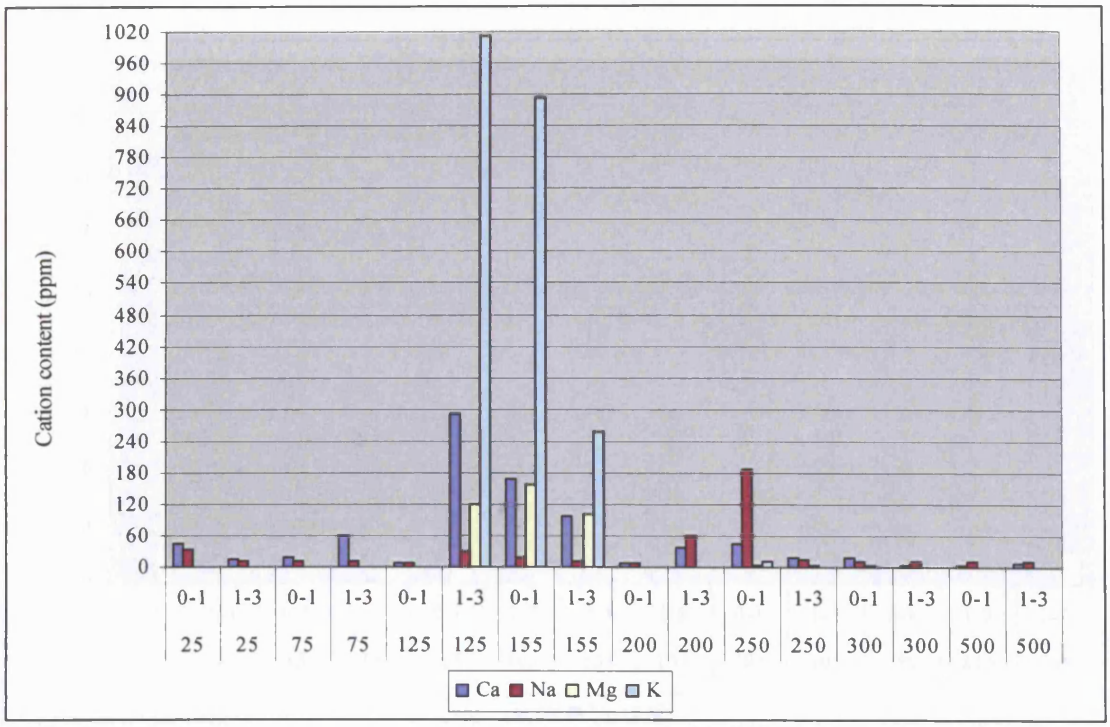

Figure (13Hb): The main cation content of drilled samples from the Corinthian Tomb, location (H) (Depth intervals: 0-1 and 1-3 cm).
Third fieldwork visit: June 2004.

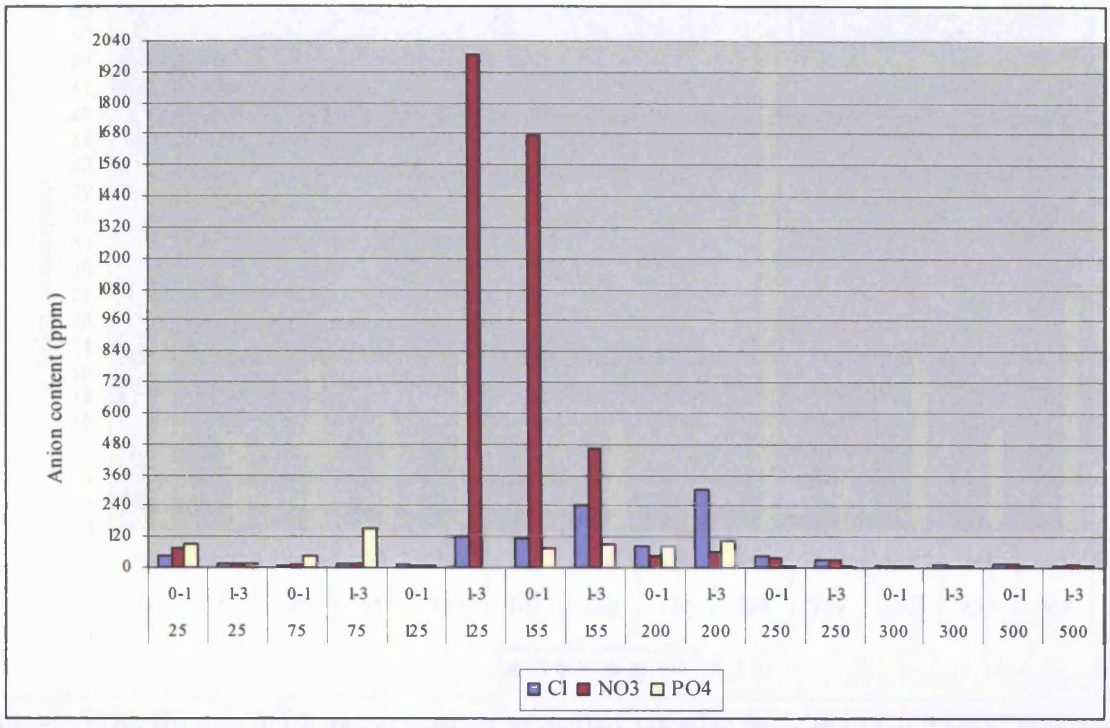

Figure (14Hb): The main anion content of drilled samples from the Corinthian Tomb, location (H) (Depth intervals: 0-1 and 1-3 cm). Third fieldwork visit: June 2004.

Appendix Hb: The anion and cation content and distribution in the drilled samples. Third fieldwork visit: June 2004.

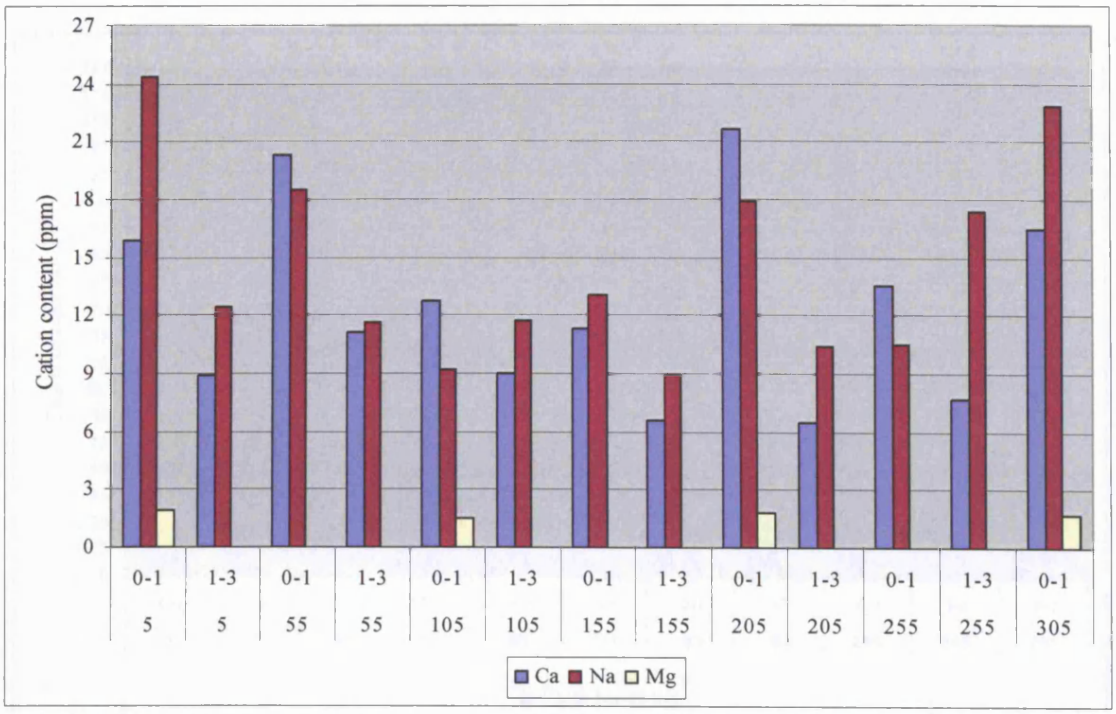

Figure (15Hb): The main cation content of drilled samples from the Deir Tomb, location (D1) (Depth intervals: 0-1 and 1-3 cm). Third fieldwork visit: June 2004.

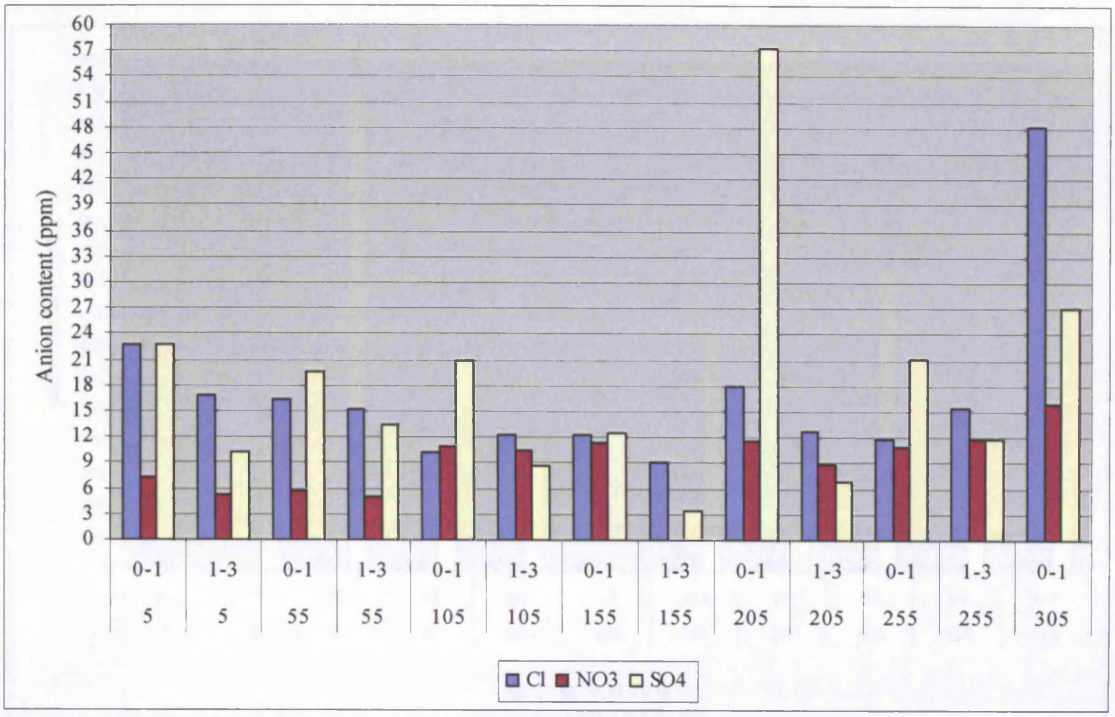

Figure (16Hb): The main anion content of drilled samples from the Deir Tomb, location (D1) (Depth intervals: 0-1 and 1-3 cm). Third fieldwork visit: June 2004.

Appendix Hb: The anion and cation content and distribution in the drilled samples. Third fieldwork visit: June 2004.

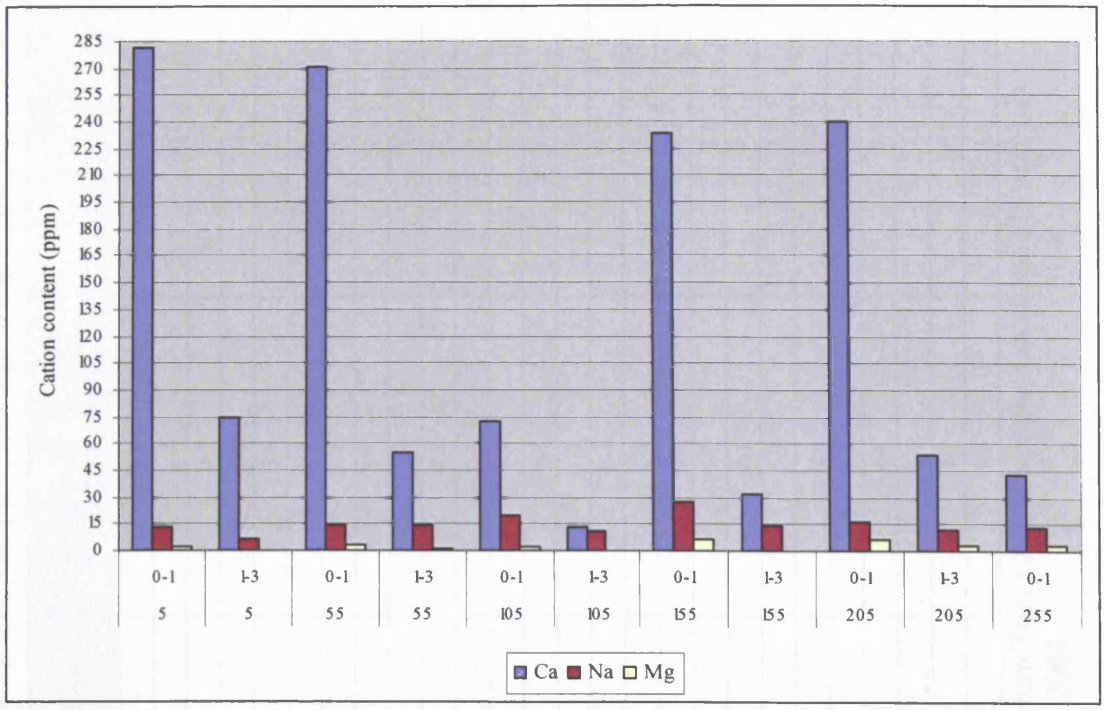

Figure (17Hb): The main cation content of drilled samples from the Deir Tomb, location (D2) (Depth intervals: 0-1 and 1-3 cm). Third fieldwork visit: June 2004.

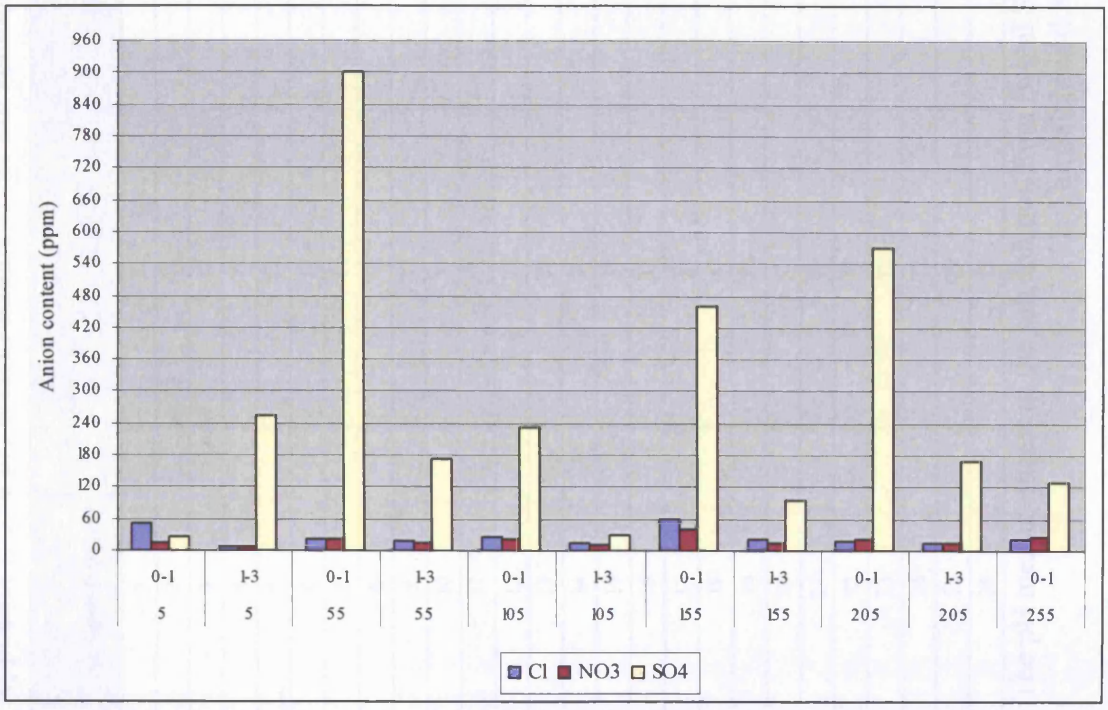

Figure (18Hb): The main anion content of drilled samples from the Deir Tomb, location (D2) (Depth intervals: 0-1 and 1-3 cm). Third fieldwork visit: June 2004.

Appendix I: The pH measurements of the salt solution from the drilled samples. Third fieldwork visit: June 2004.

Sample Number	Location	Height (cm)	Depth (cm)	pH
1	T1	5	0-1	6.6
2	T1	5	1-3	6.7
3	T1	55	0-1	6.5
4	T1	55	1-3	6.4
5	T1	105	0-1	7.2
6	T1	105	1-3	6.7
7	T1	155	0-1	7.0
8	T1	155	1-3	7.0
9	T1	205	0-1	7.3
10	T1	205	1-3	6.7
11	T1	305	0-1	7.3
12	T1	305	1-3	7.2
13	T1	405	0-1	7.4
14	T1	405	1-3	7.6
15	T1	505	0-1	7.5
16	T1	505	1-3	7.6
17	T1	550	0-1	7.6
18	T1	550	1-3	7.3
19	T2	305	0-1	7.2
20	T2	305	1-3	7.7
21	T2	405	0-1	7.4
22	T2	405	1-3	7.4
23	T2	505	0-1	7.5
24	T2	505	1-3	7.2
25	T2	550	0-1	7.4
26	T2	550	1-3	7.1

Table (I1): The pH measurements of the salt solution from Bab al Siq Triclinium Tomb drilled sample, Locations (T1 and T2). Third fieldwork visit June 2004.

Appendix I: The pH measurements of the salt solution from the drilled samples. Third fieldwork visit: June 2004.

Sample Number	Location	Height (cm)	Depth (cm)	pH
27	T3	405	0-1	6.6
28	T3	405	1-3	7.3
29	T3	505	0-1	7.1
30	T3	505	1-3	7.1
31	T3	550	0-1	7.3
32	T3	550	1-3	7.1

Table (I2): The pH measurements of the salt solution from Bab al Siq Triclinium Tomb drilled sample, location (T3). Third fieldwork visit June 2004.

Sample Number	Location	Height (cm)	Depth (cm)	pH
102	H	25	0-1	7.6
103	H	25	1-3	8.0
104	H	75	0-1	7.6
105	H	75	1-3	7.6
106	H	125	0-1	7.5
65	H	125	1-3	7.2
115	H	155	0-1	7.4
116	H	155	1-3	7.5
107	H	200	0-1	7.3
108	H	200	1-3	7.3
109	H	250	0-1	7.5
110	H	250	1-3	7.6
111	H	300	0-1	7.4
112	H	300	1-3	7.1
113	H	500	0-1	7.4
114	H	500	1-3	7.3

Table (I3): The pH measurements of the salt solution from the Corinthian Tomb drilled sample, Location (H). Third fieldwork visit June 2004.

Appendix I: The pH measurements of the salt solution from the drilled samples. Third fieldwork visit: June 2004.

Sample Number	Location	Height (cm)	Depth (cm)	pH
70	C1	5	0-1	7.6
71	C1	5	1-3	7.5
72	C1	55	0-1	7.6
73	C1	55	1-3	7.0
74	C1	105	0-1	7.6
75	C1	105	1-3	7.4
76	C1	155	0-1	7.3
77	C1	155	1-3	7.2
78	C1	205	0-1	7.5
79	C1	205	1-3	7.5
80	C1	305	0-1	7.5
81	C1	305	1-3	7.4
82	C1	355	0-1	7.3
83	C1	355	1-3	7.5
84	C1	405	0-1	7.7
85	C1	405	1-3	7.7
86	C1	505	0-1	7.4
87	C1	505	1-3	7.5
88	C1	550	0-1	7.5
89	C1	550	1-3	7.5

Table (I4): The pH measurements of the salt solution from the Palace Tomb drilled sample, Location (C1). Third fieldwork visit June 2004.

Appendix I: The pH measurements of the salt solution from the drilled samples. Third fieldwork visit: June 2004.

Sample Number	Location	Height (cm)	Depth (cm)	pH
57	C2	105	0-1	7.2
58	C2	105	1-3	7.1
59	C2	155	0-1	7.0
60	C2	155	1-3	6.8
61	C2	205	0-1	7.2
62	C2	205	1-3	7.2
63	C2	255	0-1	7.5
64	C2	255	1-3	7.0
66	C2	305	0-1	6.6
67	C2	305	1-3	6.9
68	C2	345	0-1	7.2
69	C2	345	1-3	7.0
90	C3	105	0-1	7.6
91	C3	105	1-3	7.6
92	C3	155	0-1	7.8
93	C3	155	1-3	7.6
94	C3	205	0-1	7.6
95	C3	205	1-3	7.5
96	C3	255	0-1	7.5
97	C3	255	1-3	7.6
98	C3	305	0-1	7.5
99	C3	305	1-3	8.5
100	C3	350	0-1	7.7
101	C3	350	1-3	7.3

Table (I5): The pH measurements of the salt solution from the Palace Tomb drilled sample, Locations (C2 and C3). Third fieldwork visit June 2004.

Appendix I: The pH measurements of the salt solution from the drilled samples. Third fieldwork visit: June 2004.

Sample Number	Location	Height (cm)	Depth (cm)	pH
33	D1	5	0-1	7.7
34	D1	5	1-3	7.7
35	D1	55	0-1	8.0
36	D1	55	1-3	7.5
37	D1	105	0-1	7.7
38	D1	105	1-3	7.7
39	D1	155	0-1	7.7
40	D1	155	1-3	7.5
41	D1	205	0-1	7.5
42	D1	205	1-3	7.7
43	D1	255	0-1	7.6
44	D1	255	1-3	7.5
45	D1	305	0-1	7.5
46	D2	5	0-1	7.2
47	D2	5	1-3	7.2
48	D2	55	0-1	6.9
49	D2	55	1-3	7.2
50	D2	105	0-1	7.3
51	D2	105	1-3	7.5
52	D2	155	0-1	7.3
56	D2	155	1-3	7.5
53	D2	205	0-1	7.4
54	D2	205	1-3	7.4
55	D2	255	0-1	7.6

Table (I6): The pH measurements of the salt solution from the Deir Tomb drilled sample, Locations (D and D2). Third fieldwork visit June 2004.

Appendix J: Temperature and relative humidity spot readings. Fourth fieldwork visit: April 2005.

Time	T (°C)	RH%	Time	T (°C)	RH%	Time	T (°C)	RH%	Time	T (°C)	RH%	Time	T (°C)	RH%	Time	T (°C)	RH%
07.40	19.6	47.2	09.50	21.3	44.2	12.00	24.3	40.0	14.10	25.4	36.0	16.20	23.2	37.8	18.30	19.7	38.8
07.45	19.8	47.1	09.55	21.3	45.0	12.05	24.5	39.9	14.15	25.4	35.7	16.25	23.2	37.9	18.35	19.8	37.9
07.50	19.8	47.2	10.00	22.0	44.5	12.10	24.5	39.8	14.20	25.5	35.8	16.30	23.0	37.9	18.40	19.8	37.8
07.55	19.8	47.0	10.05	22.0	43.7	12.15	24.5	40.0	14.25	25.5	35.5	16.35	23.0	38.0	18.45	19.7	37.9
08.00	19.8	46.8	10.10	22.0	43.2	12.20	25.0	39.6	14.30	25.4	35.0	16.40	22.5	38.2	18.50	19.5	37.8
08.05	20.0	46.3	10.15	22.0	43.2	12.25	25.0	39.4	14.35	25.4	35.1	16.45	22.5	38.2	18.55	19.5	37.6
08.10	20.1	46.0	10.20	22.1	43.0	12.30	25.1	39.0	14.40	25.4	35.3	16.50	22.0	37.3	19.00	19.5	37.0
08.15	20.1	46.0	10.25	22.1	43.0	12.35	25.1	38.8	14.45	25.3	35.6	16.55	22.1	37.4	19.05	19.4	38.1
08.20	20.2	46.2	10.30	22.1	42.8	12.40	25.1	38.8	14.50	25.4	35.4	17.00	22.1	37.3	19.10	19.3	38.2
08.25	20.2	46.2	10.35	22.1	42.7	12.45	25.2	38.4	14.55	25.4	35.0	17.05	22.0	37.0	19.15	19.0	38.6
08.30	20.2	46.0	10.40	22.2	42.6	12.50	25.2	38.5	15.00	24.7	35.2	17.10	21.5	37.1	19.20	18.8	39.3
08.35	20.2	45.8	10.45	22.2	42.2	12.55	25.0	38.5	15.05	24.7	35.1	17.15	21.5	36.9	19.25	18.8	39.4
08.40	20.2	45.8	10.50	22.2	42.1	13.00	24.5	38.0	15.10	24.6	35.3	17.20	21.5	36.8	19.30	18.8	39.4
08.45	20.3	45.6	10.55	22.2	42.0	13.05	24.5	38.2	15.15	24.6	35.2	17.25	21.2	36.9	19.35	18.8	39.5
08.50	20.4	45.6	11.00	22.2	42.2	13.10	24.5	38.1	15.20	24.5	35.2	17.30	21.2	36.8	19.40	18.8	39.5
08.55	20.4	45.0	11.05	22.3	41.8	13.15	25.0	37.8	15.25	24.2	35.6	17.35	21.0	36.8	19.45	18.8	39.1
09.00	20.4	45.1	11.10	22.3	41.6	13.20	25.0	37.7	15.30	24.1	35.7	17.40	20.6	36.5	19.50	18.5	39.4
09.05	20.5	45.3	11.15	22.5	41.5	13.25	25.0	37.7	15.35	24.1	35.8	17.45	20.1	36.6	19.55	18.5	39.6
09.10	20.7	45.2	11.20	22.5	41.7	13.30	25.1	37.2	15.40	24.0	36.6	17.50	20.6	37.8	20.00	18.4	37.9
09.15	20.7	45.3	11.25	23.1	41.3	13.35	25.1	37.0	15.45	23.8	36.7	17.55	20.0	33.9	20.05	18.4	37.8
09.20	20.7	45.0	11.30	23.2	41.1	13.40	25.2	37.1	15.50	23.8	36.9	18.00	20.0	38.2	20.10	18.3	37.5
09.25	20.8	44.9	11.35	23.3	40.5	13.45	25.4	36.8	15.55	23.8	36.7	18.05	20.1	37.6	20.15	18.2	38.4
09.30	20.7	44.4	11.40	23.4	40.6	13.50	25.4	36.8	16.00	23.7	36.8	18.10	19.8	38.3	20.20	18.2	38.8
09.35	20.8	44.5	11.45	23.6	40.5	13.55	25.4	36.4	16.05	23.5	37.3	18.15	19.8	38.8	20.25	18.0	38.4
09.40	21.3	44.2	11.50	24.0	40.4	14:00	25.3	36.4	16.10	23.4	37.1	18.20	19.8	38.8	20.30	18.0	38.1
09.45	21.3	44.2	11.55	24.3	40.3	14.05	25.4	36.0	16.15	23.3	37.6	18.25	19.7	38.8	20.35	18.1	38.3

Table (J1): Temperature and relative humidity spot readings. Location: Bab al Siq Triclinium Tomb.
Fourth fieldwork visit: 1-2 April 2005, between 07.40-20.35.

Appendix J: Temperature and relative humidity spot readings. Fourth fieldwork visit: April 2005.

Time	T (°C)	RH%	Time	T (°C)	RH%	Time	T (°C)	RH%	Time	T (°C)	RH%	Time	T (°C)	RH%
20.40	18.1	39.2	22.50	16.4	39.0	01.00	14.4	44.6	03.10	11.8	49.6	05.20	15.7	48.0
20.45	18.0	39.6	22.55	16.4	39.2	01.05	14.4	44.7	03.15	11.7	50.2	05.25	15.9	48.0
20.50	18.2	38.8	23.00	16.2	40.1	01.10	14.3	44.8	03.20	11.7	50.5	05.30	16.2	48.2
20.55	18.0	38.7	23.05	16.2	40.3	01.15	14.0	45.3	03.25	12.0	50.6	05.35	16.3	48.2
21.00	17.7	38.4	23.10	16.0	40.4	01.20	14.0	45.6	03.30	12.0	50.4	05.40	16.8	48.0
21.05	17.7	37.0	23.15	16.0	40.4	01.25	14.0	45.6	03.35	12.4	50.4	05.45	16.7	48.0
21.10	17.6	37.3	23.20	16.1	40.6	01.30	13.8	45.8	03.40	12.4	50.2	05.50	16.8	47.9
21.15	17.5	37.4	23.25	16.0	40.8	01.35	13.6	45.9	03.45	12.8	50.2	05.55	17.2	47.8
21.20	17.7	37.2	23.30	15.6	40.7	01.40	13.5	45.9	03.50	12.8	50.0	06.00	17.6	47.9
21.25	17.4	37.6	23.35	15.6	40.8	01.45	13.4	46.1	03.55	12.9	49.9	06.05	18.2	47.8
21.30	17.4	37.7	23.40	15.8	40.7	01.50	13.2	46.2	04.00	13.2	49.8	06.10	18.4	47.5
21.35	17.4	37.3	23.45	15.7	40.8	01.55	13.0	46.3	04.05	13.4	49.6	06.15	18.8	47.4
21.40	17.4	37.4	23.50	15.8	40.6	02.00	13.0	46.8	04.10	13.6	49.5	06.20	18.8	47.5
21.45	17.4	37.3	23.55	15.6	40.7	02.05	13.0	46.9	04.15	13.5	49.1	06.25	18.8	47.3
21.50	17.4	37.0	00.00	15.4	40.9	02.10	12.7	47.2	04.20	13.8	49.1	06.30	18.8	47.3
21.55	17.5	37.4	00.05	15.2	41.2	02.15	12.8	47.6	04.25	13.8	49.2	06.35	18.5	47.1
22.00	17.4	37.9	00.10	15.4	41.2	02.20	12.8	47.9	04.30	13.7	49.0	06.40	18.4	46.9
22.05	17.5	37.8	00.15	15.21	41.5	02.25	12.4	47.9	04.35	13.89	48.8	06.45	18.6	47.0
22.10	17.3	37.6	00.20	15.0	41.7	02.30	12.4	48.2	04.40	14.2	48.9	06.50	18.6	47.2
22.15	17.3	37.7	00.25	15.0	41.6	02.35	11.9	48.4	04.45	14.2	48.7	06.55	18.8	46.8
22.20	17.3	38.4	00.30	15.0	41.7	02.40	11.8	48.6	04.50	14.1	48.7	07.00	18.9	46.7
22.25	17.1	38.4	00.35	15.0	42.4	02.45	11.9	48.7	04.55	14.5	48.9			
22.30	17.1	38.5	00.40	14.6	42.5	02.50	11.9	48.7	05.00	14.6	48.4			
22.35	17.1	38.6	00.45	14.7	42.6	02.55	12.0	48.9	05.05	14.7	48.4			
22.40	17.1	38.7	00.50	14.9	42.7	03.00	12.0	49.1	05.10	15.2	48.2			
22.45	16.8	38.6	00.55	14.5	42.5	03.05	11.8	49.2	05.15	15.6	48.1			

Table (J2): Temperature and relative humidity spot readings. Location: Bab al Siq Triclinium Tomb.
Fourth fieldwork visit: 1-2 April, between 20.40-07.00.

Appendix J: Temperature and relative humdity spot readings. Fourth fieldwork visit: April 2005.

Time	T (°C)	RH%	Time	T (°C)	RH%	Time	T (°C)	RH%	Time	T (°C)	RH%	Time	T (°C)	RH%	Time	T (°C)	RH%
07.40	19.0	45.5	09.50	19.7	43.9	12.00	21.6	43.2	14.10	24.0	40.5	16.20	24.5	38.9	18.30	22.4	45.2
07.45	19.0	45.4	09.55	19.8	43.9	12.05	21.6	43.1	14.15	24.3	40.5	16.25	24.6	39.3	18.35	22.4	45.2
07.50	19.1	45.0	10.00	19.8	44.0	12.10	21.8	42.7	14.20	24.5	40.4	16.30	24.5	39.9	18.40	22.0	45.3
07.55	19.2	45.0	10.05	20.2	44.1	12.15	21.8	42.7	14.25	24.5	40.5	16.35	24.4	40.5	18.45	22.0	45.1
08.00	19.2	44.6	10.10	20.2	44.3	12.20	22.0	42.8	14.30	24.5	40.5	16.40	24.4	40.9	18.50	21.5	45.6
08.05	19.3	44.4	10.15	20.2	44.5	12.25	22.3	42.6	14.35	24.6	40.6	16.45	24.2	40.8	18.55	21.5	45.8
08.10	19.2	44.5	10.20	20.5	44.6	12.30	22.3	42.5	14.40	24.6	40.4	16.50	24.2	41.0	19.00	21.0	46.8
08.15	19.2	44.3	10.25	20.5	44.9	12.35	22.3	42.1	14.45	24.6	40.3	16.55	24.2	41.3	19.05	21.0	46.9
08.20	19.4	44.0	10.30	20.5	44.7	12.40	22.3	42.3	14.50	24.5	40.1	17.00	24.0	41.2	19.10	20.5	47.0
08.25	19.2	44.1	10.35	20.6	44.6	12.45	22.4	42.3	14.55	24.6	40.0	17.05	24.0	41.4	19.15	20.5	47.2
08.30	19.2	44.2	10.40	20.7	44.5	12.50	22.5	42.1	15.00	25.2	39.8	17.10	23.9	41.9	19.20	20.1	47.3
08.35	19.3	44.0	10.45	20.8	44.4	12.55	22.5	42.5	15.05	25.2	39.8	17.15	23.9	42.3	19.25	20.1	47.5
08.40	19.3	43.8	10.50	20.8	44.2	13.00	22.9	42.2	15.10	25.2	39.6	17.20	24.0	42.4	19.30	20.0	47.6
08.45	19.3	43.8	10.55	20.8	44.0	13.05	22.9	42.3	15.15	25.0	38.8	17.25	24.0	42.6	19.35	19.8	47.8
08.50	19.3	43.6	11.00	20.8	44.1	13.10	23.0	42.1	15.20	25.1	38.4	17.30	23.8	42.8	19.40	19.9	48.0
08.55	19.5	43.5	11.05	20.9	44.3	13.15	23.0	42.0	15.25	25.0	38.3	17.35	23.8	42.9	19.45	19.4	48.2
09.00	19.5	43.4	11.10	21.0	44.0	13.20	23.4	41.6	15.30	24.8	38.4	17.40	23.7	42.9	19.50	19.4	48.3
09.05	19.5	43.4	11.15	21.0	44.0	13.25	23.4	41.8	15.35	24.8	38.6	17.45	23.7	43.0	19.55	19.4	48.1
09.10	19.5	43.4	11.20	21.1	44.1	13.30	23.4	41.5	15.40	24.8	38.5	17.50	23.7	43.3	20.00	19.4	48.7
09.15	19.5	43.2	11.25	21.1	43.9	13.35	23.4	41.3	15.45	24.8	38.5	17.55	23.4	43.3	20.05	19.3	48.9
09.20	19.5	43.3	11.30	21.2	43.9	13.40	23.5	41.1	15.50	24.6	38.8	18.00	23.4	43.8	20.10	19.3	49.6
09.25	19.5	43.2	11.35	21.3	43.8	13.45	23.6	41.0	15.55	24.6	38.4	18.05	23.4	43.8	20.15	19.3	50.2
09.30	19.6	44.1	11.40	21.3	43.7	13.50	23.6	40.9	16.00	24.6	38.7	18.10	23.3	44.2	20.20	19.2	50.9
09.35	19.6	44.0	11.45	21.2	43.3	13.55	23.6	40.7	16.05	24.6	38.4	18.15	23.0	44.3	20.25	19.2	51.2
09.40	19.6	44.0	11.50	21.3	43.3	14:00	24.0	40.7	16.10	24.5	38.4	18.20	22.7	45.0	20.30	19.2	51.9
09.45	19.7	43.8	11.55	21.4	43.2	14.05	24.0	40.6	16.15	24.5	38.6	18.25	22.7	45.1	20.35	19.2	52.2

Table (J3): Temperature and relative humidity spot readings. Location: Palace Tomb.
Fourth fieldwork visit: 2-3 April 2005, between 07.40-20.35.

Appendix J: Temperature and relative humidity spot readings. Fourth fieldwork visit: April 2005.

Time	T (°C)	RH%	Time	T (°C)	RH%	Time	T (°C)	RH%	Time	T (°C)	RH%	Time	T (°C)	RH%
20.40	19.2	52.2	22.50	17.4	56.4	01.00	13.0	62.0	03.10	10.1	62.5	05.20	11.6	58.6
20.45	19.2	52.6	22.55	17.4	56.8	01.05	12.5	62.4	03.15	10.1	62.4	05.25	11.6	58.4
20.50	19.1	52.8	23.00	17.2	57.1	01.10	12.5	62.5	03.20	10.1	62.2	05.30	11.9	58.3
20.55	18.8	52.5	23.05	17.0	57.3	01.15	12.0	62.6	03.25	10.0	62.0	05.35	11.9	58.1
21.00	18.8	52.5	23.10	17.0	57.4	01.20	11.8	62.8	03.30	10.0	61.5	05.40	12.3	58.0
21.05	18.7	52.6	23.15	16.8	58.0	01.25	11.7	62.9	03.35	10.0	61.4	05.45	12.5	58.1
21.10	18.7	52.8	23.20	16.5	58.4	01.30	11.3	63.3	03.40	9.9	61.7	05.50	12.5	57.8
21.15	18.6	53.0	23.25	16.5	58.6	01.35	11.0	63.1	03.45	10.0	61.2	05.55	12.5	57.8
21.20	18.7	53.2	23.30	16.4	58.9	01.40	10.4	63.2	03.50	9.9	61.0	06.00	12.4	57.6
21.25	18.7	53.2	23.35	16.0	59.3	01.45	10.3	63.5	03.55	10.0	61.1	06.05	12.9	57.5
21.30	18.5	53.6	23.40	16.0	59.8	01.50	10.1	63.7	04.00	10.0	60.0	06.10	13.0	57.4
21.35	18.5	53.5	23.45	15.7	60.0	01.55	10.1	63.9	04.05	10.2	60.5	06.15	13.1	57.0
21.40	18.5	53.4	23.50	15.7	60.2	02.00	9.9	64.1	04.10	10.3	60.4	06.20	13.3	57.2
21.45	18.5	53.9	23.55	15.7	59.8	02.05	9.9	64.3	04.15	10.3	60.2	06.25	13.6	57.1
21.50	18.5	54.2	00.00	15.7	59.8	02.10	10.0	63.8	04.20	10.4	59.9	06.30	13.8	56.7
21.55	18.5	54.8	00.05	15.4	59.7	02.15	10.1	63.9	04.25	10.6	60.0	06.35	14.0	56.7
22.00	18.5	55.0	00.10	15.1	60.1	02.20	10.0	63.4	04.30	10.6	59.8	06.40	14.2	56.6
22.05	18.1	55.3	00.15	15.1	60.2	02.25	9.9	63.4	04.35	10.6	59.4	06.45	14.2	56.3
22.10	18.1	55.5	00.20	14.8	60.1	02.30	10.0	63.2	04.40	11.0	59.6	06.50	14.6	56.4
22.15	18.0	55.5	00.25	14.9	60.0	02.35	10.1	63.3	04.45	11.0	59.4	06.55	14.6	56.4
22.20	17.6	55.4	00.30	14.7	60.4	02.40	9.8	63.9	04.50	11.0	59.0	07.00	14.9	56.2
22.25	17.6	55.3	00.35	14.8	60.6	02.45	9.9	63.2	04.55	11.1	59.1			
22.30	17.4	55.3	00.40	14.4	60.8	02.50	9.9	63.0	05.00	11.2	59.2			
22.35	17.3	56.4	00.45	14.0	61.1	02.55	9.9	63.1	05.05	11.1	59.0			
22.40	17.4	56.5	00.50	13.5	61.2	03.00	10.0	62.9	05.10	11.3	58.9			
22.45	17.4	56.4	00.55	13.1	61.0	03.05	10.0	62.4	05.15	11.6	58.7			

Table (J4): Temperature and relative humidity spot readings. Location: Palace Tomb.
Fourth fieldwork visit: 2-3 April 2005, between 20.40-07.00.

Appendix J: Temperature and relative humidity spot readings. Fourth fieldwork visit: April 2005.

Time	T (°C)	RH%	Time	T (°C)	RH%	Time	T (°C)	RH%	Time	T (°C)	RH%	Time	T (°C)	RH%	Time	T (°C)	RH%
07.40	15.8	55.7	09.50	16.5	51.4	12.00	18.4	46.5	14.10	21.2	41.9	16.20	19.8	39.6	18.30	17.7	41.2
07.45	15.8	55.4	09.55	16.5	51.4	12.05	18.4	46.4	14.15	22.0	40.8	16.25	19.8	39.4	18.35	17.6	39.9
07.50	15.8	55.3	10.00	16.5	51.0	12.10	18.6	46.0	14.20	22.0	40.6	16.30	19.8	39.4	18.40	17.7	39.9
07.55	15.9	55.5	10.05	16.6	51.1	12.15	18.9	46.3	14.25	22.0	40.6	16.35	19.9	39.2	18.45	17.4	38.9
08.00	16.0	55.2	10.10	16.3	50.9	12.20	18.9	46.2	14.30	22.1	40.5	16.40	20.0	39.0	18.50	17.3	40.6
08.05	16.0	55.1	10.15	16.8	50.4	12.25	19.2	45.8	14.35	22.3	40.3	16.45	20.0	38.4	18.55	17.3	40.7
08.10	16.0	55.0	10.20	16.8	50.1	12.30	19.2	45.5	14.40	22.3	39.7	16.50	19.4	39.0	19.00	17.2	40.9
08.15	16.1	55.0	10.25	16.8	50.1	12.35	19.2	45.4	14.45	22.4	39.6	16.55	19.4	39.1	19.05	17.2	41.3
08.20	16.2	55.1	10.30	16.8	50.0	12.40	19.3	44.9	14.50	22.4	39.4	17.00	19.4	39.1	19.10	17.2	41.5
08.25	16.2	55.2	10.35	17.2	49.4	12.45	19.3	44.8	14.55	22.5	38.7	17.05	19.6	38.8	19.15	17.2	41.8
08.30	16.3	54.7	10.40	17.4	49.3	12.50	19.3	44.6	15.00	22.4	38.4	17.10	19.6	38.6	19.20	17.2	41.0
08.35	16.2	54.6	10.45	17.4	49.1	12.55	19.4	44.8	15.05	22.4	38.1	17.15	19.3	38.0	19.25	17.2	40.4
08.40	16.2	54.1	10.50	17.5	49.0	13.00	19.4	44.2	15.10	22.4	38.0	17.20	19.0	37.6	19.30	17.2	40.6
08.45	16.2	53.6	10.55	17.4	49.2	13.05	19.6	44.1	15.15	22.4	37.9	17.25	19.0	37.3	19.35	17.2	41.0
08.50	16.2	53.8	11.00	17.3	49.3	13.10	19.6	43.8	15.20	22.0	38.0	17.30	19.0	37.9	19.40	17.0	42.2
08.55	16.2	53.7	11.05	17.6	48.9	13.15	19.9	43.7	15.25	22.1	38.0	17.35	18.6	38.4	19.45	17.0	42.6
09.00	16.0	53.4	11.10	17.6	48.7	13.20	20.0	43.6	15.30	22.0	38.2	17.40	18.6	38.6	19.50	17.1	42.6
09.05	16.2	53.0	11.15	18.2	48.2	13.25	20.0	43.4	15.35	21.6	38.2	17.45	18.4	38.6	19.55	17.1	42.8
09.10	16.2	53.0	11.20	18.3	48.0	13.30	19.9	43.3	15.40	21.6	38.3	17.50	18.3	38.5	20.00	17.1	42.4
09.15	16.3	52.8	11.25	18.3	48.1	13.35	20.3	43.0	15.45	21.5	38.0	17.55	18.3	38.6	20.05	17.1	42.9
09.20	16.3	52.7	11.30	18.3	48.0	13.40	20.3	43.1	15.50	21.4	37.9	18.00	18.3	39.4	20.10	16.7	43.3
09.25	16.3	52.7	11.35	18.3	47.8	13.45	20.3	42.2	15.55	21.5	38.6	18.05	18.0	39.9	20.15	16.7	43.6
09.30	16.3	52.7	11.40	18.2	47.4	13.50	20.4	42.2	16.00	21.0	38.6	18.10	18.0	39.0	20.20	16.7	43.2
09.35	16.3	52.4	11.45	18.3	47.3	13.55	20.5	42.0	16.05	21.0	38.9	18.15	18.0	40.1	20.25	16.7	43.1
09.40	16.4	52.1	11.50	18.3	47.2	14:00	21.0	41.7	16.10	20.4	39.2	18.20	17.6	40.8	20.30	16.7	42.4
09.45	16.4	51.9	11.55	18.3	47.1	14.05	21.2	42.0	16.15	20.0	39.0	18.25	17.7	40.5	20.35	16.7	42.1

Table (J5): Temperature and relative humidity spot readings. Location: Deir Tomb.
Fourth fieldwork visit: 3-4 June 2005, between 07.40-20.35.

Appendix J: Temperature and relative humidity spot readings. Fourth fieldwork visit: April 2005.

Time	T (°C)	RH%	Time	T (°C)	RH%	Time	T (°C)	RH%	Time	T (°C)	RH%	Time	T (°C)	RH%
20.40	16.7	43.2	22.50	16.2	45.0	01.00	15.3	49.1	03.10	14.0	50.6	05.20	17.5	47.6
20.45	16.6	43.3	22.55	16.2	45.1	01.05	15.0	49.3	03.15	14.2	50.4	05.25	17.9	47.5
20.50	16.6	43.6	23.00	16.2	45.2	01.10	14.7	49.0	03.20	14.2	50.5	05.30	17.9	47.0
20.55	16.6	43.9	23.05	16.2	45.6	01.15	14.7	49.4	03.25	14.3	50.2	05.35	18.3	47.0
21.00	16.4	44.1	23.10	16.2	46.3	01.20	14.7	48.9	03.30	14.6	50.0	05.40	18.6	47.1
21.05	16.4	44.1	23.15	16.3	46.7	01.25	14.7	49.1	03.35	14.6	49.8	05.45	18.6	47.0
21.10	16.0	44.6	23.20	16.1	46.0	01.30	14.7	49.2	03.40	15.0	49.8	05.50	18.9	46.9
21.15	15.8	44.9	23.25	16.2	46.3	01.35	14.7	49.3	03.45	15.0	49.5	05.55	19.2	47.0
21.20	15.8	44.8	23.30	16.0	46.1	01.40	14.2	49.0	03.50	15.0	49.8	06.00	19.3	46.8
21.25	15.9	44.9	23.35	16.0	46.2	01.45	14.2	49.1	03.55	15.1	49.4	06.05	19.6	46.5
21.30	15.9	45.1	23.40	16.0	46.2	01.50	14.2	49.0	04.00	15.2	49.3	06.10	20.4	46.6
21.35	15.9	45.2	23.45	16.0	46.3	01.55	14.0	50.4	04.05	15.3	48.8	06.15	20.4	46.2
21.40	16.0	45.3	23.50	16.0	46.8	02.00	13.2	50.6	04.10	15.3	48.7	06.20	21.0	46.0
21.45	16.0	45.4	23.55	15.9	47.1	02.05	13.6	50.4	04.15	15.6	48.0	06.25	21.1	46.2
21.50	16.2	45.6	00.00	15.9	47.2	02.10	13.6	50.5	04.20	15.6	48.5	06.30	21.6	46.3
21.55	15.8	45.6	00.05	15.8	47.6	02.15	13.9	51.2	04.25	15.6	48.1	06.35	21.8	46.1
22.00	15.8	45.9	00.10	15.8	47.8	02.20	14.0	50.9	04.30	15.7	47.9	06.40	21.8	46.0
22.05	15.7	45.4	00.15	15.8	47.7	02.25	14.1	51.0	04.35	15.7	48.0	06.45	22.1	46.1
22.10	15.7	45.6	00.20	15.8	48.1	02.30	14.1	50.9	04.40	15.8	47.5	06.50	22.3	46.5
22.15	15.7	45.8	00.25	15.4	48.2	02.35	14.1	50.9	04.45	15.9	47.2	06.55	22.3	46.3
22.20	16.0	46.0	00.30	15.4	48.2	02.40	14.2	50.7	04.50	15.9	47.6	07.00	22.3	46.2
22.25	16.0	45.8	00.35	15.4	48.0	02.45	14.1	50.9	04.55	16.1	47.7			
22.30	16.0	45.8	00.40	15.3	48.3	02.50	14.3	50.8	05.00	16.2	47.5			
22.35	16.1	45.6	00.45	15.5	48.7	02.55	14.2	50.2	05.05	16.5	47.4			
22.40	16.1	45.4	00.50	15.3	48.6	03.00	14.0	51.0	05.10	16.6	47.3			
22.45	16.1	45.6	00.55	15.3	48.9	03.05	13.9	51.2	05.15	17.3	47.4			

Table (J6): Temperature and relative humidity spot readings. Location: Deir Tomb.
Fourth fieldwork visit: 3-4 April 2005, between 20.40-07.00.

Appendix K: Wind speed spot readings. Fourth fieldwork visit: April 2005.

Location	Date	Height (cm)	Time	Maximum wind speed (m/s)	Minimum wind speed (m/s)	Average wind speed (m/s)	Location	Date	Height (cm)	Time	Maximum wind speed (m/s)	Minimum wind speed (m/s)	Average wind speed (m/s)
T1	1.4.2005	5	05.00	1.9	0.8	1.3	T1	1.4.2005	205	05.05	2.2	0.8	1.3
T1	1.4.2005	5	06.00	0.9	0.2	0.7	T1	1.4.2005	205	06.05	0.9	0.3	0.7
T1	1.4.2005	5	07.00	0.8	0.2	0.5	T1	1.4.2005	205	07.05	0.8	0.1	0.5
T1	1.4.2005	5	08.00	0.7	0.2	0.4	T1	1.4.2005	205	08.05	0.6	0.2	0.4
T1	1.4.2005	5	09.00	0.6	0.3	0.4	T1	1.4.2005	205	09.05	1.0	0.3	0.7
T1	1.4.2005	5	10.00	0.8	0.4	0.5	T1	1.4.2005	205	10.05	1.0	0.4	0.7
T1	1.4.2005	5	11.00	0.8	0.4	0.6	T1	1.4.2005	205	11.05	1.1	0.4	0.7
T1	1.4.2005	5	12.00	0.6	0.1	0.4	T1	1.4.2005	205	12.05	0.8	0.2	0.4
T1	1.4.2005	5	13.00	0.6	0.2	0.5	T1	1.4.2005	205	13.05	0.9	0.3	0.6
T1	1.4.2005	5	14.00	1.3	0.7	0.8	T1	1.4.2005	205	14.05	1.5	0.4	0.9
T1	1.4.2005	5	15.00	1.4	0.6	0.9	T1	1.4.2005	205	15.05	1.7	0.6	0.9
T1	1.4.2005	5	16.00	1.7	0.7	1.1	T1	1.4.2005	205	16.05	2.2	0.6	1.4
T1	1.4.2005	5	17.00	1.6	0.9	1.3	T1	1.4.2005	205	17.05	2.4	0.7	1.6
T1	1.4.2005	5	18.00	2.8	0.8	1.3	T1	1.4.2005	205	18.05	2.8	0.6	1.6
T1	1.4.2005	5	19.00	3.1	0.9	2.1	T1	1.4.2005	205	19.05	3.3	0.9	2.1
T1	3.4.2005	5	05.00	1.4	0.4	0.8	T1	3.4.2005	205	05.05	1.2	0.4	0.8
T1	3.4.2005	5	06.00	0.9	0.3	0.6	T1	3.4.2005	205	06.05	0.8	0.3	0.5
T1	3.4.2005	5	07.00	0.8	0.2	0.5	T1	3.4.2005	205	07.05	0.9	0.2	0.5
T1	3.4.2005	5	08.00	0.2	0.1	0.2	T1	3.4.2005	205	08.05	0.4	0.1	0.3
T1	3.4.2005	5	09.00	0.2	0.1	0.2	T1	3.4.2005	205	09.05	0.5	0.0	0.2
T1	3.4.2005	5	10.00	0.6	0.3	0.4	T1	3.4.2005	205	10.05	0.9	0.3	0.6
T1	3.4.2005	5	11.00	0.6	0.4	0.6	T1	3.4.2005	205	11.05	1.0	0.1	0.6
T1	3.4.2005	5	12.00	0.2	0.0	0.1	T1	3.4.2005	205	12.05	0.4	0.1	0.3
T1	3.4.2005	5	13.00	0.5	0.3	0.4	T1	3.4.2005	205	13.05	0.7	0.3	0.4
T1	3.4.2005	5	14.00	1.2	0.3	0.7	T1	3.4.2005	205	14.05	1.4	0.5	0.8
T1	3.4.2005	5	15.00	1.9	0.4	1.2	T1	3.4.2005	205	15.05	1.8	0.7	1.3
T1	3.4.2005	5	16.00	2.2	0.6	1.5	T1	3.4.2005	205	16.05	2.5	0.7	1.6
T1	3.4.2005	5	17.00	2.7	0.6	1.6	T1	3.4.2005	205	17.05	3.0	0.5	1.8
T1	3.4.2005	5	18.00	2.3	0.8	1.7	T1	3.4.2005	205	18.05	2.9	0.8	1.9
T1	3.4.2005	5	19.00	2.9	0.8	1.7	T1	3.4.2005	205	19.05	3.2	1.0	1.9

Table (K1): Wind speed spot readings. Location: Bab al Siq Triclinium Tomb (T1). Fourth fieldwork visit: April 2005.

Appendix K: Wind speed spot readings. Fourth fieldwork visit: April 2005.

Location	Date	Height (cm)	Time	Maximum wind speed (m/s)	Minimum wind speed (m/s)	Average wind speed (m/s)	Location	Date	Height (cm)	Time	Maximum wind speed (m/s)	Minimum wind speed (m/s)	Average wind speed (m/s)
T1	1.4.2005	305	05.10	1.5	0.6	1.2	T2	1.4.2005	305	05.15	1.6	0.6	1.3
T1	1.4.2005	305	06.10	1.1	0.4	0.8	T2	1.4.2005	305	06.15	1.0	0.5	0.8
T1	1.4.2005	305	07.10	0.8	0.3	0.6	T2	1.4.2005	305	07.15	1.0	0.3	0.8
T1	1.4.2005	305	08.10	0.7	0.2	0.5	T2	1.4.2005	305	08.15	0.8	0.2	0.5
T1	1.4.2005	305	09.10	0.9	0.3	0.7	T2	1.4.2005	305	09.15	0.9	0.3	0.7
T1	1.4.2005	305	10.10	1.1	0.4	0.7	T2	1.4.2005	305	10.15	1.4	0.5	0.8
T1	1.4.2005	305	11.10	0.9	0.3	0.6	T2	1.4.2005	305	11.15	0.9	0.3	0.6
T1	1.4.2005	305	12.10	0.6	0.2	0.4	T2	1.4.2005	305	12.15	0.6	0.2	0.5
T1	1.4.2005	305	13.10	0.8	0.2	0.6	T2	1.4.2005	305	13.15	1.2	0.3	0.6
T1	1.4.2005	305	14.10	1.3	0.6	0.9	T2	1.4.2005	305	14.15	1.7	0.7	1.0
T1	1.4.2005	305	15.10	2.0	0.7	1.3	T2	1.4.2005	305	15.15	2.4	0.7	1.5
T1	1.4.2005	305	16.10	2.0	0.7	1.4	T2	1.4.2005	305	16.15	2.3	0.8	1.6
T1	1.4.2005	305	17.10	2.7	0.6	1.9	T2	1.4.2005	305	17.15	3.0	0.7	1.9
T1	1.4.2005	305	18.10	3.1	0.9	2.0	T2	1.4.2005	305	18.15	3.5	1.0	2.3
T1	1.4.2005	305	19.10	3.6	1.0	2.2	T2	1.4.2005	305	19.15	3.1	1.1	2.4
T1	3.4.2005	305	05.10	1.3	0.4	1.0	T2	3.4.2005	305	05.15	1.5	0.5	1.0
T1	3.4.2005	305	06.10	1.1	0.4	0.8	T2	3.4.2005	305	06.15	1.2	0.5	0.9
T1	3.4.2005	305	07.10	0.8	0.2	0.6	T2	3.4.2005	305	07.15	0.8	0.2	0.6
T1	3.4.2005	305	08.10	0.7	0.2	0.4	T2	3.4.2005	305	08.15	0.7	0.4	0.5
T1	3.4.2005	305	09.10	0.9	0.3	0.7	T2	3.4.2005	305	09.15	1.0	0.4	0.7
T1	3.4.2005	305	10.10	1.0	0.3	0.7	T2	3.4.2005	305	10.15	1.3	0.5	0.8
T1	3.4.2005	305	11.10	0.8	0.3	0.6	T2	3.4.2005	305	11.15	0.9	0.3	0.6
T1	3.4.2005	305	12.10	0.6	0.1	0.4	T2	3.4.2005	305	12.15	0.6	0.2	0.5
T1	3.4.2005	305	13.10	0.8	0.2	0.6	T2	3.4.2005	305	13.15	0.9	0.2	0.6
T1	3.4.2005	305	14.10	1.0	0.5	0.9	T2	3.4.2005	305	14.15	1.4	0.5	0.9
T1	3.4.2005	305	15.10	1.6	0.7	1.1	T2	3.4.2005	305	15.15	1.9	0.6	1.1
T1	3.4.2005	305	16.10	1.7	0.8	1.4	T2	3.4.2005	305	16.15	2.0	0.9	1.5
T1	3.4.2005	305	17.10	2.6	0.5	1.6	T2	3.4.2005	305	17.15	2.7	0.7	1.8
T1	3.4.2005	305	18.10	3.4	0.7	1.9	T2	3.4.2005	305	18.15	3.6	0.8	1.9
T1	21.6.2004	305	19.10	3.2	0.9	2.2	T2	3.4.2005	305	19.15	3.8	1.0	2.3

Table (K2): Wind speed spot readings. Location: Bab al Siq Triclinium Tomb (T1 and T2). Fourth fieldwork visit: April 2005.

Appendix K: Wind speed spot readings. Fourth fieldwork visit: April 2005.

Location	Date	Height (cm)	Time	Maximum wind speed (m/s)	Minimum wind speed (m/s)	Average wind speed (m/s)
T3	1.4.2005	305	05.20	1.4	0.6	1.1
T3	1.4.2005	305	06. 20	1.1	0.5	0.8
T3	1.4.2005	305	07. 20	1.0	0.3	0.8
T3	1.4.2005	305	08. 20	0.9	0.3	0.6
T3	1.4.2005	305	09. 20	0.9	0.3	0.7
T3	1.4.2005	305	10. 20	1.5	0.5	1.0
T3	1.4.2005	305	11. 20	0.9	0.3	0.7
T3	1.4.2005	305	12. 20	0.6	0.1	0.5
T3	1.4.2005	305	13. 20	1.2	0.2	0.7
T3	1.4.2005	305	14. 20	1.7	0.7	1.0
T3	1.4.2005	305	15. 20	2.3	0.6	1.5
T3	1.4.2005	305	16. 20	2.0	0.7	1.5
T3	1.4.2005	305	17. 20	3.1	0.9	2.0
T3	1.4.2005	305	18. 20	3.1	1.2	2.1
T3	1.4.2005	305	19. 20	3.7	1.0	2.3
T3	3.4.2005	305	05.20	1.4	0.3	1.0
T3	3.4.2005	305	06. 20	1.3	0.5	0.9
T3	3.4.2005	305	07. 20	0.7	0.3	0.7
T3	3.4.2005	305	08. 20	0.7	0.2	0.5
T3	3.4.2005	305	09..20	0.9	0.3	0.6
T3	3.4.2005	305	10. 20	1.4	0.4	0.9
T3	3.4.2005	305	11. 20	0.9	0.2	0.5
T3	3.4.2005	305	12. 20	0.4	0.2	0.4
T3	3.4.2005	305	13. 20	1.0	0.2	0.7
T3	3.4.2005	305	14. 20	1.5	0.5	0.8
T3	3.4.2005	305	15. 20	1.7	0.7	1.0
T3	3.4.2005	305	16. 20	2.3	1.0	1.5
T3	3.4.2005	305	17. 20	2.8	0.8	1.9
T3	3.4.2005	305	18. 20	3.5	1.0	2.1
T3	3.4.2005	305	19. 20	3.7	1.2	2.4

Table (K3): Wind speed spot readings. Location: Bab al Siq Triclinium Tomb (T3). Fourth fieldwork visit: April 2005.

Appendix K: Wind speed spot readings. Fourth fieldwork visit: April 2005.

Location	Date	Height (cm)	Time	Maximum wind speed (m/s)	Minimum wind speed (m/s)	Average wind speed (m/s)	Location	Date	Height (cm)	Time	Maximum wind speed (m/s)	Minimum wind speed (m/s)	Average wind speed (m/s)
H	2.4.2005	350	05.00	1.1	0.4	0.8	H	2.4.2005	450	05.05	1.2	0.4	0.8
H	2.4.2005	350	06.00	1.0	0.4	0.8	H	2.4.2005	450	06.05	0.9	0.4	0.8
H	2.4.2005	350	07.00	0.8	0.3	0.7	H	2.4.2005	450	07.05	1.0	0.4	0.8
H	2.4.2005	350	08.00	0.7	0.2	0.5	H	2.4.2005	450	08.05	0.7	0.3	0.6
H	2.4.2005	350	09.00	0.7	0.3	0.6	H	2.4.2005	450	09.05	0.8	0.2	0.6
H	2.4.2005	350	10.00	0.9	0.3	0.7	H	2.4.2005	450	10.05	1.0	0.4	0.8
H	2.4.2005	350	11.00	0.8	0.2	0.5	H	2.4.2005	450	11.05	0.9	0.2	0.6
H	2.4.2005	350	12.00	0.6	0.2	0.4	H	2.4.2005	450	12.05	0.6	0.2	0.4
H	2.4.2005	350	13.00	0.6	0.1	0.4	H	2.4.2005	450	13.05	0.8	0.2	0.4
H	2.4.2005	350	14.00	1.1	0.5	0.9	H	2.4.2005	450	14.05	1.3	0.4	0.9
H	2.4.2005	350	15.00	1.9	0.6	1.1	H	2.4.2005	450	15.05	2.0	0.7	1.1
H	2.4.2005	350	16.00	2.1	0.7	1.4	H	2.4.2005	450	16.05	2.2	0.8	1.6
H	2.4.2005	350	17.00	3.0	0.8	1.6	H	2.4.2005	450	17.05	3.0	0.9	1.6
H	2.4.2005	350	18.00	3.2	0.9	2.1	H	2.4.2005	450	18.05	3.4	0.8	2.3
H	2.4.2005	350	19.00	3.4	0.9	2.7	H	2.4.2005	450	19.05	3.5	0.9	2.9
H	4.4.2005	350	05.00	0.9	0.4	0.7	H	4.4.2005	450	05.05	1.0	0.3	0.7
H	4.4.2005	350	06.00	0.8	0.3	0.6	H	4.4.2005	450	06.05	0.8	0.3	0.7
H	4.4.2005	350	07.00	0.7	0.2	0.5	H	4.4.2005	450	07.05	0.8	0.3	0.6
H	4.4.2005	350	08.00	0.6	0.2	0.4	H	4.4.2005	450	08.05	0.7	0.3	0.5
H	4.4.2005	350	09.00	0.7	0.3	0.5	H	4.4.2005	450	09.05	0.9	0.3	0.6
H	4.4.2005	350	10.00	1.0	0.3	0.8	H	4.4.2005	450	10.05	0.9	0.3	0.7
H	4.4.2005	350	11.00	1.0	0.2	0.6	H	4.4.2005	450	11.05	0.8	0.2	0.5
H	4.4.2005	350	12.00	0.5	0.2	0.4	H	4.4.2005	450	12.05	0.5	0.2	0.4
H	4.4.2005	350	13.00	0.6	0.1	0.3	H	4.4.2005	450	13.05	0.8	0.2	0.4
H	4.4.2005	350	14.00	1.1	0.6	0.7	H	4.4.2005	450	14.05	1.1	0.4	0.8
H	4.4.2005	350	15.00	1.1	0.6	0.8	H	4.4.2005	450	15.05	1.5	0.7	0.9
H	4.4.2005	350	16.00	1.7	0.5	1.1	H	4.4.2005	450	16.05	2.0	0.8	1.5
H	4.4.2005	350	17.00	2.0	0.8	1.4	H	4.4.2005	450	17.05	3.0	0.7	1.5
H	4.4.2005	350	18.00	2.4	0.9	1.9	H	4.4.2005	450	18.05	3.2	0.9	1.8
H	4.4.2005	350	19.00	3.1	0.9	2.2	H	4.4.2005	450	19.05	3.7	0.8	2.2

Table (K4): Wind speed spot readings. Location: Corinthian Tomb (H). Fourth fieldwork visit: April 2005.

Appendix K: Wind speed spot readings. Fourth fieldwork visit: April 2005.

Location	Date	Height (cm)	Time	Maximum wind speed (m/s)	Minimum wind speed (m/s)	Average wind speed (m/s)	Location	Date	Height (cm)	Time	Maximum wind speed (m/s)	Minimum wind speed (m/s)	Average wind speed (m/s)
C1	2.4.2005	350	05.15	1.7	0.4	1.4	C1	2.4.2005	450	05.20	1.6	0.5	1.3
C1	2.4.2005	350	06.15	1.6	0.4	0.9	C1	2.4.2005	450	06. 20	1.7	0.4	1.0
C1	2.4.2005	350	07.15	1.0	0.3	0.8	C1	2.4.2005	450	07. 20	1.2	0.3	0.8
C1	2.4.2005	350	08.15	0.9	0.2	0.6	C1	2.4.2005	450	08. 20	0.8	0.3	0.8
C1	2.4.2005	350	09.15	1.0	0.3	0.8	C1	2.4.2005	450	09. 20	1.1	0.3	0.8
C1	2.4.2005	350	10.15	1.4	0.5	0.9	C1	2.4.2005	450	10. 20	1.5	0.5	0.9
C1	2.4.2005	350	11.15	1.2	0.4	0.8	C1	2.4.2005	450	11. 20	1.1	0.3	0.8
C1	2.4.2005	350	12.15	0.8	0.2	0.5	C1	2.4.2005	450	12. 20	0.9	0.2	0.6
C1	2.4.2005	350	13.15	0.9	0.2	0.6	C1	2.4.2005	450	13. 20	1.0	0.3	0.6
C1	2.4.2005	350	14.15	1.6	0.5	1.0	C1	2.4.2005	450	14. 20	1.6	0.5	1.0
C1	2.4.2005	350	15.15	2.6	0.6	1.5	C1	2.4.2005	450	15. 20	2.8	0.6	1.6
C1	2.4.2005	350	16.15	2.8	0.6	1.5	C1	2.4.2005	450	16. 20	3.0	0.7	1.7
C1	2.4.2005	350	17.15	3.1	0.6	2.1	C1	2.4.2005	450	17. 20	3.3	0.7	2.1
C1	2.4.2005	350	18.15	3.6	0.8	2.3	C1	2.4.2005	450	18. 20	3.8	1.0	2.4
C1	2.4.2005	350	19.15	3.8	1.0	2.6	C1	2.4.2005	450	19. 20	4.0	1.0	2.9
C1	4.4.2005	350	05.15	1.6	0.3	1.2	C1	4.4.2005	450	05.20	1.5	0.4	1.1
C1	4.4.2005	350	06.15	1.6	0.4	0.9	C1	4.4.2005	450	06. 20	1.4	0.3	0.9
C1	4.4.2005	350	07.15	1.0	0.4	0.7	C1	4.4.2005	450	07. 20	1.1	0.2	0.8
C1	4.4.2005	350	08.15	0.9	0.3	0.7	C1	4.4.2005	450	08. 20	0.8	0.2	0.6
C1	4.4.2005	350	09.15	0.9	0.2	0.7	C1	4.4.2005	450	09. 20	1.0	0.3	0.7
C1	4.4.2005	350	10.15	1.5	0.4	0.9	C1	4.4.2005	450	10. 20	1.2	0.3	0.8
C1	4.4.2005	350	11.15	1.1	0.3	0.7	C1	4.4.2005	450	11. 20	1.1	0.3	0.7
C1	4.4.2005	350	12.15	0.8	0.2	0.5	C1	4.4.2005	450	12. 20	0.8	0.1	0.5
C1	4.4.2005	350	13.15	1.0	0.2	0.5	C1	4.4.2005	450	13. 20	0.9	0.2	0.6
C1	4.4.2005	350	14.15	1.5	0.4	1.0	C1	4.4.2005	450	14. 20	1.7	0.4	0.9
C1	4.4.2005	350	15.15	2.3	0.6	1.4	C1	4.4.2005	450	15. 20	2.7	0.6	1.5
C1	4.4.2005	350	16.15	3.1	0.5	1.6	C1	4.4.2005	450	16. 20	3.1	0.6	1.6
C1	4.4.2005	350	17.15	2.9	0.5	2.0	C1	4.4.2005	450	17. 20	3.2	0.6	2.0
C1	4.4.2005	350	18.15	3.3	0.7	2.2	C1	4.4.2005	450	18. 20	3.9	0.7	2.2
C1	4.4.2005	350	19.15	3.5	0.9	2.4	C1	4.4.2005	450	19. 20	3.8	1.2	2.6

Table (K5): Wind speed spot readings. Location: Palace Tomb (C1). Fourth fieldwork visit: April 2005.

Appendix K: Wind speed spot readings. Fourth fieldwork visit: April 2005.

Location	Date	Height (cm)	Time	Maximum wind speed (m/s)	Minimum wind speed (m/s)	Average wind speed (m/s)	Location	Date	Height (cm)	Time	Maximum wind speed (m/s)	Minimum wind speed (m/s)	Average wind speed (m/s)
C2	2.4.2005	350	05.25	2.0	0.4	1.6	C2	2.4.2005	450	05.30	2.4	0.4	1.8
C2	2.4.2005	350	06.25	1.8	0.4	1.0	C2	2.4.2005	450	06.30	2.0	0.5	1.2
C2	2.4.2005	350	07.25	1.4	0.4	0.9	C2	2.4.2005	450	07.30	1.7	0.4	1.0
C2	2.4.2005	350	08.25	1.0	0.3	0.7	C2	2.4.2005	450	08.30	1.1	0.4	0.8
C2	2.4.2005	350	09.25	1.3	0.3	0.8	C2	2.4.2005	450	09.30	1.4	0.4	0.9
C2	2.4.2005	350	10.25	1.6	0.5	1.0	C2	2.4.2005	450	10.30	1.6	0.5	1.0
C2	2.4.2005	350	11.25	1.1	0.3	0.7	C2	2.4.2005	450	11.30	1.1	0.4	0.8
C2	2.4.2005	350	12.25	1.0	0.3	0.6	C2	2.4.2005	450	12.30	1.0	0.3	0.6
C2	2.4.2005	350	13.25	1.1	0.2	0.6	C2	2.4.2005	450	01.30	1.1	0.3	0.7
C2	2.4.2005	350	14.25	1.7	0.6	1.1	C2	2.4.2005	450	14.30	1.8	0.5	1.2
C2	2.4.2005	350	15.25	2.8	0.6	1.5	C2	2.4.2005	450	15.30	2.8	0.6	1.7
C2	2.4.2005	350	16.25	3.0	0.6	1.6	C2	2.4.2005	450	16.30	3.2	0.7	1.8
C2	2.4.2005	350	17.25	3.3	0.6	2.2	C2	2.4.2005	450	17.30	3.5	0.6	2.2
C2	2.4.2005	350	18.25	3.7	0.8	2.5	C2	2.4.2005	450	18.30	3.9	0.8	2.7
C2	2.4.2005	350	19.25	4.0	1.0	2.7	C2	2.4.2005	450	19.30	4.1	1.0	2.8
C2	4.4.2005	350	05.25	2.0	0.4	1.6	C2	4.4.2005	450	05.30	2.0	0.4	1.6
C2	4.4.2005	350	06.25	1.7	0.4	1.0	C2	4.4.2005	450	06.30	1.7	0.4	1.0
C2	4.4.2005	350	07.25	1.3	0.4	0.8	C2	4.4.2005	450	07.30	1.3	0.4	0.8
C2	4.4.2005	350	08.25	1.0	0.3	0.7	C2	4.4.2005	450	08.30	1.1	0.3	0.8
C2	4.4.2005	350	09.25	1.1	0.3	0.8	C2	4.4.2005	450	09.30	1.2	0.3	0.8
C2	4.4.2005	350	10.25	1.6	0.4	0.8	C2	4.4.2005	450	10.30	1.7	0.4	0.9
C2	4.4.2005	350	11.25	1.0	0.3	0.7	C2	4.4.2005	450	11.30	1.1	0.3	0.7
C2	4.4.2005	350	12.25	0.8	0.2	0.5	C2	4.4.2005	450	12.30	0.8	0.3	0.6
C2	4.4.2005	350	13.25	1.1	0.2	0.6	C2	4.4.2005	450	01.30	1.2	0.3	0.7
C2	4.4.2005	350	14.25	1.6	0.5	1.0	C2	4.4.2005	450	14.30	1.7	0.5	1.1
C2	4.4.2005	350	15.25	2.8	0.5	1.4	C2	4.4.2005	450	15.30	2.9	0.6	1.4
C2	4.4.2005	350	16.25	2.8	0.5	1.6	C2	4.4.2005	450	16.30	3.0	0.5	1.6
C2	4.4.2005	350	17.25	3.1	0.5	2.0	C2	4.4.2005	450	17.30	3.3	0.5	2.1
C2	4.4.2005	350	18.25	3.6	0.8	2.2	C2	4.4.2005	450	18.30	4.0	0.8	2.4
C2	4.4.2005	350	19.25	3.7	0.9	2.6	C2	4.4.2005	450	19.30	4.1	0.9	2.7

Table (K6): Wind speed spot readings. Location: Palace Tomb (C2). Fourth fieldwork visit: April 2005.

Appendix K: Wind speed spot readings. Fourth fieldwork visit: April 2005.

Location	Date	Height (cm)	Time	Maximum wind speed (m/s)	Minimum wind speed (m/s)	Average wind speed (m/s)	Location	Date	Height (cm)	Time	Maximum wind speed (m/s)	Minimum wind speed (m/s)	Average wind speed (m/s)
C3	2.4.2005	350	05.35	1.0	0.2	0.7	C3	2.4.2005	450	05.40	1.0	0.2	0.7
C3	2.4.2005	350	06.35	0.9	0.2	0.6	C3	2.4.2005	450	06.40	1.0	0.2	0.7
C3	2.4.2005	350	07.35	0.8	0.2	0.5	C3	2.4.2005	450	07.40	0.9	0.2	0.6
C3	2.4.2005	350	08.35	0.6	0.2	0.5	C3	2.4.2005	450	08.40	0.6	0.2	0.4
C3	2.4.2005	350	09.35	0.9	0.2	0.6	C3	2.4.2005	450	09.40	1.0	0.3	0.7
C3	2.4.2005	350	10.35	1.0	0.3	0.7	C3	2.4.2005	450	10.40	1.2	0.3	0.7
C3	2.4.2005	350	11.35	1.0	0.3	0.7	C3	2.4.2005	450	11.40	1.1	0.3	0.7
C3	2.4.2005	350	12.35	0.5	0.1	0.3	C3	2.4.2005	450	12.40	0.6	0.2	0.4
C3	2.4.2005	350	13.35	0.6	0.1	0.4	C3	2.4.2005	450	13.40	0.7	0.2	0.5
C3	2.4.2005	350	14.35	1.1	0.4	0.7	C3	2.4.2005	450	14.40	1.2	0.4	0.8
C3	2.4.2005	350	15.35	1.4	0.4	0.8	C3	2.4.2005	450	15.40	1.4	0.4	0.9
C3	2.4.2005	350	16.35	1.5	0.6	1.0	C3	2.4.2005	450	16.40	1.5	0.5	1.1
C3	2.4.2005	350	17.35	1.8	0.5	1.3	C3	2.4.2005	450	17.40	1.7	0.5	1.3
C3	2.4.2005	350	18.35	2.0	0.6	1.5	C3	2.4.2005	450	18.40	2.1	0.6	1.6
C3	2.4.2005	350	19.35	2.0	0.5	1.6	C3	2.4.2005	450	19.40	2.2	0.5	1.7
C3	4.4.2005	350	05.35	1.0	0.2	0.7	C3	4.4.2005	450	05.40	1.1	0.2	0.7
C3	4.4.2005	350	06.35	0.9	0.2	0.6	C3	4.4.2005	450	06.40	0.9	0.2	0.7
C3	4.4.2005	350	07.35	0.9	0.3	0.6	C3	4.4.2005	450	07.40	0.9	0.2	0.5
C3	4.4.2005	350	08.35	0.6	0.2	0.4	C3	4.4.2005	450	08.40	0.7	0.2	0.5
C3	4.4.2005	350	09.35	0.8	0.2	0.5	C3	4.4.2005	450	09.40	0.9	0.2	0.5
C3	4.4.2005	350	10.35	0.9	0.2	0.6	C3	4.4.2005	450	10.40	1.0	0.2	0.6
C3	4.4.2005	350	11.35	1.0	0.3	0.7	C3	4.4.2005	450	11.40	1.1	0.3	0.7
C3	4.4.2005	350	12.35	0.5	0.1	0.3	C3	4.4.2005	450	12.40	0.4	0.0	0.3
C3	4.4.2005	350	13.35	0.6	0.1	0.4	C3	4.4.2005	450	13.40	0.6	0.2	0.4
C3	4.4.2005	350	14.35	1.1	0.3	0.7	C3	4.4.2005	450	14.40	1.2	0.4	0.8
C3	4.4.2005	350	15.35	1.3	0.4	0.7	C3	4.4.2005	450	15.40	1.3	0.4	0.9
C3	4.4.2005	350	16.35	1.5	0.5	1.0	C3	4.4.2005	450	16.40	1.5	0.5	1.0
C3	4.4.2005	350	17.35	1.6	0.5	1.0	C3	4.4.2005	450	17.40	1.7	0.5	1.1
C3	4.4.2005	350	18.35	1.9	0.5	1.4	C3	4.4.2005	450	18.40	1.9	0.6	1.4
C3	4.4.2005	350	19.35	1.9	0.5	1.5	C3	4.4.2005	450	19.40	2.0	0.5	1.6

Table (K7): Wind speed spot readings. Location: Palace Tomb (C3). Fourth fieldwork visit: April 2005.

Appendix K: Wind speed spot readings. Fourth fieldwork visit: April 2005.

Location	Date	Height (cm)	Time	Maximum wind speed (m/s)	Minimum wind speed (m/s)	Average wind speed (m/s)	Location	Date	Height (cm)	Time	Maximum wind speed (m/s)	Minimum wind speed (m/s)	Average wind speed (m/s)
D1	5.4.2005	55	05.00	0.9	0.2	0.6	D1	5.4.2005	255	05.05	0.9	0.3	0.6
D1	5.4.2005	55	06.00	0.8	0.2	0.5	D1	5.4.2005	255	06.05	0.8	0.2	0.6
D1	5.4.2005	55	07.00	0.8	0.1	0.5	D1	5.4.2005	255	07.05	0.7	0.2	0.5
D1	5.4.2005	55	08.00	0.6	0.1	0.4	D1	5.4.2005	255	08.05	0.6	0.1	0.5
D1	5.4.2005	55	09.00	0.9	0.2	0.6	D1	5.4.2005	255	09.05	1.0	0.2	0.6
D1	5.4.2005	55	10.00	0.9	0.2	0.6	D1	5.4.2005	255	10.05	1.0	0.2	0.6
D1	5.4.2005	55	11.00	0.9	0.2	0.6	D1	5.4.2005	255	11.05	0.9	0.2	0.6
D1	5.4.2005	55	12.00	0.3	0.1	0.2	D1	5.4.2005	255	12.05	0.4	0.1	0.2
D1	5.4.2005	55	13.00	0.6	0.1	0.4	D1	5.4.2005	255	13.05	0.6	0.2	0.4
D1	5.4.2005	55	14.00	0.8	0.3	0.6	D1	5.4.2005	255	14.05	0.9	0.3	0.7
D1	5.4.2005	55	15.00	1.0	0.4	0.7	D1	5.4.2005	255	15.05	1.1	0.4	0.7
D1	5.4.2005	55	16.00	1.2	0.5	0.8	D1	5.4.2005	255	16.05	1.3	0.6	0.8
D1	5.4.2005	55	17.00	1.3	0.4	1.0	D1	5.4.2005	255	17.05	1.4	0.4	1.1
D1	5.4.2005	55	18.00	1.4	0.5	1.3	D1	5.4.2005	255	18.05	1.6	0.5	1.3
D1	5.4.2005	55	19.00	1.5	0.4	1.3	D1	5.4.2005	255	19.05	1.6	0.4	1.4
D1	6.4.2005	55	05.00	0.9	0.2	0.6	D1	6.4.2005	255	05.05	1.0	0.2	0.6
D1	6.4.2005	55	06.00	0.8	0.2	0.5	D1	6.4.2005	255	06.05	0.8	0.3	0.6
D1	6.4.2005	55	07.00	0.7	0.1	0.5	D1	6.4.2005	255	07.05	0.8	0.2	0.5
D1	6.4.2005	55	08.00	0.7	0.1	0.5	D1	6.4.2005	255	08.05	0.7	0.2	0.5
D1	6.4.2005	55	09.00	1.0	0.2	0.6	D1	6.4.2005	255	09.05	1.1	0.3	0.7
D1	6.4.2005	55	10.00	1.0	0.3	0.7	D1	6.4.2005	255	10.05	1.1	0.3	0.8
D1	6.4.2005	55	11.00	0.9	0.3	0.5	D1	6.4.2005	255	11.05	0.9	0.2	0.5
D1	6.4.2005	55	12.00	0.3	0.1	0.3	D1	6.4.2005	255	12.05	0.3	0.0	0.2
D1	6.4.2005	55	13.00	0.6	0.2	0.4	D1	6.4.2005	255	13.05	0.7	0.2	0.5
D1	6.4.2005	55	14.00	0.8	0.3	0.6	D1	6.4.2005	255	14.05	0.9	0.3	0.7
D1	6.4.2005	55	15.00	1.1	0.4	0.8	D1	6.4.2005	255	15.05	1.2	0.5	0.8
D1	6.4.2005	55	16.00	1.3	0.5	0.8	D1	6.4.2005	255	16.05	1.4	0.5	0.9
D1	6.4.2005	55	17.00	1.4	0.5	1.0	D1	6.4.2005	255	17.05	1.4	0.4	1.2
D1	6.4.2005	55	18.00	1.4	0.5	1.3	D1	6.4.2005	255	18.05	1.5	0.5	1.4
D1	6.4.2005	55	19.00	1.5	0.5	1.4	D1	6.4.2005	255	19.05	1.6	0.5	1.5

Table (K8): Wind speed spot readings. Location: Deir Tomb (D1). Fourth fieldwork visit: April 2005.

Appendix K: Wind speed spot readings. Fourth fieldwork visit: April 2005.

Location	Date	Height (cm)	Time	Maximum wind speed (m/s)	Minimum wind speed (m/s)	Average wind speed (m/s)	Location	Date	Height (cm)	Time	Maximum wind speed (m/s)	Minimum wind speed (m/s)	Average wind speed (m/s)
D2	5.4.2005	55	05.10	0.8	0.2	0.5	D2	5.4.2005	255	05.15	0.9	0.2	0.6
D2	5.4.2005	55	06.10	0.8	0.2	0.5	D2	5.4.2005	255	06.15	0.8	0.2	0.5
D2	5.4.2005	55	07.10	0.7	0.1	0.4	D2	5.4.2005	255	07.15	0.7	0.2	0.5
D2	5.4.2005	55	08.10	0.6	0.1	0.4	D2	5.4.2005	255	08.15	0.5	0.2	0.4
D2	5.4.2005	55	09.10	0.8	0.2	0.5	D2	5.4.2005	255	09.15	0.9	0.3	0.6
D2	5.4.2005	55	10.10	0.9	0.2	0.6	D2	5.4.2005	255	10.15	0.9	0.3	0.7
D2	5.4.2005	55	11.10	0.8	0.2	0.5	D2	5.4.2005	255	11.15	0.8	0.2	0.5
D2	5.4.2005	55	12.10	0.3	0.1	0.2	D2	5.4.2005	255	12.15	0.4	0.1	0.2
D2	5.4.2005	55	13.10	0.5	0.1	0.3	D2	5.4.2005	255	13.15	0.4	0.1	0.4
D2	5.4.2005	55	14.10	0.6	0.2	0.4	D2	5.4.2005	255	14.15	0.7	0.3	0.5
D2	5.4.2005	55	15.10	0.8	0.4	0.5	D2	5.4.2005	255	15.15	0.9	0.4	0.6
D2	5.4.2005	55	16.10	1.1	0.6	0.8	D2	5.4.2005	255	16.15	1.1	0.6	0.8
D2	5.4.2005	55	17.10	1.3	0.4	1.0	D2	5.4.2005	255	17.15	1.3	0.4	1.0
D2	5.4.2005	55	18.10	1.4	0.6	1.1	D2	5.4.2005	255	18.15	1.5	0.6	1.1
D2	5.4.2005	55	19.10	1.4	0.4	1.2	D2	5.4.2005	255	19.15	1.5	0.5	1.2
D2	6.4.2005	55	05.10	0.9	0.2	0.6	D2	6.4.2005	255	05.15	0.9	0.3	0.6
D2	6.4.2005	55	06.10	0.7	0.3	0.5	D2	6.4.2005	255	06.15	0.8	0.3	0.5
D2	6.4.2005	55	07.10	0.7	0.2	0.5	D2	6.4.2005	255	07.15	0.8	0.2	0.4
D2	6.4.2005	55	08.10	0.6	0.2	0.4	D2	6.4.2005	255	08.15	0.6	0.2	0.4
D2	6.4.2005	55	09.10	0.9	0.2	0.5	D2	6.4.2005	255	09.15	0.9	0.2	0.6
D2	6.4.2005	55	10.10	0.9	0.3	0.6	D2	6.4.2005	255	10.15	1.0	0.3	0.7
D2	6.4.2005	55	11.10	0.8	0.3	0.6	D2	6.4.2005	255	11.15	0.8	0.2	0.5
D2	6.4.2005	55	12.10	0.3	0.0	0.2	D2	6.4.2005	255	12.15	0.2	0.1	0.1
D2	6.4.2005	55	13.10	0.5	0.2	0.3	D2	6.4.2005	255	13.15	0.6	0.2	0.4
D2	6.4.2005	55	14.10	0.7	0.3	0.5	D2	6.4.2005	255	14.15	0.9	0.3	0.5
D2	6.4.2005	55	15.10	0.8	0.5	0.6	D2	6.4.2005	255	15.15	0.8	0.6	0.6
D2	6.4.2005	55	16.10	1.1	0.6	0.8	D2	6.4.2005	255	16.15	1.1	0.5	0.9
D2	6.4.2005	55	17.10	1.1	0.6	0.8	D2	6.4.2005	255	17.15	1.1	0.7	0.9
D2	6.4.2005	55	18.10	1.4	0.5	1.1	D2	6.4.2005	255	18.15	1.8	0.5	1.0
D2	6.4.2005	55	19.10	1.4	0.6	1.2	D2	6.4.2005	255	19.15	1.9	0.5	1.2

Table (K9): Wind speed spot readings. Location: Deir Tomb (D2). Fourth fieldwork visit: April 2005.

Appendix K: Wind speed spot readings. Fourth fieldwork visit: April 2005.

Location	Date	Height (cm)	Time	Maximum wind speed (m/s)	Minimum wind speed (m/s)	Average wind speed (m/s)
Nabateans Hotel (10minutes from the archaeological site).	1.4.2005	500	20.00	3.1	1.3	2.7
	1.4.2005	500	21.00	4.5	1.6	3.1
	1.4.2005	500	22.00	5.1	1.9	4.1
	1.4.2005	500	23.00	5.9	1.9	4.2
	1.4.2005	500	00.00	6.0	2.1	4.4
	2.4.2005	500	01.00	6.1	2.0	4.6
	2.4.2005	500	02.00	4.2	1.6	2.6
	2.4.2005	500	03.00	2.1	1.0	1.8
	2.4.2005	500	04.00	1.6	0.8	1.2
	3.4.2005	500	20.00	2.9	1.1	2.3
	3.4.2005	500	21.00	3.7	1.2	2.6
	3.4.2005	500	22.00	4.1	1.6	3.1
	3.4.2005	500	23.00	4.9	2.1	3.7
	3.4.2005	500	00.00	5.2	2.2	4.0
	4.4.2005	500	01.00	5.6	2.2	4.4
	4.4.2005	500	02.00	3.5	1.4	2.8
	4.4.2005	500	03.00	2.0	0.9	1.4
	4.4.2005	500	04.00	1.0	0.7	0.9
	5.4.2005	500	20.00	2.0	1.0	1.5
	5.4.2005	500	21.00	2.9	1.2	2.3
	5.4.2005	500	22.00	4.1	2.0	2.9
	5.4.2005	500	23.00	4.5	2.3	3.2
	5.4.2005	500	00.00	5.0	2.2	3.5
	6.4.2005	500	01.00	5.5	1.0	2.0
	6.4.2005	500	02.00	3.1	1.0	1.9
	6.4.2005	500	03.00	1.7	0.7	1.0
	6.4.2005	500	04.00	1.0	0.6	0.8

Table (K10): Wind speed spot readings. Location: Nabateans Hotel (10 minutes walking distance from the archaeological site). Fourth fieldwork visit: April 2005.

Appendix L: The anion and cation content of the drilled samples. Fourth fieldwork visit: April 2005.

Sample number	Location	Height (cm)	Depth (cm)	Ca (ppm)	Na (ppm)	Mg (ppm)	K (ppm)	Fe (ppm)	Al (ppm)	Ti (ppm)	Zn (ppm)	F (ppm)	Br (ppm)	Cl (ppm)	NO_3 (ppm)	PO_4 (ppm)	SO_4 (ppm)	cation charge with Al	Cation charge without Al	Anion charge	Sum of cations & anions (ppm)	Soluble salt content in the sample (%) of dry weight
1	T1	5	0-1	4.29	5.64	0.73	1.35	0.45	1.82	0.12	0.17	0.97	0.00	7.89	10.56	0.00	5.96	0.78	0.58	0.57	39.95	0.20
2	T1	5	1-3	2.91	5.18	0.56	0.99	0.29	1.32	0.13	0.07	0.49	0.00	5.24	13.08	0.00	4.58	0.60	0.45	0.48	34.84	0.17
3	T1	55	0-1	2.99	4.8	0.33	0.83	0.31	2.53	0.10	0.04	0.60	0.00	4.36	7.14	0.00	3.85	0.70	0.42	0.35	27.88	0.14
4	T1	55	1-3	2.32	4.71	0.27	0.58	0.3	2.66	0.13	0.04	0.64	0.00	5.78	7.95	0.00	4.03	0.67	0.37	0.41	29.41	0.15
5	T1	105	0-1	4.44	5.38	0.61	0.94	0.39	1.38	0.14	0.03	0.78	0.00	5.82	14.47	0.00	3.70	0.70	0.55	0.52	38.08	0.19
6	T1	105	1-3	2.07	6.28	0.41	1.04	0.3	0.94	0.17	0.03	0.63	0.00	6.31	8.49	0.00	0.00	0.56	0.46	0.35	26.67	0.13
7	T1	155	0-1	5.98	9.39	2.02	2.06	0.2	0.76	0.08	0.03	0.44	0.00	12.52	19.89	0.00	4.41	1.02	0.94	0.79	57.78	0.29
8	T1	155	1-3	4.26	8.64	1.27	1.54	0.28	1.25	0.15	0.02	0.68	0.00	10.59	15.44	0.00	4.40	0.89	0.75	0.68	48.52	0.24
9	T1	205	0-1	4.89	15.8	2.16	3.2	0.44	1.36	0.08	0.03	0.61	0.00	18.56	21.57	0.00	5.29	1.36	1.21	1.01	73.99	0.37
10	T1	205	1-3	2.05	9.44	0.88	1.74	0.24	1.09	0.05	0.02	1.39	0.00	12.77	13.82	0.00	4.83	0.76	0.64	0.76	48.32	0.24
11	T1	305	0-1	5.29	4.57	0.87	1.35	0.09	0.10	0.00	0.01	0.41	0.00	4.26	18.60	0.00	6.28	0.58	0.57	0.57	41.83	0.21
12	T1	305	1-3	4.46	5.19	0.69	1.00	0.05	0.08	0.02	0.01	0.54	0.00	4.95	7.51	0.00	7.36	0.54	0.53	0.44	31.86	0.16
13	T1	405	0-1	8.17	4.46	0.80	1.13	0.05	0.02	0.00	0.01	0.36	0.00	3.58	8.25	0.00	6.40	0.70	0.70	0.39	33.23	0.17
14	T1	405	1-3	7.94	4.53	0.89	1.59	0.13	0.13	0.01	0.01	0.00	0.00	4.15	8.37	0.00	4.52	0.73	0.72	0.35	32.27	0.16
15	T1	505	0-1	12.88	6.18	0.96	1.03	0.10	0.98	0.04	0.01	0.48	0.00	4.36	15.32	0.00	8.09	1.13	1.02	0.56	50.43	0.25
16	T1	505	1-3	6.06	5.30	0.39	0.52	0.05	0.89	0.02	0.01	0.63	0.00	4.60	8.38	0.00	6.19	0.68	0.58	0.43	33.04	0.17
17	T1	550	0-1	1.18	5.26	0.15	0.56	0.11	1.30	0.08	0.01	0.04	0.00	4.26	7.61	0.00	0.00	0.46	0.32	0.24	20.56	0.10
18	T1	550	1-3	2.74	4.03	0.21	0.61	0.10	1.03	0.07	0.01	0.28	0.00	3.78	11.38	0.00	0.00	0.46	0.35	0.30	24.24	0.12

Table (L1): The anion and cation content of drilled samples from the Bib al Siq Triclinium Tomb, location (T1). Fourth fieldwork visit: April 2005.

Appendix L: The anion and cation content of the drilled samples. Fourth fieldwork visit: April 2005.

Sample number	Location	Height (cm)	Depth (cm)	Ca (ppm)	Na (ppm)	Mg (ppm)	K (ppm)	Fe (ppm)	Al (ppm)	Ti (ppm)	Zn (ppm)	F (ppm)	Br (ppm)	Cl (ppm)	NO_3 (ppm)	PO_4 (ppm)	SO_4 (ppm)	Cation charge with Al	Cation charge without Al	Anion charge	Sum of cations & anions (ppm)	Soluble salt content in the sample (%) of dry weight
19	T2	405	0-1	12.21	7.33	1.29	2.97	0.07	0.08	0.00	0.01	0.83	0.00	11.81	14.64	0.00	15.32	1.12	1.11	0.93	66.56	0.33
20	T2	405	1-3	15.55	9.60	0.96	4.29	0.04	0.49	0.01	0.01	0.85	0.00	16.69	15.96	0.00	34.38	1.44	1.39	1.49	98.83	0.49
21	T2	455	0-1	13.56	6.30	0.80	0.75	0.07	0.74	0.07	0.01	0.37	0.00	5.22	8.54	0.00	29.96	1.12	1.04	0.93	66.39	0.33
22	T2	455	1-3	6.18	5.77	0.38	0.73	0.07	0.91	0.11	0.01	0.52	0.00	6.18	8.69	0.00	8.98	0.72	0.62	0.53	38.53	0.19
23	T2	505	0-1	0.88	3.17	0.10	0.34	0.20	0.82	0.03	0.00	0.44	0.00	3.27	5.80	0.00	0.00	0.30	0.21	0.21	15.05	0.08
24	T2	505	1-3	0.00	4.65	0.06	0.45	0.32	1.14	0.04	0.01	0.61	0.00	4.31	5.93	0.00	0.00	0.36	0.23	0.25	17.52	0.09
25	T2	550	0-1	2.68	5.53	0.16	0.78	0.43	0.36	0.01	0.01	0.70	0.00	4.70	6.75	0.00	3.88	0.46	0.42	0.36	25.99	0.13
26	T2	550	1-3	2.36	3.50	0.13	0.30	0.30	0.39	0.01	0.01	0.37	0.00	3.69	7.49	0.00	0.00	0.34	0.30	0.24	18.55	0.09
27	T3	405	0-1	33.12	22.07	6.85	88.25	0.05	0.05	0.00	0.01	0.78	0.00	36.74	97.97	0.00	135.51	5.44	5.43	5.48	421.40	2.11
28	T3	405	1-3	22.87	13.73	3.99	75.01	0.03	0.01	0.00	0.01	0.65	0.00	20.51	73.37	0.00	105.95	3.99	3.99	4.00	316.13	1.58
29	T3	455	0-1	83.55	14.52	3.60	175.81	0.02	0.01	0.00	0.02	0.00	0.00	28.94	27.30	0.00	0.00	9.60	9.60	1.26	333.77	1.67
30	T3	455	1-3	105.03	16.49	4.32	234.24	0.04	0.03	0.00	0.02	0.98	0.00	36.52	43.69	0.00	0.00	12.31	12.31	1.79	441.36	2.21
31	T3	505	0-1	5.43	16.81	0.38	37.92	0.07	0.25	0.02	0.01	0.48	0.00	32.43	44.46	0.00	19.19	2.03	2.00	2.06	157.45	0.79
32	T3	505	1-3	2.43	22.90	0.52	29.35	0.07	0.29	0.02	0.01	0.69	0.00	37.69	40.99	0.00	8.79	1.95	1.92	1.94	143.75	0.72
33	T3	550	0-1	6.34	38.84	4.50	19.51	0.04	0.21	0.00	0.01	0.63	0.00	74.51	26.41	0.00	20.87	2.90	2.88	3.00	191.87	0.96
34	T3	550	1-3	4.59	39.85	4.85	23.92	0.05	0.24	0.02	0.02	0.61	0.00	78.21	42.77	0.00	12.55	3.00	2.97	3.19	207.68	1.04

Table (L1): The anion and cation content of drilled samples from the Bib al Siq Triclinium Tomb, locations (T2 and T3). Fourth fieldwork visit: April 2005.

Appendix L: The anion and cation content of the drilled samples. Fourth fieldwork visit: April 2005.

Sample number	Location	Height (cm)	Depth (cm)	Ca (ppm)	Na (ppm)	Mg (ppm)	K (ppm)	Fe (ppm)	Al (ppm)	Tl (ppm)	Zn (ppm)	F (ppm)	Br (ppm)	Cl (ppm)	NO_3 (ppm)	PO_4 (ppm)	SO_4 (ppm)	Cation charge with Al	Cation charge without Al	Anion Charge	Sum of cations & anions (ppm)	Soluble salt content in the sample (%) of dry weight
35	C1	5	0-1	150.23	14.12	2.24	11.83	0.04	0.08	0.01	0.03	0.39	0.39	19.60	17.35	0.00	293.00	8.61	8.60	6.96	509.31	2.55
36	C1	5	1-3	53.52	12.09	1.70	8.43	0.06	0.23	0.04	0.02	0.14	0.14	19.12	19.38	0.00	133.31	3.58	3.55	3.64	248.18	1.24
37	C1	55	0-1	1.59	5.55	0.26	0.75	1.07	2.06	0.40	0.01	0.02	0.02	5.10	7.25	1.63	3.76	0.64	0.41	0.39	29.47	0.15
38	C1	55	1-3	0.00	5.14	0.12	0.61	1.34	2.30	0.51	0.01	0.59	0.59	4.80	5.62	0.00	0.00	0.56	0.30	0.26	21.63	0.11
39	C1	105	0-1	24.73	86.23	2.32	15.19	0.03	0.42	0.02	0.01	0.00	0.00	138.69	28.82	0.00	55.06	5.61	5.56	5.52	351.52	1.76
40	C1	105	1-3	25.52	200.97	4.64	40.92	0.02	0.15	0.00	0.01	0.08	0.08	347.18	74.33	0.00	55.80	11.46	11.44	12.16	749.70	3.75
41	C1	155	0-1	0.65	5.10	0.20	0.62	2.25	4.03	0.30	0.01	0.07	0.07	4.50	17.43	0.00	3.20	0.82	0.37	0.48	38.43	0.19
42	C1	155	1-3	0.11	5.30	0.07	0.58	1.43	3.54	0.34	0.00	0.02	0.02	5.53	6.53	0.00	0.00	0.71	0.32	0.26	23.47	0.12
43	C1	205	0-1	15.59	33.53	4.61	26.02	0.07	0.16	0.01	0.01	0.04	0.04	60.25	58.14	0.00	55.02	3.30	3.28	3.79	253.49	1.27
44	C1	205	1-3	11.20	17.61	2.92	12.37	0.15	0.45	0.03	0.01	0.65	0.65	35.57	45.20	0.00	23.00	1.94	1.89	2.25	149.81	0.75
45	C1	255	0-1	13.39	140.20	16.42	72.84	0.05	0.14	0.00	0.01	0.00	0.00	274.85	147.58	0.00	6.35	10.00	9.98	10.26	671.83	3.36
46	C1	255	1-3	10.87	226.81	15.36	71.17	0.07	0.22	0.00	0.05	0.00	0.00	407.23	141.72	0.00	6.07	13.52	13.50	13.90	879.57	4.40
47	C1	305	0-1	4.70	5.45	0.70	0.70	0.59	0.76	0.05	0.00	0.73	0.73	5.63	8.51	0.00	4.49	0.65	0.57	0.44	33.04	0.17
48	C1	305	1-3	3.76	4.93	0.71	0.98	0.70	0.89	0.06	0.00	0.98	0.98	11.74	27.89	0.00	11.03	0.61	0.51	1.07	64.65	0.32
49	C1	355	0-1	2.82	5.35	0.51	0.74	0.51	0.60	0.04	0.00	5.10	5.10	687.41	678.22	0.00	7.33	0.52	0.45	30.81	1,393.73	6.97
50	C1	355	1-3	8.87	5.19	0.78	0.76	0.36	0.54	0.03	0.01	0.70	0.70	5.01	10.12	0.00	16.21	0.83	0.77	0.69	49.28	0.25
51	C1	405	0-1	11.03	8.09	1.32	0.81	0.24	0.21	0.02	0.00	1.40	0.00	9.82	24.60	0.00	18.06	1.06	1.04	1.12	75.60	0.38
52	C1	405	1-3	4.90	6.65	1.25	0.90	0.59	0.95	0.06	0.03	0.59	0.00	9.24	20.07	0.00	4.80	0.79	0.68	0.72	50.03	0.25
53	C1	505	0-1	7.19	14.54	2.27	2.16	0.75	1.18	0.07	0.39	0.48	0.00	23.79	28.16	4.27	10.20	1.40	1.27	1.50	95.45	0.48
54	C1	505	1-3	6.78	17.59	2.28	1.56	0.14	0.35	0.02	0.02	0.34	0.00	28.42	31.57	0.00	8.95	1.38	1.34	1.52	98.02	0.49
55	C1	550	0-1	5.49	5.58	0.67	0.80	0.69	0.54	0.03	0.01	0.62	0.00	4.17	27.95	0.00	11.12	0.68	0.62	0.83	57.67	0.29
56	C1	550	1-3	0.97	5.29	0.26	0.47	0.56	0.13	0.02	0.01	0.34	0.00	5.86	7.43	0.00	4.86	0.35	0.34	0.40	26.20	0.13

Table (L3): The anion and cation content of drilled samples from the Palace Tomb, locations (C1).
Fourth fieldwork visit: April 2005.

Appendix L: The anion and cation content of the drilled samples. Fourth fieldwork visit: April 2005.

Sample Number	Location	Height (cm)	Depth (cm)	Ca (ppm)	Na (ppm)	Mg (ppm)	K (ppm)	Fe (ppm)	Al (ppm)	Ti (ppm)	Zn (ppm)	F (ppm)	Br (ppm)	Cl (ppm)	NO_3 (ppm)	PO_4 (ppm)	SO_4 (ppm)	Cation charge with Al	Cation charge without Al	Anion charge	Sum of cations & anions (ppm)	Soluble salt content in the sample (%) of dry weight
57	C2	105	0-1	157.98	5.78	0.65	2.69	0.22	0.03	0.01	0.03	0.13	0.00	6.59	7.75	0.00	382.39	8.27	8.27	8.28	564.25	2.82
58	C2	105	1-3	100.88	7.44	1.38	9.46	0.16	0.04	0.01	0.02	0.86	0.00	8.91	13.12	0.00	262.05	5.72	5.72	5.97	404.33	2.02
59	C2	155	0-1	157.14	24.02	10.17	61.35	0.14	0.24	0.01	0.03	0.20	0.00	31.47	102.62	0.00	355.93	11.32	11.29	9.97	743.32	3.72
60	C2	155	1-3	257.04	23.40	8.35	80.56	0.04	0.00	0.00	0.12	0.23	0.00	31.56	136.53	0.00	554.74	16.60	16.60	14.66	1,092.57	5.46
61	C2	205	0-1	218.26	32.01	23.33	37.64	0.09	0.55	0.01	0.03	0.00	0.00	0.00	112.48	0.00	520.69	15.23	15.17	12.66	945.09	4.73
62	C2	205	1-3	162.76	24.11	11.54	25.09	0.03	0.37	0.01	0.03	3.79	0.00	0.00	86.60	0.00	391.30	10.81	10.77	9.75	705.63	3.53
63	C2	255	0-1	28.27	29.43	5.71	96.48	0.45	0.55	0.06	0.01	2.53	0.00	0.00	177.62	0.00	78.56	5.71	5.65	4.63	419.67	2.10
64	C2	255	1-3	44.32	29.42	7.94	354.90	0.14	0.40	0.06	0.01	2.90	0.00	0.00	562.74	0.00	124.08	13.27	13.23	11.81	1,126.91	5.63
65	C2	305	0-1	35.52	50.87	3.38	398.74	0.15	0.14	0.01	0.01	2.59	0.00	0.00	663.86	0.00	89.52	14.48	14.46	12.71	1,244.79	6.22
66	C2	305	1-3	29.01	50.74	12.23	342.63	1.11	0.09	0.03	0.01	1.96	0.00	0.00	522.81	0.00	64.24	13.47	13.46	9.87	1,024.86	5.12
67	C2	345	0-1	4.09	11.31	11.02	10.75	0.19	1.54	0.10	0.01	0.91	0.00	0.00	44.05	0.00	22.22	2.06	1.89	1.22	106.19	0.53
68	C2	345	1-3	27.55	58.60	3.23	268.82	0.05	0.06	0.00	0.01	1.67	0.00	0.00	450.85	0.00	68.42	11.07	11.06	8.78	879.26	4.40
69	C3	105	0-1	22.84	24.30	4.36	10.17	0.01	0.01	0.00	0.00	0.68	0.00	0.00	70.62	0.00	8.71	2.82	2.82	1.36	141.70	0.71
70	C3	105	1-3	19.37	17.80	2.45	5.19	0.02	0.28	0.03	0.00	0.22	0.00	0.00	50.00	0.00	9.80	2.11	2.08	1.02	105.16	0.53
71	C3	155	0-1	56.36	11.24	1.80	1.92	0.04	0.20	0.01	0.01	0.03	0.00	0.00	23.37	0.00	127.85	3.52	3.50	3.04	222.83	1.11
72	C3	155	1-3	19.90	7.57	0.84	1.38	0.02	0.06	0.00	0.01	0.76	0.00	0.00	37.50	0.00	47.01	1.43	1.42	1.62	115.05	0.58
73	C3	205	0-1	20.96	11.30	1.89	1.98	0.20	0.61	0.03	0.01	0.64	0.00	0.00	34.92	0.00	31.69	1.82	1.75	1.26	104.23	0.52
74	C3	205	1-3	45.25	11.22	2.52	1.58	0.04	0.28	0.01	0.01	2.03	0.00	0.00	49.70	0.00	80.99	3.03	3.00	2.60	193.63	0.97
75	C3	255	0-1	6.78	5.36	0.55	1.15	0.30	0.34	0.02	0.00	0.04	0.00	0.00	9.72	0.00	2.17	0.70	0.66	0.20	26.43	0.13
76	C3	255	1-3	25.94	7.80	1.02	1.01	0.06	0.03	0.00	0.01	0.57	0.00	0.00	23.58	0.00	51.75	1.75	1.75	1.49	111.77	0.56
77	C3	305	0-1	2.67	5.21	0.26	0.65	0.12	0.38	0.01	0.00	0.40	0.00	0.00	35.65	0.00	4.58	0.44	0.40	0.69	49.93	0.25
78	C3	305	1-3	2.51	5.65	0.29	0.66	0.20	0.36	0.01	0.00	0.01	0.00	0.00	7.75	0.00	3.51	0.46	0.42	0.20	20.95	0.10
79	C3	350	0-1	3.05	6.40	0.47	0.54	0.38	0.55	0.02	0.00	0.36	0.00	0.00	29.29	0.00	4.34	0.56	0.50	0.58	45.40	0.23
80	C3	350	1-3	3.53	4.39	0.32	0.51	0.23	0.24	0.01	0.00	1.34	0.00	0.00	29.31	0.00	4.42	0.44	0.41	0.64	44.30	0.22

Table (L4): The anion and cation content of drilled samples from the Palace Tomb, locations (C2 and C3). Fourth fieldwork visit: April 2005.

Appendix L: The anion and cation content of the drilled samples. Fourth fieldwork visit: April 2005.

Sample number	Location	Height (cm)	Depth (cm)	Ca (ppm)	Na (ppm)	Mg (ppm)	K (ppm)	Fe (ppm)	Al (ppm)	Ti (ppm)	Zn (ppm)	F (ppm)	Br (ppm)	Cl (ppm)	NO_3 (ppm)	PO_4 (ppm)	SO_4 (ppm)	cation charge with AL	Cation charge without AL	Anion Charge	Sum of cations & anions (ppm)	Soluble salt content in the sample (%)
81	H	25	0-1	18.12	5.10	2.53	1.04	0.37	9.72	0.17	0.24	0.05	0.00	0.23	0.25	0.00	0.38	2.47	1.39	0.02	38.20	0.19
82	H	25	1-3	9.95	6.29	1.01	0.58	0.23	4.08	0.07	0.08	0.04	0.00	0.21	0.23	0.00	0.34	1.33	0.88	0.02	23.11	0.12
83	H	75	0-1	70.04	7.82	2.58	2.01	0.01	0.00	0.00	0.01	0.04	0.00	0.38	0.49	0.00	5.20	4.10	4.10	0.13	88.58	0.44
84	H	75	1-3	116.34	6.92	2.65	1.06	0.03	0.13	0.00	0.02	0.06	0.00	0.41	0.40	0.00	7.83	6.37	6.36	0.18	135.85	0.68
85	H	125	0-1	6.07	4.76	0.75	0.93	0.23	1.31	0.06	0.01	0.05	0.00	0.21	0.27	0.00	0.16	0.75	0.60	0.02	14.81	0.07
86	H	125	1-3	4.44	5.72	0.49	0.66	0.05	0.61	0.03	0.01	0.03	0.00	0.19	0.18	0.00	0.17	0.60	0.53	0.01	12.58	0.06
87	H	155	0-1	4.60	5.74	0.55	0.86	0.18	0.57	0.05	0.01	0.03	0.00	0.19	0.20	0.00	0.16	0.62	0.56	0.01	13.14	0.07
88	H	155	1-3	3.51	5.50	0.42	0.50	0.07	0.62	0.04	0.01	0.04	0.00	0.17	0.41	0.00	0.14	0.53	0.46	0.02	11.43	0.06
89	H	200	0-1	44.06	224.87	0.99	2.17	0.02	0.28	0.00	0.01	0.00	0.00	16.29	0.51	0.00	3.49	12.15	12.12	0.54	292.69	1.46
90	H	200	1-3	43.38	51.01	0.98	1.84	0.01	0.13	0.00	0.02	0.00	0.00	3.48	0.38	0.00	3.37	4.53	4.52	0.17	104.60	0.52
91	H	250	0-1	19.92	11.38	4.72	2.99	0.12	0.16	0.02	0.00	0.04	0.00	1.48	1.29	0.00	0.17	1.98	1.96	0.07	42.29	0.21
92	H	250	1-3	16.10	9.37	2.72	1.77	0.44	0.56	0.19	0.00	0.00	0.00	1.07	0.77	0.00	0.16	1.56	1.50	0.05	33.15	0.17
93	H	300	0-1	3.43	4.65	0.27	0.78	0.24	3.42	0.18	0.00	0.04	0.00	0.20	0.18	0.00	0.11	0.81	0.43	0.01	13.50	0.07
94	H	300	1-3	1.22	5.24	0.16	0.61	0.30	4.45	0.30	0.01	0.03	0.00	0.19	0.44	0.00	0.17	0.83	0.34	0.02	13.12	0.07
95	H	500	0-1	7.49	12.40	1.16	2.79	0.04	0.45	0.02	0.01	0.00	0.00	0.87	0.43	0.00	0.37	1.13	1.08	0.04	26.03	0.13
96	H	500	1-3	3.27	9.09	1.33	3.04	0.02	0.13	0.01	0.11	0.08	0.00	0.83	0.51	0.00	0.13	0.76	0.75	0.04	18.55	0.09
97	H	550	0-1	15.25	13.24	2.95	7.75	0.07	0.17	0.01	0.00	0.01	0.00	1.30	1.32	0.00	0.46	1.80	1.78	0.07	42.53	0.21
98	H	550	1-3	14.65	13.39	3.01	8.15	0.04	0.10	0.00	0.00	0.03	0.00	1.20	1.06	0.00	0.31	1.78	1.77	0.06	41.94	0.21

Table (L5): The anion and cation content of drilled samples from the Corinthian Tomb, location (H).
Fourth fieldwork visit: April 2005.

Appendix L: The anion and cation content of the drilled samples. Fourth fieldwork visit: April 2005.

Sample Number	Location	Height (cm)	Depth (cm)	Ca (ppm)	Na (ppm)	Mg (ppm)	K (ppm)	Fe (ppm)	Al (ppm)	Tl (ppm)	Zn (ppm)	F (ppm)	Br (ppm)	Cl (ppm)	NO_3 (ppm)	PO_4 (ppm)	SO_4 (ppm)	Cation charge with Al	Cation charge without Al	Anion charge	Sum of cations & anions (ppm)	Soluble Salt Content in the sample (%) of dry weight
99	D1	5	0-1	8.51	12.32	1.54	0.82	0.22	8.63	0.30	0.01	0.04	0.00	0.50	0.28	0.00	0.21	2.08	1.12	0.03	33.38	0.17
100	D1	5	1-3	2.77	7.14	0.27	0.48	0.01	0.14	0.01	0.00	0.10	0.00	0.46	0.90	0.00	0.14	0.50	0.48	0.04	12.42	0.06
101	D1	55	0-1	39.51	7.54	3.46	1.00	0.24	2.08	0.11	0.01	0.03	0.00	0.32	0.48	0.00	3.26	2.85	2.62	0.09	58.04	0.29
102	D1	55	1-3	6.21	7.05	0.51	0.42	0.06	1.02	0.03	0.01	0.00	0.00	0.21	0.21	0.00	0.54	0.79	0.68	0.02	16.27	0.08
103	D1	105	0-1	6.77	6.76	1.03	0.78	0.06	0.39	0.08	0.00	0.05	0.00	0.26	0.95	0.00	0.34	0.78	0.74	0.03	17.47	0.09
104	D1	105	1-3	3.07	8.07	0.32	0.65	0.05	0.55	0.02	0.00	0.12	0.00	0.37	1.13	0.00	0.22	0.61	0.55	0.04	14.57	0.07
105	D1	155	0-1	5.49	11.12	0.69	0.74	0.06	1.01	0.02	0.00	0.09	0.00	0.53	0.77	0.00	0.36	0.95	0.84	0.04	20.88	0.10
106	D1	155	1-3	3.91	8.01	0.24	0.38	0.02	0.50	0.01	0.00	0.09	0.00	0.45	0.75	0.00	0.14	0.63	0.57	0.03	14.50	0.07
107	D1	205	0-1	5.82	10.24	0.51	0.83	0.08	0.97	0.04	0.01	0.05	0.00	0.30	0.95	0.00	0.41	0.91	0.80	0.03	20.21	0.10
108	D1	205	1-3	6.50	8.00	0.34	0.68	0.09	1.38	0.04	0.00	0.07	0.00	0.30	0.39	0.00	0.46	0.88	0.73	0.03	18.25	0.09
109	D1	255	0-1	6.69	10.65	0.76	1.23	0.28	4.13	0.10	0.03	0.09	0.00	0.42	0.96	0.00	0.46	1.36	0.90	0.04	25.80	0.13
110	D1	255	1-3	2.36	5.82	0.16	0.47	0.08	1.66	0.05	0.02	0.02	0.00	0.20	1.04	0.00	0.15	0.59	0.41	0.03	12.03	0.06
111	D1	305	0-1	4.39	7.63	0.80	1.44	0.55	1.00	0.07	0.01	0.01	0.00	0.25	0.22	0.00	0.21	0.79	0.68	0.02	16.58	0.08
112	D2	5	0-1	10.70	16.95	0.80	4.16	0.13	0.31	0.03	0.00	0.01	0.00	1.00	0.84	0.00	0.82	1.48	1.45	0.06	35.75	0.18
113	D2	5	1-3	3.59	7.71	0.41	1.43	0.35	0.85	0.04	0.01	0.01	0.00	0.39	1.15	0.00	0.32	0.69	0.60	0.04	16.26	0.08
114	D2	55	0-1	95.06	9.18	3.00	1.67	0.02	0.12	0.01	0.02	0.02	0.00	0.57	0.98	0.00	7.39	5.45	5.44	0.19	118.04	0.59
115	D2	55	1-3	13.90	8.06	0.84	1.09	0.01	0.13	0.01	0.00	0.12	0.00	0.51	0.98	0.00	1.17	1.16	1.15	0.06	26.82	0.13
116	D2	105	0-1	149.89	107.30	14.82	10.73	0.02	0.00	0.00	0.03	0.02	0.00	6.28	3.92	0.00	0.00	13.64	13.64	0.24	293.01	1.47
117	D2	105	1-3	123.36	19.39	6.97	2.42	0.02	0.07	0.00	0.02	0.01	0.00	1.42	1.24	0.00	0.00	7.64	7.63	0.06	154.92	0.77
118	D2	155	0-1	47.95	8.91	3.86	1.95	0.02	0.12	0.01	0.01	0.12	0.00	0.83	1.07	0.00	3.69	3.16	3.15	0.12	68.54	0.34
119	D2	155	1-3	37.04	49.62	1.97	18.31	0.01	0.04	0.00	0.01	0.03	0.00	3.59	0.54	0.00	2.96	4.64	4.64	0.17	114.12	0.57
120	D2	205	0-1	38.36	31.46	2.86	12.57	0.08	0.30	0.02	0.01	0.02	0.00	1.89	0.86	0.00	2.77	3.88	3.85	0.13	91.20	0.46
121	D2	205	1-3	8.35	6.05	0.88	0.59	0.02	0.20	0.02	0.01	0.02	0.00	0.33	0.86	0.00	0.55	0.79	0.77	0.04	17.88	0.09
122	D2	255	0-1	61.87	14.00	1.90	3.71	0.08	0.14	0.02	0.01	0.01	0.00	0.91	1.11	0.00	4.77	3.97	3.95	0.14	88.53	0.44
123	D2	255	1-3	6.47	5.55	0.93	0.49	0.03	0.18	0.01	0.01	0.01	0	0.35	0.79	0	0.56	0.67	0.65	0.03	15.38	0.08
124	D2	305	0-1	35.64	11.54	1.87	3.56	0.05	0.16	0.02	0.01	0	0	0.88	1.24	0	3.99	2.55	2.53	0.13	58.96	0.29

Table (L6): The anion and cation content of drilled samples from the Deir Tomb, locations (D1 and D2). Fourth fieldwork visit April 2005.

Appendix Lb: The anion and cation content and distribution in the drilled samples. Fourth fieldwork visit: April 2005.

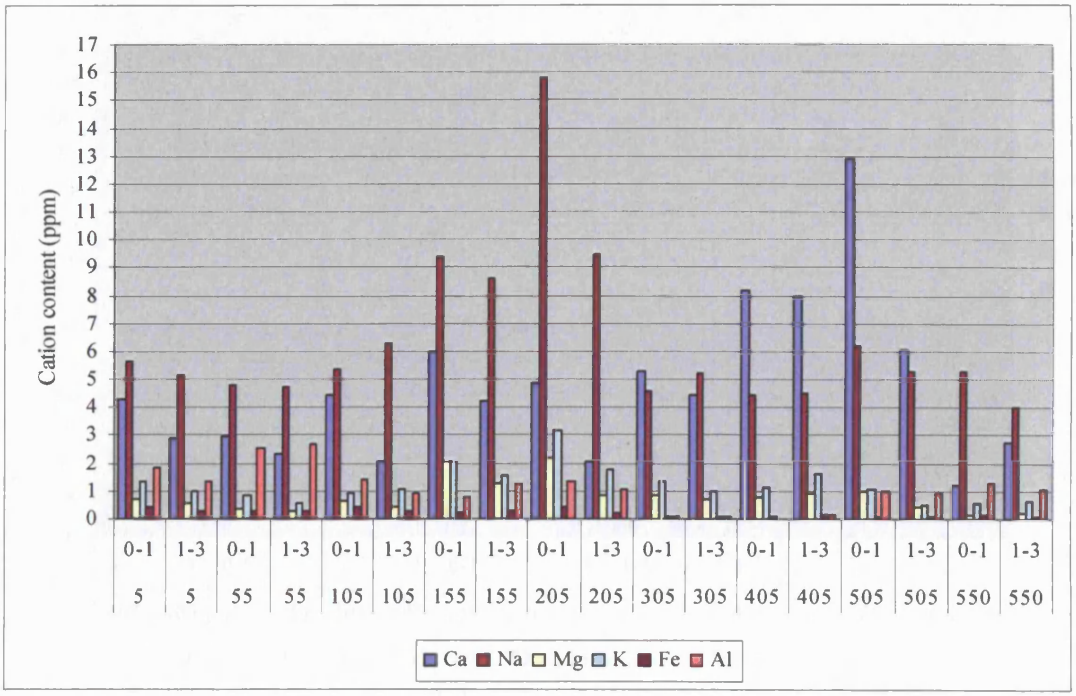

Figure (1Lb): The main cation content of drilled samples from the Bab al Siq Triclinium Tomb, location (T1) (Depth intervals: 0-1 and 1-3 cm).
Fourth fieldwork visit: April 2005.

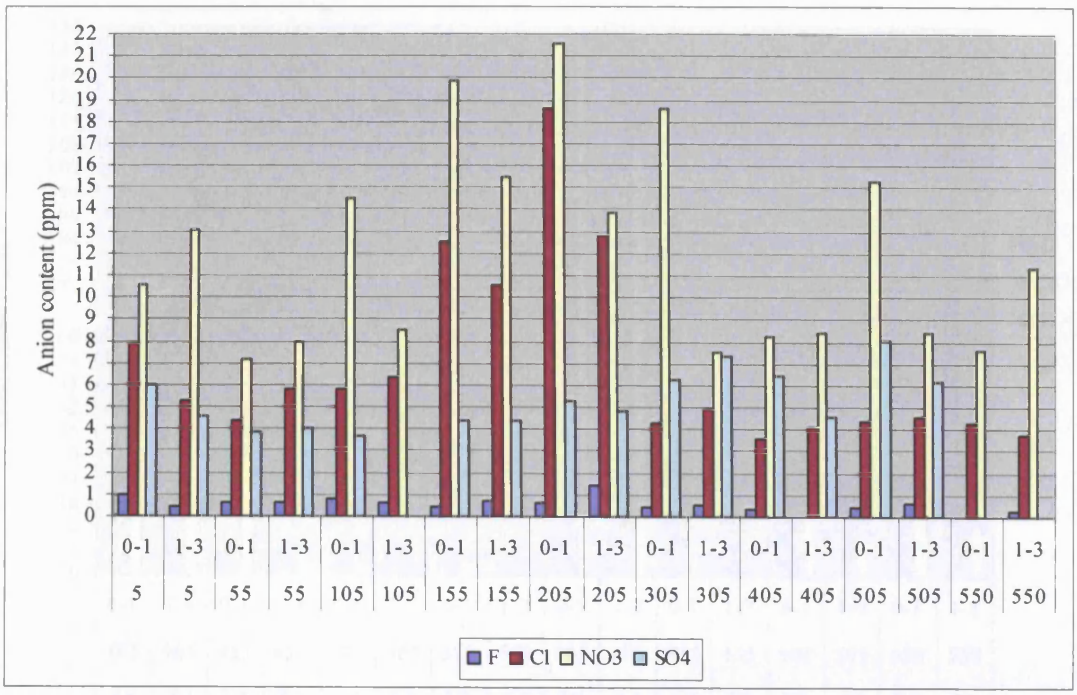

Figure (2Lb): The main anion content of drilled samples from the Bab al Siq Triclinium Tomb, location (T1) (Depth intervals: 0-1 and 1-3 cm).
Fourth fieldwork visit: April 2005.

Appendix Lb: The anion and cation content and distribution in the drilled samples. Fourth fieldwork visit: April 2005.

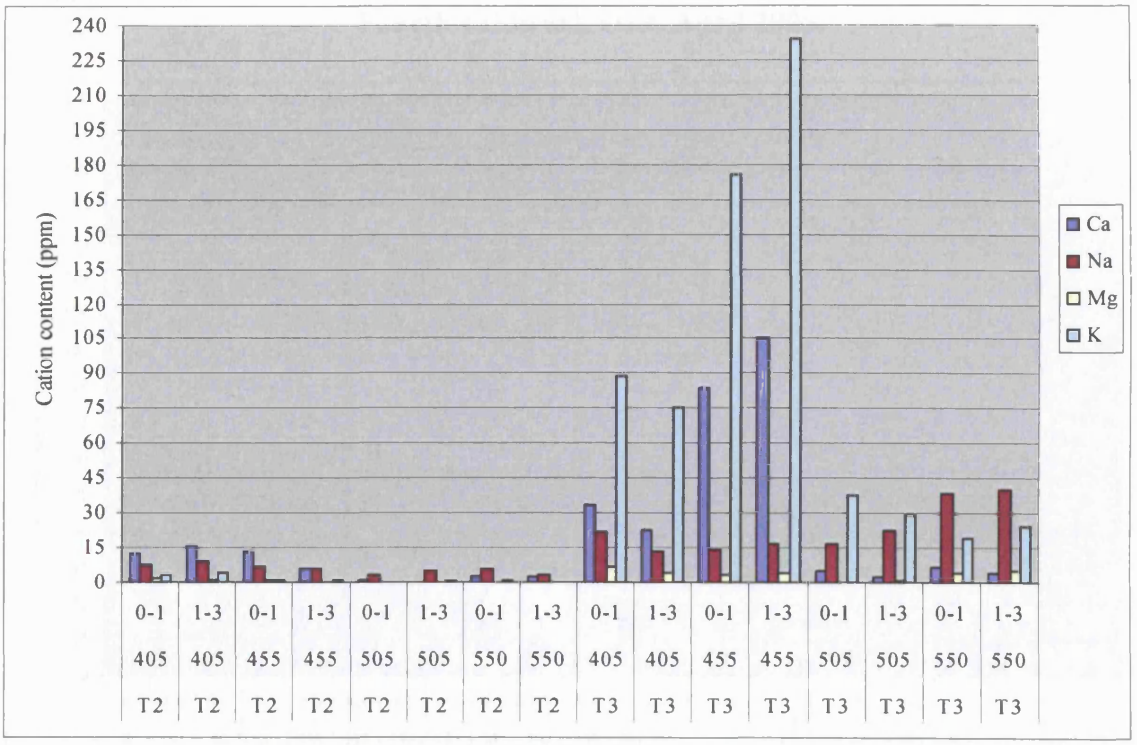

Figure (3Lb): The main cation content of drilled samples from the Bab al Siq Triclinium Tomb, locations (T2 and T3) (Depth intervals: 0-1 and 1-3 cm). Fourth fieldwork visit: April 2005.

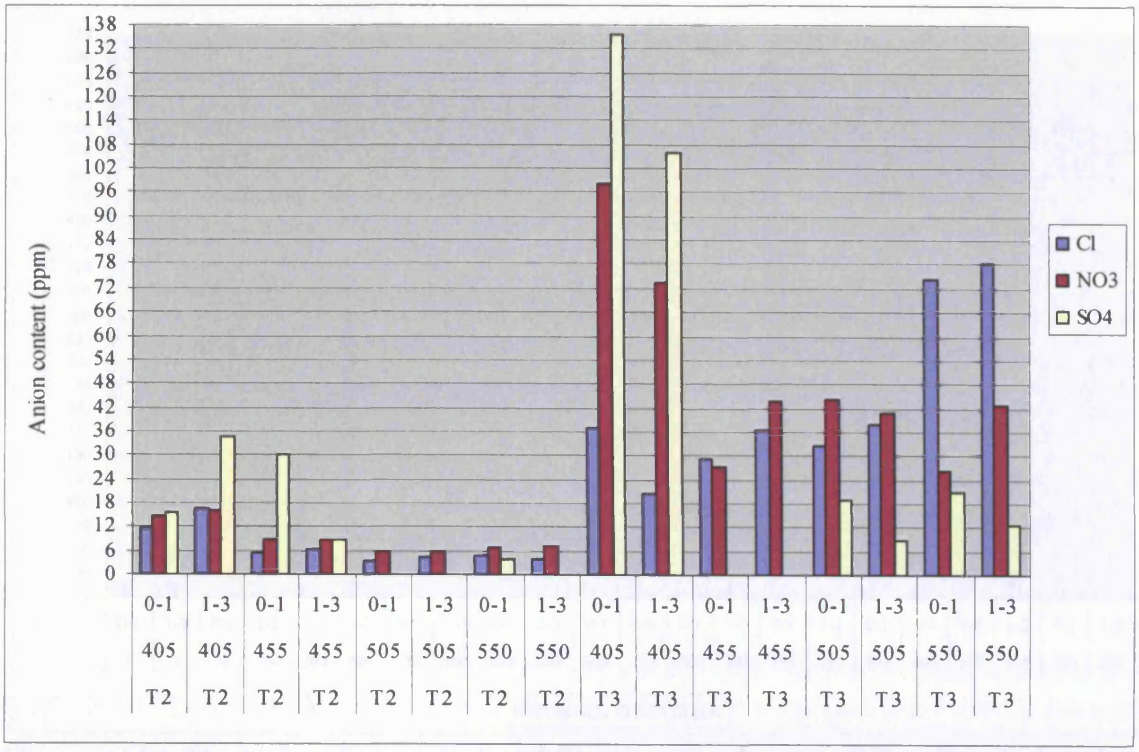

Figure (4Lb): The main anion content of drilled samples from the Bab al Siq Triclinium Tomb, locations (T2 and T3) (Depth intervals: 0-1 and 1-3 cm). Fourth fieldwork visit: April 2005.

Appendix Lb: The anion and cation content and distribution in the drilled samples. Fourth fieldwork visit: April 2005.

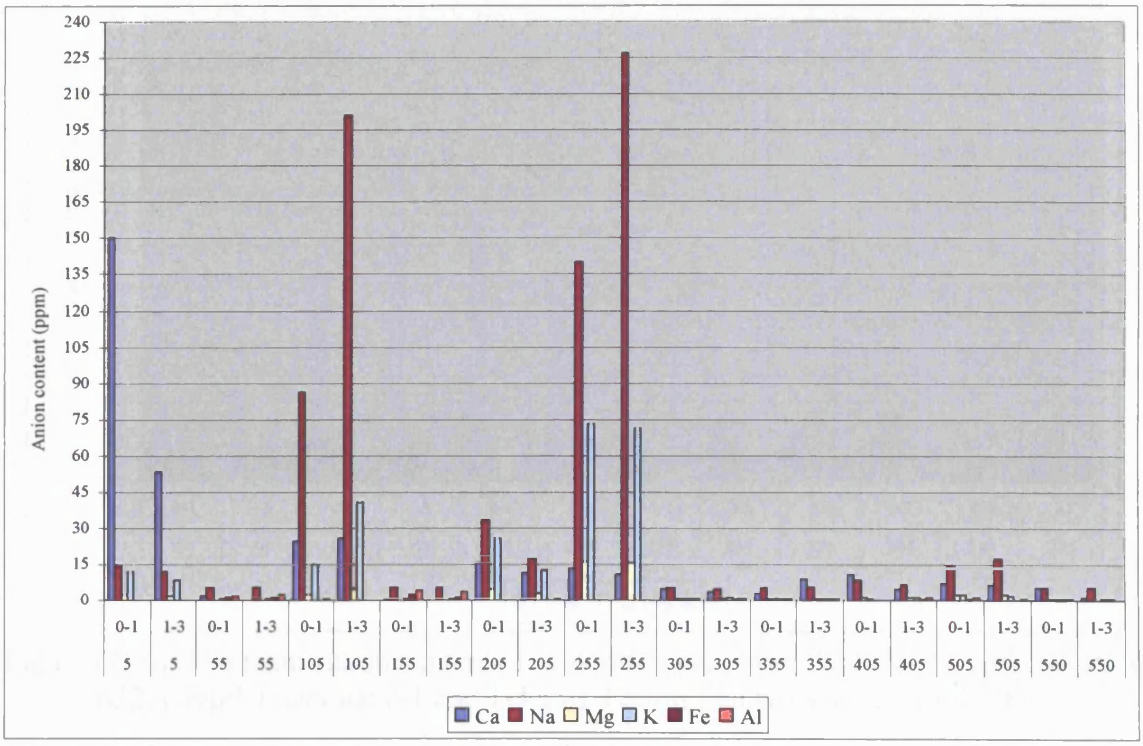

Figure (5Lb): The main cation content of drilled samples from the Palace Tomb, location (C1) (Depth intervals: 0-1 and 1-3 cm). Fourth fieldwork visit: April 2005.

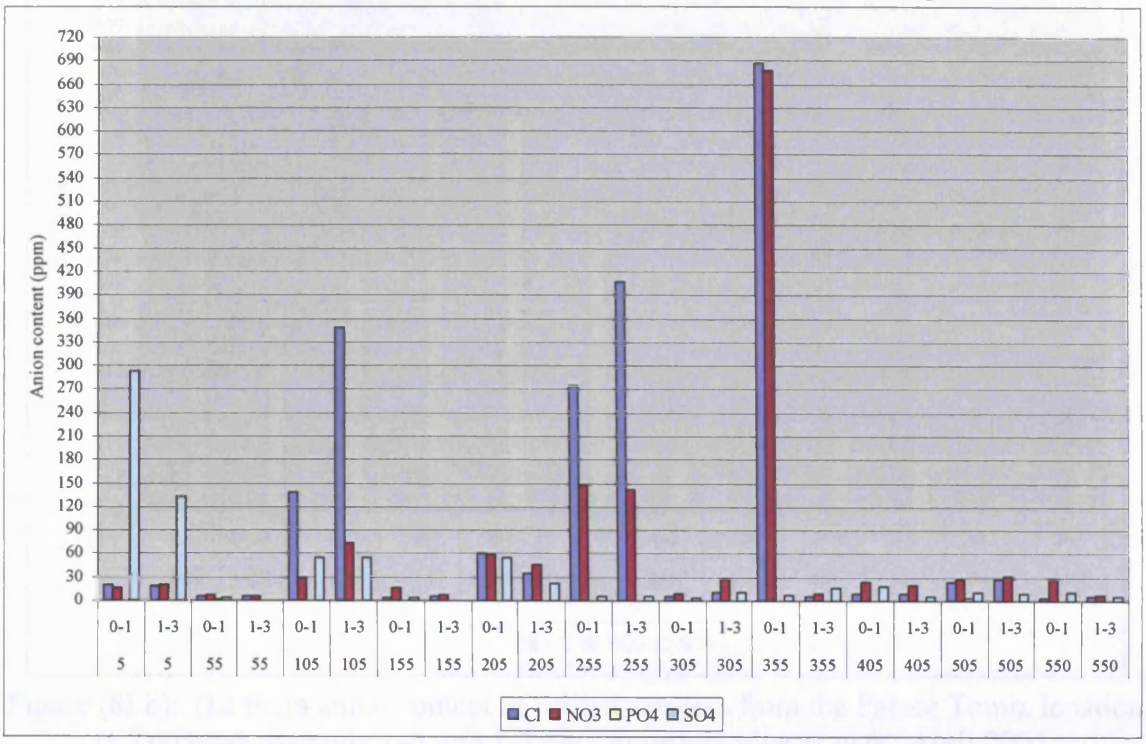

Figure (6Lb): The main anion content of drilled samples from the Palace Tomb, location (C1) (Depth intervals: 0-1 and 1-3 cm). Fourth fieldwork visit: April 2005.

Appendix Lb: The anion and cation content and distribution in the drilled samples. Fourth fieldwork visit: April 2005.

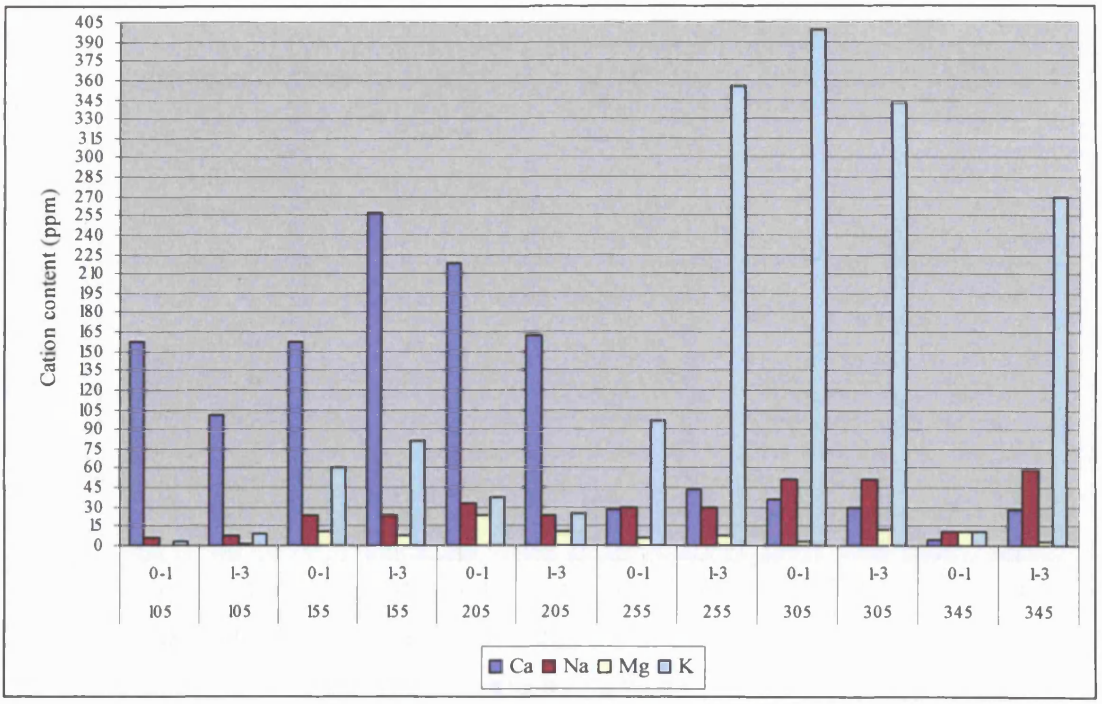

Figure (7Lb): The main cation content of drilled samples from the Palace Tomb, location (C2) (Depth intervals: 0-1 and 1-3 cm). Fourth fieldwork visit: April 2005.

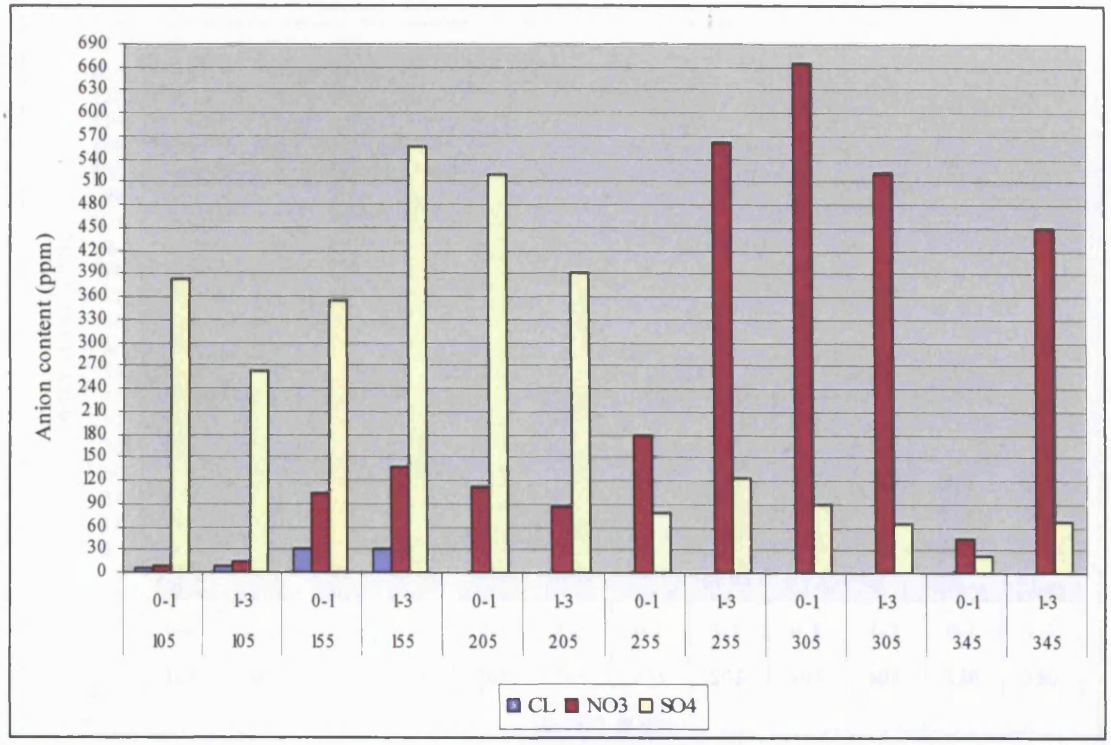

Figure (8Lb): The main anion content of drilled samples from the Palace Tomb, location (C2) (Depth intervals: 0-1 and 1-3 cm). Fourth fieldwork visit: April 2005.

Appendix Lb: The anion and cation content and distribution in the drilled samples. Fourth fieldwork visit: April 2005.

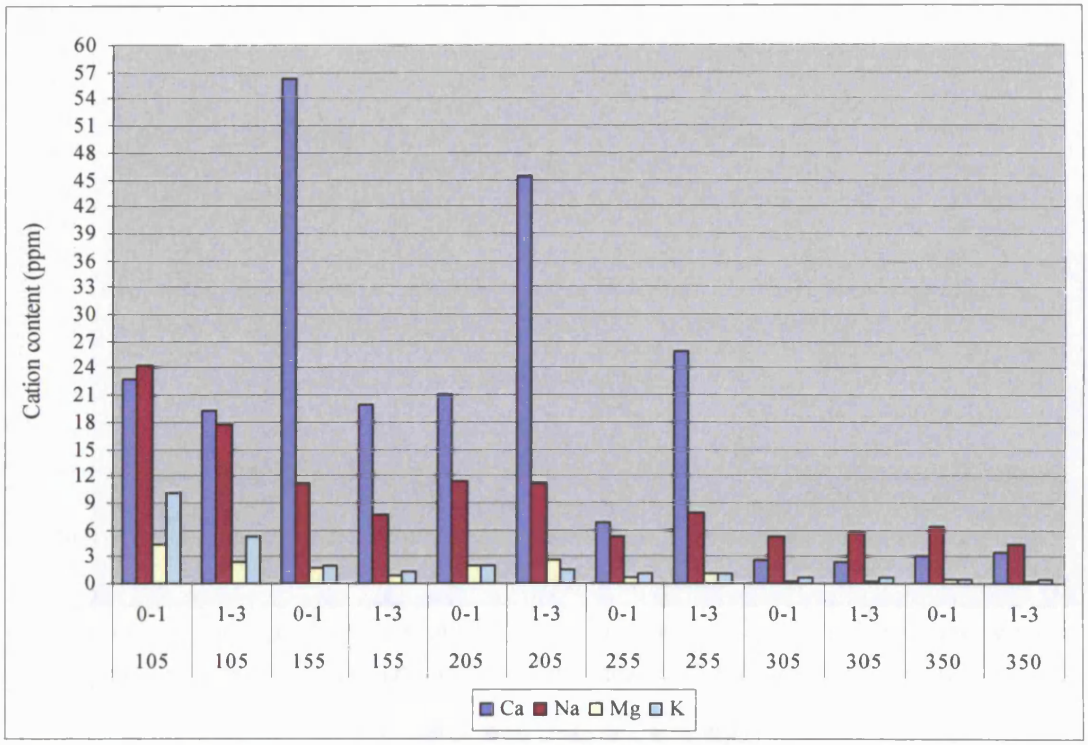

Figure (9Lb): The main cation content of drilled samples from the Palace Tomb, location (C3) (Depth intervals: 0-1 and 1-3 cm). Fourth fieldwork visit: April 2005.

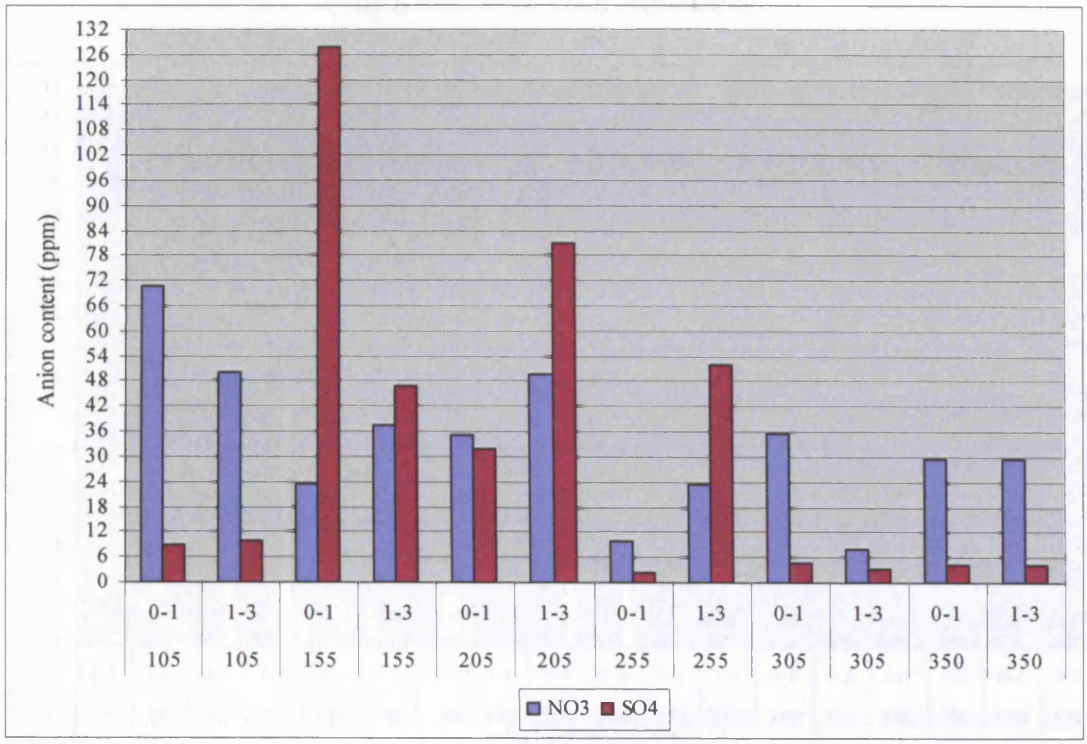

Figure (10Lb): The main anion content of drilled samples from the Palace Tomb, location (C3) (Depth intervals: 0-1 and 1-3 cm). Fourth fieldwork visit: April 2005.

Appendix Lb: The anion and cation content and distribution in the drilled samples. Fourth fieldwork visit: April 2005.

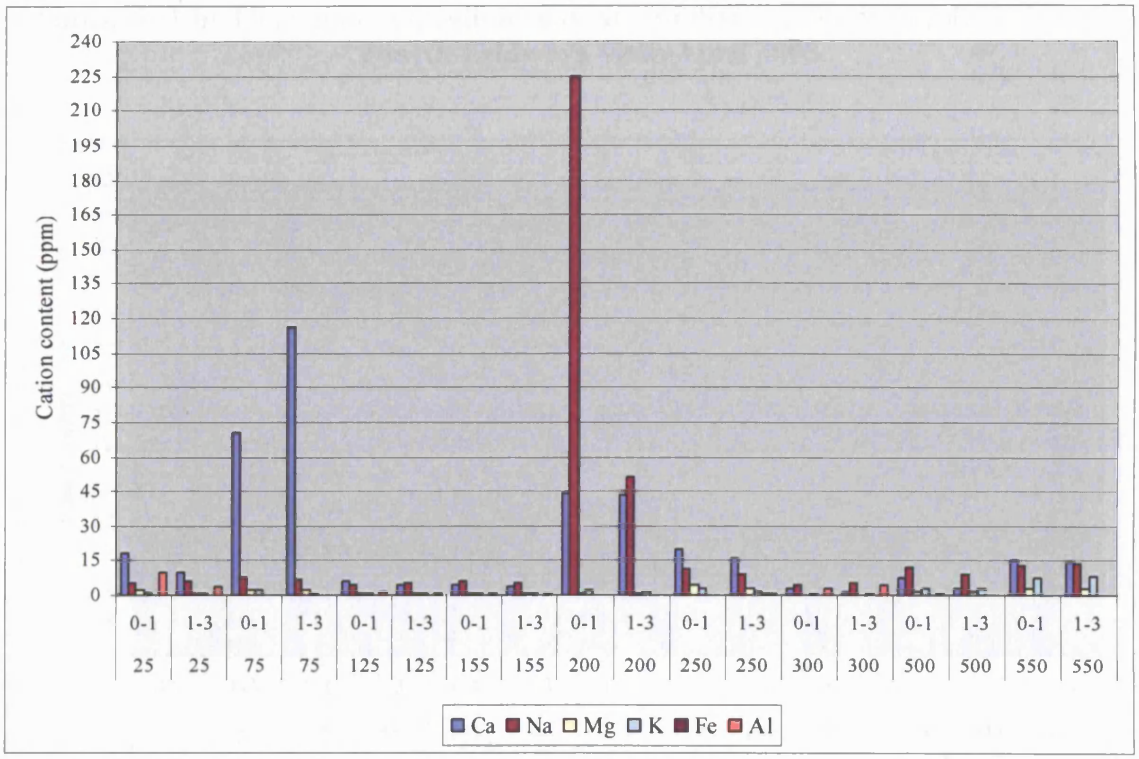

Figure (11Lb): The main cation content of drilled samples from the Corinthian Tomb, location (H) (Depth intervals: 0-1 and 1-3 cm).
Fourth fieldwork visit: April 2005.

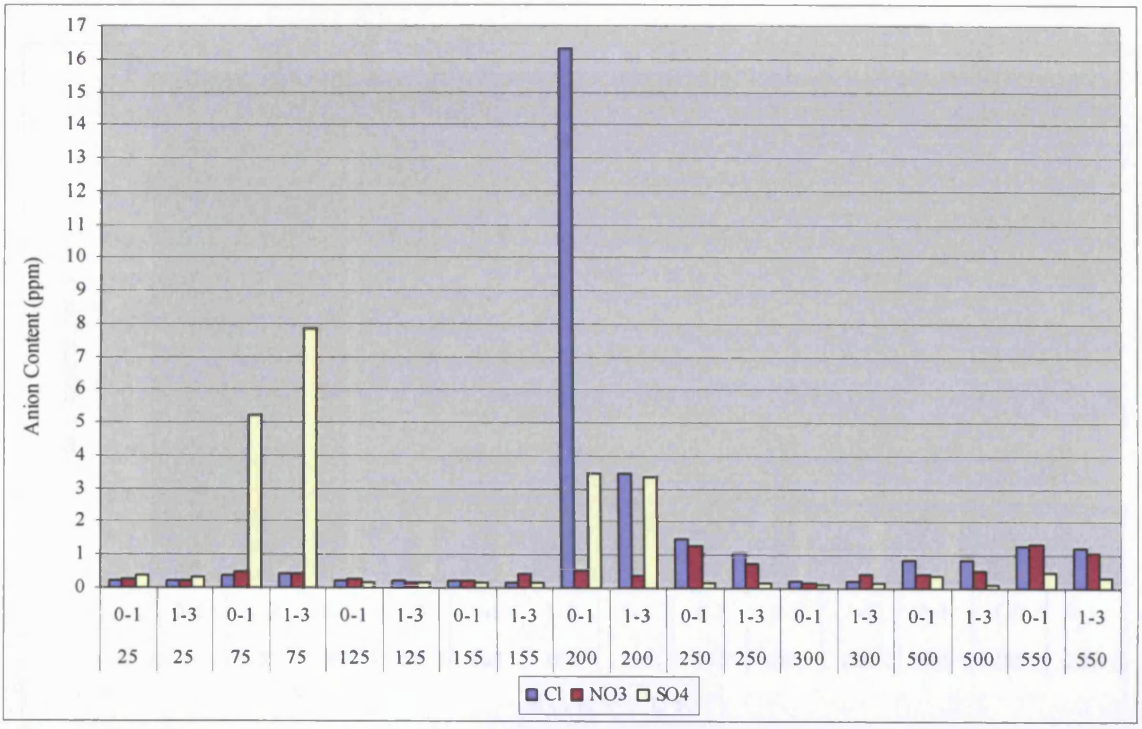

Figure (12 Lb): The main anion content of drilled samples from the Corinthian Tomb, location (H) (Depth intervals: 0-1 and 1-3 cm).
Fourth fieldwork visit: April 2005.

Appendix Lb: The anion and cation content and distribution in the drilled samples. Fourth fieldwork visit: April 2005.

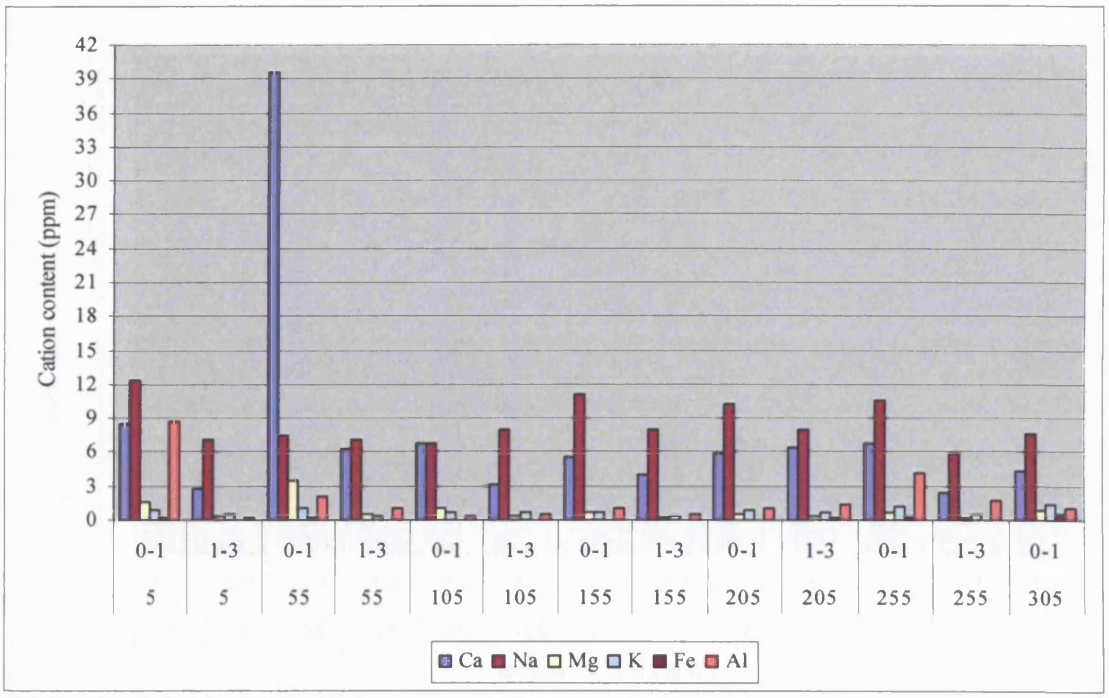

Figure (13Lb): The main cation content of drilled samples from the Deir Tomb, location (D1) (Depth intervals: 0-1 and 1-3 cm). Fourth fieldwork visit: April 2005.

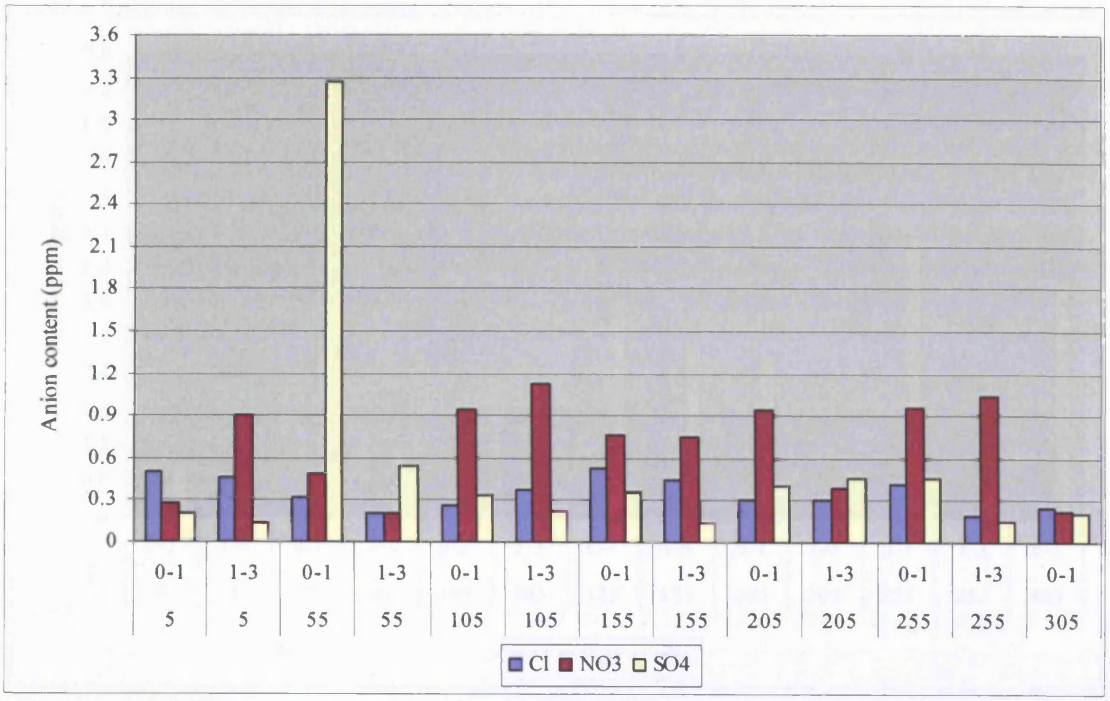

Figure (14Lb): The main anion content of drilled samples from the Deir Tomb, location (D1) (Depth intervals: 0-1 and 1-3 cm). Fourth fieldwork visit: April 2005.

Appendix Lb: The anion and cation content and distribution in the drilled samples. Fourth fieldwork visit: April 2005.

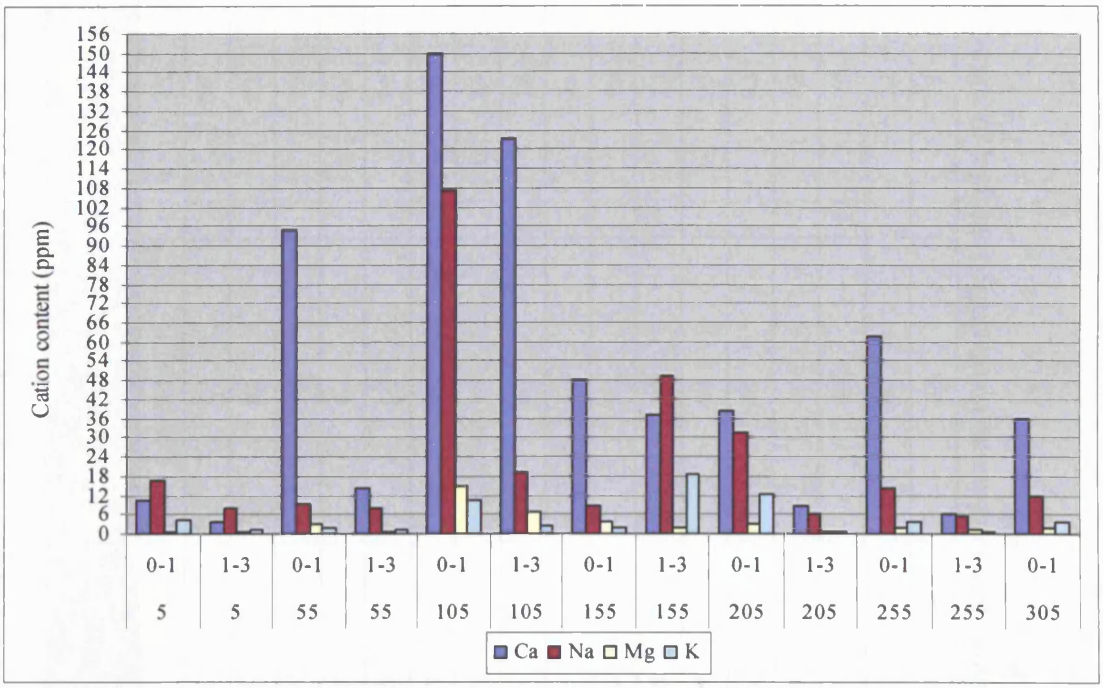

Figure (15Lb): The main cation content of drilled samples from the Deir Tomb, location (D2) (Depth intervals: 0-1 and 1-3 cm). Fourth fieldwork visit: April 2005.

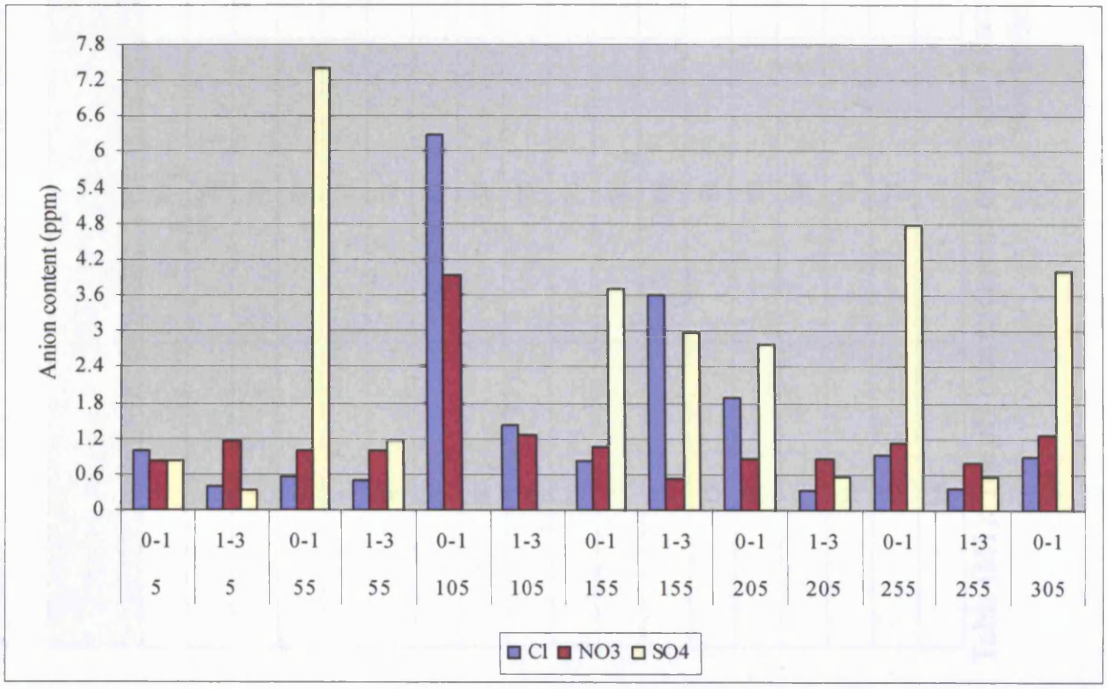

Figure (16Lb): The main anion content of drilled samples from the Deir Tomb, location (D2) (Depth intervals: 0-1 and 1-3 cm). Fourth fieldwork visit: April 2005.

Appendix M: The pH measurements of the salt solution from the drilled samples. Fourth fieldwork visit: April 2005.

Sample Number	Location	Height (cm)	Depth (cm)	pH
1	T1	5	0-1	7.4
2	T1	5	1-3	7.1
3	T1	55	0-1	7.3
4	T1	55	1-3	7.2
5	T1	105	0-1	7.1
6	T1	105	1-3	7.2
7	T1	155	0-1	7.3
8	T1	155	1-3	7.4
9	T1	205	0-1	7.3
10	T1	205	1-3	7.1
11	T1	305	0-1	7.0
12	T1	305	1-3	7.1
13	T1	405	0-1	7.3
14	T1	405	1-3	7.3
15	T1	505	0-1	7.5
16	T1	505	1-3	7.2
17	T1	550	0-1	7.2
18	T1	550	1-3	7.1

Table (M1): The pH measurements of the salt solution from Bab al Siq Triclinium Tomb drilled sample, location (T1). Fourth fieldwork visit: April 2005.

Appendix M: The pH measurements of the salt solution from the drilled samples. Fourth fieldwork visit: April 2005.

Sample Number	Location	Height (cm)	Depth (cm)	pH
19	T2	405	0-1	7.2
20	T2	405	1-3	7.1
21	T2	455	0-1	7.2
22	T2	455	1-3	7.2
23	T2	505	0-1	7.1
24	T2	505	1-3	7.1
25	T2	550	0-1	7.1
26	T2	550	1-3	7.1
27	T3	405	0-1	7.1
28	T3	405	1-3	6.8
29	T3	455	0-1	7.0
30	T3	455	1-3	7.7
31	T3	505	0-1	7.8
32	T3	505	1-3	7.0
33	T3	550	0-1	7.0
34	T3	550	1-3	6.9

Table (M2): The pH measurements of the salt solution from Bab al Siq Triclinium Tomb drilled sample, locations (T2 and T3). Fourth fieldwork visit: April 2005.

Appendix M: The pH measurements of the salt solution from the drilled samples. Fourth fieldwork visit: April 2005.

Sample Number	Location	Height (cm)	Depth (cm)	pH
35	H	25	0-1	8.1
36	H	25	1-3	8.0
37	H	75	0-1	8.5
38	H	75	1-3	8.2
39	H	125	0-1	7.7
40	H	125	1-3	7.8
41	H	155	0-1	7.9
42	H	155	1-3	8.0
43	H	200	0-1	8.6
44	H	200	0-1	8.2
45	H	250	0-1	7.7
46	H	250	1-3	8.0
47	H	300	0-1	8.0
48	H	300	1-3	7.8
49	H	500	0-1	8.2
50	H	500	1-3	8.1
51	H	550	0-1	8.1
52	H	550	1-3	8.3

Table (M3): The pH measurements of the salt solution from the Corinthian Tomb drilled sample, location (H). Fourth fieldwork visit: April 2005.

Appendix M: The pH measurements of the salt solution from the drilled samples. Fourth fieldwork visit: April 2005.

Sample Number	Location	Height (cm)	Depth (cm)	pH
53	C1	5	0-1	7.3
54	C1	5	1-3	7.0
55	C1	55	0-1	7.1
56	C1	55	1-3	7.2
57	C1	105	0-1	7.0
58	C1	105	1-3	6.8
59	C1	155	0-1	7.4
60	C1	155	1-3	7.3
61	C1	205	0-1	6.9
62	C1	205	1-3	6.8
63	C1	255	0-1	6.9
64	C1	255	1-3	7.0
65	C1	305	0-1	6.6
66	C1	305	1-3	6.0
67	C1	355	0-1	7.2
68	C1	355	1-3	7.1
69	C1	405	0-1	7.0
70	C1	405	1-3	7.0
71	C1	505	0-1	6.9
72	C1	505	1-3	6.8
73	C1	550	0-1	6.7
74	C1	550	1-3	6.9

Table (M4): The pH measurements of the salt solution from the Palace Tomb drilled sample, location (C1). Fourth fieldwork visit: April 2005.

Appendix M: The pH measurements of the salt solution from the drilled samples. Fourth fieldwork visit: April 2005.

Sample Number	Location	Height (cm)	Depth (cm)	pH
75	C2	105	0-1	8.2
76	C2	105	1-3	7.9
77	C2	155	0-1	7.5
78	C2	155	1-3	7.6
79	C2	205	0-1	7.4
80	C2	205	1-3	7.1
81	C2	255	0-1	7.3
82	C2	255	1-3	7.2
83	C2	305	0-1	7.4
84	C2	305	1-3	7.6
85	C2	345	0-1	7.5
86	C2	345	1-3	7.3
87	C3	105	0-1	7.6
88	C3	105	1-3	7.7
89	C3	155	0-1	7.2
90	C3	155	1-3	6.8
91	C3	205	0-1	7.3
92	C3	205	1-3	7.2
93	C3	255	0-1	7.6
94	C3	255	1-3	7.3
95	C3	305	0-1	6.7
96	C3	305	1-3	7.3
97	C3	350	0-1	6.9
98	C3	350	1-3	6.8

Table (M5): The pH measurements of the salt solution from the Palace Tomb drilled sample, locations (C2 and C3). Fourth fieldwork visit: April 2005.

Appendix M: The pH measurements of the salt solution from the drilled samples. Fourth fieldwork visit: April 2005.

Sample Number	Location	Height (cm)	Depth (cm)	pH
99	D1	5	0-1	8.3
100	D1	5	1-3	7.8
101	D1	55	0-1	8.5
102	D1	55	1-3	8.3
103	D1	105	0-1	8.6
104	D1	105	1-3	8.3
105	D1	155	0-1	8.7
106	D1	155	1-3	8.4
107	D1	205	0-1	8.5
108	D1	205	1-3	8.5
109	D1	255	0-1	8.7
110	D1	255	1-3	8.4
111	D1	305	0-1	8.5
112	D2	5	0-1	8.8
113	D2	5	1-3	8.5
114	D2	55	0-1	8.5
115	D2	55	1-3	8.9
116	D2	105	0-1	8.8
117	D2	105	1-3	8.5
118	D2	155	0-1	8.4
119	D2	155	1-3	8.4
120	D2	205	0-1	8.6
121	D2	205	1-3	8.5
122	D2	255	0-1	8.6
123	D2	255	1-3	8.6
124	D2	305	0-1	8.4

Table (M6): The pH measurements of the salt solution from the Deir Tomb drilled sample, locations (D and D2). Fourth fieldwork visit: April 2005.

Appendix N: Thermodynamic analysis of the salt content in samples from the Palace Tomb (C1) using ECOS.

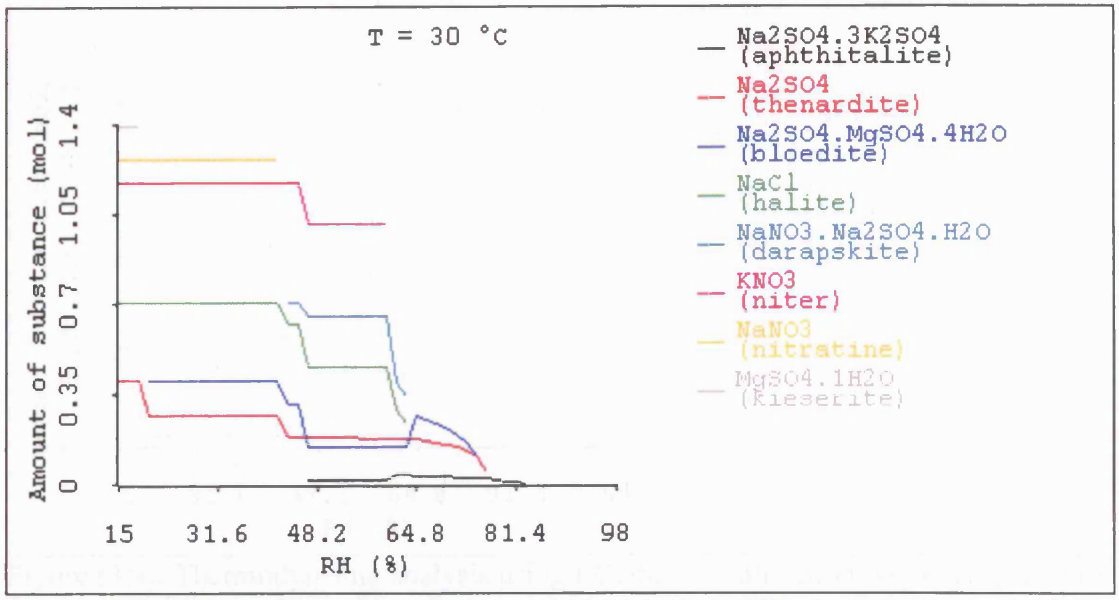

Figure (1N): Thermodynamic analysis using ECOS. Crystallisation sequence of soluble salts: relative humidity against amount of substance (mol). Sampling height: (5 cm) sampling depth interval: (1-3 cm). First fieldwork visit: August 2003.

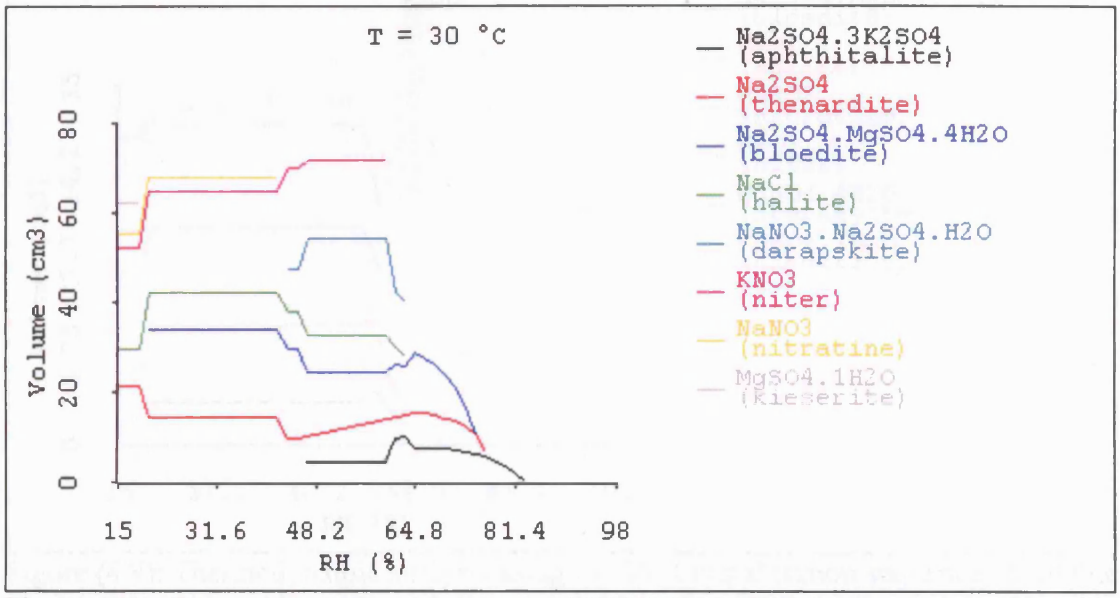

Figure (2N): Thermodynamic analysis using ECOS. Crystallisation sequence of soluble salts: relative humidity against volume of substance (cm^3). Sampling height: (5 cm) sampling depth interval: (1-3 cm). First fieldwork visit: August 2003.

Appendix N: Thermodynamic analysis of the salt content in samples from the Palace Tomb (C1) using ECOS.

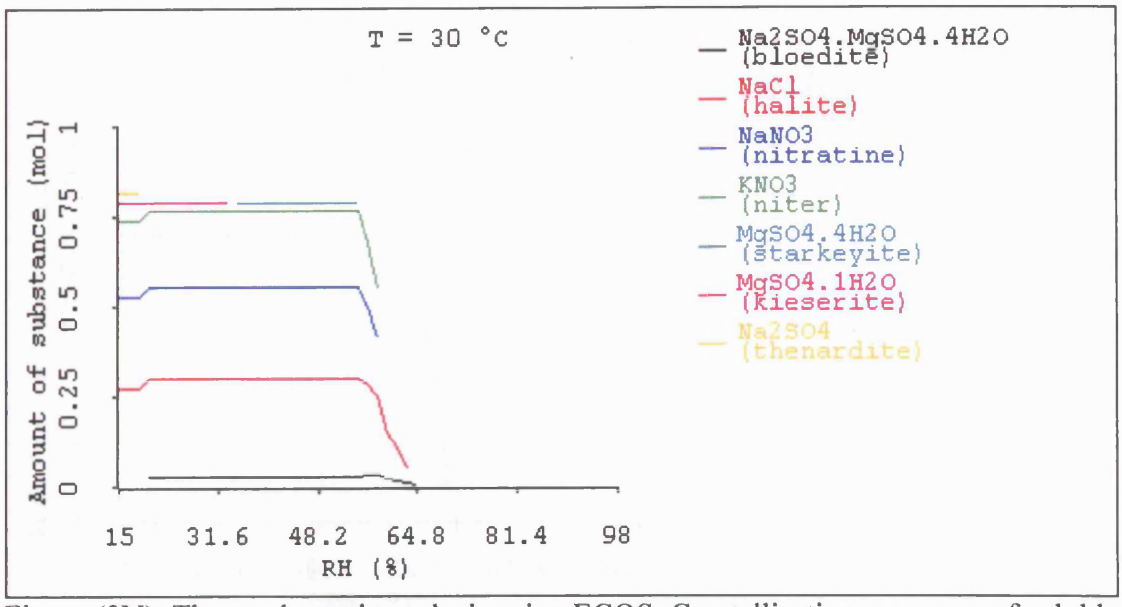

Figure (3N): Thermodynamic analysis using ECOS. Crystallisation sequence of soluble salts: relative humidity against amount of substance (mol). Sampling height: (5 cm) sampling depth interval: (3-5 cm). First fieldwork visit: August 2003.

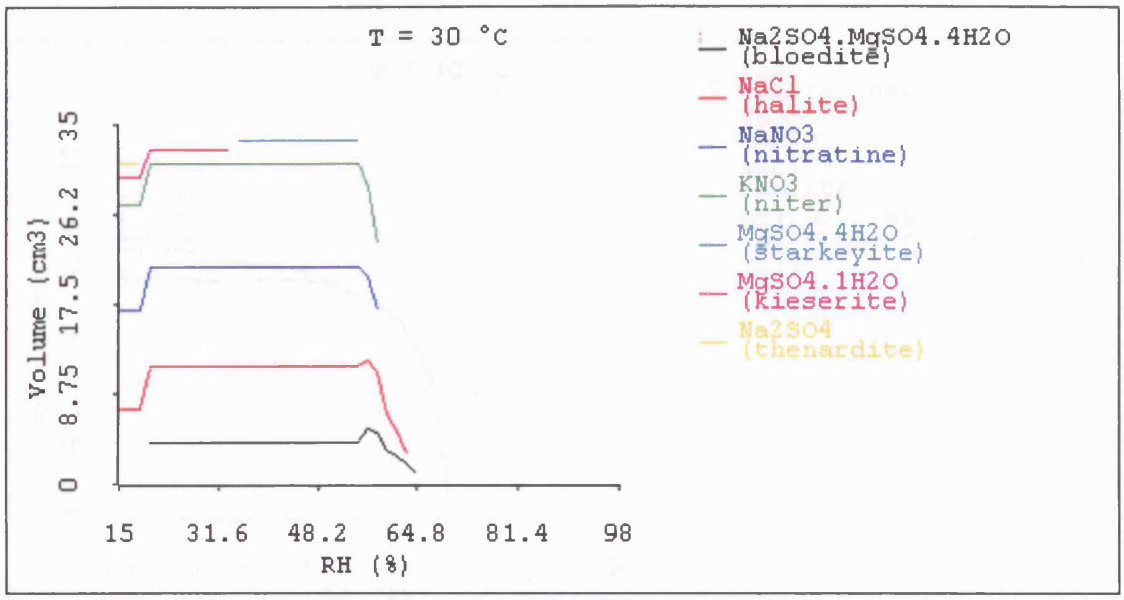

Figure (4N): Thermodynamic analysis using ECOS. Crystallisation sequence of soluble salts: relative humidity against volume of substance (cm^3). Sampling height: (5 cm) sampling depth interval: (3-5 cm). First fieldwork visit: August 2003.

Appendix N: Thermodynamic analysis of the salt content in samples from the Palace Tomb (C1) using ECOS.

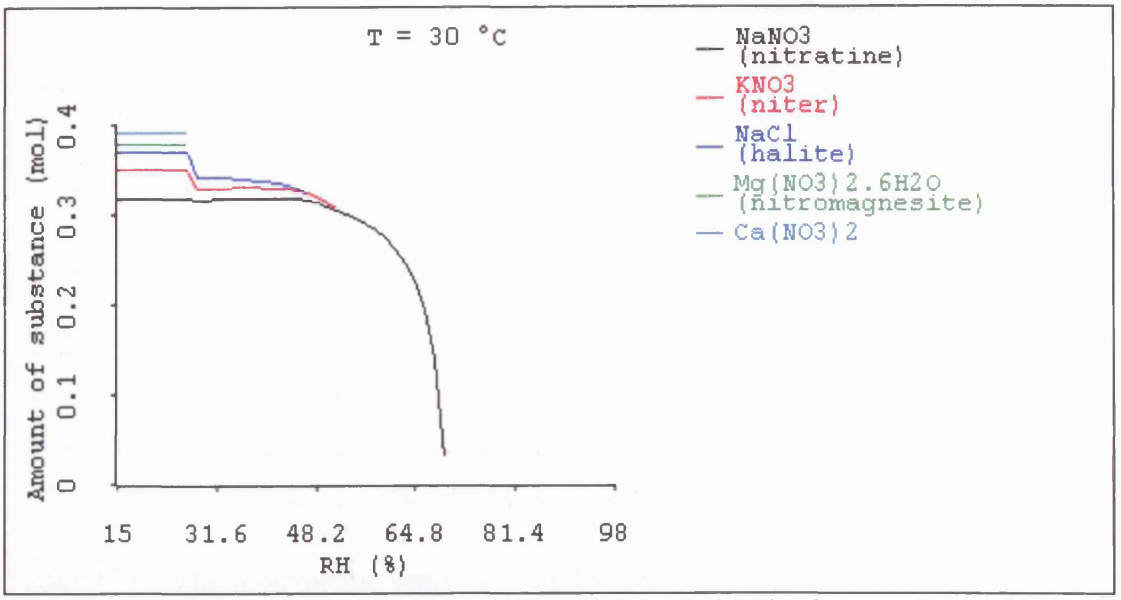

Figure (5N): Thermodynamic analysis using ECOS. Crystallisation sequence of soluble salts: relative humidity against amount of substance (mol). Sampling height: (105 cm) sampling depth interval: (0-1 cm). First fieldwork visit: August 2003.

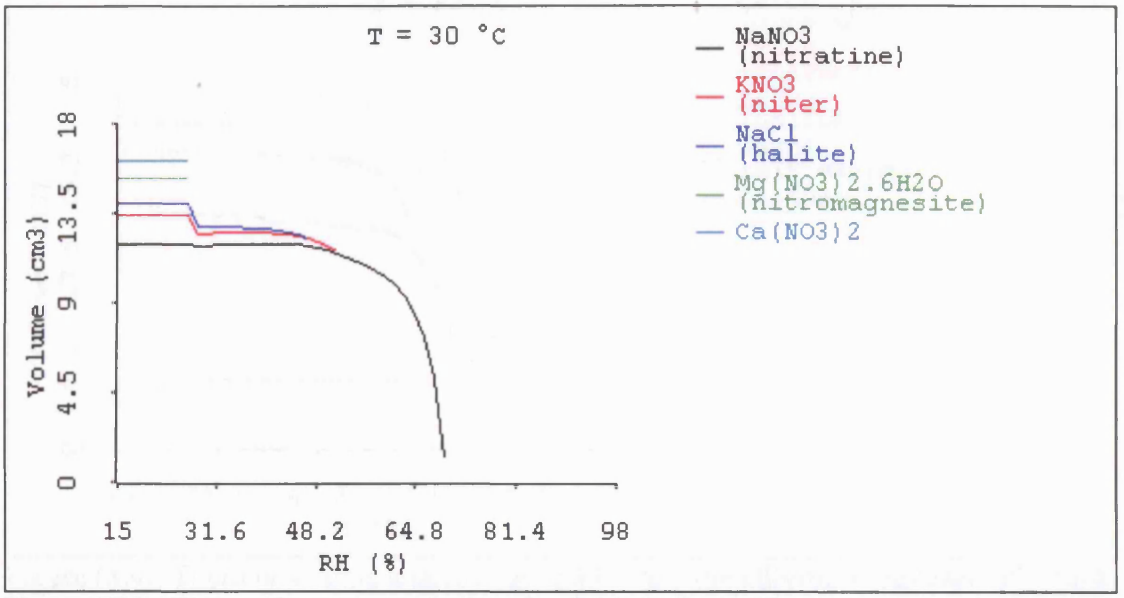

Figure (6N): Thermodynamic analysis using ECOS. Crystallisation sequence of soluble salts: relative humidity against volume of substance (cm^3). Sampling height: (105 cm) sampling depth interval: (0-1 cm). First fieldwork visit: August 2003.

Appendix N: Thermodynamic analysis of the salt content in samples from the Palace Tomb (C1) using ECOS.

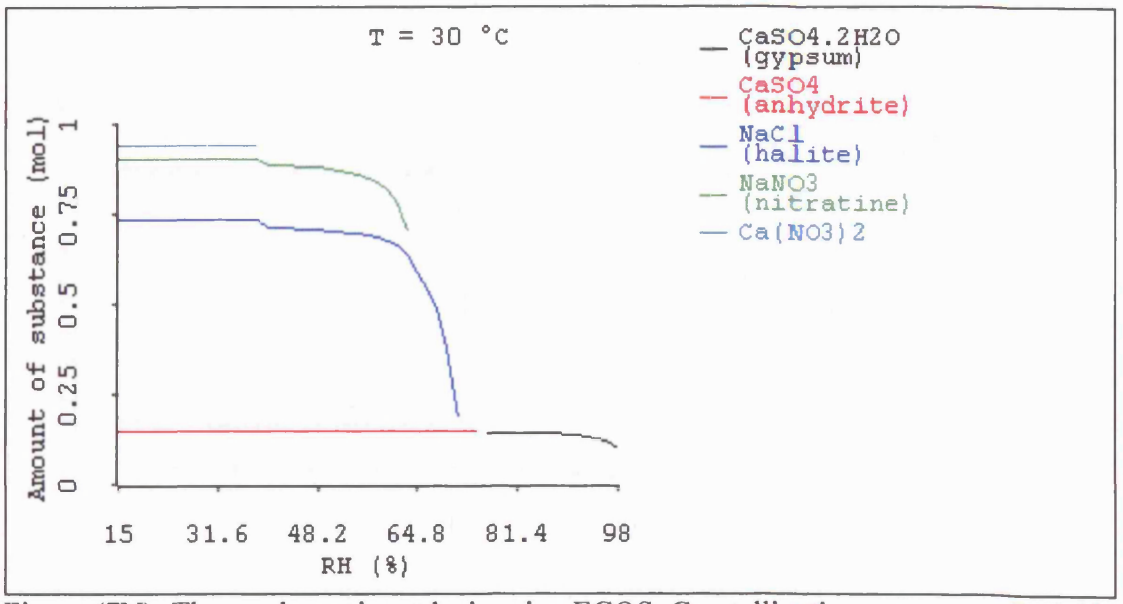

Figure (7N): Thermodynamic analysis using ECOS. Crystallisation sequence of soluble salts: relative humidity against amount of substance (mol). Sampling height: (105 cm) sampling depth interval: (1-3 cm). First fieldwork visit: August 2003.

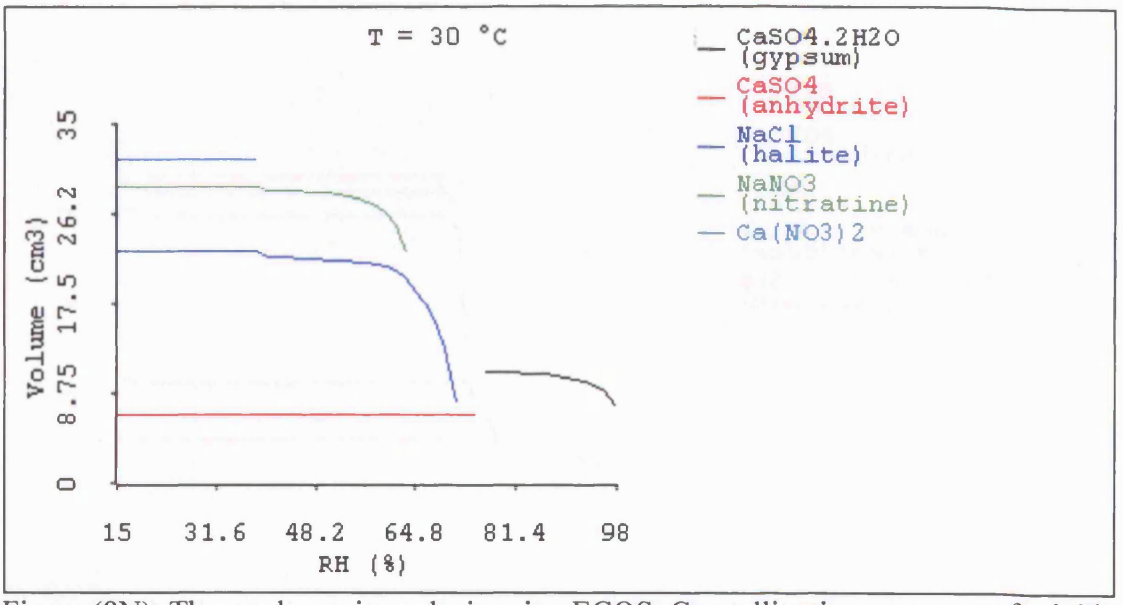

Figure (8N): Thermodynamic analysis using ECOS. Crystallisation sequence of soluble salts: relative humidity against volume of substance (cm^3). Sampling height: (105 cm) sampling depth interval: (1-3 cm). First fieldwork visit: August 2003.

Appendix N: Thermodynamic analysis of the salt content in samples from the Palace Tomb (C1) using ECOS.

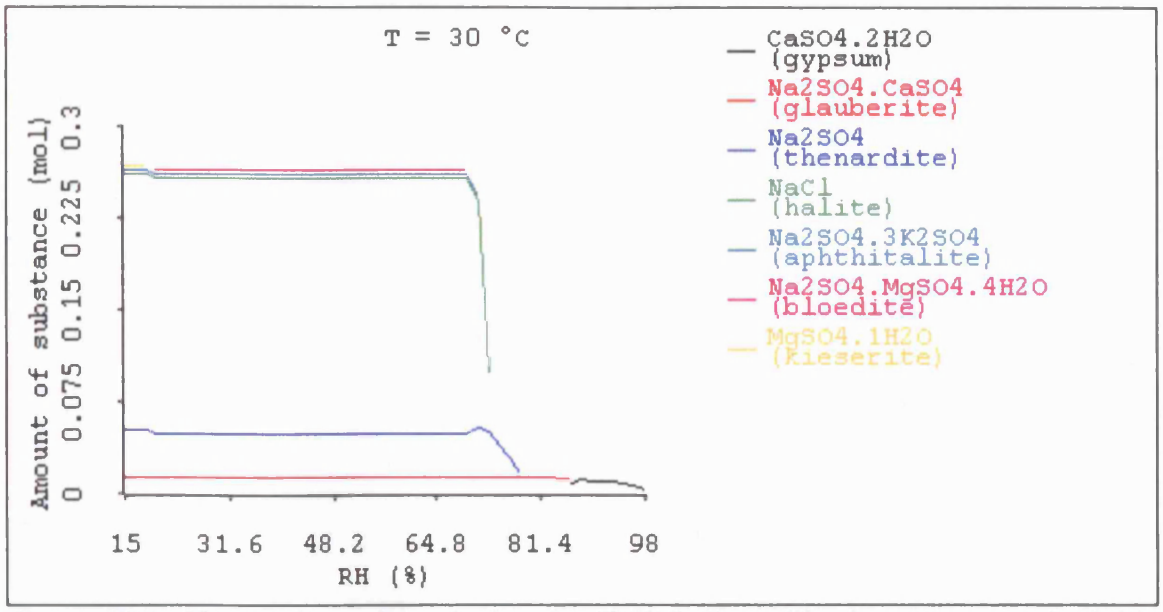

Figure (9N): Thermodynamic analysis using ECOS. Crystallisation sequence of soluble salts: relative humidity against amount of substance (mol). Sampling height: (105 cm) sampling depth interval: (3-5 cm). First fieldwork visit: August 2003.

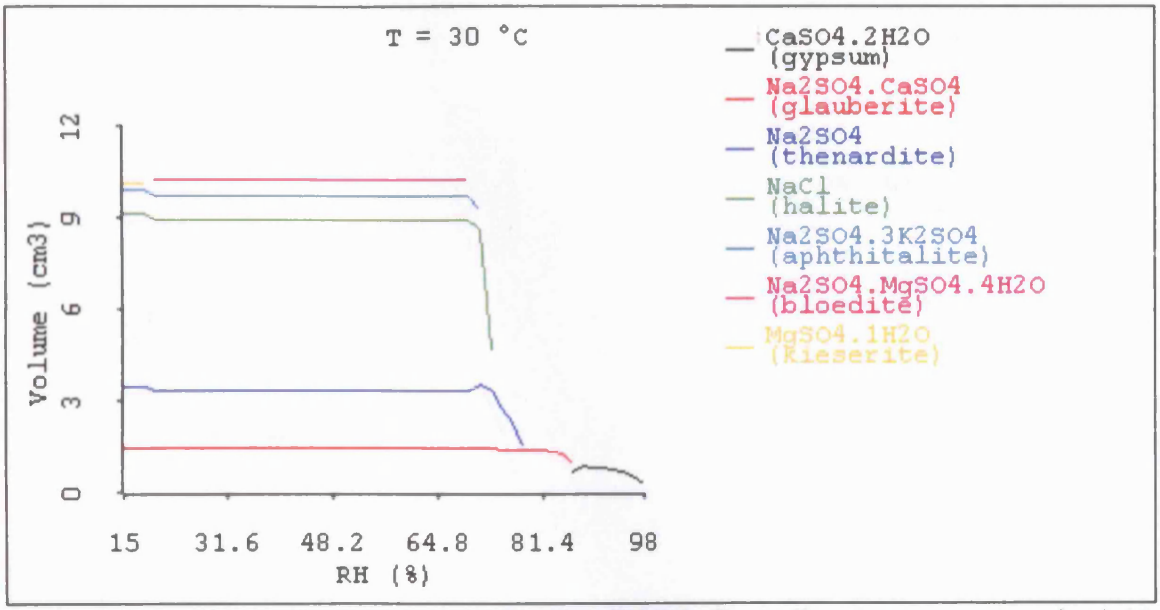

Figure (10N): Thermodynamic analysis using ECOS. Crystallisation sequence of soluble salts: relative humidity against volume of substance (cm^3). Sampling height: (105 cm) sampling depth interval: (3-5 cm). First fieldwork visit: August 2003.

Appendix N: Thermodynamic analysis of the salt content in samples from the Palace Tomb (C1) using ECOS.

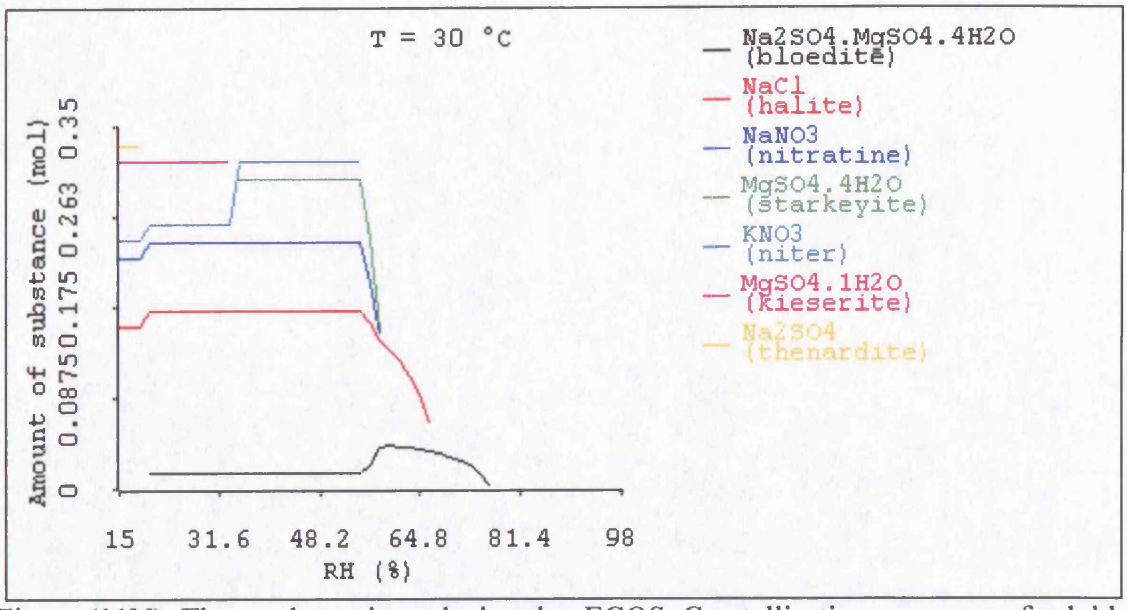

Figure (11N): Thermodynamic analysis using ECOS. Crystallisation sequence of soluble salts: relative humidity against amount of substance (mol). Sampling height: (355 cm) sampling depth interval: (0-1 cm). First fieldwork visit: August 2003.

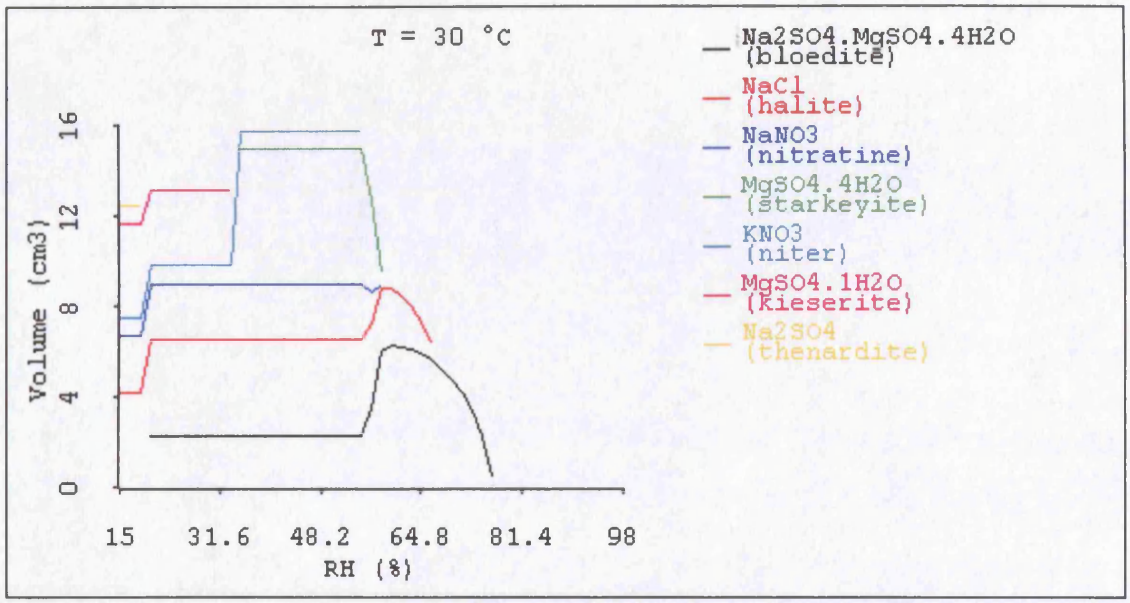

Figure (11N): Thermodynamic analysis using ECOS. Crystallisation sequence of soluble salts: relative humidity against volume of substance (cm^3). Sampling height: (355 cm) sampling depth interval: (0-1 cm). First fieldwork visit: August 2003.

Appendix N: Thermodynamic analysis of the salt content in samples from the Palace Tomb (C1) using ECOS.

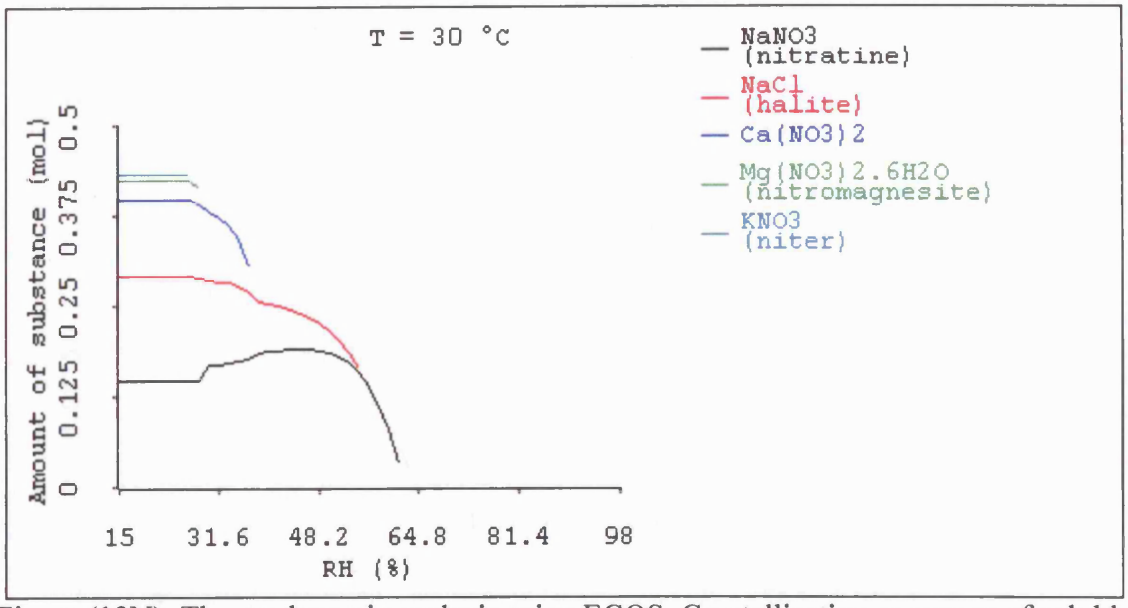

Figure (13N): Thermodynamic analysis using ECOS. Crystallisation sequence of soluble salts: relative humidity against amount of substance (mol). Sampling height: (355 cm) sampling depth interval: (1-3 cm). First fieldwork visit: August 2003.

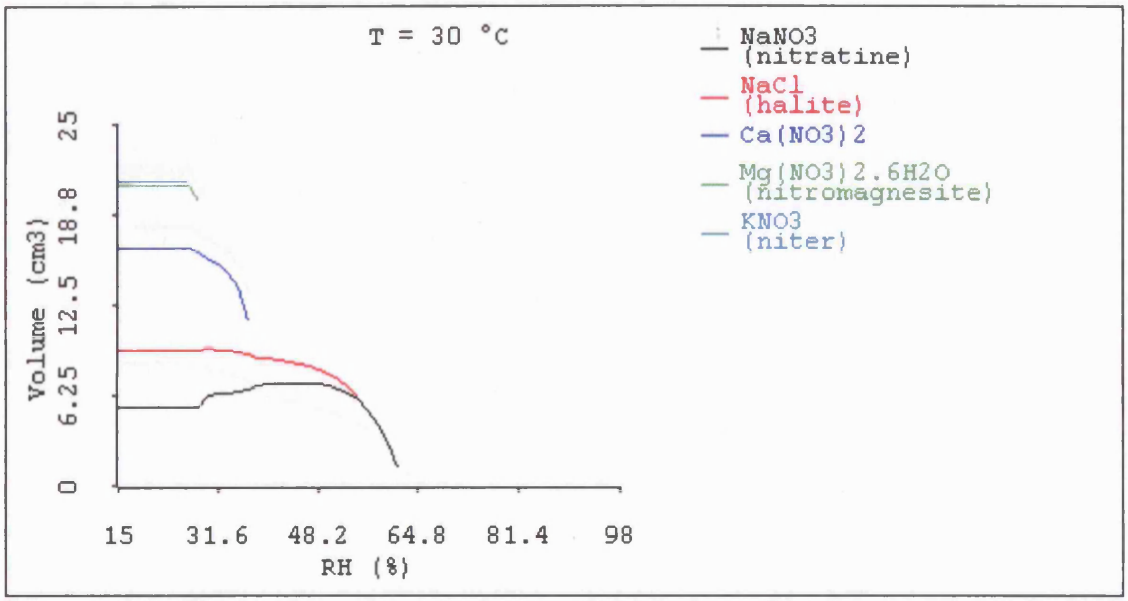

Figure (13N): Thermodynamic analysis using ECOS. Crystallisation sequence of soluble salts: relative humidity against volume of substance (cm^3). Sampling height: (355 cm) sampling depth interval: (1-3 cm). First fieldwork visit: August 2003.

Appendix N: Thermodynamic analysis of the salt content in samples from the Palace Tomb (C1) using ECOS.

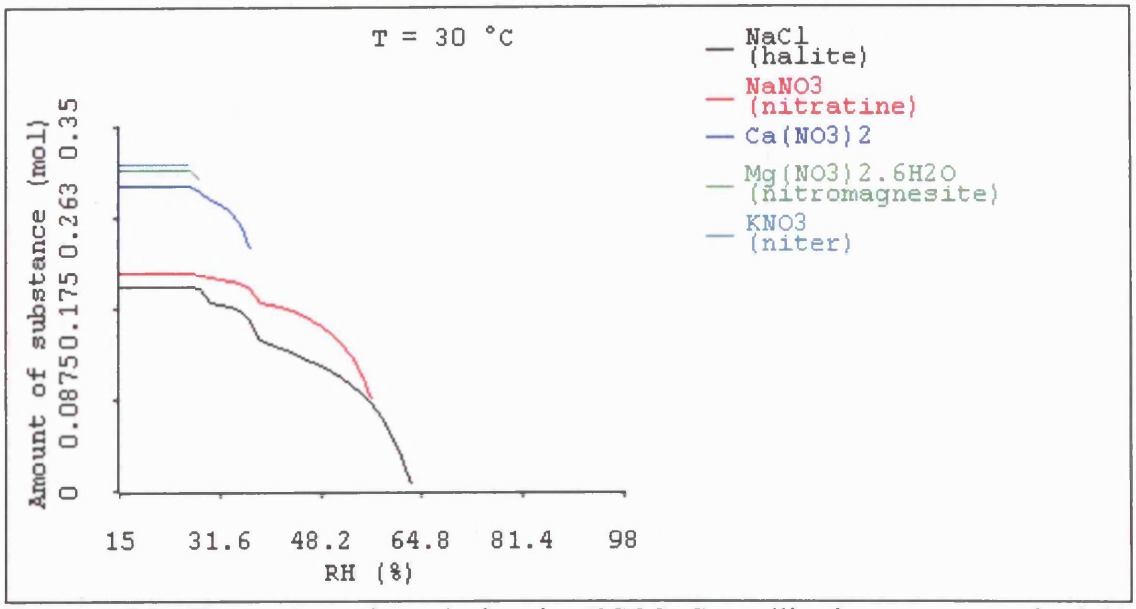

Figure (15N): Thermodynamic analysis using ECOS. Crystallisation sequence of soluble salts: relative humidity against amount of substance (mol). Sampling height: (355 cm) sampling depth interval: (3-5 cm). First fieldwork visit: August 2003.

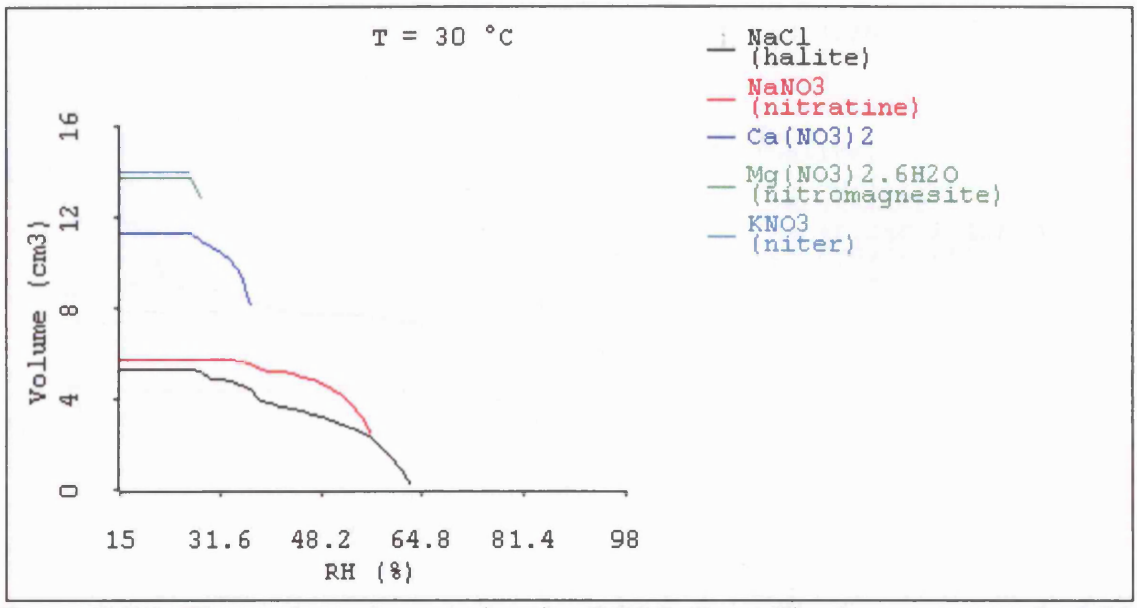

Figure (16N): Thermodynamic analysis using ECOS. Crystallisation sequence of soluble salts: relative humidity against volume of substance (cm^3). Sampling height: (355 cm) sampling depth interval: (3-5 cm). First fieldwork visit: August 2003.

Appendix N: Thermodynamic analysis of the salt content in samples from the Palace Tomb (C1) using ECOS.

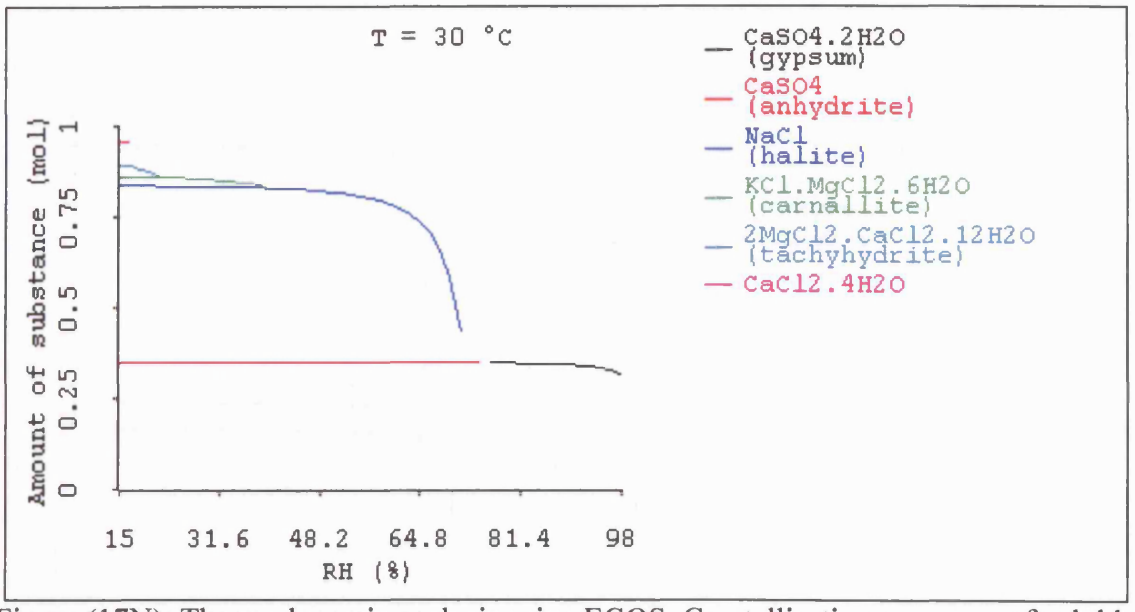

Figure (17N): Thermodynamic analysis using ECOS. Crystallisation sequence of soluble salts: relative humidity against amount of substance (mol). Sampling height: (505 cm) sampling depth interval: (0-1 cm). First fieldwork visit: August 2003.

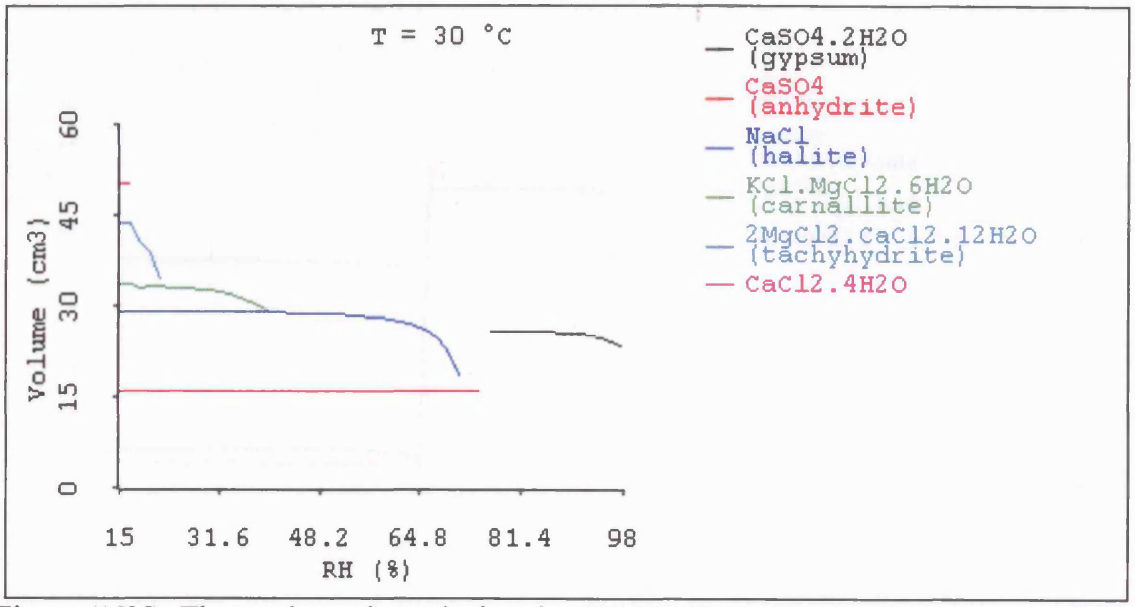

Figure (18N): Thermodynamic analysis using ECOS. Crystallisation sequence of soluble salts: relative humidity against volume of substance (cm^3). Sampling height: (505 cm) sampling depth interval: (0-1 cm). First fieldwork visit: August 2003.

Appendix N: Thermodynamic analysis of the salt content in samples from the Palace Tomb (C1) using ECOS.

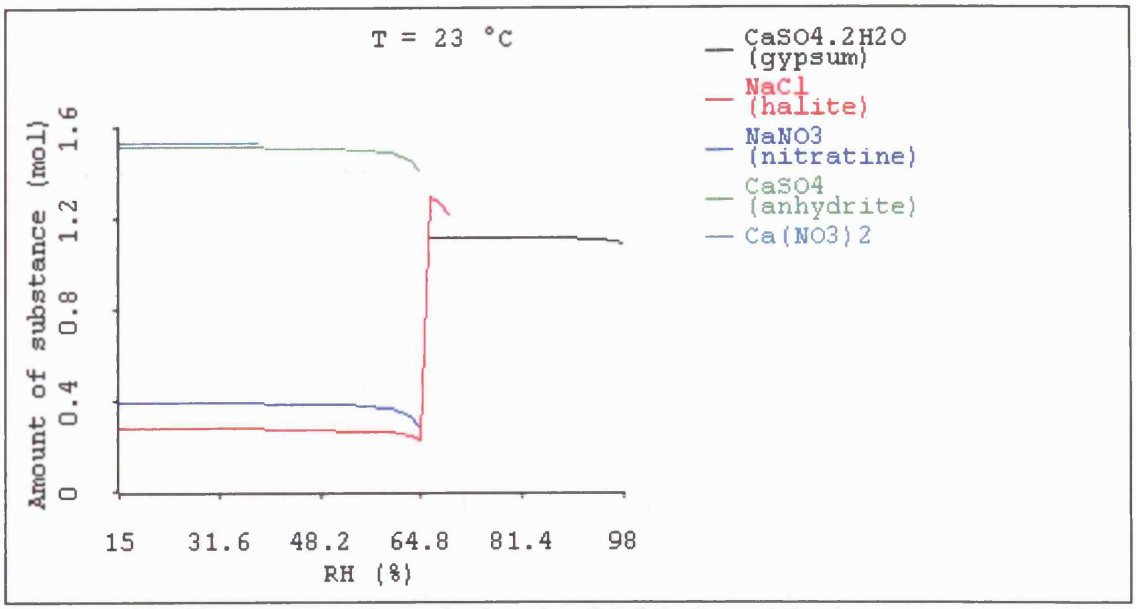

Figure (19N): Thermodynamic analysis using ECOS. Crystallisation sequence of soluble salts: relative humidity against amount of substance (mol). Sampling height: (505 cm) sampling depth interval: (1-3 cm). First fieldwork visit: August 2003.

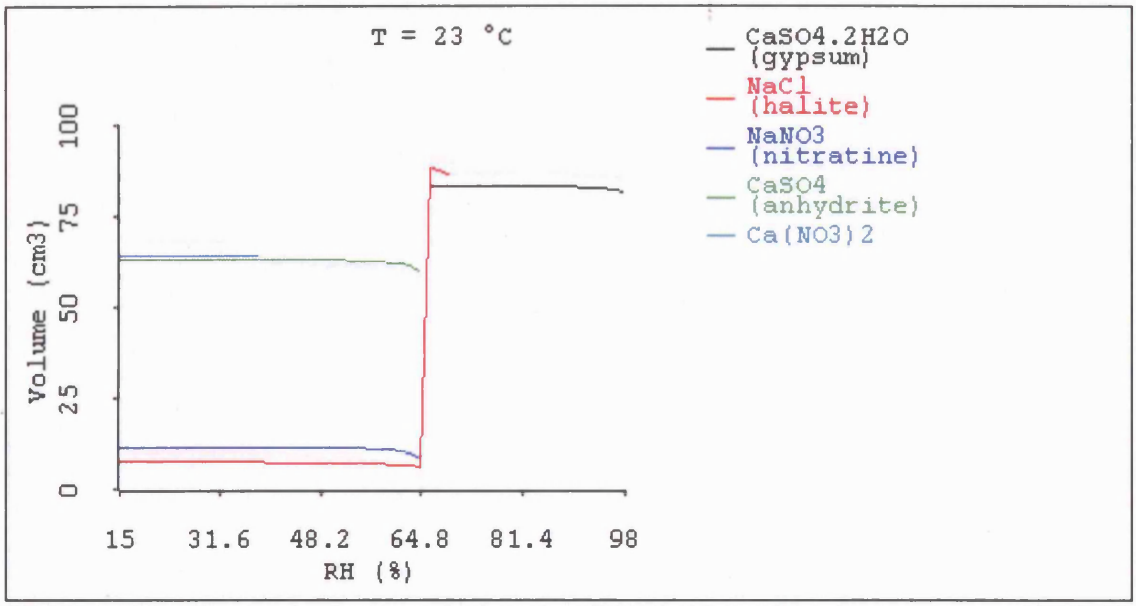

Figure (20N): Thermodynamic analysis using ECOS. Crystallisation sequence of soluble salts: relative humidity against volume of substance (cm^3). Sampling height: (505 cm) sampling depth interval: (1-3 cm). First fieldwork visit: August 2003.

Appendix N: Thermodynamic analysis of the salt content in samples from the Palace Tomb (C1) using ECOS.

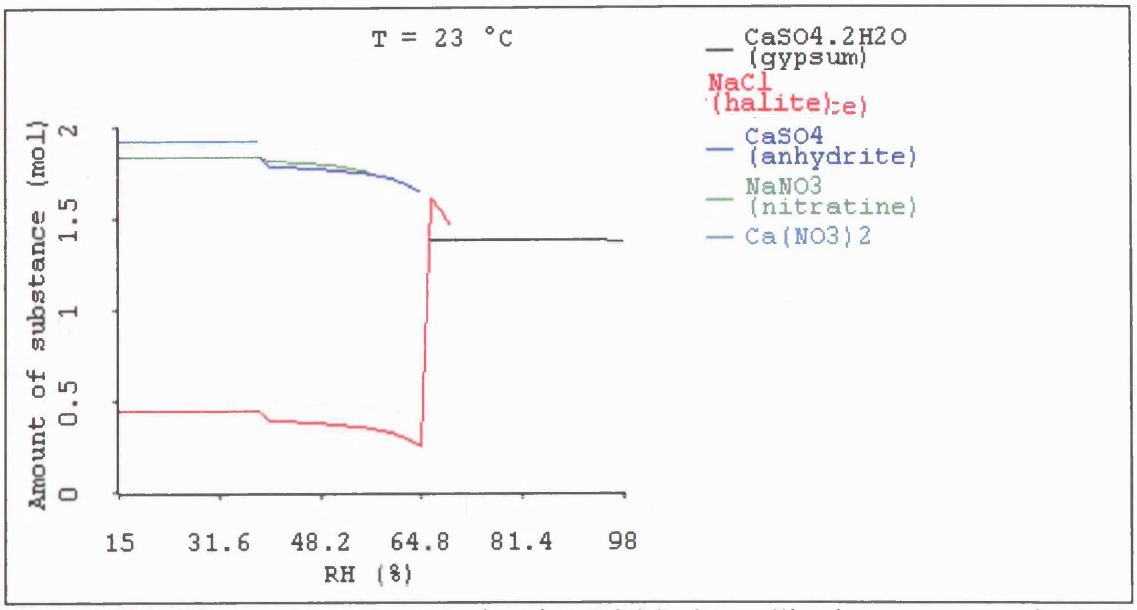

Figure (21N): Thermodynamic analysis using ECOS. Crystallisation sequence of soluble salts: relative humidity against amount of substance (mol). Sampling height: (5 cm) sampling depth interval: (0-1 cm). Third fieldwork visit: June 2004.

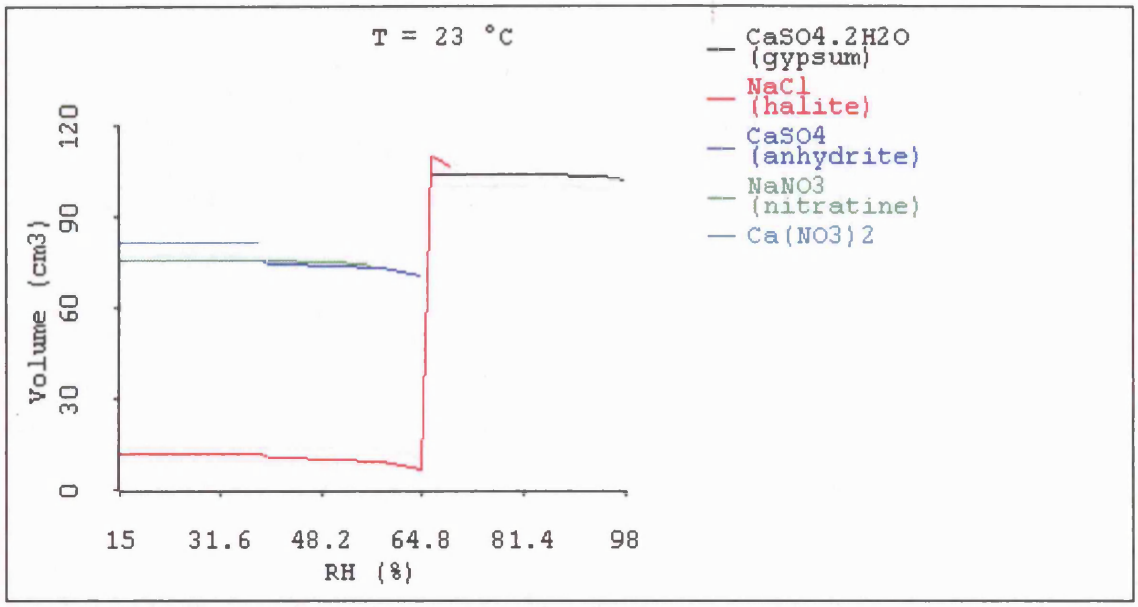

Figure (22N): Thermodynamic analysis using ECOS. Crystallisation sequence of soluble salts: relative humidity against volume of substance (cm^3). Sampling height: (5 cm) sampling depth interval: (0-1 cm). Third fieldwork visit: June 2004.

Appendix N: Thermodynamic analysis of the salt content in samples from the Palace Tomb (C1) using ECOS.

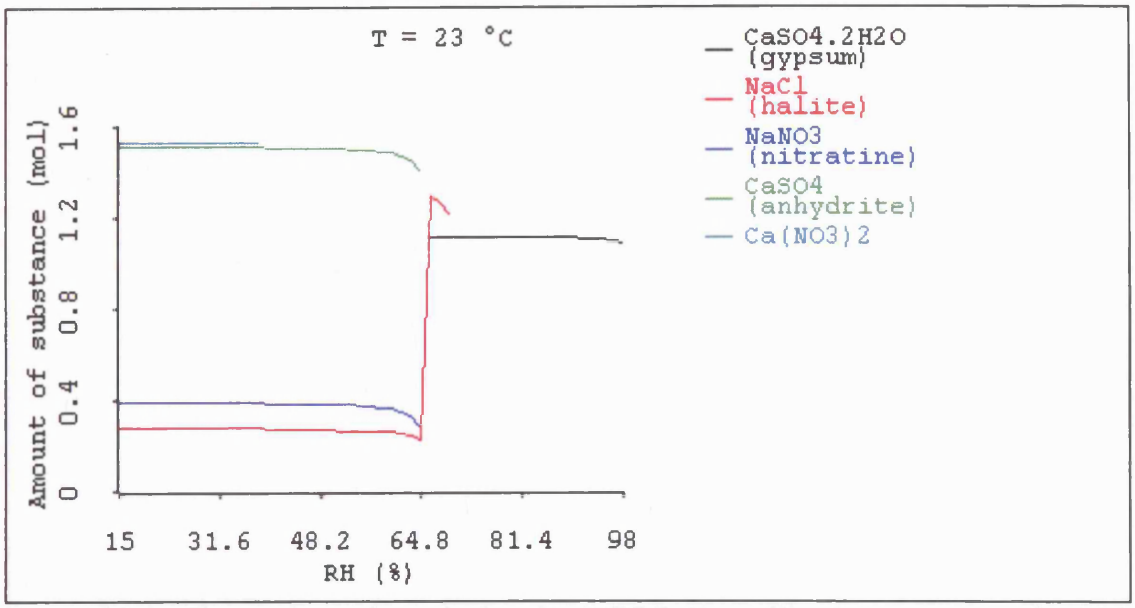

Figure (23N): Thermodynamic analysis using ECOS. Crystallisation sequence of soluble salts: relative humidity against amount of substance (mol). Sampling height: (5 cm) sampling depth interval: (1-3 cm). Third fieldwork visit: June 2004.

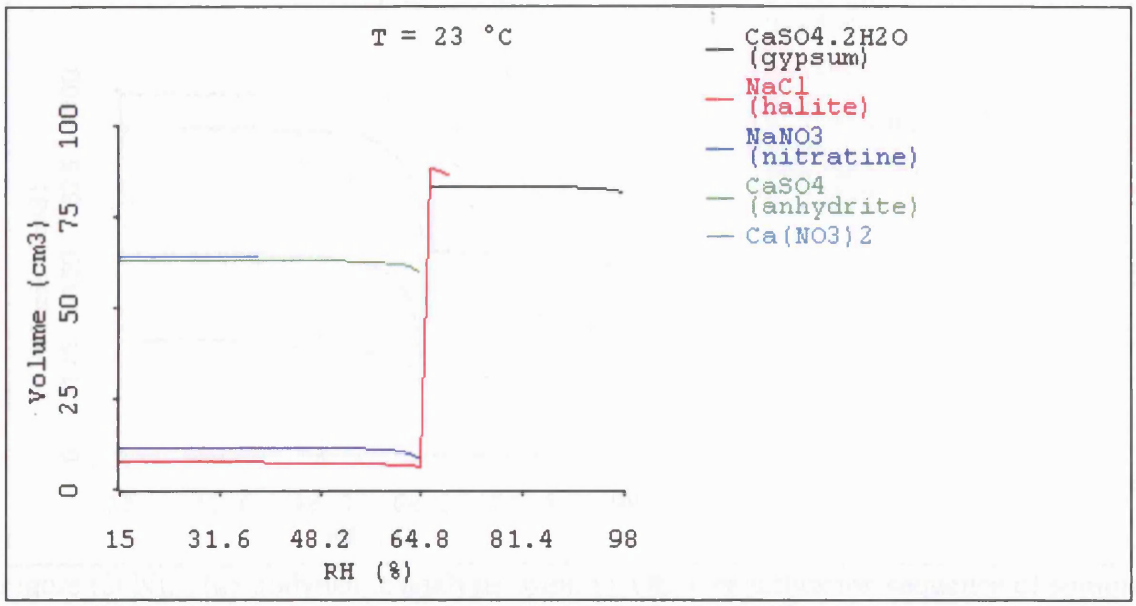

Figure (24N): Thermodynamic analysis using ECOS. Crystallisation sequence of soluble salts: relative humidity against volume of substance (cm^3). Sampling height: (5 cm) sampling depth interval: (1-3 cm). Third fieldwork visit: June 2004.

Appendix N: Thermodynamic analysis of the salt content in samples from the Palace Tomb (C1) using ECOS.

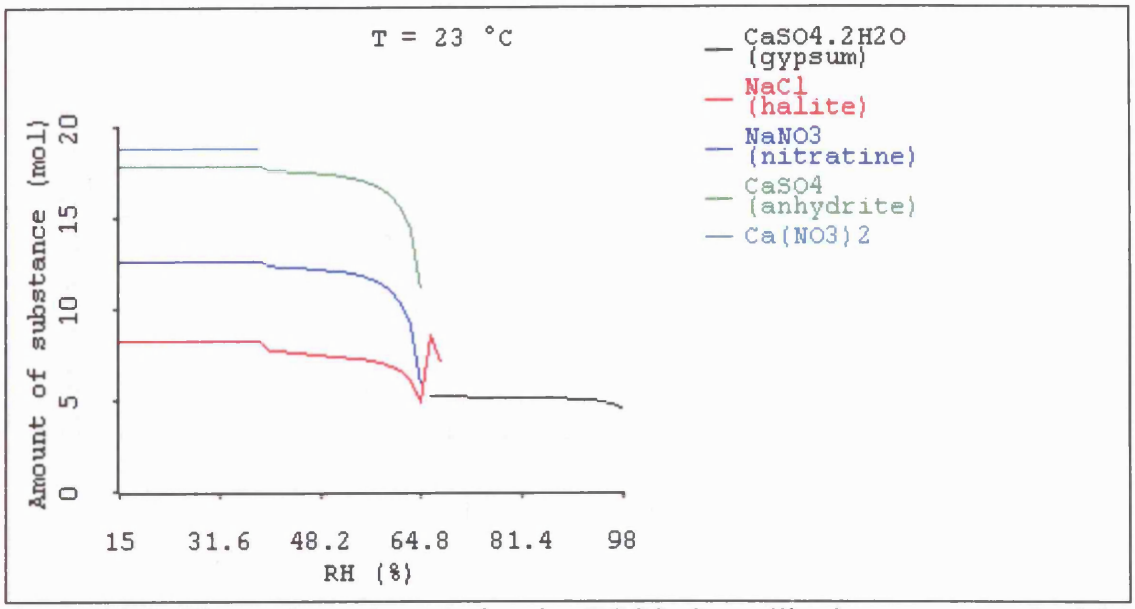

Figure (25N): Thermodynamic analysis using ECOS. Crystallisation sequence of soluble salts: relative humidity against amount of substance (mol). Sampling height: (105 cm) sampling depth interval: (0-1 cm). Third fieldwork visit: June 2004.

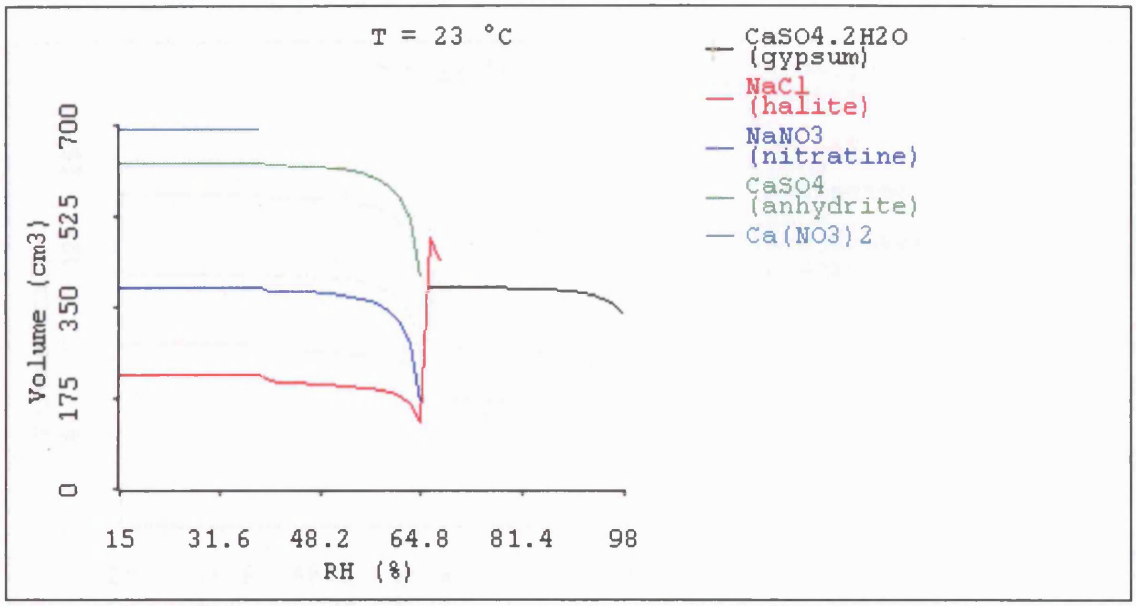

Figure (26N): Thermodynamic analysis using ECOS. Crystallisation sequence of soluble salts: relative humidity against volume of substance (cm^3). Sampling height: (105 cm) sampling depth interval: (0-1 cm). Third fieldwork visit: June 2004.

Appendix N: Thermodynamic analysis of the salt content in samples from the Palace Tomb (C1) using ECOS.

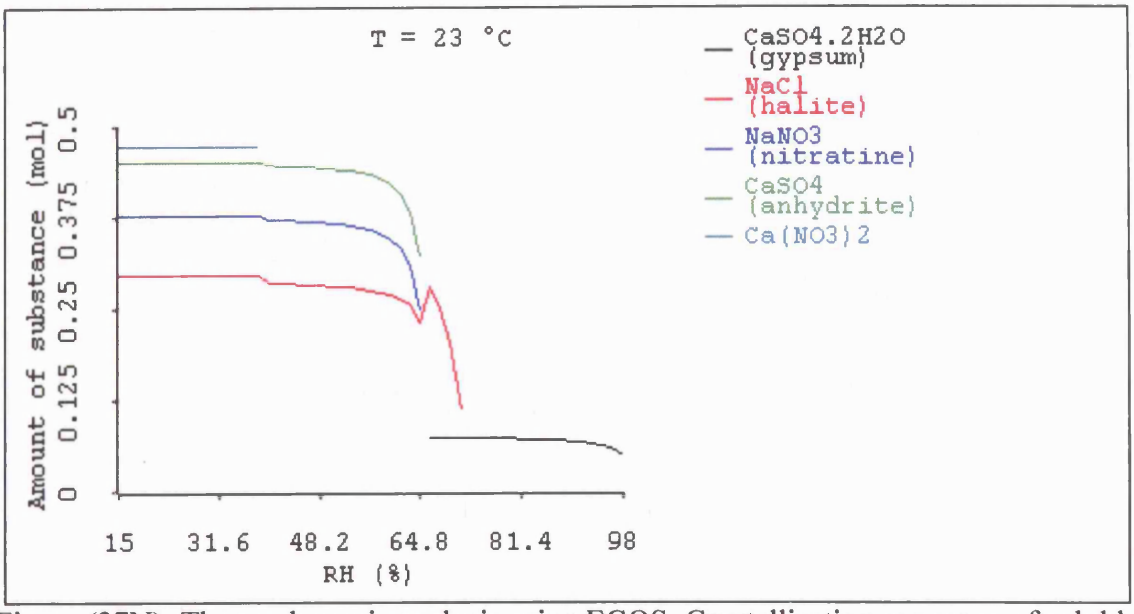

Figure (27N): Thermodynamic analysis using ECOS. Crystallisation sequence of soluble salts: relative humidity against amount of substance (mol). Sampling height: (105 cm) sampling depth interval: (1-3 cm). Third fieldwork visit: June 2004.

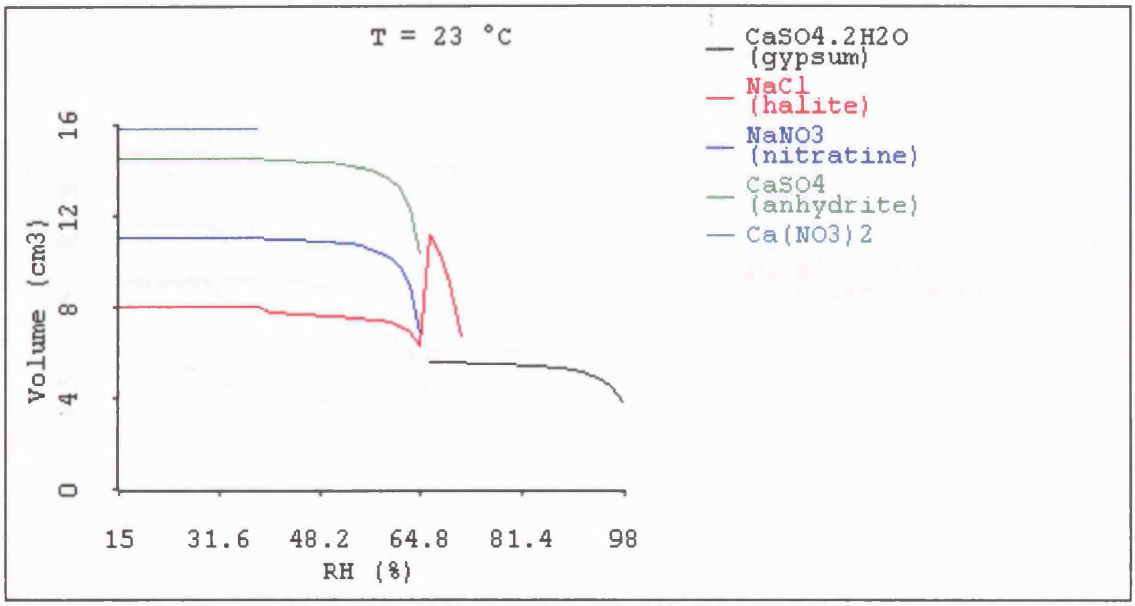

Figure (28N): Thermodynamic analysis using ECOS. Crystallisation sequence of soluble salts: relative humidity against volume of substance (cm^3). Sampling height: (105 cm) sampling depth interval: (1-3 cm). Third fieldwork visit: June 2004.

Appendix N: Thermodynamic analysis of the salt content in samples from the Palace Tomb (C1) using ECOS.

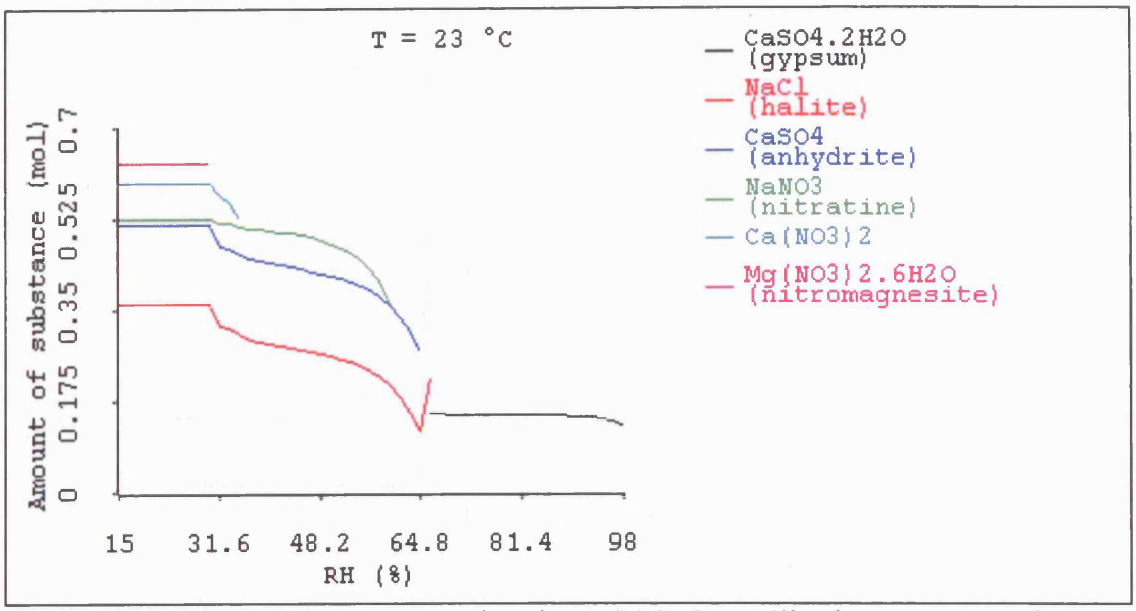

Figure (29N): Thermodynamic analysis using ECOS. Crystallisation sequence of soluble salts: relative humidity against amount of substance (mol). Sampling height: (355 cm) sampling depth interval: (0-1 cm). Third fieldwork visit: June 2004.

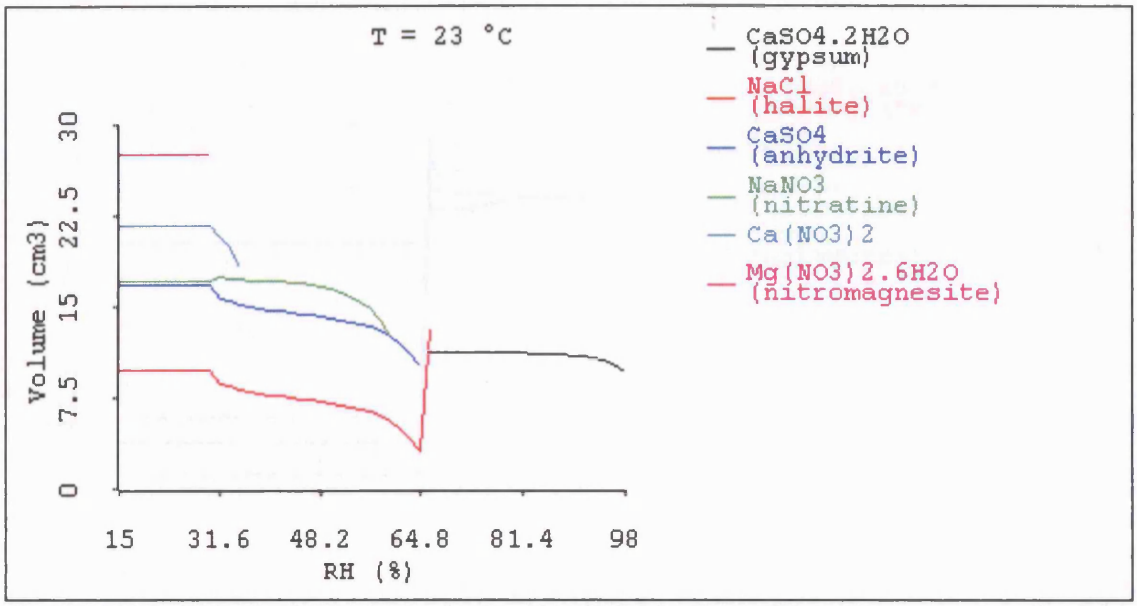

Figure (30N): Thermodynamic analysis using ECOS. Crystallisation sequence of soluble salts: relative humidity against volume of substance (cm^3). Sampling height: (355 cm) sampling depth interval: (0-1 cm). Third fieldwork visit: June 2004.

Appendix N: Thermodynamic analysis of the salt content in samples from the Palace Tomb (C1) using ECOS.

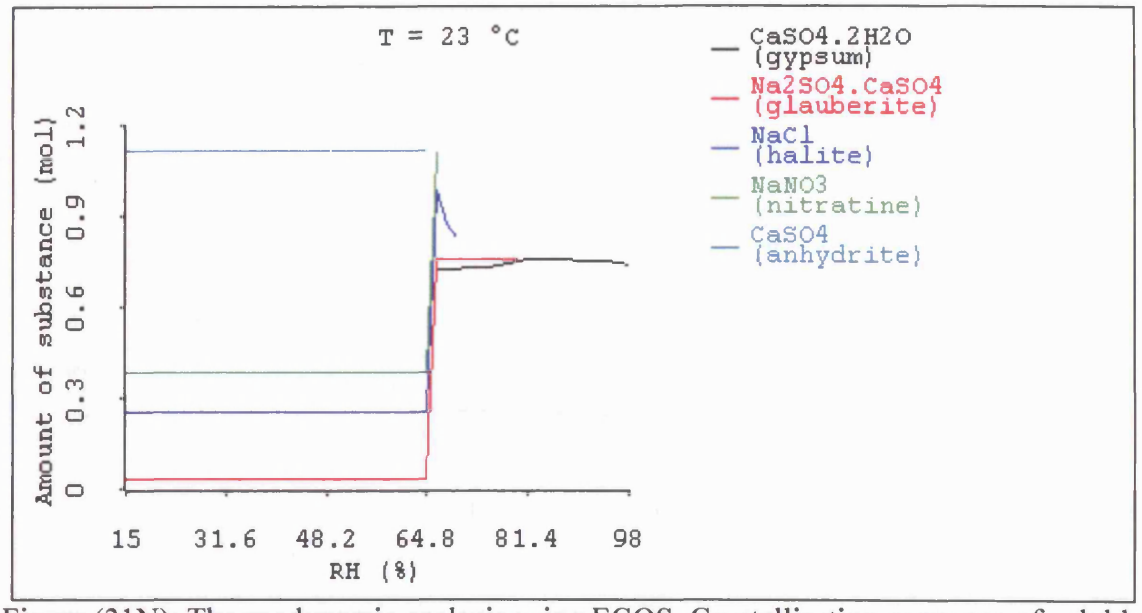

Figure (31N): Thermodynamic analysis using ECOS. Crystallisation sequence of soluble salts: relative humidity against amount of substance (mol). Sampling height: (355 cm) sampling depth interval: (1-3 cm). Third fieldwork visit: June 2004.

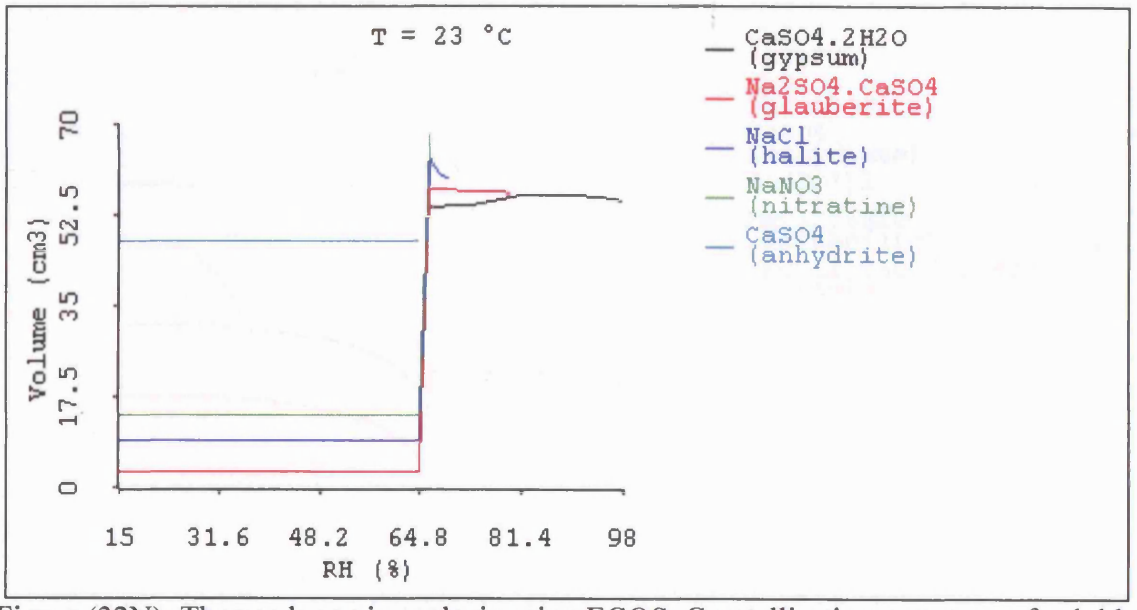

Figure (32N): Thermodynamic analysis using ECOS. Crystallisation sequence of soluble salts: relative humidity against volume of substance (cm^3). Sampling height: (355 cm) sampling depth interval: (1-3 cm). Third fieldwork visit: June 2004.

Appendix N: Thermodynamic analysis of the salt content in samples from the Palace Tomb (C1) using ECOS.

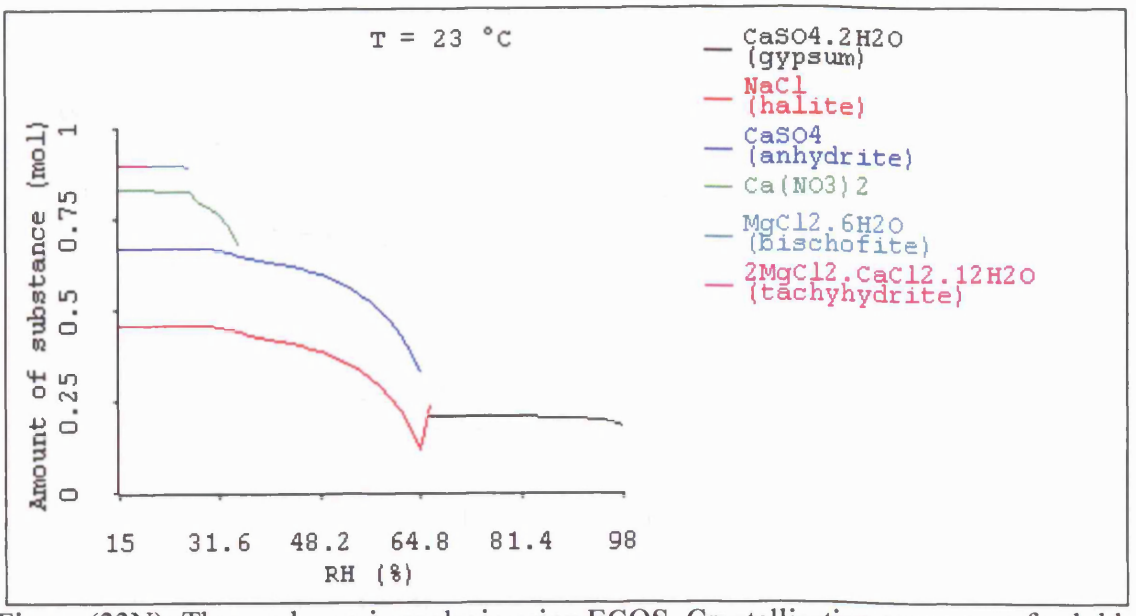

Figure (33N): Thermodynamic analysis using ECOS. Crystallisation sequence of soluble salts: relative humidity against amount of substance (mol). Sampling height: (505 cm) sampling depth interval: (0-1 cm). Third fieldwork visit: June 2004.

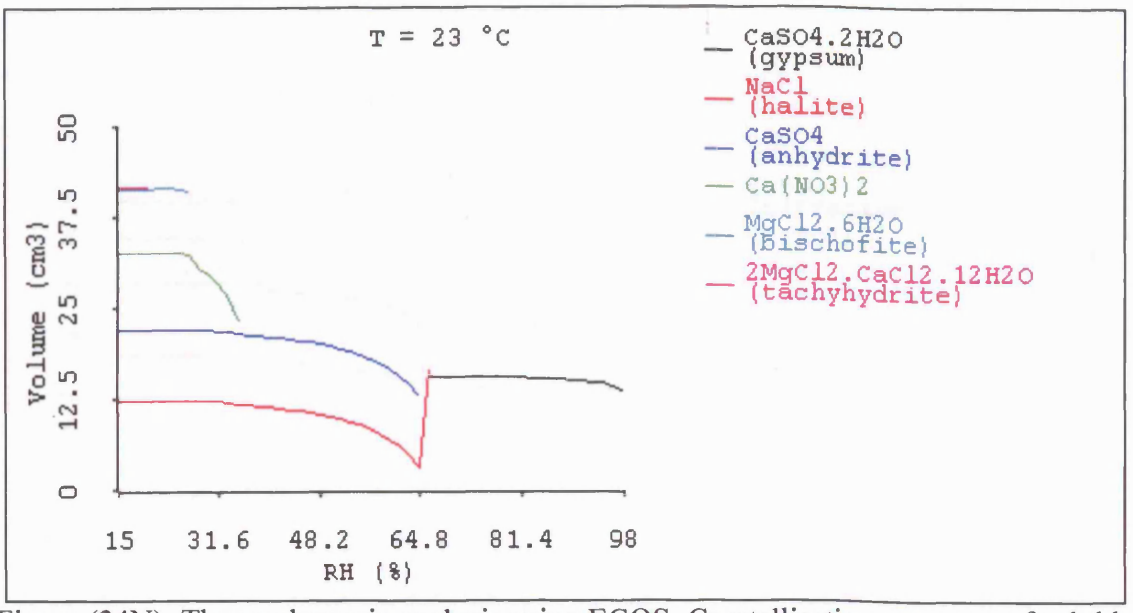

Figure (34N): Thermodynamic analysis using ECOS. Crystallisation sequence of soluble salts: relative humidity against volume of substance (cm^3). Sampling height: (505 cm) sampling depth interval: (0-1 cm). Third fieldwork visit: June 2004.

Appendix N: Thermodynamic analysis of the salt content in samples from the Palace Tomb (C1) using ECOS.

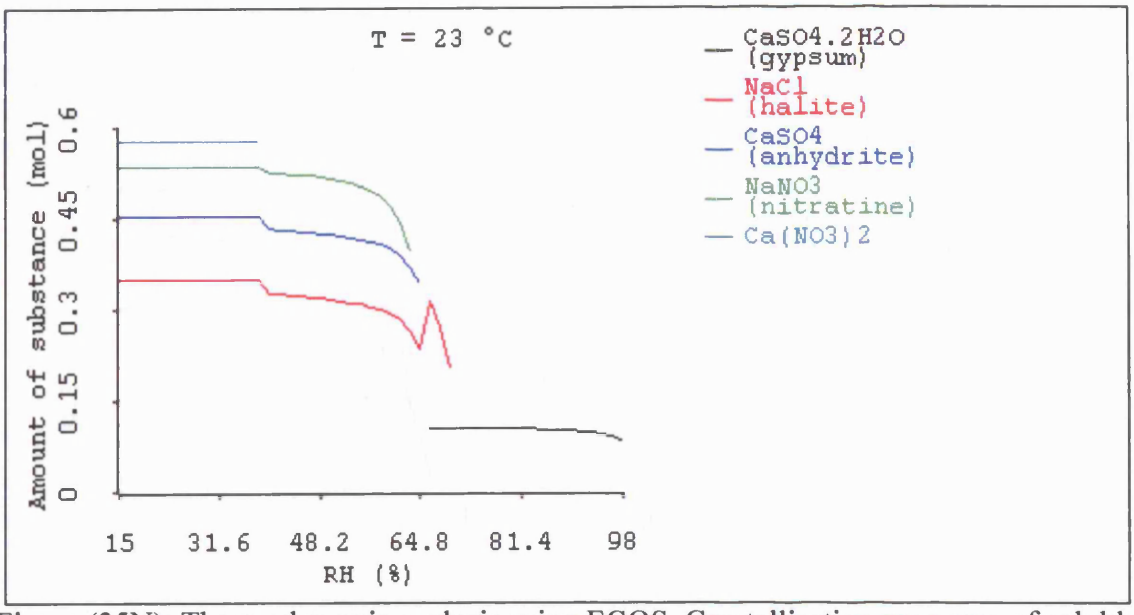

Figure (35N): Thermodynamic analysis using ECOS. Crystallisation sequence of soluble salts: relative humidity against amount of substance (mol). Sampling height: (505 cm) sampling depth interval: (1-3 cm). Third fieldwork visit: June 2004.

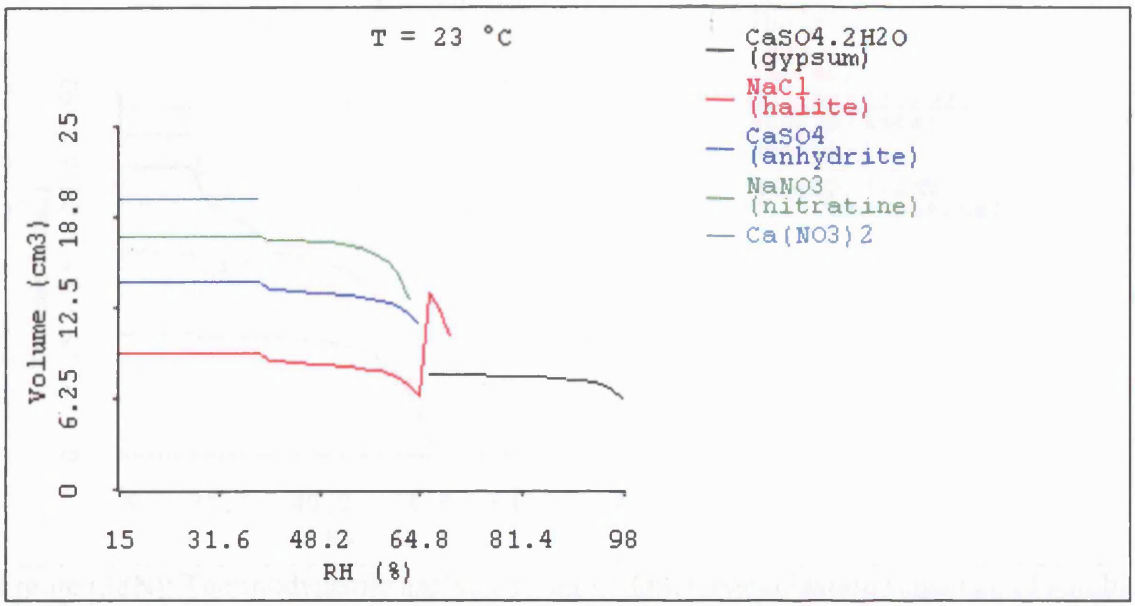

Figure (36N): Thermodynamic analysis using ECOS. Crystallisation sequence of soluble salts: relative humidity against volume of substance (cm^3). Sampling height: (505 cm) sampling depth interval: (1-3 cm). Third fieldwork visit: June 2004.

Appendix N: Thermodynamic analysis of the salt content in samples from the Palace Tomb (C1) using ECOS.

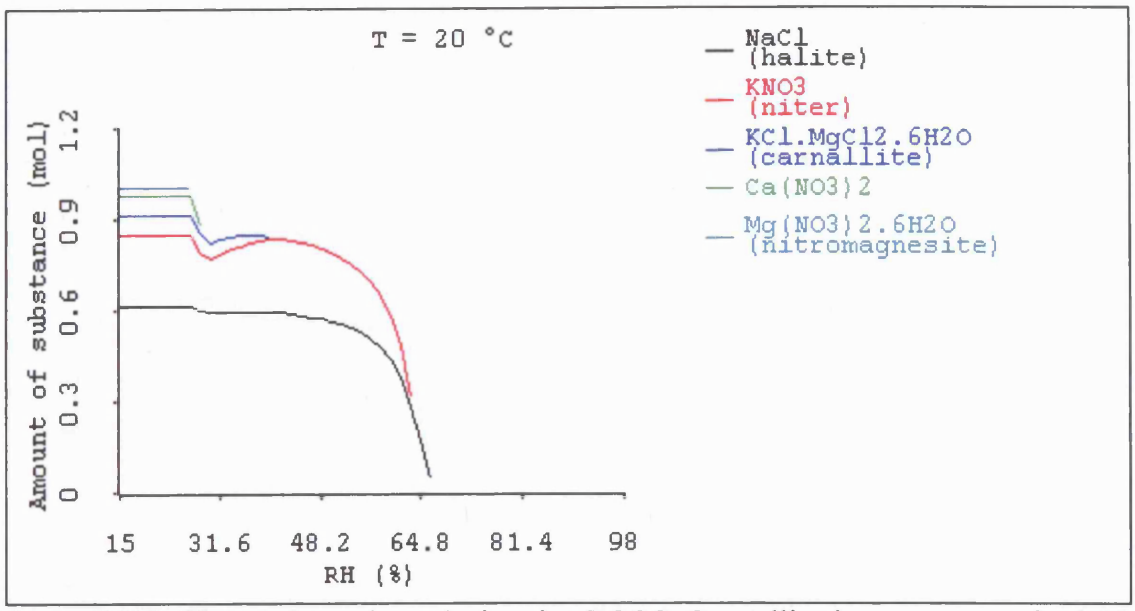

Figure (37N): Thermodynamic analysis using ECOS. Crystallisation sequence of soluble salts: relative humidity against amount of substance (mol). Sampling height: (5 cm) sampling depth interval: (0-1 cm). Fourth fieldwork visit: April 2005.

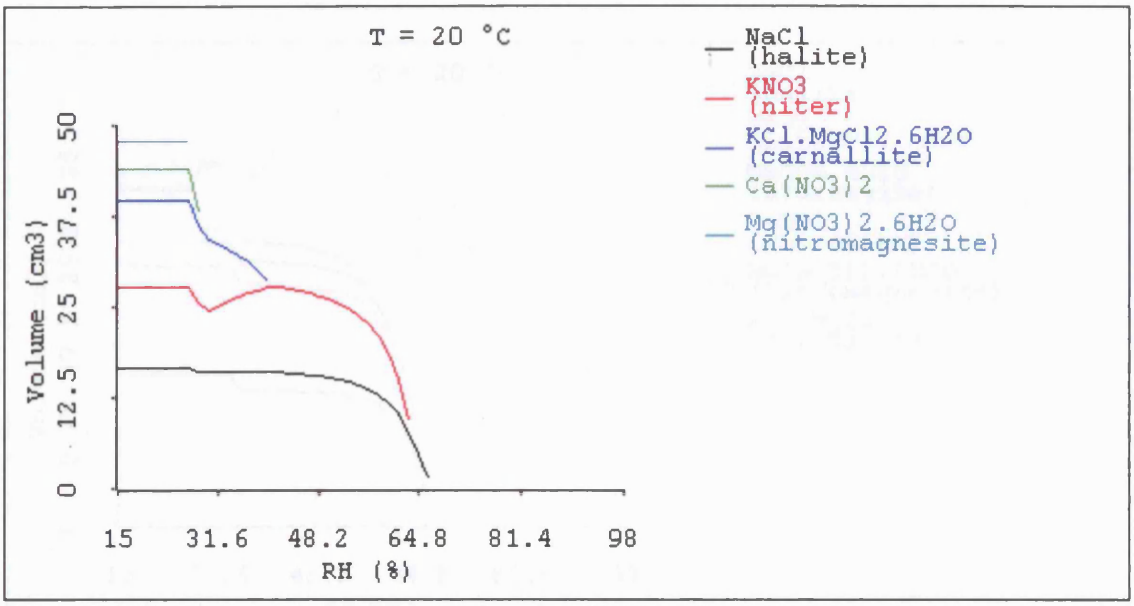

Figure (38N): Thermodynamic analysis using ECOS. Crystallisation sequence of soluble salts: relative humidity against volume of substance (cm^3). Sampling height: (5 cm) sampling depth interval: (0-1 cm). Fourth fieldwork visit: April 2005.

Appendix N: Thermodynamic analysis of the salt content in samples from the Palace Tomb (C1) using ECOS.

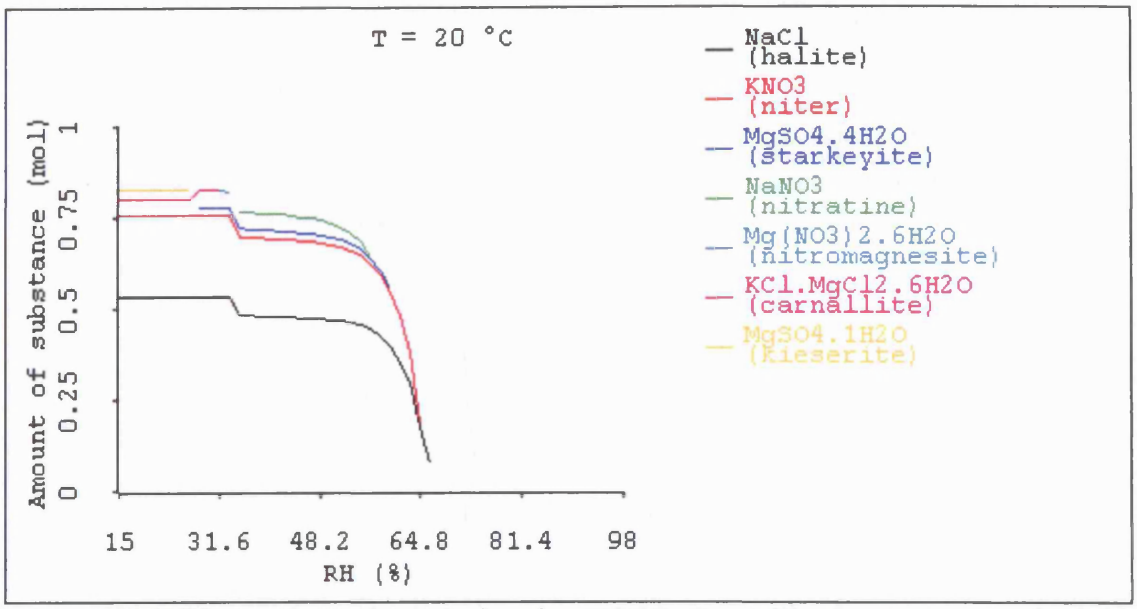

Figure (39N): Thermodynamic analysis using ECOS. Crystallisation sequence of soluble salts: relative humidity against amount of substance (mol). Sampling height: (5 cm) sampling depth interval: (1-3 cm). Fourth fieldwork visit: April 2005.

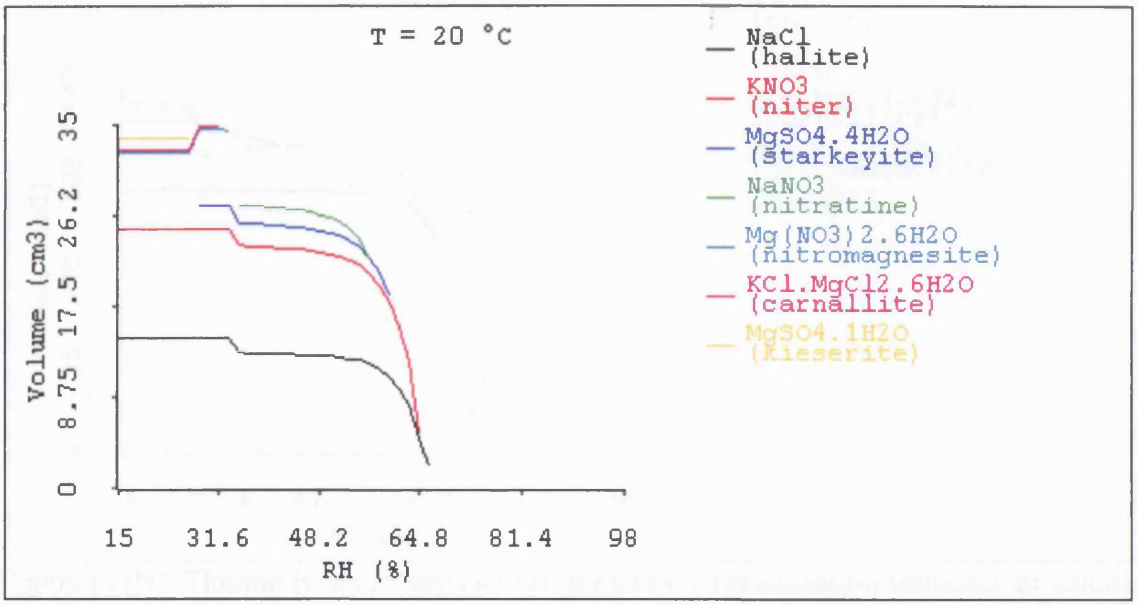

Figure (40N): Thermodynamic analysis using ECOS. Crystallisation sequence of soluble salts: relative humidity against volume of substance (cm^3). Sampling height: (5 cm) sampling depth interval: (1-3 cm). Fourth fieldwork visit: April 2005.

Appendix N: Thermodynamic analysis of the salt content in samples from the Palace Tomb (C1) using ECOS.

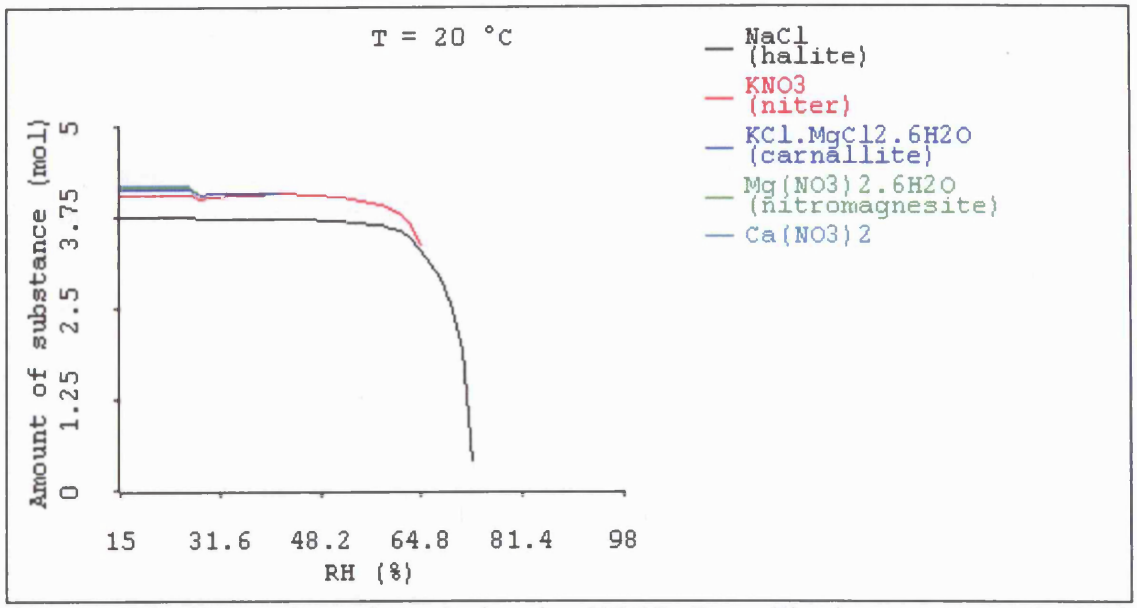

Figure (41N): Thermodynamic analysis using ECOS. Crystallisation sequence of soluble salts: relative humidity against amount of substance (mol). Sampling height: (105 cm) sampling depth interval: (0-1 cm). Fourth fieldwork visit: April 2005.

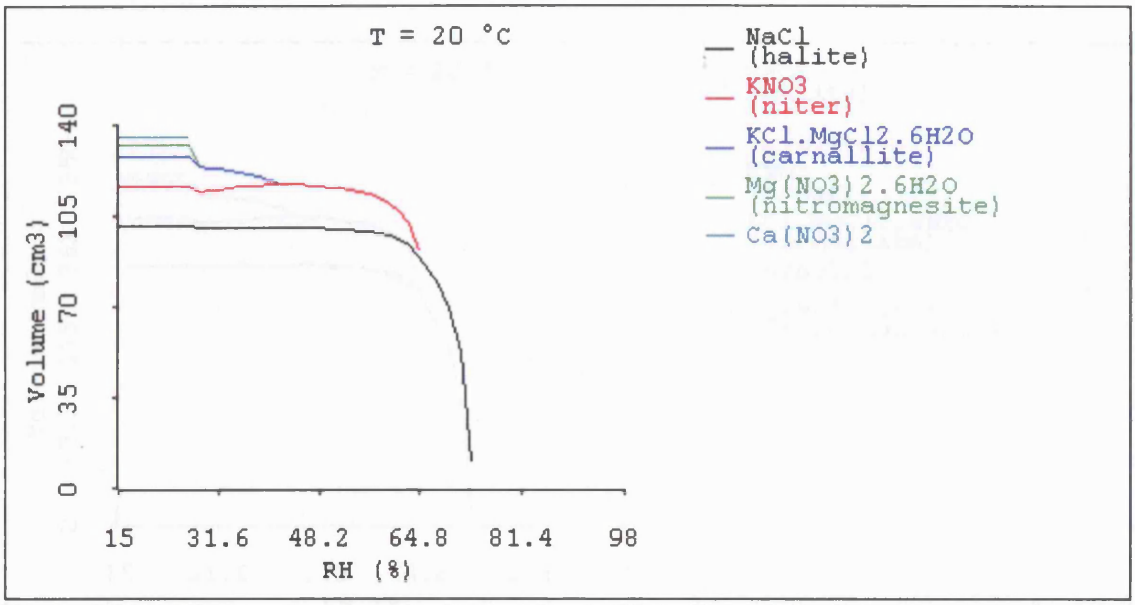

Figure (42N): Thermodynamic analysis using ECOS. Crystallisation sequence of soluble salts: relative humidity against volume of substance (cm^3). Sampling height: (105 cm) sampling depth interval: (0-1 cm). Fourth fieldwork visit: April 2005.

Appendix N: Thermodynamic analysis of the salt content in samples from the Palace Tomb (C1) using ECOS.

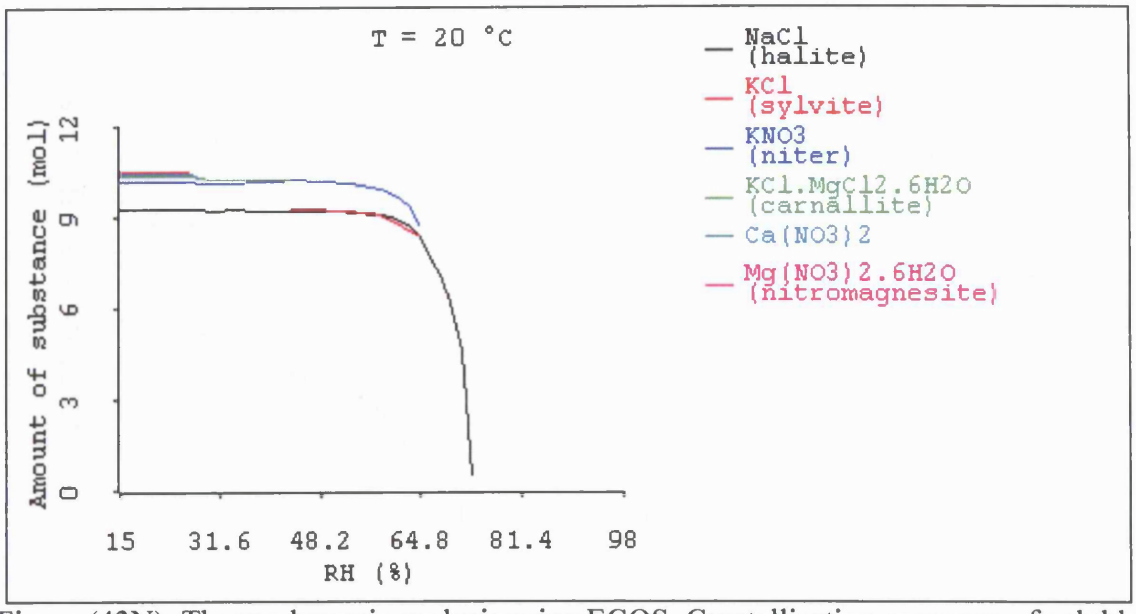

Figure (43N): Thermodynamic analysis using ECOS. Crystallisation sequence of soluble salts: relative humidity against amount of substance (mol). Sampling height: (105 cm) sampling depth interval: (1-3 cm). Fourth fieldwork visit: April 2005.

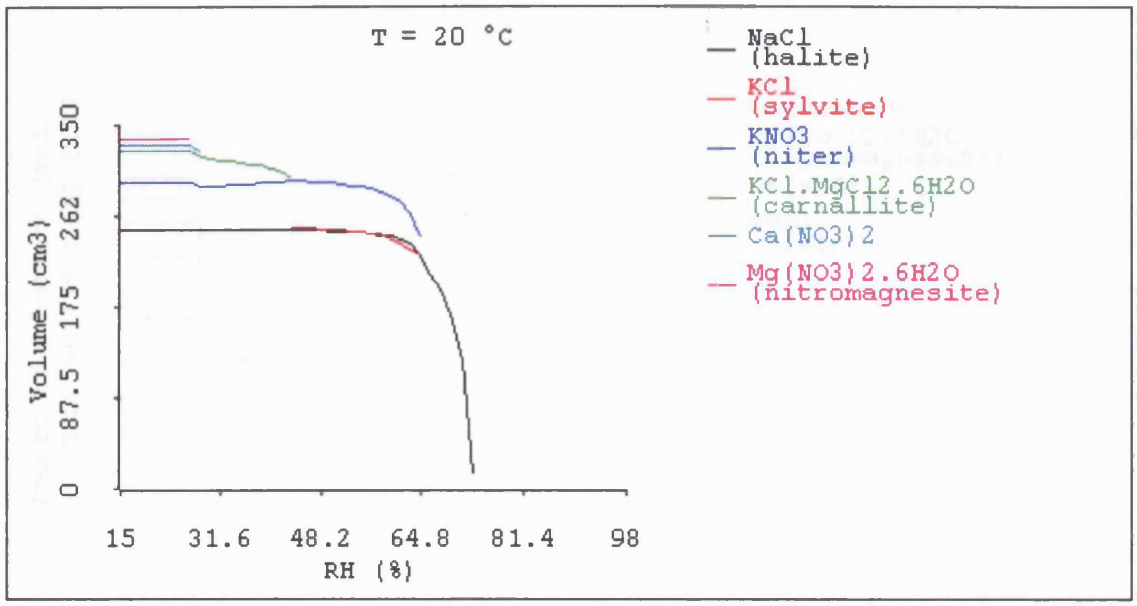

Figure (44N): Thermodynamic analysis using ECOS. Crystallisation sequence of soluble salts: relative humidity against volume of substance (cm^3). Sampling height: (105 cm) sampling depth interval: (1-3 cm). Fourth fieldwork visit: April 2005.

Appendix N: Thermodynamic analysis of the salt content in samples from the Palace Tomb (C1) using ECOS.

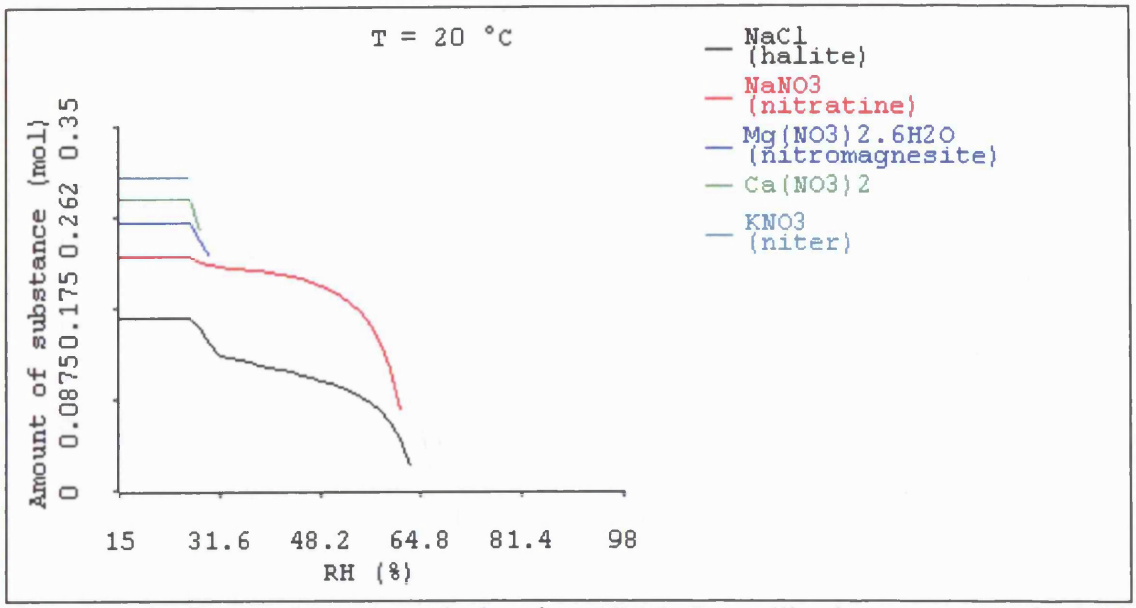

Figure (45N): Thermodynamic analysis using ECOS. Crystallisation sequence of soluble salts: relative humidity against amount of substance (mol). Sampling height: (355 cm) sampling depth interval: (1-3 cm). Fourth fieldwork visit: April 2005.

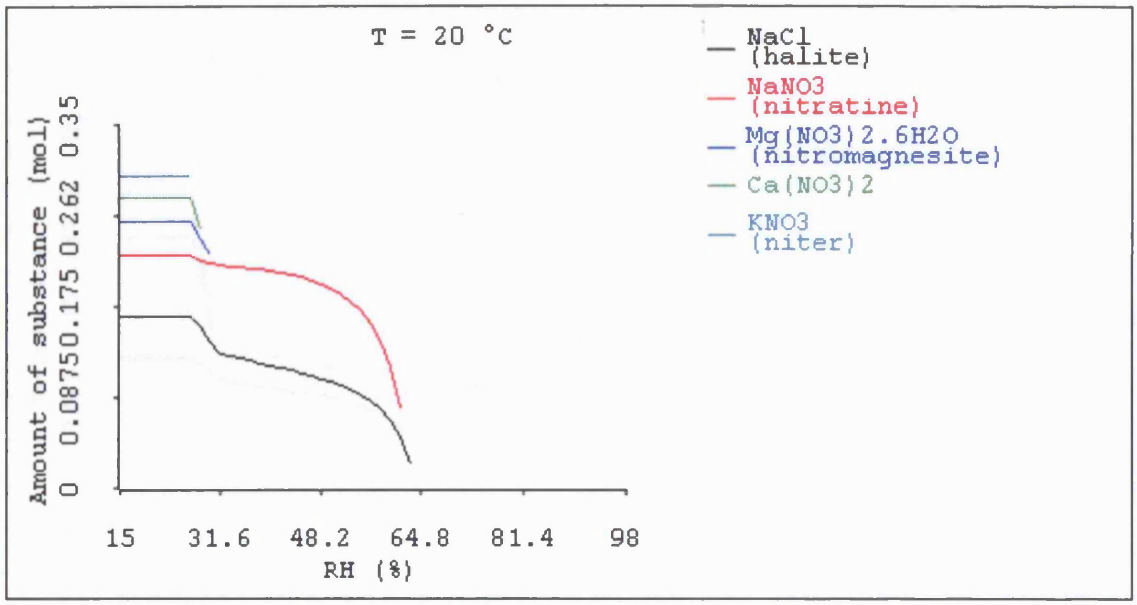

Figure (46N): Thermodynamic analysis using ECOS. Crystallisation sequence of soluble salts: relative humidity against volume of substance (cm^3). Sampling height: (355 cm) sampling depth interval: (1-3 cm). Fourth fieldwork visit: April 2005.

Appendix N: Thermodynamic analysis of the salt content in samples from the Palace Tomb (C1) using ECOS.

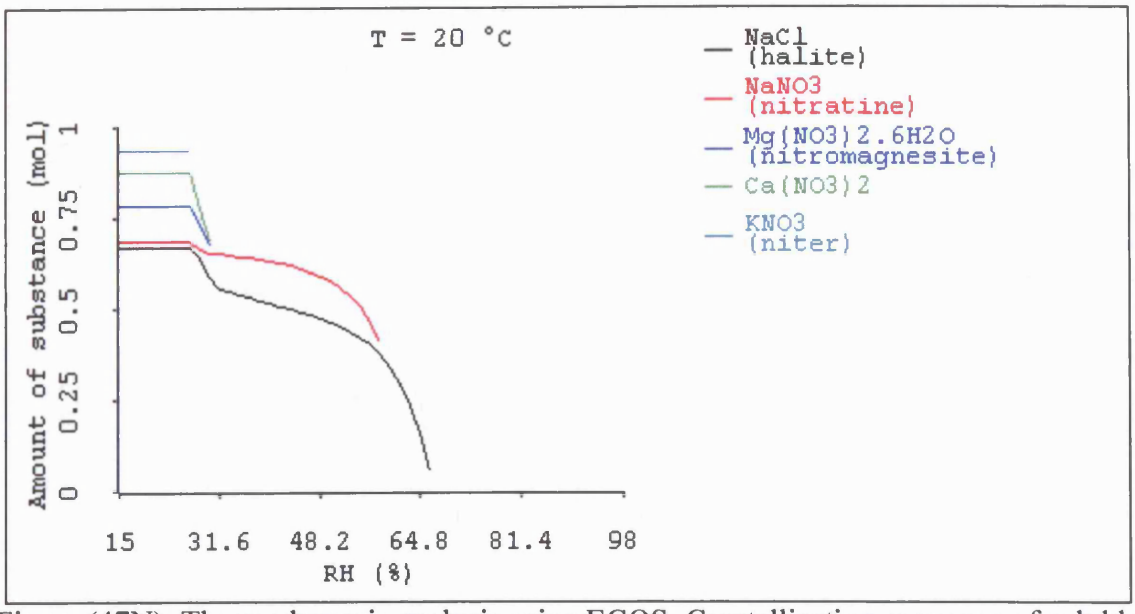

Figure (47N): Thermodynamic analysis using ECOS. Crystallisation sequence of soluble salts: relative humidity against amount of substance (mol). Sampling height: (505 cm) sampling depth interval: (0-1 cm). Fourth fieldwork visit: April 2005.

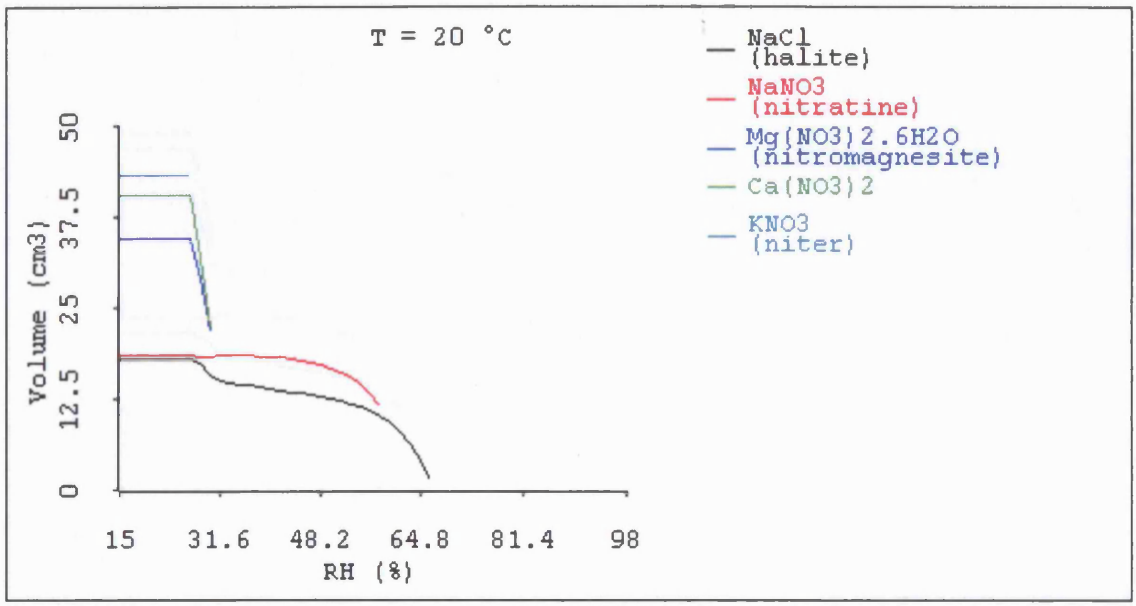

Figure (48N): Thermodynamic analysis using ECOS. Crystallisation sequence of soluble salts: relative humidity against volume of substance (cm^3). Sampling height: (505 cm) sampling depth interval: (0-1 cm). Fourth fieldwork visit: April 2005.

Appendix N: Thermodynamic analysis of the salt content in samples from the Palace Tomb (C1) using ECOS.

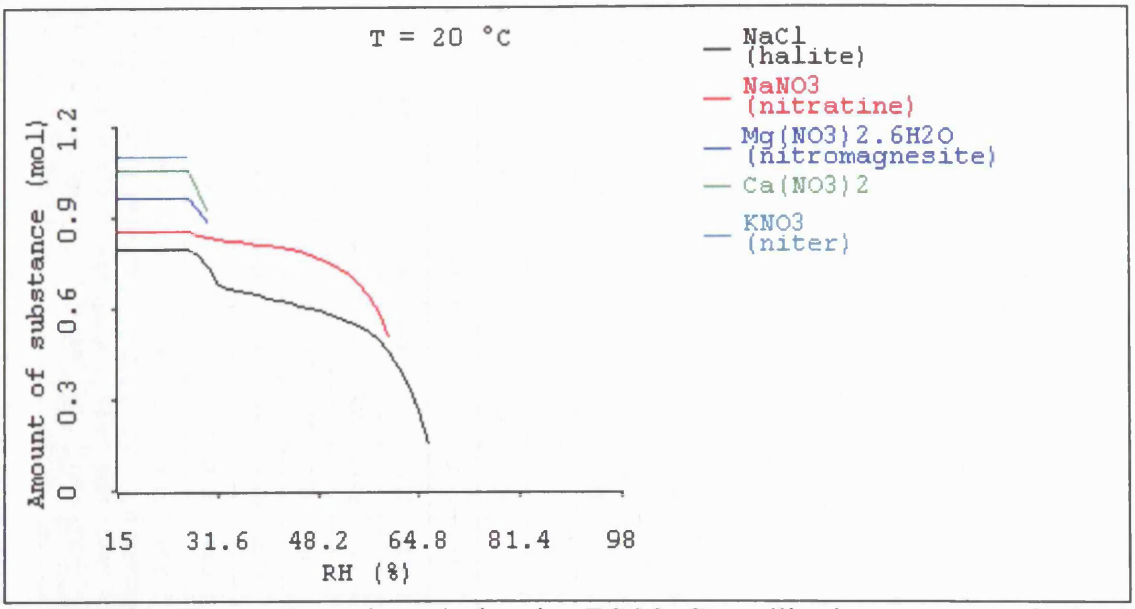

Figure (49N): Thermodynamic analysis using ECOS. Crystallisation sequence of soluble salts: relative humidity against amount of substance (mol). Sampling height: (505 cm) sampling depth interval: (1-3 cm). Fourth fieldwork visit: April 2005.

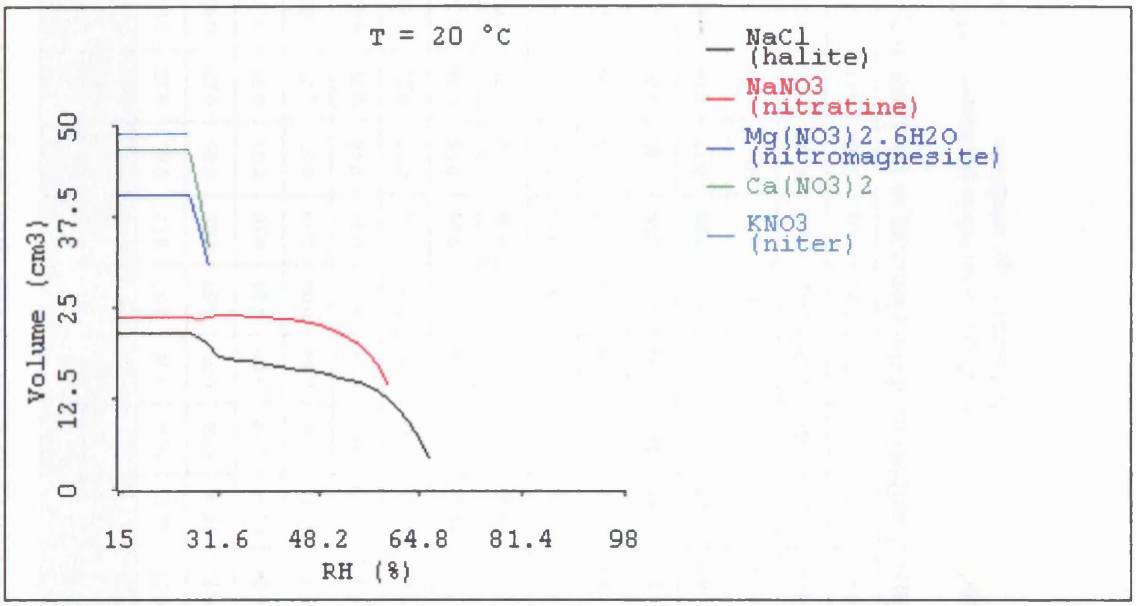

Figure (50N): Thermodynamic analysis using ECOS. Crystallisation sequence of soluble salts: relative humidity against volume of substance (cm^3). Sampling height: (505 cm) sampling depth interval: (1-3 cm). Fourth fieldwork visit: April 2005.

Appendix O: Distribution of elements in the laboratory tested specimens (expressed as oxides, %). X-ray fluorescence results.

Sample Code	Na_2O %	MgO %	Al_2O_3 %	SiO_2 %	P_2O_5 %	SO_3 %	Cl %	K_2O %	CaO %	TiO_2 %	MnO %	Fe_2O_3 %	Co_3O_4 µg/g	NiO µg/g	CuO µg/g	ZnO µg/g	SrO µg/g	ZrO_2 µg/g	Ba µg/g	PbO µg/g	Sum %
U	0.73	0.00	6.11	88.13	0.04	0.09	0.00	0.11	0.05	0.22	0.00	0.19	6.00	5.60	54.00	7.5	186.6	151.00	16.50	17.50	95.69
U_r01	0.00	0.00	6.17	88.06	0.04	0.09	0.00	0.10	0.05	0.22	0.00	0.19	0.00	9.80	52.60	6.4	184.9	158.90	14.40	18.40	94.93
U_r02	0.81	0.07	6.24	88.39	0.04	0.09	0.00	0.10	0.05	0.21	0.00	0.19	4.60	10.80	61.00	6.4	186.9	156.80	14.90	19.30	96.21
M	0.00	0.00	9.23	85.81	0.06	0.09	0.00	0.10	0.17	0.22	0.01	2.87	22.40	9.00	30.50	21.2	283.9	105.10	15.60	40.00	98.58
M_r01	0.83	0.08	9.45	86.39	0.07	0.09	0.00	0.11	0.16	0.22	0.01	2.88	29.50	7.10	30.80	18.6	285.7	103.80	16.70	39.30	100.32
M_r02	0.56	0.10	9.29	85.88	0.07	0.09	0.00	0.12	0.17	0.22	0.01	2.88	26.60	5.30	32.70	20.3	282.4	104.30	19.90	40.30	99.42
D	0.92	0.12	7.13	88.62	0.07	0.09	0.00	0.08	0.08	0.36	0.00	0.47	6.00	13.40	55.00	9.9	303.8	244.20	19.40	20.90	97.95
D_r01	0.74	0.11	7.10	88.90	0.07	0.09	0.00	0.08	0.09	0.36	0.00	0.48	9.30	11.30	50.00	8.5	306.5	248.10	14.40	19.40	98.04
D_r02	0.94	0.09	7.08	88.55	0.07	0.08	0.00	0.09	0.08	0.35	0.00	0.47	7.40	7.90	49.40	10.3	305.7	237.40	9.10	20.30	97.83
S	0.89	0.26	4.89	92.02	0.00	0.07	0.00	1.93	0.16	0.09	0.01	0.82	13.50	11.70	30.80	10.6	75.7	43.90	268.70	16.70	101.16
S_r01	0.00	0.07	4.62	91.65	0.01	0.06	0.00	1.90	0.16	0.09	0.01	0.82	0.00	10.20	31.60	12.8	75.7	41.70	275.70	14.80	99.40
S_r02	0.88	0.23	4.67	91.45	0.00	0.06	0.00	1.88	0.17	0.09	0.01	0.82	22.20	8.30	31.00	11.2	74.8	46.60	274.70	15.60	100.28
L	0.09	0.33	0.40	1.21	0.01	0.00	0.01	0.01	50.27	0.00	0.00	0.00	0.04	0.76	11.00	4.30	575.8	13.8	10.4	14.4	53.14
L_r01	0.08	0.35	0.39	1.21	0.01	0.00	0.01	0.01	50.48	0.00	0.00	0.00	0.04	0.77	11.00	4.40	574.8	8.4	10	14.1	53.36
L_r02	0.09	0.40	0.40	1.17	0.01	0.00	0.01	0.01	50.12	0.01	0.00	0.00	0.04	0.75	12.20	4.20	573	7.9	11	13.7	53.00

Table (O1): The original distribution of the elements in the laboratory test samples before the start of the tests (expressed as oxides, %).

Appendix key legend: U: Upper Umm Ishrin sandstone M: Middle Umm Ishrin sandstone D: Disi sandstone
S: Locharbriggs sandstone L: Monks Park limestone

Appendix P: Distribution of major elements in the laboratory tested specimens. X-ray diffraction results.

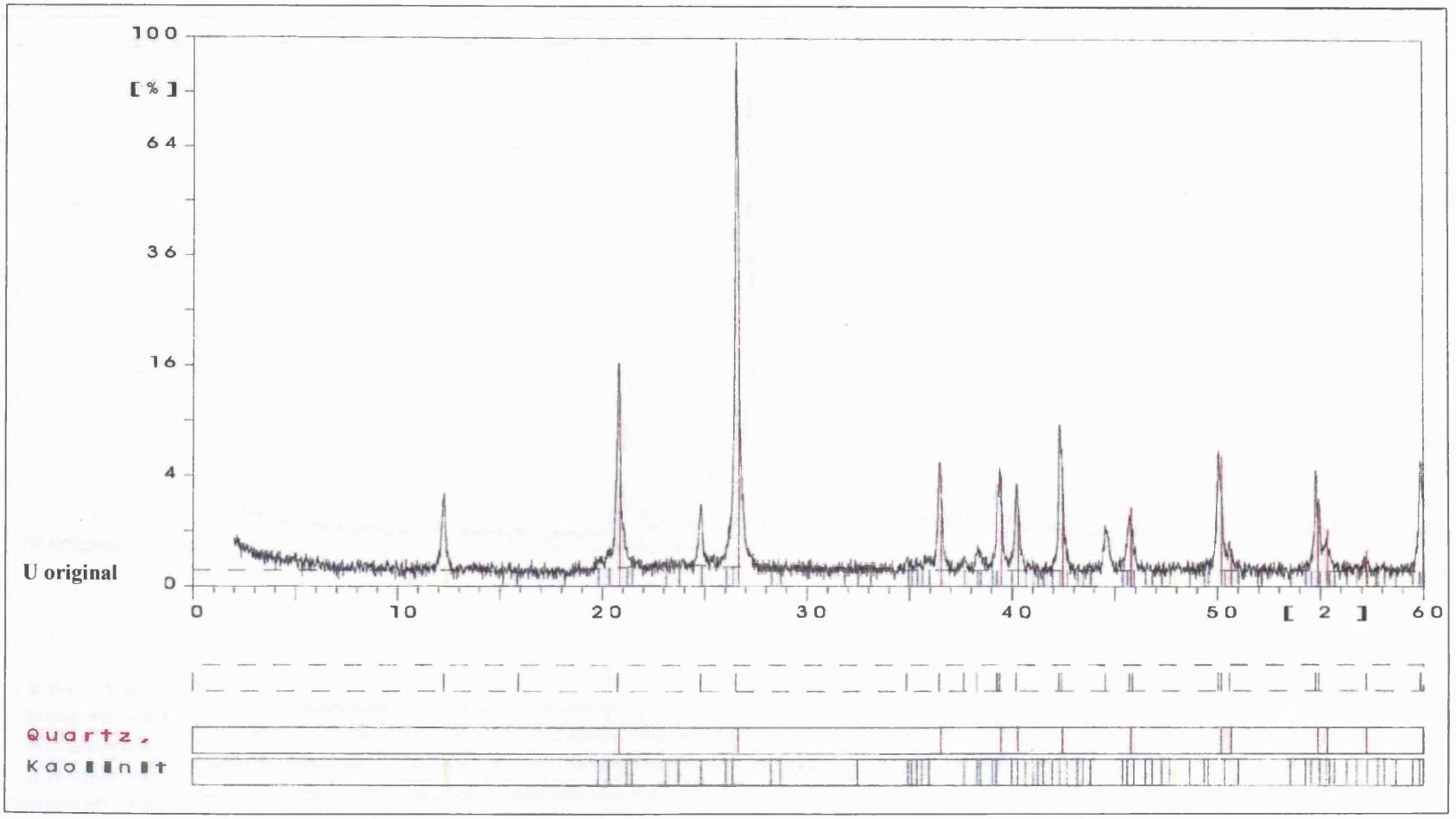

Figure (P1): The X-ray diffraction pattern of the Upper Umm Ishrin sandstone specimens. Analysis type: Non-preferred orientated sample.

Appendix P: Distribution of major elements in the laboratory tested specimens. X-ray diffraction results.

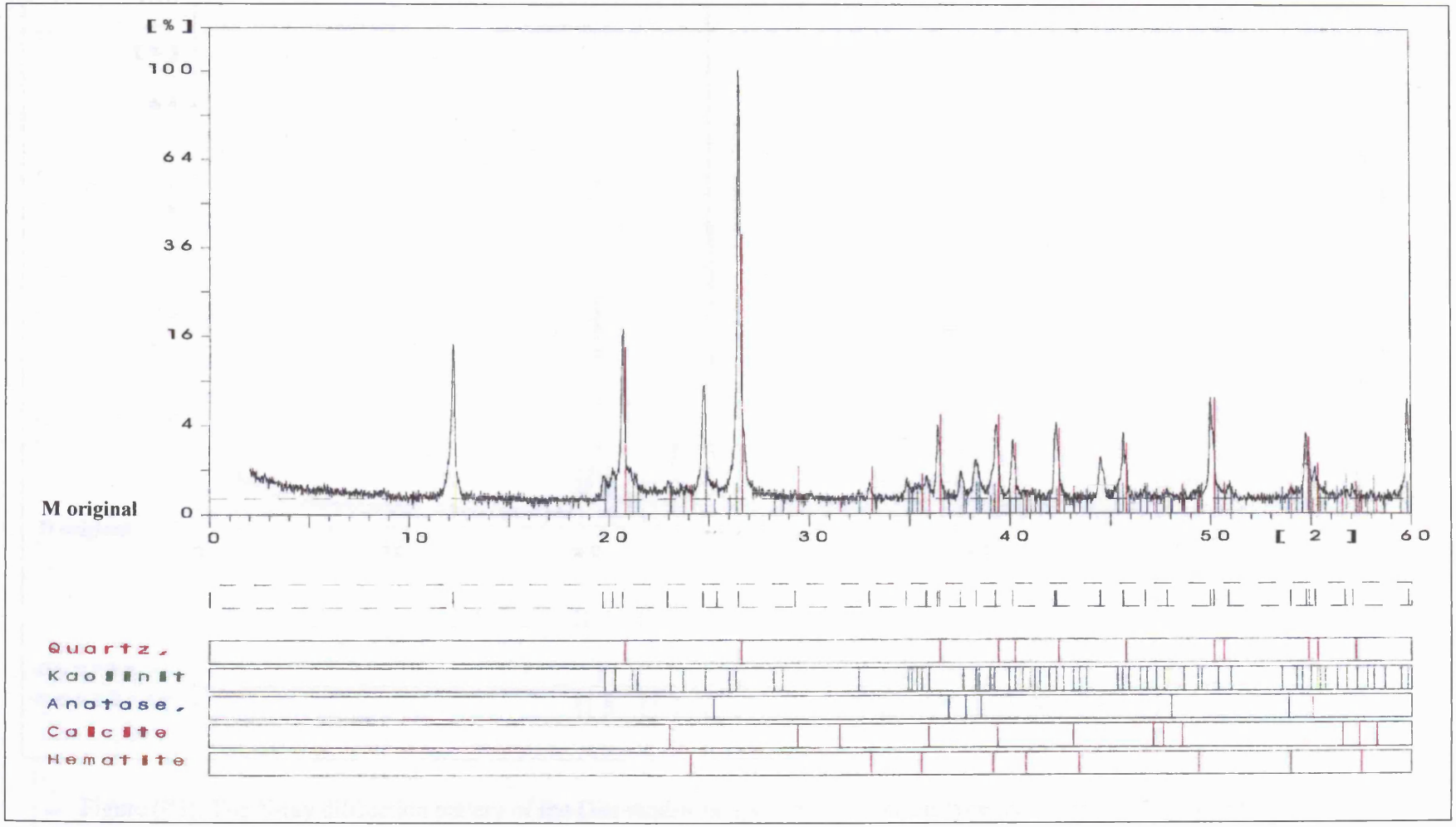

Figure (P2): The X-ray diffraction pattern of the Middle Umm Ishrin sandstone specimens. Analysis type: Non-preferred orientated sample.

Appendix P: Distribution of major elements in the laboratory tested specimens. X-ray diffraction results.

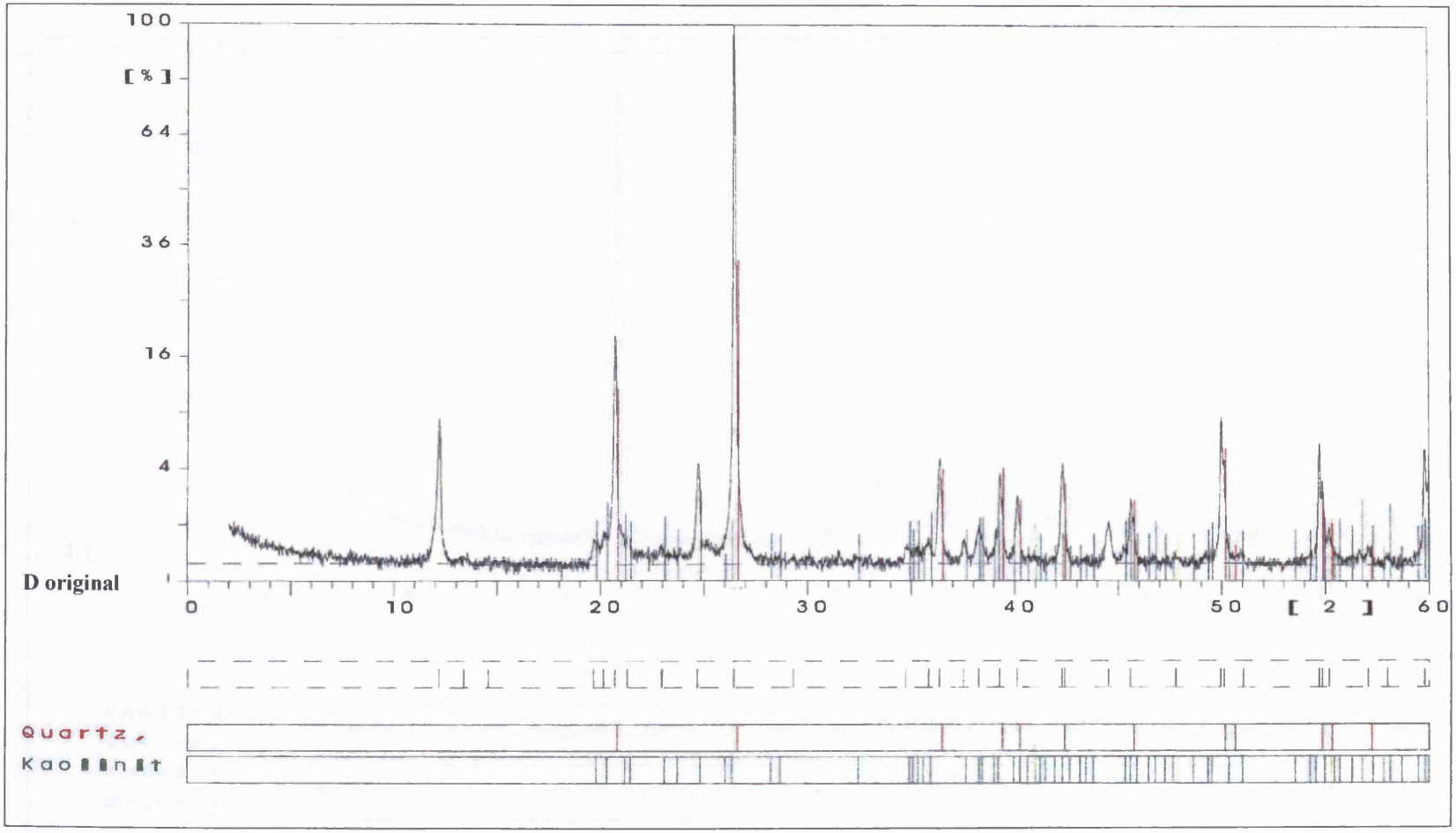

Figure (P3): The X-ray diffraction pattern of the Disi sandstone specimens. Analysis type: Non-preferred orientated sample.

Appendix P: Distribution of major elements in the laboratory tested specimens. X-ray diffraction results.

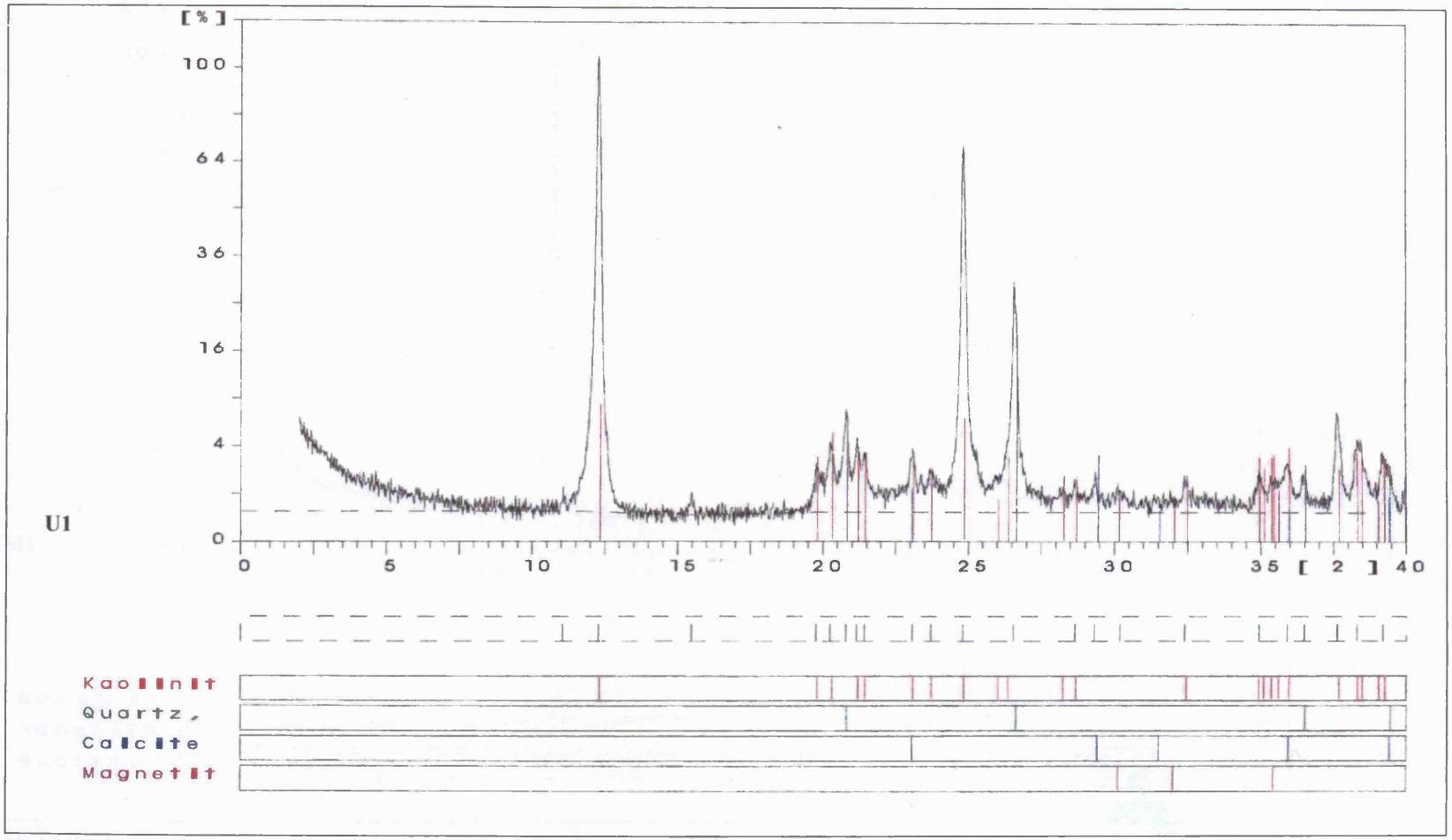

Figure (P4): The X-ray diffraction pattern of the Upper Umm Ishrin sandstone specimens. Analysis type: preferred orientated sample.

Appendix P: Distribution of major elements in the laboratory tested specimens. X-ray diffraction results.

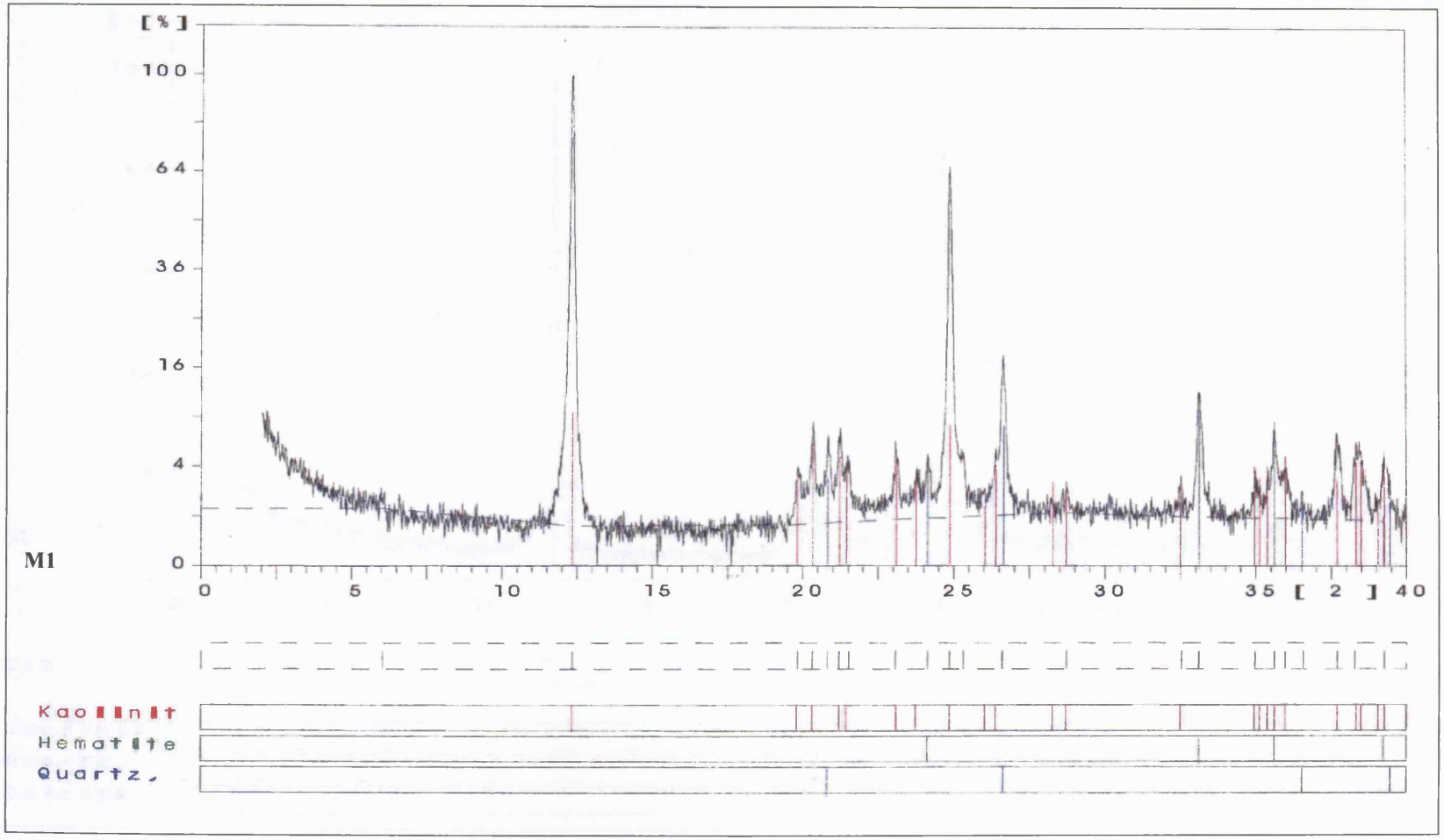

Figure (P5): The X-ray diffraction pattern of the Middle Umm Ishrin sandstone specimens. Analysis type: preferred orientated sample.

Appendix P: Distribution of major elements in the laboratory tested specimens. X-ray diffraction results.

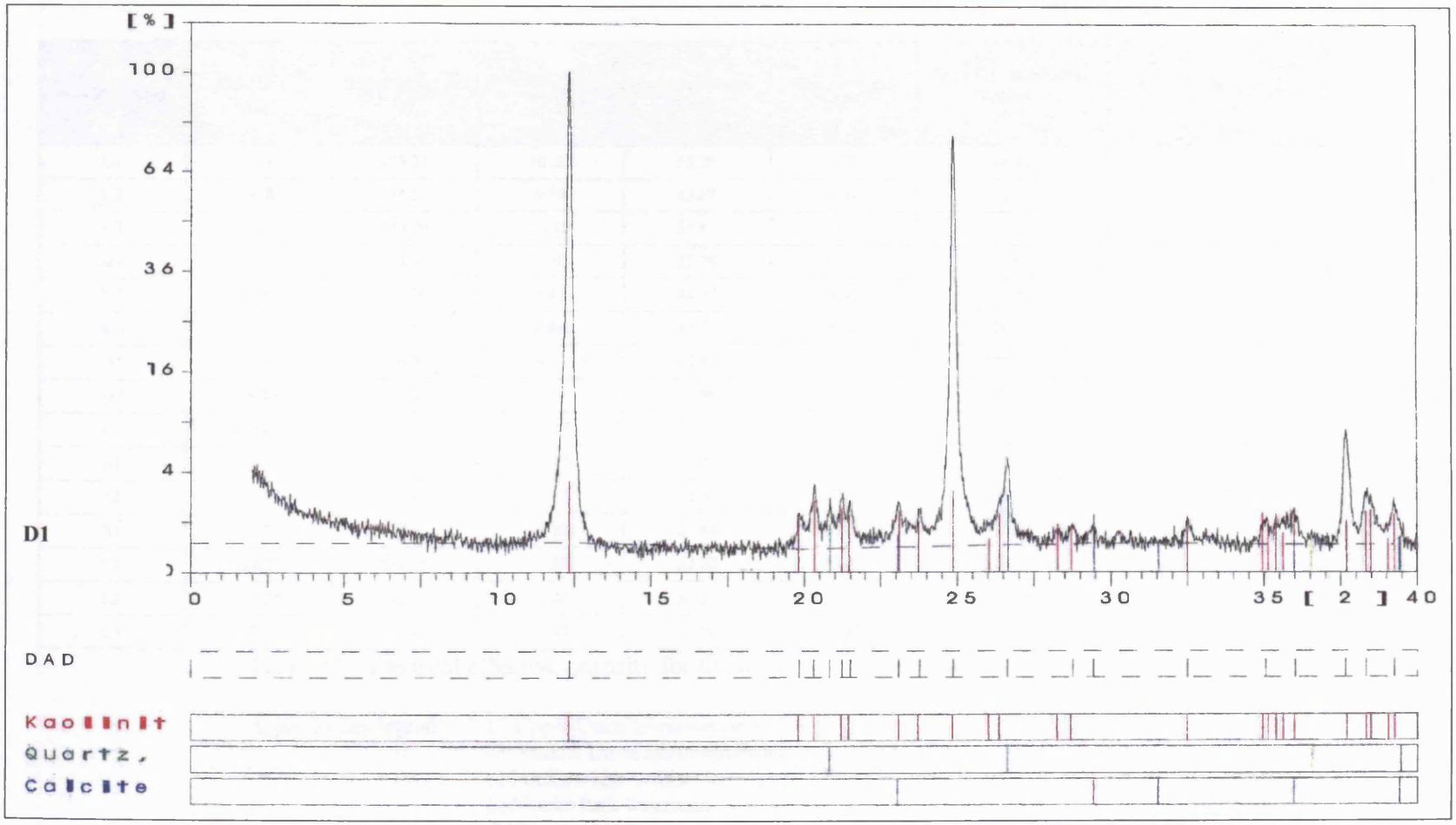

Figure (P6): The X-ray diffraction pattern of the Disi sandstone specimens. Analysis type: preferred orientated sample.

Appendix Q: Results of total effective porosity (%) of the laboratory tested specimens.

Sample number	Dry weight (g)	Saturated weight (g)	Weight of the water (g)	Sample volume (cm^3)	Water volume (cm^3)	Sample total effective porosity (%)	Average total effective porosity (%)
U1	123.11	133.33	10..22	55.30	10..22	18.48	19.08
U2	104.87	114.21	9.34	45.62	9.34	20.47	
U3	124.08	134.20	10.12	55.81	10.12	18.29	
M1	123.68	134.60	10.92	55.78	10.92	20.69	20.40
M2	95.58	103.99	8.41	41.33	8.41	20.35	
M3	84.26	91.06	6.80	33.71	6.80	20.17	
D1	100.88	110.32	9.44	43.85	9.44	21.52	20.98
D2	98.75	107.34	8.59	42.40	8.59	20.26	
D3	134.03	146.20	12.17	58.24	12.17	20.90	
S1	110.09	121.36	11.27	54.02	11.27	20.86	20.87
S2	107.23	117.95	10.72	52.36	10.72	20.47	
S3	105.78	116.67	10.89	51.84	10.89	21.01	
L1	124.27	137.07	12.80	57.80	12.80	22.15	21.92
L2	121.25	133.69	12.44	56.32	12.44	22.09	
L3	127.10	140.47	13.37	62.09	13.37	21.53	

Table (Q): The total effective porosity for the laboratory test specimens.

Appendix key legend:
U: Upper Umm Ishrin sandstone
M: Middle Umm Ishrin sandstone
S: Locharbriggs sandstone
L: Monks Park limestone
D: Disi sandstone

Appendix R: Water absorption measurements for the laboratory tested specimens.

Sample number	Original dry weight (g)	Dry mass after 24 hours of drying at 105°C (g)	Dry mass after 46 hours of drying at 105°C (g)	Dry mass after 47 hours of drying at 105°C (g)	Dry mass after 48 hours of drying at 105°C (g) (A)	Saturated mass after 24 hours of immersing in de-ionized water (g)	Saturated mass after 48 hours of immersing in de-ionized water (g) (B)	Saturated mass after immersing and boiling for 5hours and cooling naturally for 14 hours (g) (C)	Absorption after immersion [(B-A)/A]*100 (%)	Absorption after immersion and boiling [(C-A)/A]*100 (%)
U1	109.03	108.44	108.18	108.18	108.17	114.09	114.01	115.52	5.40	6.79
U2	133.09	132.67	132.58	132.54	132.54	139.22	139.04	140.51	4.90	6.01
U3	104.78	104.34	104.24	104.22	104.22	111.71	111.56	113.41	7.00	8.80
M1	100.16	100.14	100.12	100.12	100.12	105.04	105.03	105.32	4.90	5.19
M2	132.66	132.61	132.60	132.58	132.58	138.13	138.09	138.38	4.20	4.40
M3	84.21	84.17	84.17	84.14	84.14	90.41	90.39	90.73	7.40	7.80
D1	108.22	108.17	108.14	108.13	108.13	114.21	114.14	114.58	5.56	5.96
D2	103.65	103.58	103.56	103.54	103.54	110.87	110.85	111.02	7.06	7.22
D3	98.75	98.72	98.72	98.71	98.70	105.01	105.52	105.93	6.90	7.32
S1	107.34	107.11	107.03	107.01	107.00	115.26	115.38	119.18	7.80	11.40
S2	110.04	109.89	109.77	109.74	109.74	118.02	118.08	122.35	7.60	11.50
S3	105.66	105.39	105.31	105.31	105.31	112.96	113.02	115.29	7.30	9.50
L1	131.11	130.99	130.92	130.92	130.91	140.04	142.78	143.33	9.10	9.50
L2	121.19	121.01	120.90	120.89	120.89	130.87	132.62	133.80	9.70	10.70
L3	124.19	123.97	123.91	123.88	123.88	135.34	137.14	138.28	11.00	12.00

Table (R1): Water absorption measurement for the laboratory test specimens.

Appendix key legend: U: Upper Umm Ishrin sandstone M: Middle Umm Ishrin sandstone D: Disi sandstone
S: Locharbriggs sandstone L: Monks Park limestone

Appendix S: Drying- wetting measurements for the laboratory tested specimens.

Sample Number	Original dry Weight (g)	Dry weight 1st Cycle (g)	Dry weight 2nd cycle (g)	Dry weight 3rd cycle (g)	Dry weight 4th cycle (g)	Dry Weight 5th cycle (g)	Dry Weight 6th cycle (g)	Dry weight 7th cycle (g)	Dry weight 8th cycle (g)	Dry weight 9th cycle (g)	Dry weight 10th cycle (g)	Dry weight 11th cycle (g)	Dry weight 12th cycle (g)	Dry weight 13th cycle (g)	Dry weight 14th cycle (g)	Dry weight 15th cycle (g)
U1	105.59	104.09	103.88	103.69	103.56	103.54	103.55	103.52	103.43	103.40	103.39	103.37	103.38	103.37	103.36	103.37
U2	114.12	114.08	114.00	114.01	113.47	113.45	113.39	113.40	113.37	113.36	113.24	113.14	112.87	112.88	112.80	112.79
U3	98.43	98.22	98.11	97.99	97.78	97.71	97.76	97.51	97.44	97.41	97.31	97.02	96.79	96.76	96.75	96.74
M1	86.67	85.95	85.84	85.73	85.66	85.64	85.60	85.56	85.49	85.40	85.10	85.11	84.89	84.83	84.69	84.33
M2	91.65	91.41	91.39	91.31	91.26	91.25	91.22	90.87	90.39	90.25	90.15	90.13	90.14	90.15	90.13	90.14
M3	131.12	131.04	131.07	130.99	131.02	131.00	130.99	131.00	131.00	130.96	130.95	130.95	130.96	130.95	130.94	130.95
D1	107.44	107.22	107.10	106.89	106.85	106.74	106.73	106.70	106.54	106.47	106.49	106.40	106.35	106.30	106.14	106.09
D2	85.14	85.01	84.51	84.33	83.25	83.01	82.87	82.23	82.01	81.54	81.29	81.19	80.29	80.22	79.89	79.71
D3	99.21	99.12	98.74	98.41	98.12	97.54	97.35	96.54	96.12	95.57	95.50	94.32	93.01	92.17	90.28	89.56
S1	110.47	110.10	110.09	110.09	110.07	110.07	110.06	110.14	110.07	110.07	110.08	110.13	110.18	110.19	110.20	110.19
S2	105.62	105.45	105.41	105.39	105.32	105.32	105.31	105.30	105.26	105.25	105.25	105.24	105.26	105.25	105.24	105.22
S3	107.85	107.53	107.50	107.42	107.37	107.37	107.37	107.36	107.31	107.31	107.30	107..29	107.30	107.29	107.23	107.24
L1	133.61	133.34	133.34	133.33	133.28	133.28	133.26	133.29	133.25	133.25	133.25	133.25	133.25	133.24	133.24	133.24
L2	125.10	125.12	125.06	125.00	124.97	124.94	124.93	124.95	124.93	124.92	124.93	124.92	124.99	125.00	124.98	124.99
L3	131.25	131.10	131.10	131.10	131.09	131.08	131.06	131.05	131.02	131.02	131.03	131.03	131.02	131.03	131.01	131.00

Table (S1): The dry weight of the laboratory test specimens during the drying-wetting test.

Sample Number	ΔM (mass loss or gain) after the drying - wetting test (%)	Sample Number	ΔM (mass loss or gain) after the drying - wetting test (%)	Sample Number	ΔM (mass loss or gain) after the drying - wetting test (%)	Sample Number	ΔM (mass loss or gain) after the drying - wetting test (%)	Sample Number	ΔM (mass loss or gain) after the drying - wetting test (%)
U1	-2.10	M1	-2.70	D1	-1.28	S1	-0.25	S1	-0.28
U2	-1.71	M2	-1.65	D2	-6.37	S2	-0.39	S2	-0.09
U3	-1.71	M3	-0.13	D3	-9.23	S3	-0.57	S3	-0.19

Table (S2): The mass loss or gain after the drying - wetting test.

Appendix key legend: U: Upper Umm Ishrin sandstone M: Middle Umm Ishrin sandstone D: Disi sandstone S: Locharbriggs sandstone L: Monks Park limestone

Appendix S: Drying- wetting measurements for the laboratory tested specimens.

Sample Number	Original dry Weight (g)	Wet weight 1st Cycle (g)	Wet weight 2nd cycle (g)	Wet weight 3rd cycle (g)	Wet weight 4th cycle (g)	Wet Weight 5th cycle (g)	Wet Weight 6th cycle (g)	Wet weight 7th cycle (g)	Wet weight 8th cycle (g)	Wet weight 9th cycle (g)	Wet weight 10th cycle (g)	Wet weight 11th cycle (g)	Wet weight 12th cycle (g)	Wet weight 13th cycle (g)	Wet weight 14th cycle (g)	Wet weight 15th cycle (g)
U1	105.59	111.69	111.05	111.19	110.09	110.58	110.06	110.70	110.48	110.40	110.46	109.48	110.49	110.50	110. 44	110.41
U2	114.12	120.23	120.18	120.01	120.58	120.55	120.40	120.33	120.39	120.35	120.20	120.01	119.74	119.61	119.58	119.43
U3	98.43	104.47	104.33	104.12	103.87	103.80	103.71	103.61	103.52	103.41	103.38	103.10	102.91	102.84	102.80	102.67
M1	86.67	92.56	92.49	92.41	92.29	92.36	92.33	92.15	92.14	92.08	91.79	91.75	91.62	91.53	91.43	91.28
M2	91.65	98.64	98.61	98.55	98.47	98.45	98.36	97.87	97.85	97.59	97.58	97.49	97.45	97.34	97.08	96.87
M3	131.12	138.32	138.22	138.30	138.25	138.14	138.17	138.21	138.23	138.22	138.14	138.10	138.08	137.98	137.84	137.82
D1	107.44	113.325	113.25	112.86	112.80	112.74	112.71	112.64	112.62	112.64	112.45	112.47	112.44	112.32	112.28	112.19
D2	85.14	91.58	90.89	90.74	90.71	90.66	90.28	89.81	89.59	89.03	88.93	87.86	86.69	85.74	85.47	85.31
D3	99.21	106.28	106.13	105.84	105.51	105.32	104.85	104.12	103.57	103.25	103.01	101.28	100.28	97.58	95.87	94.74
S1	110.47	118.69	118.66	118.67	118.97	118.86	118.86	119.25	118.86	119.02	118.59	119.14	119.09	119.16	119.13	119.09
S2	105.62	113.55	113.49	113.56	113.33	113.59	113.60	113.68	113.66	113.65	113.55	113.69	113.72	113.66	113.60	113.49
S3	107.85	115.46	115.45	115.45	115.60	115.54	115.37	115.53	115.56	115.59	115.49	115.52	115.56	115.63	115.64	115.53
L1	133.61	145.08	145.08	145.45	145.18	144.97	145.10	145.19	145.18	145.02	145.07	145.16	145.19	145.19	145.19	145.19
L2	125.10	136.98	136.91	137.01	136.89	136.95	136.94	136.99	137.01	136.99	137.00	137.08	137.07	137.14	137.20	137.26
L3	131.25	143.88	143.14	143.13	143.25	143.19	143.22	143.30	143.30	143.26	143.22	143.19	143.12	143.18	143.19	143.23

Table (S3): The wet weight of the laboratory test specimens during the drying-wetting test.

Appendix key legend:
U: Upper Umm Ishrin sandstone
M: Middle Umm Ishrin sandstone
D: Disi sandstone
S: Locharbriggs sandstone
L: Monks Park limestone

Modified salt crystallisation test results

Appendix T and U key legend

U: sandstone sample from upper Umm Ishrin sandstone formation (Deir Tomb).

M: sandstone sample from middle Umm Ishrin sandstone formation (Palace Tomb).

D: sandstone sample from Disi sandstone formation (Bab al Siq Triclinium Tomb).

S: laboratory test sandstone: Locharbriggs sandstone, UK.

L: laboratory test limestone: Monks Park limestone, UK.

Ds: de-ionised water.

First run conditions: low relative humidity and low wind speed.

Second run conditions: low relative humidity and high wind speed.

Third run conditions: low relative humidity and fluctuating wind speed.

Fourth run conditions: high relative humidity and low wind speed.

Fifth run conditions: high relative humidity and high wind speed.

Sixth run conditions: high relative humidity and fluctuating wind speed.

ΔW: weight loss or gain

Appendix T: Modified salt crystallisation test results.
Sodium sulfate solution: First run.

Sample number	Original Dry Weight + weight of the label (g)	Weight after 1st cycle (g)	Weight after the 2nd cycle (g)	Weight after the 3rd cycle (g)	Weight after the 4th cycle (g)	Weight after the 5th cycle (g)	Weight after the 6th cycle (g)	Weight after the 7th cycle (g)	Weight after the 8th cycle (g)	Weight after the 9th cycle (g)	Weight after the 10th cycle (g)	Weight after the 11th cycle (g)	Weight after the 12th cycle (g)	Weight after the 13th cycle (g)	Weight after the 14th cycle (g)	Weight after the 15th cycle (g)	Weight after the 16th cycle (g)	ΔW (%)
L3	120.680	133.095	132.166	126.766	128.858	123.902	122.207	120.529	115.170	104.578	103.668	101.886	95.704	86.172	67.994	49.587	33.657	-66.34
L4	120.887	134.747	128.958	115.259	117.931	92.087	83.982	73.981	66.384	56.791	44.194	29.804	0.000	0.000	0.000	0.000	0.000	-100.00
S3	107.177	113.016	113.469	116.345	116.261	113.990	115.884	113.328	108.957	111.702	108.720	107.828	105.360	107.324	103.541	99.874	87.894	-12.11
S4	107.850	113.768	114.190	115.009	114.727	112.673	113.048	111.555	103.596	105.901	101.054	83.831	77.127	71.800	58.799	47.963	40.410	-59.59
U2	110.259	110.998	107.896	100.218	99.898	90.254	65.235	13.254	5.287	0.000	0.000	0.000	0.000	0.000	0.000	0.000	0.000	-100.00
M2	123.271	126.691	123.625	111.701	111.655	85.686	10.604	0.000	0.000	0.000	0.000	0.000	0.000	0.000	0.000	0.000	0.000	-100.00
D2	104.596	105.012	43.853	4.408	0.000	0.000	0.000	0.000	0.000	0.000	0.000	0.000	0.000	0.000	0.000	0.000	0.000	-100.00

Table (T1): The dry weight of the sandstone and limestone samples immersed in saturated sodium sulfate solution and dried for 24-hours at low relative humidity and low wind speed conditions.

Sample number	Original Dry Weight + weight of the label (g)	Wet Weight before the 1st cycle (g)	Wet Weight before the 2nd cycle (g)	Wet Weight before the 3rd cycle (g)	Wet Weight before the 4th cycle (g)	Wet Weight before the 5th cycle (g)	Wet Weight before the 6th cycle (g)	Wet Weight before the 7th cycle (g)	Wet Weight before the 8th cycle (g)	Wet Weight before the 9th cycle (g)	Wet Weight before the 10th cycle 100 (g)	Wet Weight before the 11th cycle (g)	Wet Weight before the 12th cycle (g)	Wet Weight before the 13th cycle (g)	Wet Weight before the 14th cycle (g)	Wet Weight before the 15th cycle (g)	Wet Weight before the 16th cycle (g)
L3	120.680	137.740	136.289	133.838	131.745	131.399	127.698	126.099	120.521	109.691	108.579	108.344	102.389	90.902	68.981	53.698	37.001
L4	120.887	140.199	135.381	122.996	122.041	102.044	90.048	82.715	70.885	62.628	49.646	35.499	0.000	0.000	0.000	0.000	0.000
S3	107.177	117.937	119.488	122.782	120.624	126.118	122.667	119.707	114.309	123.125	120.615	118.748	114.837	122.272	129.795	108.541	99.025
S4	107.850	117.611	119.247	121.409	119.051	121.939	123.403	119.565	119.661	120.467	116.022	106.852	88.348	103.043	94.185	58.213	49.632
U2	110.259	115.589	113.785	106.471	106.002	97.107	74.023	20.014	13.698	0.000	0.000	0.000	0.000	0.000	0.000	0.000	0.000
M2	123.271	129.379	128.294	121.902	116.919	98.859	22.376	0.000	0.000	0.000	0.000	0.000	0.000	0.000	0.000	0.000	0.000
D2	104.596	111.680	52.436	12.409	0.000	0.000	0.000	0.000	0.000	0.000	0.000	0.000	0.000	0.000	0.000	0.000	0.000

Table (T2): The wet weight of the sandstone and limestone samples after immersing in saturated sodium sulfate solution and before the drying cycle (low relative humidity and low wind speed).

Appendix T: Modified salt crystallisation test results
Sodium sulfate solution: Second run.

Sample number	Original Dry Weight + weight of the label (g)	Weight after 1st cycle (g)	Weight after the 2nd cycle (g)	Weight after the 3rd cycle (g)	Weight after the 4th cycle (g)	Weight after the 5th cycle (g)	Weight after the 6th cycle (g)	Weight after the 7th cycle (g)	Weight after the 8th cycle (g)	Weight after the 9th cycle (g)	Weight after the 10th cycle (g)	Weight after the 11th cycle (g)	Weight after the 12th cycle (g)	Weight after the 13th cycle (g)	Weight after the 14th cycle (g)	Weight after the 15th cycle (g)	Weight after the 16th cycle (g)	ΔW (%)
L3	123.633	140.398	137.183	131.014	128.995	113.355	99.940	98.193	95.147	95.929	95.761	90.397	88.726	88.395	86.247	85.651	84.571	-15.43
L4	119.009	133.351	129.930	125.365	124.893	118.987	117.940	116.044	114.487	112.337	101.736	89.619	87.119	87.187	86.010	85.233	81.545	-18.46
S3	108.152	114.397	114.379	113.103	112.569	117.665	116.964	114.146	112.416	110.423	111.032	110.058	105.877	88.158	63.920	59.728	40.596	-59.40
S4	105.541	111.597	112.421	109.621	113.910	114.467	114.042	108.873	90.989	92.004	92.447	92.879	90.336	68.158	57.732	48.202	40.733	-61.40
U2	93.444	96.524	76.259	56.999	36.001	18.591	5.871	0.000	0.000	0.000	0.000	0.000	0.000	0.000	0.000	0.000	0.000	-100.00
M2	86.455	87.592	68.323	42.387	40.968	13.547	3.030	0.000	0.000	0.000	0.000	0.000	0.000	0.000	0.000	0.000	0.000	-100.00
D2	100.180	102.344	77.966	13.905	2.894	0.000	0.000	0.000	0.000	0.000	0.000	0.000	0.000	0.000	0.000	0.000	0.000	-100.00

Table (T3): The dry weight of the sandstone and limestone samples immersed in saturated sodium sulfate solution and dried for 24-hours at low relative humidity and high wind speed conditions

Sample number	Original Dry Weight + weight of the label (g)	Wet Weight before the 1st cycle (g)	Wet Weight before the 2nd cycle (g)	Wet Weight before the 3rd cycle (g)	Wet Weight before the 4th cycle (g)	Wet Weight before the 5th cycle (g)	Wet Weight before the 6th cycle (g)	Wet Weight before the 7th cycle (g)	Wet Weight before the 8th cycle (g)	Wet Weight before the 9th cycle (g)	Wet Weight before the 10th cycle 100 (g)	Wet Weight before the 11th cycle (g)	Wet Weight before the 12th cycle (g)	Wet Weight before the 13th cycle (g)	Wet Weight before the 14th cycle (g)	Wet Weight before the 15th cycle (g)	Wet Weight before the 16th cycle (g)
L3	123.633	143.584	143.103	137.889	142.057	123.668	102.177	101.184	98.726	99.667	100.261	94.411	91.868	90.430	90.668	88.062	88.249
L4	119.009	138.137	135.177	131.808	135.110	123.619	121.654	118.830	117.562	117.743	107.386	92.448	90.273	89.918	89.917	87.359	84.006
S3	108.152	117.787	119.105	122.414	131.163	125.765	125.289	121.757	121.528	127.480	124.672	129.191	122.126	101.895	73.520	79.582	66.359
S4	105.541	118.266	116.555	118.526	131.726	125.320	124.229	124.278	107.663	111.369	115.426	122.775	118.767	79.765	67.443	55.030	46.560
U2	93.444	96.994	80.147	49.017	45.547	24.547	12.217	0.000	0.000	0.000	0.000	0.000	0.000	0.000	0.000	0.000	0.000
M2	86.455	90.147	73.159	49.287	48.889	20.144	9.147	0.000	0.000	0.000	0.000	0.000	0.000	0.000	0.000	0.000	0.000
D2	100.180	100.478	88.459	22.547	10.214	2.014	0.000	0.000	0.000	0.000	0.000	0.000	0.000	0.000	0.000	0.000	0.000

Table (T4): The wet weight of the sandstone and limestone samples after immersing in saturated sodium sulfate solution and before the drying cycle (low relative humidity and high wind speed).

Appendix T: Modified salt crystallisation test results
Sodium sulfate solution: Third run.

Sample number	Original Dry Weight + weight of the label (g)	Weight after 1st cycle (g)	Weight after the 2nd cycle (g)	Weight after the 3rd cycle (g)	Weight after the 4th cycle (g)	Weight after the 5th cycle (g)	Weight after the 6th cycle (g)	Weight after the 7th cycle (g)	Weight after the 8th cycle (g)	Weight after the 9th cycle (g)	Weight after the 10th cycle (g)	Weight after the 11th cycle (g)	Weight after the 12th cycle (g)	Weight after the 13th cycle (g)	Weight after the 14th cycle (g)	Weight after the 15th cycle (g)	Weight after the 16th cycle (g)	ΔW (%)
L3	130.796	141.537	143.986	143.695	142.537	142.056	141.829	140.580	139.963	138.053	135.616	134.041	129.724	110.557	95.009	80.247	70.547	-29.45
L4	119.613	134.350	132.327	124.832	117.425	110.646	106.276	100.482	97.745	63.536	46.030	15.218	0.000	0.000	0.000	0.000	0.000	-100.00
S3	110.195	115.573	115.076	116.844	114.361	114.828	111.311	111.144	108.153	110.426	107.446	105.672	68.350	57.705	50.147	42.014	27.874	-74.70
S4	107.570	112.682	113.132	113.207	112.545	115.142	111.212	111.806	109.112	107.532	106.446	103.345	88.503	81.472	72.149	55.014	45.012	-58.15
U2	108.657	110.367	90.140	72.325	60.218	51.021	33.214	12.014	0.000	0.000	0.000	0.000	0.000	0.000	0.000	0.000	0.000	-100.00
M2	93.590	96.856	84.211	68.748	54.125	40.939	13.594	0.000	0.000	0.000	0.000	0.000	0.000	0.000	0.000	0.000	0.000	-100.00
D2	115.919	111.418	12.915	0.000	0.000	0.000	0.000	0.000	0.000	0.000	0.000	0.000	0.000	0.000	0.000	0.000	0.000	-100.00

Table (T5): The dry weight of the sandstone and limestone samples immersed in saturated sodium sulfate solution and dried for 24-hours at low relative humidity and fluctuating wind speed conditions

Sample number	Original Dry Weight + weight of the label (g)	Wet Weight before the 1st cycle (g)	Wet Weight before the 2nd cycle (g)	Wet Weight before the 3rd cycle (g)	Wet Weight before the 4th cycle (g)	Wet Weight before the 5th cycle (g)	Wet Weight before the 6th cycle (g)	Wet Weight before the 7th cycle (g)	Wet Weight before the 8th cycle (g)	Wet Weight before the 9th cycle (g)	Wet Weight before the 10th cycle 100 (g)	Wet Weight before the 11th cycle (g)	Wet Weight before the 12th cycle (g)	Wet Weight before the 13th cycle (g)	Wet Weight before the 14th cycle (g)	Wet Weight before the 15th cycle (g)	Wet Weight before the 16th cycle (g)
L3	130.796	143.731	146.196	146.160	146.045	144.523	143.547	143.947	143.624	141.119	139.170	137.694	134.399	123.970	106.471	92.147	79.841
L4	119.613	138.544	138.253	129.526	123.304	114.504	110.178	103.610	102.949	67.548	50.585	17.850	7.019	0.000	0.000	0.000	0.000
S3	110.195	120.505	119.770	122.533	121.691	122.893	117.473	118.130	116.094	118.093	116.570	116.401	85.566	70.094	62.014	52.147	42.961
S4	107.570	117.460	117.646	118.423	118.234	120.988	117.639	118.044	117.892	117.569	115.570	113.981	96.100	90.148	78.014	66.621	51.298
U2	108.657	116.014	95.555	77.198	64.447	56.874	35.214	13.014	0.000	0.000	0.000	0.000	0.000	0.000	0.000	0.000	0.000
M2	93.590	99.540	88.778	74.451	59.112	46.577	22.257	8.061	0.000	0.000	0.000	0.000	0.000	0.000	0.000	0.000	0.000
D2	115.919	119.020	13.950	0.000	0.000	0.000	0.000	0.000	0.000	0.000	0.000	0.000	0.000	0.000	0.000	0.000	0.000

Table (T6): The wet weight of the sandstone and limestone samples after immersing in saturated sodium sulfate solution and before the drying cycle (low relative humidity and fluctuating wind speed).

Appendix T: Modified salt crystallisation test results
Sodium sulfate solution: Fourth run.

Sample number	Original Dry Weight + weight of the label (g)	Weight after 1st cycle (g)	Weight after the 2nd cycle (g)	Weight after the 3rd cycle (g)	Weight after the 4th cycle (g)	Weight after the 5th cycle (g)	Weight after the 6th cycle (g)	Weight after the 7th cycle (g)	Weight after the 8th cycle (g)	Weight after the 9th cycle (g)	Weight after the 10th cycle (g)	Weight after the 11th cycle (g)	Weight after the 12th cycle (g)	Weight after the 13th cycle (g)	Weight after the 14th cycle (g)	Weight after the 15th cycle (g)	Weight after the 16th cycle (g)	ΔW (%)
L3	122.495	135.643	137.154	135.625	134.385	132.309	129.950	129.489	131.104	127.771	127.033	127.277	126.598	125.599	125.518	125.637	125.323	2.31
L4	121.291	134.345	135.529	133.774	132.603	130.862	128.860	128.087	125.869	120.377	118.622	118.122	114.157	112.538	111.937	111.706	111.421	-8.14
S3	109.788	115.533	116.586	115.168	114.402	112.327	111.250	109.754	105.079	101.532	99.703	97.491	95.828	81.819	80.175	78.932	75.364	-31.35
S4	107.747	112.915	114.426	113.844	114.062	113.661	112.336	110.859	109.138	108.123	106.846	104.180	103.247	103.503	98.508	96.932	84.218	-21.84
U2	114.258	115.369	114.879	114.025	97.651	84.569	74.269	70.254	64.129	47.985	24.658	12.698	4.546	0.000	0.000	0.000	0.000	-100
M2	87.396	88.555	86.951	49.787	31.324	23.670	20.054	10.900	5.143	0.000	0.000	0.000	0.000	0.000	0.000	0.000	0.000	-100
D2	140.986	143.595	146.356	131.247	119.347	111.762	82.573	78.240	59.367	36.297	0.000	0.000	0.000	0.000	0.000	0.000	0.000	-100

Table (T7): The dry weight of the sandstone and limestone samples immersed in saturated sodium sulfate solution and dried for 24-hours at high relative humidity and low wind speed conditions.

Sample number	Original Dry Weight + weight of the label (g)	Wet Weight before the 1st cycle (g)	Wet Weight before the 2nd cycle (g)	Wet Weight before the 3rd cycle (g)	Wet Weight before the 4th cycle (g)	Wet Weight before the 5th cycle (g)	Wet Weight before the 6th cycle (g)	Wet Weight before the 7th cycle (g)	Wet Weight before the 8th cycle (g)	Wet Weight before the 9th cycle (g)	Wet Weight before the 10th cycle 100 (g)	Wet Weight before the 11th cycle (g)	Wet Weight before the 12th cycle (g)	Wet Weight before the 13th cycle (g)	Wet Weight before the 14th cycle (g)	Wet Weight before the 15th cycle (g)	Wet Weight before the 16th cycle (g)
L3	122.495	138.686	140.784	140.133	137.288	136.323	134.771	135.275	133.722	132.171	132.134	131.271	130.081	130.058	128.459	129.223	128.878
L4	121.291	138.122	140.152	139.164	137.118	135.355	133.927	133.369	130.981	124.826	123.170	121.756	118.178	116.172	115.279	115.384	115.326
S3	109.788	120.830	120.987	120.899	120.209	117.968	118.120	116.651	112.402	107.436	104.449	103.066	102.902	87.103	83.718	82.352	78.981
S4	107.747	117.697	119.214	118.724	117.785	117.351	117.357	116.618	115.373	113.231	112.079	109.329	108.449	107.490	104.023	102.865	89.014
U2	114.258	119.579	119.004	118.951	102.239	86.214	77.891	72.014	67.214	49.334	27.014	14.057	5.993	0.000	0.000	0.000	0.000
M2	87.396	93.164	92.632	57.132	33.851	22.695	20.987	12.549	6.514	0.000	0.000	0.000	0.000	0.000	0.000	0.000	0.000
D2	140.986	150.342	152.759	141.051	127.290	122.354	93.594	86.960	69.979	45.034	0.000	0.000	0.000	0.000	0.000	0.000	0.000

Table (T8): The wet weight of the sandstone and limestone samples after immersing them in saturated sodium sulfate solution and before the drying cycle (high relative humidity and low wind speed).

Appendix T: Modified salt crystallisation test results
Sodium sulfate solution: Fifth run.

Sample number	Original Dry Weight+ weight of the label (g)	Weight after 1st cycle (g)	Weight after the 2nd cycle (g)	Weight after the 3rd cycle (g)	Weight after the 4th cycle (g)	Weight after the 5th cycle (g)	Weight after the 6th cycle (g)	Weight after the 7th cycle (g)	Weight after the 8th cycle (g)	Weight after the 9th cycle (g)	Weight after the 10th cycle (g)	Weight after the 11th cycle (g)	Weight after the 12th cycle (g)	Weight after the 13th cycle (g)	Weight after the 14th cycle (g)	Weight after the 15th cycle (g)	Weight after the 16th cycle (g)	ΔW (%)
L3	121.194	134.964	139.459	139.519	139.919	140.200	141.306	140.123	140.659	140.701	141.336	139.334	140.746	140.348	139.342	139.812	138.092	13.87
L4	137.146	139.102	144.804	144.103	144.607	144.302	145.491	144.166	145.296	144.723	144.465	144.323	144.453	145.158	143.961	144.053	143.637	4.73
S3	107.447	111.482	113.188	113.915	112.899	111.756	110.250	106.335	103.405	101.009	99.721	97.322	95.826	92.757	89.342	84.913	82.034	-23.65
S4	109.769	110.235	113.056	112.040	111.160	110.300	110.299	104.811	100.878	100.118	97.902	92.945	92.735	88.163	85.554	81.207	77.580	-29.32
U2	107.452	108.328	107.961	105.361	100.323	92.147	80.228	65.652	40.147	13.657	5.210	0.000	0.000	0.000	0.000	0.000	0.000	-100
M2	99.324	101.002	100.621	97.321	93.327	84.327	80.974	67.398	44.328	18.741	3.547	0.000	0.000	0.000	0.000	0.000	0.000	-100
D2	108.647	109.658	107.321	104.364	96.547	81.297	73.147	55.541	39.741	10.321	0.000	0.000	0.000	0.000	0.000	0.000	0.000	-100

Table (T9): The dry weight of the sandstone and limestone samples immersed in saturated sodium sulfate solution and dried for 24-hours at high relative humidity and high wind speed conditions

Sample number	Original Dry Weight + weight of the label (g)	Wet Weight before the 1st cycle (g)	Wet Weight before the 2nd cycle (g)	Wet Weight before the 3rd cycle (g)	Wet Weight before the 4th cycle (g)	Wet Weight before the 5th cycle (g)	Wet Weight before the 6th cycle (g)	Wet Weight before the 7th cycle (g)	Wet Weight before the 8th cycle (g)	Wet Weight before the 9th cycle (g)	Wet Weight before the 10th cycle 100 (g)	Wet Weight before the 11th cycle (g)	Wet Weight before the 12th cycle (g)	Wet Weight before the 13th cycle (g)	Wet Weight before the 14th cycle (g)	Wet Weight before the 15th cycle (g)	Wet Weight before the 16th cycle (g)
L3	121.194	140.332	139.459	142.322	144.029	143.696	143.066	144.320	143.885	143.336	143.629	142.000	143.482	143.331	142.882	143.823	143.417
L4	137.146	144.727	144.804	145.328	147.182	148.255	147.005	147.957	149.070	147.528	147.872	147.367	148.157	148.434	147.744	147.999	147.422
S3	107.447	119.242	113.188	115.367	120.723	120.778	117.007	115.899	109.048	106.318	104.940	99.327	102.250	98.904	96.657	93.686	87.448
S4	109.769	117.276	113.056	112.874	118.922	117.984	117.084	122.479	107.915	104.909	101.344	94.210	96.505	93.534	90.563	87.512	84.041
U2	107.452	111.214	108.397	107.214	95.322	93.641	82.029	68.951	41.399	15.698	6.547	0.000	0.000	0.000	0.000	0.000	0.000
M2	99.324	104.598	102.025	99.324	94.687	86.047	83.009	69.981	47.635	22.017	5.033	0.000	0.000	0.000	0.000	0.000	0.000
D2	108.647	113.899	108.987	105.556	100.369	83.331	75.558	58.688	41.027	12.554	0.000	0.000	0.000	0.000	0.000	0.000	0.000

Table (T10): The wet weight of the sandstone and limestone samples after immersing in saturated sodium sulfate solution and before the drying cycle (high relative humidity and high wind speed).

Appendix T: Modified salt crystallisation test results
Sodium sulfate solution: Sixth run.

Sample number	Original Dry Weight+ weight of the label (g)	Weight after 1st cycle (g)	Weight after the 2nd cycle (g)	Weight after the 3rd cycle (g)	Weight after the 4th cycle (g)	Weight after the 5th cycle (g)	Weight after the 6th cycle (g)	Weight after the 7th cycle (g)	Weight after the 8th cycle (g)	Weight after the 9th cycle (g)	Weight after the 10th cycle (g)	Weight after the 11th cycle (g)	Weight after the 12th cycle (g)	Weight after the 13th cycle (g)	Weight after the 14th cycle (g)	Weight after the 15th cycle (g)	Weight after the 16th cycle (g)	ΔW (%)
L3	124.690	137.085	136.867	134.187	124.576	115.080	109.448	106.916	103.890	99.400	94.945	90.991	89.153	86.537	86.467	83.848	77.641	-37.73
L4	125.245	134.835	136.303	137.390	136.609	136.713	135.320	134.783	135.924	135.667	135.343	133.862	132.588	130.966	128.110	125.023	124.936	- 0.25
S3	110.851	116.924	116.601	116.337	118.152	114.277	114.326	116.726	112.081	111.249	110.124	108.675	102.484	99.741	95.376	91.572	88.127	-20.50
S4	107.690	113.130	112.846	112.547	111.243	112.913	109.550	109.352	103.337	103.591	102.260	98.474	94.282	90.099	87.285	84.697	82.322	-23.56
U2	101.258	103.251	87.954	75.584	40.147	35.574	13.014	2.010	0.000	0.000	0.000	0.000	0.000	0.000	0.000	0.000	0.000	-100
M2	88.323	89.724	67.395	37.726	12.593	0.000	0.000	0.000	0.000	0.000	0.000	0.000	0.000	0.000	0.000	0.000	0.000	-100
D2	108.049	108.492	71.326	37.685	0.000	0.000	0.000	0.000	0.000	0.000	0.000	0.000	0.000	0.000	0.000	0.000	0.000	-100

Table (T11): The dry weight of the sandstone and limestone samples immersed in saturated sodium sulfate solution and dried for 24-hours at high relative humidity and fluctuating wind speed conditions.

Sample number	Original Dry Weight + weight of the label (g)	Wet Weight before the 1st cycle (g)	Wet Weight before the 2nd cycle (g)	Wet Weight before the 3rd cycle (g)	Wet Weight before the 4th cycle (g)	Wet Weight before the 5th cycle (g)	Wet Weight before the 6th cycle (g)	Wet Weight before the 7th cycle (g)	Wet Weight before the 8th cycle (g)	Wet Weight before the 9th cycle (g)	Wet Weight before the 10th cycle 100 (g)	Wet Weight before the 11th cycle (g)	Wet Weight before the 12th cycle (g)	Wet Weight before the 13th cycle (g)	Wet Weight before the 14th cycle (g)	Wet Weight before the 15th cycle (g)	Wet Weight before the 16th cycle (g)
L3	124.690	143.194	142.047	139.046	130.806	118.396	114.516	112.017	107.954	103.945	98.790	95.044	92.481	90.106	89.467	87.615	81.577
L4	125.245	137.860	139.746	140.100	140.287	139.610	139.053	138.693	138.537	139.153	138.369	137.687	135.456	133.950	131.617	129.426	127.852
S3	110.851	122.088	121.981	121.710	120.835	120.160	120.379	119.550	118.161	115.771	114.543	112.046	104.085	103.169	98.026	94.340	91.149
S4	107.690	118.172	118.191	117.026	117.156	115.617	114.247	114.565	111.850	109.427	106.626	104.687	97.047	92.783	89.208	87.572	84.896
U2	101.258	106.214	91.241	78.988	43.654	38.957	18.014	4.387	0.000	0.000	0.000	0.000	0.000	0.000	0.000	0.000	0.000
M2	88.323	94.634	74.646	44.215	16.991	0.000	0.000	0.000	0.000	0.000	0.000	0.000	0.000	0.000	0.000	0.000	0.000
D2	108.049	115.216	80.810	41.367	0.000	0.000	0.000	0.000	0.000	0.000	0.000	0.000	0.000	0.000	0.000	0.000	0.000

Table (T12): The wet weight of the sandstone and limestone samples after immersing in saturated sodium sulfate solution and before the drying cycle (high relative humidity and fluctuating wind speed).

Appendix T: Modified salt crystallisation test results
Petra salts solution: First run.

Sample number	Original Dry Weight+ weight of the label (g)	Weight after 1st cycle (g)	Weight after the 2nd cycle (g)	Weight after the 3rd cycle (g)	Weight after the 4th cycle (g)	Weight after the 5th cycle (g)	Weight after the 6th cycle (g)	Weight after the 7th cycle (g)	Weight after the 8th cycle (g)	Weight after the 9th cycle (g)	Weight after the 10th cycle (g)	Weight after the 11th cycle (g)	Weight after the 12th cycle (g)	Weight after the 13th cycle (g)	Weight after the 14th cycle (g)	Weight after the 15th cycle (g)	Weight after the 16th cycle (g)	ΔW (%)
L1	133.385	133.976	135.348	135.870	137.674	136.834	137.952	138.592	138.486	139.850	140.145	139.922	139.902	140.297	140.516	139.874	139.777	4.79
L2	121.637	122.251	123.001	123.401	125.501	124.152	125.131	125.960	125.659	127.887	126.955	126.944	126.899	127.783	127.750	127.698	127.598	4.90
S1	105.070	105.231	105.594	105.970	105.976	105.664	105.862	105.965	105.633	105.931	105.803	106.077	106.174	106.271	105.142	105.098	105.071	0.50
S2	110.256	110.641	110.894	110.951	111.086	111.539	111.526	111.441	111.514	111.579	111.360	111.545	111.728	111.943	111.723	111.657	111.545	1.17
U1	124.215	124.745	125.214	125.421	125.359	124.997	125.125	125.008	124.899	125.000	124.877	124.741	124.254	124.322	123.754	123.701	123.124	-0.87
M1	162.466	162.872	163.154	163.416	163.412	163.815	163.478	163.257	163.027	163.245	162.471	161.902	161.725	162.475	159.257	157.874	156.214	-3.85
D1	154.086	153.500	153.120	152.338	151.529	150.410	149.234	149.058	148.564	148.053	147.441	146.825	146.178	144.698	143.657	142.245	141.981	-7.85

Table (T13): The dry weight of the sandstone and limestone samples immersed in Petra salt solution and dried for 24-hours at low relative humidity and low wind speed conditions

Sample number	Original Dry Weight + weight of the label (g)	Wet Weight before the 1st cycle (g)	Wet Weight before the 2nd cycle (g)	Wet Weight before the 3rd cycle (g)	Wet Weight before the 4th cycle (g)	Wet Weight before the 5th cycle (g)	Wet Weight before the 6th cycle (g)	Wet Weight before the 7th cycle (g)	Wet Weight before the 8th cycle (g)	Wet Weight before the 9th cycle (g)	Wet Weight before the 10th cycle 100 (g)	Wet Weight before the 11th cycle (g)	Wet Weight before the 12th cycle (g)	Wet Weight before the 13th cycle (g)	Wet Weight before the 14th cycle (g)	Wet Weight before the 15th cycle (g)	Wet Weight before the 16th cycle (g)
L1	133.385	145.708	146.109	146.115	146.780	146.830	147.348	147.478	147.667	147.368	147.611	147.821	147.737	148.006	148.071	147.967	148.014
L2	121.637	137.051	137.545	137.592	138.346	138.213	138.450	138.658	138.735	138.817	138.829	138.870	138.629	138.842	139.227	139.325	138.874
S1	105.070	113.589	113.759	113.830	113.914	114.093	114.177	113.758	114.309	113.730	113.854	113.908	114.034	113.826	114.180	114.241	114.008
S2	110.256	119.169	119.754	119.313	119.651	119.628	119.716	119.566	119.661	119.340	119.421	119.250	119.389	119.530	119.774	119.547	119.621
U1	124.215	130.354	130.457	130.547	130.214	130.589	130.874	130.323	130.028	130.229	129.887	129.786	129.569	129.874	129.008	129.112	128.968
M1	162.466	170.163	170.240	170.206	170.664	170.819	171.114	170.758	170.835	170.246	169.782	169.225	169.094	168.873	167.381	166.988	167.012
D1	154.086	162.318	162.086	160.918	160.448	159.139	158.176	157.513	157.123	155.603	155.947	154.844	154.054	152.534	151.583	150.028	149.849

Table (T14): The wet weight of the sandstone and limestone samples after immersing them in saturated Petra salt solution and before the drying cycle (low relative humidity and low wind speed).

Appendix T: Modified salt crystallisation test results
Petra salts solution: Second run.

Sample number	Original Dry Weight+ weight of the label (g)	Weight after 1st cycle (g)	Weight after the 2nd cycle (g)	Weight after the 3rd cycle (g)	Weight after the 4th cycle (g)	Weight after the 5th cycle (g)	Weight after the 6th cycle (g)	Weight after the 7th cycle (g)	Weight after the 8th cycle (g)	Weight after the 9th cycle (g)	Weight after the 10th cycle (g)	Weight after the 11th cycle (g)	Weight after the 12th cycle (g)	Weight after the 13th cycle (g)	Weight after the 14th cycle (g)	Weight after the 15th cycle (g)	Weight after the 16th cycle (g)	ΔW (%)
L1	117.939	118.981	119.876	120.369	121.083	122.337	121.972	121.699	120.921	120.359	120.538	120.057	120.058	119.998	119.833	119.557	119.338	1.23
L2	121.642	122.678	123.849	124.524	124.776	125.829	125.801	125.542	125.659	125.642	125.408	125.251	125.184	125.180	125.085	125.003	125.100	2.88
S1	106.425	106.796	107.080	107.344	104.557	107.699	107.839	107.949	107.879	107.359	107.165	107.064	107.167	106.852	106.732	106.547	106.461	0.03
S2	110.270	110.728	110.027	111.376	111.150	111.721	111.867	111.716	111.703	111.544	111.601	111.584	111.358	111.304	111.609	111.332	111.145	0.79
U1	101.146	101.326	101.421	101.867	101.023	101.521	101.530	101.013	100.991	100.596	100.704	99.198	98.435	98.400	98.536	98.654	99.014	-2.11
M1	107.658	107.869	107.963	107.103	106.857	106.156	106.178	105.478	105.050	105.243	104.726	105.064	104.370	104.119	103.842	103.922	103.813	-3.57
D1	122.232	122.076	121.312	120.976	120.040	119.499	119.118	118.618	117.960	117.465	117.063	116.635	114.371	113.363	113.480	112.485	112.328	-8.10

Table (T15): The dry weight of the sandstone and limestone samples immersed in Petra salt solution and dried for 24-hours at low relative humidity and high wind speed conditions.

Sample number	Original Dry Weight+ weight of the label (g)	Wet Weight before the 1st cycle (g)	Wet Weight before the 2nd cycle (g)	Wet Weight before the 3rd cycle (g)	Wet Weight before the 4th cycle (g)	Wet Weight before the 5th cycle (g)	Wet Weight before the 6th cycle (g)	Wet Weight before the 7th cycle (g)	Wet Weight before the 8th cycle (g)	Wet Weight before the 9th cycle (g)	Wet Weight before the 10th cycle (g)	Wet Weight before the 11th cycle (g)	Wet Weight before the 12th cycle (g)	Wet Weight before the 13th cycle (g)	Wet Weight before the 14th cycle (g)	Wet Weight before the 15th cycle (g)	Wet Weight before the 16th cycle (g)
L1	117.939	133.315	133.813	134.237	134.463	134.806	134.578	134.673	134.248	134.320	133.254	133.917	133.797	133.997	133.392	134.120	133.897
L2	121.642	136.642	137.939	138.092	118.930	138.558	138.620	138.525	138.226	138.511	138.335	138.259	138.135	138.012	137.880	138.191	138.214
S1	106.425	113.411	114.412	114.245	114.417	114.262	114.639	114.355	114.444	114.764	114.684	114.783	114.884	114.616	114.739	114.124	114.109
S2	110.270	118.112	118.936	118.942	118.705	118.825	118.936	118.895	118.850	119.127	118.703	118.823	118.994	118.980	118.968	119.203	118.885
U1	101.146	106.412	106.982	107.025	106.853	107.088	107.125	106.879	107.258	106.547	106.321	105.687	105.367	105.222	105.298	105.338	105.080
M1	107.658	111.979	112.391	112.757	112.612	112.564	112.647	112.672	112.377	112.815	110.471	109.567	109.636	109.566	109.274	109.186	108.843
D1	122.232	128.346	128.655	128.374	127.729	127.009	126.363	125.555	125.408	125.001	124.482	122.978	122.709	122.264	122.029	121.764	121.339

Table (T16): The wet weight of the sandstone and limestone samples after immersing them in saturated Petra salt solution and before the drying cycle (low relative humidity and high wind speed).

Appendix T: Modified salt crystallisation test results
Petra salts solution: Third run.

Sample number	Original Dry Weight+ weight of the label (g)	Weight after 1st cycle (g)	Weight after the 2nd cycle (g)	Weight after the 3rd cycle (g)	Weight after the 4th cycle (g)	Weight after the 5th cycle (g)	Weight after the 6th cycle (g)	Weight after the 7th cycle (g)	Weight after the 8th cycle (g)	Weight after the 9th cycle (g)	Weight after the 10th cycle (g)	Weight after the 11th cycle (g)	Weight after the 12th cycle (g)	Weight after the 13th cycle (g)	Weight after the 14th cycle (g)	Weight after the 15th cycle (g)	Weight after the 16th cycle (g)	ΔW (%)
L1	122.962	123.754	124.224	124.990	125.743	126.084	126.113	126.940	126.352	126.213	126.693	126.556	126.032	125.874	125.121	124.874	124.545	1.28
L2	123.123	123.653	124.232	1250.118	125.824	126.233	126.219	126.174	125.828	125.731	126.056	125.646	124.821	124.138	124.111	123.853	123.712	0.48
S1	108.989	109.214	109.388	109.680	109.819	109.942	110.126	109.870	109.311	109.225	108.695	108.555	108.463	107.951	108.025	107.887	107.552	-1.32
S2	103.912	104.580	104.670	104.862	104.903	104.964	104.821	104.974	104.817	104.000	103.968	103.963	103.974	104.020	103.921	103.852	103.222	-0.66
U1	110.269	110.398	110.502	110.457	110.698	110.128	109.547	108.238	108.232	107.258	107.333	107.149	106.297	106.214	106.007	105.885	105.676	-4.16
M1	105.241	105.509	105.780	105.660	105.809	105.943	105.834	105.509	105.207	105.288	103.790	103.034	102.937	102.842	103.004	102.854	102.631	-2.80
D1	133.732	132.045	131.573	130.699	130.511	129.848	129.182	128.461	125.877	124.100	121.297	121.024	120.422	120.061	119.147	118.001	117.541	-12.11

Table (T17): The dry weight of the sandstone and limestone samples immersed in Petra salt solution and dried for 24-hours at low relative humidity and fluctuating wind speed conditions.

Sample number	Original Dry Weight + weight of the label (g)	Wet Weight before the 1st cycle (g)	Wet Weight before the 2nd cycle (g)	Wet Weight before the 3rd cycle (g)	Wet Weight before the 4th cycle (g)	Wet Weight before the 5th cycle (g)	Wet Weight before the 6th cycle (g)	Wet Weight before the 7th cycle (g)	Wet Weight before the 8th cycle (g)	Wet Weight before the 9th cycle (g)	Wet Weight before the 10th cycle (g)	Wet Weight before the 11th cycle (g)	Wet Weight before the 12th cycle (g)	Wet Weight before the 13th cycle (g)	Wet Weight before the 14th cycle (g)	Wet Weight before the 15th cycle (g)	Wet Weight before the 16th cycle (g)
L1	122.962	139.057	139.516	139.564	140.052	139.922	139.800	139.842	139.520	139.881	140.106	139.773	140.355	139.869	139.547	139.741	139.454
L2	123.123	138.444	138.597	139.179	139.393	139.424	139.250	139.499	139.496	139.672	139.730	139.559	139.480	139.433	139.442	139.238	139.654
S1	108.989	116.079	116.360	116.481	116.385	116.622	116.296	116.432	116.823	116.502	115.951	115.446	115.557	115.478	115.547	115.114	115.102
S2	103.912	111.239	111.566	111.348	111.441	111.444	111.751	111.790	111.637	111.505	111.357	111.282	111.712	111.612	111.547	111.521	111.255
U1	110.269	115.201	115.186	115.087	115.100	115.001	114.903	114.889	114.579	114.547	115.214	114.214	113.323	113.300	113.212	112.321	112.101
M1	105.241	109.820	109.766	109.567	109.928	109.785	109.685	109.536	109.958	110.037	109.718	109.505	109.844	109.646	109.149	109.002	108.889
D1	133.732	140.612	139.587	138.462	138.319	137.771	137.013	136.218	133.781	131.611	128.634	128.322	127.497	127.114	126.547	125.547	124.417

Table (T18): The wet weight of the sandstone and limestone samples after immersing them in saturated Petra salt solution and before the drying cycle (low relative humidity and fluctuating wind speed).

Appendix T: Modified salt crystallisation test results
Petra salts solution: Fourth run.

Sample number	Original Dry Weight+ weight of the label (g)	Weight after 1st cycle (g)	Weight after the 2nd cycle (g)	Weight after the 3rd cycle (g)	Weight after the 4th cycle (g)	Weight after the 5th cycle (g)	Weight after the 6th cycle (g)	Weight after the 7th cycle (g)	Weight after the 8th cycle (g)	Weight after the 9th cycle (g)	Weight after the 10th cycle (g)	Weight after the 11th cycle (g)	Weight after the 12th cycle (g)	Weight after the 13th cycle (g)	Weight after the 14th cycle (g)	Weight after the 15th cycle (g)	Weight after the 16th cycle (g)	ΔW (%)
L1	123.351	128.692	128.331	127.480	128.567	130.632	131.249	130.607	131.290	131.364	131.656	130.771	130.836	130.406	130.026	129.522	129.478	4.96
L2	121.549	125.186	125.722	126.434	127.489	128.774	130.062	129.269	130.510	129.010	128.725	128.292	130.899	128.982	128.744	127.807	127.744	5.10
S1	109.811	112.514	112.879	112.873	113.194	113.889	113.581	113.095	113.628	113.307	113.080	113.368	113.562	113.194	113.390	113.362	113.114	3.01
S2	107.585	110.171	110.653	110.514	110.783	111.249	110.167	111.407	111.764	111.098	110.922	111.055	111.220	110.935	111.101	111.140	111.105	3.27
U1	123.458	127.025	127.079	127.001	126.867	126.954	126.960	126.801	126.885	126.754	125.524	124.695	123.222	123.124	123.002	122.985	122.859	-0.48
M1	96.668	99.656	99.885	99.644	99.312	99.578	99.582	99.227	99.707	98.833	97.387	97.992	96.837	96.473	95.062	95.036	94.651	-2.09
D1	141.186	142.998	142.012	141.175	141.059	141.181	141.259	140.107	140.191	140.074	138.323	136.694	134.809	132.717	129.723	126.416	124.214	-12.02

Table (T19): The dry weight of the sandstone and limestone samples immersed in Petra salt solution and dried for 24-hours at high relative humidity and low wind speed conditions.

Sample number	Original Dry Weight + weight of the label (g)	Wet Weight before the 1st cycle (g)	Wet Weight before the 2nd cycle (g)	Wet Weight before the 3rd cycle (g)	Wet Weight before the 4th cycle (g)	Wet Weight before the 5th cycle (g)	Wet Weight before the 6th cycle (g)	Wet Weight before the 7th cycle (g)	Wet Weight before the 8th cycle (g)	Wet Weight before the 9th cycle (g)	Wet Weight before the 10th cycle 100 (g)	Wet Weight before the 11th cycle (g)	Wet Weight before the 12th cycle (g)	Wet Weight before the 13th cycle (g)	Wet Weight before the 14th cycle (g)	Wet Weight before the 15th cycle (g)	Wet Weight before the 16th cycle (g)
L1	123.351	137.466	138.019	138.422	138.734	139.150	139.233	139.630	139.830	139.622	139.563	139.699	140.196	139.899	139.883	139.772	139.689
L2	121.549	137.069	137.659	137.997	138.788	139.155	139.430	139.482	139.377	139.316	139.190	139.255	139.577	139.582	139.322	139.853	139.547
S1	109.811	118.472	118.305	118.253	118.545	118.750	118.713	119.301	118.707	118.389	118.210	118.560	118.725	118.808	118.586	119.165	119.020
S2	107.585	115.610	116.201	116.254	116.678	116.518	116.507	116.866	116.992	116.590	116.307	116.213	116.386	116.370	116.389	116.772	116.521
U1	123.458	130.214	130.354	130.324	130.587	130.334	131.025	131.000	130.687	130.874	130.885	130.652	129.217	129.854	128.147	129.021	129.554
M1	96.668	103.403	103.451	103.089	102.678	102.583	102.871	102.911	102.630	102.015	101.321	101.105	100.428	100.071	99.978	99.436	98.329
D1	141.186	148.889	148.261	147.691	147.208	146.697	146.283	146.560	145.684	143.541	143.070	141.341	138.194	137.128	133.852	131.514	130.214

Table (T20): The wet weight of the sandstone and limestone samples after immersing them in saturated Petra salt solution and before the drying cycle (high relative humidity and low wind speed).

Appendix T: Modified salt crystallisation test results
Petra salts solution: Fifth run.

Sample number	Original Dry Weight+ weight of the label (g)	Weight after 1st cycle (g)	Weight after the 2nd cycle (g)	Weight after the 3rd cycle (g)	Weight after the 4th cycle (g)	Weight after the 5th cycle (g)	Weight after the 6th cycle (g)	Weight after the 7th cycle (g)	Weight after the 8th cycle (g)	Weight after the 9th cycle (g)	Weight after the 10th cycle (g)	Weight after the 11th cycle (g)	Weight after the 12th cycle (g)	Weight after the 13th cycle (g)	Weight after the 14th cycle (g)	Weight after the 15th cycle (g)	Weight after the 16th cycle (g)	ΔW (%)
L1	135.119	142.197	143.059	143.525	142.978	145.352	145.884	145.430	145.834	146.014	145.999	145.120	144.904	143.587	143.147	142.821	142.314	5.32
L2	128.522	130.711	133.860	132.867	131.540	132.967	133.405	133.702	134.501	135.939	135.065	135.904	134.759	133.874	133.135	133.120	133.007	3.49
S1	108.849	113.202	113.961	113.079	113.711	113.118	113.714	113.012	112.622	112.329	112.512	112.272	111.633	110.990	110.308	110.229	110.129	1.83
S2	107.454	112.253	111.562	110.851	110.499	110.070	110.687	110.115	109.878	110.151	110.517	109.255	109.906	109.682	109.395	109.092	108.944	1.38
U1	105.654	111.548	111.625	111.222	111.259	110.017	109.879	109.028	108.748	107.338	107.478	105.471	104.411	104.038	103.159	102.266	101.517	-3.91
M1	112.241	118.365	118.401	118.444	118.028	117.228	116.749	115.447	114.418	114.003	113.479	112.214	111.279	110.217	110.004	109.299	109.019	-2.87
D1	110.254	116.145	116.597	115.887	115.007	110.558	108.547	106.973	104.471	103.010	101.521	100.547	99.698	95.247	94.357	93.219	91.294	-17.20

Table (T21): The dry weight of the sandstone and limestone samples immersed in Petra salt solution and dried for 24-hours at high relative humidity and high wind speed conditions.

Sample number	Original Dry Weight + weight of the label (g)	Wet Weight before the 1st cycle (g)	Wet Weight before the 2nd cycle (g)	Wet Weight before the 3rd cycle (g)	Wet Weight before the 4th cycle (g)	Wet Weight before the 5th cycle (g)	Wet Weight before the 6th cycle (g)	Wet Weight before the 7th cycle (g)	Wet Weight before the 8th cycle (g)	Wet Weight before the 9th cycle (g)	Wet Weight before the 10th cycle 100 (g)	Wet Weight before the 11th cycle (g)	Wet Weight before the 12th cycle (g)	Wet Weight before the 13th cycle (g)	Wet Weight before the 14th cycle (g)	Wet Weight before the 15th cycle (g)	Wet Weight before the 16th cycle (g)
L1	135.119	148.489	147.059	147.895	147.200	146.429	151.891	152.343	151.761	151.715	151.808	150.147	152.261	152.354	150.209	149.603	148.450
L2	128.522	139.916	139.860	139.899	139.419	139.683	140.323	140.189	140.467	140.292	140.335	140.448	140.617	140.463	140.127	140.227	141.728
S1	108.849	120.014	119.961	118.579	119.657	119.464	119.386	119.428	120.119	119.336	119.401	119.323	118.919	119.424	118.700	118.761	117.534
S2	107.454	117.956	117.562	117.019	116.888	116.909	117.611	117.508	117.079	116.839	116.865	117.579	116.778	116.298	116.496	116.060	116.029
U1	105.654	113.687	113.547	113.028	113.478	112.587	112.002	112.214	112.254	112.364	111.547	110.547	110.214	110.008	108.547	105.547	104.987
M1	112.241	120.566	120.442	120.345	120.591	120.020	120.103	119.874	119.547	119.017	118.549	118.050	116.879	116.357	115.697	114.487	114.434
D1	110.254	118.988	118.217	118.040	117.982	116.27	114.547	111.954	110.357	109.324	107.328	107.007	106.547	100.087	99.984	97.541	97.029

Table (T22): The wet weight of the sandstone and limestone samples after immersing them in saturated Petra salt solution and before the drying cycle (high relative humidity and high wind speed).

Appendix T: Modified salt crystallisation test results
Petra salts solution: Sixth run.

Sample number	Original Dry Weight+ weight of the label (g)	Weight after 1st cycle (g)	Weight after the 2nd cycle (g)	Weight after the 3rd cycle (g)	Weight after the 4th cycle (g)	Weight after the 5th cycle (g)	Weight after the 6th cycle (g)	Weight after the 7th cycle (g)	Weight after the 8th cycle (g)	Weight after the 9th cycle (g)	Weight after the 10th cycle (g)	Weight after the 11th cycle (g)	Weight after the 12th cycle (g)	Weight after the 13th cycle (g)	Weight after the 14th cycle (g)	Weight after the 15th cycle (g)	Weight after the 16th cycle (g)	ΔW (%)
L1	117.208	123.695	122.778	125.169	122.126	133.111	122.753	122.749	121.704	121.905	120.098	120.387	119.862	119.367	118.947	118.690	118.322	0.95
L2	124.517	127.767	127.224	131.244	129.244	137.632	130.786	130.047	130.185	130.340	130.190	130.750	129.440	130.668	129.986	128.661	128.040	3.11
S1	109.663	111.448	110.924	112.195	112.036	116.553	112.276	111.256	111.320	111.695	111.026	111.459	111.247	110.022	110.683	109.680	109.675	0.01
S2	109.932	111.850	111.230	111.373	110.108	115.832	110.071	110.307	110.719	110.939	111.205	111.817	111.703	111.750	111.766	110.883	110.427	0.28
U1	104.210	106.214	106.028	105.741	105.333	109.148	105.051	104.327	103.598	103.471	103.214	102.241	102.342	101.147	100.214	98.327	97.888	-6.07
M1	100.542	102.647	101.670	100.896	100.731	104.346	100.185	99.288	99.207	98.443	98.398	97.459	97.361	97.000	96.345	96.155	95.332	-5.18
D1	106.699	108.826	108.896	108.366	107.460	109.920	104.510	103.231	101.356	99.877	98.121	97.878	96.851	96.630	93.696	91.362	89.273	-16.33

Table (T23): The dry weight of the sandstone and limestone samples immersed in Petra salt solution and dried for 24-hours at high relative humidity and fluctuating wind speed conditions.

Sample number	Original Dry Weight + weight of the label (g)	Wet Weight before the 1st cycle (g)	Wet Weight before the 2nd cycle (g)	Wet Weight before the 3rd cycle (g)	Wet Weight before the 4th cycle (g)	Wet Weight before the 5th cycle (g)	Wet Weight before the 6th cycle (g)	Wet Weight before the 7th cycle (g)	Wet Weight before the 8th cycle (g)	Wet Weight before the 9th cycle (g)	Wet Weight before the 10th cycle 100 (g)	Wet Weight before the 11th cycle (g)	Wet Weight before the 12th cycle (g)	Wet Weight before the 13th cycle (g)	Wet Weight before the 14th cycle (g)	Wet Weight before the 15th cycle (g)	Wet Weight before the 16th cycle (g)
L1	117.208	133.396	133.752	134.195	134.636	134.510	134.563	134.401	134.411	134.092	134.665	135.469	134.847	134.814	134.533	134.983	134.021
L2	124.517	138.096	137.933	138.752	139.284	138.917	139.025	138.915	138.904	139.329	138.962	139.557	139.572	139.191	139.415	139.383	139.558
S1	109.663	118.112	118.283	118.162	117.772	118.455	117.926	117.889	117.871	117.496	117.416	117.855	117.673	117.609	117.540	118.033	118.048
S2	109.932	117.571	117.924	117.569	117.585	117.589	117.380	116.857	117.227	116.942	117.156	117.707	117.797	117.673	117.288	117.164	117.350
U1	104.210	112.541	112.218	110.658	110.257	110.889	110.547	110.367	109.547	109.547	109.471	108.214	108.874	108.512	106.321	103.214	101.995
M1	100.542	107.363	106.147	105.053	105.748	106.780	105.522	104.365	104.202	103.294	104.089	102.434	102.797	102.788	100.482	101.486	100.827
D1	106.699	113.194	113.507	113.487	114.028	111.595	109.179	109.602	108.360	105.913	105.883	104.975	103.617	102.347	100.310	98.235	96.344

Table (T24): The wet weight of the Sandstone and Limestone samples after immersing them in saturated Petra salt solution and before the drying cycle (high relative humidity and fluctuating wind speed).

Appendix T: Modified salt crystallisation test results
De-ionised water: First run.

Sample number	Original Dry Weight+ weight of the label (g)	Weight after 1st cycle (g)	Weight after the 2nd cycle (g)	Weight after the 3rd cycle (g)	Weight after the 4th cycle (g)	Weight after the 5th cycle (g)	Weight after the 6th cycle (g)	Weight after the 7th cycle (g)	Weight after the 8th cycle (g)	Weight after the 9th cycle (g)	Weight after the 10th cycle (g)	Weight after the 11th cycle (g)	Weight after the 12th cycle (g)	Weight after the 13th cycle (g)	Weight after the 14th cycle (g)	Weight after the 15th cycle (g)	Weight after the 16th cycle (g)	ΔW (%)
Lds	128.727	128.746	128.744	128.825	129.018	128.770	128.785	128.752	129.471	129.879	129.249	129.177	129.127	129.184	129.104	129.052	129.039	0.24
Sds	110.329	110.152	110.178	110.150	110.133	110.071	110.095	110.101	110.565	110.530	110.324	110.214	110.117	110.148	110.073	110.061	110.055	-0.25
Uds	108.236	108.124	108.002	107.952	107.842	107.810	106.976	106.802	106.791	106.665	106.546	106.209	106.358	106.302	106.288	106.225	106.202	-1.88
Mds	105.523	104.889	103.966	103.314	102.250	102.417	98.912	98.332	97.123	96.080	95.025	93.384	93.925	93.374	92.870	92.778	92.687	-12.16
Dds	103.166	103.094	102.994	102.931	102.899	102.820	102.855	102.759	102.667	102.701	102.509	102.450	102.377	102.334	102.264	102.256	102.246	-0.89

Table (T25): The dry weight of the sandstone and limestone samples immersed in de-ionised water and dried for 24-hours at low relative humidity and low wind speed conditions.

Sample number	Original Dry Weight+ weight of the label (g)	Wet Weight before the 1st cycle (g)	Wet Weight before the 2nd cycle (g)	Wet Weight before the 3rd cycle (g)	Wet Weight before the 4th cycle (g)	Wet Weight before the 5th cycle (g)	Wet Weight before the 6th cycle (g)	Wet Weight before the 7th cycle (g)	Wet Weight before the 8th cycle (g)	Wet Weight before the 9th cycle (g)	Wet Weight before the 10th cycle 100 (g)	Wet Weight before the 11th cycle (g)	Wet Weight before the 12th cycle (g)	Wet Weight before the 13th cycle (g)	Wet Weight before the 14th cycle (g)	Wet Weight before the 15th cycle (g)	Wet Weight before the 16th cycle (g)
Lds	128.727	139.351	139.058	138.850	138.983	138.782	138.820	139.002	138.902	138.151	138.955	138.864	138.954	139.131	139.303	139.147	139.301
Sds	110.329	117.942	118.091	117.680	117.976	117.478	117.719	117.591	118.251	117.838	117.947	117.885	117.643	117.679	117.611	117.666	117.712
Uds	108.236	114.051	114.327	113.546	113.874	113.957	112.254	112.000	112.213	112.478	112.445	112.247	112.112	112.364	112.412	112.321	112.280
Mds	105.523	111.329	110.132	108.825	108.751	107.407	104.965	103.961	103.688	102.030	100.628	99.881	99.385	99.417	98.488	98.127	98.001
Dds	103.166	109.080	109.245	108.953	108.640	108.435	108.465	108.475	108.744	108.770	108.204	108.289	107.965	108.176	107.889	107.743	107.702

Table (T26): The wet weight of the sandstone and limestone samples after immersing them in de-ionised water and before the drying cycle (low relative humidity and low wind speed).

Appendix T: Modified salt crystallisation test results
De-ionised water: Second run.

Sample number	Original Dry Weight+ weight of the label (g)	Weight after 1st cycle (g)	Weight after the 2nd cycle (g)	Weight after the 3rd cycle (g)	Weight after the 4th cycle (g)	Weight after the 5th cycle (g)	Weight after the 6th cycle (g)	Weight after the 7th cycle (g)	Weight after the 8th cycle (g)	Weight after the 9th cycle (g)	Weight after the 10th cycle (g)	Weight after the 11th cycle (g)	Weight after the 12th cycle (g)	Weight after the 13th cycle (g)	Weight after the 14th cycle (g)	Weight after the 15th cycle (g)	Weight after the 16th cycle (g)	ΔW (%)
Lds	122.178	122.123	122.064	122.062	122.032	122.028	121.986	121.952	121.952	121.910	121.903	121.886	121.878	121.860	121.838	121.807	121.798	-0.31
Sds	105.701	105.573	105.558	105.612	105.624	105.625	105.552	105.543	105.603	105.520	105.537	105.519	105.538	105.532	105.502	105.464	105.545	-0.15
Uds	85.254	85.252	85.003	84.898	84.558	84.421	84.214	84.125	84.001	83.269	83.016	82.958	82.798	82.251	82.007	81.897	81.587	-4.29
Mds	90.965	90.790	90.678	90.164	89.902	89.790	89.691	89.579	89.229	89.144	88.981	88.838	88737	88.627	88.397	88.331	88.115	-3.13
Dds	134.038	132.495	131.459	130.102	129.624	128.496	127.865	127.262	127.209	125.854	125.459	124.994	124.737	123.921	123.456	122.954	122.204	-8.83

Table (T27): The dry weight of the sandstone and limestone samples immersed in de-ionised water and dried for 24-hours at low relative humidity and high wind speed conditions.

Sample number	Original Dry Weight+ weight of the label (g)	Wet Weight before the 1st cycle (g)	Wet Weight before the 2nd cycle (g)	Wet Weight before the 3rd cycle (g)	Wet Weight before the 4th cycle (g)	Wet Weight before the 5th cycle (g)	Wet Weight before the 6th cycle (g)	Wet Weight before the 7th cycle (g)	Wet Weight before the 8th cycle (g)	Wet Weight before the 9th cycle (g)	Wet Weight before the 10th cycle 100 (g)	Wet Weight before the 11th cycle (g)	Wet Weight before the 12th cycle (g)	Wet Weight before the 13th cycle (g)	Wet Weight before the 14th cycle (g)	Wet Weight before the 15th cycle (g)	Wet Weight before the 16th cycle (g)
Lds	122.178	136.562	136.313	136.557	136.213	136.143	136.226	136.438	136.438	136.215	135.189	136.438	136.156	136.120	136.189	135.916	136.286
Sds	105.701	113.930	113.948	113.969	114.089	113.657	114.358	113.903	114.031	113.641	113.689	113.663	114.310	113.799	113.965	113.753	113.905
Uds	85.254	90.258	90.324	89.564	89.547	89.222	89.122	89.101	88.869	88.328	83.000	87.883	87.457	87.323	86.956	86.909	86.417
Mds	90.965	96.645	96.062	96.408	95.485	95.178	95.548	95.278	94.633	94.419	94.321	94.496	93.944	93.946	93.897	93.601	93.433
Dds	134.038	142.864	141.685	139.695	139.293	138.429	137.773	137.556	136.135	135.207	134.978	134.668	134.023	133.580	132.732	132.245	131.777

Table (T28): The wet weight of the sandstone and limestone samples after immersing them in de-ionised water and before the drying cycle (low relative humidity and high wind speed).

Appendix T: Modified salt crystallisation test results
De-ionised water: Third run.

Sample number	Original Dry Weight+ weight of the label (g)	Weight after 1st cycle (g)	Weight after the 2nd cycle (g)	Weight after the 3rd cycle (g)	Weight after the 4th cycle (g)	Weight after the 5th cycle (g)	Weight after the 6th cycle (g)	Weight after the 7th cycle (g)	Weight after the 8th cycle (g)	Weight after the 9th cycle (g)	Weight after the 10th cycle (g)	Weight after the 11th cycle (g)	Weight after the 12th cycle (g)	Weight after the 13th cycle (g)	Weight after the 14th cycle (g)	Weight after the 15th cycle (g)	Weight after the 16th cycle (g)	ΔW (%)
Lds	119.945	119.877	119.845	119.852	119.808	119.782	119.746	119.721	119.726	119.693	119.682	119.654	119.628	119.620	119.515	119.503	119.480	-0.39
Sds	110.052	110.030	109.983	110.007	109.963	109.963	109.954	109.932	109.940	109.920	109.935	109.927	109.903	109.931	109.923	109.906	109.912	-0.13
Uds	102.697	102.536	102.369	102.005	101.899	101.812	101.786	101.658	101.556	101.501	101.123	100.343	100.229	99.200	98.808	98.479	98.265	-4.32
Mds	92.634	92.264	92.008	91.783	91.560	91.342	90.832	90.487	90.211	90.035	89.644	89.399	89.102	88.770	88.596	88.327	82.548	4.41
Dds	115.754	113.043	112.311	111.478	110.661	109.857	108.133	107.494	106.419	105.959	105.413	104.706	102.637	101.755	100.335	99.547	99.368	-14.16

Table (T29): The dry weight of the sandstone and limestone samples immersed in de-ionised water and dried for 24-hours at low relative humidity and fluctuating wind speed conditions

Sample number	Original Dry Weight+ weight of the label (g)	Wet Weight before the 1st cycle (g)	Wet Weight before the 2nd cycle (g)	Wet Weight before the 3rd cycle (g)	Wet Weight before the 4th cycle (g)	Wet Weight before the 5th cycle (g)	Wet Weight before the 6th cycle (g)	Wet Weight before the 7th cycle (g)	Wet Weight before the 8th cycle (g)	Wet Weight before the 9th cycle (g)	Wet Weight before the 10th cycle 100 (g)	Wet Weight before the 11th cycle (g)	Wet Weight before the 12th cycle (g)	Wet Weight before the 13th cycle (g)	Wet Weight before the 14th cycle (g)	Wet Weight before the 15th cycle (g)	Wet Weight before the 16th cycle (g)
Lds	119.945	134.368	134.334	134.164	134.040	134.120	134.051	134.134	133.925	134.250	134.084	134.079	134.270	133.938	133.902	133.725	133.421
Sds	110.052	117.716	117.800	117.891	117.570	117.602	117.773	117.460	117.789	117.627	117.825	117.546	117.557	117.780	117.541	117.488	117.402
Uds	102.697	107.700	106.712	106.498	106.214	106.187	106.142	106.059	105.871	105.887	105.567	105.357	104.987	104.900	104.471	104.017	103.886
Mds	92.634	97.673	97.833	97.307	96.891	96.556	96.280	96.015	95.515	95.576	95.096	94.931	94.682	94.370	94.012	93.856	93.014
Dds	115.754	122.305	120.253	119.526	118.273	117.687	115.743	114.983	114.569	113.422	112.357	112.087	109.602	108.817	107.547	106.514	106.323

Table (T30): The wet weight of the sandstone and limestone samples after immersing them in de-ionised water and before the drying cycle (low relative humidity and fluctuating wind speed).

Appendix T: Modified salt crystallisation test results
De-ionised water: Fourth run.

Sample number	Original Dry Weight+ weight of the label (g)	Weight after 1st cycle (g)	Weight after the 2nd cycle (g)	Weight after the 3rd cycle (g)	Weight after the 4th cycle (g)	Weight after the 5th cycle (g)	Weight after the 6th cycle (g)	Weight after the 7th cycle (g)	Weight after the 8th cycle (g)	Weight after the 9th cycle (g)	Weight after the 10th cycle (g)	Weight after the 11th cycle (g)	Weight after the 12th cycle (g)	Weight after the 13th cycle (g)	Weight after the 14th cycle (g)	Weight after the 15th cycle (g)	Weight after the 16th cycle (g)	ΔW (%)
Lds	119.206	120.197	120.184	120.152	120.123	120.145	120.107	120.092	120.117	120.131	120.064	120.092	120.194	120.093	120.032	120.054	120.021	0.86
Sds	106.032	107.222	107.241	107.271	107.223	107.219	107.639	107.181	107.219	107.217	107.114	107.341	107.841	107.497	107.397	107.305	107.222	1.12
Uds	113.265	113. 957	113.802	113.796	113.602	113.264	113.202	113.354	113.346	113.221	113.129	113.008	113.258	113.101	112.819	112.702	112.574	-0.61
Mds	105.025	105.930	105.861	105.777	105.591	105.558	104.911	104.432	104.396	104.327	104.206	104.161	104.382	104.081	103.917	103.788	103.610	-1.35
Dds	101.499	102.108	101.613	101.303	100.994	99.655	99.280	99.023	98.779	98.470	98.062	97.815	97.534	96.001	96.600	96.131	95.521	-5.89

Table (T31): The dry weight of the sandstone and limestone samples immersed in de-ionised water and dried for 24-hours at high relative humidity and low wind speed conditions.

Sample number	Original Dry Weight+ weight of the label (g)	Wet Weight before the 1st cycle (g)	Wet Weight before the 2nd cycle (g)	Wet Weight before the 3rd cycle (g)	Wet Weight before the 4th cycle (g)	Wet Weight before the 5th cycle (g)	Wet Weight before the 6th cycle (g)	Wet Weight before the 7th cycle (g)	Wet Weight before the 8th cycle (g)	Wet Weight before the 9th cycle (g)	Wet Weight before the 10th cycle 100 (g)	Wet Weight before the 11th cycle (g)	Wet Weight before the 12th cycle (g)	Wet Weight before the 13th cycle (g)	Wet Weight before the 14th cycle (g)	Wet Weight before the 15th cycle (g)	Wet Weight before the 16th cycle (g)
Lds	119.206	134.522	134.222	134.313	134.190	134.374	134.302	134.148	134.212	134.155	134.132	134.247	134.265	134.270	134.131	134.309	134.119
Sds	106.032	113.789	113.688	113.695	113.802	113.731	113.646	113.645	113.703	113.770	113.673	113.744	113.825	113.991	113.906	113.706	113.628
Uds	113.265	118.579	118.574	118.954	118.214	118.005	118.877	118.333	118.000	118.141	118.017	117.984	117.745	117.624	117.214	116.879	116.549
Mds	105.025	110.790	111.079	110.900	111.702	110.602	110.458	110.389	110.156	110.287	110.136	110.024	109.957	109.969	109.089	109.780	109.587
Dds	101.499	105.842	105.410	105.036	104.922	104.521	104.125	103.994	103.835	103.537	102.827	102.716	102.372	102.296	101.524	101.107	100.488

Table (T32): The wet weight of the sandstone and limestone samples after immersing them in de-ionised water and before the drying cycle (high relative humidity and low wind speed).

Appendix T: Modified salt crystallisation test results
De-ionised water: Fifth run.

Sample number	Original Dry Weight+ weight of the label (g)	Weight after 1st cycle (g)	Weight after the 2nd cycle (g)	Weight after the 3rd cycle (g)	Weight after the 4th cycle (g)	Weight after the 5th cycle (g)	Weight after the 6th cycle (g)	Weight after the 7th cycle (g)	Weight after the 8th cycle (g)	Weight after the 9th cycle (g)	Weight after the 10th cycle (g)	Weight after the 11th cycle (g)	Weight after the 12th cycle (g)	Weight after the 13th cycle (g)	Weight after the 14th cycle (g)	Weight after the 15th cycle (g)	Weight after the 16th cycle (g)	ΔW (%)
Lds	130.214	130.621	130.607	130.611	130.571	130.541	130.539	130.535	130.578	130.501	130.490	130.585	130.529	130.525	130.524	130.520	130.525	0.24
Sds	105.589	105.921	105.932	105.901	105.848	105.912	105.947	105.901	105.843	105.824	105.854	105.901	105.904	105.921	105.908	105.889	105.907	0.30
Uds	98.654	99.324	99.301	93.257	99.231	99.230	99.210	99.147	99.150	99.110	98.894	98.749	98.412	97.987	97.457	97.238	97.219	-1.45
Mds	107.681	107.541	107.488	107.402	107.215	107.325	107.212	107.108	106.871	106.741	106.703	106.7.05	106.648	106.354	106.301	106.259	106.207	-1.37
Dds	114.258	114.201	114.140	113.854	113.802	113.458	113.147	112.478	112.684	112.217	111.583	110.457	109.561	109.007	108.413	106.957	106.201	-7.05

Table (T33): The dry weight of the sandstone and limestone samples immersed in de-ionised water and dried for 24-hours at high relative humidity and high wind speed conditions

Sample number	Original Dry Weight+ weight of the label (g)	Wet Weight before the 1st cycle (g)	Wet Weight before the 2nd cycle (g)	Wet Weight before the 3rd cycle (g)	Wet Weight before the 4th cycle (g)	Wet Weight before the 5th cycle (g)	Wet Weight before the 6th cycle (g)	Wet Weight before the 7th cycle (g)	Wet Weight before the 8th cycle (g)	Wet Weight before the 9th cycle (g)	Wet Weight before the 10th cycle 100 (g)	Wet Weight before the 11th cycle (g)	Wet Weight before the 12th cycle (g)	Wet Weight before the 13th cycle (g)	Wet Weight before the 14th cycle (g)	Wet Weight before the 15th cycle (g)	Wet Weight before the 16th cycle (g)
Lds	130.214	143.984	143.547	143.627	143.457	143.347	143.571	143.601	143.324	143.297	143.324	143.307	143.412	143.361	143.211	143.116	143.010
Sds	105.589	112.847	112.852	112.863	112.861	112.843	112.880	112.841	112.824	112.827	112.827	112.713	112.775	112.741	112.732	112.720	117.710
Uds	98.654	104.209	103.967	103.955	104.015	104.011	103.896	104.002	103.687	103.614	103.478	103.323	103.028	103.004	102.846	102.743	102.457
Mds	107.681	113.138	113.016	112.883	112.687	112.653	112.487	112.338	112.149	111.587	111.298	111.020	111.004	110.961	112.021	111.851	111.637
Dds	114.258	118.879	118.687	118.014	117.943	117.638	117.547	117.621	117.212	116.217	116.021	116.247	115.214	114.372	113.364	111.050	110.548

Table (T34): The wet weight of the sandstone and limestone samples after immersing them in de-ionised water and before the drying cycle (high relative humidity and high wind speed).

Appendix T: Modified salt crystallisation test results
De-ionised water: Sixth run.

Sample number	Original Dry Weight+ weight of the label (g)	Weight after 1st cycle (g)	Weight after the 2nd cycle (g)	Weight after the 3rd cycle (g)	Weight after the 4th cycle (g)	Weight after the 5th cycle (g)	Weight after the 6th cycle (g)	Weight after the 7th cycle (g)	Weight after the 8th cycle (g)	Weight after the 9th cycle (g)	Weight after the 10th cycle (g)	Weight after the 11th cycle (g)	Weight after the 12th cycle (g)	Weight after the 13th cycle (g)	Weight after the 14th cycle (g)	Weight after the 15th cycle (g)	Weight after the 16th cycle (g)	ΔW (%)
Lds	128.898	128.972	128.918	129.139	128.906	135.747	129.122	129.033	128.935	128.916	129.007	128.951	128.955	128.947	128.922	128.897	128.871	-0.02
Sds	106.532	106.751	106.712	106.738	106.711	111.177	106.804	106.772	106.749	106.761	106.760	106.758	106.782	106.747	106.748	106.740	106.733	0.19
Uds	112.214	112.884	112.024	111.412	111.388	115.217	110.988	110.747	110.738	110.549	110.557	110.323	110.019	109.967	109.800	109.718	109.703	-2.24
Mds	88.032	88.531	87.374	87.200	87.072	89.446	86.886	86.802	86.751	86.650	86.589	86.509	86.446	86.379	86.329	86.184	86.075	-2.22
Dds	108.625	108.859	103.981	101.366	98.095	97.046	95.934	94.713	93.473	93.405	92.757	92541	92.531	91.760	91.450	91.884	91.302	-15.49

Table (T35): The dry weight of the sandstone and limestone samples immersed in de-ionised water and dried for 24-hours at high relative humidity and fluctuating wind speed conditions.

Sample number	Original Dry Weight+ weight of the label (g)	Wet Weight before the 1st cycle (g)	Wet Weight before the 2nd cycle (g)	Wet Weight before the 3rd cycle (g)	Wet Weight before the 4th cycle (g)	Wet Weight before the 5th cycle (g)	Wet Weight before the 6th cycle (g)	Wet Weight before the 7th cycle (g)	Wet Weight before the 8th cycle (g)	Wet Weight before the 9th cycle (g)	Wet Weight before the 10th cycle 100 (g)	Wet Weight before the 11th cycle (g)	Wet Weight before the 12th cycle (g)	Wet Weight before the 13th cycle (g)	Wet Weight before the 14th cycle (g)	Wet Weight before the 15th cycle (g)	Wet Weight before the 16th cycle (g)
Lds	128.898	138.757	138.849	139.095	138.650	138.941	138.996	138.961	138.847	139.071	139.017	138.991	138.999	138.946	139.291	87.615	139.052
Sds	106.532	114.342	114.991	114.592	114.491	114.743	114.879	114.494	114.450	114.797	114.719	114.796	115.299	114.630	114.592	136.426	114.892
Uds	112.214	118.021	117.687	117.521	117.444	117.214	116.016	115.547	115.479	115.148	115.107	114.879	114.698	114.428	114.016	114.007	113.934
Mds	88.032	93.256	92.959	92.923	92.591	92.270	92.412	92.289	92.050	92.064	92.056	92.031	92.011	91.773	91.669	91.565	91.482
Dds	108.625	111.126	109.780	107.201	103.406	101.537	100.214	99.390	98.589	98.610	98.303	97.707	97.773	96.920	96.899	96.693	96.659

Table (T36): The wet weight of the sandstone and limestone samples after immersing them in de-ionised water and before the drying cycle (high relative humidity and fluctuating wind speed).

Appendix U: Microclimate conditions during the modified salt crystallisation test.
First run: low relative humidity - low wind speed.

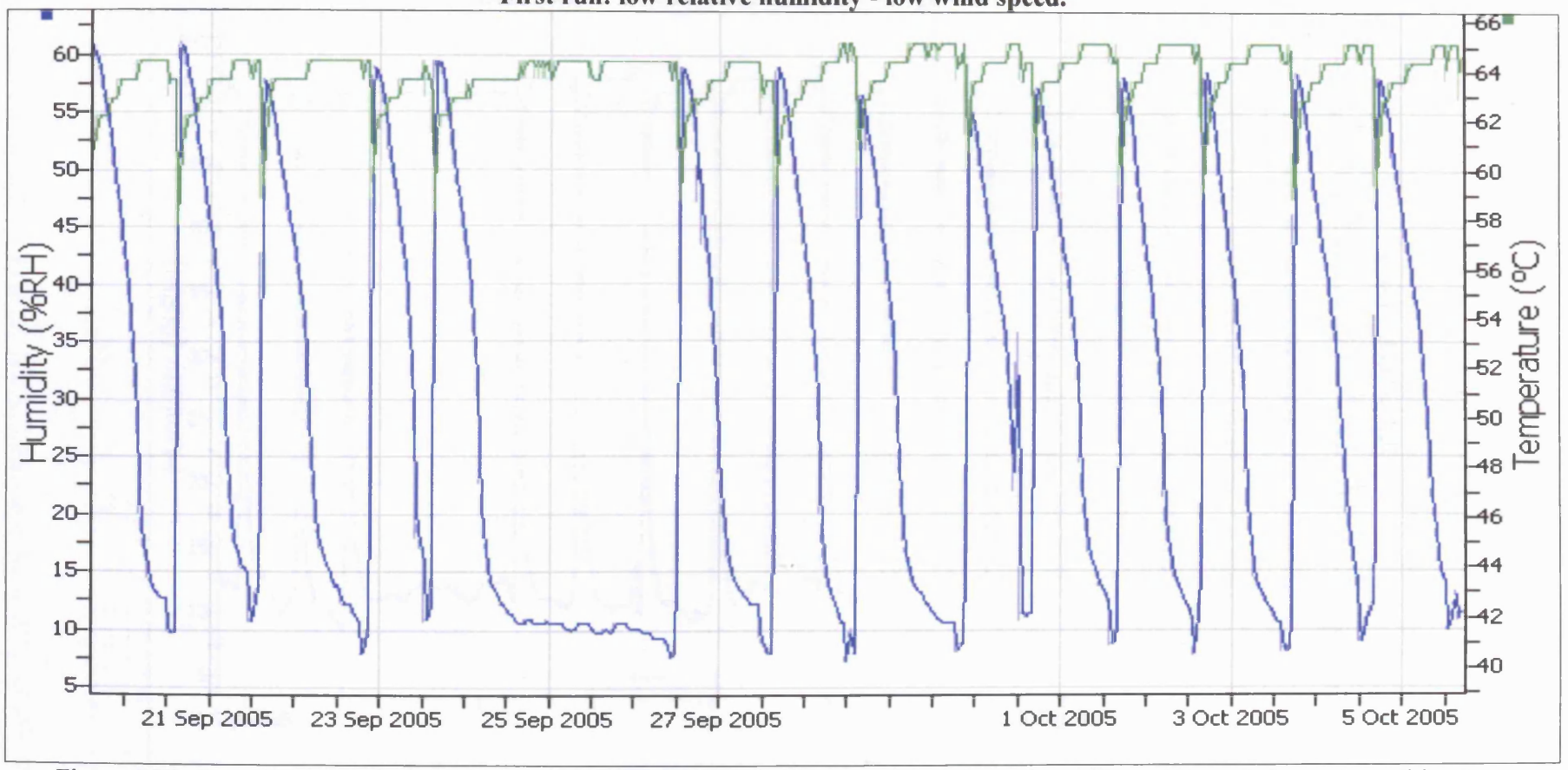

Figure (U1): Temperature and relative humidity readings during the first run (low relative humidity and low wind speed conditions).

Appendix U: Microclimate conditions during the modified salt crystallisation test.
Second run: low relative humidity - high wind speed.

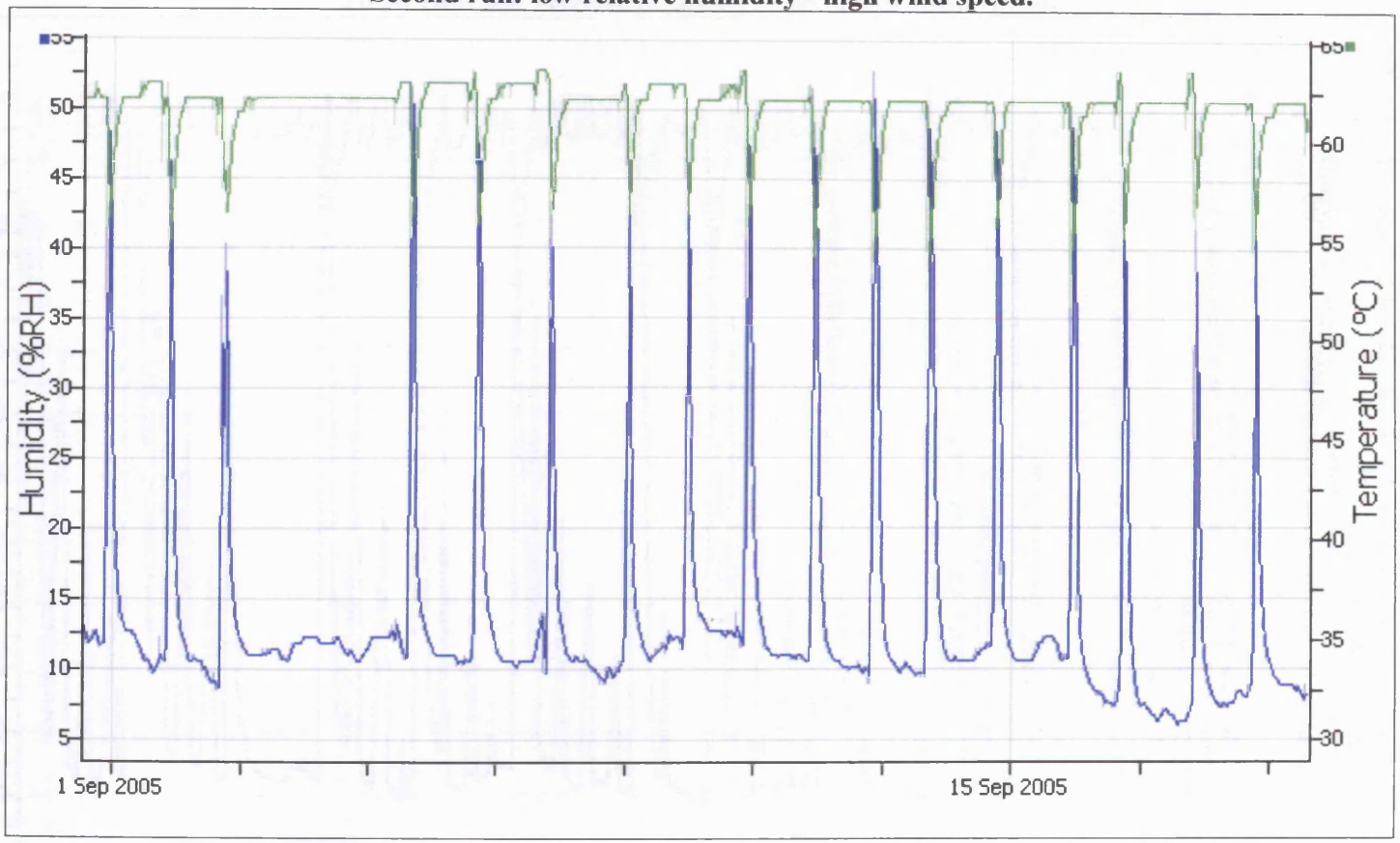

Figure (U2): Temperature and relative humidity readings during the second run (low relative humidity and high wind speed conditions).

Appendix U: Microclimate conditions during the modified salt crystallisation test.
Third run: low relative humidity - fluctuated wind speed.

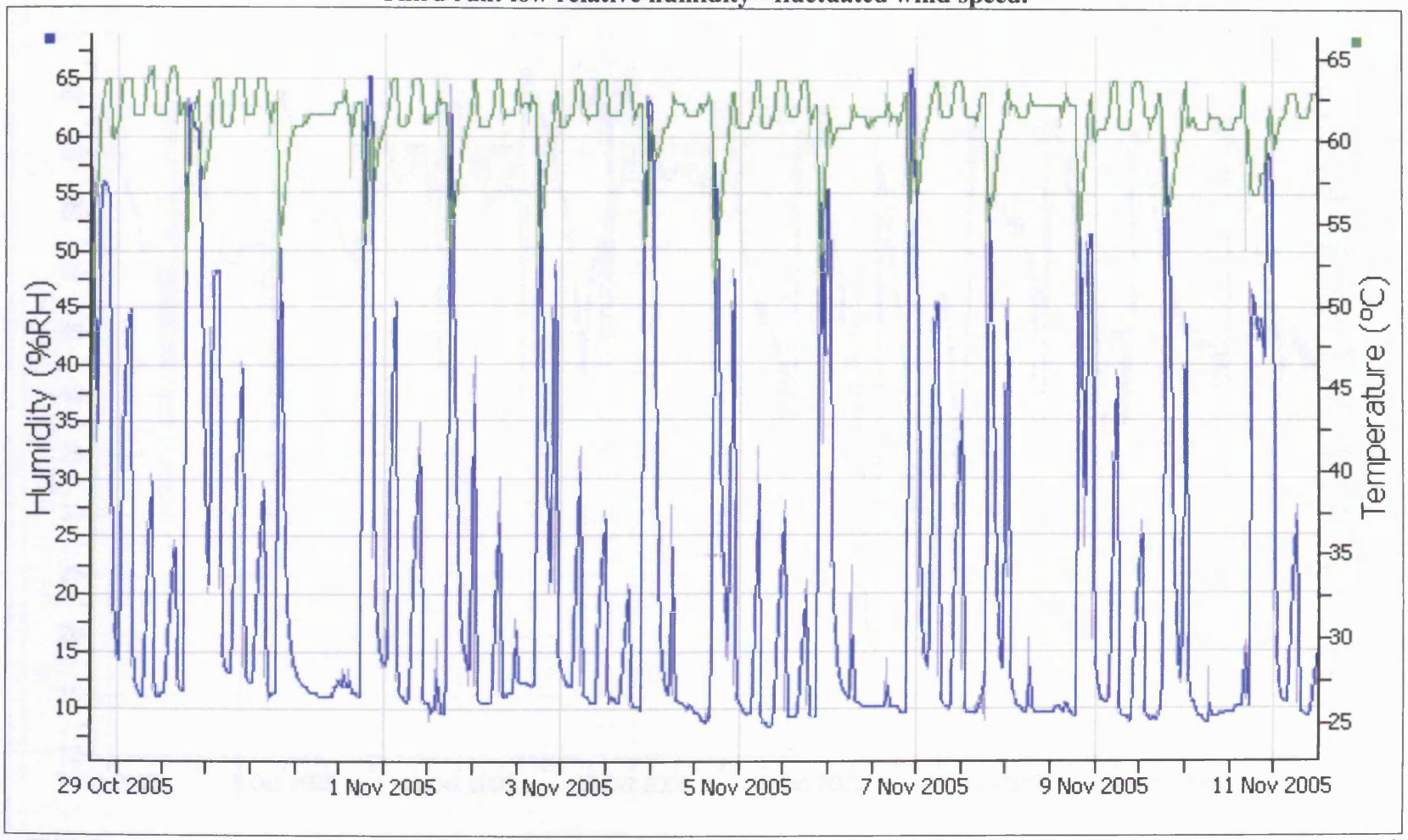

Figure (U3): Temperature and relative humidity readings during the third run (low relative humidity and fluctuating wind speed conditions).

Appendix U: Microclimate conditions during the modified salt crystallisation test.
Fourth run: high relative humidity - low wind speed.

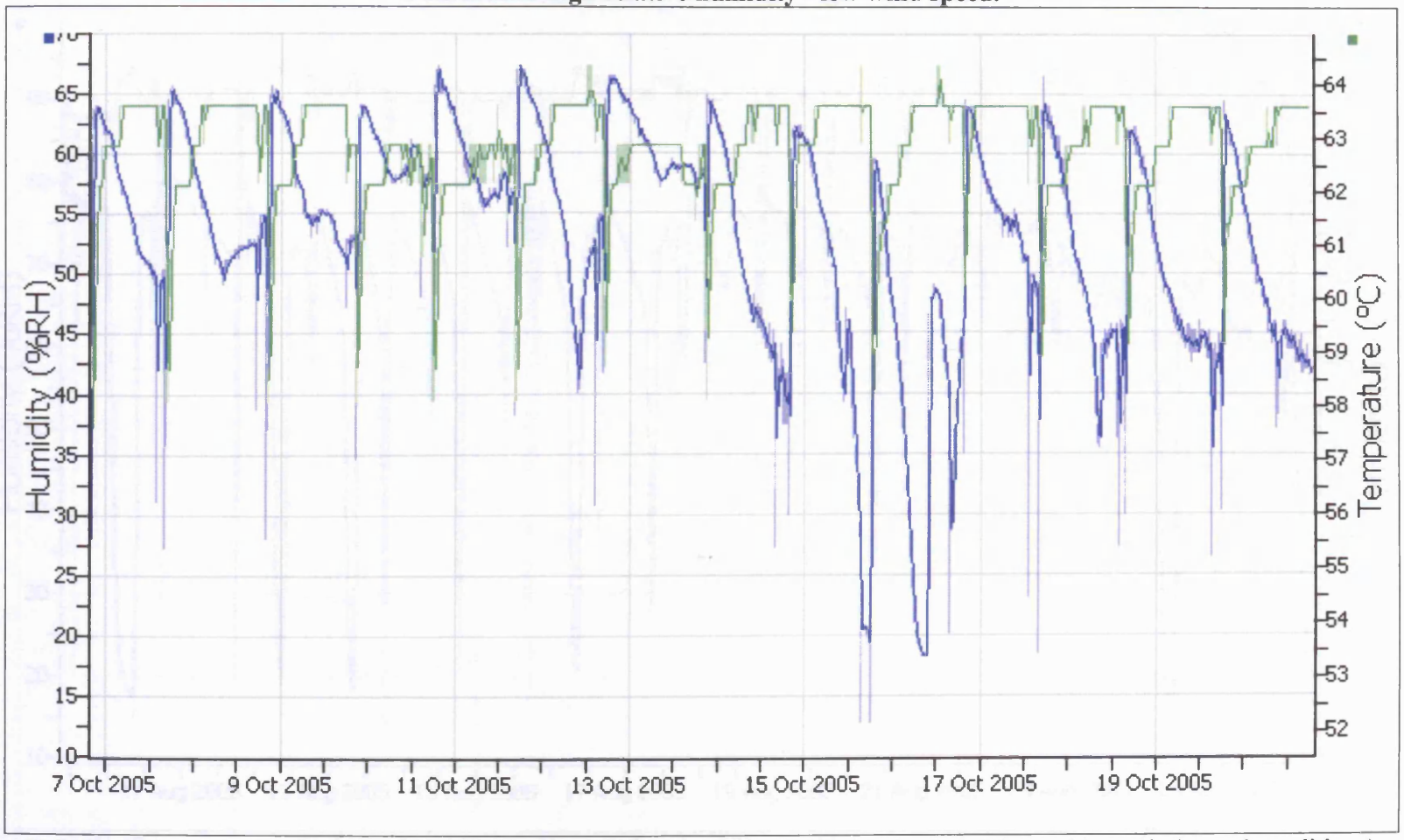

Figure (U4): Temperature and relative humidity readings during the fourth run (high relative humidity and low wind speed conditions).

Appendix U: Microclimate conditions during the modified salt crystallisation test.
Fifth run: high relative humidity - high wind speed.

Figure (U5): Temperature and relative humidity readings during the fifth run (high relative humidity and high wind speed conditions).

Appendix U: Microclimate conditions during the modified salt crystallisation test.
Sixth run: high relative humidity - low wind speed.

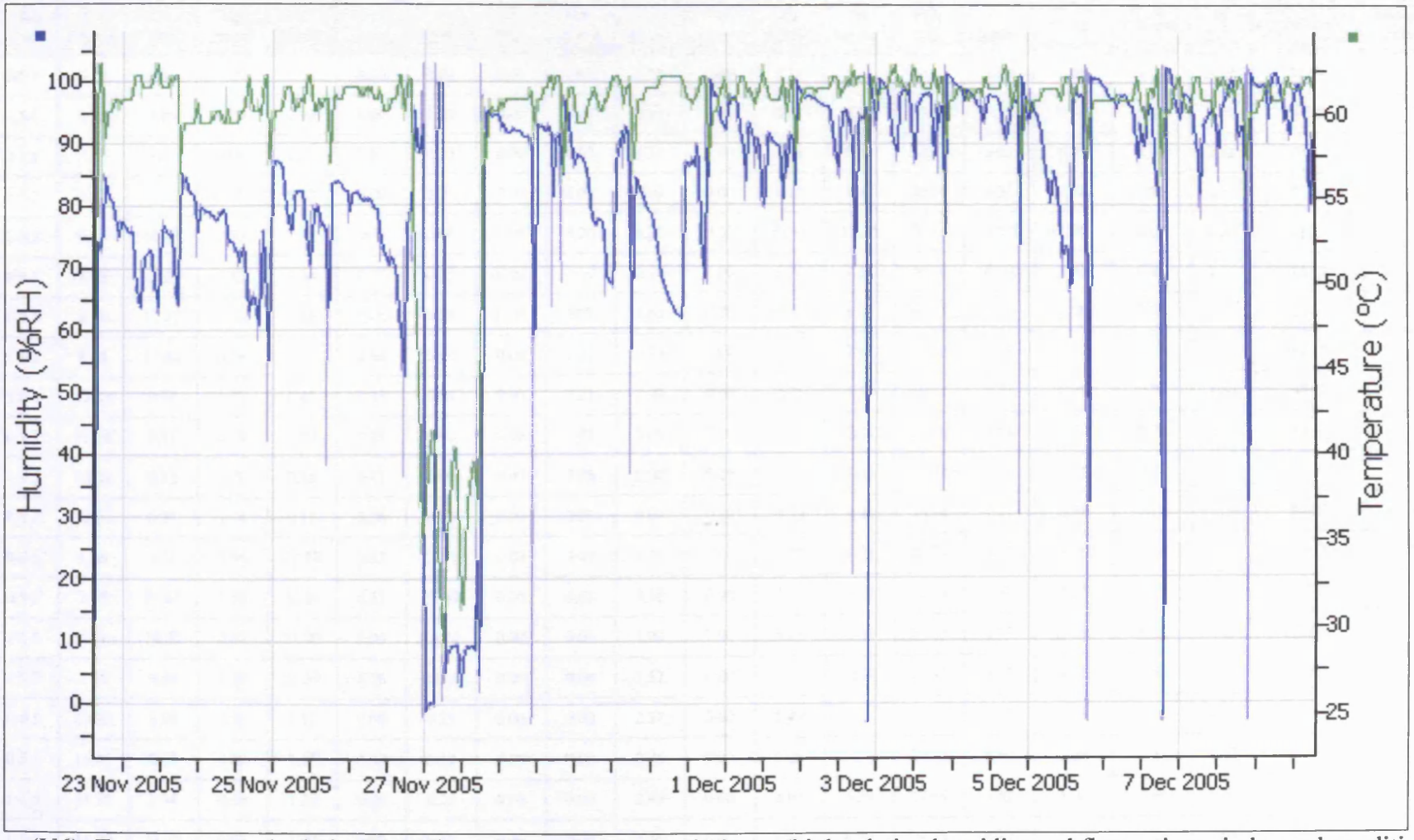

Figure (U6): Temperature and relative humidity readings during the sixth run (high relative humidity and fluctuating wind speed conditions).

Appendix V: The anion and cation content of the drilled samples at the end of the modified salt crystallisation test.
Experiment run: Original samples before the test.

Sample code	Depth (cm)	Ca (ppm)	Na (ppm)	Mg (ppm)	K (ppm)	Fe (ppm)	Al (ppm)	Ti (ppm)	Zn (ppm)	F (ppm)	Br (ppm)	Cl (ppm)	NO_3 (ppm)	PO_4 (ppm)	SO_4 (ppm)	cation charge with Al	Cation charge without Al	Anion charge	Sum of cations & anions (ppm)	Soluble salt content in the sample (%)
D original	0-0.5	6.45	9.05	0.00	0.60	0.00	0.84	0.00	0.00	2.37	0.00	7.27	5.32	30.87	8.62	0.82	0.73	1.57	71.39	0.36
D original	0.5-1	4.09	9.25	0.00	0.90	0.00	1.22	0.00	0.00	0.95	0.00	8.88	5.56	30.79	5.78	0.77	0.63	1.48	67.42	0.34
D original	1-1.5	5.15	9.61	0.00	0.80	0.00	1.73	0.00	0.00	3.34	0.00	7.98	5.09	30.71	6.00	0.89	0.70	1.58	70.41	0.35
D original	1.5-2	4.67	10.57	0.00	0.63	0.00	1.21	0.00	0.01	3.63	0.00	8.16	5.44	30.34	6.34	0.84	0.71	1.60	71.00	0.36
M original	0-0.5	9.45	10.48	0.53	1.72	0.00	0.00	0.00	0.00	1.23	0.00	11.49	17.20	30.45	8.82	1.02	1.02	1.81	91.37	0.46
M original	0.5-1	8.40	8.31	0.43	1.26	0.27	0.55	0.00	0.00	2.76	0.00	9.70	7.54	30.70	6.50	0.92	0.86	1.65	76.42	0.38
M original	1-1.5	8.16	11.07	0.36	1.76	0.16	0.29	0.00	0.01	1.63	0.00	11.11	8.01	30.15	8.91	1.00	0.97	1.67	81.62	0.41
M original	1.5-2	8.04	11.62	0.26	1.45	0.30	0.41	0.00	0.01	3.75	0.00	10.92	7.41	30.56	7.42	1.02	0.97	1.74	82.15	0.41
U original	0-0.5	12.04	0.34	1.22	0.41	0.33	0.00	0.00	1.21	0.00	0.00	4.21	6.59	30.21	9.21	0.78	0.78	1.37	65.77	0.33
U original	0.5-1	11.08	0.51	1.09	0.23	0.21	0.00	0.00	1.45	0.00	0.00	3.24	5.54	30.18	8.64	0.72	0.72	1.31	62.17	0.31
U original	1-1.5	10.21	0.32	1.3	0.18	0.41	0.00	0.00	1.98	0.00	0.00	4.05	5.32	30.28	8.21	0.71	0.71	1.33	62.26	0.31
U original	1.5-2	12.04	0.21	1.14	0.17	0.28	0.00	0.00	2.01	0.00	0.00	3.69	4.96	30.04	7.21	0.78	0.78	1.28	61.75	0.31
S original	0-0.5	1.86	6.54	0.96	22.78	5.82	17.51	0.00	0.02	1.76	0.00	5.29	4.23	30.73	4.20	3.19	1.24	1.37	101.70	0.51
S original	0.5-1	3.97	11.45	1.56	28.20	8.51	22.49	0.00	0.03	3.18	0.00	7.79	5.13	30.75	9.69	4.35	1.85	1.64	132.75	0.66
S original	1-1.5	2.31	10.02	0.82	21.00	5.09	14.74	0.00	0.03	1.03	0.00	8.71	5.09	30.18	5.53	2.98	1.34	1.45	104.55	0.52
S original	1.5-2	2.40	9.49	1.19	25.39	8.26	20.43	0.00	0.04	1.57	0.00	6.19	14.77	29.91	5.23	3.85	1.58	1.55	124.87	0.62
L original	0-0.5	19.22	8.99	0.86	1.11	0.00	0.13	0.00	0.00	2.77	0.00	5.49	6.82	29.73	7.57	1.46	1.45	1.51	82.69	0.41
L original	0.5-1	16.45	8.30	0.69	1.15	0.00	0.12	0.00	0.00	2.75	0.00	6.06	6.30	29.58	5.90	1.28	1.27	1.47	77.30	0.39
L original	1-1.5	11.54	7.34	0.59	1.20	0.00	0.23	0.00	0.00	2.99	0.00	4.67	5.59	29.69	5.52	1.00	0.97	1.43	69.36	0.35
L original	1.5-2	14.00	11.73	0.65	1.99	0.00	0.40	0.00	0.00	4.16	0.00	8.69	6.90	29.75	8.33	1.36	1.32	1.69	86.60	0.43

Table (V1): The anion and cation content of drilled samples from the original salt crystallisation specimens prior to the start of the tests.

Appendix V: The anion and cation content of the drilled samples at the end of the modified salt crystallisation test. Experiment run: First run (low relative humidity - low wind speed).

Sample code	Salt solution	Depth (cm)	Ca (ppm)	Na (ppm)	Mg (ppm)	K (ppm)	Fe (ppm)	Al (ppm)	Ti (ppm)	Zn (ppm)	F (ppm)	Br (ppm)	Cl (ppm)	NO_3 (ppm)	PO_4 (ppm)	SO_4 (ppm)	cation charge with Al	cation charge without Al	Anion charge	Sum of cations & anions (ppm)	Soluble salt content in the sample (%)
D1.1	Petra mixture	0-0.5	20.14	60.74	4.21	55.54	0.01	0.54	0.00	0.00	2.14	0.00	70.37	105.47	23.01	104.16	5.47	5.41	6.70	446.33	2.23
D1.1	Petra mixture	0.5-1	18.14	51.24	3.71	41.14	0.00	0.61	0.00	0.00	3.17	0.00	65.41	40.55	22.58	60.21	4.56	4.49	4.63	306.76	1.53
D1.1	Petra mixture	1-1.5	17.21	65.24	2.47	22.21	0.01	0.12	0.00	0.00	3.54	0.00	40.54	54.24	21.47	30.53	4.48	4.47	3.52	257.58	1.29
D1.1	Petra mixture	1.5-2	15.74	66.06	3.01	16.01	0.03	0.14	0.00	0.00	4.81	0.00	41.52	49.51	20.96	31.34	4.33	4.31	3.54	249.13	1.25
M.1.1	Petra mixture	0-0.5	35.15	75.24	6.21	69.84	0.01	0.30	0.00	0.00	4.28	0.00	40.12	140.38	24.02	140.21	7.36	7.33	7.30	535.76	2.68
M.1.1	Petra mixture	0.5-1	30.64	40.19	4.25	33.25	0.02	0.65	0.00	0.01	3.64	0.00	36.08	50.21	23.04	80.54	4.55	4.48	4.42	302.52	1.51
M.1.1	Petra mixture	1-1.5	30.01	36.47	3.54	30.14	0.00	0.14	0.00	0.00	3.14	0.00	33.65	56.02	22.87	81.24	4.16	4.14	4.43	297.22	1.49
M.1.1	Petra mixture	1.5-2	26.87	48.87	3.67	44.21	0.00	0.11	0.00	0.01	2.68	0.00	34.62	55.27	22.65	98.67	4.91	4.90	4.78	337.63	1.69
S.1.1	Petra mixture	0-0.5	8.24	89.58	5.69	338.61	0.49	1.76	0.00	0.03	4.40	0.00	64.00	152.90	34.76	505.79	13.65	13.45	16.14	1,206.25	6.03
S.1.1	Petra mixture	0.5-1	6.15	42.76	3.67	151.52	3.59	11.83	0.00	0.03	3.69	0.00	37.16	81.77	34.91	145.15	7.79	6.47	6.69	522.23	2.61
S.1.1	Petra mixture	1-1.5	7.43	57.75	4.04	225.42	4.33	13.47	0.00	0.03	3.72	0.00	43.83	104.38	34.24	241.65	10.63	9.13	9.23	740.29	3.70
S.1.1	Petra mixture	1.5-2	6.22	56.08	3.44	219.19	4.67	12.64	0.00	0.04	3.99	0.00	39.79	86.38	33.83	239.61	10.21	8.80	8.79	705.88	3.53
L.2.1	Petra mixture	0-0.5	30.04	142.63	6.52	411.94	0.00	0.00	0.00	0.01	2.17	0.00	100.05	231.62	33.49	478.20	18.77	18.77	17.69	1,436.67	7.18
L.2.1	Petra mixture	0.5-1	33.54	86.16	5.12	253.15	0.00	0.00	0.00	0.01	0.76	0.00	54.54	119.50	32.72	361.50	12.32	12.32	12.07	947.00	4.74
L.2.1	Petra mixture	1-1.5	33.61	81.65	4.61	199.92	0.00	0.00	0.00	0.01	2.81	0.00	61.30	121.18	32.84	253.51	10.72	10.72	10.15	791.44	3.96
L.2.1	Petra mixture	1.5-2	29.80	80.81	5.58	179.58	0.00	0.00	0.00	0.01	2.16	0.00	70.00	146.25	32.75	219.21	10.05	10.05	10.05	766.15	3.83
L.3.1	Sodium sulfate	0-0.5	31.08	320.04	1.83	49.41	0.00	0.00	0.00	0.01	3.15	0.00	20.52	41.60	33.00	673.43	16.89	16.89	16.49	1,174.07	5.87
L.3.1	Sodium sulfate	0.5-1	35.73	191.33	1.65	30.33	0.05	0.00	0.00	0.01	2.36	0.00	15.58	37.34	32.93	386.63	11.02	11.02	10.26	733.94	3.67
L.3.1	Sodium sulfate	1-1.5	29.88	189.49	1.65	32.80	0.00	0.00	0.00	0.01	2.62	0.00	18.39	39.52	32.59	388.85	10.71	10.71	10.42	735.80	3.68
L.3.1	Sodium sulfate	1.5-2	25.39	183.76	1.51	33.83	0.00	0.00	0.00	0.01	2.19	0.00	21.21	49.34	32.38	356.76	10.25	10.25	9.96	706.38	3.53
S.3.1	Sodium sulfate	0-0.5	12.75	481.86	0.28	11.99	0.00	0.07	0.00	0.00	3.90	0.00	12.61	12.84	33.34	1,012.47	21.93	21.92	22.91	1,582.11	7.91
S.3.1	Sodium sulfate	0.5-1	7.29	191.48	0.13	11.29	0.00	0.27	0.00	0.00	3.71	0.00	11.55	10.39	32.44	385.40	9.02	8.99	9.74	653.95	3.27
S.3.1	Sodium sulfate	1-1.5	7.00	248.77	0.34	13.14	1.24	3.92	0.00	0.00	0.00	0.02	0.07	9.39	32.48	502.20	12.01	11.57	11.64	818.57	4.09

Table (V2): The anion and cation content of drilled samples from the salt crystallisation test: first run (low relative humidity and low wind speed conditions).

Appendix V: The anion and cation content of the drilled samples at the end of the modified salt crystallisation test. Experiment run: Second run (low relative humidity - high wind speed).

Sample code	Salt solution	Depth (cm)	Ca (ppm)	Na (ppm)	Mg (ppm)	K (ppm)	Fe (ppm)	Al (ppm)	Tl (ppm)	Zn (ppm)	F (ppm)	Br (ppm)	Cl (ppm)	NO_3 (ppm)	PO_4 (ppm)	SO_4 (ppm)	cation charge with Al	cation charge without Al	Anion charge	Sum of cations & anions (ppm)	Soluble salt content in the sample (%)
S.1.2	Petra mixture	0-0.5	29.57	66.29	4.70	96.99	0.53	2.59	0.00	0.05	5.06	0.00	53.87	153.86	26.34	113.21	7.53	7.24	7.46	553.06	2.77
S.1.2	Petra mixture	0.5-1	15.80	28.04	2.54	55.62	2.36	7.37	0.00	0.09	3.57	0.00	23.94	58.37	27.49	65.52	4.55	3.73	4.04	290.71	1.45
S.1.2	Petra mixture	1-1.5	13.62	28.88	2.61	65.90	4.53	10.95	0.00	0.10	2.55	0.00	23.34	55.32	26.47	70.94	5.22	4.00	4.00	305.21	1.53
S.1.2	Petra mixture	1.5-2	14.67	34.76	2.14	57.02	0.06	0.50	0.00	0.05	3.17	0.00	26.89	59.81	23.83	70.83	3.94	3.88	4.12	293.73	1.47
M.1.2	Petra mixture	0-0.5	48.40	85.51	5.13	79.46	0.05	0.38	0.00	0.05	3.40	0.00	39.46	137.26	24.10	231.68	8.63	8.59	9.09	654.88	3.27
M.1.2	Petra mixture	0.5-1	30.60	28.28	1.61	23.87	0.05	0.00	0.00	0.03	4.20	0.00	20.92	46.10	23.66	108.74	3.50	3.50	4.57	288.06	1.44
M.1.2	Petra mixture	1-1.5	26.80	38.46	2.00	38.29	1.24	1.02	0.00	0.02	3.34	0.00	22.50	54.77	23.86	106.07	4.31	4.20	4.66	318.37	1.59
L.2.2	Petra mixture	0-0.5	58.19	74.97	7.72	123.46	0.00	0.00	0.00	0.01	2.28	0.00	64.13	215.48	23.61	159.93	9.96	9.96	9.48	729.78	3.65
L.2.2	Petra mixture	0.5-1	31.02	74.31	4.93	78.97	0.00	0.00	0.00	0.01	2.83	0.00	56.32	188.02	23.32	68.18	7.21	7.21	6.93	527.91	2.64
L.2.2	Petra mixture	1-1.5	38.94	67.59	6.02	90.90	0.00	0.00	0.00	0.01	2.06	0.00	53.42	186.58	23.54	103.43	7.70	7.70	7.52	572.49	2.86
L.2.2	Petra mixture	1.5-2	40.49	67.68	6.37	108.53	0.00	0.00	0.00	0.01	2.41	0.00	54.43	204.26	23.56	123.37	8.26	8.26	8.27	631.11	3.16
S.3.2	Sodium sulfate	0-0.5	4.23	213.03	0.00	0.62	0.00	0.00	0.00	0.03	2.33	0.00	4.91	4.59	24.37	473.25	9.49	9.49	10.96	727.36	3.64
S.3.2	Sodium sulfate	0.5-1	2.82	1130.74	0.00	0.33	0.00	0.00	0.00	0.01	3.09	0.00	6.02	10.80	6.54	2,454.73	49.33	49.33	51.85	3,615.08	18.08
S.3.2	Sodium sulfate	1-1.5	4.05	243.22	0.00	0.58	0.00	0.00	0.00	0.01	3.78	0.00	8.19	5.01	6.51	501.74	10.80	10.80	11.17	773.09	3.87
D.1.2	Petra mixture	0-0.5	47.78	135.07	3.06	18.96	0.00	0.07	0.00	0.02	3.47	0.00	14.68	37.82	6.46	379.21	9.00	8.99	9.31	646.60	3.23
D.1.2	Petra mixture	0.5-1	31.02	57.91	2.92	26.27	0.00	0.00	0.00	0.01	3.27	0.00	22.02	52.78	24.14	159.66	4.98	4.98	5.73	380.00	1.90
D.1.2	Petra mixture	1-1.5	32.39	74.16	3.05	29.41	0.00	0.12	0.00	0.01	2.38	0.00	20.44	56.47	6.51	195.06	5.86	5.85	5.88	420.00	2.10
D.1.2	Petra mixture	1.5-2	22.68	28.76	2.17	24.01	0.00	0.11	0.00	0.01	2.22	0.00	16.26	53.63	6.30	79.11	3.19	3.18	3.29	235.26	1.18
L.3.2	Sodium sulfate	0-0.5	27.80	375.00	1.01	2.09	0.00	0.00	0.00	0.01	1.73	0.00	6.85	19.98	24.60	806.23	17.84	17.84	18.18	1,265.30	6.33
L.3.2	Sodium sulfate	0.5-1	27.50	603.12	1.08	3.02	0.00	0.00	0.00	0.01	3.49	0.00	9.71	12.73	24.54	1288.74	27.77	27.77	28.28	1,973.94	9.87

Table (V3): The anion and cation content of drilled samples from the salt crystallisation test: second run (low relative humidity and high wind speed conditions).

Appendix V: The anion and cation content of the drilled samples at the end of the modified salt crystallisation test. Experiment run: Third run (low relative humidity - fluctuated wind speed).

Sample code	Salt solution	Depth (cm)	Ca (ppm)	Na (ppm)	Mg (ppm)	K (ppm)	Fe (ppm)	Al (ppm)	Ti (ppm)	Zn (ppm)	F (ppm)	Br (ppm)	Cl (ppm)	NO_3 (ppm)	PO_4 (ppm)	SO_4 (ppm)	cation charge with Al	cation charge without Al	Anion charge	Sum of cations & anions (ppm)	Soluble salt content in the sample (%)
M.1.3	Petra mixture	0-0.25	49.83	84.50	3.39	58.98	0.00	0.05	0.00	0.02	1.38	0.00	38.44	146.53	15.61	202.49	7.96	7.95	8.23	601.22	3.01
M.1.3	Petra mixture	0.25-0.5	23.67	34.43	1.87	21.26	1.47	2.70	0.00	0.04	1.58	0.00	22.32	57.96	24.63	64.36	3.73	3.43	3.77	256.29	1.28
M.1.3	Petra mixture	0.5-0.75	20.40	25.24	1.33	15.43	0.73	1.09	0.00	0.03	2.44	0.00	20.61	44.01	24.78	49.17	2.77	2.65	3.23	205.26	1.03
M.1.3	Petra mixture	0.75-1	21.76	22.44	1.38	17.59	0.00	0.03	0.00	0.03	1.65	0.00	18.02	48.49	24.69	46.04	2.63	2.63	3.12	202.12	1.01
L.3.3	Sodium sulfate	0-0.5	24.43	247.19	0.81	1.53	0.00	0.00	0.00	0.02	1.55	0.00	7.20	10.10	24.85	502.58	12.08	12.08	11.70	820.26	4.10
L.3.3	Sodium sulfate	0.5-1	23.33	106.53	0.61	0.93	0.00	0.00	0.00	0.01	1.80	0.00	6.98	10.84	24.38	205.45	5.87	5.87	5.52	380.86	1.90
L.3.3	Sodium sulfate	1-1.5	25.23	150.93	0.62	1.05	0.00	0.01	0.00	0.01	1.73	0.00	7.14	10.24	24.51	295.04	7.90	7.90	7.38	516.51	2.58
L.3.3	Sodium sulfate	1.5-2	36.94	542.98	0.69	1.27	0.03	0.02	0.00	0.02	1.23	0.00	6.27	12.33	24.62	1,063.60	25.55	25.55	23.37	1,690.00	8.45
S.1.3	Petra mixture	0-0.5	26.40	69.12	4.31	75.92	1.65	6.57	0.00	0.05	2.20	0.00	36.50	97.54	2.56	166.41	7.41	6.68	6.27	489.23	2.45
S.1.3	Petra mixture	0.5-1	15.31	33.17	2.15	50.57	3.16	9.72	0.00	0.05	4.41	0.00	24.05	56.14	8.74	75.64	4.87	3.79	3.67	283.11	1.42
S.1.3	Petra mixture	1-1.5	9.26	31.62	1.30	36.97	1.25	3.67	0.00	0.04	3.38	0.00	22.60	46.57	3.02	55.76	3.34	2.93	2.82	215.44	1.08
S.1.3	Petra mixture	1.5-2	11.94	28.13	1.88	58.13	2.89	8.97	0.00	0.03	3.81	0.00	22.14	49.67	8.74	71.04	4.56	3.56	3.38	267.37	1.34
D.1.3	Petra mixture	0-0.5	41.79	38.90	5.53	62.01	0.00	0.02	0.00	0.07	4.14	0.00	39.43	127.87	23.97	116.76	5.82	5.82	6.58	460.49	2.30
D.1.3	Petra mixture	0.5-1	9.48	17.46	1.24	16.53	0.02	0.31	0.00	0.03	2.10	0.00	15.34	36.85	23.70	33.23	1.79	1.76	2.58	156.29	0.78
D.1.3	Petra mixture	1-1.5	14.24	13.10	0.67	12.86	0.00	0.07	0.00	0.02	2.18	0.00	12.61	25.76	23.53	41.22	1.67	1.66	2.49	146.26	0.73
D.1.3	Petra mixture	1.5-2	17.50	18.61	1.24	19.48	0.00	0.05	0.00	0.03	2.10	0.00	13.21	29.91	23.65	39.29	2.29	2.28	2.53	165.07	0.83
S.3.3	Sodium sulfate	0-0.5	5.20	464.84	0.08	1.43	0.00	0.31	0.00	0.03	4.00	0.00	10.49	7.82	24.02	997.57	20.56	20.53	22.17	1,515.79	7.58
S.3.3	Sodium sulfate	0.5-1	4.38	420.63	0.00	1.01	0.00	0.00	0.00	0.02	3.81	0.00	9.21	6.54	24.03	892.39	18.54	18.54	19.91	1,362.02	6.81

Table (V4): The anion and cation content of drilled samples from the salt crystallisation test: third run (low relative humidity and fluctuating wind speed conditions).

Appendix V: The anion and cation content of the drilled samples at the end of the modified salt crystallisation test. Experiment run: Fourth run (high relative humidity - low wind speed).

Sample code	Salt solution	Depth (cm)	Ca (ppm)	Na (ppm)	Mg (ppm)	K (ppm)	Fe (ppm)	Al (ppm)	Ti (ppm)	Zn (ppm)	F (ppm)	Br (ppm)	Cl (ppm)	NO_3 (ppm)	PO_4 (ppm)	SO_4 (ppm)	cation charge with Al	cation charge without Al	Anion charge	Sum of cations & anions (ppm)	Soluble salt content in the sample (%)
L.3.4	Sodium sulfate	0-0.5	18.37	551.76	0.78	2.03	0.00	0.00	0.00	0.00	1.86	0.00	9.58	17.92	24.14	1,193.33	25.03	25.03	26.28	1,819.77	9.10
L.3.4	Sodium sulfate	0.5-1	17.55	280.21	1.00	1.83	0.00	0.00	0.00	0.00	4.01	0.00	7.23	11.89	24.08	577.49	13.19	13.19	13.40	925.29	4.63
L.3.4	Sodium sulfate	1-1.5	15.77	248.69	1.01	1.51	0.00	0.00	0.00	0.00	2.33	0.00	6.67	9.61	24.02	528.53	11.73	11.73	12.23	838.14	4.19
L.3.4	Sodium sulfate	1.5-2	24.41	327.13	1.14	1.80	0.00	0.01	0.00	0.01	2.01	0.00	5.99	16.99	24.21	697.62	15.59	15.59	15.85	1,101.32	5.51
S.3.4	Sodium sulfate	0-0.5	13.20	669.54	0.41	8.13	0.00	0.37	0.00	0.00	3.61	0.00	8.56	9.80	24.81	1,420.58	30.06	30.02	30.97	2,159.01	10.80
S.3.4	Sodium sulfate	0.5-1	8.42	194.47	0.71	14.69	2.19	7.32	0.00	0.01	4.61	0.00	11.19	9.56	2.97	406.17	10.21	9.40	9.27	662.31	3.31
S.3.4	Sodium sulfate	1-1.5	4.90	149.80	0.20	7.23	0.45	1.76	0.00	0.03	4.29	0.00	10.92	7.48	23.92	300.24	7.17	6.97	7.66	511.22	2.56
S.3.4	Sodium sulfate	1.5-2	4.26	143.07	0.30	10.73	0.00	0.09	0.00	0.04	4.73	0.00	10.00	8.15	8.63	298.44	6.75	6.74	7.15	488.44	2.44
M.1.4	Petra mixture	0-0.5	36.09	54.67	3.10	53.73	0.13	0.32	0.00	0.02	3.33	0.00	31.65	92.00	29.02	134.48	5.85	5.81	6.27	438.54	2.19
M.1.4	Petra mixture	0.5-1	24.25	40.20	3.78	57.18	0.00	0.00	0.00	0.02	3.13	0.00	38.23	122.70	23.69	65.84	4.73	4.73	5.34	379.02	1.90
M.1.4	Petra mixture	1-1.5	35.34	37.37	3.70	44.57	0.02	0.05	0.00	0.02	2.64	0.00	31.18	102.21	23.91	103.47	4.84	4.83	5.58	384.48	1.92
M.1.4	Petra mixture	1.5-2	32.69	38.21	3.73	43.37	0.00	0.00	0.00	0.02	3.11	0.00	34.30	110.66	23.72	105.35	4.71	4.71	5.86	395.16	1.98
D.1.4	Petra mixture	0-0.5	25.64	61.98	6.22	85.04	0.00	1.11	0.00	0.03	3.36	0.00	53.14	190.05	7.61	93.64	6.79	6.67	6.93	527.82	2.64
D.1.4	Petra mixture	0.5-1	13.25	42.88	4.49	55.71	0.00	0.41	0.00	0.02	3.16	0.00	38.82	116.68	7.58	56.71	4.37	4.32	4.56	339.71	1.70
D.1.4	Petra mixture	1-1.5	15.57	49.50	4.98	68.88	0.00	2.22	0.00	0.02	3.46	0.00	42.25	134.49	7.71	72.90	6.75	6.74	7.15	488.44	2.44
D.1.4	Petra mixture	1.5-2	12.37	44.83	4.86	60.90	0.00	2.36	0.00	0.15	3.15	0.00	36.87	128.43	7.76	66.40	5.35	5.10	5.30	401.98	2.01
L.1.4	Petra mixture	0-0.5	86.12	84.67	9.92	158.85	0.00	0.00	0.00	0.02	3.88	0.00	74.73	293.94	24.05	269.39	4.79	4.53	4.91	368.08	1.84
L.1.4	Petra mixture	0.5-1	46.21	81.99	7.12	88.20	0.07	0.00	0.00	0.01	1.82	0.00	73.40	234.19	22.95	82.73	12.86	12.86	13.42	1,005.57	5.03
L.1.4	Petra mixture	1-1.5	29.35	79.51	6.37	90.01	0.00	0.00	0.00	0.01	3.37	0.00	73.07	236.28	23.76	71.18	8.72	8.72	8.39	638.69	3.19
L.1.4	Petra mixture	1.5-2	40.54	91.80	6.03	94.65	0.00	0.00	0.00	0.01	4.94	0.00	85.16	254.60	23.65	59.05	7.75	7.75	8.28	612.91	3.06
S.2.4	Petra mixture	0-0.5	52.08	29.22	3.18	63.25	0.42	1.55	0.00	0.03	3.06	0.00	24.84	72.07	25.15	161.23	8.93	8.93	8.75	660.43	3.30
S.2.4	Petra mixture	0.5-1	19.59	23.78	2.08	46.74	2.03	6.49	0.00	0.04	2.16	0.00	21.34	51.95	24.77	61.72	4.17	3.45	3.62	262.69	1.31
S.2.4	Petra mixture	1-1.5	22.55	26.43	2.10	45.20	1.86	5.17	0.00	0.04	4.41	0.00	22.75	40.01	25.19	73.33	4.25	3.68	3.84	269.04	1.35
S.2.4	Petra mixture	1.5-2	27.09	23.34	2.11	44.57	3.21	7.63	0.00	0.04	3.90	0.00	20.23	34.61	25.06	87.24	4.65	3.80	3.94	279.03	1.40

Table (V5): The anion and cation content of drilled samples from the salt crystallisation test: Fourth run (high relative humidity and low wind speed conditions).

Appendix V: The anion and cation content of the drilled samples at the end of the modified salt crystallisation test. Experiment run: Fifth run (high relative humidity - high wind speed).

Sample code	Salt solution	Depth (cm)	Ca (ppm)	Na (ppm)	Mg (ppm)	K (ppm)	Fe (ppm)	Al (ppm)	Ti (ppm)	Zn (ppm)	F (ppm)	Br (ppm)	Cl (ppm)	NO_3 (ppm)	PO_4 (ppm)	SO_4 (ppm)	cation charge with Al	cation charge without Al	Anion charge	Sum of cations & anions (ppm)	Soluble salt content in the sample (%)
S.1.5	Petra mixture	0-0.5	57.09	25.73	2.40	60.93	0.17	1.32	0.00	0.08	3.02	0.00	27.35	68.98	27.99	157.46	5.88	5.73	6.21	432.52	2.16
S.1.5	Petra mixture	0.5-1	25.15	22.73	2.10	41.52	0.84	3.04	0.00	0.02	3.55	0.00	23.88	56.02	7.17	65.07	3.85	3.51	3.35	251.09	1.26
S.1.5	Petra mixture	1-1.5	25.12	24.81	2.36	41.35	0.53	2.07	0.00	0.04	3.75	0.00	25.88	56.14	23.87	76.57	3.83	3.60	4.18	282.49	1.41
S.1.5	Petra mixture	1.5-2	16.69	21.02	2.02	39.96	2.78	8.99	0.00	0.04	3.73	0.00	17.52	26.50	24.75	50.77	4.04	3.04	2.96	214.77	1.07
D.1.5	Petra mixture	0-0.5	22.74	36.93	3.64	51.03	0.02	0.05	0.00	0.02	3.45	0.00	34.71	106.06	6.43	64.57	4.35	4.34	4.42	329.65	1.65
D.1.5	Petra mixture	0.5-1	13.32	27.77	3.14	38.19	0.00	0.08	0.00	0.02	3.10	0.00	25.72	68.67	6.34	47.78	3.12	3.11	3.19	234.13	1.17
D.1.5	Petra mixture	1-1.5	13.20	29.01	3.69	39.23	0.00	0.00	0.00	0.01	2.58	0.00	26.99	74.00	22.99	49.80	3.23	3.23	3.85	261.50	1.31
D.1.5	Petra mixture	1.5-2	20.46	35.26	4.30	47.31	0.00	0.00	0.00	0.05	3.09	0.00	31.55	94.59	23.08	64.59	4.12	4.12	4.65	324.28	1.62
M.1.5	Petra mixture	0-0.5	28.35	87.08	6.55	83.12	0.00	0.25	0.00	0.06	2.90	0.00	52.58	161.70	24.29	158.34	7.90	7.87	8.31	605.22	3.03
M.1.5	Petra mixture	0.5-1	27.30	68.36	5.64	79.20	0.16	0.65	0.00	0.09	2.61	0.00	46.44	146.84	23.87	146.72	6.91	6.84	7.63	547.88	2.74
M.1.5	Petra mixture	1-1.5	10.37	31.37	2.05	35.24	0.21	0.77	0.00	0.04	2.01	0.00	22.43	57.88	23.19	60.62	3.05	2.96	3.67	246.18	1.23
M.1.5	Petra mixture	1.5-2	17.14	38.51	2.48	42.35	0.00	0.05	0.00	0.04	1.76	0.00	25.02	71.88	23.25	81.70	3.82	3.81	4.39	304.18	1.52
S.3.5	Sodium sulfate	0-0.5	6.04	952.76	0.12	7.15	0.00	0.00	0.00	0.16	2.71	0.00	12.33	23.33	23.81	2,028.88	41.94	41.94	43.88	3,057.29	15.29
S.35	Sodium sulfate	0.5-1	3.15	243.25	0.00	7.27	0.00	0.00	0.00	0.03	2.47	0.00	11.66	30.54	6.39	478.25	10.92	10.92	11.12	783.01	3.92
S.3.3	Sodium sulfate	1-1.5	3.76	362.90	0.00	7.01	0.00	0.00	0.00	0.02	3.44	0.00	10.48	32.02	23.77	739.07	16.15	16.15	17.14	1,182.47	5.91
S.3.5	Sodium sulfate	1.5-2	4.41	252.04	0.05	7.00	0.00	0.00	0.00	0.03	3.76	0.00	12.19	36.02	23.86	584.40	11.37	11.37	14.05	923.76	4.62
L.3.5	Sodium sulfate	0-0.5	20.95	813.00	0.99	3.07	0.00	0.00	0.00	0.01	4.58	0.00	10.28	26.61	6.41	1,726.53	36.57	36.57	37.13	2,612.43	13.06
L.3.5	Sodium sulfate	0.5-1	19.94	286.31	0.99	2.64	0.00	0.00	0.00	0.01	2.34	0.00	7.40	11.40	23.75	601.55	13.60	13.60	13.80	956.33	4.78
L.3.5	Sodium sulfate	1-1.5	22.19	326.98	1.01	2.43	0.00	0.00	0.00	0.01	4.23	0.00	8.82	12.40	24.09	823.08	15.48	15.48	18.58	1,225.24	6.13
L.3.5	Sodium sulfate	1.5-2	25.74	216.92	1.43	2.69	0.00	0.00	0.00	0.00	3.20	0.00	8.43	21.15	23.73	447.82	10.91	10.91	10.83	751.11	3.76

Table (V6): The anion and cation content of drilled samples from the salt crystallisation test: fifth run (high relative humidity and high wind speed conditions).

Appendix V: The anion and cation content of the drilled samples at the end of the modified salt crystallisation test. Experiment run: sixth run (high relative humidity – fluctuating wind speed).

Sample code	Salt solution	Depth (cm)	Ca (ppm)	Na (ppm)	Mg (ppm)	K (ppm)	Fe (ppm)	Al (ppm)	Ti (ppm)	Zn (ppm)	F (ppm)	Br (ppm)	Cl (ppm)	NO_3 (ppm)	PO_4 (ppm)	SO_4 (ppm)	cation charge with Al	cation charge without Al	Anion charge	Sum of cations & anions (ppm)	Soluble salt content in the sample (%)
S.3.6	Sodium sulfate	0-0.5	5.61	165.26	0.11	5.76	0.00	0.34	0.00	0.01	1.87	0.00	7.72	6.51	30.76	318.26	7.66	7.62	8.02	542.21	2.71
S.3.6	Sodium sulfate	0.5-1	3.65	66.88	0.14	10.42	0.60	2.10	0.00	0.01	3.27	0.00	9.49	5.23	31.05	124.78	3.62	3.39	4.10	257.62	1.29
S.3.6	Sodium sulfate	1-1.5	4.91	81.23	0.50	17.48	1.53	5.06	0.00	0.03	3.28	0.00	9.10	5.43	33.51	165.30	4.88	4.32	5.02	327.36	1.64
L.3.6	Sodium sulfate	0-0.5	20.16	325.32	0.86	2.93	0.00	0.00	0.00	0.01	2.21	0.00	9.48	10.61	31.03	661.13	15.30	15.30	15.31	1,063.74	5.32
L.3.6	Sodium sulfate	0.5-1	30.97	256.73	1.05	1.84	0.00	0.00	0.00	0.01	1.76	0.00	6.87	9.35	31.48	530.12	12.85	12.85	12.47	870.18	4.35
M.1.6	Petra mixture	0-0.5	63.63	43.78	2.45	36.12	0.00	0.00	0.00	0.02	2.39	0.00	24.70	75.49	30.47	191.40	6.21	6.21	6.99	470.45	2.35
M.1.6	Petra mixture	0.5-1	19.74	25.97	1.76	25.05	0.00	0.00	0.00	0.01	2.12	0.00	19.27	56.61	30.03	57.30	2.90	2.90	3.71	237.86	1.19
L.2.6	Sodium sulfate	0-0.5	49.54	99.67	9.69	126.50	0.00	0.00	0.00	0.06	3.10	0.00	75.14	290.31	30.23	161.91	10.84	10.84	11.29	846.15	4.23
L.2.6	Petra mixture	0.5-1	32.74	70.08	4.70	90.87	0.00	0.00	0.00	0.01	2.11	0.00	55.63	198.22	29.91	71.49	7.39	7.39	7.31	555.76	2.78
L.2.6	Petra mixture	1-1.5	30.54	57.23	3.44	78.82	0.00	0.00	0.00	0.01	1.76	0.00	47.38	166.49	29.90	49.51	6.31	6.31	6.09	465.08	2.33
L.2.6	Petra mixture	1.5-2	37.66	55.59	4.68	82.81	0.00	0.00	0.00	0.01	1.46	0.00	47.13	165.37	29.72	83.73	6.80	6.80	6.76	508.16	2.54
D.1.6	Petra mixture	0-0.5	43.35	37.95	3.45	35.10	0.00	0.00	0.00	0.04	2.28	0.00	24.53	76.80	29.70	129.60	5.00	5.00	5.69	382.80	1.91
D.1.6	Petra mixture	0.5-1	18.37	24.90	1.70	19.96	0.00	0.00	0.00	0.03	2.69	0.00	18.06	43.07	29.44	49.79	2.65	2.65	3.31	208.01	1.04
D.1.6	Petra mixture	1-1.5	9.77	29.62	1.85	21.55	0.00	0.00	0.00	0.02	3.29	0.00	21.29	49.14	30.14	35.37	2.48	2.48	3.26	202.04	1.01
S.2.6	Petra mixture	0-0.5	79.79	43.20	5.34	87.67	0.00	0.00	0.00	0.02	3.36	0.00	40.97	127.00	29.87	228.07	8.54	8.54	9.08	645.29	3.23
S.2.6	Petra mixture	0.5-1	23.74	29.63	2.47	55.87	0.97	3.60	0.00	0.05	3.84	0.00	30.72	45.70	37.15	90.00	4.54	4.14	4.85	323.74	1.62
S.2.6	Petra mixture	1-1.5	12.50	25.73	1.55	44.89	1.09	3.41	0.00	0.04	3.28	0.00	26.96	36.79	36.88	53.91	3.44	3.06	3.81	247.03	1.24
S.2.6	Petra mixture	1.5-2	10.36	27.16	1.85	50.39	1.28	3.90	0.00	0.03	3.29	0.00	28.22	56.79	31.71	43.13	3.62	3.19	3.79	258.11	1.29
L.4.6	Petra mixture	1-1.5	19.23	318.49	0.70	1.77	0.00	0.00	0.00	0.00	3.94	0.00	9.55	8.47	29.82	638.40	14.92	14.92	14.85	1,030.37	5.15
L.4.6	Sodium sulfate	1.5-2	22.13	266.56	0.68	1.49	0.00	0.00	0.00	0.00	3.69	0.00	8.40	7.99	34.21	537.22	12.79	12.79	12.83	882.37	4.41
L.4.6	Sodium sulfate	0-0.5	21.64	250.40	0.69	1.60	0.00	0.00	0.00	0.00	3.46	0.00	7.18	8.14	29.68	500.84	12.07	12.07	11.89	823.63	4.12
L.4.6	Sodium sulfate	0.5-1	45.83	258.80	1.33	1.93	0.01	0.00	0.00	0.01	2.75	0.00	8.74	9.88	29.41	508.56	13.70	13.70	12.07	867.25	4.34
Ds.6	Di-ionized water	0-05	2.61	8.85	0.00	0.57	0.20	2.47	0.00	0.02	2.70	0.00	7.09	6.83	0.56	11.27	0.81	0.54	0.70	43.17	0.22
Ds.6	Di-ionized water	0.5-1	2.59	9.10	0.00	0.55	0.14	2.80	0.00	0.01	2.48	0.00	6.14	6.59	12.62	11.70	0.86	0.55	1.05	54.72	0.27

Table (V7): The anion and cation content of drilled samples from the salt crystallisation test: sixth run (high relative humidity and fluctuating wind speed conditions).

Appendix W: Distribution of the main anions and cations in the powder samples collected from the Locharbriggs sandstone specimens at the end of the modified salt crystallisation test.

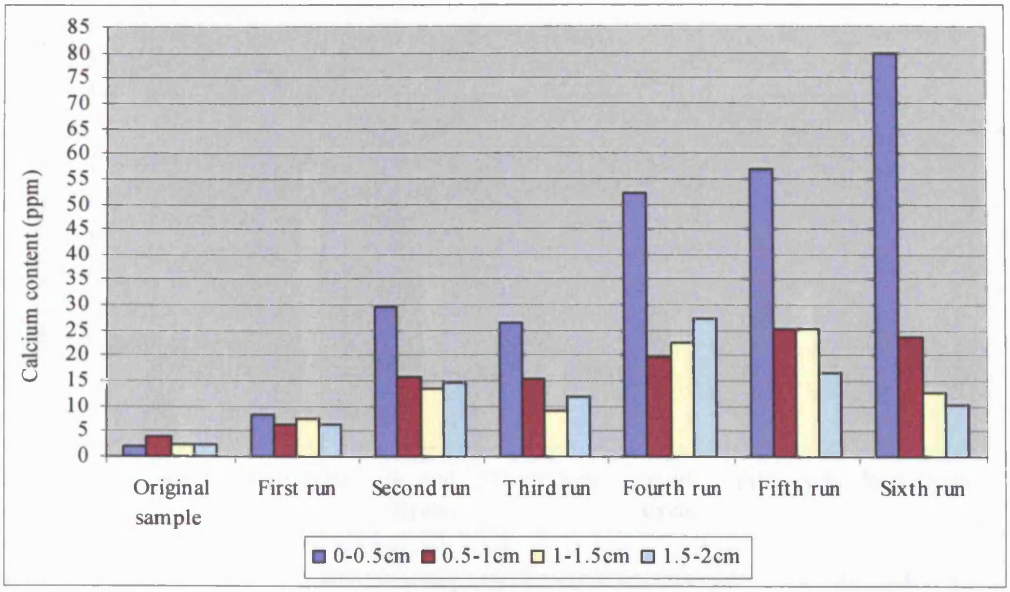

Figure (W1): The calcium concentration, as weight %, in the Locharbriggs sandstone powder samples collected from different depth intervals at end of the Petra salt simulation test.

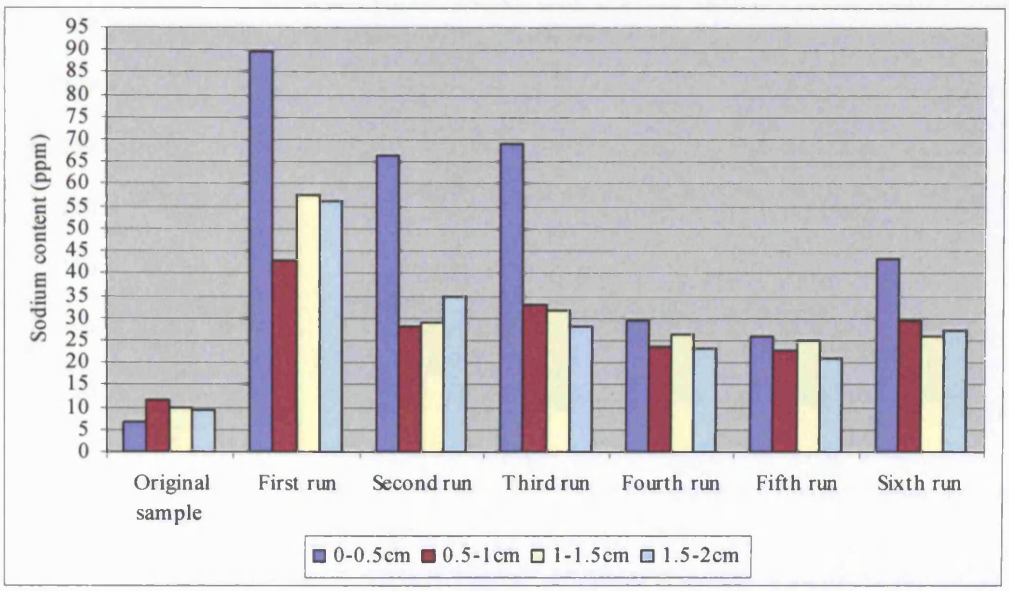

Figure (W2): The sodium concentration, as weight %, in the Locharbriggs sandstone powder samples collected from different depth intervals at end of the Petra salt simulation test.

Appendix W: Distribution of the main anions and cations in the powder samples collected from the Locharbriggs sandstone specimens at the end of the modified salt crystallisation test.

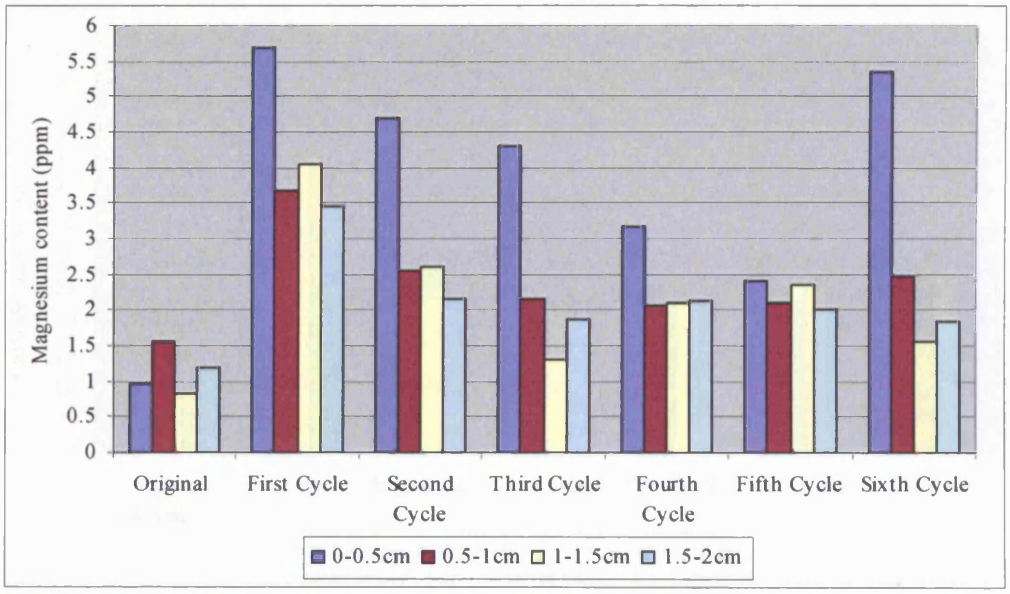

Figure (W3): The magnesium concentration, as weight %, in the Locharbriggs sandstone powder samples collected from different depth intervals at end of the Petra salt simulation test.

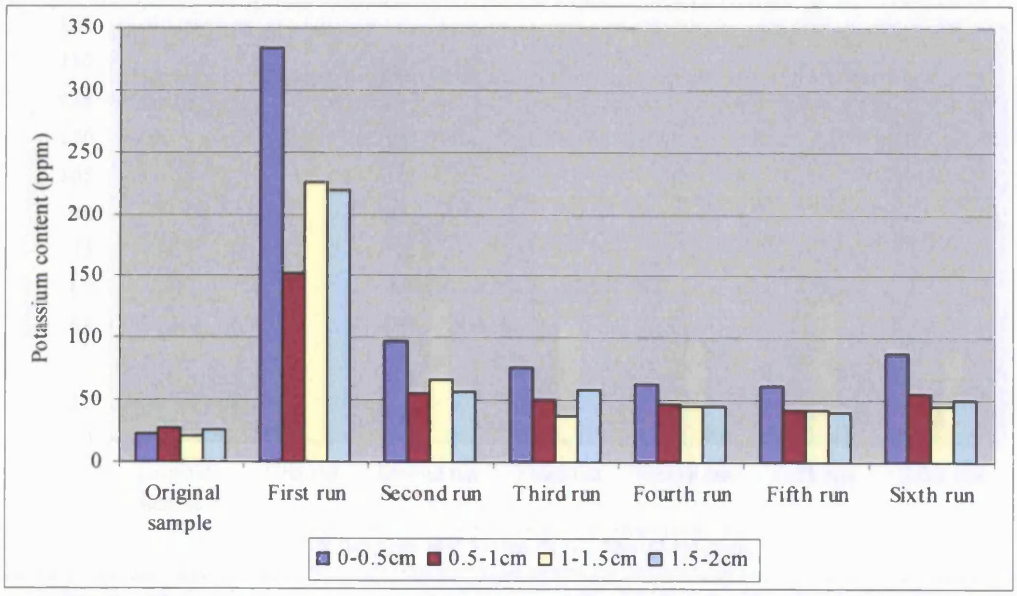

Figure (W4): The potassium concentration, as weight %, in the Locharbriggs sandstone powder samples collected from different depth intervals at end of the Petra salt simulation test.

Appendix W: Distribution of the main anions and cations in the powder samples collected from the Locharbriggs sandstone specimens at the end of the modified salt crystallisation test.

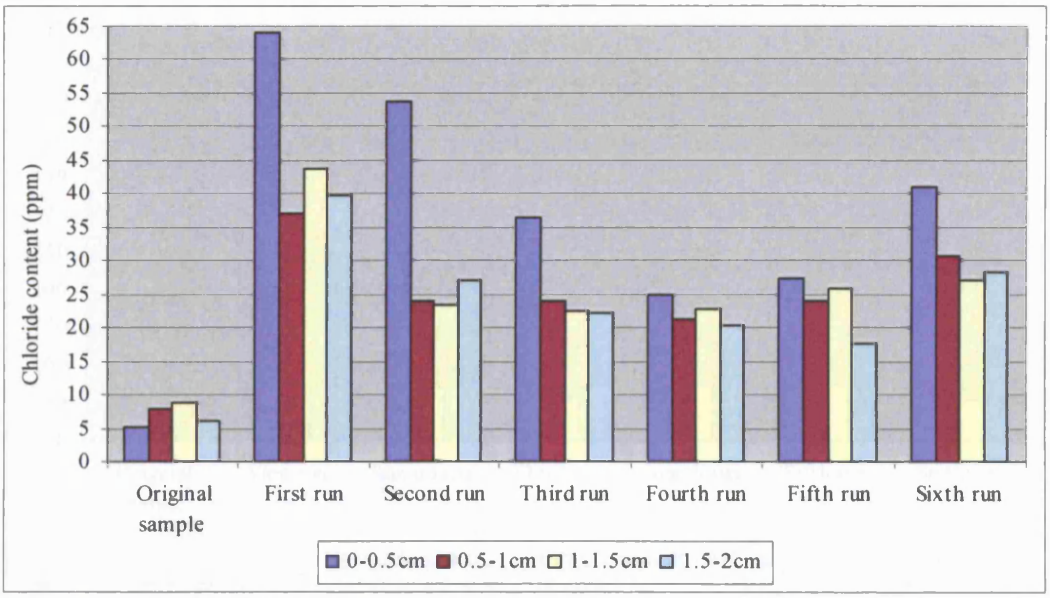

Figure (W5): The chloride concentration, as weight %, in the Locharbriggs sandstone powder samples collected from different depth intervals at end of the Petra salt simulation test.

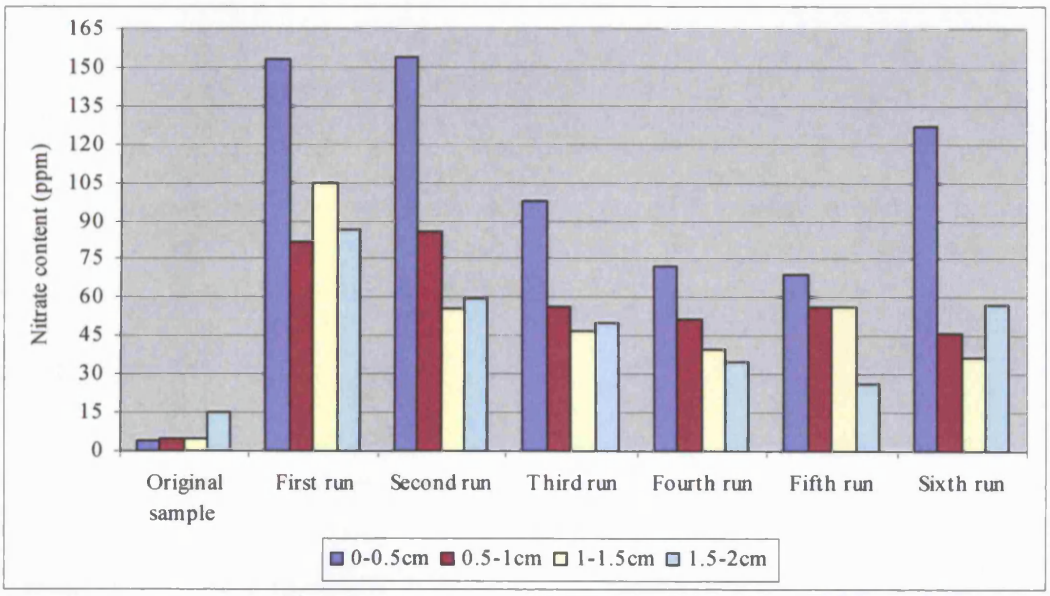

Figure (W6): The nitrate concentration, as weight %, in the Locharbriggs sandstone powder samples collected from different depth intervals at end of the Petra salt simulation test.

Appendix W: Distribution of the main anions and cations in the powder samples collected from the Locharbriggs sandstone specimens at the end of the modified salt crystallisation test.

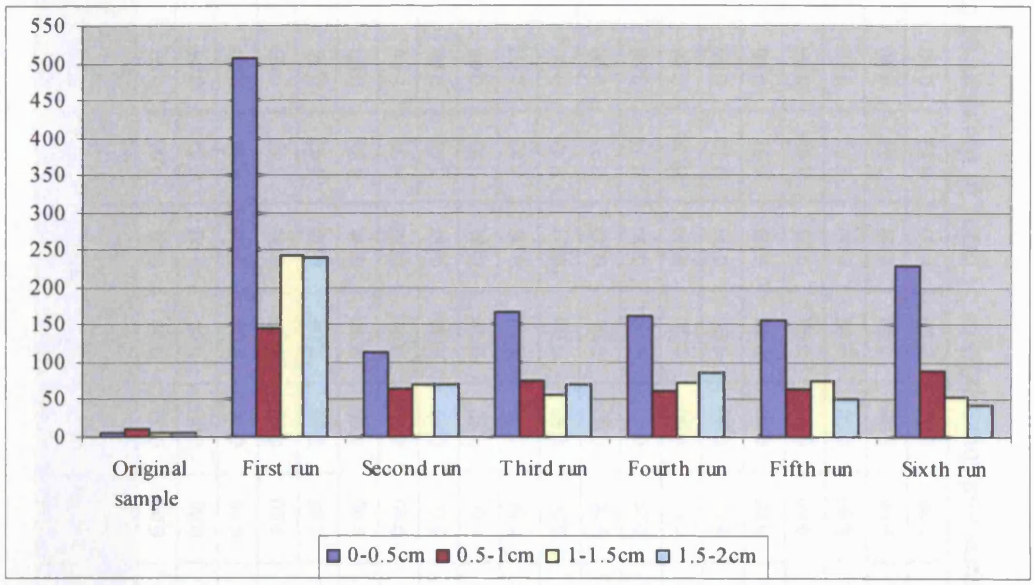

Figure (W7): The sulfate concentration, as weight %, in the Locharbriggs sandstone powder samples collected from different depth intervals at end of the Petra salt simulation test.

Appendix X: The anion and cation content from the thin sections at the end of the modified salt crystallisation test. Experiment run: Original samples before the test

Sample code	Depth (mm)	Si %	Na %	Ca %	Mg %	K %	Al %	S %	Cl %	O %	Na/Si ×100% %	Ca/Si ×100% %	Mg/Si ×100% %	K/Si ×100% %	Al/Si ×100% %	S/Si ×100% %	Cl/Si ×100% %
D original	0-2	44.38	0.00	0.00	0.00	0.00	2.51	0.00	0.31	52.80	0.00	0.00	0.00	0.00	5.66	0.00	0.70
D original	2-4	43.93	0.00	0.00	0.00	0.00	2.80	0.00	0.32	52.71	0.00	0.00	0.00	0.00	6.37	0.00	0.73
D original	4-6	43.12	0.00	0.32	0.00	0.00	2.94	0.00	0.00	52.27	0.00	0.74	0.00	0.00	6.82	0.00	0.00
D original	6-8	44.16	0.00	0.00	0.00	0.00	2.45	0.00	0.45	52.62	0.00	0.00	0.00	0.00	5.55	0.00	1.02
D original	8-10	44.42	0.00	0.00	0.00	0.00	2.19	0.00	0.27	52.68	0.00	0.00	0.00	0.00	4.93	0.00	0.61
D original	10-12	44.42	0.00	0.00	0.00	0.00	2.16	0.00	0.26	52.67	0.00	0.00	0.00	0.00	4.86	0.00	0.59
D original	12-14	44.40	0.00	0.00	0.00	0.00	2.04	0.00	0.27	52.61	0.00	0.00	0.00	0.00	4.59	0.00	0.61
D original	14-16	43.68	0.00	0.30	0.00	0.00	2.47	0.00	0.28	52.42	0.00	0.69	0.00	0.00	5.65	0.00	0.64
D original	16-18	44.29	0.00	0.23	0.00	0.00	1.69	0.00	0.44	52.43	0.00	0.52	0.00	0.00	3.82	0.00	0.99
D original	18-20	43.58	0.00	0.00	0.00	0.00	2.97	0.00	0.28	52.65	0.00	0.00	0.00	0.00	6.82	0.00	0.64
M original	0-2	42.41	0.00	0.21	0.00	0.00	3.15	0.00	0.27	51.82	0.00	0.50	0.00	0.00	7.43	0.00	0.64
M original	2-4	42.00	0.00	0.00	0.00	0.00	3.34	0.00	0.26	51.72	0.00	0.00	0.00	0.00	7.95	0.00	0.62
M original	4-6	42.82	0.00	0.00	0.00	0.00	3.15	0.00	0.00	52.13	0.00	0.00	0.00	0.00	7.36	0.00	0.00
M original	6-8	41.63	0.00	0.00	0.00	0.00	4.32	0.00	0.00	51.89	0.00	0.00	0.00	0.00	10.38	0.00	0.00
M original	8-10	41.85	0.00	0.00	0.00	0.00	3.82	0.00	0.00	51.81	0.00	0.00	0.00	0.00	9.13	0.00	0.00
M original	10-12	42.71	0.00	0.00	0.00	0.00	2.95	0.00	0.00	51.96	0.00	0.00	0.00	0.00	6.91	0.00	0.00
M original	12-14	41.81	0.00	0.00	0.00	0.00	3.73	0.00	0.00	51.73	0.00	0.00	0.00	0.00	8.92	0.00	0.00
M original	14-16	41.81	0.00	0.00	0.00	0.00	3.73	0.00	0.00	51.73	0.00	0.00	0.00	0.00	8.92	0.00	0.00
M original	16-18	42.36	0.00	0.00	0.00	0.00	3.25	0.00	0.00	51.88	0.00	0.00	0.00	0.00	7.67	0.00	0.00
M original	18-20	42.37	0.00	0.00	0.00	0.00	3.44	0.00	0.00	51.88	0.00	0.00	0.00	0.00	8.12	0.00	0.00

Table (X1): The main cations and anions of the original Petra sandstone specimens and their ratio to Si prior to the start of the tests.

Appendix X: The anion and cation content from the thin sections at the end of the modified salt crystallisation test.

Experiment run: Original samples before the test

Sample code	Depth (mm)	Si %	Na %	Ca %	Mg %	K %	Al %	S %	Cl %	O %	Na/Si ×100% %	Ca/Si ×100% %	Mg/Si ×100% %	K/Si ×100% %	Al/Si ×100% %	S/Si ×100% %	Cl/Si ×100% %
S original	0-2	43.11	0.00	0.45	0.00	1.98	2.02	0.00	0.41	51.61	0.00	1.04	0.00	4.59	4.69	0.00	0.95
S original	2-4	43.09	0.00	0.39	0.00	2.08	2.01	0.00	0.31	51.61	0.00	0.91	0.00	4.83	4.66	0.00	0.72
S original	4-6	44.21	0.00	0.00	0.00	1.82	1.57	0.00	0.27	52.13	0.00	0.00	0.00	4.12	3.55	0.00	0.61
S original	6-8	44.02	0.00	0.00	0.00	1.80	1.43	0.00	0.38	51.92	0.00	0.00	0.00	4.09	3.25	0.00	0.86
S original	8-10	43.56	0.00	0.00	0.00	2.19	1.70	0.00	0.41	51.71	0.00	0.00	0.00	5.03	3.90	0.00	0.94
S original	10-12	43.33	0.00	0.00	0.00	2.256	1.89	0.00	0.33	51.66	0.00	0.00	0.00	5.21	4.36	0.00	0.76
S original	12-14	43.99	0.00	0.00	0.00	1.68	1.57	0.00	0.00	52.46	0.00	0.00	0.00	3.82	3.57	0.00	0.00
S original	14-16	44.94	0.00	0.00	0.00	1.13	1.01	0.00	0.00	52.46	0.00	0.00	0.00	2.51	2.25	0.00	0.00
S original	16-18	44.27	0.00	0.00	0.00	1.41	1.40	0.00	0.30	52.12	0.00	0.00	0.00	3.19	3.16	0.00	0.68
S original	18-20	44.26	0.00	0.00	0.00	1.14	1.54	0.00	0.21	52.09	0.00	0.00	0.00	2.58	3.48	0.00	0.47

Table (X2): The main cations and anions of the original Locharbriggs sandstone specimen, and their ratio to (Si) prior to the start of the tests.

Sample code	Depth (mm)	Ca %	Na %	Si %	Mg %	K %	Al %	S %	Cl %	O %	Na/Ca ×100% %	Si/Ca ×100% %	Mg/Ca ×100% %	K/Ca ×100% %	Al/Ca ×100% %	S/Ca ×100% %	Cl/Ca ×100% %
L original	0-2	66.58	0.00	1.71	0.00	0.00	0.00	0.43	0.55	29.52	0.00	2.57	0.00	0.00	0.00	0.65	0.83
L original	2-4	66.33	0.00	1.83	0.62	0.00	0.00	0.00	0.71	29.32	0.00	2.76	0.93	0.00	0.00	0.00	1.07
L original	4-6	67.79	0.00	1.47	0.00	0.00	0.00	0.00	0.53	29.06	0.00	2.17	0.00	0.00	0.00	0.00	0.78
L original	6-8	66.94	0.00	1.84	0.00	0.00	0.00	0.00	0.88	29.15	0.00	2.75	0.00	0.00	0.00	0.00	1.31
L original	8-10	67.1	0.00	1.71	0.00	0.00	0.00	0.00	0.55	29.16	0.00	2.55	0.00	0.00	0.00	0.00	0.82
L original	10-12	68.11	0.00	0.00	0.79	0.00	0.00	0.00	1.22	28.19	0.00	0.00	1.16	0.00	0.00	0.00	1.79
L original	12-14	66.45	0.00	4.39	0.00	0.00	0.00	0.00	0.73	29.28	0.00	6.61	0.00	0.00	0.00	0.00	1.10
L original	14-16	67.14	0.00	1.64	0.00	0.00	0.00	0.43	0.00	29.64	0.00	2.44	0.00	0.00	0.00	0.64	0.00
L original	16-18	67.14	0.00	3.96	0.00	0.00	0.00	0.00	0.44	29.28	0.00	5.90	0.00	0.00	0.00	0.00	0.66
L original	18-20	66.63	0.00	1.62	0.61	0.00	0.00	0.00	0.00	29.36	0.00	2.43	0.92	0.00	0.00	0.00	0.00

Table (X3): The main cations and anions of the original Monks Park limestone specimen, and their ratio to (Ca) prior to the start of the tests.

Appendix X: The anion and cation content from the thin sections at the end of the modified salt crystallisation test. Experiment run: First Run.

Sample code	Depth (mm)	Salt solution	Si %	Na %	Ca %	Mg %	K %	Al %	S %	Cl %	O %	Na/Si ×100% %	Ca/Si ×100% %	Mg/Si ×100% %	K/Si ×100% %	Al/Si ×100% %	S/Si ×100% %	Cl/Si ×100% %
S.3.1	0-2	Sodium sulfate	40.37	2.36	0.34	0.00	1.51	1.49	1.68	0.51	51.25	5.85	0.84	0.00	3.74	3.69	4.16	1.26
S.3.1	2-4	Sodium sulfate	41.69	1.77	0.00	0.00	1.21	1.39	1.14	0.57	51.51	4.25	0.00	0.00	2.90	3.33	2.73	1.37
S.3.1	4-6	Sodium sulfate	41.31	2.15	0.30	0.00	1.45	1.31	1.33	0.78	51.38	5.20	0.73	0.00	3.51	3.17	3.22	1.89
S.3.1	6-8	Sodium sulfate	40.27	2.30	0.00	0.00	2.26	1.65	1.70	0.66	51.15	5.71	0.00	0.00	5.61	4.10	4.22	1.64
S.3.1	8-10	Sodium sulfate	40.82	2.27	0.00	0.00	1.91	1.65	1.50	0.62	51.32	5.56	0.00	0.00	4.68	4.04	3.67	1.52
S.3.1	10-12	Sodium sulfate	39.35	3.05	0.30	0.00	1.64	1.14	2.63	0.58	51.31	7.75	0.76	0.00	4.17	2.90	6.68	1.47
S.3.1	12-14	Sodium sulfate	41.44	1.76	0.30	0.00	1.72	1.36	1.33	0.60	51.49	4.25	0.72	0.00	4.15	3.28	3.21	1.45
S.3.1	14-16	Sodium sulfate	43.06	0.87	0.00	0.00	1.68	1.57	0.69	0.00	52.13	2.02	0.00	0.00	3.90	3.65	1.60	0.00
S.3.1	16-18	Sodium sulfate	42.02	1.52	0.00	0.00	1.62	1.53	1.16	0.33	51.83	3.62	0.00	0.00	3.86	3.64	2.76	0.79
S.3.1	18-20	Sodium sulfate	41.06	1.99	0.00	0.00	1.20	1.40	1.72	0.44	51.69	4.85	0.00	0.00	2.92	3.41	4.19	1.07
S.1.1	0-2	Petra salt solution	42.67	0.91	0.00	0.00	2.25	1.75	0.00	0.91	51.07	2.13	0.00	0.00	5.27	4.10	0.00	2.13
S.1.1	2-4	Petra salt solution	41.85	0.82	0.27	0.00	3.08	1.87	0.30	0.99	50.80	1.96	0.65	0.00	7.36	4.47	0.72	2.37
S.1.1	4-6	Petra salt solution	42.53	0.71	0.00	0.00	2.61	1.71	0.00	0.68	50.98	1.67	0.00	0.00	6.14	4.02	0.00	1.60
S.1.1	6-8	Petra salt solution	42.36	0.69	0.00	0.00	2.57	1.67	0.39	0.62	51.23	1.63	0.00	0.00	6.07	3.94	0.92	1.46
S.1.1	8-10	Petra salt solution	41.69	0.75	0.00	0.00	3.02	2.17	0.35	0.61	50.97	1.80	0.00	0.00	7.24	5.21	0.84	1.46
S.1.1	10-12	Petra salt solution	41.26	0.78	0.34	0.00	2.82	2.08	0.42	0.72	50.72	1.89	0.82	0.00	6.83	5.04	1.02	1.75
S.1.1	12-14	Petra salt solution	42.28	0.48	0.00	0.00	2.79	1.93	0.00	0.59	50.91	1.14	0.00	0.00	6.60	4.56	0.00	1.40
S.1.1	14-16	Petra salt solution	42.35	0.55	0.00	0.00	2.59	1.89	0.00	0.61	51.11	1.30	0.00	0.00	6.12	4.46	0.00	1.44
S.1.1	16-18	Petra salt solution	42.08	0.46	0.00	0.00	2.89	2.13	0.34	0.48	51.21	1.09	0.00	0.00	6.87	5.06	0.81	1.14
S.1.1	18-20	Petra salt solution	42.99	0.40	0.00	0.00	2.34	1.68	0.37	0.56	51.65	0.93	0.00	0.00	5.44	3.91	0.86	1.30

Table (X4): The main cations and anions of Locharbriggs sandstone specimens, and their ratio to (Si) at the end of the first run.

Appendix X: The anion and cation content from the thin sections at the end of the modified salt crystallisation test. Experiment run: First run.

Sample code	Depth (mm)	Salt solution	Si %	Na %	Ca %	Mg %	K %	Al %	S %	Cl %	O %	Na/Si ×100% %	Ca/Si ×100% %	Mg/Si ×100% %	K/Si ×100% %	Al/Si ×100% %	S/Si ×100% %	Cl/Si ×100% %
M.1.1	0-2	Petra salt solution	42.02	0.51	0.57	0.00	0.00	3.93	0.00	0.54	51.92	1.21	1.36	0.00	0.00	9.35	0.00	1.29
M.1.1	2-4	Petra salt solution	41.81	0.53	0.56	0.00	0.00	2.42	0.00	0.69	51.04	1.27	1.34	0.00	0.00	5.79	0.00	1.65
M.1.1	4-6	Petra salt solution	41.46	0.00	0.39	0.00	0.00	2.93	0.00	0.00	50.91	0.00	0.94	0.00	0.00	7.07	0.00	0.00
M.1.1	6-8	Petra salt solution	41.28	0.00	0.41	0.00	0.00	2.84	0.00	0.00	51.00	0.00	0.99	0.00	0.00	6.88	0.00	0.00
M.1.1	8-10	Petra salt solution	41.31	0.00	0.48	0.00	0.00	3.55	0.00	0.00	51.35	0.00	1.16	0.00	0.00	8.59	0.00	0.00
M.1.1	10-12	Petra salt solution	41.96	0.40	0.42	0.00	0.00	3.23	0.00	0.34	51.58	0.95	1.00	0.00	0.00	7.70	0.00	0.81
M.1.1	12-14	Petra salt solution	42.26	0.00	0.48	0.00	0.00	3.46	0.00	0.00	51.95	0.00	1.14	0.00	0.00	8.19	0.00	0.00
M.1.1	14-16	Petra salt solution	41.52	0.37	0.44	0.00	0.00	4.01	0.00	0.00	51.72	0.89	1.06	0.00	0.00	9.66	0.00	0.00
M.1.1	16-18	Petra salt solution	42.55	0.00	0.43	0.00	0.00	3.14	0.00	0.00	51.98	0.00	1.01	0.00	0.00	7.38	0.00	0.00
M.1.1	18-20	Petra salt solution	42.64	0.00	0.34	0.00	0.00	3.46	0.00	0.00	52.18	0.00	0.80	0.00	0.00	8.11	0.00	0.00
D.1.1	0-2	Petra salt solution	42.08	0.88	0.63	0.00	0.67	2.86	0.00	0.56	51.63	2.09	1.50	0.00	1.59	6.80	0.00	1.33
D.1.1	2-4	Petra salt solution	42.35	0.63	0.44	0.00	0.75	2.79	0.45	0.64	51.96	1.49	1.04	0.00	1.77	6.59	1.06	1.51
D.1.1	4-6	Petra salt solution	42.72	0.48	0.46	0.00	0.74	2.55	0.41	0.58	52.05	1.12	1.08	0.00	1.73	5.97	0.96	1.36
D.1.1	6-8	Petra salt solution	43.83	0.49	0.00	0.00	0.54	2.66	0.00	0.64	52.23	1.12	0.00	0.00	1.23	6.07	0.00	1.46
D.1.1	8-10	Petra salt solution	43.05	0.54	0.41	0.00	0.66	2.29	0.32	0.68	50.05	1.25	0.95	0.00	1.53	5.32	0.74	1.58
D.1.1	10-12	Petra salt solution	42.08	0.54	0.54	0.00	0.61	2.73	0.45	0.68	51.89	1.28	1.28	0.00	1.45	6.49	1.07	1.62
D.1.1	12-14	Petra salt solution	42.60	0.45	0.31	0.00	0.54	2.45	0.00	0.54	51.91	1.06	0.73	0.00	1.27	5.75	0.00	1.27
D.1.1	14-16	Petra salt solution	43.54	0.42	0.36	0.00	0.43	2.21	0.00	0.63	52.19	0.96	0.83	0.00	0.99	5.08	0.00	1.45
D.1.1	16-18	Petra salt solution	42.78	0.57	0.52	0.00	0.49	2.69	0.00	0.63	51.91	1.33	1.22	0.00	1.15	6.29	0.00	1.47
D.1.1	18-20	Petra salt solution	43.26	0.47	0.00	0.00	0.39	2.68	0.30	0.55	52.35	1.09	0.00	0.00	0.90	6.20	0.69	1.27

Table (X5): The main cations and anions of Petra sandstone specimens, and their ratio to (Si) at the end of the first run.

Appendix X: The anion and cation content from the thin sections at the end of the modified salt crystallisation test. Experiment run: Second run.

Sample code	Depth (mm)	Salt solution	Si %	Na %	Ca %	Mg %	K %	Al %	S %	Cl %	O %	Na/Si ×100% %	Ca/Si ×100% %	Mg/Si ×100% %	K/Si ×100% %	Al/Si ×100% %	S/Si ×100% %	Cl/Si ×100% %
S.3.2	0-2	Sodium sulfate	42.69	0.80	0.00	0.00	2.04	1.82	0.37	0.81	51.49	1.87	0.00	0.00	4.78	4.26	0.87	1.90
S.3.2	2-4	Sodium sulfate	42.77	0.90	0.00	0.00	1.65	1.70	0.38	0.47	51.60	2.10	0.00	0.00	3.86	3.97	0.89	1.10
S.3.2	4-6	Sodium sulfate	42.88	1.08	0.00	0.00	1.73	1.73	0.49	0.25	51.85	2.52	0.00	0.00	4.03	4.03	1.14	0.58
S.3.2	6-8	Sodium sulfate	42.64	0.93	0.00	0.00	1.92	1.84	0.38	0.36	51.59	2.18	0.00	0.00	4.50	4.32	0.89	0.84
S.3.2	8-10	Sodium sulfate	42.50	0.87	0.00	0.00	2.18	1.82	0.00	0.45	50.92	2.05	0.00	0.00	5.13	4.28	0.00	1.06
S.3.2	10-12	Sodium sulfate	41.90	0.86	0.00	0.00	2.68	2.47	0.32	0.51	51.26	2.05	0.00	0.00	6.40	5.89	0.76	1.22
S.3.2	12-14	Sodium sulfate	42.63	0.49	0.20	0.00	1.79	1.92	0.42	0.39	51.69	1.15	0.47	0.00	4.20	4.50	0.99	0.91
S.1.2	0-2	Petra salt solution	42.91	0.38	0.36	0.00	1.99	1.67	0.26	0.54	51.55	0.89	0.84	0.00	4.64	3.89	0.61	1.26
S.1.2	2-4	Petra salt solution	43.02	0.36	0.35	0.00	2.08	1.70	0.14	0.59	51.52	0.84	0.81	0.00	4.83	3.95	0.33	1.37
S.1.2	4-6	Petra salt solution	43.32	0.35	0.34	0.00	2.11	1.37	0.00	0.58	51.58	0.81	0.78	0.00	4.87	3.16	0.00	1.34
S.1.2	6-8	Petra salt solution	43.49	0.39	0.00	0.00	2.15	1.78	0.00	0.47	51.71	0.90	0.00	0.00	4.94	4.09	0.00	1.08
S.1.2	8-10	Petra salt solution	43.93	0.00	0.00	0.00	2.05	1.68	0.00	0.38	51.96	0.00	0.00	0.00	4.67	3.82	0.00	0.87
S.1.2	10-12	Petra salt solution	43.12	0.39	0.00	0.00	2.52	1.99	0.00	0.44	51.54	0.90	0.00	0.00	5.84	4.62	0.00	1.02
S.1.2	12-14	Petra salt solution	43.09	0.00	0.00	0.00	2.64	1.96	0.00	0.35	51.50	0.00	0.00	0.00	6.13	4.55	0.00	0.81
S.1.2	14-16	Petra salt solution	43.58	0.00	0.00	0.00	2.17	1.74	0.00	0.36	51.76	0.00	0.00	0.00	4.98	3.99	0.00	0.83
S.1.2	16-18	Petra salt solution	43.71	0.00	0.00	0.00	2.34	1.94	0.00	0.00	52.01	0.00	0.00	0.00	5.35	4.44	0.00	0.00

Table (X6): The main cations and anions of Locharbriggs sandstone specimens, and their ratio to (Si) at the end of the second run.

Appendix X: The anion and cation content from the thin sections at the end of the modified salt crystallisation test. Experiment run: Second run.

Sample code	Depth (mm)	Salt solution	Si %	Na %	Ca %	Mg %	K %	Al %	S %	Cl %	O %	Na/Si ×100% %	Ca/Si ×100% %	Mg/Si ×100% %	K/Si ×100% %	Al/Si ×100% %	S/Si ×100% %	Cl/Si ×100% %
M.1.2	0-2	Petra salt solution	40.78	1.37	0.65	0.00	0.48	2.93	0.77	1.10	51.25	3.36	1.59	0.00	1.18	7.18	1.89	2.70
M.1.2	2-4	Petra salt solution	39.85	1.08	0.45	0.00	0.39	4.63	0.66	1.02	51.31	2.71	1.13	0.00	0.98	11.62	1.66	2.56
M.1.2	4-6	Petra salt solution	41.91	0.88	0.50	0.00	0.00	3.06	0.44	0.84	51.80	2.10	1.19	0.00	0.00	7.30	1.05	2.00
M.1.2	6-8	Petra salt solution	41.44	0.98	0.44	0.00	0.26	3.54	0.45	0.77	51.72	2.36	1.06	0.00	0.63	8.54	1.09	1.86
M.1.2	8-10	Petra salt solution	42.27	1.72	1.13	0.00	0.65	1.07	0.25	1.65	50.80	4.07	2.67	0.00	1.54	2.53	0.59	3.90
M.1.2	10-12	Petra salt solution	42.12	1.10	0.47	0.00	0.32	3.05	0.00	1.60	51.34	2.61	1.12	0.00	0.76	7.24	0.00	3.80
M.1.2	12-14	Petra salt solution	41.76	0.65	0.29	0.00	0.22	3.98	0.32	0.47	51.97	1.56	0.69	0.00	0.53	9.53	0.77	1.13
M.1.2	14-16	Petra salt solution	41.70	0.93	0.43	0.00	0.23	3.16	0.41	0.88	51.65	2.23	1.03	0.00	0.55	7.58	0.98	2.11
M.1.2	16-18	Petra salt solution	42.23	0.81	0.31	0.00	0.34	3.13	0.00	1.05	51.54	1.92	0.73	0.00	0.81	7.41	0.00	2.49
D.1.2	0-2	Petra salt solution	45.21	0.44	0.00	0.00	0.24	0.86	0.00	0.44	52.72	0.97	0.00	0.00	0.53	1.90	0.00	0.97
D.1.2	2-4	Petra salt solution	45.45	0.28	0.22	0.00	0.00	0.89	0.00	0.40	52.76	0.62	0.48	0.00	0.00	1.96	0.00	0.88
D.1.2	4-6	Petra salt solution	44.96	0.37	0.20	0.00	0.00	1.37	0.00	0.47	52.64	0.82	0.44	0.00	0.00	3.05	0.00	1.05
D.1.2	6-8	Petra salt solution	45.36	0.25	0.00	0.00	0.00	1.25	0.00	0.34	52.84	0.55	0.00	0.00	0.00	2.76	0.00	0.75
D.1.2	8-10	Petra salt solution	45.36	0.00	0.00	0.00	0.18	1.25	0.00	0.37	52.83	0.00	0.00	0.00	0.40	2.76	0.00	0.82
D.1.2	10-12	Petra salt solution	45.54	0.00	0.34	0.00	0.00	0.88	0.00	0.00	52.77	0.00	0.75	0.00	0.00	1.93	0.00	0.00
D.1.2	12-14	Petra salt solution	45.60	0.00	0.00	0.00	0.00	0.88	0.00	0.37	52.74	0.00	0.00	0.00	0.00	1.93	0.00	0.81
D.1.2	14-16	Petra salt solution	45.79	0.00	0.00	0.00	0.00	0.69	0.00	0.73	52.79	0.00	0.00	0.00	0.00	1.51	0.00	1.59

Table (X7): The main cations and anions of Petra sandstone specimens, and their ratio to (Si) at the end of the second run.

Appendix X: The anion and cation content from the thin sections at the end of the modified salt crystallisation test. Experiment run: Second run.

Sample code	Depth (mm)	Salt solution	Ca %	Na %	Si %	Mg %	K %	Al %	S %	Cl %	O %	Na/Ca ×100% %	Si/Ca ×100% %	Mg/Ca ×100% %	K/Ca ×100% %	Al/Ca ×100% %	S/Ca ×100% %	Cl/Ca ×100% %
L.3.2	0-2	Sodium sulfate	67.45	0.67	0.79	0.50	0.00	0.00	0.00	0.53	28.76	0.99	1.17	0.74	0.00	0.00	0.00	0.79
L.3.2	2-4	Sodium sulfate	67.41	0.00	0.95	0.55	0.00	0.00	0.00	0.40	28.86	0.00	1.41	0.82	0.00	0.00	0.00	0.59
L.3.2	4-6	Sodium sulfate	68.41	0.00	0.81	0.00	0.00	0.00	0.00	0.53	28.67	0.00	1.18	0.00	0.00	0.00	0.00	0.77
L.3.2	6-8	Sodium sulfate	66.67	0.59	0.69	0.59	0.00	0.00	0.00	0.38	28.67	0.88	1.03	0.88	0.00	0.00	0.00	0.57
L.3.2	8-10	Sodium sulfate	68.95	0.00	0.65	0.00	0.00	0.00	0.00	0.00	28.73	0.00	0.94	0.00	0.00	0.00	0.00	0.00
L.3.2	10-12	Sodium sulfate	67.24	0.00	0.52	0.00	0.00	0.00	0.00	0.38	28.53	0.00	0.77	0.00	0.00	0.00	0.00	0.57
L.3.2	12-14	Sodium sulfate	66.94	0.94	0.68	0.00	0.00	0.00	0.00	0.41	28.52	1.40	1.02	0.00	0.00	0.00	0.00	0.61

Table (X8): The main cations and anions of Monks Park limestone specimen, and their ratio to (Ca) at the end of the second run.

Appendix X: The anion and cation content from the thin sections at the end of the modified salt crystallisation test. Experiment run: Third run.

Sample code	Depth (mm)	Salt solution	Si %	Na %	Ca %	Mg %	K %	Al %	S %	Cl %	O %	Na/Si ×100% %	Ca/Si ×100% %	Mg/Si ×100% %	K/Si ×100% %	Al/Si ×100% %	S/Si ×100% %	Cl/Si ×100% %
S.4.3	0-2	Sodium sulfate	43.73	0.00	0.00	0.00	1.75	1.88	0.00	0.00	52.02	0.00	0.00	0.00	4.00	4.30	0.00	0.00
S.4.3	2-4	Sodium sulfate	43.99	0.00	0.00	0.00	2.05	1.81	0.00	0.00	52.15	0.00	0.00	0.00	4.66	4.11	0.00	0.00
S.4.3	4-6	Sodium sulfate	44.10	0.00	0.00	0.00	1.61	1.69	0.00	0.00	52.19	0.00	0.00	0.00	3.65	3.83	0.00	0.00
S.4.3	6-8	Sodium sulfate	44.31	0.00	0.00	0.00	1.45	1.68	0.00	0.28	52.28	0.00	0.00	0.00	3.27	3.79	0.00	0.63
S.4.3	8-10	Sodium sulfate	43.56	0.00	0.00	0.00	1.74	1.69	0.00	0.27	52.09	0.00	0.00	0.00	3.99	3.88	0.00	0.62
S.4.3	10-12	Sodium sulfate	43.70	0.38	0.00	0.00	1.95	1.93	0.00	0.00	52.04	0.87	0.00	0.00	4.46	4.42	0.00	0.00
S.4.3	12-14	Sodium sulfate	43.37	0.30	0.00	0.00	1.93	1.70	0.00	0.29	51.64	0.69	0.00	0.00	4.45	3.92	0.00	0.67
S.1.3	0-2	Petra salt solution	43.14	0.23	0.30	0.00	1.51	1.55	0.00	0.27	51.51	0.53	0.70	0.00	3.50	3.59	0.00	0.63
S.1.3	2-4	Petra salt solution	43.81	0.29	0.00	0.00	1.68	1.67	0.00	0.32	51.93	0.66	0.00	0.00	3.83	3.81	0.00	0.73
S.1.3	4-6	Petra salt solution	44.02	0.25	0.00	0.00	1.42	1.27	0.00	0.32	51.78	0.57	0.00	0.00	3.23	2.89	0.00	0.73
S.1.3	6-8	Petra salt solution	43.07	0.36	0.00	0.00	2.12	1.83	0.00	0.27	51.38	0.84	0.00	0.00	4.92	4.25	0.00	0.63
S.1.3	8-10	Petra salt solution	43.83	0.23	0.00	0.14	1.63	1.47	0.00	0.36	51.76	0.52	0.00	0.32	3.72	3.35	0.00	0.82
S.1.3	10-12	Petra salt solution	43.19	0.32	0.00	0.00	1.78	1.90	0.00	0.34	51.62	0.74	0.00	0.00	4.12	4.40	0.00	0.79
S.1.3	12-14	Petra salt solution	42.91	0.26	0.00	0.00	2.10	2.03	0.00	0.30	51.47	0.61	0.00	0.00	4.89	4.73	0.00	0.70
S.1.3	14-16	Petra salt solution	43.18	0.26	0.00	0.00	2.13	1.96	0.00	0.30	51.62	0.60	0.00	0.00	4.93	4.54	0.00	0.69
S.1.3	16-18	Petra salt solution	43.67	0.30	0.00	0.00	1.85	1.75	0.00	0.33	51.86	0.69	0.00	0.00	4.24	4.01	0.00	0.76
S.1.3	18-20	Petra salt solution	43.47	0.26	0.00	0.00	2.02	1.86	0.00	0.28	51.78	0.60	0.00	0.00	4.65	4.28	0.00	0.64

Table (X9): The main cations and anions of Locharbriggs sandstone specimens, and their ratio to (Si) at the end of the third run.

Appendix X: The anion and cation content from the thin sections at the end of the modified salt crystallisation test. Experiment run: Third run.

Sample code	Depth (mm)	Salt solution	Si %	Na %	Ca %	Mg %	K %	Al %	S %	Cl %	O %	Na/Si ×100% %	Ca/Si ×100% %	Mg/Si ×100% %	K/Si ×100% %	Al/Si ×100% %	S/Si ×100% %	Cl/Si ×100% %
M.1.3	0-2	Petra salt solution	41.39	0.00	0.00	0.00	0.00	4.73	0.00	0.25	51.86	0.00	0.00	0.00	0.00	11.43	0.00	0.60
M.1.3	2-4	Petra salt solution	42.18	0.00	0.00	0.00	0.00	4.02	0.00	0.00	52.11	0.00	0.00	0.00	0.00	9.53	0.00	0.00
M.1.3	4-6	Petra salt solution	42.21	0.00	0.00	0.00	0.00	3.95	0.00	0.00	52.09	0.00	0.00	0.00	0.00	9.36	0.00	0.00
M.1.3	6-8	Petra salt solution	42.18	0.00	0.00	0.00	0.00	3.96	0.00	0.00	52.07	0.00	0.00	0.00	0.00	9.39	0.00	0.00
M.1.3	8-10	Petra salt solution	42.55	0.00	0.00	0.00	0.00	3.52	0.00	0.00	52.12	0.00	0.00	0.00	0.00	8.27	0.00	0.00
M.1.3	10-12	Petra salt solution	42.69	0.00	0.00	0.00	0.00	3.10	0.00	0.00	52.01	0.00	0.00	0.00	0.00	7.26	0.00	0.00
M.1.3	12-14	Petra salt solution	42.39	0.00	0.00	0.00	0.00	3.44	0.00	0.00	52.04	0.00	0.00	0.00	0.00	8.12	0.00	0.00
M.1.3	14-16	Petra salt solution	41.80	0.00	0.00	0.00	0.00	3.93	0.00	0.00	51.80	0.00	0.00	0.00	0.00	9.40	0.00	0.00
M.1.3	16-18	Petra salt solution	41.22	0.00	0.00	0.00	0.00	4.77	0.00	0.00	51.80	0.00	0.00	0.00	0.00	11.57	0.00	0.00
M.1.3	18-20	Petra salt solution	41.93	0.00	0.00	0.00	0.00	3.89	0.00	0.00	51.90	0.00	0.00	0.00	0.00	9.28	0.00	0.00

Table (X9): The main cations and anions of Petra sandstone specimens, and their ratio to (Si) at the end of the third run.

Sample code	Depth (mm)	Salt solution	Ca %	Na %	Si %	Mg %	K %	Al %	S %	Cl %	O %	Na/Ca ×100% %	Si/Ca ×100% %	Mg/Ca ×100% %	K/Ca ×100% %	Al/Ca ×100% %	S/Ca ×100% %	Cl/Ca ×100% %
L.3.3	0-2	Sodium sulfate	68.73	0.56	0.26	0.00	0.00	0.00	0.26	0.00	28.97	0.81	0.38	0.00	0.00	0.00	0.38	0.00
L.3.3	2-4	Sodium sulfate	68.42	0.00	1.07	0.00	0.00	0.00	0.00	0.41	28.87	0.00	1.56	0.00	0.00	0.00	0.00	0.60
L.3.3	4-6	Sodium sulfate	66.94	0.84	1.07	0.56	0.00	0.00	0.00	0.49	28.94	1.25	1.60	0.84	0.00	0.00	0.00	0.73
L.3.3	6-8	Sodium sulfate	65.05	0.00	1.59	0.75	0.00	0.00	0.00	0.73	29.24	0.00	2.44	1.15	0.00	0.00	0.00	1.12
L.3.3	8-10	Sodium sulfate	67.03	0.00	1.07	0.61	0.00	0.00	0.00	0.55	28.87	0.00	1.60	0.91	0.00	0.00	0.00	0.82
L.3.3	10-12	Sodium sulfate	66.79	1.00	1.03	0.50	0.00	0.00	0.00	0.64	28.85	1.50	1.54	0.75	0.00	0.00	0.00	0.96
L.3.3	12-14	Sodium sulfate	68.85	0.00	0.81	0.00	0.00	0.00	0.34	0.46	29.06	0.00	1.18	0.00	0.00	0.00	0.49	0.67

Table (X10): The main cations and anions of Monks Park limestone specimen, and their ratio to (Ca) at the end of the third run.

Appendix X: The anion and cation content from the thin sections at the end of the modified salt crystallisation test. Experiment run: Fourth run.

Sample code	Depth (mm)	Salt solution	Si %	Na %	Ca %	Mg %	K %	Al %	S %	Cl %	O %	Na/Si ×100% %	Ca/Si ×100% %	Mg/Si ×100% %	K/Si ×100% %	Al/Si ×100% %	S/Si ×100% %	Cl/Si ×100% %
S.4.4	0-2	Sodium sulfate	44.05	0.57	0.29	0.00	1.25	1.43	0.00	0.35	52.04	1.29	0.66	0.00	2.84	3.25	0.00	0.79
S.4.4	2-4	Sodium sulfate	42.93	0.53	0.00	0.00	2.42	1.95	0.00	0.29	51.45	1.23	0.00	0.00	5.64	4.54	0.00	0.68
S.4.4	4-6	Sodium sulfate	43.64	0.63	0.00	0.00	2.10	1.73	0.00	0.00	51.90	1.44	0.00	0.00	4.81	3.96	0.00	0.00
S.4.4	6-8	Sodium sulfate	44.29	0.49	0.00	0.00	1.25	1.19	0.33	0.00	52.44	1.11	0.00	0.00	2.82	2.69	0.75	0.00
S.4.4	8-10	Sodium sulfate	43.29	0.67	0.00	0.00	1.70	1.45	0.35	0.25	51.84	1.55	0.00	0.00	3.93	3.35	0.81	0.58
S.4.4	10-12	Sodium sulfate	42.99	0.81	0.00	0.00	1.95	1.71	0.55	0.00	52.00	1.88	0.00	0.00	4.54	3.98	1.28	0.00
S.4.4	12-14	Sodium sulfate	42.93	0.77	0.00	0.00	1.81	1.73	0.56	0.28	51.92	1.79	0.00	0.00	4.22	4.03	1.30	0.65
S.4.4	14-16	Sodium sulfate	44.65	0.56	0.00	0.00	1.03	1.05	0.00	0.00	52.32	1.25	0.00	0.00	2.31	2.35	0.00	0.00
S.4.4	16-18	Sodium sulfate	43.43	0.65	0.00	0.00	1.50	1.35	0.33	0.27	51.88	1.50	0.00	0.00	3.45	3.11	0.76	0.62
S.1.4	0-2	Petra salt solution	42.92	0.59	0.44	0.00	1.83	1.68	0.00	0.54	51.35	1.37	1.03	0.00	4.26	3.91	0.00	1.26
S.1.4	2-4	Petra salt solution	43.57	0.38	0.29	0.00	2.06	1.50	0.00	0.56	51.64	0.87	0.67	0.00	4.73	3.44	0.00	1.29
S.1.4	4-6	Petra salt solution	43.46	0.40	0.00	0.00	2.18	1.81	0.00	0.44	51.71	0.92	0.00	0.00	5.02	4.16	0.00	1.01
S.1.4	6-8	Petra salt solution	43.91	0.38	0.00	0.00	1.60	1.66	0.00	0.48	51.97	0.87	0.00	0.00	3.64	3.78	0.00	1.09
S.1.4	8-10	Petra salt solution	43.63	0.40	0.00	0.00	1.69	1.56	0.00	0.33	51.76	0.92	0.00	0.00	3.87	3.58	0.00	0.76
S.1.4	10-12	Petra salt solution	43.03	0.44	0.00	0.00	2.47	2.11	0.00	0.38	51.56	1.02	0.00	0.00	5.74	4.90	0.00	0.88
S.1.4	12-14	Petra salt solution	42.54	0.34	0.00	0.00	2.35	2.36	0.00	0.59	51.31	0.80	0.00	0.00	5.52	5.55	0.00	1.39
S.1.4	14-16	Petra salt solution	43.23	0.41	0.00	0.00	2.35	1.94	0.00	0.46	51.30	0.95	0.00	0.00	5.44	4.49	0.00	1.06
S.1.4	16-18	Petra salt solution	43.42	0.53	0.00	0.00	1.81	1.75	0.00	0.36	51.70	1.22	0.00	0.00	4.17	4.03	0.00	0.83
S.1.4	18-20	Petra salt solution	43.03	0.33	0.39	0.00	2.06	1.82	0.00	0.35	51.50	0.77	0.91	0.00	4.79	4.23	0.00	0.81

Table (X11): The main cations and anions of Locharbriggs sandstone specimens, and their ratio to (Si) at the end of the fourth run.

Appendix X: The anion and cation content from the thin sections at the end of the modified salt crystallisation test. Experiment run: Fourth run.

Sample code	Depth (mm)	Salt solution	Si %	Na %	Ca %	Mg %	K %	Al %	S %	Cl %	O %	Na/Si ×100% %	Ca/Si ×100% %	Mg/Si ×100% %	K/Si ×100% %	Al/Si ×100% %	S/Si ×100% %	Cl/Si ×100% %
M.1.4	0-2	Petra salt solution	44.64	0.00	0.94	0.00	0.38	0.83	0.00	0.34	52.23	0.00	2.11	0.00	0.85	1.86	0.00	0.76
M.1.4	2-4	Petra salt solution	46.62	0.20	0.00	0.00	0.00	0.00	0.00	0.00	53.18	0.43	0.00	0.00	0.00	0.00	0.00	0.00
M.1.4	4-6	Petra salt solution	44.45	0.49	0.82	0.00	0.37	0.77	0.00	0.53	52.06	1.10	1.84	0.00	0.83	1.73	0.00	1.19
M.1.4	6-8	Petra salt solution	44.16	0.74	0.80	0.00	0.38	0.92	0.00	0.67	51.90	1.68	1.81	0.00	0.86	2.08	0.00	1.52
M.1.4	8-10	Petra salt solution	43.50	0.65	0.81	0.00	0.52	1.49	0.00	0.86	51.68	1.49	1.86	0.00	1.20	3.43	0.00	1.98
M.1.4	10-12	Petra salt solution	42.97	0.98	0.00	0.00	0.47	1.75	0.00	1.51	51.34	2.28	0.00	0.00	1.09	4.07	0.00	3.51
M.1.4	12-14	Petra salt solution	44.18	0.72	1.15	0.00	0.00	0.69	0.00	1.61	51.65	1.63	2.60	0.00	0.00	1.56	0.00	3.64
D.1.4	0-2	Petra salt solution	42.34	0.76	0.23	0.00	0.74	3.00	0.24	0.91	51.78	1.79	0.54	0.00	1.75	7.09	0.57	2.15
D.1.4	2-4	Petra salt solution	41.40	0.80	0.26	0.00	0.92	2.92	0.00	0.80	51.18	1.93	0.63	0.00	2.22	7.05	0.00	1.93
D.1.4	4-6	Petra salt solution	42.82	0.75	0.00	0.00	0.66	2.47	0.00	0.77	51.84	1.75	0.00	0.00	1.54	5.77	0.00	1.80
D.1.4	6-8	Petra salt solution	42.93	0.97	0.00	0.00	0.65	2.70	0.00	0.56	51.94	2.26	0.00	0.00	1.51	6.29	0.00	1.30
D.1.4	8-10	Petra salt solution	43.12	0.54	0.24	0.00	0.45	2.71	0.00	0.56	52.10	1.25	0.56	0.00	1.04	6.28	0.00	1.30
D.1.4	10-12	Petra salt solution	42.83	0.88	0.22	0.00	0.60	2.91	0.00	0.66	51.90	2.05	0.51	0.00	1.40	6.79	0.00	1.54
D.1.4	12-14	Petra salt solution	42.71	0.72	0.23	0.00	0.75	3.06	0.00	0.65	51.88	1.69	0.54	0.00	1.76	7.16	0.00	1.52
D.1.4	14-16	Petra salt solution	43.79	0.55	0.00	0.00	0.54	2.35	0.00	0.49	52.28	1.26	0.00	0.00	1.23	5.37	0.00	1.12
D.1.4	16-18	Petra salt solution	42.34	0.76	0.23	0.00	0.74	3.00	0.24	0.91	52.09	1.79	0.54	0.00	1.75	7.09	0.57	2.15
D.1.4	18-20	Petra salt solution	41.40	0.80	0.26	0.00	0.92	2.92	0.00	0.80	52.18	1.93	0.63	0.00	2.22	7.05	0.00	1.93

Table (X12): The main cations and anions of Petra sandstone specimens, and their ratio to (Si) at the end of the fourth run.

Appendix X: The anion and cation content from the thin sections at the end of the modified salt crystallisation test. Experiment run: Fourth run.

Sample code	Depth (mm)	Salt solution	Ca %	Na %	Si %	Mg %	K %	Al %	S %	Cl %	O %	Na/Ca ×100% %	Si/Ca ×100% %	Mg/Ca ×100% %	K/Ca ×100% %	Al/Ca ×100% %	S/Ca ×100% %	Cl/Ca ×100% %
L.3.4	0-2	Sodium sulfate	60.98	2.40	2.51	0.48	0.00	0.00	1.44	0.45	30.78	3.94	4.12	0.79	0.00	0.00	2.36	0.74
L.3.4	2-4	Sodium sulfate	59.43	4.10	2.03	0.00	0.00	0.00	2.43	0.00	31.31	6.90	3.42	0.00	0.00	0.00	4.09	0.00
L.3.4	4-6	Sodium sulfate	62.18	2.89	1.91	0.00	0.00	0.00	1.52	0.00	30.55	4.65	3.07	0.00	0.00	0.00	2.44	0.00
L.3.4	6-8	Sodium sulfate	60.40	3.02	2.80	0.52	0.00	0.00	1.46	0.00	31.08	5.00	4.64	0.86	0.00	0.00	2.42	0.00
L.3.4	8-10	Sodium sulfate	62.74	2.20	2.05	0.45	0.00	0.00	1.21	0.00	30.50	3.51	3.27	0.72	0.00	0.00	1.93	0.00
L.3.4	10-12	Sodium sulfate	63.99	1.85	1.62	0.62	0.00	0.00	0.90	0.33	29.99	2.89	2.53	0.97	0.00	0.00	1.41	0.52
L.3.4	12-14	Sodium sulfate	64.07	2.43	1.55	0.00	0.00	0.00	1.01	0.40	29.87	3.79	2.42	0.00	0.00	0.00	1.58	0.62
L.3.4	14-16	Sodium sulfate	62.50	2.56	1.39	0.63	0.00	0.00	1.23	0.47	30.02	4.10	2.22	1.01	0.00	0.00	1.97	0.75
L.3.4	16-18	Sodium sulfate	63.17	2.46	1.79	0.00	0.00	0.00	1.28	0.00	30.31	3.89	2.83	0.00	0.00	0.00	2.03	0.00
L.3.4	18-20	Sodium sulfate	63.21	2.36	1.63	0.00	0.00	0.00	1.32	0.38	30.16	3.73	2.58	0.00	0.00	0.00	2.09	0.60

Table (X13): The main cations and anions of Monks Park limestone specimen, and their ratio to (Ca) at the end of the fourth run.

Appendix X: The anion and cation content from the thin sections at the end of the modified salt crystallisation test. Experiment run: Fifth run.

Sample code	Depth (mm)	Salt solution	Si %	Na %	Ca %	Mg %	K %	Al %	S %	Cl %	O %	Na/Si ×100% %	Ca/Si ×100% %	Mg/Si ×100% %	K/Si ×100% %	Al/Si ×100% %	S/Si ×100% %	Cl/Si ×100% %
S.3.5	0-2	Sodium sulfate	42.08	0.82	0.30	0.00	2.03	1.82	0.49	0.31	51.35	1.95	0.71	0.00	4.82	4.33	1.16	0.74
S.3.5	2-4	Sodium sulfate	42.10	0.99	0.00	0.00	2.14	1.91	0.43	0.31	51.32	2.35	0.00	0.00	5.08	4.54	1.02	0.74
S.3.5	4-6	Sodium sulfate	42.31	0.83	0.00	0.00	2.22	2.06	0.44	0.00	51.60	1.96	0.00	0.00	5.25	4.87	1.04	0.00
S.3.5	6-8	Sodium sulfate	42.00	0.80	0.28	0.00	2.44	2.18	0.34	0.25	51.30	1.90	0.67	0.00	5.81	5.19	0.81	0.60
S.3.5	8-10	Sodium sulfate	43.01	0.82	0.00	0.00	1.92	1.62	0.41	0.00	51.85	1.91	0.00	0.00	4.46	3.77	0.95	0.00
S.3.5	10-12	Sodium sulfate	42.71	0.80	0.00	0.00	1.75	1.73	0.54	0.35	51.75	1.87	0.00	0.00	4.10	4.05	1.26	0.82
S.3.5	12-14	Sodium sulfate	43.05	0.74	0.00	0.00	2.01	1.74	0.35	0.33	51.79	1.72	0.00	0.00	4.67	4.04	0.81	0.77
S.3.5	14-16	Sodium sulfate	42.83	0.65	0.28	0.00	1.49	1.53	0.00	0.39	51.43	1.52	0.65	0.00	3.48	3.57	0.00	0.91
S.3.5	16-18	Sodium sulfate	43.37	0.76	0.00	0.00	2.05	1.70	0.00	0.53	51.60	1.75	0.00	0.00	4.73	3.92	0.00	1.22
S.3.5	18-20	Sodium sulfate	43.13	0.74	0.21	0.00	1.84	1.74	0.00	0.51	51.50	1.72	0.49	0.00	4.27	4.03	0.00	1.18
S.1.5	0-2	Petra salt solution	40.57	0.53	0.32	0.00	3.97	1.57	1.36	0.37	50.89	1.31	0.79	0.00	9.79	3.87	3.35	0.91
S.1.5	2-4	Petra salt solution	42.37	0.33	0.00	0.00	2.61	1.60	0.00	0.39	51.02	0.78	0.00	0.00	6.16	3.78	0.00	0.92
S.1.5	4-6	Petra salt solution	43.99	0.00	0.00	0.00	2.01	1.40	0.00	0.35	51.88	0.00	0.00	0.00	4.57	3.18	0.00	0.80
S.1.5	6-8	Petra salt solution	41.92	0.49	0.00	0.00	3.28	2.29	0.39	0.41	51.22	1.17	0.00	0.00	7.82	5.46	0.93	0.98
S.1.5	8-10	Petra salt solution	41.88	0.36	0.00	0.00	3.38	2.30	0.00	0.41	50.94	0.86	0.00	0.00	8.07	5.49	0.00	0.98
S.1.5	10-12	Petra salt solution	41.52	0.40	0.31	0.00	3.64	1.95	0.68	0.45	51.06	0.96	0.75	0.00	8.77	4.70	1.64	1.08
S.1.5	12-14	Petra salt solution	40.07	0.61	0.00	0.00	4.71	2.01	1.45	0.37	50.78	1.52	0.00	0.00	11.75	5.02	3.62	0.92
S.1.5	14-16	Petra salt solution	40.84	0.66	0.00	0.00	3.71	2.20	0.69	0.60	50.69	1.62	0.00	0.00	9.08	5.39	1.69	1.47
S.1.5	16-18	Petra salt solution	41.48	0.39	0.00	0.00	3.75	2.17	0.42	0.55	50.84	0.94	0.00	0.00	9.04	5.23	1.01	1.33
S.1.5	18-20	Petra salt solution	41.82	0.53	0.00	0.00	3.27	1.94	0.52	0.46	51.11	1.27	0.00	0.00	7.82	4.64	1.24	1.10

Table (X14): The main cations and anions of Locharbriggs sandstone specimens, and their ratio to (Si) at the end of the fifth run.

Appendix X: The anion and cation content from the thin sections at the end of the modified salt crystallisation test. Experiment run: sixth run.

Sample code	Depth (mm)	Salt solution	Si %	Na %	Ca %	Mg %	K %	Al %	S %	Cl %	O %	Na/Si ×100% %	Ca/Si ×100% %	Mg/Si ×100% %	K/Si ×100% %	Al/Si ×100% %	S/Si ×100% %	Cl/Si ×100% %
S.3.6	0-2	Sodium sulfate	41.58	0.73	0.00	0.00	2.08	1.78	0.44	0.25	51.36	1.76	0.00	0.00	5.00	4.28	1.06	0.60
S.3.6	2-4	Sodium sulfate	41.69	0.74	0.00	0.00	2.11	1.84	0.44	0.21	51.38	1.78	0.00	0.00	5.06	4.41	1.06	0.50
S.3.6	4-6	Sodium sulfate	41.28	0.86	0.00	0.00	2.13	1.81	0.47	0.25	51.62	2.08	0.00	0.00	5.16	4.38	1.14	0.61
S.3.6	6-8	Sodium sulfate	41.55	0.84	0.21	0.00	2.01	1.80	0.00	0.21	51.36	2.02	0.51	0.00	4.84	4.33	0.00	0.51
S.3.6	8-10	Sodium sulfate	42.01	0.80	0.14	0.00	1.98	1.71	0.45	0.20	51.41	1.90	0.33	0.00	4.71	4.07	1.07	0.48
S.3.6	10-12	Sodium sulfate	41.74	0.83	0.00	0.00	2.14	1.80	0.51	0.24	51.26	1.99	0.00	0.00	5.13	4.31	1.22	0.57
S.3.6	12-14	Sodium sulfate	41.52	0.97	0.00	0.00	1.87	1.69	0.63	0.00	51.28	2.34	0.00	0.00	4.50	4.07	1.52	0.00
S.3.6	14-16	Sodium sulfate	41.22	0.92	0.00	0.00	1.90	1.66	0.61	0.00	51.30	2.23	0.00	0.00	4.61	4.03	1.48	0.00
S.3.6	16-18	Sodium sulfate	41.36	1.02	0.00	0.00	1.84	1.62	0.74	0.00	51.31	2.47	0.00	0.00	4.45	3.92	1.79	0.00
S.3.6	18-20	Sodium sulfate	41.27	1.01	0.00	0.00	1.74	1.60	0.74	0.00	51.41	2.45	0.00	0.00	4.22	3.88	1.79	0.00
S.1.6	0-2	Petra salt solution	40.02	0.47	0.00	0.00	2.21	1.65	0.65	0.41	50.87	1.17	0.00	0.00	5.52	4.12	1.62	1.02
S.1.6	2-4	Petra salt solution	40.52	0.45	0.23	0.00	2.98	1.80	0.40	0.39	50.78	1.11	0.57	0.00	7.35	4.44	0.99	0.96
S.1.6	4-6	Petra salt solution	41.02	0.38	0.00	0.00	3.02	1.78	0.21	0.36	50.37	0.93	0.00	0.00	7.36	4.34	0.51	0.88
S.1.6	6-8	Petra salt solution	40.87	0.36	0.18	0.00	3.25	1.88	0.33	0.37	50.69	0.88	0.44	0.00	7.95	4.60	0.81	0.91
S.1.6	8-10	Petra salt solution	40.59	0.37	0.25	0.00	3.17	1.90	0.00	0.34	51.02	0.91	0.62	0.00	7.81	4.68	0.00	0.84
S.1.6	10-12	Petra salt solution	40.38	0.35	0.00	0.00	3.12	1.79	0.00	0.33	51.01	0.87	0.00	0.00	7.73	4.43	0.00	0.82
S.1.6	12-14	Petra salt solution	40.27	0.33	0.00	0.00	3.08	1.91	0.00	0.29	50.91	0.82	0.00	0.00	7.65	4.74	0.00	0.72
S.1.6	14-16	Petra salt solution	40.24	0.31	0.25	0.00	3.14	1.87	0.21	0.33	50.84	0.77	0.62	0.00	7.80	4.65	0.52	0.82
S.1.6	16-18	Petra salt solution	40.52	0.33	0.18	0.00	3.04	1.82	0.22	0.35	50.47	0.81	0.44	0.00	7.50	4.49	0.54	0.86
S.1.6	18-20	Petra salt solution	40.25	0.35	0.17	0.00	2.78	1.56	0.21	0.32	50.41	0.87	0.42	0.00	6.91	3.88	0.52	0.80

Table (X15): The main cations and anions of Locharbriggs sandstone specimens, and their ratio to (Si) at the end of the sixth run.

Appendix Y: The main ions/Si weight ratio in the Locharbriggs sandstone specimens at the end of the modified salt crystallisation test.

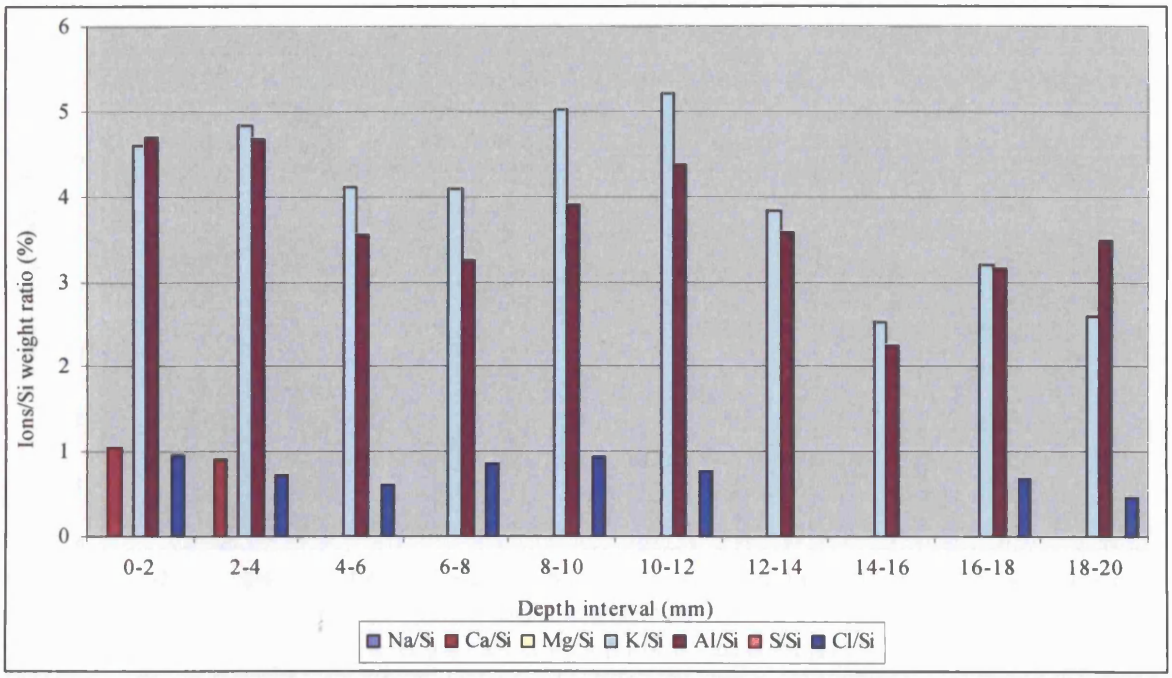

Figure (Y1): The main ions/Si ratio in the Locharbriggs sandstone original specimens (prior to the start of the test).

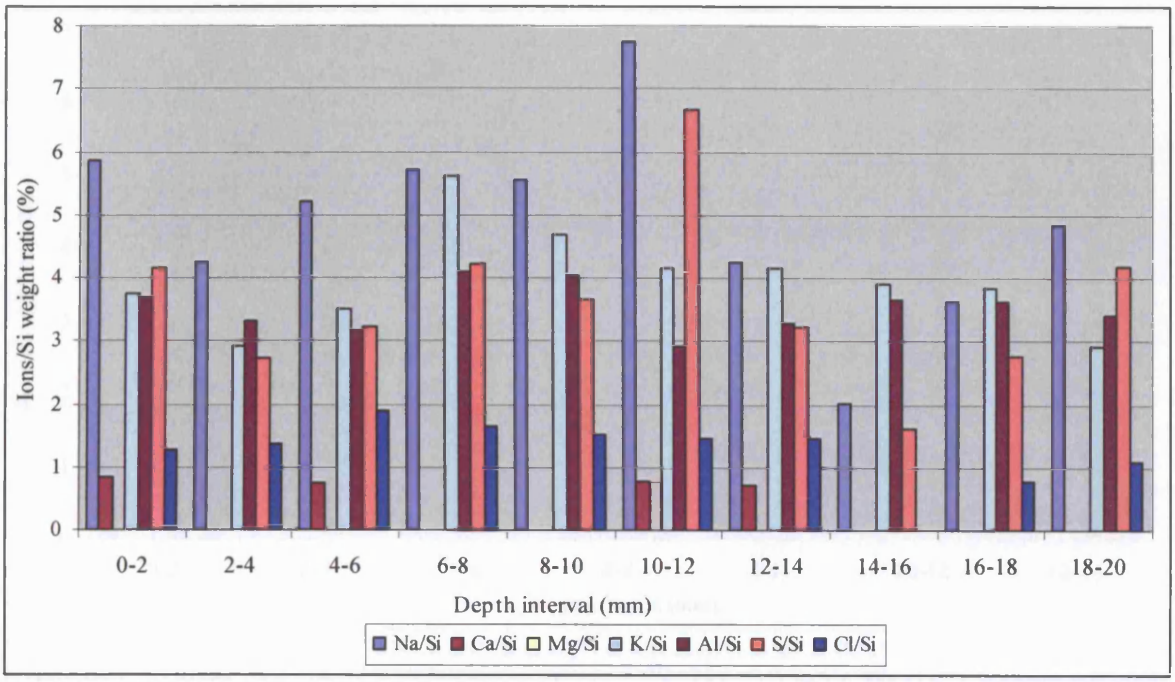

Figure (Y2): The main ions/Si ratio in the Locharbriggs sandstone at the end of the first run. Solution: saturated sodium sulfate.

Appendix Y: The main ions/Si weight ratio in the Locharbriggs sandstone specimens at the end of the modified salt crystallisation test.

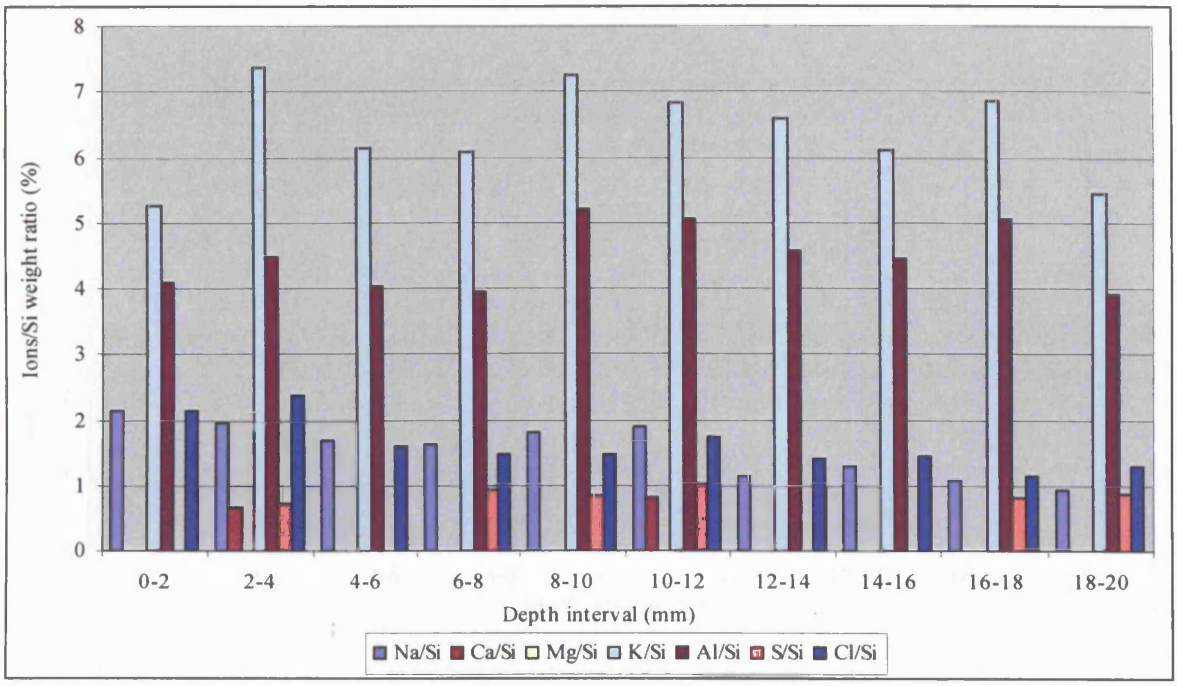

Figure (Y3): The main ions/Si ratio in the Locharbriggs sandstone at the end of the first run. Solution: saturated Petra salt solution.

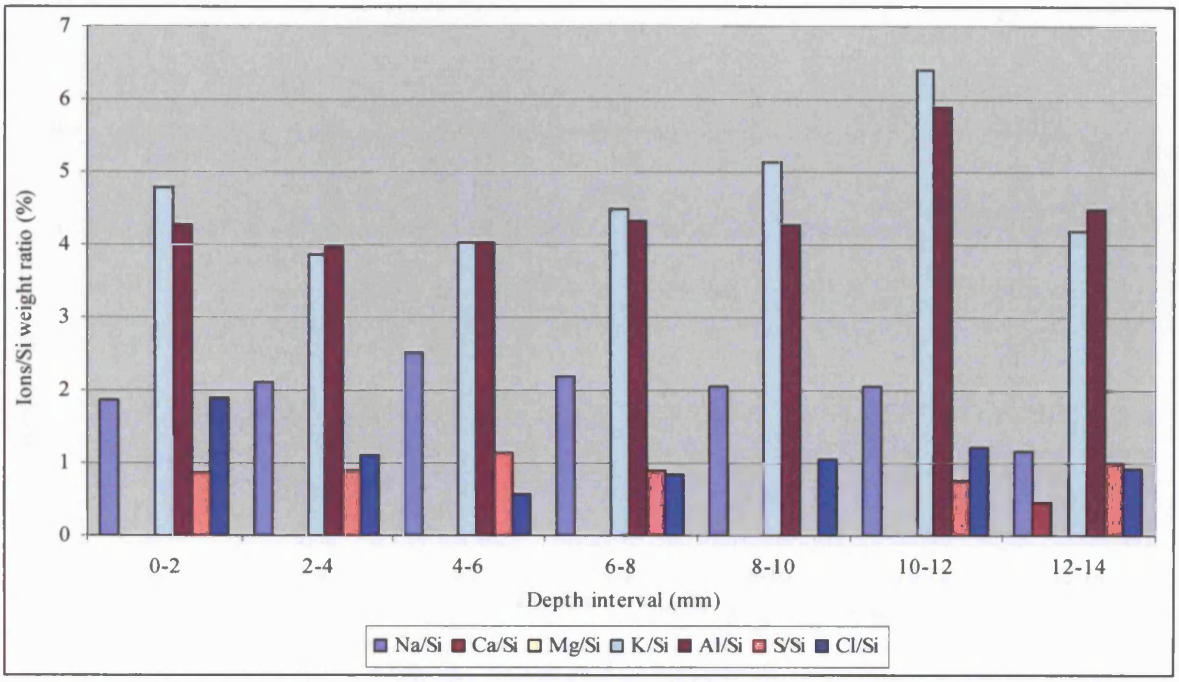

Figure (Y4): The main ions/Si ratio in the Locharbriggs sandstone at the end of the second run. Solution: saturated sodium sulfate.

Appendix Y: The main ions/Si weight ratio in the Locharbriggs sandstone specimens at the end of the modified salt crystallisation test.

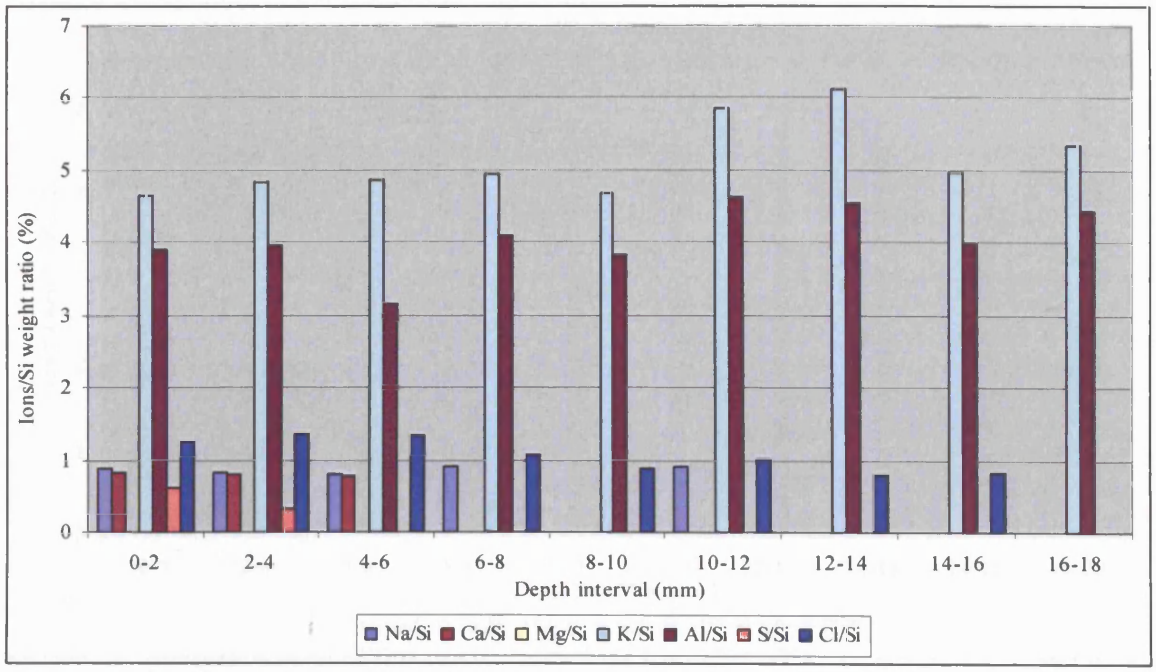

Figure (Y5): The main ions/Si ratio in the Locharbriggs sandstone at the end of the second run. Solution: saturated Petra salt solution.

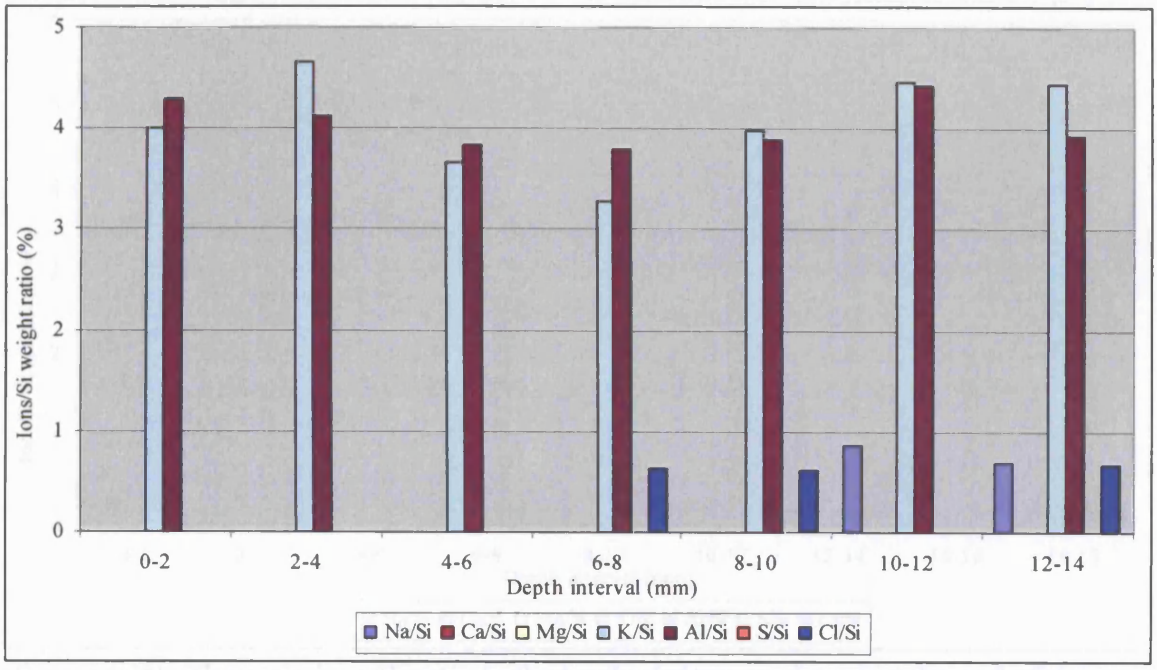

Figure (Y6): The main ions/Si ratio in the Locharbriggs sandstone at the end of the third run. Solution: saturated sodium sulfate.

Appendix Y: The main ions/Si weight ratio in the Locharbriggs sandstone specimens at the end of the modified salt crystallisation test.

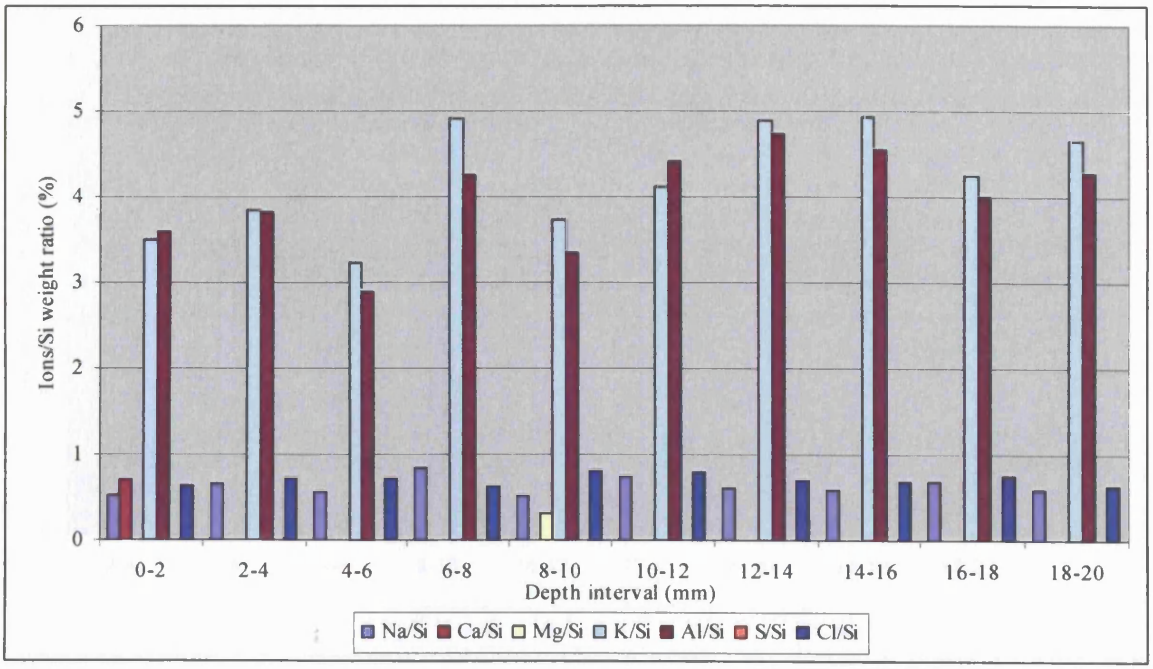

Figure (Y7): The main ions/Si ratio in the Locharbriggs sandstone at the end of the third run. Solution: saturated Petra salt solution.

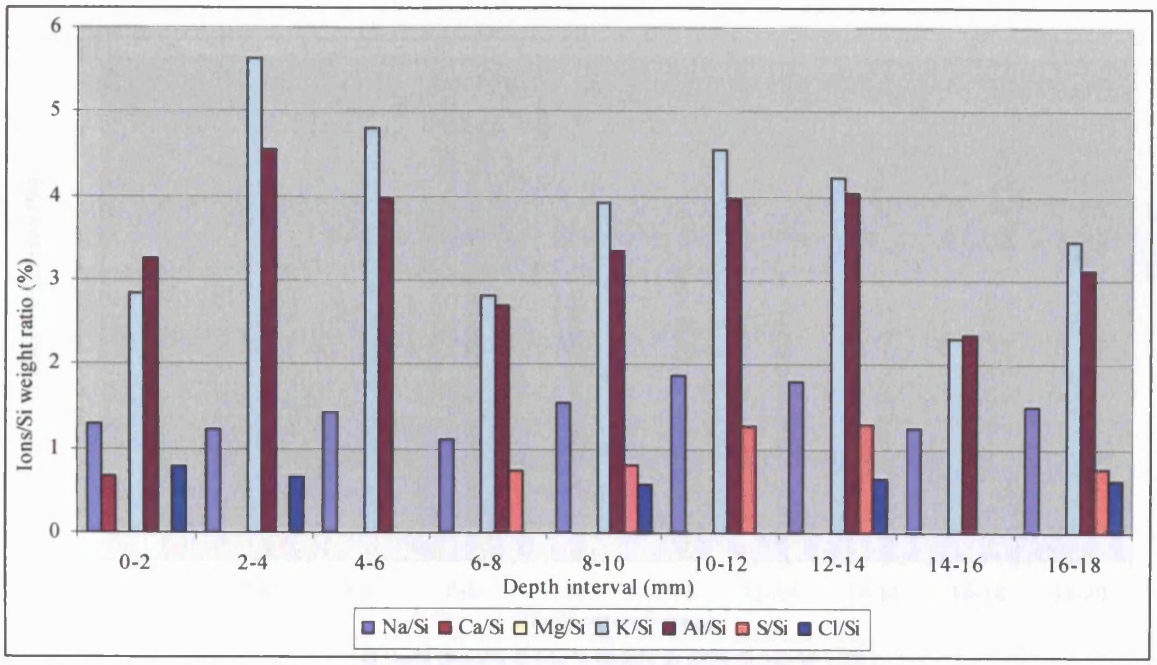

Figure (Y8): The main ions/Si ratio in the Locharbriggs sandstone at the end of the fourth run. Solution: saturated sodium sulfate.

Appendix Y: The main ions/Si weight ratio in the Locharbriggs sandstone specimens at the end of the modified salt crystallisation test.

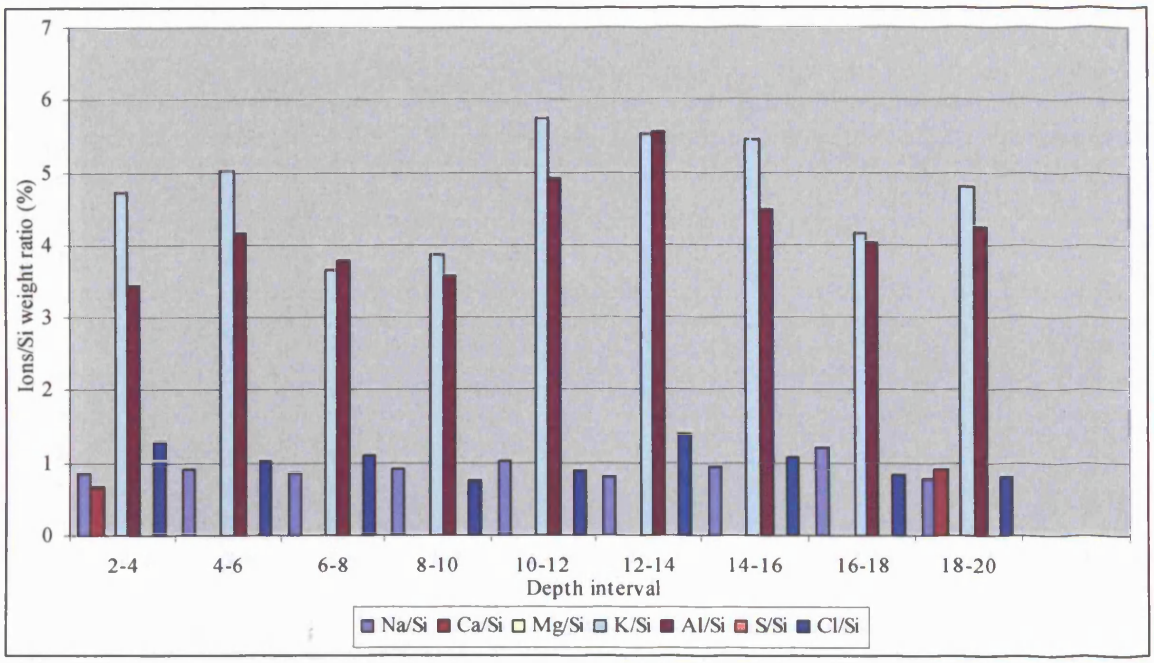

Figure (Y9): The main ions/Si ratio in the Locharbriggs sandstone at the end of the fourth run. Solution: saturated Petra salt solution.

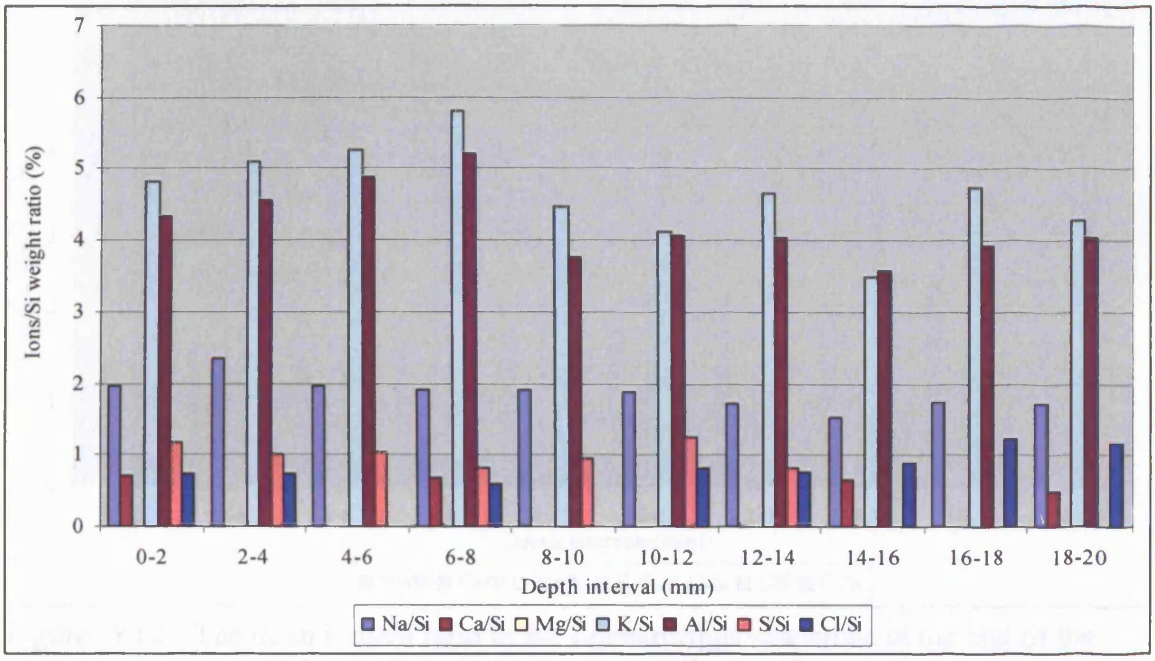

Figure (Y10): The main ions/Si ratio in the Locharbriggs sandstone at the end of the fifth run. Solution: saturated sodium sulfate.

Appendix Y: The main ions/Si weight ratio in the Locharbriggs sandstone specimens at the end of the modified salt crystallisation test.

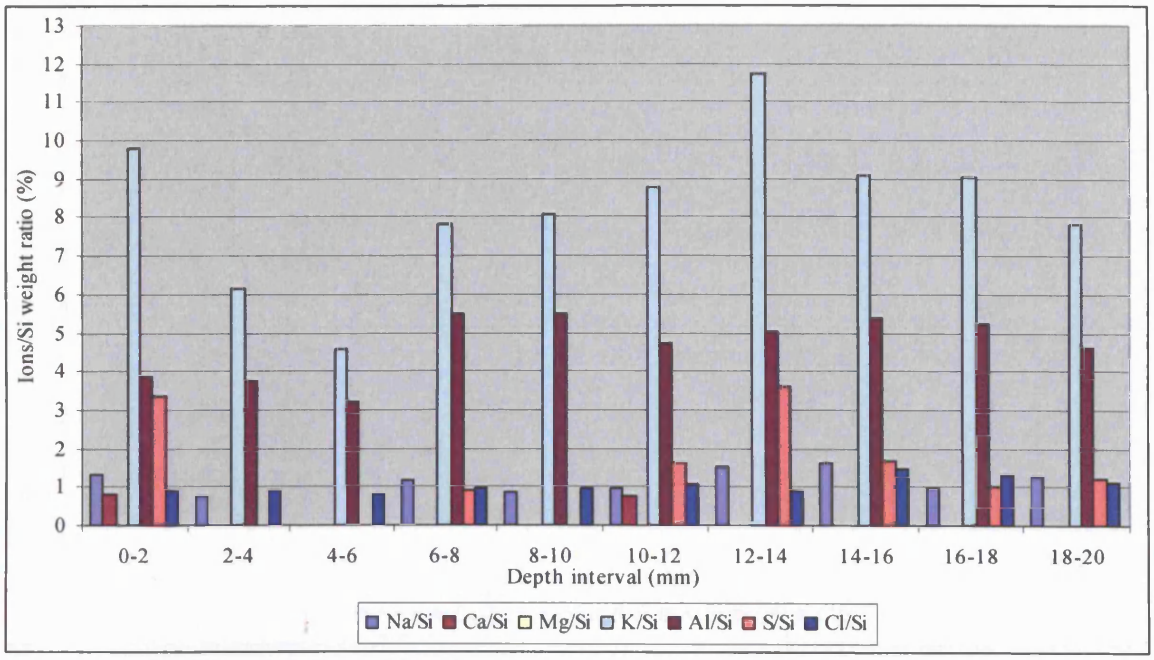

Figure (Y11): The main ions/Si ratio in the Locharbriggs sandstone at the end of the fifth run. Solution: saturated Petra salt solution.

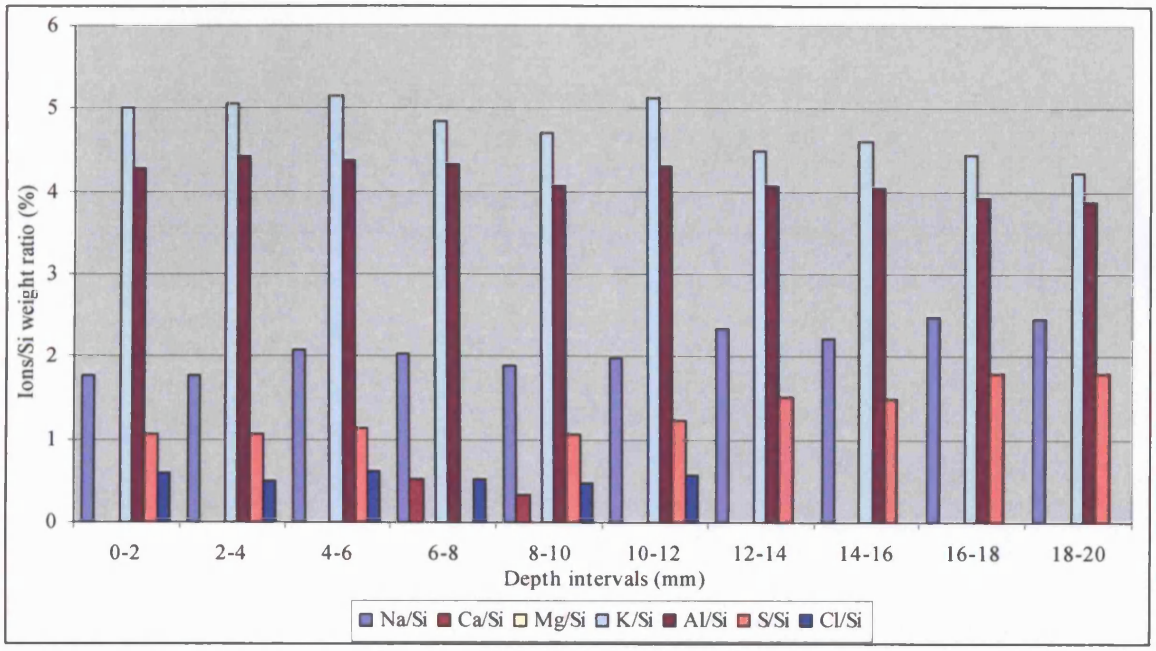

Figure (Y12): The main ions/Si ratio in the Locharbriggs sandstone at the end of the sixth run. Solution: saturated sodium sulfate.

Appendix Y: The main ions/Si weight ratio in the Locharbriggs sandstone specimens at the end of the modified salt crystallisation test.

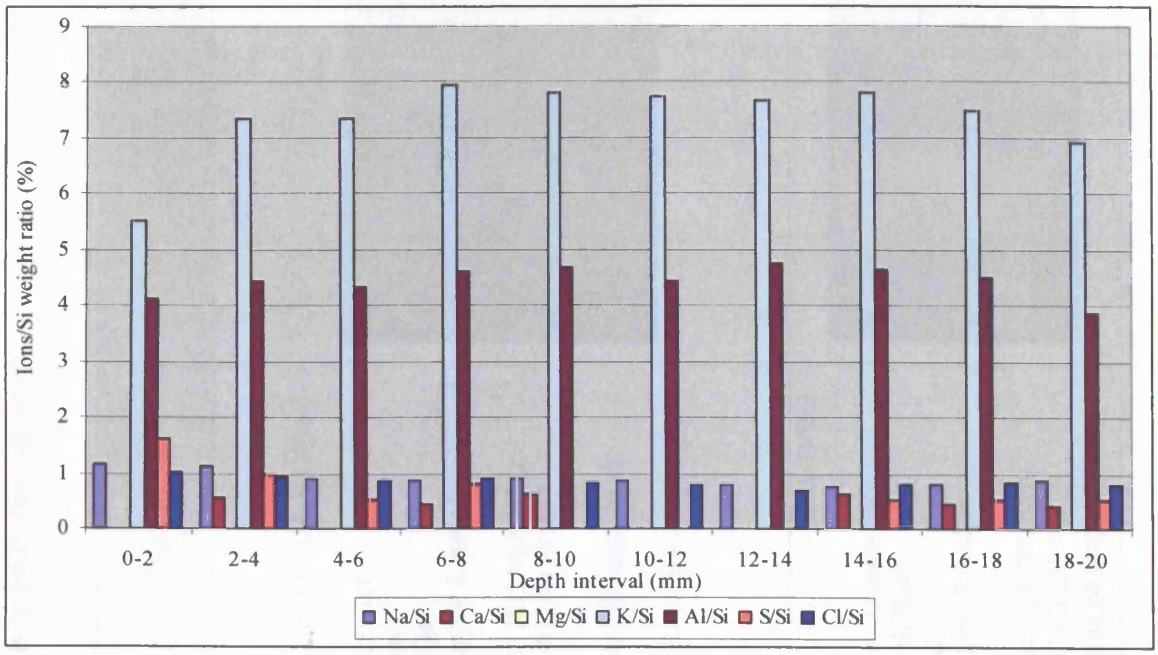

Figure (Y13): The main ions/Si ratio in the Locharbriggs sandstone at the end of the sixth run. Solution: saturated Petra salt solution.

Appendix Za: Specifications of the instruments used in the research.

Instruments	Location	Specification	Supplier	Image
Ion Chromatography (IC) Dionex modular system	Department of Earth Sciences, University College London, London, UK.	The instrument is a Dionex modular system comprising of the following components: ED 50 electrochemical detector IP 25 isocratic pump EG 50 eluant generator AG 50 thermal compartment AS 50 auto sampler The separation of the ions was performed by an AS 17 anion separator using 15 mM KOH eluant Software: Chameleon For more details see: http://www1.dionex.com/en-us/webdocs/30193_ICS-3000_DataSheet_V26_releasedJC092605.pdf	Dionex (UK) Ltd. (Main Office) 4 Albany Court Camberley GU 16 7QL Surrey United Kingdom Phone: 44 (01276) 691722 Fax: 44 (01276) 691837 e-mail: info@dionex.co.uk Website: http://www.dionex.co.uk	
Ion Chromatography (IC) Dionex DX 100	Geology Department, Royal Holloway University, Egham, UK.	AS14A anion column AMMS II anion micromembrane suppressor Eluant: 1.8 mM carbonate/1.7 mM bicarbonate Regenerant: 0.05M H2SO4 Detection: Bipolar heated conductivity cell, digital signal processing over the range of 0-500 µS Software: PeakNet-IA	Dionex (UK) Ltd. - Leeds Office 6 Pavilion Business Park Royds Hall Road LS12 6AJ Leeds United Kingdom Phone: 44 (113) 279 8579 Fax: 44 (113) 231 1597 e-mail: info@dionex.co.uk	

Appendix Za: Specifications of the instruments used in the research.

Instruments	Location	Specification	Supplier	Image
Inductively Coupled Plasma - Atomic Emission Spectrometry (ICP-AES) Perkin Elmer Optima 3300RL	Geology Department, Royal Holloway University, Egham, UK	Segmented array Charge-coupled-device Detector Subarrays 235 Pixels per subarray 20 - 80 Injector tube (quartz) 1.50 mm id Plasma power 0.8–1.2 kW Coolant argon flow 11.0–15.0 l min21 Nebulizer argon pressure 280 kPa (40 psi) Sample uptake 1.0 ml min21 Autosampler AS91 Sample positions 98 Sample read delay 60 s Autosampler wash delay 20 s Integration time 3 s Number of integration 3	PerkinElmer LAS (UK) Ltd Chalfont Road Seer Green Beaconsfield Bucks HP9 2FX Tel. 0800-89 60 46 Fax 0800-89 17 14 http://uk.instruments.perkinelmer.com	
Polarizing Transmitted Light Microscope Leica DMLP	Institute of Archaeology, University College London, London, UK	Polarizing transmitted light microscope Built-in 12V/100W illumination system Objective magnifications 1.6x - 250x RL/TL polarizers Field of view 2.5mm. Used magnification: 40x Dimension Width: 365mm. Height: 505mm. For more details see: http://www.spectronic.co.uk/dmlsp_lp.pdf	Leica Microsystems (UK) Ltd Davy Avenue Knowlhill Milton Keynes MK5 8LB Tel.:+44 1 908 246 246 Fax.:+44 1 908 609992 www.leica-microsystems.com	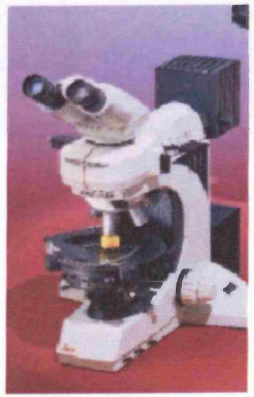

Appendix Za: Specifications of the instruments used in the research.

Instruments	Location	Specification	Supplier	Image
Environmental Scanning Electron Microscopy (ESEM) Philips XL 30	Institute of Archaeology, University College London, London, UK	Resolution: 2 nm Accelerating voltage: 0.2 to 30 kV Electron gun: Field-Emission Magnification: 15 to 500,000 Stage movements: Tilt -15° to +75° Z 50 mm X 50 mm Y 50 mm Image media: Digital storage Detectors: Wet Mode Gaseous secondary electron detector Set of environmental secondary detectors Solid state backscattered electron detector High Vacuum Mode:Everhart-Thornley secondary electron detector Solid state backscattered electron Digital EDS Prism X-ray detector with IMIX-PC system. Peltier cooling stage Specimen chamber CCD camera Software: INCA Microanalysis version 16. Oxford instrument: Oxford Instruments Analytical, Bucks, UK.	FEI UK Ltd. Cambridge Business Park Cowley Road CB4 0HF Cambridge United Kingdom Tel: +44 1223 468560 Fax: +44 1223 468599	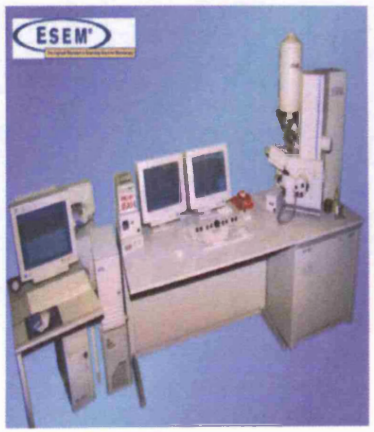

Appendix Za: Specifications of the instruments used in the research.

Instruments	Location	Specification	Supplier	Image
X-ray Fluorescence (XRF) SPECTRO X-LAP 2000	Institute of Archaeology, University College London, London, UK	**Excitation** X-ray end-window tube with Pd anode Max. power 400W Max. voltage 55Kv **Sample chamber**: Sample trays for 32mm (20 position) and 40mm (12 position). **Detector:** Si (Li) detector (12mm^2 active area, 3mm effective thickness). 8 mm Moxtek dura beryllium™ radiation entrance window. Energy resolution < 154eV, measured at the Mn Kα line with an input count rate of 104 pulses. **Digital Pulse Processor**. **Software**: Menu-based X-LAP Pro software. Height: 1060mm. Width: 950mm. Depth: 710mm. **Analytical method** : Pellet analysis (Torboquant).	SPECRO A. I. Inc Scientific & Medical Products Ltd. Shirley House 12 Gatley Road Cheadle Cheshire SK8 1PY Tel.: +44.161.491 3068 Fax: +44.161.428 7521 Email: scimed@dircon.co.uk Website: http://www.spectro.co.uk	

Appendix Za: Specifications of the instruments used in the research.

Instruments	Location	Specification	Supplier	Image
Diffractometer Philips PW 1710	Department of Earth Sciences, University College London, London, UK	Type: Phillips PW 1710 Diffractometer. The machine was fitted with a curved graphite crystal monocharomator using Ni-filtered Cu K-alpha radiation. 40Kv, 30mA. Scanning angles: 2-40° for clay mineral analysis and 2-60° for the whole rock analysis at 0.5° per minute, 0.5 ° divergences, 2mm receiving, and 0.5° scatter. Analysis of the mineral phase was carried out using the Philips PC-APD software.	Unknown	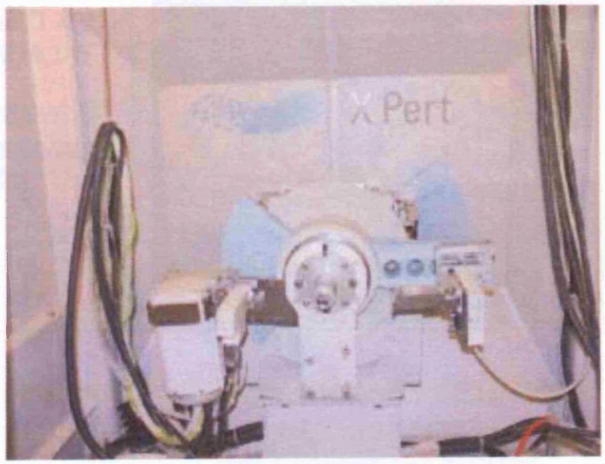

Appendix Za: Specifications of the instruments used in the research.

Instruments	Location	Specification	Supplier	Image
Microclimate Generator A 92 MCG	Institute of Archaeology, University College London, London, UK	A 92 MCG-TG Microclimate Generator Size: the size of desktop case.	Microclimate Technologies International 114 Bowes Road, Units 1 & 2 Concord, ON, CANADA L4K 1J7 Tel: +146 647 833 1531 http://www.microclimate.ca/productdata/mcgsmall.htm	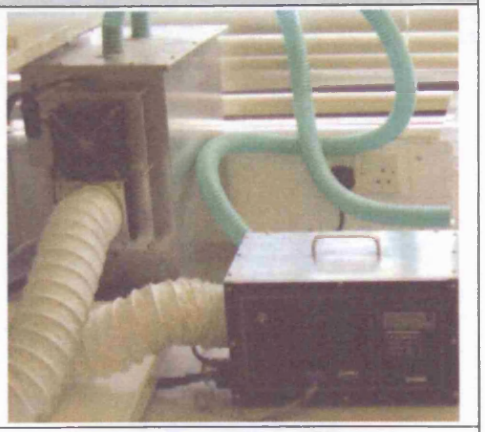
Anemometer Lutron Am-4201 hand anemometer	Department of Geography, University College London, London, UK	Display: 18 mm (0.7") LCD (Liquid Crystal Display), 3 1/2 digits. Measurements: m/s (meters per second) km/h (kilometers per hour) ft/min (feet per minute) knots (nautical miles per hour) Operating temperature: 0°C to 50°C Operating humidity: Less than 80% RH Dimensions: 168mm x 80mm x 35 mm Air velocity sensor structure: Conventional twisted vane arms and low friction ball-bearing design	Lutron Electronic Enterprise Co Ltd Min Chuan W. Rd., 4F No 106 Ta Tung Chu Taipei Taiwan 103	

Appendix Za: Specifications of the instruments used in the research.

Instruments	Location	Specification	Supplier	Image
Data loggers Tinytag Plus data logger (TGP-1500)	Institute of Archaeology, University College London, London, UK	Memory size: 32K (Non-volatile) No. of readings: app. 16000/channel. Resolution: 8bit. Trigger start: Magnatic reed switch. Delayed start: Relative/actual up to 45days. Logging interval: 1 sec-10days. Stop option: when full. IP Rating: IP68[2] Function range: -20 -+85°C Dimensions: 35mm×57mm × 80mm Sensor 1 Temperature: Range: -30-+50°C. Type: 10K NTC Thermistor Accuracy: ± 0.2°C. Sensor 2 Relative Humidity Range : 0-100% Type: Capacitive Accuracy: ±3%RH.	Gemini Data Loggers (UK) Ltd. Scientific House Terminus Road Chichester West Sussex PO19 8UJ United Kingdom Tel: +44 1243 813000 Fax: +44 1243 531948 Email: sales@geminidataloggers.com Web: www.geminidataloggers.com	

Appendix Za: Specifications of the instruments used in the research.

Instruments	Location	Specification	Supplier	Image
Data loggers Tinytag extra Temperature/ extra Relative Humidity (TXG-3580)	Institute of Archaeology, University College London, London, UK	Memory size: 16K (Non-volatile) No. of readings: app. 7900/channel. Resolution: 8bit. Trigger start: Magnatic reed switch. Delayed start: Relative/actual up to 45days. Logging interval: 1 sec-10days. Stop option: when full. Function range: -20 -+85°C IP Rating: IP68[2] Dimensions: 40mm×60mm × 82mm Sensor 1 Temperature: Range: -30-+85°C. Type: 10K NTC Thermistor Accuracy: ± 0.2°C. Sensor 2 Relative Humidity Range : 0-100% Type: Capacitive Accuracy: ±3%RH.	Gemini Data Loggers (UK) Ltd. Scientific House Terminus Road Chichester West Sussex PO19 8UJ United Kingdom Tel: +44 1243 813000 Fax: +44 1243 531948 Email: sales@geminidataloggers.com Web: www.geminidataloggers.com	

Appendix Za: Specifications of the instruments used in the research.

Instruments	Location	Specification	Supplier	Image
Electrical power supply EMS 24v SA	Institute of Archaeology, University College London, London, UK	Electrical power supply out put: 24v SA EMS power	EMS (Manufacturing) Ltd Merlin House Lancaster Road High Wycombe Buckinghamshire HP12 3PY England	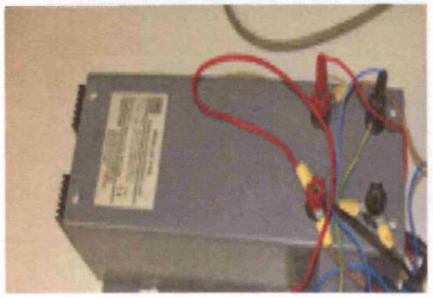
Multifunction Time Delay Relays Crouzet TAR1	Institute of Archaeology, University College London, London, UK	Type: Multifunction Time Delay Relays. Brand: Crouzet. Supply Voltage (ac-dc): 20 - 30 Vdc; 20 - 260 Vac. Time Range: 1s-100hr. Reset Accuracy: 100ms. Contact Rating - Resistive Load: 8A at 250VacA Height: 78mm. Width: 22.5mm. Depth: 95mm.	RS Components Ltd Birchington Road Corby Northants NN17 9RS, UK Tel: 08457 201201 Fax: 0845 850 9911 Web: http://rswww.com	

Appendix Za: Specifications of the instruments used in the research.

Instruments	Location	Specification	Supplier	Image
Gallenkamp vacuum oven	Institute of Archaeology, University College London, London, UK	Temperature range, °C: 30 to 200 at ambient temperature less than 25°C. Internal dimensions: (wxdxh), mm: 366x29x260. Power rating, max W: 1000.	VWR International Ltd BDH Laboratory Supplies Poole Dorset United Kingdom BH15 1TD Tel: 01202669700	
Electrical Air Pump Hailea ACO-328	Institute of Archaeology, University College London, London, UK	Air flow: 75l/min Power composition: 55W. Wieght: 2,8kg. Dimension: 199x108x133mm	Hailea Group Sinili Industrial zone Sinili Road, Raoping County, Chaozhou, Guangdong China (Mainland) Tel: ++ 867688899999 Fax: ++ 867688883813 Website: www.hailea.com	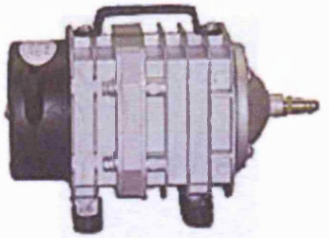

Appendix Za: Specifications of the instruments used in the research.

Instruments	Location	Specification	Supplier	Image
Temperature Controlled Water Bath Grant (W28)	Institute of Archaeology, University College London, London, UK	Type: Grant W28 Thermostatted Water Bath. Capacity 28 litres. Internal LWD: 505x 300 x 200mm Temperature: +5 ambient to 150°C	Grant Instruments Cambridge Ltd Barrington CB2 5QZ England Tel:02076360811 Fax: 02076362410	
Gas wash bottles	Institute of Archaeology, University College London, London, UK	Gas wash bottles: manufactured from chemically resistant borosilicate glass. Two sizes of these bottles were used in this research: 3L and 500ml. Boday height : 260mm.	VWR International Ltd BDH Laboratory Supplies Poole Dorset United Kingdom BH15 1TD Tel: 01202669700	

Appendix Za: Specifications of the instruments used in the research.

Instruments	Location	Specification	Supplier	Image
2/2 General Purpose Solenoid Valve	Institute of Archaeology, University College London, London, UK	Type: Solenoid Valves. Brand : Burkert: Supply Voltage: 24 Vdc Port size: ½ in. Pressure range: 0 – 10bar Orifice diameter: 10mm. Ambient Temperature: +55°C. Coil material: Epoxy Encapsulated/	RS Components Ltd Birchington Road Corby Northants NN17 9RS, UK Tel: 08457 201201 Web: http://rswww.com Fax: 0845 850 9911	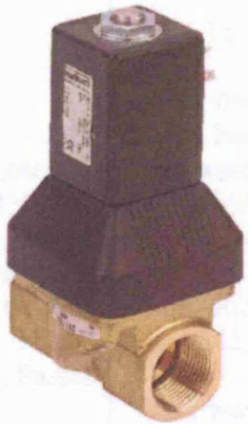
SL60-A Evaporative Coolers	Institute of Archaeology, University College London, London, UK	Multifunction cooler, humidifier, fan, air and air cleaner. Power composition: 60W. Dimensions: 389mm×279mm×635mm. Water level indicator. 230V-50Hz.	Expert Climate Control. 34 New John Street West Birmingham B19 5NB Tel: 0121 333 6373 Fax: 0121 333 6166	

Appendix Zb: Specifications of the salts used in the simulation tests.

Salt	Specification	Supplier
Sodium sulfate anhydrous GPR	Chemical formula: Na_2SO_4 Molecular weight: 142.04 Assay (on dried material): 99.0-100.5% Maximum limit of impurities Loss on drying (130 °C): 1% Chloride(Cl): 0.002% Arsenic (As): 0.0002% Heavy metal (as Pb): 0.001% Iron (Fe): 0.001%	Merck Ltd Hunter Boulevard Magan Park Lutterworth Leicestershire LE17 4XN Tel: 0800223344 Fax: 01455558586 Web: www.vwr.com
Sodium chloride GPR	Chemical formula: NaCl Molecular weight: 58.44 Minimum assay (argentometric, calculated on dried material :99.5% Maximum limit of impurities Loss on drying at (130 °C): 0.5% Hexacyanoferrate ($Fe(CN)_6$: Passes test Sulfate: 0.01% Ammonium (NH_4): 0.002% Heavy metal (as Pb): 0.0005% Iron (Fe): 0.0002% Potassium (K): 0.02%	Merck Ltd Hunter Boulevard Magan Park Lutterworth Leicestershire LE17 4XN Tel: 0800223344 Fax: 01455558586 Web: www.vwr.com

Appendix Zb: Specifications of the salts used in the simulation tests.

Salt	Specification	Supplier	Salt	Specification	Supplier
Sodium nitrate	Chemical formula:$NaNO_3$ Molecular weight: 84.99g/mol Assay (acidimetric): ≥99.5 Insoluble matter: ≤ 0.005 pH value (5%; water): 5.5-8.0 Chloride(Cl): ≤0.0005 Iodate: ≤0.0005 Magnesium (Mg): ≤0.002 Ammonium(NH_4): ≤0.002 Nitrite (NO_2): ≤0.001 Phosphate (PO_4): ≤0.0005 Sulfate (SO_4): ≤0.003 Heavy metal (as Pb): ≤0.0005 Calcium (Ca): ≤0.002 Iron (Fe): ≤0.0003 Potassium (K): ≤0.01	VWR International Ltd BDH Laboratory Supplies Poole Dorset United Kingdom BH15 1TD Tel: 01202669700	Calcium-nitrate 4 hydrate	Chemical formula: $Ca(NO_3)_2*4H_2O$ Molecular weight: 236.15 g/mol Assay (complexometric): ≥ 98.0 Chloride(Cl): ≤0.005 Sulfate (SO_4): ≤0.02 Heavy metal (as Pb): ≤0.002 Iron (Fe): ≤0.001 Ammonium(NH_4): ≤0.0005 Substance not precipitated by Ammonium oxalate (as sulfate).	VWR International Ltd BDH Laboratory Supplies Poole Dorset United Kingdom BH15 1TD Tel: 01202669700

Appendix Zb: Specifications of the salts used in the simulation tests.

Salt	Specification	Supplier	Salt	Specification	Supplier
Potassium sulfate GPR	Chemical formula: K_2SO_4 Molecular weight: 174..24 Assay (preciptative titration ≥:99% Maximum limit of impurities Chloride(Cl): 0.002% Heavy metal (as Pb): 0.002% Iron (Fe): 0.001% Sodium (Na): 0.2	VWR International Ltd BDH Laboratory Supplies Poole Dorset United Kingdom BH15 1TD Tel: 01202669700	Calcium sulfate anhydrous	Chemical formula: $CaSO_4$ Molecular weight: 136.14 Minimum assay: 96% Loss in ignition: 3%.	VWR International Ltd BDH Laboratory Supplies Poole Dorset United Kingdom BH15 1TD Tel: 01202669700
Magnesium sulfate dried	Chemical formula: $MgSO_4$ Molecular weight: Minimum assay (argentometric, calculated on dried material : 99-101 Chloride: ≤ 0.02 Heavy metal (as Pb): ≤ 0.001 Iron (Fe): ≤ 0.001	VWR International Ltd BDH Laboratory Supplies Poole Dorset United Kingdom BH15 1TD Tel: 01202669700			